

Plasma Confinement

R. D. Hazeltine

University of Texas at Austin

J. D. Meiss

University of Colorado at Boulder



Addison-Wesley Publishing Company

The Advanced Book Program

Redwood City, California • Menlo Park, California • Reading, Massachusetts
New York • Don Mills, Ontario • Wokingham, United Kingdom • Amsterdam
Bonn • Sydney • Singapore • Tokyo • Madrid • San Juan

Frontiers in Physics

DAVID PINES/Editor

Volumes of the Series published from 1961 to 1973 are not officially numbered. The parenthetical numbers shown are designed to aid librarians and bibliographers to check the completeness of their holdings.
Titles published in this series prior to 1987 appear under either the W. A. Benjamin or the Benjamin/Cummings imprint; titles published since 1986 appear under the Addison-Wesley imprint.

- (1) N. Bloembergen Nuclear Magnetic Relaxation: A Reprint Volume, 1961
- (2) G. F. Chew S-Matrix Theory of Strong Interactions: A Lecture Note and Reprint Volume, 1961
- (3) R. P. Feynman Quantum Electrodynamics: A Lecture Note and Reprint Volume, 1961
- (4) R. P. Feynman The Theory of Fundamental Processes: A Lecture Note Volume, 1961
- (5) L. Van Hove, N. M. Hugenholtz and L. P. Howland Problem in Quantum Theory of Many-Particle Systems: A Lecture Note and Reprint Volume, 1961
- (6) D. Pines The Many-Body Problem: A Lecture Note and Reprint Volume, 1961
- (7) H. Frauenfelder The Mössbauer Effect: A Review—With a Collection of Reprints, 1962
- (8) L. P. Kadanoff Quantum Statistical Mechanics: Green's Function Methods in Equilibrium and Nonequilibrium Problems, 1962
- (9) G. E. Pake Paramagnetic Resonance: An Introductory Monograph, 1962 [cr. (42)—2nd edition]
- (10) P. W. Anderson Concepts in Solids: Lectures on the Theory of Solids, 1963
- (11) S. C. Frautschi Regge Poles and S-Matrix Theory, 1963
- (12) R. Hofstadter Electron Scattering and Nuclear and Nucleon Structure: A Collection of Reprints with an Introduction, 1963
- (13) A. M. Lane Nuclear Theory: Pairing Force Correlations to Collective Motion, 1964
- (14) R. Omnes Mandelstam Theory and Regge Poles: An Introduction for Experimentalists, 1963
- (15) M. Froissart Complex Angular Momenta and Particle Physics: A Lecture Note and Reprint Volume, 1963
- (16) H. L. Frisch The Equilibrium Theory of Classical Fluids: A Lecture Note and Reprint Volume, 1964
- (17) M. Gell-Mann The Eightfold Way (A Review—With a Collection of Reprints), 1964
- (18) M. Jacob Strong-Interaction Physics: A Lecture Note Volume, 1964
- (19) G. F. Chew Theory of Interacting Fermi Systems, 1964
- (20) J. R. Schrieffer Theory of Superconductivity, 1964 (revised 3rd printing, 1983)
- (21) N. Bloembergen Nonlinear Optics: A Lecture Note and Reprint Volume, 1965
- (22) R. Brout Phase Transitions, 1965
- (23) I. M. Khalatnikov An Introduction to the Theory of Superfluidity, 1965
- (24) P. G. deGennes Superconductivity of Metals and Alloys, 1966
- (25) W. A. Harrison Pseudopotentials in the Theory of Metals, 1966
- (26) V. Barger Phenomenological Theories of High Energy Scattering: An Experimental Evaluation, 1967
- (27) P. Choquard The Anharmonic Crystal, 1967

Table of Contents

Editor's Foreword

xi

Preface

xiii

1	Introduction	1
1.1	The Science of Plasma Confinement	1
1.2	Goals and Synopsis	2
1.3	Confinement Demands of Controlled Fusion	3
1.4	Magnetized Plasma Confinement	7
1.5	Character of Toroidal Confinement	10
1.6	Understanding Confinement	17
2	Review of Fundamentals	19
2.1	Tensor Calculus	19
2.2	Lagrangian and Hamiltonian mechanics	26
2.3	Maxwell-Lorentz equations	29
2.4	Charged Particle Motion	33
3	Confined Plasma Equilibrium	45
3.1	Flux Surfaces	45
3.2	Magnetic Flux Coordinates	52
3.3	Applications of Flux Coordinates	57
3.4	Special Cases of Flux Coordinates	62
3.5	Scalar Pressure Equilibrium	66
3.6	Explicit Force Balance	71
3.7	Ampère's Law	74
3.8	Tensor Pressure Equilibrium*	78
3.9	Magnetic Field	81
3.10	Plasma Current	82
3.11	Equilibrium Electric Field	87
3.12	Large Aspect Ratio Approximation	89
3.13	Summary	96

4	Kinetic Description of a Magnetized Plasma	105
4.1	General Kinetic Equation	105
4.2	Drift-kinetic Equation	113
4.3	Gyrokinetic Equation*	123
4.4	Guiding-center Phase Space	134
4.5	Application: Flow of a Magnetized Plasma	144
4.6	Summary	152
5	Coulomb Collisions	157
5.1	General Collision Operator	157
5.2	Coulomb Operator	163
5.3	Application: The Equilibrium Distribution	176
5.4	Summary	185
6	Fluid Description of Magnetized Plasma	191
6.1	Moments of Distribution Function	191
6.2	Moments of Kinetic Equation	194
6.3	Small Gyroradius Ordering	199
6.4	MHD Closure	211
6.5	Generalization of MHD	218
6.6	Application of the Drift Model: Drift Waves	228
6.7	Summary	235
7	Stability of Confined Plasmas	241
7.1	General Stability Considerations	241
7.2	Ideal MHD Waves	245
7.3	Shear-Alfvén Law	247
7.4	Flute Reduction	252
7.5	Cylindrical Reduced MHD	260
7.6	Ideal MHD Stability*	272
7.7	Asymptotic Matching	279
7.8	Boundary Layer Theory	282
7.9	Kinetic Effects*	291
7.10	Ballooning Representation	298
7.11	Ideal Stability	303
7.12	Model Equation*	307
7.13	Non-Ideal Stability*	314
7.14	Summary	314
8	Collisional Transport	321
8.1	Introduction: Classical Perpendicular Transport	321
8.2	Fluid Evolution in a Torus	327
8.3	Axisymmetric Geometry	332
8.4	Entropy Production*	338
8.5	Tokamak Transport: Basic Features	342

8.6 Tokamak Transport: Analysis and Results*	351
8.7 Summary	370
9 Nonlinear Processes	375
9.1 Magnetic Islands	375
9.2 Coherent Nonlinear Islands*	382
9.3 Multiple Helicity Fields: Island Overlap Criterion	386
9.4 Anomalous Particle Transport	391
9.5 Ambipolarity and Rotation*	394
9.6 Summary	398

Chapter 1

Introduction

1.1 The Science of Plasma Confinement

A sufficiently cold plasma can be confined by glass tubing; a sufficiently large plasma is confined gravitationally. This book is concerned with the confinement of terrestrial, very hot plasmas, which would be quenched by direct contact with ordinary container walls. Primarily of interest in application to controlled fusion research, such plasmas are confined magnetically: the magnetic field, itself ultimately confined by mechanical forces on the field coils, acts as an insulating and stress-bearing containment vessel. So our subject is more specifically *magnetic confinement*: the behavior of bounded, magnetized plasma.

The international research program in magnetic plasma confinement, now some forty years old, stems almost entirely from interest in controlled fusion. It is therefore not surprising that the perspective and emphasis of that program pervades this book. Yet this is not a book about controlled fusion. Beyond a brief survey later in the present chapter, we rarely refer to the specific confinement criteria set by fusion, and make no attempt to cover the multitude of scientific, engineering and environmental issues involved in this potential energy source. Furthermore, mindful of the application of fusion-confinement ideas to such fields as astrophysics and solar physics, we have tried to adopt as broad and fundamental a viewpoint as possible. Thus we approach plasma confinement as a scientific issue with both extrinsic and intrinsic interest.

Given the potent electrodynamics of an assemblage of charged particles, to what extent can they be kept away from, or at least insulated from, material walls? How do such fundamental physical processes as Coulomb collisions, fluid instability, and turbulence limit confinement? The attack on questions of this sort has yet to generate complete or final answers. But it has produced a body of science: a collection of observations, insights and methods that illuminate part of the physical world. This scientific domain is the subject of our book.

1.2 Goals and Synopsis

No book of reasonable size can attempt to cover the entire discipline of plasma confinement. Our coverage will be skimpy in several areas; some aspects of the subject are not treated at all. Our most important omission concerns experimental confinement physics. The design and operation of experimental confinement devices, the development of plasma diagnostic methods, and the vast technology of confinement, heating and plasma-current drive are areas of obvious critical importance to controlled fusion—and areas that have shown exciting progress in recent years. They deserve, in fact require, treatment in a separate volume.

Thus, in keeping with the interests of its authors, this book primarily treats the *theory* of magnetic confinement. However, we have tried to make it more than a collection of theoretical methods. Instead we emphasize the relatively small set of physical ideas that lie at the heart of the confinement problem. Most of these ideas have a significance that is not only theoretically pervasive but also borne out, at least qualitatively, by experimental observation. In developing these concepts and demonstrating their application to various issues of confined plasma evolution, we attempt to display the scaffold of plasma confinement physics.

Chapter 2 contains a review of certain ideas and methods that are used throughout the book. It is intended to indicate how much mathematical and physical background is assumed, and perhaps to jog memories. The treatment is very terse; students who find much of this material new should probably seek more detailed coverage elsewhere. Chapter 3, essentially a much more detailed and careful version of §1.4 below, concerns confined plasma equilibrium. The next three chapters concern how a system as complicated as a confined plasma is to be efficiently and convincingly described. The kinetic description is considered first: in Chapter 4 we derive and discuss the basic (drift- and gyro-) kinetic equations, and in Chapter 5, the collision operator. These treatments include applications of the methods discussed, so that, by the end of Chapter 5, key features of the confined plasma distribution function have been established. The fluid description of confined plasma is taken up in Chapter 6; special attention is given to the question of deriving a closed set of equations for the plasma and electromagnetic field. (Indeed, the closure issue, never trivial in plasma physics, is a theme of this book.) The results and methods of Chapters 4–6 are applied, in the three last three chapters, to the central confinement issues: linear stability, collisional transport and nonlinear resistive MHD, as well as kinetic and nonzero gyroradius considerations, are organized around the “shear-Alfvén law.” The techniques for studying transport are introduced in Chapter 8. The emphasis here is on basic physical ideas—such as the importance of collisionless orbits, or the role of momentum conservation—rather than detailed results. Finally, Chapter 9

provides a brief introduction to some of the nonlinear processes, including magnetic island evolution, and quasilinear transport, which seem critically to affect confined plasma behavior.

1.3 Confinement Demands of Controlled Fusion

A nuclear reaction liberates energy when the mass of the reactant nuclei exceeds that of the reaction products. Stored nuclear energy is a function of atomic weight, with a broad minimum in the vicinity of the element iron and maxima at both ends. The variation is sharpest at the lower end, for the lightest elements; thus much more energy per nucleon is freed by hydrogen fusion than by fission of uranium.

Hydrogen survives because of electrostatic repulsion: the repulsive Coulomb force between nuclei easily overrides nuclear attraction at atomic or molecular distances. The potency of this barrier results primarily from the infinite range of the Coulomb field, which impedes quantum tunneling. In fact tunneling becomes effective only after most of the Coulomb barrier has been classically penetrated, requiring large kinetic energy of the reactants. Thus fusion cross sections are negligibly small for kinetic energies less than several kilo-electron Volts (keV). For this reason, and because the density of fusion reactions depends on the product of the cross section with particle velocity, the interesting energy range for thermonuclear fusion is between ten and thirty keV.

Fusion in our sun relies on the proton-proton interaction, whose cross section, adequate in a body of stellar dimensions, is too small for laboratory reactions. Terrestrial fusion research depends upon hydrogen isotopes that are much more reactive, if unfortunately less abundant. Table 1 lists

Reactants	Products
D-D	T (1 Mev) + p (3 Mev)
D-D	He ³ (0.8 Mev) + n (2.5 Mev)
D-T	He ⁴ (3.5 Mev) + n (14 Mev)
D-He ³	He ⁴ (3.7 Mev) + p (14.7 Mev)

Table 1. Fusion reactions with relatively large cross-sections (Rose and Clark, 1961)

the most important reactions. The deuterium-tritium (D-T) reaction is emphasized because of its relatively favorable cross section; D-T reactors would operate at a temperature close to 10 keV. (Note that we always measure temperature in units of energy.) Other reactions that appear feasible for energy production, such as D-D and D-He³, may have economic

or environmental advantages but are more demanding with respect to confinement. For example, the D-D reaction is advantageous because of the relative abundance of deuterium (tritium is rare and would have to be bred from lithium) and because it provides a greater fraction of its energy in the form of charged particles, whose energy can be captured to sustain the reaction, or “directly” converted to output power. But a D-D reactor would apparently have to operate at temperatures exceeding 25 keV.

Some explanation of the term “thermal,” or “thermonuclear” fusion is appropriate here. One can imagine penetrating the Coulomb barrier by means of energetic, oppositely directed particle beams, at low temperature. Indeed, non-thermal schemes of this general sort have been proposed and remain objects of research. However, especially because the Coulomb cross section for elastic scattering always greatly exceeds fusion cross sections, most research attention has been devoted to a population of reactants whose velocity distribution approximates a Maxwellian: a *thermal* population, with temperature close to the optimal reaction energy. In this book we study thermal plasmas exclusively. On the other hand we treat seriously both the process of relaxation to a Maxwellian as well as the non-Maxwellian components of the steady-state distribution; the latter are critically important.

Power Balance and the Lawson Criterion

Fusion confinement requirements are conveniently quantified in terms of energy and particle *confinement times*. The energy confinement time, τ_E , is operationally defined in terms of a steady state plasma. One measures the plasma energy content, U , as well as the rate at which energy must be added to sustain the steady state. Unavoidable energy losses due to radiation losses (see below) are subtracted from the latter to provide a net rate of energy input, W_{in} . Then we have

$$\tau_E \equiv U/W_{\text{in}} .$$

The particle confinement time, τ_p , is defined analogously, in terms of particle content and replacement rate.

In a steady-state, self-sustained fusion plasma, the energy input would come from fusion reactions. We denote the power input by fusion reactions by F_{in} . Note that F_{in} measures the rate at which fusion energy is deposited in the plasma; it is smaller than the rate of fusion energy production, because only the kinetic energy of charged reaction products, such as alpha particles, can be contained. Neutron energy is too quickly lost to the walls of the containing vessel to contribute to F_{in} . We express the radiation losses by R_b , where the subscript refers to bremsstrahlung radiation. Cyclotron radiation losses are conventionally omitted because their longer wavelength allows at least partial reflection at the plasma boundary. Thus $W_{\text{in}} =$

$F_{\text{in}} - R_b$ and fusion plasma power balance is expressed as

$$F_{\text{in}} - R_b = U/\tau_E . \quad (1)$$

It was noted by Lawson that, while the energy content is proportional to plasma density, n , both quantities on the left-hand side of (1) vary with the square of the density (Rose and Clark, 1961). That F_{in} is proportional to n^2 follows immediately from the binary nature of fusion reactions; for R_b it is a consequence of the role of ions in accelerating electrons to produce bremsstrahlung—and the fact that plasma quasineutrality makes the electron and ion densities vary together. It follows that the density enters (1) only through the combination $n\tau_E$, the "Lawson parameter".

The critical value of the Lawson Parameter, $(n\tau_E)_c$, satisfies (1). It is evident that smaller values of $n\tau_E$ correspond to energy losses too severe for self-sustained fusion; larger values could presumably be cured by artificially enhanced losses. Thus the *Lawson criterion* for self-sustained, or "ignited" fusion states that the product of density and confinement time must equal or exceed $(n\tau_E)_c$.

Using the known fusion-reaction, energy-deposition and bremsstrahlung rates, it is possible to evaluate $(n\tau_E)_c$. The result is sensitive to the particular fusion reaction considered, as well as to various plasma parameters (such as impurity content) that are not easy to predict, so that a simple, general specification is difficult. Nonetheless most estimates are in rough agreement; for the important case of D-T reactions, one finds

$$(n\tau_E)_c \approx 5 \times 10^{14} \text{ sec/cm}^3 . \quad (2)$$

Confinement Q

Another measure of confinement quality, alternative to $n\tau_E$, realistically allows for nuclear energy production that is short of *ignition*, or self-sustained fusion. Thus a certain fusion device might produce excess energy only in the presence of continuous energy input, the deposited fusion energy being insufficient to maintain thermonuclear temperature. If the ratio (fusion power produced)/(operating power supplied) is sufficiently large, the device is a useful fusion reactor. Sometimes this ratio is called "engineering Q ".

A more commonly used ratio is simplified by including in the denominator only the *plasma heating power* that is required to sustain nuclear reactions. This ratio is denoted by

$$Q \equiv (\text{fusion power produced}) / (\text{heating power supplied}) .$$

Here the numerator is some multiple, $\alpha > 1$, of the deposited power F_{in} :

$$\text{fusion power produced} = \alpha F_{\text{in}} .$$

For the case of D-T fusion, where 80% of the fusion energy is carried off by 14 Mev neutrons, $\alpha \approx 5$.

The denominator of Q is a fraction, $\gamma < 1$, of the total externally supplied power, P_{in} , where P_{in} includes heating power as well as the power needed to magnetize the plasma, drive plasma currents required for equilibrium and so on:

$$\text{heating power supplied} = \gamma P_{in}. \quad (3)$$

The value of γ is very sensitive to reactor concept and design; it could in principle approach unity, but might be as small as 10%. One object of magnetized plasma research is to find confinement schemes consistent with $\gamma \approx 1$.

Evidently the ignited state corresponds to $Q = \infty$. Finite Q -values have scientific interest or even, if sufficiently large, power-production relevance. For example, a Q value of five or more in a D-T plasma yields fusion heating comparable to external heating; such a plasma, although far from economic application, might reveal much about plasma ignition physics.

Most fusion reactors designs presume ignition, although, as we have observed, this is not economically essential. On the other hand, the confinement quality required by high Q differs little from what is required for ignition: large values of the Lawson parameter, approaching $(n\tau_E)_c$, are required to make Q much bigger than unity.

Summary

Fusion makes two demands on the quality of confinement: the temperature must exceed some critical temperature for significant fusion yield; and the product of density and confinement time must approach, or, for ignition, exceed the critical Lawson value. The critical temperature is close to ten keV (or, for reactions other than D-T, a few tens of keV), while the critical value of the Lawson parameter is several times 10^{14} sec/cm^3 .

It is possible to satisfy both demands without any plasma confinement in the usual sense. For "inertial confinement fusion", as it is called, τ_E is measured in microseconds and fixed essentially by inertia of the reactants; the density is correspondingly large. A controlled energy release is made possible by limiting the total reactant mass for each, essentially explosive, fusion cycle. The fusion devices considered in this book allow for steady-state, or nearly steady-state operation. Then densities are limited by the maximum containable plasma pressure—ultimately fixed by mechanical stresses on the confining magnetic field coils. A typical reactor might have $n \approx 10^{14}/\text{cm}^3$, with confinement times measured in seconds. Experimental densities and confinement times approach these figures.

1.4 Magnetized Plasma Confinement

Nonequilibrium Physics

A charged particle subject to magnetic force executes a helical orbit about an axis parallel to the local direction of the magnetic field; one says that the particle gyrates about the field line, while moving uniformly along it. We suppose at first that the field is uniform, so each field line is straight. By increasing the strength of the field, we can make the particle's Larmor radius or gyroradius indefinitely small, thereby restricting the particle orbit to the neighborhood of a single line. In so far as the field line avoids hitting boundaries, the particle is confined.

An obvious weakness of this scheme is its two-dimensional character: confinement in the direction of the field is not addressed. But before considering the third dimension, we note a more fundamental problem: consistency with classical thermodynamics. Since the equilibrium distribution of charged particles depends only on particle energy, it is unaffected by magnetic fields. Thus thermodynamic equilibrium is inconsistent with magnetic confinement.

For concreteness, consider the "canonical" two-dimensional confinement structure: an infinite circular cylinder (solenoid) with radius a and uniform, axial magnetic field. If the field is strong enough to make all gyroradii small compared to a , then single particle motion will be effectively axial. For magnetic confinement however, we must require in addition that field lines within a gyroradius of the wall are unpopulated. Thus the confined distribution must have a density gradient, with maximum near the cylindrical axis and vanishing density at the radius a . It is this gradient that contradicts thermodynamic equilibrium. Evidently any initial gradient is worn away by, *inter alia*, the random Coulomb interactions of discrete charges.

Single-particle confinement is straightforward, even in three-dimensions, because it involves only external forces. Plasma confinement, on the other hand, invokes electromagnetic interactions. At the very least, binary Coulomb collisions will relax density and temperature gradients; often collective interactions—plasma instability and turbulence—produce the same effect much more rapidly. The nonequilibrium character of magnetized plasma confinement has a controlling influence on confinement physics.

Toroidicity

Confinement in the third dimension is addressed, in different ways, by two broad classes of devices: open confinement systems and closed confinement systems.

In an open system, the confinement vessel is roughly cylindrical in

shape, and the field is essentially axial. Field lines intersect the material walls at either end of the vessel. Thus particles moving in the direction of the cylindrical axis are not confined in the usual sense, and a strategy is needed to “plug” the ends of the cylinder, or otherwise ameliorate the effects of end loss. The most common technique relies on the conservation of particle energy and magnetic moment, implying that particles with sufficient perpendicular energy will be reflected by positive gradients in the field magnitude. Hence confinement in the third dimension can be addressed by strong field regions, magnetic mirrors, at each end of the cylinder. The burden of mirror confinement is to insure that particles approaching a plug have enough perpendicular energy to be reflected by it.

The vast majority of plasma confinement devices are closed. In this case the field lines are bent, through appropriate coil geometry, in such a way that each is effectively endless. A field line without ends can be hoop-shaped, closing on itself, or it can fill some two- or three-dimensional region of space without self-intersections. In any case it can be shown that the magnetization of the entire plasma requires the boundary of the confinement region to be topologically equivalent to a torus: a closed confinement system is necessarily toroidal.

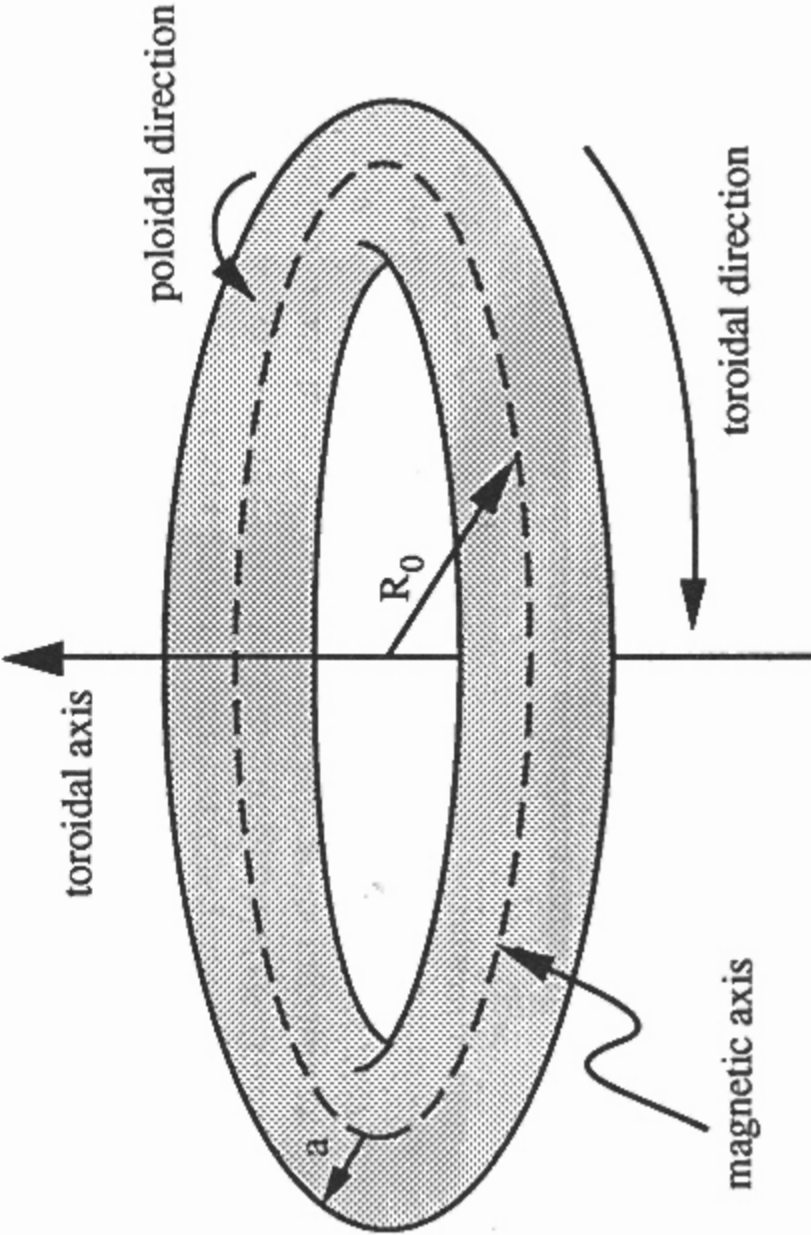


Figure 1. Simplest features of a torus.

A simple torus is depicted in Figure 1. The toroidal axis is vertical by convention; it is encircled by the magnetic axis, a single toroidal field line that generally locates the peak of the plasma density profile. The magnetic axis exemplifies a closed toroidal curve; any such curve can be loosely identified with the toroidal direction. Similarly, closed poloidal curves, enclosing the magnetic axis, indicate the local poloidal direction. One says

that toroidal curves traverse the torus the long way, and poloidal curves, the short way. Such statements reflect the essence of a torus: the existence of two topologically distinct round trips.

The torus in Figure 1. is axisymmetric—symmetric with respect to rotation about the major axis. Of course the same geometric concepts also apply to an asymmetric torus, such as the generic torus depicted in Figure 2.

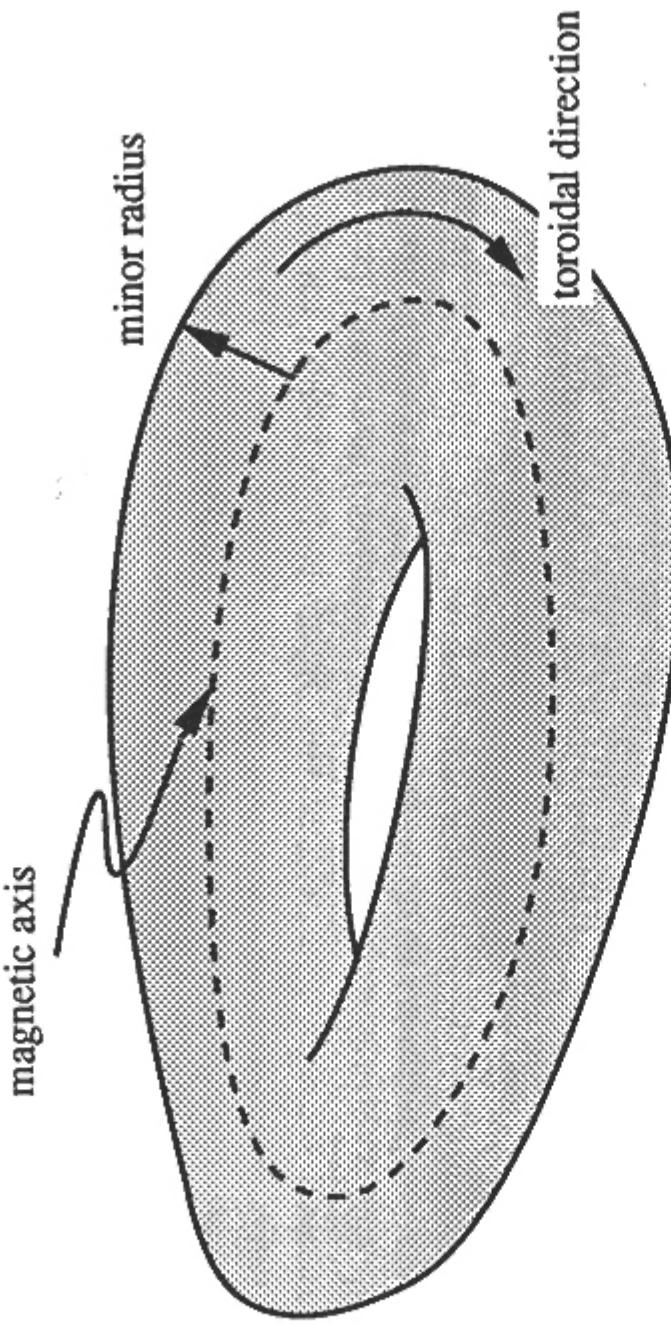


Figure 2. Features of a generic torus.

Corresponding to the two closed curves are two radii: the *major radius*, R , measuring distance from the toroidal axis, and the *minor radius*, r , measuring distance from the magnetic axis. The major radius of the magnetic axis is denoted by R_0 , while the minor radius of the confinement region is denoted by a . The ratio R_0/a , characterizing the “fatness” of the torus, is the toroidal *aspect ratio*.

A consequence of toroidicity is that the confining field cannot be uniform. For example, the magnitude of a purely toroidal, axisymmetric magnetic field, formed by bending a solenoid upon itself, varies inversely with major radius. Field variation and curvature are responsible for most of the difficulties in confining thermonuclear plasma.

Nonuniformity affects even single-particle confinement: the guiding-center drifts associated with non-uniform fields allow charged particles to stray from the field lines. In the simplest case of closed toroidal field lines, the drift is vertical (orthogonal to B and to ∇B), and in opposite directions for oppositely charged species. The electric field resulting from such uncompensated drifts would quickly sweep any confined plasma outward in major radius, so that confinement based on strictly toroidal, axisymmetric field is not possible.

However, vertical drifts can be rendered innocuous. By imposing strong poloidal motion on the guiding center trajectories, one controls the net ex-

cursion away from the magnetic axis. Such compensation is considered explicitly in Chapter 3. The required poloidal motion can result from gradients in the magnitude of purely toroidal field lines, but more commonly it is provided by field lines that have poloidal as well as toroidal components. Notice that in this case the lines are roughly helical, a typical line winding around a toroidal surface much like copper wire is wound on a ferromagnetic core. A toroidal surface that is covered in this way by lines of magnetic field is called a magnetic surface, or flux surface.

Thus toroidicity poses no insurmountable threat to single-particle confinement; the problem again stems from particle interactions. First, classical dissipation, resulting from Coulomb collisions, is enhanced by particle drifts, even when collisionless drifts are perfectly compensated. This issue is a major theme of Chapter 8. More severely, line-curvature threatens plasma confinement by its potentially unstable interaction with plasma pressure gradients. Indeed, the most dangerous electromagnetic instabilities usually involve curvature of the field. This topic is taken up in Chapter 7.

1.5 Character of Toroidal Confinement

Confinement Parameters

We have noted that the boundary surface of any closed magnetic confinement system is necessarily toroidal. Since the field lines are not to intercept material walls they must lie on this surface. It follows that the magnetic field on the surface can always be expressed as

$$\mathbf{B} = \mathbf{B}_P + \mathbf{B}_T \quad (4)$$

where \mathbf{B}_P and \mathbf{B}_T are the poloidal and toroidal components respectively. This decomposition is intended to be descriptive; more rigorous definitions of \mathbf{B}_P and \mathbf{B}_T will be found in Chapter 3. As we have noted, (4) suggests the picture of a single, helical field line, winding endlessly around the toroidal surface.

Systems have been envisioned in which all confinement forces are provided only at the boundary, the plasma pressure being nearly uniform inside. Much more commonly however, confinement is distributed in minor radius, in the sense that a smooth pressure gradient is supported. Then (4) applies not only to the plasma boundary, but to a sequence of nested tori, each bounding and confining some fraction of the plasma. The innermost such torus is evidently a single toroidal field line, the magnetic axis. Every other toroidal surface has the crucial property of being nowhere penetrated by magnetic field lines. The lines lie everywhere in the surfaces, which are therefore called magnetic surfaces, or flux surfaces. It should be pointed out that this picture of nested toroidal flux surfaces, however basic to con-

finement theory, is considerably idealized; we consider its relation to real confining fields in Chapter 3.

We next introduce, qualitatively, the two key parameters describing a toroidal confinement device: the safety factor, and the plasma beta.

The *safety factor*, denoted by q , measures the field line pitch. A field line will, upon a single circuit of the magnetic axis (poloidal circuit), perform q circuits of the toroidal axis (toroidal circuits). Thus small q corresponds to a tightly wound helix; the limiting case of infinite q describes a purely toroidal line. An approximate, useful formula can be inferred from consideration of the simple cylindrical torus (as in Figure 1):

$$\frac{2\pi R_0}{2\pi r} q \approx \frac{B_T}{B_P} \Rightarrow q \approx q_c \equiv \frac{r}{R_0} \frac{B_T}{B_P}$$

where q_c is called the “cylindrical safety factor.”

The more elaborate definition of Chapter 3 shows that the safety factor has a fixed value on each toroidal surface. But it obviously varies within the confining volume: not all field lines have the same pitch. Indeed, the variation of q from one surface to the next, called magnetic shear, has crucial effects on plasma stability. In particular, rational values of q , corresponding to surfaces with closed field lines, are especially vulnerable to electromagnetic perturbation. In the present chapter we associate a q -value with some confinement geometry, globally, by referring implicitly to an average or typical value.

The parameter *beta* measures the efficiency of magnetic confinement, in terms of the ratio

$$\beta \equiv \text{Plasma thermal energy/Magnetic field energy} \quad (5)$$

Like q , this quantity will vary throughout the confinement region, one should strictly distinguish “maximum beta,” “average beta,” and so on; for simplicity we will ignore such distinctions here.

Economical fusion reactors require high beta: the numerator roughly measures fusion yield, while the denominator measures input energy. Experimental devices have beta-values ranging from less than one percent to perhaps 30%.

Plasma diamagnetism, the depression of magnetic fields by plasma pressure, increases with beta. Thus higher beta devices have stronger diamagnetic currents—currents that usually play a critical role in the confinement mechanism. For this reason high beta devices tend to be relatively “self-confining,” in the sense of relying less on external coils to produce the desired field. However, the relation between beta and plasma current is easily exaggerated. The point is that diamagnetic current, while indeed measured by beta, is always perpendicular to the local field; plasma current parallel to B is unrelated to diamagnetism or beta. Thus large parallel currents can exist even at zero beta, and certain low-beta devices make critical use of plasma current.

Confinement Systems

We next briefly survey some representative toroidal devices. Our discussion is emphatically incomplete: its purpose is simply to impart some sense of the variety and nature of actual confinement geometries.

A convenient initial characterization involves the safety-factor. When q is infinite ($\mathbf{B}_P = 0$), each line is a hoop encircling the toroidal axis. Equilibrium is possible in this case only if the lines are asymmetric: the hoops cannot be simple circles. Devices with this geometry are called bumpy tori, or, more generally, closed field-line devices. The opposite limit, with vanishing toroidal field, does not globally describe an operating machine, although q vanishes locally in certain devices discussed below.

The most common confinement geometries have both poloidal and toroidal field components, with values of q within an order of magnitude of unity. In this case only exceptional field lines close on themselves; the typical field line eventually covers its toroidal surface ergodically (i.e., comes arbitrarily close to every point on the surface). There are two broad categories of such devices, which we shall call self-excited and externally excited. Self-excited devices tend to have to low q ,

$$q < 1 ,$$

and relatively large beta:

$$\beta \sim 10 .$$

Their characteristic feature is the reliance on self-generated magnetic fields—plasma currents—to provide the primary confining force. (We will find in Chapter 3 that part of the confining force must always be provided external coils.) The smaller q -values reflect the fact that poloidal fields are most easily generated by toroidal plasma current, rather than external field coils. Examples are the stabilized Z-pinch, the spheromak, and various compact toroid geometries. The first of these has received by far the greatest attention; its most popular manifestation is the reversed-field pinch (RFP). In the RFP, plasma currents parallel to the toroidal minor axis not only generate the poloidal field, but also diamagnetically alter the toroidal field, allowing \mathbf{B}_T to change sign near the plasma boundary. (Such “field reversal” improves fluid stability.) In fact all three of these devices usually have small toroidal fields—small or vanishing q —in the boundary region.

The most common versions of all three concepts are axisymmetric. The spheromak, as well as most compact toroid devices, has nearly unit aspect ratio. Z-pinch devices have aspect ratios of 5 or more.

The externally excited category has, typically,

$$q > 1 ,$$

and smaller beta. It includes describes most stellarator devices, as well as the presently most important confinement geometry, the tokamak.

The stellarator derives both poloidal and toroidal fields from external coils, whose helical windings are necessarily asymmetric. For reasons of stability, stellarator experiments often strive to reduce plasma currents as much as possible; a common intention is to provide direct external control of the full confining field.

The tokamak is an axisymmetric device with q -values close to, but usually somewhat larger than, unity. With regard to our two confinement categories, it has a certain hybrid character. Its poloidal field is driven by plasma current, much like the Z-pinch. On the other hand its large external coils evoke the external coil investment of a stellarator. This hybrid quality is especially clear with regard to tokamak beta: the overall beta is small (typically a few per cent or less) because of the large B_T , but the so-called poloidal beta,

$$\beta_P \equiv \text{Plasma thermal energy/Poloidal field energy ,}$$

$$\approx (B_T/B_P)^2 \beta ,$$

can approach unity. Thus, in terms of simple force balance, the poloidal field does most of the work in tokamak confinement. The toroidal field enhances stability, as well as improving thermal insulation.

Tokamaks have earned a central role in the fusion research program for several reasons. Most importantly, they work well, attaining confinement parameters of fusion-research interest in a reliable and even reasonably predictable manner. They appear to have fundamental advantages as well, essentially because guiding-center orbits are better behaved in symmetric geometry. Finally, of course, tokamak axisymmetry tends to simplify machine design and construction.

The disadvantages of the tokamak are mostly associated with the large toroidal current required. First, driving the tokamak current in a reactor environment is problematic. Inductive drive—changing the magnetic flux that links the tokamak minor radius—is technically simple but unfortunately pulsed; engineering constraints would favor steady-state operation. The more sophisticated, noninductive, current-drive schemes tend to affect unfavorably the parameter γ in (3)—a key economic consideration. Second, the tokamak current appears to drive certain plasma instabilities that have deleterious effects. For these reasons stellarator confinement, being inherently steady-state and nearly current-free, remains of considerable interest.

It is worth remarking here that plasma current plays a dual role in experimental fusion devices. We have emphasized its contributions to the confining magnetic field, such as the poloidal field in a tokamak. But the current also heats the plasma, through Ohmic dissipation. Many devices rely exclusively on Ohmic heating, although, since classical dissipation decreases with temperature, this strategy becomes questionable at thermonuclear temperatures. Alternative external heat sources, such as energetic particle beams or electromagnetic radiation, are usually applied addition-

ally, or subsequently, to Ohmic heating. Thus one speaks of the non-Ohmic power sources as providing “auxiliary” heating.

Confined Plasma Behavior

There is a well-known prescription for developing, from some physical model of plasma dynamics, an understanding of confinement. First, one identifies a confined equilibrium—or better, a family of equilibria—by solving the system obtained when time derivatives in the model are equated to zero. The equilibrium analysis must also neglect classical dissipation; otherwise the only equilibrium is the thermodynamic one. Second, one studies the stability of the various equilibria, by determining how each responds to small perturbations. Usually such stability analyses are linear. The stability analysis may include dissipative terms, but it must ignore the very slow time scale associated with dissipation. Of course this analysis is an enormous task; however, if the initial family of equilibria is sufficiently large or sufficiently ingenious, one can in principle identify a stable equilibrium. Finally, restoring the dissipative time-scale, one studies the rate at which the stably confined plasma decays—or how potent a source is needed to maintain a steady-state. What matters here are such collisionally-induced processes as particle diffusion, resistivity and heat conduction: plasma transport mechanisms.

This traditional decomposition of plasma confinement theory—equilibrium, stability, and transport—is clearly sensible. A glance at our table of contents shows that it has influenced the structure of this book. But it must be pointed out at the start that its implicit picture of a confined plasma corresponds poorly to what is observed in experiments. In discussing the disparity, we consider tokamak experiments specifically. The tokamak is not only the most elaborately diagnosed machine but also seems most closely to approach the traditional ideal.

What is the experimental nature of tokamak-plasma equilibrium? In many respects it is faithful to the prescriptions of equilibrium theory; in fact, theory is reliable enough to help interpret experimental data and to tailor desired equilibrium configurations. Indeed, the growing correspondence between plasma confinement theory and experiment is unmistakable and encouraging.

Unfortunately, however, experiments show that the tokamak equilibrium is not stable. Virtually every tokamak discharge displays characteristic, recurrent instabilities, involving a wide range of space-time scales and most of the physical quantities—electromagnetic fields, plasma densities and temperatures—characterizing the configuration. Even the most quiescent operating regimes (“H-modes”) display spontaneous electromagnetic disturbance. Occasionally the instabilities grow to catastrophic size, annihilating the discharge. More commonly, the equilibrium survives—not

because it is stable, but because the amplitude of unstable disturbances remains bounded at acceptable levels: one has a simmering pot, rather than a boiling one.

A model for such behavior is of that of linear instability, followed by nonlinear saturation. In some cases, further evolution of the saturated configuration soon restores the initial, unstable state; the resulting nonlinear oscillation typically displays coherent structure in space as well as time. Other forms of perturbation, simultaneously observed, have a noisy, chaotic character. In other words, the experimental picture shows the variety of nonlinear behaviors expected, from nonlinear dynamics, in driven, dissipative systems.

There is nothing surprising in this experimental circumstance, which does not directly violate the assumptions of the traditional model. Indeed, theory has never found a tokamak equilibrium of proven stability; and the character of the perturbations, both coherent and turbulent, is consistent with predictions of conventional confinement science. But the noisy, dynamic reality of tokamak confinement qualifies each step in the traditional sequence:

With regard to equilibrium, we see that the steady-state assumption is an idealization. It is a useful idealization because, or in so far as, the fluctuations remain small.

With regard to (linear) stability, we see that linear theory, despite the valuable insights it provides regarding the origins of noise or oscillation, cannot predict realistic dynamics. Tokamak plasma evolution expresses almost exclusively nonlinear physics.

With regard to transport, we see that classical dissipation, in the sense of §1.4, is unlikely to account for observed plasma transport. Indeed, relatively direct measures of confinement confirm that tokamak transport is strongly enhanced over the classical predictions.

Types of Fluctuations

Tokamak fluctuations fall into two broad categories.

First, one observes fine-scale, incoherent, electrostatic noise, accompanied by significant fluctuation in plasma density, but little magnetic fluctuation. Except near the plasma boundary, the fluctuations are small in amplitude—a few per-cent or less of the ambient thermal energy. But electrostatic noise is pervasive, and it character changes little from one machine to the next. It is often ascribed to unstable drift waves—a class of linear modes, discussed in Chapter 6, that are supported by plasma gradients—

and sometimes referred to as “drift-wave turbulence.” Indeed, the noise spectrum, although very broad, is centered in the vicinity of the drift-wave frequency. The noise is commonly, and very plausibly, associated with enhanced plasma transport.

Second, one observes a variety of electromagnetic disturbances, in which variation of the magnetic field is prominent. For partly historical reasons, we shall refer to this class of disturbances as MHD activity. They are diagnosed by various magnetic field measurements, as well as local X-ray detection of the temperature fluctuations: the soft X-ray signal from a tokamak plasma responds mainly to temperature variation. There are three subcategories:

(i) *MHD noise* consists of small scale, incoherent magnetic oscillations, often localized to certain annular regions of the torus. It has low amplitude, the relative field perturbation being measured in tenths or hundredths of a percent (most measurements are confined to the outer regions of the discharge, but there is little reason to expect larger amplitudes in the interior). Its frequencies and wavelengths can be comparable to those of electrostatic noise, to which some components of the MHD noise may be accessory. But a significant fraction, at least, of MHD noise seems quite independent from the electrostatic fluctuations. We include Mirnov oscillations—magnetic fluctuations mainly associated with the start-up phase of a tokamak discharge—in this category, although they have somewhat larger amplitude and are rather better understood. In fact Mirnov oscillations could as well be considered a variant manifestation of the next category of perturbation.

(ii) *Sawtooth oscillations* are expressed by periodic, coherent magnetic pulses, generated near the interior of the confined plasma. They are strictly nonlinear phenomena, with elaborate spatial structure indicating rearrangement of the confining field. The magnetic perturbation is prominently accompanied by local variation in plasma temperature; the name, “sawtooth,” refers to the temporal shape of the X-ray signal, each period of which consists of a relatively slow rise followed by a very sharp drop. The temperature variation can be as large as 10%. Sawtooth oscillations are believed to seriously corrupt confinement near the tokamak minor axis, thus limiting the maximum temperature accessible.

(iii) *Plasma disruptions* are violent electromagnetic events that generally terminate the discharge. The unbridled motions of the plasma column that precede annihilation have been compared to magnetic storms in the solar corona. Although only partially understood, disruptions are experimentally avoidable. But they appear to impose limits on the maximum achievable plasma density and current; indeed, the hottest, most dense discharges seem especially prone to disrupt. Furthermore the associated current interruptions are fast enough to generate enormous inductive pulses outside the plasma—a dangerous circumstance in the reactor context.

1.6 Understanding Confinement

The most important recent advances in controlled fusion research stem from dramatic improvements in experimental proficiency, especially with regard to diagnostic development. Some of the resulting new information, such as the existence of high-confinement operating modes in auxiliary heated tokamaks, is quite unexpected. Other diagnostic gains serve to resolve structural details of phenomena, such as tokamak sawtooth oscillations, previously seen in rough outline.

A striking benefit of the improved diagnostic information has been enlarged contact, and even agreement, between theory and experiment. Examples of such improvement concern, *inter alia*, stability criteria, plasma-impurity profiles, and (ion) diffusion rates. Yet equally striking is the persistent lack of definitive, predictive understanding.

Consider for example sawtooth oscillations. Theory predicts that the tokamak current should drive instability; thus for example the relative immunity of current-free stellarators to sawtooth activity is not surprising. Indeed, theoretical studies correctly anticipated the observed conditions and spatial locations conducive to such instability. Nonetheless a thoroughly persuasive analysis of sawtooth oscillation remains elusive. Questions persist even with regard to its linear phase, and the mechanics and time-scales of its nonlinear collapse remain deeply controversial.

This state of affairs is especially unfortunate because the phenomena in question directly affect the design and operation of fusion reactors. For example, as we have noted, the danger of disruptions limits the operating parameters of present tokamaks; a level of understanding sufficient to evade such limits would provide important freedom to the reactor designer. A more practical issue concerns predictability: if disruptions or other unstable motions cannot be prevented, what becomes essential is a predictive understanding of when they occur, and how their intensity is affected by machine parameters. In particular, reactor design would benefit enormously from credible *scaling laws*; describing the effect of changing parameters, such as major radius or magnetic field intensity, on energy confinement times.

In other words, understanding the physics of plasma confinement would bring certain practical benefit to the controlled fusion quest; confinement physics matters. Why is it so hard? The point seems to be that a confined plasma is both *complicated* and *nonlinear*.

It is complicated not only as system with many degrees of freedom, far from thermal equilibrium, but also because of the variety of its interactions with the external world. For example, in addition to external electromagnetic interactions, confined plasma ordinarily exchanges energy and matter with container walls. Without an effective quarantine on such *wall-interaction*, the plasma physics issues treated in this book become mixed with atomic- and surface-physics processes, whose effects and rela-

tive importance remain incompletely understood.

Complexity dictates the strategy of confined plasma science. It clearly establishes the long-term importance of numerical plasma simulation. Just as importantly, it calls for stringent but informed *selectivity*—a recognition that any attempt to account for all the processes that might bear on some set of observations is unlikely to produce either comprehensible or predictive physics.

The nonlinearity of confined plasma physics brings with it the unpredictability and analytic intractability familiar from investigations of simpler nonlinear systems. Thus it affects not only the strategy of theory but also its ambitions, which must often stop far short of detailed realism. On the other hand, as a thoroughly diagnosed and richly interacting system, confined plasma also brings opportunities for advances in the science of nonlinear dynamics.

In summary, plasma confinement physics represents an attempt to understand and reliably predict the behavior of a complicated nonlinear system. It has developed to this end a compelling body of ideas and methods, as well as clear-cut accomplishments. But much remains to be understood.

Further Reading on Controlled Thermonuclear Fusion:

Rose and Clark, 1961

Ribe, 1975

Kapitsa, 1979

Teller, 1981

Gross, 1984

Chapter 2

Review of Fundamentals

This chapter surveys the basic mathematical techniques used in the book. We also review the basic physical laws that describe plasmas, including the description of the motion of an individual charged particle in slowly varying electromagnetic fields. The treatment is terse, and the reader is urged to consult any of the standard texts on mathematical physics and basic plasma physics for more detailed discussions (see the references at the end of the chapter).

Note that some topics mentioned here, such as symplectic forms and Christoffel symbols, are relatively advanced. They occur only rarely in later chapters and are not essential to understanding this book's main conclusions.

2.1 Tensor Calculus

The major complication in the treatment of confined plasmas, as compared to homogeneous plasmas, is geometrical. A confined plasma is necessarily inhomogeneous, and often anisotropic due to the confining magnetic fields. Just as in relativity, a basic understanding of tensor calculus is helpful in simplifying the resulting formulae.

Coordinate Systems

Physical space can be represented by many equivalent coordinate systems. We can refer all of these coordinate systems to the Cartesian system $\mathbf{x} = (x, y, z)$ or (x^1, x^2, x^3) by giving a set of functions $\xi^i(\mathbf{x}) = \xi^i(x, y, z)$ for $i = 1, 2, 3$ —that is, a set of three generalized coordinates. By convention, coordinates are denoted with superscript indices. The ξ^i form a

non-degenerate coordinate system only if the Jacobian,

$$J \equiv \nabla\xi^1 \cdot \nabla\xi^2 \times \nabla\xi^3 = \det\left(\frac{\partial\xi^i}{\partial x^j}\right) \quad (1)$$

does not vanish. The coordinate system is right-handed when $J > 0$.

Cylindrical coordinates are given by the set $(\xi^1, \xi^2, \xi^3) = (R, \varphi, Z)$. Here the Z axis is the cylindrical axis, R is the cylindrical radius, and φ is the azimuthal angle. The coordinates are defined by

$$\begin{aligned} R &= \sqrt{x^2 + y^2}, \\ \varphi &= \tan^{-1}(y/x), \end{aligned} \quad (2)$$

$$Z = z.$$

The Jacobian for this coordinate system is $J = 1/R$.

As we will find in Chapter 3, toroidal coordinates are especially useful for magnetic confinement. The primitive toroidal coordinate system (r_0, θ_0, ζ_0) is defined by specifying the toroidal axis as the Z -axis of a cylindrical system (R, φ, Z) , and then defining the minor radius r_0 , and two angles θ_0 and ζ_0 , according to

$$\begin{aligned} r_0 &= \sqrt{(R - R_0)^2 + Z^2}, \\ \theta_0 &= \tan^{-1}\left(\frac{Z}{R - R_0}\right), \\ \zeta_0 &= -\varphi. \end{aligned} \quad (3)$$

Here θ_0 is the *poloidal angle* and ζ_0 is the *toroidal angle*. The negative sign in the latter definition is required in order to make (r_0, θ_0, ζ_0) right handed; the Jacobian is $1/(r_0 R)$. The symmetry axis of the coordinate system is the line $R = 0$. The surfaces on which r_0 is constant are a set of nested, two dimensional tori, each described by the two angle coordinates. The innermost torus, $r_0 = 0$, is degenerate: it is a circle enclosing the symmetry axis, and is called the *minor axis*. A *toroidal circuit* is any closed loop that encircles the symmetry axis of the torus once. Similarly a *poloidal circuit* is a closed loop that encircles the minor axis exactly once. There are clearly many distinct such circuits, but all are topologically equivalent, in the sense of being continuously deformable into each other. These two closed paths are precisely the two distinct “round trips” permitted in toroidal topology, as discussed in Chapter 1.

A *general toroidal coordinate* system is described by a set of suitably smooth functions $(\psi(\mathbf{x}), \theta(\mathbf{x}), \zeta(\mathbf{x}))$ such that the Jacobian

$$J = \nabla\psi \cdot \nabla\theta \times \nabla\zeta \quad (4)$$

is positive and finite everywhere. The *poloidal angle*, $\theta(\mathbf{x})$, must be a function of position that is single-valued on any toroidal circuit, but that

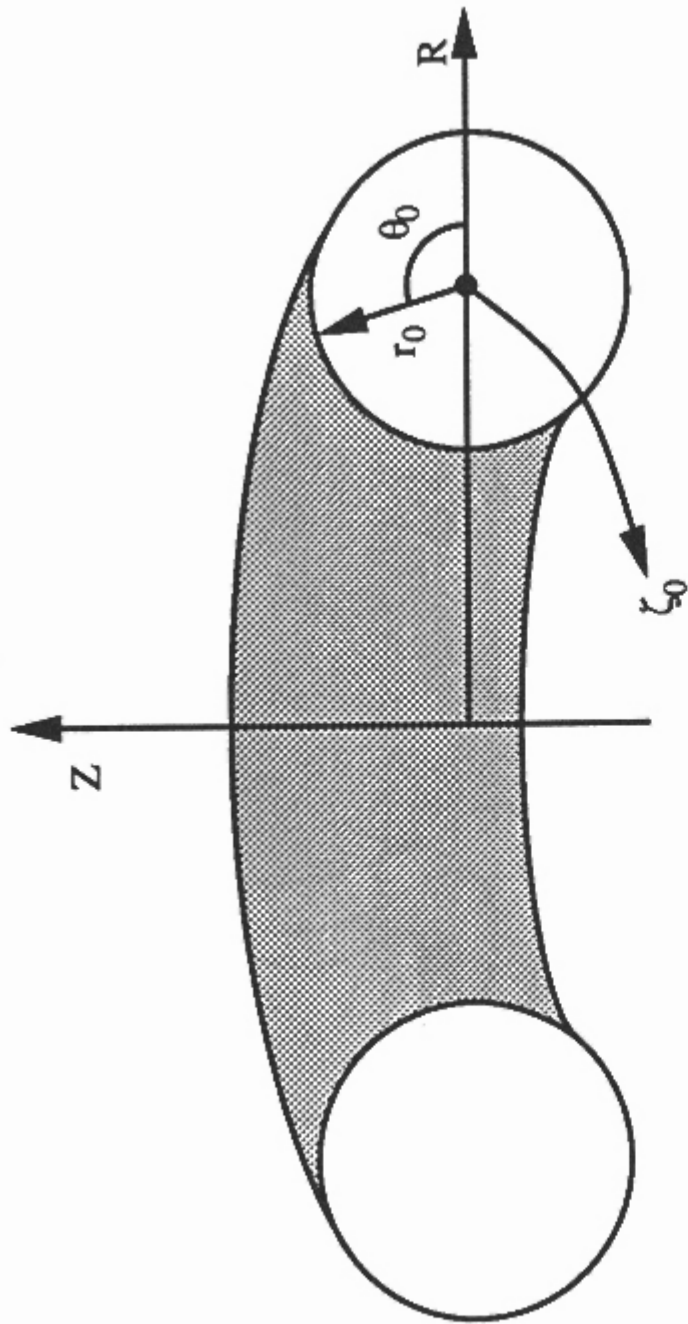


Figure 1. Primitive toroidal coordinates

changes by 2π over a poloidal circuit. The *toroidal angle*, $\zeta(\mathbf{x})$, is defined analogously, with interchange of the words “poloidal” and “toroidal.” Thus if we define these coordinates in terms of the primitive toroidal coordinates, they obey

$$\begin{aligned}\theta(r_0, \theta_0 + 2m\pi, \zeta_0 + 2n\pi) &= \theta(r_0, \theta_0, \zeta_0) + 2m\pi \\ \zeta(r_0, \theta_0 + 2m\pi, \zeta_0 + 2n\pi) &= \zeta(r_0, \theta_0, \zeta_0) + 2n\pi\end{aligned}\quad (5)$$

for any integers m and n .

Finally the generalized radial coordinate, $\psi(\mathbf{x})$ must be single valued

$$\psi(r_0, \theta_0 + 2m\pi, \zeta_0 + 2n\pi) = \psi(r_0, \theta_0, \zeta_0). \quad (6)$$

Thus the surfaces on which $\psi(\mathbf{x})$ is constant define a sequence of nested tori. The innermost torus is again a toroidal circuit (not necessarily the circle $r_0 = 0$); it is called the minor axis of this coordinate system. For a given set of nested tori, any two radial coordinates, ψ and ψ' are related by a monotonic function $\psi'(\psi)$. We denote by “ r ” any such radial coordinate that vanishes on the minor axis, increases monotonically outward, and has the dimensions of length; thus r can be loosely identified with minor radius. The variety of well-behaved toroidal coordinates is easily understood. If (ψ, θ, ζ) is an acceptable set of general toroidal coordinates, then (5) implies that the angle coordinates can be written as

$$\theta = \theta_0 + p_1(r_0, \theta_0, \zeta_0), \quad \zeta = \zeta_0 + p_2(r_0, \theta_0, \zeta_0), \quad (7)$$

where p_1 and p_2 are periodic functions of (θ_0, ζ_0) . A similar relationship must hold between *any* pair of generalized toroidal coordinates.

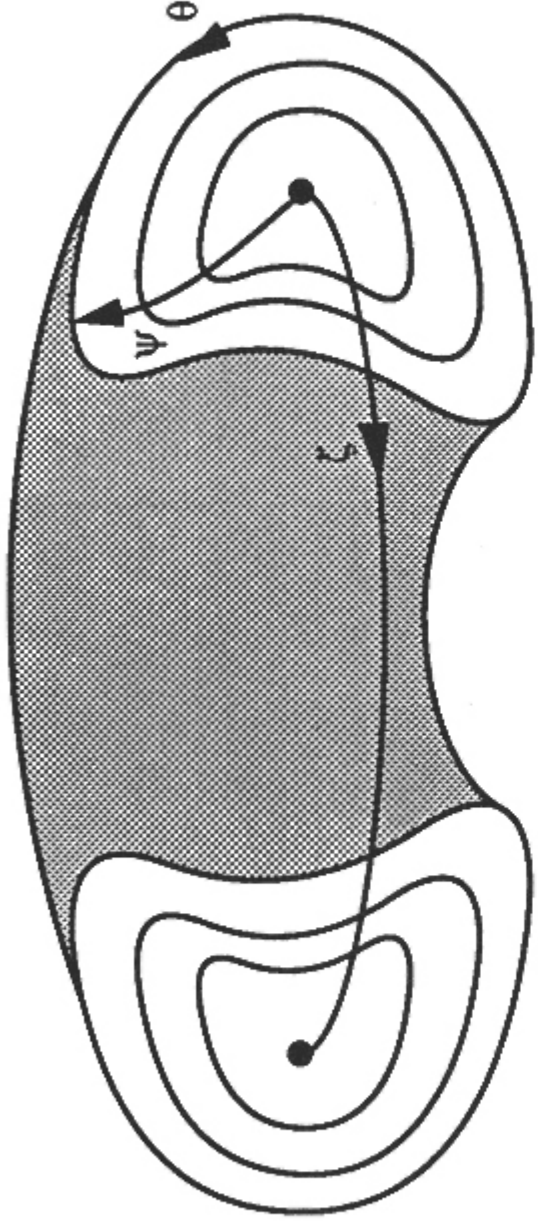


Figure 2. General toroidal coordinates

Covariant and Contravariant Components

A vector field, $\mathbf{A}(\mathbf{x}, t)$, represents a direction and magnitude attached to each point in space and time. While a vector is indicated by bold type, its magnitude is usually denoted by the same symbol using plain type: $A = |\mathbf{A}|$. The corresponding unit vector, $\mathbf{a} = \mathbf{A}/A$, is indicated by a lower case letter, or sometimes as $\hat{\mathbf{a}}$. The components of vectors can be represented in terms of a basis set, which is a linearly independent set of vectors spanning the set of directions. The simplest basis is the Cartesian basis, $\hat{\mathbf{x}}, \hat{\mathbf{y}}, \hat{\mathbf{z}}$ a set of mutually orthogonal, constant unit vectors. In this case we expand

$$\mathbf{A} = A_1 \hat{\mathbf{x}} + A_2 \hat{\mathbf{y}} + A_3 \hat{\mathbf{z}} . \quad (8)$$

The coefficients of the vector written in terms of a unit vector basis, the A_i above, are known as the ordinary, or vector, components of the vector \mathbf{A} . More general bases can also be represented in terms of a set of three vector fields that span the set of directions at every point in space.

The *covariant basis* of a coordinate system $\xi^i(x, y, z)$ is given by the three vectors $\nabla \xi^i$. For example, the covariant basis in Cartesian coordinates is the set of unit vectors $\nabla x = \hat{\mathbf{x}}, \nabla y = \hat{\mathbf{y}}, \nabla z = \hat{\mathbf{z}}$. In general basis vectors are linearly independent because the Jacobian is non-zero. The covariant representation for a vector is its expansion in this basis:

$$\mathbf{A} = A_i \nabla \xi^i , \quad (9)$$

where the summation over repeated indices is understood. Here A_i is the i^{th} covariant component of \mathbf{A} . We can express the covariant components of a vector in terms of the vector products

$$A_1 = \frac{1}{j} \nabla \xi^2 \times \nabla \xi^3 \cdot \mathbf{A} , \quad A_2 = \frac{1}{j} \nabla \xi^3 \times \nabla \xi^1 \cdot \mathbf{A} , \quad A_3 = \frac{1}{j} \nabla \xi^1 \times \nabla \xi^2 \cdot \mathbf{A} ,$$

or in compact notation

$$A_i = \frac{\epsilon_{ijk}}{2j} \nabla \xi^j \times \nabla \xi^k \cdot \mathbf{A} , \quad (10)$$

where we use the “summation convention”: repeated indices are to be summed, and where ϵ_{ijk} is the antisymmetric matrix with non-zero components $\epsilon_{123} = \epsilon_{231} = 1$ and $\epsilon_{312} = \epsilon_{132} = \epsilon_{213} = \epsilon_{321} = -1$. Thus, for example the covariant components of the Cartesian basis vectors are

$$(\nabla x^k)_i = \delta_{ki} \quad (\text{Cartesian Coordinates}).$$

The term “covariant” arises from the transformation properties of the components. Given the covariant components in one coordinate system ξ^i , the components in another coordinate system, $\tilde{\xi}^i$, are obtained by the chain rule for derivatives:

$$\mathbf{A} = A_i \nabla \xi^i = A_i \frac{\partial \xi^i}{\partial \tilde{\xi}^j} \nabla \tilde{\xi}^j = \tilde{A}_j \nabla \tilde{\xi}^j.$$

Thus the new covariant components are

$$\tilde{A}_j = A_i \frac{\partial \xi^i}{\partial \tilde{\xi}^j}. \quad (11)$$

For example, if ξ represents Cartesian coordinates, then the j th covariant component of a basis vector ∇x^k is given by

$$(\nabla x^k)_j = \delta_{kj} \frac{\partial x^i}{\partial \xi^j} \quad (\text{General Coordinates}) \quad (12)$$

Thus the covariant components “vary with” the basis vectors, in the sense that the x^i is in the numerator above.

By contrast, *contravariant* components “vary against” the basis vectors. They are designated by superscripts, and are most easily obtained by the scalar products

$$A^i = \mathbf{A} \cdot \nabla \xi^i. \quad (13)$$

This implies the transformation property inverse to (11):

$$\tilde{A}^j = A^i \frac{\partial \tilde{\xi}^j}{\partial \xi^i}. \quad (14)$$

A contravariant basis can be easily constructed. For example the contravariant basis vector corresponding to ξ^1 must have contravariant components $(1,0,0)$. Equation (13) then gives three equations for this vector, which have the solution $(1/j)\nabla \xi^2 \times \nabla \xi^3$. Similar formulae apply to the other two contravariant basis vectors. Thus any vector can be expanded in a contravariant basis as

$$\begin{aligned} \mathbf{A} &= \frac{1}{j} (A^1 \nabla \xi^2 \times \nabla \xi^3 + A^2 \nabla \xi^3 \times \nabla \xi^1 + A^3 \nabla \xi^1 \times \nabla \xi^2) \\ &= \frac{\epsilon_{ijk}}{2j} A^i \nabla \xi^j \times \nabla \xi^k. \end{aligned} \quad (15)$$

The relationship between covariant and contravariant components is given by the *metric tensor*. Combining (9) and (13) gives

$$A^i = A_j \nabla \xi^j \cdot \nabla \xi^i \equiv g^{ij} A_j. \quad (16)$$

Thus

$$g^{ij} \equiv \nabla \xi^i \cdot \nabla \xi^j = \frac{\partial \xi^i}{\partial x^k} \frac{\partial \xi^j}{\partial x^k}. \quad (17)$$

As the superscripts indicate, these are the contravariant components of a tensor \mathbf{g} . Since we also demand that

$$A_i = g_{ij} A^j, \quad (18)$$

the covariant components of \mathbf{g} are given by the inverse of the matrix (17); i.e.,

$$g_{ij} = \frac{\partial x^k}{\partial \xi^i} \frac{\partial x^k}{\partial \xi^j}. \quad (19)$$

It is clear from the definition of the Jacobian (1) that the determinant of $g_{ij} \equiv g$ is the inverse of the square of the Jacobian

$$g = 1/j^2. \quad (20)$$

Since the volume element transforms with Jacobian, (20) implies

$$d^3x = \sqrt{g} d\xi^1 d\xi^2 d\xi^3. \quad (21)$$

The metric tensor can be recognized as the length element; since in Cartesian coordinates a length element is $ds^2 = dx^2 + dy^2 + dz^2$, the chain rule gives $ds = (\partial x / \partial \xi^i) d\xi^i$, and so

$$ds^2 = g_{ij} d\xi^i d\xi^j.$$

Vector Calculus

All the usual vector operations can be extended to a general coordinate system. Rewriting the dot product in terms of contravariant and covariant components gives

$$\mathbf{A} \cdot \mathbf{B} = A_i \nabla \xi^i \cdot \nabla \xi^j B_j = A_i g^{ij} B_j = A_i B^i \quad (22)$$

in agreement with the usual definition of scalar product. The cross product

$$\mathbf{W} = \mathbf{A} \times \mathbf{B}$$

has the contravariant components

$$W^i = \nabla \xi^i \cdot \nabla \xi^j \times \nabla \xi^k A_j B_k = \epsilon_{ijk} A_j B_k \quad (23)$$

and covariant components

$$W_i = \frac{\epsilon_{ijk}}{j} A^j B^k . \quad (24)$$

Differential operators also have simple representations in a general coordinate system. Using the chain rule, the gradient operator can be written as

$$\nabla = \nabla \xi^i \frac{\partial}{\partial \xi^i} . \quad (25)$$

This directly implies that the gradient of a scalar has a natural covariant representation

$$S_{;i} \equiv (\nabla S)_i = \frac{\partial S}{\partial \xi^i} . \quad (26)$$

The comma notation, defined in (26), is used to denote the *covariant derivative* of the scalar.

More generally the covariant derivative of a vector (or indeed, of a tensor) is the covariant component of the directional derivative. It differs from the partial derivative of a component because the coordinate system typically varies with position. For example, the derivative of a vector \mathbf{A} in the direction ξ^j is given by

$$\frac{\partial}{\partial \xi^j} \mathbf{A} = \frac{\partial A_i}{\partial \xi^j} \nabla \xi^i + A_i \frac{\partial}{\partial \xi^j} \nabla \xi^i .$$

where we have used the covariant components, (9). The comma subscript is used to denote the covariant components of such a derivative:

$$\frac{\partial \mathbf{A}}{\partial \xi^j} = A_{i,j} \nabla \xi^i ; \quad (27)$$

thus

$$A_{i,j} \equiv \left(\frac{\partial}{\partial \xi^j} \mathbf{A} \right)_i = \frac{\partial A_i}{\partial \xi^j} + \Gamma_{j,i}^k A_k . \quad (28)$$

Here the last term involves the *Christoffel symbol* or affine connection, defined by

$$\Gamma_{j,i}^k \equiv \left(\frac{\partial}{\partial \xi^j} \nabla \xi^k \right)_i . \quad (29)$$

Simple manipulations using (29) and (12) show that

$$\Gamma_{j,i}^k = \frac{\partial x^\ell}{\partial \xi^j} \frac{\partial^2 \xi^k}{\partial \xi^\ell \partial x^m} (\nabla x^m)_i = \frac{\partial^2 \xi^k}{\partial x^m \partial x^\ell} \frac{\partial x^m}{\partial \xi^\ell} \frac{\partial x^\ell}{\partial \xi^j} .$$

This shows immediately that $\Gamma_{j,i}^k$ is symmetric in its two lower indices. This book uses the Christoffel symbol infrequently.

Similarly the derivative of a vector expressed in terms of its contravariant components is denoted

$$A_{,j}^i \equiv \left(\frac{\partial}{\partial \xi^j} \mathbf{A} \right)^i = \frac{\partial A^i}{\partial \xi^j} - \Gamma_{jk}^i A^k . \quad (30)$$

Finally, a useful expression for the Christoffel symbol is obtained by noting that the derivative of the scalar product can be expressed in two ways:

$$\frac{\partial}{\partial \xi^i} (\mathbf{A} \cdot \mathbf{A}) = \frac{\partial}{\partial \xi^i} (A^j g_{jk} A^k) = A_{,i}^j g_{jk} A^k + A^j g_{jk} A_{,i}^k .$$

Using the Christoffel symbol to expand the last expression, and expanding the second using the product rule gives an equation relating derivatives of the metric tensor to Γ . Its solution is

$$\Gamma_{jk}^i = -\frac{1}{2} g^{im} \left(\frac{\partial g_{mi}}{\partial \xi^j} + \frac{\partial g_{mj}}{\partial \xi^i} - \frac{\partial g_{ji}}{\partial \xi^m} \right) . \quad (31)$$

Certain vector derivatives (including those most commonly used) can be evaluated without knowledge of the Christoffel symbols. For example, the divergence of a vector is

$$\nabla \cdot \mathbf{A} = \nabla \xi^m \cdot \frac{\partial}{\partial \xi^m} \left(\frac{\epsilon_{ijk}}{2j} A^i \nabla \xi^j \times \nabla \xi^k \right) = J \frac{\partial}{\partial \xi^i} \left(\frac{1}{J} A^i \right) . \quad (32)$$

Verification of this is left as an exercise. Finally the curl of a vector

$$\mathbf{B} = \nabla \times \mathbf{A}$$

has contravariant components given by

$$B^i = \nabla \xi^i \cdot \nabla \xi^j \times \left(\frac{\partial}{\partial \xi^j} \nabla \xi^m A_m \right) = J \epsilon_{ijk} \frac{\partial}{\partial \xi^j} A_k . \quad (33)$$

2.2 Lagrangian and Hamiltonian mechanics

In this section we recall some of the fundamentals of mechanics, using notation appropriate for general coordinate systems.

The dynamics of most fundamental physical systems can be derived from an elegant variational principle, Hamilton's principle. This description is obtained by representing the complete mechanical configuration of the system as a single point, \mathbf{x} , in an n dimensional configuration space. Here n is called the number of *degrees of freedom*, of the system. For example a point particle moving under the action of forces in three dimensional space has three degrees of freedom, while an extended, rigid body has six.

We assume that the dynamics of the system would be completely defined if, in addition to the configuration, \mathbf{x} , we are given the velocity vector, $\dot{\mathbf{x}}$: the dynamics takes place on the space of all configurations and velocities. The *Lagrangian*, $L(\mathbf{x}, \dot{\mathbf{x}}, t)$, gives all the information required to construct the dynamics. For a simple particle system the Lagrangian is the difference between the kinetic and potential energies, though it can be more complicated when, for example, there is a magnetic field.

Consider a path $\mathbf{x}(t)$, $t_0 < t < t_1$, in the configuration space. For each point on the path, the velocity is defined as the time derivative of \mathbf{x} . The action $S[\mathbf{x}]$, is a functional on the space of such paths; the action of a path is defined by

$$S[\mathbf{x}] = \int_{t_0}^{t_1} L(\mathbf{x}(t), \dot{\mathbf{x}}(t), t) dt . \quad (34)$$

Hamilton's principle asserts that the dynamically allowed paths are stationary points of the action, for the class of paths with given initial and final conditions, $\mathbf{x}(t_0) = \mathbf{x}_0$ and $\mathbf{x}(t_1) = \mathbf{x}_1$. Demanding that the path be stationary gives the Euler-Lagrange equations of motion

$$0 = -\frac{d}{dt} \frac{\partial L}{\partial \dot{x}^i} + \frac{\partial L}{\partial x^i} . \quad (35)$$

In general these are a set of second order differential equations for each configuration point; their solution requires that an initial condition $(\mathbf{x}(0), \dot{\mathbf{x}}(0))$ be given.

The Lagrangian formulation is covariant under arbitrary coordinate transformations. Suppose we change coordinates to a new system $\xi^i(\mathbf{x})$. In the new coordinate system the velocity has components $\dot{\xi}^i = \nabla \xi^i \cdot \dot{\mathbf{x}}$ and the Lagrangian for the new variables is equal in value to the old Lagrangian: $L(\xi, \dot{\xi}, t) \equiv L(\mathbf{x}(\xi), \dot{\mathbf{x}}(\xi), \xi, t)$. Thus the equations of motion differ from (35) only in that derivatives with respect to ξ^i replace those with respect to x^i .

Equations in Hamiltonian form are obtained by the Legendre transformation from velocity to canonical momentum:

$$H(\mathbf{P}, \mathbf{x}) = \mathbf{P} \cdot \dot{\mathbf{x}} - L(\mathbf{x}, \dot{\mathbf{x}}, t) . \quad (36)$$

Implicit in the transformation (36) is that H is a function only of (\mathbf{P}, \mathbf{x}) , or that H is independent of the velocity: $\partial H / \partial \dot{\mathbf{x}} = 0$. This provides the definition of the canonical momenta

$$\mathbf{P} = \frac{\partial}{\partial \dot{\mathbf{x}}} L(\mathbf{x}, \dot{\mathbf{x}}, t) . \quad (37)$$

Since the Hamiltonian must be a function of (\mathbf{P}, \mathbf{x}) , it exists only if the equation for the momenta can be inverted to obtain $\dot{\mathbf{x}}(\mathbf{P}, \mathbf{x}, t)$; this is true locally whenever L satisfies the Legendre condition $\partial^2 L / \partial \dot{\mathbf{x}}^2 \neq 0$. In some

cases $\dot{\mathbf{x}}(\mathbf{p}, \mathbf{x}, t)$ may have several branches, and in singular cases the inversion might not exist.

The $2n$ -dimensional space with coordinates (\mathbf{p}, \mathbf{x}) is called *phase space*. The coordinates (\mathbf{p}, \mathbf{x}) are called *canonical coordinates* on the phase space.

To derive Hamilton's equations, we can use Hamilton's principle (34), but substitute the definition of H for the Lagrangian. In this case the momentum $\mathbf{p}(\mathbf{x}, \dot{\mathbf{x}}, t)$ is defined on the path $\mathbf{x}(t)$ by (37). More elegantly and more generally, this variational principle can be extended to a *phase space action principle* that gives (37) automatically. To accomplish this we formally assume that $\mathbf{p}(t)$ is independent of $\mathbf{x}(t)$: a path in phase space is defined by any choice of the functions $(\mathbf{p}(t), \mathbf{x}(t))$. The action must now be written as

$$S[\mathbf{p}, \mathbf{x}] = \int_{t_0}^{t_1} [\mathbf{p} \cdot \dot{\mathbf{x}} - H(\mathbf{p}, \mathbf{x}, t)] dt . \quad (38)$$

The phase space action principle asserts that the (38) should be stationary with respect to arbitrary variations in phase space paths, subject to given initial and final configurations $\mathbf{x}(t_0) = \mathbf{x}_0$ and $\mathbf{x}(t_1) = \mathbf{x}_1$. The initial and final momenta can float freely since no integration by parts is required upon variations with respect to \mathbf{p} . Since \mathbf{p} and \mathbf{x} are independent, we vary (38) with respect to both, to obtain Hamilton's equations in well known form

$$\dot{p}^i = -\frac{\partial H}{\partial x^i}, \quad \dot{x}^i = \frac{\partial H}{\partial p_i} . \quad (39)$$

Since Hamilton's equations are obtained from a scalar action, (38), they can be written in a coordinate free way: canonical coordinates are by no means necessary for a Hamiltonian description. Let $\mathbf{z}(\mathbf{p}, \mathbf{x})$ represent a general coordinate system on the phase space. The Hamiltonian is a function $H(\mathbf{z}, t)$ on a phase space and the dynamics are represented by first order differential equations for the coordinates \mathbf{z} . The action in the new coordinate system is equal in value to the original action, but is evaluated in the new coordinates:

$$S[\mathbf{z}] = \int_{t_0}^{t_1} [\mathcal{A}(\mathbf{z}) \cdot \dot{\mathbf{z}} - H(\mathbf{z}, t)] dt . \quad (40)$$

Here the generalized "momenta", $\mathcal{A}_i(\mathbf{z}) = p_k(\mathbf{z}) dx^k / dz^i$, can have $2n$ non-zero components. The equations of motion are obtained by variation with respect to all $2n$ z^i 's,

$$\begin{aligned} \delta S &= \int \left(\frac{\partial \mathcal{A}_i}{\partial z^j} \frac{dz^i}{dt} + \mathcal{A}_j \frac{d}{dt} - \frac{\partial H}{\partial z^j} \right) \delta z^j dt = 0 \\ &\Rightarrow \left(\frac{\partial \mathcal{A}_i}{\partial z^j} - \frac{\partial \mathcal{A}_j}{\partial z^i} \right) \frac{d z^i}{dt} - \frac{\partial H}{\partial z^j} = 0 , \end{aligned}$$

which can be written

$$\omega_{ij} \dot{z}^j = \frac{\partial H}{\partial z_i}. \quad (41)$$

Here the matrix ω_{ij} , the *symplectic form*, is defined by

$$\omega_{ij} = \frac{\partial A_j}{\partial z_i} - \frac{\partial A_i}{\partial z_j}. \quad (42)$$

In canonical coordinates (\mathbf{p}, \mathbf{x}) the symplectic form is

$$\omega \begin{bmatrix} \dot{\mathbf{p}} \\ \dot{\mathbf{x}} \end{bmatrix} = \begin{bmatrix} 0 & \mathbf{I} \\ -\mathbf{I} & 0 \end{bmatrix} \begin{bmatrix} \dot{\mathbf{p}} \\ \dot{\mathbf{x}} \end{bmatrix}. \quad (43)$$

but more generally it is the anti-symmetric matrix defined in (42). We will consider below several cases, where the non-canonical form of the variational principle arises naturally; guiding-center particle motion is an example.

2.3 Maxwell-Lorentz equations

General Form

A plasma is a gas of charged and neutral particles viewed on scale lengths large compared to the Debye length. We will recall the fundamental laws governing plasma dynamics in this section. Although the statement of these laws is reasonably concise, the laws are too complicated to solve in general. Hence a prominent concern of this book is the construction of simplified descriptions.

Plasmas usually contain several species of charged particles, typically electrons with charge $e_e = -e$ and mass m_e and at least one species of ions with charge $e_i = Z_i e$ and mass m_i . The various species are denoted by a subscript “ s ”; thus e_s is the charge of species s . Species labels will be suppressed except when necessary. This book uses Gaussian cgs units throughout.

Each (non-relativistic) particle can be described by the Lagrangian

$$L(\mathbf{x}, \dot{\mathbf{x}}, t) = \frac{m_s}{2} |\dot{\mathbf{x}}|^2 - e_s \Phi(\mathbf{x}, t) + \frac{e_s}{c} \dot{\mathbf{x}} \cdot \mathbf{A}(\mathbf{x}, t). \quad (44)$$

where $\Phi(\mathbf{x}, t)$ is the electrostatic potential and $\mathbf{A}(\mathbf{x}, t)$ is the electromagnetic potential. The Euler-Lagrange equations of motion are (suppressing the species labels)

$$m \ddot{\mathbf{x}}_i = -e \frac{\partial \Phi}{\partial x^i} - \frac{e}{c} \frac{\partial A_i}{\partial t} + \frac{e}{c} \dot{x}^j \left(\frac{\partial A_j}{\partial x^i} - \frac{\partial A_i}{\partial x^j} \right),$$

which can be recognized as a covariant component of the Lorentz force law,

$$m \frac{d^2\mathbf{x}}{dt^2} = e\mathbf{E} + \frac{e}{c} \frac{d\mathbf{x}}{dt} \times \mathbf{B}, \quad (45)$$

once we recall that in a general coordinate system the electromagnetic fields are defined by

$$\mathbf{E}_i = \left(-\nabla\Phi - \frac{1}{c} \frac{\partial \mathbf{A}}{\partial t} \right)_i = -\frac{\partial\Phi}{\partial x^i} - \frac{1}{c} \frac{\partial A_i}{\partial t} \quad (46)$$

$$\epsilon_{ijk} B^i = \epsilon_{ijk} (\nabla \times \mathbf{A})^i = j \left(\frac{\partial A_k}{\partial x^j} - \frac{\partial A_j}{\partial x^k} \right).$$

A Hamiltonian description of the motion is obtained by defining the canonical momentum by (37)

$$\mathbf{P} = m\mathbf{v} + \frac{e}{c} \mathbf{A}, \quad (47)$$

and the Hamiltonian by (36)

$$H = \frac{1}{2m} \left| \mathbf{P} - \frac{e}{c} \mathbf{A} \right|^2 + e\Phi. \quad (48)$$

The Hamiltonian yields equations of motion completely equivalent to (45).

To exactly describe the dynamics of a plasma, we must follow the motion of all its particles, and the dynamics of the fields themselves. The latter obey Maxwell's equations

$$\begin{aligned} \nabla \cdot \mathbf{E} &= 4\pi\rho_e \\ \nabla \times \mathbf{B} - \frac{1}{c} \frac{\partial \mathbf{E}}{\partial t} &= \frac{4\pi}{c} \mathbf{J} \\ \nabla \times \mathbf{E} + \frac{1}{c} \frac{\partial \mathbf{B}}{\partial t} &= 0 \\ \nabla \cdot \mathbf{B} &= 0. \end{aligned} \quad (49)$$

The interactions of the fields with the particles occurs only through the plasma charge density ρ_e and current \mathbf{J} . If the plasma consists of particles of species s at positions $(\mathbf{x}_s^i, \mathbf{v}_s^i)$ for $i = 1, \dots, n$, then the number density is

$$n_s(\mathbf{x}, t) = \sum_{i=1}^n \delta(\mathbf{x} - \mathbf{x}_s^i(t)),$$

The charge density is

$$\rho_e(\mathbf{x}, t) = \sum_s e_s n_s(\mathbf{x}, t), \quad (50)$$

The current density \mathbf{J} is obtained from the mean velocities

$$\mathbf{n}_s \cdot \mathbf{v}_s(\mathbf{x}, t) = \sum_{i=1}^n \mathbf{v}_s^i(t) \delta(\mathbf{x} - \mathbf{x}_s^i(t)),$$

as

$$\mathbf{J}(\mathbf{x}, t) = \sum_s e_s \mathbf{v}_s(\mathbf{x}, t) \mathbf{n}_s(\mathbf{x}, t). \quad (51)$$

Charge conservation follows from the definitions (50) and (51) as well as from the first and second Maxwell equations

$$\frac{\partial \rho}{\partial t} + \nabla \cdot \mathbf{J} = 0. \quad (52)$$

The Maxwell-Lorentz equations are invariant under the gauge transformation

$$\mathbf{A} \rightarrow \mathbf{A} + \nabla G, \Phi \rightarrow \Phi - \frac{1}{c} \frac{\partial G}{\partial t},$$

because the definitions of \mathbf{E} and \mathbf{B} are invariant. Similarly the action based on the charged particle Lagrangian (44) is gauge invariant because

$$-\Phi(\mathbf{x}, t) + \frac{1}{c} \dot{\mathbf{x}} \cdot \mathbf{A}(\mathbf{x}, t) \rightarrow -\Phi(\mathbf{x}, t) + \frac{1}{c} \dot{\mathbf{x}} \cdot \mathbf{A}(\mathbf{x}, t) + \frac{1}{c} \frac{d}{dt} G(\mathbf{x}, t)$$

and the addition of a total time derivative to the action does not change the equations of motion. Note that the Hamiltonian itself is not gauge invariant; in fact the canonical momentum (47) clearly depends on the choice of gauge.

Approximations

The Lorentz force law (45) together with the Maxwell equations (49) give a complete description of plasma motions. Though formally exact, these equations are almost useless, since it is neither possible, nor even desirable, to know the positions and velocities of each individual particle in the plasma. Much of the analysis in plasma physics is devoted toward deriving approximate sets of equations that are tractable. *Kinetic theory* approximations replace the Lorentz force law with an equation for smoothed particle distributions in phase space. *Fluid theory* approximations attempt to derive equations directly for the plasma density and current, usually requiring only minimal information about the particle distribution, such as

its width. In later chapters we will discuss some of the models appropriate to confinement.

One of the basic approximations is that of *quasineutrality*. It should be recalled that even a small local charge imbalance would yield huge electric fields. For plasmas close to thermal equilibrium, one expects the electrostatic energy to be roughly comparable to the thermal energy, or $e\Phi \sim T$.¹ In this case, Poisson's equation, the first of (49), implies that (for unit ionic charge)

$$\frac{1}{L^2} \Phi \sim 4\pi e(n_e - n_i) \Rightarrow \frac{(n_e - n_i)}{n_e} \sim \left(\frac{\lambda_D}{L} \right)^2 .$$

where L is the length scale for potential variation and λ_D is the Debye length

$$\lambda_D \equiv \sqrt{\frac{T}{4\pi n_e e^2}} . \quad (53)$$

Thus for length scales L much larger than the Debye length, the charge density is effectively zero. Recall here that the ordering $L \gg \lambda_D$ serves to define what is meant by a “plasma.” The implication is that electrons and ions are effectively bound together. Thus the “electrostatic” quasineutrality approximation is to replace Poisson’s equation by $\rho_c = 0$, or $n_e = n_i$.

Another aspect of quasineutrality is the neglect of the charge term in (52), yielding

$$\nabla \cdot \mathbf{J} = 0 . \quad (54)$$

this can be called “electromagnetic” quasineutrality, and requires a separate discussion. Using Ampère’s law to estimate $J \sim eB/L$, charge conservation implies

$$\nabla \cdot \mathbf{J} \sim \frac{e(n_e - n_i)}{\tau} \sim \left(\frac{\lambda_D}{L} \right)^2 \frac{en}{\tau} \Rightarrow \frac{L \nabla \cdot \mathbf{J}}{J} \sim \left(\frac{v_e}{c} \right)^2 \frac{1}{\Omega_e \tau} .$$

where τ is the time scale of interest, and

$$v_e = \sqrt{\frac{2T_e}{m_e}}, \quad \Omega_e = \frac{eB}{mc}, \quad (55)$$

are the electron thermal velocity and gyrofrequency. Since v_e/c is not always negligible in confinement experiments (indeed when the temperature is 10 keV, $v_e \sim c/7$), (54) is appropriate only for processes that are slow compared to the electron gyrofrequency. On the other hand, for processes faster than Ω_e , quasineutrality is rarely an issue.

An additional, often valid, approximation is to replace the Maxwell equations by their pre-Maxwell version, neglecting the displacement current. This approximation is valid providing the time scales of interest are

¹We use energy units for temperature, so that Boltzman’s constant is unity.

slow compared to that for electromagnetic waves ($\tau \gg c/L$). Thus we often use the approximate Ampère's law,

$$\nabla \times \mathbf{B} = \frac{4\pi}{c} \mathbf{J}. \quad (56)$$

Since the divergence of the left hand side of (56) is zero, this is also consistent with charge conservation (54).

2.4 Charged Particle Motion

Gyration

In uniform, time-independent fields the Lorentz equations (45) are easily solved. Define the unit vector in the direction of the magnetic field by $\mathbf{b} = \mathbf{B}/B$. Letting $d\mathbf{x}/dt = \mathbf{v} = v_{\parallel}\mathbf{b} + \mathbf{v}_{\perp}$ with $\mathbf{v}_{\perp} = \mathbf{b} \times (\mathbf{v} \times \mathbf{b})$, and separating (45) into parallel and perpendicular components, we find

$$\begin{aligned} \mathbf{v}_{\parallel}(t) &= \mathbf{v}_{\parallel}(0) + \frac{e}{m} E_{\parallel} t \\ \mathbf{v}_{\perp}(t) &= v_{\perp} [\mathbf{e}_2 \cos(\Omega t) - \mathbf{e}_3 \sin(\Omega t)] + c \frac{\mathbf{E} \times \mathbf{B}}{B^2}, \end{aligned} \quad (57)$$

where the unit vectors \mathbf{e}_2 and \mathbf{e}_3 form an orthonormal triplet with \mathbf{b} :

$$\mathbf{b} \cdot \mathbf{e}_2 \times \mathbf{e}_3 = 1. \quad (58)$$

but are otherwise arbitrary. The last term in the perpendicular velocity is referred to as the $\mathbf{E} \times \mathbf{B}$ drift. Integrating (57) once more gives

$$\begin{aligned} \mathbf{x}(t) &= \mathbf{X}(t) + \mathbf{r}(t) \\ \mathbf{r}(t) &= \rho [\mathbf{e}_2 \sin(\Omega t) + \mathbf{e}_3 \cos(\Omega t)], \end{aligned} \quad (59)$$

where $\rho = v_{\perp}/\Omega$ is the *gyroradius*. The first term represents the non-gyrating part of the motion; we define it by its derivative

$$\dot{\mathbf{X}}(t) = c \frac{\mathbf{E} \times \mathbf{B}}{B^2} + \mathbf{b} \frac{e}{m} E_{\parallel} t. \quad (60)$$

Thus the motion is a superposition of gyration, a parallel acceleration, and a transverse drift.

Various other simple cases of gyromotion can be solved exactly (Lehnert, 1964). However, in general the Lorentz equations are nonlinear, and exact solution is usually impossible.

Guiding Center Motion

More generally the fields are vary both in magnitude and direction. When the magnetic field varies slowly, in the sense that

$$1 \gg \delta \sim \frac{\rho|\nabla B|}{B}, \quad \frac{1}{\Omega B} \frac{dB}{dt}, \quad (61)$$

and when the electric field is correspondingly constrained (see below), then the motion of a charged particle can be obtained using a perturbation expansion. The expansion assumes that electromagnetic forces are more important than inertia, or that charge dominates mass: the essential physical idea is that gyration is faster than any other process. A systematic perturbation series is obtained by replacing the ratio m/e by $\delta m/e$ where δ is a formal small parameter. Thus the Lorentz equation becomes

$$\delta \frac{d^2 \mathbf{x}}{dt^2} = \frac{e}{m} \mathbf{E} + \frac{e}{mc} \frac{d\mathbf{x}}{dt} \times \mathbf{B}. \quad (62)$$

Following the form of the uniform field solution (59), let

$$\mathbf{x}(t) = \mathbf{X}(t) + \delta \mathbf{r}_1(\gamma(t), t) + \delta^2 \mathbf{r}_2(\gamma(t), t) + \dots \quad (63)$$

Here $\mathbf{X}(t)$ represents the non-gyrating part of the motion, or the motion of the guiding center.

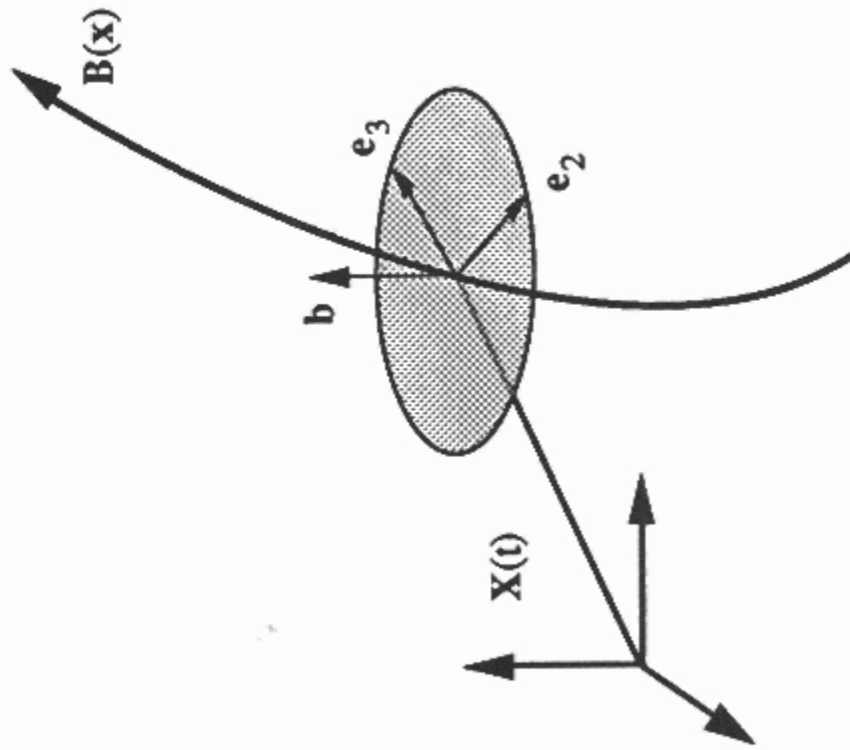


Figure 3. Guiding center variables

Rather than specify the form of \mathbf{X} a priori, we assume that the guiding-center velocity has an expansion in δ :

$$\dot{\mathbf{X}}(t) = \mathbf{u}_0 + \delta \mathbf{u}_1(t) + \dots \quad (64)$$

The gyromotion is represented by the vectors \mathbf{r}_i that rapidly rotate with the phase $\gamma(t)$, as in (59). We expect to find that $\dot{\gamma}(t) = \Omega t$ to lowest order; since $\Omega = eB/mc$, it should be replaced by Ω/δ according to our scaling. Note that the gyrofrequency will depend on position through $|\mathbf{B}|$. Since there will also be corrections to the phase, we assume

$$\dot{\gamma} = \frac{1}{\delta} \omega_0(t) + \omega_1(t) + \dots . \quad (65)$$

The coordinates \mathbf{r}_i may depend on the slow time scale as well, through their second arguments. In order to define uniquely the splitting between guiding-center position and gyration, we assume that the *gyroaverage* of each of the \mathbf{r}_i is zero:

$$\langle \mathbf{r}_i \rangle \equiv \frac{1}{2\pi} \int_0^{2\pi} d\gamma \mathbf{r}_i(\gamma, t) = 0 . \quad (66)$$

Thus the gyroaverage of \mathbf{x} is the guiding-center position $\langle \mathbf{x} \rangle = \mathbf{X}$. This expansion is an example of a *multiple time scale*, or *averaging* perturbation expansion; in particular we follow the general method of Krylov, Bogoliubov and Mitropolsky (Bogoliubov, 1961).

To carry out the expansion we recall that the field amplitudes are evaluated at the particle positions, and vary slowly. Hence they can be expanded as well:

$$\mathbf{B}(\mathbf{x}, t) = \mathbf{B}(\mathbf{X}, t) + \delta(\mathbf{r}_1 \cdot \nabla) \mathbf{B}(\mathbf{X}, t) + \dots . \quad (67)$$

The electric field will be expanded similarly, with an additional caveat: we will be forced to assume that the parallel electric field is small,

$$E_{\parallel} = \mathbf{E} \cdot \mathbf{b} = \delta E_{\parallel}(\mathbf{X}, t) + \delta^2(\mathbf{r}_1 \cdot \nabla) E_{\parallel}(\mathbf{X}, t) + \dots . \quad (68)$$

The particle velocity has the expansion

$$\frac{d\mathbf{x}}{dt} = \dot{\mathbf{X}} + \frac{\partial \mathbf{r}_1}{\partial \gamma} \dot{\gamma} + \delta \frac{\partial \mathbf{r}_1}{\partial t} + \dots$$

$$= \mathbf{u}_0 + \delta \mathbf{u}_1 + \dots + \frac{\partial \mathbf{r}_1}{\partial \gamma} (\omega_0 + \delta \omega_1 + \dots) + \delta \frac{\partial \mathbf{r}_1}{\partial t} + \dots \quad (69)$$

and there is a similar, but more complicated expansion for the acceleration.

Substitution of the expansion into the Lorentz equation gives, order by order, the equations for the guiding-center velocity, gyrophase, and gyration. The lowest order is $\mathcal{O}(\delta^0)$, which gives

$$\omega_0^2 \frac{\partial^2 \mathbf{r}_1}{\partial \gamma^2} - \frac{e}{mc} \omega_0 \frac{\partial \mathbf{r}_1}{\partial \gamma} \times \mathbf{B}(\mathbf{X}) = c \mathbf{E}(\mathbf{X}) + \frac{e}{mc} \mathbf{u}_0 \times \mathbf{B}(\mathbf{X}) . \quad (70)$$

From this equation we can determine ω_0 , \mathbf{u}_0 and \mathbf{r}_1 . Since the left hand side of the equation will occur often, we give it a name:

$$\mathcal{G} \equiv \omega_0^2 \frac{\partial^2}{\partial \gamma^2} + \frac{e}{mc} \omega_0 \mathbf{B}(\mathbf{X}) \times \frac{\partial}{\partial \gamma} . \quad (71)$$

The operator \mathcal{G} is a linear, second order differential operator. It is symmetric with respect to the gyroaverage: $\langle \mathbf{r} \cdot \mathcal{G} \mathbf{s} \rangle = \langle \mathbf{s} \cdot \mathcal{G} \mathbf{r} \rangle$.

To find \mathbf{r}_1 , we first solve the homogeneous equation $\mathcal{G}\mathbf{r}_1 = 0$, a second order differential equation with the independent variable γ . The slow time enters parametrically, and for present purposes can be considered fixed. The general solution of the homogeneous equation is

$$\mathbf{r}_1(\gamma, t) = \mathbf{R}(t) + \rho [\mathbf{e}_2(t) \sin(\gamma + \varphi) + \mathbf{e}_3(t) \cos(\gamma + \varphi)]$$

providing

$$\frac{e}{mc} \mathbf{e}_3 \times \mathbf{B} = \omega_0 \mathbf{e}_2 , \quad \frac{e}{mc} \mathbf{e}_2 \times \mathbf{B} = -\omega_0 \mathbf{e}_3 . \quad (72)$$

There are six integration constants (for the second order vector operator \mathcal{G}); three are the components of the vector \mathbf{R} . The direction of the unit vector $\mathbf{e}_2(t)$ can be chosen arbitrarily in the plane perpendicular to \mathbf{B} ; the gyroradius $\rho(t)$ is also arbitrary. Finally there is an arbitrary phase φ . The consistency condition (66) implies that $\mathbf{R} = 0$, and we absorb the phase into the definition of γ , giving

$$\mathbf{r}_1(\gamma, t) = \rho [\mathbf{e}_2(t) \sin \gamma + \mathbf{e}_3(t) \cos \gamma] . \quad (73)$$

Taking the dot product of the two equations (72) with \mathbf{e}_2 and \mathbf{e}_3 shows that

$$\omega_0(t) = \frac{e}{mc} \mathbf{B}(\mathbf{X}, t) = \Omega(\mathbf{X}, t) . \quad (74)$$

which is the gyrofrequency evaluated at the position of the guiding center. Thus we have deduced that the lowest order frequency is the local gyrofrequency. The arbitrariness in the choice of the direction for $\mathbf{e}_3(t)$ at each point in space can be considered to be a gauge freedom; the guiding-center equations must be independent of this choice, and thus exhibit gauge symmetry (Littlejohn, 1988).

Before proceeding with the solution to (70), we consider the general structure of this perturbation series. At each order the equation will have the form

$$\mathcal{G}\mathbf{r}_i = \frac{e}{mc} \mathbf{u}_{i-1} \times \mathbf{B}(\mathbf{X}) + \mathbf{F}(\mathbf{u}_0, \dots, \mathbf{u}_{i-2}, \underline{\mathbf{r}_1}, \dots, \underline{\mathbf{r}_{i-1}}, \omega_0, \dots, \omega_{i-1}) . \quad (75)$$

Nominally this equation determines the γ dependence of \mathbf{r}_i ; however, it must also determine the drift velocity \mathbf{u}_{i-1} , the frequency ω_{i-1} , and the slow, explicit time dependence of \mathbf{r}_{i-1} . These are determined by solvability conditions. To ensure that the gyroaverage of \mathbf{r}_i is zero, the right-hand

side of (75) must be orthogonal to the kernel of the operator \mathcal{G} : the set of homogeneous solutions, which are a) a constant vector, b) the function $\mathbf{r}_1(\gamma)$ in (73) and c) $d\mathbf{r}_1/d\gamma$. Thus there are three solvability conditions for this equation. The first,

$$\langle \mathcal{G}\mathbf{r}_i \rangle = 0 \Rightarrow \begin{cases} \frac{e}{mc} \mathbf{u}_{i-1} \times \mathbf{B} = -\langle \mathbf{F}_\perp \rangle \\ \langle \mathbf{F}_\parallel \rangle = 0 \end{cases} \quad (76)$$

determines both the perpendicular component of \mathbf{u}_{i-1} and the parallel component of \mathbf{u}_{i-2} . Condition b),

$$\langle \mathbf{r}_1 \cdot \mathcal{G}\mathbf{r}_i \rangle = 0 \Rightarrow \langle \mathbf{r}_1 \cdot \mathbf{F} \rangle \quad (77)$$

determines ω_{i-1} . The final solvability condition

$$\left\langle \frac{d\mathbf{r}_1}{d\gamma} \cdot \mathcal{G}\mathbf{r}_i \right\rangle = 0 \Rightarrow \left\langle \frac{d\mathbf{r}_1}{d\gamma} \cdot \mathbf{F} \right\rangle \quad (78)$$

determines the time dependence of \mathbf{r}_{i-1} . Once the solvability conditions have been satisfied, we can obtain \mathbf{r}_i as the particular solution of the non-homogeneous equation (75).

We now apply these conditions to the first-order equation (70). The gyroaverage of (70) simply implies that the right-hand side of (70) is identically zero. Thus

$$\mathbf{u}_{0\perp} = c \frac{\mathbf{E} \times \mathbf{B}}{B^2}, \quad (79)$$

where all the fields are evaluated at the guiding-center position. We also arrive at the consistency condition (68), $E_\parallel = \mathcal{O}(\delta)$, since there is no other term on the right-hand side to balance this component.

For our purposes, it is sufficient to obtain the guiding-center velocity to $\mathcal{O}(\delta)$; this arises from the condition (76), the gyroaverage of the $\mathcal{O}(\delta)$ terms of (62),

$$0 = \frac{e}{mc} \mathbf{u}_1 \times \mathbf{B}(\mathbf{X}) - \frac{d\mathbf{u}_0}{dt} + \frac{e}{m} E_\parallel \mathbf{b} - \frac{e\Omega}{mc} \left\langle (\mathbf{r}_1 \cdot \nabla) \mathbf{B} \times \frac{\partial \mathbf{r}_1}{\partial \gamma} \right\rangle. \quad (80)$$

The main difficulty here is to compute the last term, using the explicit form of \mathbf{r}_1 . The easiest way to do this is to orient a rectangular coordinate system at the guiding-center position \mathbf{X} , such that $\hat{\mathbf{z}} = \mathbf{b}(\mathbf{X})$, $\hat{\mathbf{x}} = \mathbf{e}_2(\mathbf{X})$, and $\hat{\mathbf{y}} = \mathbf{e}_3(\mathbf{X})$. Substitution gives

$$\left\langle (\mathbf{r}_1 \cdot \nabla) \mathbf{B} \times \frac{\partial \mathbf{r}_1}{\partial \gamma} \right\rangle = -\frac{\rho^2}{2} \left[\hat{\mathbf{x}} \frac{\partial B_z}{\partial x} + \hat{\mathbf{y}} \frac{\partial B_z}{\partial y} - \hat{\mathbf{z}} \left(\frac{\partial B_x}{\partial x} + \frac{\partial B_y}{\partial y} \right) \right].$$

Using the fact that $\nabla \cdot \mathbf{B} = 0$, and that $B_z(\mathbf{X}) = B(\mathbf{X})$, by definition of the coordinate system, we obtain

$$\left\langle (\mathbf{r}_1 \cdot \nabla) \mathbf{B} \times \frac{\partial \mathbf{r}_1}{\partial \gamma} \right\rangle = \frac{\rho^2}{2} \nabla B(\mathbf{X}).$$

Substitution into (80) gives

$$\mathbf{u}_{1\perp} = \frac{1}{\Omega B} \mathbf{B} \times \frac{d\mathbf{u}_0}{dt} + \frac{\Omega \rho^2}{2B^2} \mathbf{B} \times \nabla B. \quad (81)$$

The perpendicular drift is thus composed of two terms, the *inertial drift*, and the *gradient-B drift*. The inertial drift can be decomposed similarly into several distinct drift motions. First note that $\mathbf{u}_0 = \mathbf{u}_{0\parallel} \mathbf{b} + \mathbf{u}_{0\perp}$. The total time derivative of the first term includes the derivative of $\mathbf{b}(\mathbf{X}, t)$ along the guiding-center orbit

$$\frac{d\mathbf{b}}{dt} = \frac{\partial \mathbf{b}}{\partial t} + \mathbf{u}_{\parallel} \mathbf{b} \cdot \nabla \mathbf{b} + \mathbf{u}_{\perp} \cdot \nabla \mathbf{b}$$

where each term above is perpendicular to \mathbf{b} , because \mathbf{b} is a unit vector. The second term represents the curvature of the magnetic field:

$$\kappa = \mathbf{b} \cdot \nabla \mathbf{b} = -\mathbf{b} \times (\nabla \times \mathbf{b}). \quad (82)$$

The last equality follows from the vector identity for $\nabla(\mathbf{b} \cdot \mathbf{b}) = 0$, and shows that κ is perpendicular to \mathbf{b} . The drift due to this term is the *curvature drift*

$$\mathbf{u}_c = \frac{u_{\parallel}^2}{\Omega B} (\mathbf{B} \times \boldsymbol{\kappa}). \quad (83)$$

The time derivative of \mathbf{u}_{\perp} is

$$\frac{d\mathbf{u}_{0\perp}}{dt} = c \left(\frac{\partial}{\partial t} + \mathbf{u}_0 \cdot \nabla \right) \frac{\mathbf{E} \times \mathbf{B}}{B^2}. \quad (84)$$

This term, when substituted into (81), yields the nonlinear *polarization drift*; its linear part is

$$\mathbf{u}_p = \frac{c}{\Omega B} \frac{\partial \mathbf{E}_\perp}{\partial t}. \quad (85)$$

The equation for the parallel velocity is obtained from the parallel component of (80):

$$m \frac{du_{0\parallel}}{dt} = e E_{\parallel} - \frac{e \rho^2 \Omega}{2c} \mathbf{b} \cdot \nabla B(\mathbf{X}). \quad (86)$$

The first term on the right-hand side is simply the parallel electrostatic force. The second term is the *mirror force*. It is a force that decelerates the parallel motion if the magnetic intensity is increasing along the field lines.

We collect the final results below for convenience:

$$\mathbf{u}_{0\perp} = c \frac{\mathbf{E} \times \mathbf{B}}{B^2}$$

$$m \frac{du_{0\parallel}}{dt} = e E_{\parallel} - \mu \mathbf{b} \cdot \nabla B(\mathbf{X})$$

$$\mathbf{u}_{1\perp} = \frac{1}{\Omega B} \mathbf{B} \times \frac{d\mathbf{u}_0}{dt} + \frac{\mu}{m \Omega} \mathbf{b} \times \nabla B.$$

Here we have defined the magnetic moment

$$\mu \equiv \frac{e}{2c} \Omega \rho^2 = \frac{mv_\perp^2}{2B} \quad (88)$$

which, as we will see in the next section, is the action for the gyration.

We have yet to impose the second and third solvability conditions to the $\mathcal{O}(\delta)$ equation. The second condition, (77), yields an expression for ω_1 that is not of much interest. The third condition, (78), implies

$$2 \left\langle \frac{\partial \mathbf{r}_1}{\partial \gamma} \cdot \frac{\partial^2 \mathbf{r}_1}{\partial t \partial \gamma} \right\rangle \Omega + \left\langle \left(\frac{\partial \mathbf{r}_1}{\partial \gamma} \right)^2 \right\rangle \Omega =$$

$$\left\langle \frac{\partial \mathbf{r}_1}{\partial \gamma} \cdot (\mathbf{r}_1 \cdot \nabla) \mathbf{E} \right\rangle + \left\langle \frac{\partial \mathbf{r}_1}{\partial \gamma} \cdot \left(\frac{\partial \mathbf{r}_1}{\partial t} \times \mathbf{B} \right) \right\rangle + \left\langle \frac{\partial \mathbf{r}_1}{\partial \gamma} \cdot \mathbf{u} \times (\mathbf{r}_1 \cdot \nabla) \mathbf{B} \right\rangle .$$

Inserting the form (73), using Faraday's law (49), and calculating all the averages yields a surprisingly simple result:

$$\frac{\Omega}{2} \frac{\partial}{\partial t} \rho^2 + \frac{1}{2} \rho^2 \left(\frac{\partial}{\partial t} + \mathbf{u} \cdot \nabla \right) \Omega = 0 .$$

This equation determines the time dependence of $\rho(t)$, the gyroradius; it implies that the quantity $\Omega \rho^2$ is conserved along the guiding-center motion

$$\frac{d}{dt} \rho^2 \Omega = 0 . \quad (89)$$

In other words, the magnetic moment, μ , is preserved through $\mathcal{O}(1)$.

The guiding-center expansion can also be carried out in a Hamiltonian formulation. In fact the most expeditious method for doing this is to use the phase space action principle. The variational principle, when expanded in δ , yields an elegant formulation for the equations of motion, and is especially useful if one desires to continue the expansion to higher order (Littlejohn, 1983).

Adiabatic Invariants

When the parameters of a Hamiltonian system are slowly changed, the orbits evolve preserving adiabatic invariants. Consider, for example, a Hamiltonian $H(p, q, \mathbf{Z}, t)$. Here \mathbf{Z} represents slowly varying dynamical variables (coordinates and momenta), so that $\partial H / \partial \mathbf{Z} = \mathcal{O}(\delta)$. Furthermore the energy itself is assumed to vary slowly with time, $\partial H / \partial t = \mathcal{O}(\delta)$. The frozen system associated with H is the same function with its \mathbf{Z} and t dependence held fixed: it is simply a one degree of freedom system with Hamiltonian $H(p, q)$ depending parametrically on \mathbf{Z} and t . Suppose that all orbits of the

frozen system are periodic. Then the action, the area enclosed by an orbit of the frozen system,

$$J(E, \mathbf{Z}, t) = \oint p(q, E, \mathbf{Z}, t) dq \quad (90)$$

is an adiabatic invariant for H : it remains nearly invariant even as \mathbf{Z} and t evolve in time. Here the function $p(q, E, \mathbf{Z}, t)$ is defined implicitly by the equation

$$E = H(p, q, \mathbf{Z}, t), \quad (91)$$

and the loop integral is over one period of the oscillation (i.e., holding E , \mathbf{Z} , and t fixed).

The first step in showing that J is an adiabatic invariant is to prove that J is an invariant to $O(1)$ by considering its time derivative along the exact orbits of H :

$$\frac{dJ}{dt} = \frac{\partial J}{\partial E} \frac{dE}{dt} + \frac{\partial J}{\partial \mathbf{Z}} \cdot \dot{\mathbf{Z}} + \frac{\partial J}{\partial t} = O(\delta). \quad (92)$$

Each of the terms in (92) is $O(\delta)$ by assumption. Equation (92) does not indicate the importance of J , since both H and \mathbf{Z} are approximate invariants in the sense of (92). The importance of the adiabatic invariant is that even when H and \mathbf{Z} change by $O(1)$, in a time $O(1/\delta)$, J remains close to its initial value. To show this we show that the average over an oscillation of the frozen motion of dJ/dt is identically zero. We expand each of the terms in (92), using (90) to obtain

$$\frac{dJ}{dt} = \frac{dE}{dt} \oint \frac{\partial p}{\partial E} dq + \dot{\mathbf{Z}} \cdot \oint \frac{\partial p}{\partial \mathbf{Z}} dq + \oint \frac{\partial p}{\partial t} dq. \quad (93)$$

Since $p(E, \mathbf{Z}, t)$ is defined implicitly by (91), we can see that

$$\frac{\partial p}{\partial E} = \frac{1}{\dot{q}}, \quad \frac{\partial p}{\partial \mathbf{Z}} = -\frac{1}{\dot{q}} \frac{\partial H}{\partial \mathbf{Z}}.$$

Furthermore, let $\langle f \rangle$ denote the *bounce average* of f over the frozen trajectory:

$$\langle f \rangle = \frac{1}{T} \oint f(q, E, \mathbf{Z}, t) \frac{dq}{\dot{q}}. \quad (94)$$

Where $T(E, \mathbf{Z}, t)$ is the period of the orbit $T = \oint \frac{dq}{\dot{q}}$. Using (94) in (93) gives

$$\frac{1}{T} \frac{dJ}{dt} = \frac{dE}{dt} - \dot{\mathbf{Z}} \cdot \left\langle \frac{\partial H}{\partial \mathbf{Z}} \right\rangle - \left\langle \frac{\partial H}{\partial t} \right\rangle. \quad (95)$$

While (95) itself does not vanish, its bounce average does. The bounce average of the first and last terms cancel explicitly since $dE/dt = \partial H/\partial t$ by Hamilton's equations. Furthermore the dynamical variables \mathbf{Z} evolve by

Hamilton's equations (41), thus $\omega \dot{\mathbf{Z}} = \partial H / \partial \mathbf{Z}$ where ω is the symplectic form (42), and is antisymmetric. The symplectic form may depend explicitly on \mathbf{Z} if they are not canonical variables, but will not depend on (q, p) if the latter are canonical variables, so $\langle \omega \rangle = \omega$. Thus the bounce average of the second term in (95) vanishes by antisymmetry, and we obtain

$$\left\langle \frac{dJ}{dt} \right\rangle = 0 . \quad (96)$$

Of course, this equation does not imply that $J(T) = J(0)$; however, it does mean that most of the change in J is oscillatory.

In fact (96) is the solvability condition for the construction of the next approximation to the adiabatic invariant: $I^{(1)} = J + \mathcal{O}(\delta)$, where $I^{(1)}$ is defined such that $dI^{(1)} / dt = \mathcal{O}(\delta^2)$. Moreover, Kruskal has shown that there is a series in powers of δ for an adiabatic invariant, I , such that the n^{th} approximation $I^{(n)}$ satisfies $dI^{(n)} / dt = \mathcal{O}(\delta^{n+1})$ for any n (Kruskal, 1962). Thus the adiabatic invariant is preserved to all orders in δ . However, the series for I is asymptotic, and does not converge in general; thus the actual rate of change of I can be non-zero even though its power series is zero (e.g., any function of the form $e^{-1/\delta}$ has a zero power series about $\delta = 0$).

The fundamental adiabatic invariant for the motion of a charged particle in a magnetic field is that associated with the gyration of the particle. If the conditions (61) and (68) for the validity of the guiding-center approximation hold, the slow dependence of the Hamiltonian is induced by the slow spatial and temporal dependences of the fields. It is easy to compute this adiabatic invariant to lowest order: it is the action associated with gyration. To compute J , use the guiding-center expansions (63) and (64), in the canonical momentum (47) to obtain

$$\mathbf{P} = mv + \frac{e}{\delta c} \mathbf{A} = m \left(\mathbf{u} + \Omega \frac{\partial \mathbf{r}}{\partial \gamma} \right) + \frac{e}{\delta c} (\mathbf{A}(\mathbf{X}) + \delta \mathbf{r} \cdot \nabla \mathbf{A}(\mathbf{X})) + \mathcal{O}(\delta) .$$

The frozen system is obtained by demanding that \mathbf{X} and t are fixed allowing only θ to change, which gives the periodic gyromotion. Thus the action is

$$J = \oint \mathbf{p} \cdot d\mathbf{q} = \int_0^{2\pi} d\gamma \mathbf{p}(\gamma) \cdot \frac{d\mathbf{q}}{d\gamma} = \int_0^{2\pi} \left(m\Omega \frac{d\mathbf{r}}{d\gamma} + \frac{e}{c} (\mathbf{r} \cdot \nabla) \mathbf{A} \right) \cdot \frac{d\mathbf{r}}{d\gamma} d\gamma + \mathcal{O}(\delta) .$$

Several terms vanish in the last equality because \mathbf{r} is periodic in γ . Substituting the form (73) for $\mathbf{r}(\gamma, t)$ yields

$$J = \pi m\Omega \rho^2 + \mathcal{O}(\delta) . \quad (97)$$

This equation implies that the lowest order adiabatic invariant is simply the magnetic moment. We showed the magnetic moment is indeed invariant to $\mathcal{O}(1)$ by another approach in (89).

In special cases, there are additional adiabatic invariants for guiding-center particles. Suppose that the conditions (61) for guiding-center motion are valid, so that the magnetic moment is an adiabatic invariant; for our current purposes suppose that it is in fact constant. Suppose further that the electric field is $O(\delta)$. Then the zero order drift velocity, the $\mathbf{E} \times \mathbf{B}$ drift, vanishes, so the predominant motion is along the field lines. The momentum associated with this motion is the canonical parallel momentum, which is

$$p_{\parallel} = m\mathbf{u}_{\parallel} + \frac{e}{c} A_{\parallel}. \quad (98)$$

The Hamiltonian for this motion is simply the energy in guiding-center coordinates:

$$H = \frac{1}{2} m\mathbf{u}_{\parallel}^2 + \mu B.$$

The parallel momentum is canonically conjugate to X_{\parallel} , a coordinate measuring position along \mathbf{B} . The Hamiltonian depends parametrically on the remaining guiding-center coordinates \mathbf{X}_{\perp} and t , but since the zero order drift velocity vanishes, each of these variations is slow. The standard adiabatic analysis applies if the parallel motion is periodic in time. This will occur if the magnetic field $B(X_{\parallel}, \mathbf{X}_{\perp})$ exhibits a local well, trapping the guiding center by the mirror force. We can then solve $H(p_{\parallel}, X_{\parallel}, \mathbf{X}_{\perp}, \mu, t) = E$ for p_{\parallel} , and compute the *longitudinal* or *bounce* adiabatic invariant:

$$\begin{aligned} J_{\parallel} &= \oint p_{\parallel}(X_{\parallel}, E, \mu, \mathbf{X}_{\perp}, t) dX_{\parallel} \\ &= \oint \sqrt{2m\mu(B_t(\mathbf{X}_{\perp}) - B(X_{\parallel}, \mathbf{X}_{\perp}))} dX_{\parallel} \end{aligned} \quad (99)$$

where B_t is the value of $B(\mathbf{X})$ at the turning point, and the integral is done along a fixed field line.

The final adiabatic invariant arises from the slow perpendicular drift \mathbf{u}_{\perp}^1 , which causes the particle to drift slowly across the magnetic field. To obtain an adiabatic invariant associated with this motion, both the magnetic moment and longitudinal invariants must be well preserved. An expression for this invariant is obtained by averaging the equations over the longitudinal motion, just as we averaged to obtain the guiding-center equations.

Further Reading

On Tensor Calculus:

Morse, 1953
Adler, 1958

On Plasma Physics:

Chen, 1974
 Ichimaru, 1973
 Krall and Trivelpiece, 1973
 Schmidt, 1979

On Guiding Center Motion:

Northrop, 1963
 Morozov, 1966

Exercises

- 1.** Define a toroidal coordinate system (ψ, θ, ζ) by the relations

$$x = \cos \zeta \frac{\sqrt{\psi^2 - 1}}{\psi - \cos \theta}, \quad y = \sin \zeta \frac{\sqrt{\psi^2 - 1}}{\psi - \cos \theta}, \quad z = \frac{\sin \theta}{\psi - \cos \theta},$$

where ψ ranges from 1 to ∞ . Show that the surfaces $\psi = \text{constant}$ are axisymmetric tori with a circular poloidal cross section. Compute the metric tensor g_{ij} , and the Jacobian J .

- 2.** Verify Equations (30), (31) and (32).

- 3.** Compute the ordinary, covariant and contravariant components of the vector field $\mathbf{A} = \hat{z}$ in cylindrical (2) and primitive toroidal (3) coordinates.

- 4.** Compute the curl of $\mathbf{A} = r_0 \nabla \zeta_0$.

- 5.** Suppose the action is given by

$$S = \int \frac{e}{c} \hat{\mathbf{A}} \cdot d\mathbf{x} - e\varphi dt.$$

Show that the symplectic form is the antisymmetric matrix $\epsilon_{ijk} B^k / jc$ and that equations of motion give the $\mathbf{E} \times \mathbf{B}$ drift.

- 6.** Discuss the motion of a charged particle in the magnetic field $\mathbf{B} = x\hat{z}$. Use of the Hamiltonian (48) may prove advantageous. Compare your results to the guiding-center equations, and explain the limitations of the latter.

Chapter 3

Confined Plasma Equilibrium

The topic of magnetized plasma equilibrium divides naturally into two subtopics. First, there are geometrical issues involving toroidicity, coordinate systems and representations of the confining field. Plasma dynamics (or even plasma physics!) plays little role in such considerations, which hinge primarily on toroidal topology and the nature of magnetic fields. The plasma enters as an active medium in the second category of issues, essentially through its ability to support and generate electrical current. Plasma currents need to be understood because of their effect on energy balance (Ohmic heating) as well as plasma instabilities, considered later. Most importantly, the magnetic fields resulting from plasma current often play an essential role in confinement.

This chapter is divided into three parts. The first part, “Magnetic field Geometry,” develops the issues specific to confinement geometry. “Plasma Current” is studied in the second part. These treatments avoid geometrical specialization or approximation. Because a much more explicit analysis is possible in the case of symmetric fields, and because of the paramount role of symmetric confinement in the fusion program, we devote a separate discussion, the third part, to “Axisymmetric Systems.”

Part 1: Magnetic Field Geometry

3.1 Flux Surfaces

Toroidicity

Suppose one is given a smooth, closed surface, S , together with some well-behaved vector field $\mathbf{C}(\mathbf{x})$ such that the component of \mathbf{C} tangent to S never vanishes. Then, according to a famous theorem of Poincaré, the surface S must be a torus.

This conclusion is traditionally pictured by imagining the field lines of \mathbf{C} as hairs, protruding from the surface. Such hair can be smoothly combed, without bald spots or “spikes,” only on a toroidal surface. This image makes the theorem unsurprising, although the rigorous proof is lengthy and not presented here (Taylor, 1974).

From the vector field \mathbf{C} one can construct on S another smooth field, $\mathbf{D}(\mathbf{x}) = \mathbf{C}(\mathbf{x}) - \mathbf{n}(\mathbf{x})[\mathbf{n}(\mathbf{x}) \cdot \mathbf{C}(\mathbf{x})]$, where $\mathbf{n}(\mathbf{x})$ is the unit vector normal to S . The new vector field has no normal component—it lies in the surface at each point—and it never vanishes on S . In this case we say that \mathbf{D} covers the surface S ; the Poincaré theorem states that only toroidal surfaces can be covered by a nonzero vector field.

The implication for plasma confinement is clear. Consider the outermost bounding surface of some magnetically confined plasma. If the plasma is assumed magnetized everywhere, the magnetic field cannot vanish on this surface. Furthermore, since particle motion is unconstrained along \mathbf{B} , the field cannot have a component normal to the surface. Thus \mathbf{B} covers the bounding surface, which must therefore be toroidal. It is noteworthy that neither Maxwell's equations nor any detailed plasma dynamics, such as force balance, enters this conclusion.

A toroidal surface densely covered by a magnetic field is called a *flux surface*. Flux surfaces provide a barrier to collisionless charged particles that is penetrable only by their relatively slow, perpendicular drift motion. While we have shown that the outermost, bounding surface must be a flux surface, it is natural to suppose the confinement region to be filled by a sequence of flux surfaces, each enclosing the next. Thus one speaks of *nested, toroidal flux surfaces*—the fundamental impediment to plasma motion and the key to confinement.

This idealized structure approximates the field configuration in successful, quiescent confinement devices. But it is not realistic in detail; we consider next the nature of real confining fields. It should be kept in mind that the present discussion concerns stationary magnetic fields exclusively.

Ergodic Field Lines and Chaos

We noted in Chapter 1 that the field lines on a magnetic surface or flux surface can be closed. For example, purely toroidal or purely poloidal lines close upon themselves after a single circuit of the torus, so that an infinity of lines is needed to cover the surface. More commonly, however, the flux surface is densely covered by a single line, winding endlessly around the torus. One says then that the surface is *ergodically covered*, or that it is an ergodic surface. (Note that the word “ergodic” is used here in the sense of densely covering, without connotation of randomness.) The distinction between closed-line surfaces and ergodic surfaces is important. For example, particles following closed field lines explore only a fraction of the toroidal

surface, while those following ergodic lines eventually approach every point on the surface. In most configurations both kinds of surface occur, although the ergodic surfaces are prevalent.

Closed field lines are exceptional because any small perturbation of the currents is likely to destroy closure. For the same reason, ergodicity on a surface should be considered fragile: the generic field line travels ergodically over a three-dimensional volume. Thus the existence of flux surfaces cannot be taken for granted; in real devices one may have instead “flux volumes” throughout which field lines, and therefore particles, freely range (Grad, 1967), (Stix, 1973).

The chaotic threading (“braiding”) of a three-dimensional region by field lines is called *magnetic chaos*¹. This wording emphasizes an important fact: flux surface deterioration rarely entails lines leading directly from the confinement interior to a container wall. Instead the errant lines perform a sort of random walk, weaving chaotically through the ergodic volume. Similarly, because of their finite streaming speed, charged particles following such lines are not immediately lost. Instead, as shown in Chapter 9, they display an enhanced rate of diffusion.

Idealized, well-behaved fields, whose lines (open or closed) remain on two-dimensional surfaces, are called *integrable*. The language comes from classical mechanics: as discussed in §2.4, field line trajectories are in fact described by Hamiltonian equations. Thus the existence of a flux surface is equivalent to, and no more generic than, the integrability of a Newtonian trajectory. The mechanical analogy explains why symmetrical geometries, such as the tokamak, are integrable: the symmetry provides the additional “constant of motion” needed for integration. Thus an ideal tokamak would have exact flux surfaces.

The mechanical analogy is also instructive regarding departures from symmetry. For it is known from mechanics that sufficiently weak, symmetry-breaking perturbations do not globally destroy integrability. Only resonant orbits are at first affected—those corresponding in the magnetic case to surfaces with closed field lines. The famous “KAM” (Kolmogorov-Arnol’d-Moser) theorem shows specifically that the total chaotic volume induced by any smooth, symmetry-breaking field perturbation is small, proportional to some power of the perturbation amplitude. Even at significant amplitude, the bands of chaos surrounding closed-line surfaces are separated by ergodic surfaces, whose survival can render the chaotic regions relatively innocuous.

We will return to the KAM theorem in Chapter 9. What needs to be understood here is the quality of realistic flux surfaces. It should be clear that all real confinement devices will have at least small regions of field chaos—narrow ergodic volumes. Furthermore, violent plasma instability, such as the major disruptions observed in tokamaks, can effect much worse

¹The term “stochastic” was used for this concept, but has been discarded because it can be confused with randomness in the sense of probability theory.

field-line behavior. But appropriate machine design, even in cases with intentional asymmetry, can control equilibrium chaos. In operating machines the chaotic regions are sufficiently sparse to make the ideal description, in terms of a sequence of nested flux surfaces, a sensible approximation.

Flux Labels

A function that is constant on flux surfaces, is called a *flux label*. Any reasonably smooth function $f(x)$ that is constant along field lines,

$$\mathbf{B} \cdot \nabla f = 0 , \quad (1)$$

must be a flux label when the field line is ergodic on the surface. Indeed, we shall find the identification

$$\mathbf{B} \cdot \nabla f = 0 \Rightarrow f \text{ is a flux label} , \quad (2)$$

to be a crucial feature of ideal confinement. Note that any monotonic flux label provides a good radial coordinate, as in (2.4). We consider next two flux labels that are usually monotonic and have special importance (Kruskal and Kulsrud, 1958).

Poloidal and Toroidal Fluxes

We define the poloidal flux, Ψ_P , in terms of the ribbon-like surface, $S_P(r)$, stretched between the magnetic axis and a line of constant θ on the surface labelled by r . Such a surface is depicted in Fig. 1, in which the torus has been cut and “unwound” for clarity. We have

$$\Psi_P(r) \equiv \int_{S_P(r)} dS \mathbf{n} \cdot \mathbf{B} \quad (3)$$

where $\mathbf{n} = \nabla\theta/|\nabla\theta|$ is the unit normal from the surface, oriented in the direction of increasing θ . It is clear that S_P intersects all the poloidal flux of \mathbf{B} within r , since no field lines cross a flux surface. More importantly it is clear that the value of Ψ_P is independent of the choice of angle coordinates: since all acceptable poloidal angles are topologically equivalent, a ribbon attached to any constant- θ line must intercept the same magnetic flux.

The toroidal flux is defined analogously,

$$\Psi_T(r) \equiv \int_{S_T(r)} dS \mathbf{n} \cdot \mathbf{B}$$

where $S_T(r)$ is a disk or cap, whose rim is attached to the surface labelled by r , with normal $\mathbf{n} = \nabla\zeta/|\nabla\zeta|$; see Fig. 1. Again, the definition can be seen to be independent of the choice of angle variables.

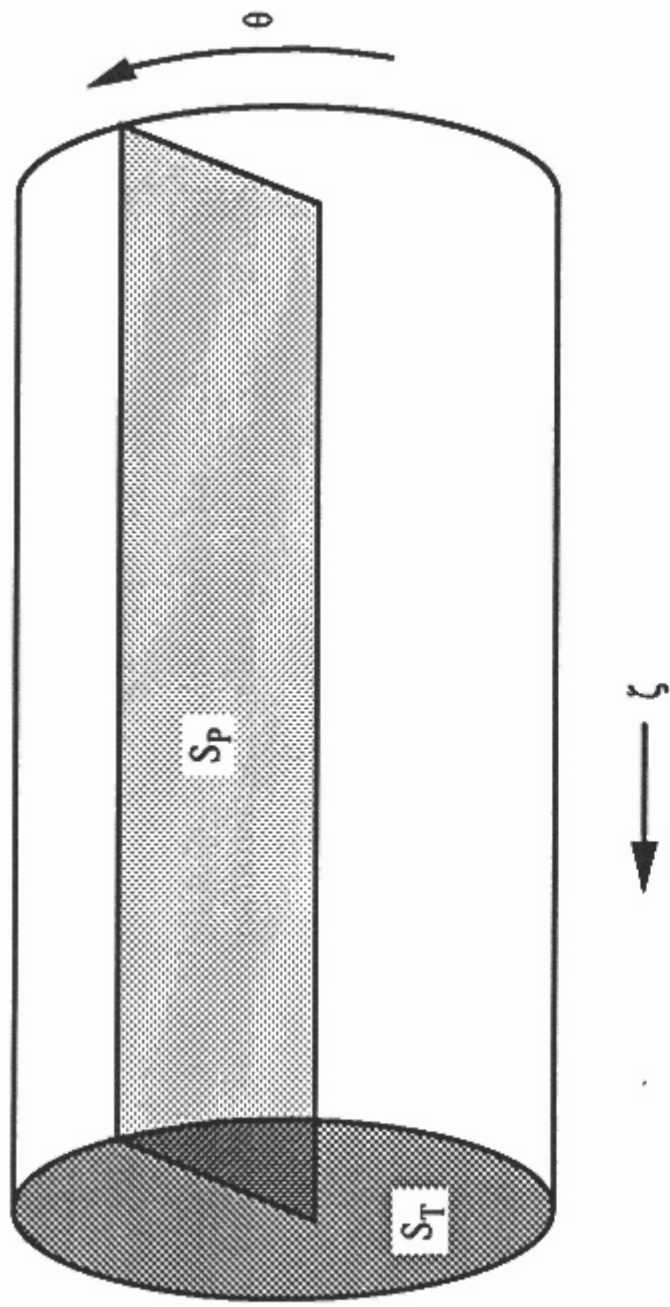


Figure 1. Toroidal and Poloidal surfaces S_T and S_P .

Calculation of either flux is easiest when they are expressed as volume integrals:

$$2\pi\Psi_P = \int_{V(r)} d^3x \mathbf{B} \cdot \nabla\theta, \quad (4)$$

$$2\pi\Psi_T = \int_{V(r)} d^3x \mathbf{B} \cdot \nabla\zeta. \quad (5)$$

Here $V(r)$ is the volume enclosed by the surface r . To confirm (4), we first use $\nabla \cdot \mathbf{B} = 0$ to express it as

$$2\pi\Psi_P = \int_{V(r)} d^3x \nabla \cdot (\mathbf{B}\theta)$$

and then apply Gauss' theorem. Note that Gauss' theorem applies to $\theta(\mathbf{x})$ only in the cut volume bounded by the flux surface and by (both sides of) S_P . Since \mathbf{B} has no component normal to the flux surface, the result is

$$2\pi\Psi_P = \left(\int_{S_P(r)} + \int_{S_P(r)+2\pi} \right) ds \mathbf{n} \cdot (\mathbf{B}\theta) \quad \blacksquare$$

where the two integrals represent both sides of S_P . The form (3) follows because θ differs by 2π across this surface. Of course a very similar proof applies to Ψ_T .

Rotational Transform

Since both Ψ_P and Ψ_T are flux labels, either can be considered as a function of the other. Indeed, the requirement that Ψ_P be expressible as a function

of Ψ_T alone,

$$\Psi_P(\mathbf{x}) = \Psi_P(\Psi_T),$$

is one way to characterize an integrable magnetic field. The derivative of this function is another flux label, called the *rotational transform* and denoted by

$$\iota \equiv 2\pi \frac{d\Psi_P}{d\Psi_T}.$$

To interpret ι , consider the “puncture plot” of points representing the successive intersections of a single field line with S_T . The change in ζ between any two successive points is 2π ; the corresponding change in θ is measured by ι . Here it should be noted that the θ -changes are not uniform; a field line might move further poloidally during one toroidal circuit than another. However, we will see that the *average* change in θ after many passes is given by $\iota/2\pi$. Thus, the rotational transform measures the average twist or pitch of field lines on a flux surface. A purely toroidal line has no rotational transform; for a purely poloidal line, $\iota = \infty$.

To verify this interpretation (Kruskal and Kulsrud, 1958), choose an ergodic flux surface and a specific field-line segment, extending from $\zeta = 0$ to $\zeta = 2\pi$, on the surface. On that segment erect a thin ribbon, normal to the surface and everywhere parallel to \mathbf{B} . The ribbon winds around the surface, eventually reaching $\zeta = 2\pi$, with a change $\Delta\theta$ in poloidal angle. At this point, we construct a closed volume by attaching two other ribbons, one along a constant θ contour, extending from $\zeta = 0$ to $\zeta = 2\pi$, and the other on a constant ζ contour, extending only across the “gap,” $\Delta\theta$, as shown in Fig. 2. It is clear that the flux entering this volume through the constant θ contour is simply $d\Psi_P$, the incremental poloidal flux contained between two neighboring flux surfaces. On the other hand, the flux through the constant ζ segment, which does not encircle the magnetic axis, is some fraction of $d\Psi_T$. We denote this leaving flux by $\delta\Psi_T$ and conclude, from $\nabla \cdot \mathbf{B} = 0$, that

$$\delta\Psi_T = d\Psi_P,$$

since no flux can penetrate the original ribbon, oriented along \mathbf{B} .

We next repeat this procedure, continuing to follow the same field line as it winds around the torus, and accumulating the flux increments $d\Psi_P$ and $\delta\Psi_T$. Note that the increments $\Delta\theta$ on successive passes will differ, although each $\delta\Psi_T = d\Psi_P$ is the same. After many circuits the field line will—with any desired accuracy—have returned to its starting point: it will have completed an integral number (m) of toroidal circuits and an integral number (n) of poloidal circuits. At that point the sum of the $\delta\Psi_T$ ’s must be $m \cdot d\Psi_T$ so we have, by the usual Gauss’ argument,

$$nd\Psi_T = md\Psi_P.$$

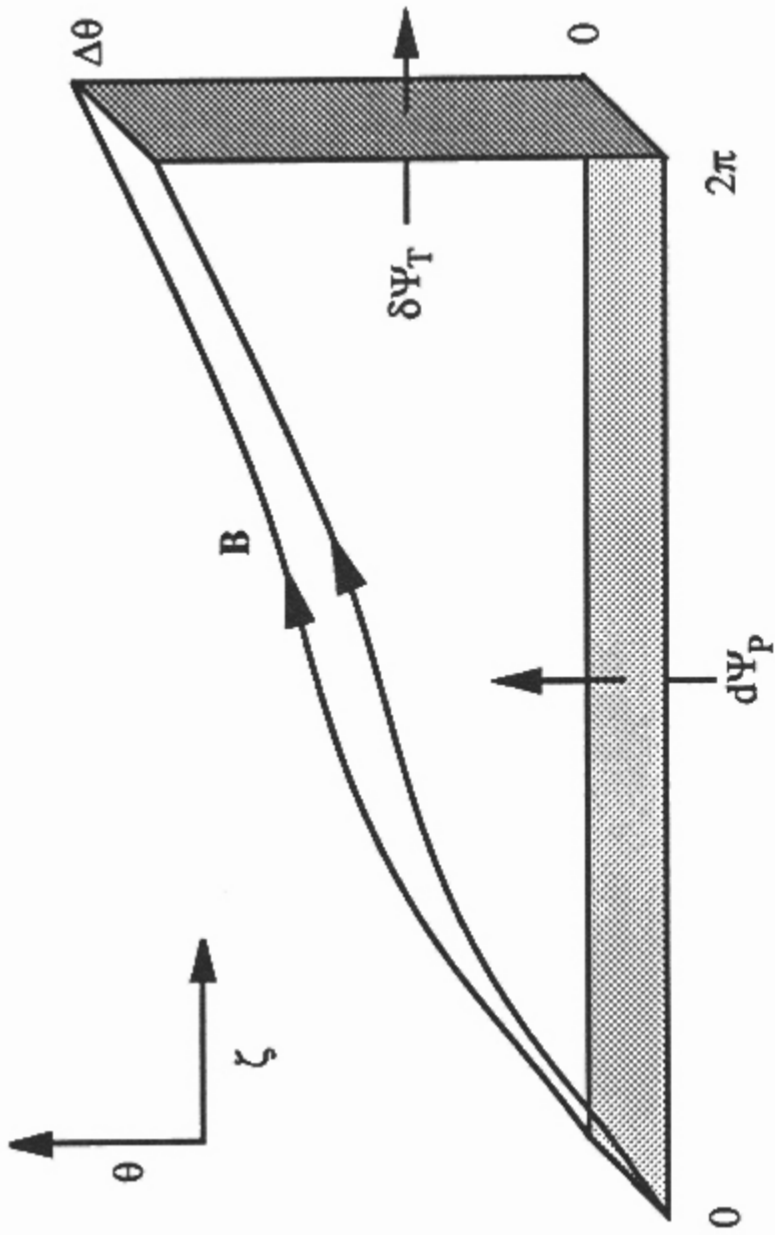


Figure 2. Calculation of the average field line pitch.

On the other hand, the ratio of circuits, n/m , evidently measures average field line pitch. Thus we may conclude

$$\text{average field line pitch} = \iota/2\pi.$$

Note in particular that when $\iota/2\pi$ is irrational, the average pitch is irrational, and the surface is densely covered by a single field line. For this reason the ergodic surfaces are also called *irrational flux surfaces*.

Most recent literature uses an inverse measure of pitch: the *safety factor*, $q \equiv 2\pi/\iota$, or

$$q \equiv \frac{d\Psi_T}{d\Psi_P}. \quad (6)$$

This book will use q almost exclusively. Its name belies an historical association with stability that remains cogent: the safety factor, and its radial derivative dq/dr , bear directly on fluid stability. The derivative measures *magnetic shear*: the change in field-line pitch from one surface to the next.

The connections between q and stability are several, but most stem from the peculiarity of surfaces on which q is rational. Our discussion of ι shows that such *rational flux surfaces* are simply the closed field-line surfaces: if $q = m/n$, then each line on the surface closes on itself after m toroidal and n poloidal circuits.² In the presence of magnetic shear, it is clear that rational surfaces, like rational numbers, are exceptional: shear is sufficient to enforce the prevalence of irrational surfaces.

² Actually, since we only showed that the average pitch is rational, it can only be proven that such surfaces must have at least two closed field lines. This minimal case is atypical. Our description applies to the integrable case.

This observation explains the sense of (2). Any nonpathological function that is a flux label on irrational surfaces must, in a sheared field, be a flux surface label everywhere.

On the other hand, it is also clear that rationality in the strict mathematical sense cannot be taken too seriously; sufficiently high-order rationals (rationals with sufficiently large denominators) are physically indistinguishable from irrationals. The sense of the word “large” in this context is a topic that will be considered in later chapters. Indeed, the subject of rational surfaces is a major theme of confinement and this book. For the present we simply anticipate that it is the low-order rationals that display exceptional properties.

3.2 Magnetic Flux Coordinates

Surface Potentials

The functions $\theta(\mathbf{x})$ and $\zeta(\mathbf{x})$ usefully describe phenomena on the surface of a torus, although neither is single-valued. More generally, a multivalued function $G(r, \theta, \zeta)$ is useful if it satisfies two requirements: (i) G should be single-valued on any path that encircles neither the toroidal axis nor the magnetic axis; (ii) the vector $\nabla G \times \nabla r$ should be single-valued on all paths. We call any (reasonably smooth) function satisfying both requirements a surface potential. The name reflects that fact that it is the gradient of G that ultimately matters.

Any linear combination (with flux-label coefficients) of θ and ζ is a surface potential. Indeed, the most general surface potential has the form

$$G(r, \theta, \zeta) = a(r)\theta + b(r)\zeta + G_0(r, \theta, \zeta), \quad (7)$$

where G_0 is an arbitrary periodic function of both angles. We can verify this form by Taylor expansion for small θ and ζ ; requirement (ii) forces all but the linear terms to vanish.

The main importance of surface potentials is in the descriptions they afford of the magnetic field. Such descriptions depend upon the following

Theorem: If F is a flux label, and $\mathbf{U}(\mathbf{x})$ is any vector field satisfying $\nabla F \cdot \nabla \times \mathbf{U} = 0$, then there exists a surface potential G such that $\nabla F \times \mathbf{U} = \nabla F \times \nabla G$.

The proof is constructive. For a given \mathbf{x} , we choose a fixed point \mathbf{z} on the surface F that contains \mathbf{x} and let

$$G(\mathbf{x}) = \int_{\mathbf{z}(F)}^{\mathbf{x}} \mathbf{U} \cdot d\mathbf{x}$$

where the integration path lies entirely on the surface. It is clear that ∇G differs from \mathbf{U} only by terms proportional to ∇F , coming from the lower endpoint. Hence $\nabla F \times (\mathbf{U} - \nabla G) = 0$, and furthermore $\nabla F \times \nabla G = \nabla F \times \mathbf{U}$ is single-valued. What remains to be shown is property (i) in the definition of a surface potential: we need to check the variation of G along paths encircling neither axis. Hence consider, for any such path C ,

$$\oint d\mathbf{x} \cdot \mathbf{U} = \int \nabla \times \mathbf{U} \cdot \mathbf{n} dS = \int \nabla \times \mathbf{U} \cdot \frac{\nabla F}{|\nabla F|} dS.$$

The last quantity vanishes by assumption, completing the proof. Note that if C were allowed to encircle the magnetic or toroidal axis, the integration surface would not be a flux surface.

General Form of Confining Field

Since \mathbf{B} is everywhere normal to ∇r it must be expressible as

$$\mathbf{B} = \nabla F \times \mathbf{U}$$

for some flux label $F(r)$ and vector field \mathbf{U} . Then $\nabla \cdot \mathbf{B} = 0$ implies that $\nabla F \cdot \nabla \times \mathbf{U} = 0$, so the theorem is applicable and we can write

$$\mathbf{B} = \nabla F \times \nabla G \quad (8)$$

where G is a surface potential.

Equation (8) is an important characterization of toroidal magnetic fields. Some readers may have seen the similar expression,

$$\mathbf{B} = \nabla \alpha \times \nabla \beta, \quad (9)$$

which holds, with suitable functions α and β , for any magnetic field. We emphasize that (8) is both stronger and less generally applicable than (9). It is stronger because we are told that the function F is constant on a sequence of nested tori, and that G is a surface potential. It is less general because it requires the existence of flux surfaces; for chaotic fields neither flux labels nor surface potentials have meaning. In any case the resemblance between (8) and (9) is superficial.

We next substitute the general form of G , given by (7), into (8). As long as F is unspecified, there is no loss of generality in choosing $b = -1$; then we have

$$\mathbf{B} = \nabla F \times \nabla(a\theta - \zeta) + \nabla F \times \nabla G_0,$$

or, since a and F are both flux labels,

$$\mathbf{B} = \nabla \zeta \times \nabla F + a \nabla F \times \nabla \theta + \nabla F \times \nabla G_0. \quad (10)$$

Equation (10) represents any magnetic field possessing toroidal flux surfaces. Furthermore it pertains for a completely general set of toroidal coordinates (r, θ, ζ) . More useful expressions for \mathbf{B} are obtained by appropriately restricting the coordinates. We consider next the most important class of special coordinates.

Flux Coordinates

We have found that the surface potential G in (8) can always be expressed as

$$G = a(r)\theta - \zeta + G_0(r, \theta, \zeta) \quad (11)$$

where G_0 is periodic. Recall, however, that for any acceptable poloidal angle θ , the alternative angle,

$$\theta' \equiv \theta + p(r, \theta, \zeta),$$

where p is periodic, is equally acceptable. It follows that the poloidal angle can always be chosen to eliminate G_0 from (11), with the result

$$\mathbf{B} = \nabla\zeta \times \nabla F + a\nabla F \times \nabla\theta. \quad (12)$$

We will show presently that (12) gives unique expressions for the two functions $a(r)$ and $F(r)$ in terms of magnetic fluxes, so that the only remaining freedom concerns the toroidal angle, ζ . This freedom is reserved for later use.

We call any representation having the form of (12) a *flux representation* of the magnetic field. The coordinates that permit this representation, while not unique, are no longer general toroidal coordinates. We will call them *flux coordinates*. When it is necessary to distinguish flux coordinates from other coordinate choices, we will use a subscript: (r_f, θ_f, ζ_f) .

Let us compute the poloidal flux from (12). The f -subscripts are suppressed. From (4) we have

$$2\pi\Psi_P = \int_{V(r)} d^3x \mathbf{B} \cdot \nabla\theta = \int_{V(r)} d^3x \nabla\zeta \times \nabla F \cdot \nabla\theta.$$

But (2.21) implies that $d^3x = \sqrt{g} dr d\theta d\zeta$, where \sqrt{g} (that is, $\sqrt{g_f}$) is the inverse of the flux coordinate Jacobian. Hence, according to (2.1), $d^3x \nabla\zeta \times \nabla F \cdot \nabla\theta = (dF/dr) dr d\theta d\zeta$ and we have

$$2\pi\Psi_P = \int_{V(r)} \frac{dF}{dr} dr d\theta d\zeta = \int_0^r \frac{dF}{dr} dr \oint d\theta \oint d\zeta = (2\pi)^2 F.$$

That is, $F = \Psi_P/2\pi$. This measure of the poloidal flux occurs frequently enough to deserve its own notation; we introduce

$$\chi = \frac{\Psi_P}{2\pi}, \quad (13)$$

to write $F = \chi$.

A similar calculation of the toroidal flux, using (12) and (5), shows that

$$2\pi\Psi_T = \int_{V(r)} d^3x \mathbf{B} \cdot \nabla \zeta = \int_{V(r)} dr d\theta d\zeta a(r) \frac{d\chi}{dr} = \int_{V(r)} d\chi d\theta d\zeta a(r).$$

It follows that $(d/d\chi)2\pi\Psi_T = (2\pi)^2 a(r)$, or $a(r) = d\Psi_T/d\Psi_P$; $a(r)$ is the safety factor, q . The flux representation can therefore be written as

$$\mathbf{B} = \nabla\chi \times \nabla(q\theta - \zeta). \quad \blacksquare \quad (14)$$

A closely related form,

$$\mathbf{B} = \frac{1}{2\pi} (\nabla\zeta \times \nabla\Psi_P + \nabla\Psi_T \times \nabla\theta) \quad (15)$$

justifies the name: we have expressed the magnetic field in terms of its fluxes.

Equation (14) shows that the quantity $q\theta - \zeta$, like χ , is constant along B. This quantity is conventionally called the *field line label*, a term that we will also use. However, this name can be misleading: the field line label is obviously not constant on irrational surfaces, which are densely covered by a single line. The point is that $q\theta - \zeta$ is single-valued only on a *cut* toroidal surface, where the angles vary between 0 and 2π ; it is not constant on any field line that crosses a cut.

Note also that $q\theta - \zeta$ would faithfully label magnetic field lines if the domain of θ and ζ were infinite. This occurs in “slab” geometry, as well as on the expanded angular domain, called the covering space, which is sometimes useful in stability theory. In either case the concept of ergodicity, as well as the distinction between rational and irrational surfaces, is lost.

The two terms of (15) correspond to a useful decomposition,

$$\mathbf{B} = \mathbf{B}_P + \mathbf{B}_T,$$

where the poloidal field is

$$\mathbf{B}_P = \frac{1}{2\pi} \nabla\zeta \times \nabla\Psi_P = \nabla\zeta \times \nabla\chi \quad (16)$$

and the toroidal field is

$$\mathbf{B}_T = \frac{1}{2\pi} \nabla\Psi_T \times \nabla\theta = q\nabla\chi \times \nabla\theta. \quad (17)$$

These vectors are not be confused with such field components as B_θ or B_ζ ; in particular, the latter do not have the dimensions of B .

The essential advantage of flux coordinates concerns field line pitch. We have noted that pitch generally varies over the flux surface, its average value

being measured by rotational transform or q . When pitch is measured in flux coordinates, however, it is constant on the surface, so that q measures as well the local pitch. An equivalent statement of this property may be helpful. Suppose the torus is appropriately slit and then unfolded into a rectangular sheet, stretched in such a way that the angle coordinates have uniform increments on a Cartesian grid. For arbitrary angle coordinates, the field lines will be curves on this grid, as in Fig. 3a. However, if flux coordinates are used, each field line will be straight, as in Fig. 3b. Indeed, flux coordinates are sometimes called “straight field-line coordinates.”

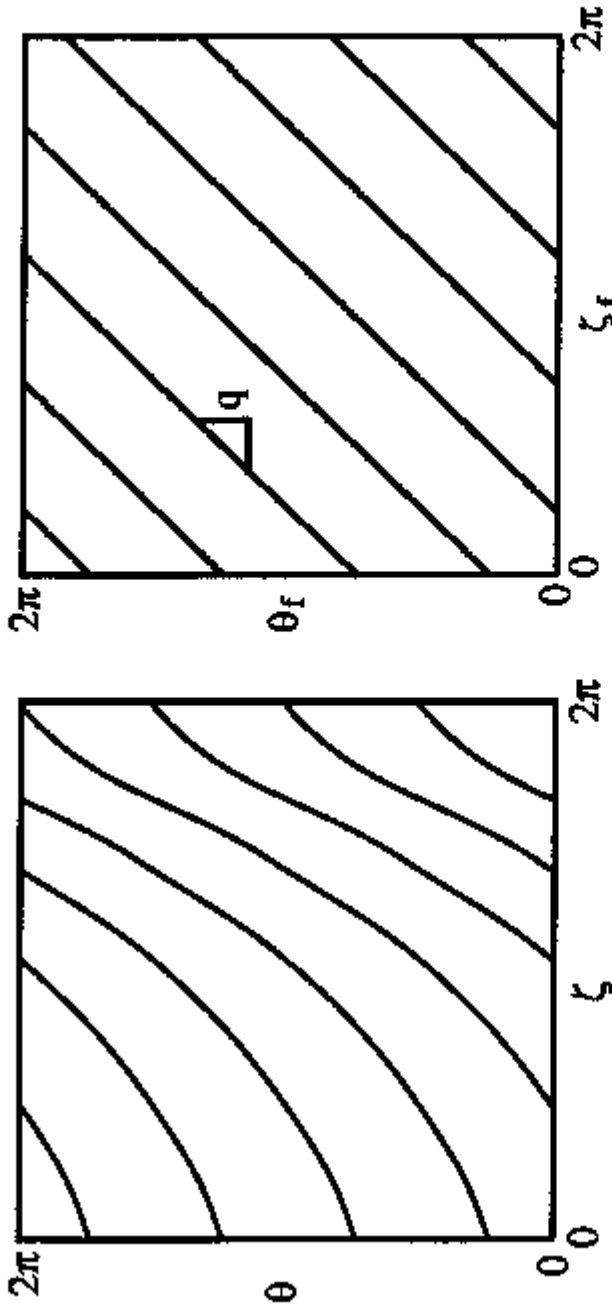


Figure 3. Field lines on a flux surface in (a) arbitrary toroidal coordinates, (b) flux coordinates.

The straight-line property, manifested in the field line label $q(\mathbf{r})\theta - \zeta$, is easily verified. Local pitch is given by the ratio $d\theta/d\zeta$, where the increments are measured along a field line: $d\theta/\mathbf{B} \cdot \nabla\theta = d\zeta/\mathbf{B} \cdot \nabla\zeta$, or

$$\frac{d\theta}{d\zeta} = \frac{\mathbf{B} \cdot \nabla\theta}{\mathbf{B} \cdot \nabla\zeta}. \quad (18)$$

For arbitrary angle coordinates, this ratio varies over the surface. However, for flux coordinates (14) implies

$$\mathbf{B} \cdot \nabla\zeta = \nabla\zeta \cdot \nabla\chi \times \nabla(q\theta) = q \nabla\zeta \cdot \nabla\chi \times \nabla\theta, \quad (19)$$

and

$$\mathbf{B} \cdot \nabla\theta = \nabla\theta \cdot \nabla\zeta \times \nabla\chi, \quad (20)$$

$$\text{so } \frac{\mathbf{B} \cdot \nabla\theta}{\mathbf{B} \cdot \nabla\zeta} = \frac{1}{q(\mathbf{r})} \quad (\text{flux coordinates}), \quad (21)$$

which is a flux label and therefore constant on the flux surface.

To avoid possible confusion we emphasize that the safety factor (at least as the term is used in this book) is always a flux label, regardless of the choice of coordinates. But (21) holds, making the *local* pitch $\mathbf{B} \cdot \nabla\theta / \mathbf{B} \cdot \nabla\zeta$ a flux label, only in the flux-coordinate case.

Components of \mathbf{B}

The relations (19) and (20) provide expressions for the contravariant field components that are often useful. We will indicate radial derivatives of any flux label with a prime:

$$\chi' = \frac{d\chi}{dr} .$$

Then we see from (2.20) that

$$\nabla\theta \cdot \nabla\zeta \times \nabla\chi = \frac{\chi'}{\sqrt{g}} .$$

We conclude, after comparing (12) and (2.13), that the confining field has contravariant components

$$B^r = 0, \quad B^\theta = \frac{\chi'}{\sqrt{g}}, \quad B^\zeta = \frac{q\chi'}{\sqrt{g}} . \quad (22)$$

Here (r, θ, ζ) are arbitrary flux coordinates; note that all the angular dependence enters through the Jacobian.

The covariant components, from (2.10), are more complicated. Note in particular that the covariant radial component is not zero:

$$B_r \equiv \sqrt{g} \nabla\theta \times \nabla\zeta \cdot B \neq 0 . \quad (23)$$

The point is that flux coordinates are not orthogonal, so that $\nabla\theta \times \nabla\zeta$ is not generally parallel to ∇r .

3.3 Applications of Flux Coordinates

Flute Perturbations

We have noted that the differential equation

$$\mathbf{B} \cdot \nabla h = 0 , \quad (24)$$

commonly requires that h be a flux label, depending only on the radial variable r . However a more interesting solution is possible in general. As suggested by (14), h might also depend upon the field line label:

$$h = h(r, q\theta - \zeta) . \quad (25)$$

If we think of h as representing height above the flux surface, then the variation allowed by (25) corresponds to ridges aligned along the field. In the simple case of sinusoidal h , the effect on a straight cylindrical surface would resemble a fluted column. Hence one says that (24) characterizes *flute perturbations*. Note that the columnar flutes one has in mind are twisted, following the pitch of the magnetic field.

A crucial observation here is that magnetically aligned flutes are more easily imposed on a straight column than on a toroidal surface. Toroidal topology requires that h be periodic in both angle variables. But a function of the form (25) cannot be periodic in both θ and ζ , i.e., cannot satisfy

$$h|_{\theta,\zeta} = h|_{\theta+2\pi,\zeta+2\pi} \quad (26)$$

unless q is rational. This important conclusion is directly clear from (25) and (26), but the physical statement is even more transparent. Indeed, if h is to have different values on different field lines, then there must be distinguishable field lines on the surface. Since irrational surfaces are densely covered by a single line, it follows that flute perturbations can occur only on rational flux surfaces.

In a sheared magnetic field, the rational surfaces are isolated, so that no physically smooth flute perturbation can exist. Exact “fluting” occurs only in shear-free systems, when q has a constant rational value. Yet sheared systems can display flute-like disturbances, satisfying

$$\mathbf{B} \cdot \nabla h \simeq 0 .$$

We shall find that flute-like structures play a major role in confined plasma stability.

It is instructive to express (25) in flux coordinates. Note first that (26) implies that h can be expanded in a Fourier series

$$h(r, \theta, \zeta) = \sum_{m,n} H_{mn}(r) \exp(im\theta - in\zeta) . \quad (27)$$

where, of course,

$$H_{mn}(r) = (2\pi)^{-2} \oint d\theta \oint d\zeta e^{-i(m\theta - n\zeta)} h(r, \theta, \zeta) . \quad (28)$$

The integers m and n are sometimes called, respectively, the *poloidal* and *toroidal mode numbers*. Their ratio m/n is the helicity of the corresponding term in (28); in this sense, helicity simply measures the twist or pitch of the flutes.

Next we use (2.26), (2.22), and (22) to write

$$\mathbf{B} \cdot \nabla h = B^{\theta} \left(\frac{\partial h}{\partial \theta} + q \frac{\partial h}{\partial \zeta} \right) . \quad (29)$$

Substitution from (27) then yields

$$\mathbf{B} \cdot \nabla h \approx B^\theta \sum_{m,n} i(m-nq) H_{mn}(r) e^{i(m\theta-n\zeta)},$$

which can vanish only if each Fourier coefficient vanishes:

$$(m - nq) H_{mn}(r) = 0. \quad (30)$$

That is,

$$H_{mn}(r) = 0, \quad \text{unless } m = nq(r). \quad (31)$$

In other words the only allowed Fourier components are the resonant components, whose helicity matches the field-line pitch on the rational surface. Again, the presence of shear will force any reasonably smooth $H_{mn}(r)$ to vanish on all surfaces: only H_{00} survives, as assumed in (2).

Equations (27)–(31) reveal nothing new about flute perturbations; in particular, (31) could be anticipated directly from (25) and (27). What is significant here is that the simple form of (30) and (31) depends strictly upon the use of flux coordinates. Any other system would mix many components H_{mn} , because the coefficient corresponding to q would depend upon the angles.

Magnetic Differential Equations

The inhomogeneous form of (24),

$$\mathbf{B} \cdot \nabla f = S(\mathbf{x}), \quad (32)$$

where S is a specified source, occurs so frequently in plasma confinement theory that it has been given a name: the magnetic differential equation (Newcomb, 1959). Specific examples, pertaining to equilibrium, stability, transport and nonlinear evolution, are studied later in this book. Here we briefly consider the Fourier representation of (32).

Using the conventions of (27) and (28), we quickly find

$$f_{mn} = -\frac{i(S/B^\theta)_{mn}}{(m - nq)}.$$

Again we note that the Fourier components are uncoupled, and therefore trivially computed, only in flux coordinates. The solvability condition (recall §2.4) for the magnetic differential equation is also evident. For finite $f_{mn}(r)$, we must require that

$$\left(\frac{S}{B^\theta}\right)_{mn} = 0 \quad (33)$$

on the rational surface where $q = m/n$.

In straight systems, it is often convenient to use the distance measured along a field line, s , as a coordinate. Then the magnetic differential equation is simply

$$B \frac{\partial f}{\partial s} = S.$$

If boundary conditions are specified at the two ends of the line, $s = \pm L$, then the solvability condition for the magnetic differential equation is obvious:

$$f(s = L) - f(s = -L) = \int_{-L}^L ds \frac{S}{B}.$$

The variable s is not often useful in toroidal geometry because of its singular dependence on position; thus, on an irrational surface, two neighboring points can have widely different values of s . If one nonetheless analyzes the magnetic differential on a torus using s , one obtains, unsurprisingly, the solvability condition

$$\oint \frac{ds}{B} S = 0 \quad (34)$$

on each rational surface. Here the loop integral is performed over the closed path defined by any field line on the surface; because the surface is rational, every line is closed. This integration path generally includes many toroidal circuits.

The explicit equivalence of (33) and (34) has been demonstrated by Newcomb (Newcomb, 1959). We will refer to either as the *Newcomb condition*. The essential conclusion—one that will be used often in this book—is that a *magnetic differential equation has solutions only if its source term satisfies the Newcomb condition on every rational surface*.

Flux Surface Average

The flux surface average of some function $A(\mathbf{x})$ is its normalized volume average, restricted to a surface \mathbf{r} :

$$\langle A \rangle \equiv \frac{\int d^3x' A(\mathbf{x}') \delta(\mathbf{r}' - \mathbf{r})}{\int d^3x' \delta(\mathbf{r}' - \mathbf{r})}.$$

The normalization ensures that

$$\langle F \rangle \equiv F,$$

for any flux label $F(\mathbf{r})$.

More useful expressions for $\langle A \rangle$ can be obtained by noticing that the volume, V , enclosed by a flux surface r is given by

$$V(r) \equiv \int_V d^3x = \int_V \sqrt{g} dr d\theta d\zeta ,$$

where we use (2.20). This implies

$$V' \equiv \frac{dV}{dr} = \oint \sqrt{g} d\theta d\zeta . \quad (35)$$

Then we find

$$\langle A \rangle = \frac{1}{V'} \oint \sqrt{g} d\theta d\zeta A(\mathbf{x}) . \quad (36)$$

In flux coordinates, (36) remains useful, but (22) allows writing

$$\langle A \rangle = \frac{d\chi}{dV} \oint \frac{d\theta_f}{\mathbf{B} \cdot \nabla \theta_f} \frac{d\zeta_f}{A(r, \theta_f, \zeta_f)} A(r, \theta_f, \zeta_f) . \quad (37)$$

This version provides an alternative statement of the Newcomb condition, (33):

$$\langle S \exp(i(n\zeta - m\theta)) \rangle = 0 ,$$

on the rational surface where $q = m/n$.

A third expression for flux surface average is obtained from (36) by using the volume V itself as the radial coordinate,

$$\langle A \rangle = \frac{1}{V} \frac{d}{dr} \int_V^r dr \oint \sqrt{g} d\theta d\zeta A(\mathbf{x}) = \frac{d}{dV} \int_V d^3x A(\mathbf{x}) . \quad (38)$$

We next use (36) and (38) to derive two crucial identities involving the flux surface average. First consider $\langle \nabla \cdot \mathbf{A} \rangle$, for any vector \mathbf{A} . Applying Gauss' theorem to the form (38) yields

$$\langle \nabla \cdot \mathbf{A} \rangle = \frac{d}{dV} \int_V dS \mathbf{A} \cdot \frac{\nabla V}{|\nabla V|} ,$$

where the integration surface is the flux surface labelled by r . Since the surface element dS satisfies $d^3x = dS dr / |\nabla r|$, the integrand above is related to that in (36) and we have

$$\langle \nabla \cdot \mathbf{A} \rangle = \frac{d}{dV} \langle \mathbf{A} \cdot \nabla V \rangle . \quad (39)$$

It follows that the flux surface average annihilates the operator $\mathbf{B} \cdot \nabla$; that is,

$$\langle \mathbf{B} \cdot \nabla f \rangle = 0 \quad (40)$$

for any single-valued function $f(\mathbf{x})$. The point is that $\mathbf{B} \cdot \nabla f = \nabla \cdot (\mathbf{B}f)$, and \mathbf{B} has no component normal to a flux surface [recall (1)].

The second identity is an easy corollary of (39):

$$\langle \nabla r \cdot \nabla \times \mathbf{A} \rangle = 0 \quad (41)$$

for any vector \mathbf{A} ; it follows because $\nabla r \cdot \nabla \times \mathbf{A} = \nabla \cdot (\mathbf{A} \times \nabla r)$.

3.4 Special Cases of Flux Coordinates

We have noted that flux coordinates—coordinates that allow \mathbf{B} to be expressed in the form of (14)—are not unique. Indeed, it is clear that any coordinate transformation, $(r, \theta, \zeta) \rightarrow (r', \theta', \zeta')$ that preserves the field line label,

$$q\theta' - \zeta' = q\theta - \zeta,$$

and where r' is a flux label, yields an equally acceptable flux coordinate set. Thus any two sets of flux coordinate angles are related by some function K , periodic in both angles, according to

$$\begin{aligned} \theta' &= \theta + \frac{1}{q} K(r, \theta, \zeta), \\ \zeta' &= \zeta + K(r, \theta, \zeta). \end{aligned} \quad (42)$$

One can use this freedom, appropriately choosing the function K , to obtain angles with convenient properties. *Hamada coordinates* and *symmetry coordinates* are the two most important examples of such specialized flux coordinates.

Hamada Coordinates

Hamada coordinates (Hamada, 1962) are chosen to make the Jacobian, $\sqrt{g_H}$, a flux label. In this case the value of $\sqrt{g_H}$ is determined by

$$\mathcal{V} = \int \sqrt{g_H} d\theta_H d\zeta_H = (2\pi)^2 \sqrt{g_H}.$$

We can then conclude from (2.20) that

$$\nabla \mathcal{V} \cdot \nabla \theta_H \times \nabla \zeta_H = (2\pi)^2. \quad (43)$$

Hamada coordinates provide important simplification in several contexts. In particular, (22) shows that each contravariant field component, and not only the ratio $B^{\zeta}/B^{\theta} = q$, becomes a flux label. Similarly the flux surface average is simplified: (36) becomes

$$\langle A \rangle = \oint \frac{d\theta_H d\zeta_H}{(2\pi)^2} A(r, \theta_H, \zeta_H). \quad (44)$$

the basic distinguishing feature of the Hamada system.

To examine whether flux coordinates satisfying (43) exist, we substitute from (42), with $(\theta', \zeta') = (\theta_H, \zeta_H)$. The result is to turn (43) into a requirement on the periodic function K . Simple manipulation reduces this requirement to

$$\mathbf{B} \cdot \nabla K = qX' [(2\pi)^2 - \nabla V \cdot \nabla \theta \times \nabla \zeta]. \quad (45)$$

Here, since θ and ζ are arbitrary but given flux-coordinate angles, the right-hand side can be presumed known.

We see that (45) is a magnetic differential equation. Since its solution prescribes Hamada coordinates, through (42), we may conclude the latter exist whenever the Newcomb condition,

$$\oint \frac{ds}{B} [(2\pi)^2 - \nabla V \cdot \nabla \theta \times \nabla \zeta] = 0 \quad (46)$$

is satisfied on each rational surface. We defer the full proof of (46) (Greene and Johnson, 1962), since it depends upon the nature of equilibrium plasma currents, a topic we have not yet considered. However, some discussion of the condition is appropriate here.

We can express (46) as $I_0 \approx I_1$, where

$$I_0 \equiv \oint \frac{ds}{B}$$

and

$$I_1 \equiv \frac{1}{(2\pi)^2} \oint \nabla V \cdot \nabla \theta \times \nabla \zeta \frac{ds}{B} .$$

To compute I_1 we note that the change in θ along a field line satisfies $ds/B = d\theta/B^\theta$ and therefore that the volume element can be expressed as

$$d^3x = \chi' dr d\alpha \frac{ds}{B} , \quad (47)$$

where $\alpha \equiv \zeta - q\theta = \zeta - m\theta/n$ is the field line label. It follows that

$$I_1 = \frac{1}{(2\pi)^2} \frac{1}{\chi'} \oint \nabla V \cdot \nabla \theta \times \nabla \zeta \delta(r - r_{mn}) \delta(\alpha - \alpha_0) d^3x .$$

Here r_{mn} labels the rational surface on which $q = m/n$, while α_0 chooses a field line on that surface. From

$$\nabla V \cdot \nabla \theta \times \nabla \zeta d^3x = V' dr d\theta d\zeta \quad (48)$$

we find

$$I_1 = \frac{1}{(2\pi)^2} \frac{V'}{\chi'} \oint d\theta d\zeta \delta(\alpha - \alpha_0) = \frac{1}{(2\pi)^2} \frac{V'}{\chi'} \oint d\theta = \frac{1}{2\pi} n \frac{dV}{d\chi} ,$$

since the line encircles the magnetic axis n times. It is significant that I_1 turns out to be a flux label. It evidently measures the specific volume—the volume per unit flux—of a flux surface.

The quantity I_0 will be seen to have wide importance, beyond the context of Hamada coordinates. It measures the specific volume of a small tube (“flux tube”) enclosing the chosen field line. The point is that the

flux through such a tube is BdA , where dA is its cross-sectional area, while the volume of a small tube segment is $dAds$. It is easy to imagine that the flux tubes enclosing different closed lines might have different specific volumes: I_0 is not obviously a flux label. This issue depends upon properties of the plasma current that are considered later. Here we demonstrate that, if I_0 is the same on each closed line, then (46) quickly follows.

First note that the flux surface average of the right-hand side of (45) clearly vanishes; this follows from, for example, (48). But (47) shows that, on a rational surface, the flux surface average can be expressed as

$$\langle A \rangle = \frac{\oint d\alpha \frac{ds}{B} A}{\oint d\alpha \frac{ds}{B}}.$$

Hence the α -average of (46),

$$\oint d\alpha I_0 = \oint d\alpha I_1 = I_1 \oint d\alpha$$

is satisfied. In the second equality we have noted that I_1 is independent of α ; if I_0 is similarly the same on each closed line, then $\oint d\alpha I_0 = I_0 \oint d\alpha$ and (46) is verified.

We conclude that the existence of Hamada coordinates hinges on the constancy of I_0 , the flux-tube specific volume, on each rational flux surface.

The relation (44) suggests an especially convenient radial variable for Hamada coordinates: $r \rightarrow v_H \equiv \mathcal{V}(r)/(2\pi)^2$. The point is that the system (v_H, θ_H, ζ_H) has unit Jacobian, $\sqrt{g} = 1$, simplifying many manipulations. This circumstance often outweighs the minor disadvantage of a radial coordinate having the dimensions of volume.

Symmetry Coordinates

Symmetry coordinates, (r_0, θ_0, ζ_0) are flux coordinates in which the toroidal angle is chosen very simply: $\zeta_0 = -\varphi$, where φ is the ordinary cylindrical angle of (2.2), measured about the toroidal axis. We will see that this choice is not consistent with the Hamada strategy: it yields a Jacobian that varies on flux surfaces. The name is chosen because symmetry coordinates become especially useful when the magnetic field is axisymmetric,

$$\frac{\partial \mathbf{B}}{\partial \zeta} = 0. \quad (49)$$

However their application is not restricted to the axisymmetric case.

Note that symmetry conditions having the form (49) are essentially coordinate-independent: the statement is simply that only two coordinates

are needed to describe a symmetric field. On the other hand, statements concerning $\nabla\zeta$, such as

$$\nabla\zeta \cdot \nabla B = 0, \quad (50)$$

are strongly coordinate dependent; (50) will not hold in an axisymmetric system for a general toroidal angle ζ . This clarifies the choice of ζ_0 , since axisymmetry can be seen to imply that

$$\nabla\zeta_0 \cdot \nabla r_0 = 0 = \nabla\zeta_0 \cdot \nabla\theta_0. \quad (51)$$

In other words, in an axisymmetric field, symmetry coordinates become *partially orthogonal*. Although the remaining inner product, $\nabla r_0 \cdot \nabla\theta_0$, does not generally vanish, (51) is sufficiently advantageous to rule out other flux coordinate choices in the symmetric case.

In terms of the metric tensor (2.17), (51) implies $g^{r\zeta} = g^{\theta\zeta} = 0$, suppressing the 0 subscript. Consideration of the inverse matrix g_{ij} then quickly shows that

$$g_{r\zeta} = 0 = g_{\theta\zeta}, \quad (52)$$

an alternative statement of partial orthogonality. From the toroidal arc length $ds_\zeta = R d\zeta$, we infer

$$g_{\zeta\zeta} = R^2 \quad (53)$$

where R is the major radius. Since partial orthogonality implies $g^{\zeta\zeta} = 1/g_{\zeta\zeta}$, we have $g^{\zeta\zeta} = 1/R^2$, or

$$|\nabla\zeta| = \frac{1}{R}, \quad (54)$$

as also follows from $\zeta = -\varphi$.

To deduce other features of symmetry coordinates, we anticipate a simple consequence of Ampère's law (see §3.9): axisymmetry makes the covariant ζ -component of \mathbf{B} a flux label. A conventional notation is

$$B_\zeta = I(r). \quad (55)$$

Hence $B^\zeta = g^{\zeta\zeta} B_\zeta = I/R^2$. Then, since symmetry coordinates are flux coordinates, (22) provides a useful formula for the Jacobian:

$$\sqrt{g_0} = q\chi' \frac{R^2}{I}. \quad (56)$$

Notice that all factors on the right-hand side of (56) are flux labels except R^2 . Since R cannot be constant on a torus, symmetry coordinates never coincide with Hamada coordinates. More importantly the flux surface average of any symmetric quantity A can be expressed as

$$\langle A \rangle = \frac{\oint d\theta R^2 A}{\oint d\theta R^2}. \quad (57)$$

Hamada coordinates and symmetry coordinates are by far the most commonly used flux coordinates in the confinement literature. However, other flux coordinate choices can be advantageous in specific applications. It is also sometimes convenient to use nonflux coordinate sets, such as the Shafranov coordinates discussed in §3.12.

Part 2: Plasma Current

3.5 Scalar Pressure Equilibrium

Pressure Surfaces

The simplest and most important class of toroidal equilibria are characterized by a balance between the plasma pressure gradient, ∇P , and the electromagnetic force $\mathbf{J} \times \mathbf{B}$, where

$$\mathbf{J} = \frac{c}{4\pi} \nabla \times \mathbf{B}, \quad (58)$$

is the plasma current density. Thus

$$\mathbf{J} \times \mathbf{B} = c \nabla P. \quad (59)$$

In Chapter 5 we will obtain (59) as an asymptotic result, valid in the limit of small gyroradius. Furthermore it is in reasonable accord with measurements in most toroidal experiments. Nonetheless its approximate nature should be kept in mind.

An equilibrium without pressure, with \mathbf{J} parallel to \mathbf{B} , is called *force-free*. Force-free equilibria have considerable importance, for two reasons. First, it can be shown that an arbitrary equilibrium, subject to reasonable constraints, will relax under resistive turbulence to a force-free state. Such constrained relaxation is in fact observed in reversed-field pinch experiments (Taylor, 1986). Second, the field configurations in a number of common confinement devices, including tokamaks, resemble those of force-free equilibria: the parallel current often greatly exceeds the perpendicular current. We do not emphasize the strictly force-free case here because magnetic confinement requires J_{\perp} .

An obvious generalization of (59),

$$\mathbf{J} \times \mathbf{B} = c \nabla \cdot \mathbf{P}. \quad (60)$$

where \mathbf{P} is the plasma pressure tensor, is also of some importance. However, we shall see in Chapter 5 that for a closed, sufficiently *isolated*, system, the pressure tensor relaxes to scalar form, $\mathbf{P} = \mathbf{I}P$, where \mathbf{I} is the unit tensor, even when the collision frequency is very small. Thus (59) is restored.

Here the word “isolated” is intended to rule out strong external energy sources, associated with certain auxiliary heating schemes, that can drive appreciable pressure anisotropy. We will examine the anisotropic case in §3.8.

Equation (59) clearly implies that the plasma pressure is constant along \mathbf{B} ,

$$\mathbf{B} \cdot \nabla P = 0. \quad (61)$$

We have noted that under typical circumstances this requirement makes P a flux label. In other words, the flux surfaces become constant pressure surfaces, or *isobars*. Commonly, the pressure is monotonic, with its maximum on the magnetic axis.

The physical mechanism underlying (61) depends upon the collision frequency regime. When the collision frequency is very small, (61) reflects rapid particle streaming along field lines; at higher collisionality it results from relaxation by acoustic waves. The point in either case is that the confinement time is long compared to parallel equilibration times.

We have observed that confinement configurations may include narrow ergodic volumes—three-dimensional bands, enclosing rational surfaces and filled by a single chaotic field line. As shown in Chapter 9, enhanced diffusion in such chaotic regions will relax the pressure gradient more rapidly than in nonchaotic regions. For steady-state or slowly evolving chaos, the expectation is that $|\nabla P|$ will be locally small in any chaotic band. We see that (61) captures this physics in oversimplified form, predicting flat pressure gradients throughout the chaotic region. The point here is that the force balance relation (59) is too primitive to describe pressure relaxation in a chaotic field; it effectively assumes infinitely rapid communication along field lines.

A related oversimplification concerns very narrow chaotic layers. It must be noted that, since (59) is not valid on scale lengths narrower than a gyroradius, predictions of flattening or singularity on such scales are not physical. We shall see in Chapter 9 that the radial width of a chaotic region varies inversely with the order of its associated rational surface. Thus, while $P(r)$ may be locally flattened near low-order rational surfaces, it is indifferent to high-order rationals and typically a smooth function of radius.

Diamagnetism

Aside from (61), the main consequence of (59) is to specify the plasma current density perpendicular to \mathbf{B} . In this regard it is convenient to introduce some notation: subscripts “ \parallel ” and “ \perp ” will always refer to the direction of \mathbf{B} . Thus we have, for any vector \mathbf{V} ,

$$\mathbf{V} = \mathbf{V}_\parallel + \mathbf{V}_\perp,$$

where, in terms of the unit vector,

$$\mathbf{b} = \frac{\mathbf{B}}{B} \quad (62)$$

$$\mathbf{V}_\perp \equiv (\mathbf{I} - \mathbf{b}\mathbf{b}) \cdot \mathbf{V} = \mathbf{b} \times (\mathbf{V} \times \mathbf{b}).$$

Thus we express (59) as

$$\mathbf{J}_\perp = \frac{c}{B} \mathbf{b} \times \nabla P, \quad (63)$$

giving the *diamagnetic current* of a scalar pressure plasma. The origin of this current in charged-particle gyration is considered in Chapter 4. Its diamagnetic effect is easily seen by noting that the direction of \mathbf{J}_\perp is such as to diminish \mathbf{B} in regions of larger pressure.

Two salient properties of the diamagnetic current are the vanishing of its (contravariant) radial component,

$$\mathbf{J}_\perp \cdot \nabla r = \mathbf{J} \cdot \nabla r \equiv J^r = 0; \quad (64)$$

and its nonvanishing divergence,

$$\nabla \cdot \mathbf{J}_\perp \neq 0. \quad (65)$$

Equation (65) is related to quasineutrality, (2.54)—the requirement that the local plasma charge density (“space-charge”) be small. Equation (64) is a special case of ambipolarity—the balancing flows of oppositely charged particles across flux surfaces.

Ambipolarity

More generally, Ampère’s law (2.56) and (41) imply that the flux-surface averaged radial current must vanish,

$$\langle J^r \rangle = 0, \quad (66)$$

independently of (59). This result is usually referred to as the ambipolarity condition, since it requires the net fluxes of oppositely charged species across a surface to be the same. It can be seen that ambipolarity in this form is broken by the Maxwell term,

$$\nabla \times \mathbf{B} = \frac{4\pi}{c} \mathbf{J} + \frac{1}{c} \frac{\partial \mathbf{E}}{\partial t},$$

and that an exact ambipolarity condition would include the displacement current. We return to this point, which is outside equilibrium theory, in Chapter 9.

Here we emphasize that the local condition, (64), is much stronger than (66), and strictly applicable only to scalar pressure equilibria. Small corrections to the lowest-order pressure appearing in (60) can allow local currents normal to the surface, without contradicting (66). However the corresponding corrections to the equilibrium magnetic field are very small and invariably ignored.

Note that quasineutrality, as expressed by (2.54), and ambipolarity are independent concepts. For example, parallel current flow is nonambipolar but quasineutral; similarly, near the plasma boundary there can occur nonquasineutral regions with ambipolar flow.

Plasma Boundary

Plasma ions striking a material wall can have a variety of effects. Often the ions are absorbed, to be liberated by the subsequent impact of other ions; such “wall-recycling” can be a significant energy sink. Ion impact can also liberate impurity ions from the wall material. Because of their relatively large ionic charge, the impurities radiate potently as they are heated, sacrificing plasma energy in the wall vicinity. Probably the most harmful effect is the liberation of neutral particles. Being unaffected by the confining field, neutrals freely penetrate the plasma, becoming widely available for charge-exchange collisions with the ambient ion species. Since each charge exchange replaces a hot ion by a cold one, energy confinement is reduced—and not only near the wall.

For these reasons a successful confinement scheme must strictly limit the plasma pressure at the wall radius.

In the presence of $\mathbf{J} \times \mathbf{B}$ forces it is possible in principle for the plasma pressure to vanish on some outermost flux surface; that is after all the main purpose of the magnetic field: In practice however no confinement scheme prevents contact between the plasma and material walls. Successful confinement devices limit such contact, especially thermal contact, in two ways. First, flux-surface integrity and appropriate current density profiles can balance most of the pressure gradient in the interior region, so that the pressure in the wall vicinity is manageable small. Second, the residual, unavoidable plasma-wall interaction is controlled, by localizing it to selected contact surfaces—surfaces fashioned to withstand the plasma heat load with minimal damage and sputtering.

The simplest contact surface is a **limiter**: an inward protrusion from the chamber wall, typically in the form of a toroidal or poloidal ring, that “scapes-off” plasma from what then becomes the outermost occupied flux surface. Thus one speaks of the “limiter radius,” a , as distinct from the chamber wall radius, $b > a$. An effective limiter allows little plasma pressure in its “shadow,” the region $a < r < b$. Proper choice of limiter composition can significantly improve plasma purity and energy confinement.

A more elaborate scheme, called a divertor, is sketched in Fig. 4. Here the magnetic field has a separatrix, so that the geometry consists of two stacked tori. The larger torus confines plasma in the usual way, while the smaller one acts as a dump for particles crossing the separatrix: the diverted lines intersect a divertor plate, the contact surface for divertor geometry. The point is that the divertor contact surface is relatively isolated, compared to the limiter case, from the main plasma. In particular, the neutral influx is sharply reduced simply by enclosing the diverted torus in a separate chamber; neutrals, oblivious to the field, are unlikely to find their way to the main plasma. By pumping on the chamber and appropriately fashioning the plate, charged-particle contamination is also controlled.

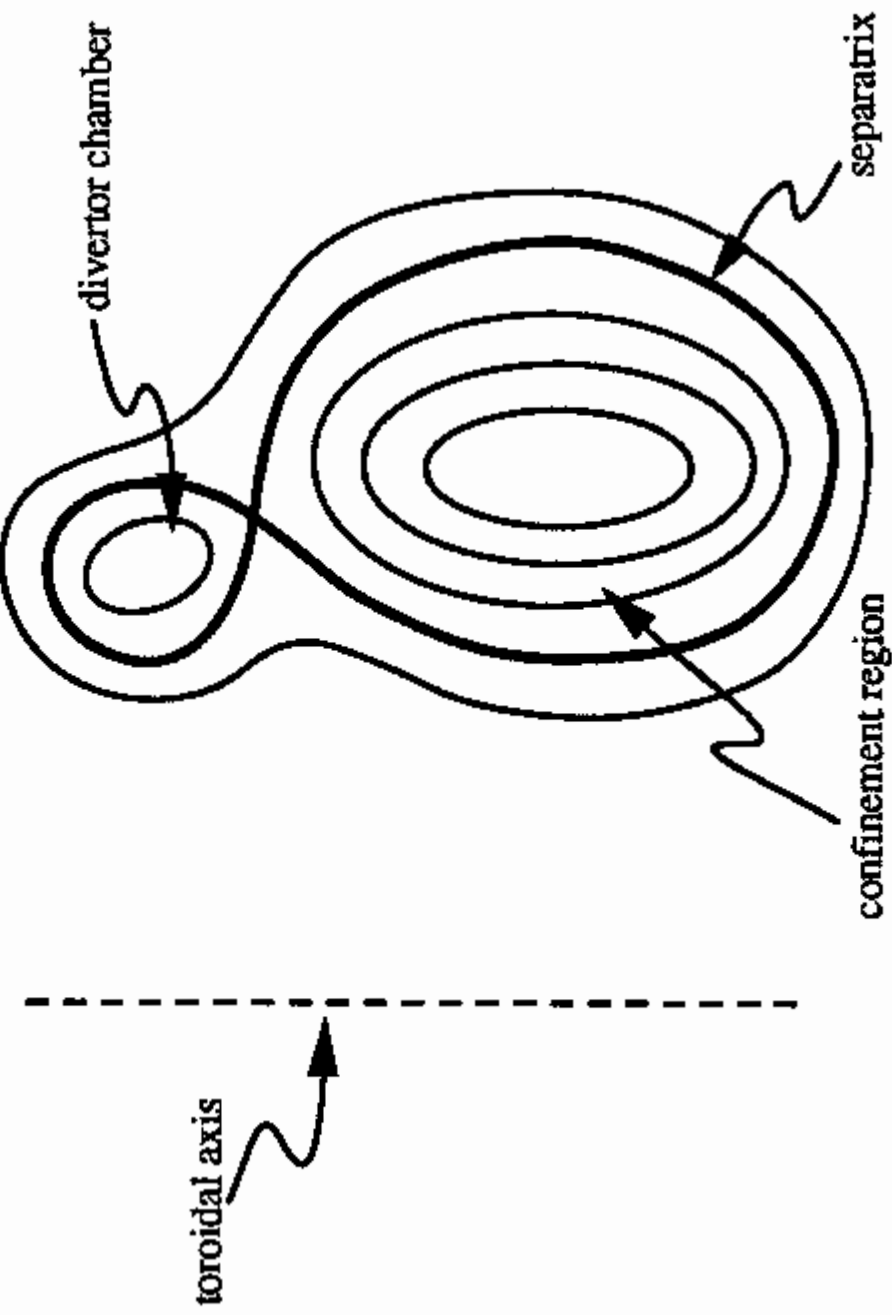


Figure 4. Divertor field line configuration, seen in poloidal cross section.

Notice that both schemes provide a bounding envelope, usually several centimeters in radial width, of sharply reduced plasma pressure: the region exterior to either the limiter radius or the separatrix radius. This envelope often displays quite complicated behavior, including strong and rapidly varying electromagnetic fields. It is presumably dominated by wall-recycling, impurities and related plasma-surface chemistry ("kitchen physics"), as well as space charge effects analogous to the Debye sheath. The overall physics of the envelope is poorly understood, although it appears to effect such globally dramatic phenomena as the tokamak "H-mode".

In classical MHD studies the envelope is treated as a simple vacuum. As an artifice to provide boundary conditions on MHD linear eigenmodes, this idealization seems reasonable, especially in the limiter case: certainly

plasma currents in the limiter shadow are negligible. However, the vacuum model is too idealized for understanding a wider class of plasma-wall issues, including the apparent effect of wall-vicinity electric fields and rotation rates on global plasma transport.

3.6 Explicit Force Balance

Parallel Current

It is convenient at this point to express the force balance relation (59) more explicitly. For generality we use Hamada coordinates, (v_H, θ_H, ζ_H) , suppressing the subscript as usual. Recall that this coordinate choice yields a unit Jacobian; thus, according to (22), both contravariant components of \mathbf{B} are flux labels. (The radial variable v_H is related to the flux-surface volume V by $v_H = V/(2\pi)^2$, as in §3.4.) Hence (15) can be expressed as

$$\mathbf{B} = B^\theta(v) \nabla \zeta \times \nabla v + B^\zeta(v) \nabla v \times \nabla \theta . \quad (67)$$

We next derive an analogous expression for the current density. The covariant radial component of (59) is

$$c P' = J^\theta B^\zeta - J^\zeta B^\theta = \chi'(q J^\theta - J^\zeta) , \quad (68)$$

where the primes denote v -derivatives. The other covariant components vanish. Similarly, (2.54) becomes

$$\frac{\partial J^\theta}{\partial \theta} + \frac{\partial J^\zeta}{\partial \zeta} = 0 . \quad (69)$$

We eliminate J^ζ from (69), using (68) and the fact that P' , q and χ' are flux labels. The result is $(\partial/\partial \theta + q \partial/\partial \zeta) J^\theta = 0$, or

$$\mathbf{B} \cdot \nabla J^\theta = 0 .$$

Hence J^θ is a flux label in Hamada coordinates. Then (68) requires J^ζ to be a flux label also, so we have

$$\mathbf{J} = J^\theta(v) \nabla \zeta \times \nabla v + J^\zeta(v) \nabla v \times \nabla \theta \quad (70)$$

the desired “flux representation” for \mathbf{J} .

As an application of (70) we derive two useful expressions for the parallel current density, $J_{||}$. First note from (67) that

$$\nabla \zeta \times \nabla v = \frac{(\mathbf{B} - B^\zeta \nabla v \times \nabla \theta)}{B^\theta} ,$$

so (70) can be expressed as

$$\mathbf{J} = J^\theta \mathbf{B} + \nabla v \times \nabla \theta (J^\zeta - \theta J^\theta),$$

or, in view of (68),

$$\mathbf{J} = J^\theta \mathbf{B} - \frac{cP'}{\chi'} \nabla v \times \nabla \theta.$$

Then, from (2.10),

$$\frac{\chi'}{B} J_\parallel = J^\theta - \frac{cP'}{B^2} B_\zeta \quad (71)$$

Analogous elimination of the $\nabla v \times \nabla \theta$ term from (70) yields

$$\frac{q\chi'}{B} J_\parallel = J^\zeta + \frac{cP'}{B^2} B_\theta. \quad (72)$$

The form of (71) and (72) suggests that part of the parallel current density is driven by the radial pressure gradient. We point out next that this suggestion is both accurate and consequential.

Return Current

We noted, in (65), that the diamagnetic current is not solenoidal. Explicitly,

$$\nabla \cdot \mathbf{J}_\perp = \frac{2c}{B^2} \nabla P \cdot \mathbf{b} \times \nabla B = \frac{cP'}{B^2} \mathbf{b} \cdot (\nabla B \times \nabla r). \quad (73)$$

Indeed this quantity can vanish in special circumstances: it is possible in principle to construct toroidal equilibria in which the field magnitude is a flux label, $B = B(r)$. However such equilibria, called “omnigenous,” are exceptional. A crucial and universal property of real devices is that the field magnitude varies on flux surfaces, and therefore that the diamagnetic current has a divergence.

The return current is a current along \mathbf{B} that neutralizes the charge accumulated by \mathbf{J}_\perp . It is the return branch of a charge-flow pattern that forms on every (nonomnigenous) flux surface. Return currents play a surprisingly important role in confinement physics; they manage to enter, often critically, not only linear stability studies but also such topics as transport theory and nonlinear plasma evolution.

The return current is calculated as part of the solution to the quasineutrality condition

$$\nabla \cdot \mathbf{J} = \nabla \cdot \left(\frac{\mathbf{B} J_\parallel}{B} \right) + \nabla \cdot \mathbf{J}_\perp = 0,$$

where the second term is given by (73). Equivalently,

$$\mathbf{B} \cdot \nabla \left(\frac{J_\parallel}{B} \right) = -\nabla \cdot \mathbf{J}_\perp, \quad (74)$$

which is a magnetic differential equation for J_{\parallel} (recall §3.3). Its solution is given by (71) [or (72)]:

$$J_{\parallel} = \frac{J^{\theta}}{\chi'} B - \frac{cP'}{\chi' B} B_{\zeta}. \quad (75)$$

Here the first term represents an arbitrary solution to the homogeneous form of (74), i.e., it is an integration constant. Since, as we will see presently, B_{ζ}/B^2 is not a flux label, the two terms in (75) cannot cancel for any $J^{\theta}(v)$: diamagnetism in a toroidal system requires a parallel flow. Its proportionality to the radial pressure gradient is the characteristic feature of return current.

Of course (75) describes more than return currents. For example, any externally driven currents, such as Ohmic currents, are included in the first term. In many devices the externally driven parallel current dominates.

One might expect (74) to yield, as its solvability condition, a significant equilibrium constraint. To see that it does not, we use (69) to write

$$\nabla \cdot \mathbf{J}_{\perp} = \frac{\partial J_{\perp}^{\theta}}{\partial \theta} + \frac{\partial J_{\perp}^{\zeta}}{\partial \zeta}.$$

Now (63) gives,

$$\mathbf{J}_{\perp} = \frac{cP'}{B^2} \mathbf{B} \times \nabla v, \quad (76)$$

where, for unit Jacobian, we find

$$(\mathbf{B} \times \nabla v)^{\theta} = B_{\zeta}, \quad (\mathbf{B} \times \nabla v)^{\zeta} = -B_{\theta}.$$

Hence we have

$$\nabla \cdot \mathbf{J}_{\perp} = cP' \left\{ \frac{\partial}{\partial \theta} \left(\frac{B_{\zeta}}{B^2} \right) - \frac{\partial}{\partial \zeta} \left(\frac{B_{\theta}}{B^2} \right) \right\}$$

or, after using (70) and (71) to eliminate B_{θ} ,

$$\nabla \cdot \mathbf{J}_{\perp} = \left(\frac{\partial}{\partial \theta} + q \frac{\partial}{\partial \zeta} \right) \left(\frac{cP' B_{\zeta}}{\chi' B^2} \right) = \mathbf{B} \cdot \nabla \left(\frac{cP' B_{\zeta}}{\chi' B^2} \right). \quad (77)$$

Since the right-hand side here manifestly satisfies (40), we conclude that the quasineutrality condition is always soluble for scalar-pressure equilibrium. (The implicit constraint, that Hamada coordinates exist, is considered presently.) Furthermore, since $\nabla \cdot \mathbf{J}_{\perp}$ [from (73)] does not generally vanish, we see that B_{ζ}/B^2 is not a flux label, as we anticipated in our discussion of (75).

Existence of Hamada Coordinates

We showed in §3.4 that Hamada coordinates can be found if the specific volume of a closed field line,

$$I_0 = \oint \frac{ds}{B}$$

is the same for each line on the rational surface. Here we use force balance, in coordinate-free form, to show that I_0 is indeed a flux label (Greene and Johnson, 1962).

Consider the usual thin toroidal annulus enclosing the rational surface, with volume ΔV and radial width $\Delta V/|\nabla V|$. The current flowing across a closed field line in this volume,

$$I(v) = \oint ds |\mathbf{J}_\perp| \frac{\Delta V}{|\nabla V|},$$

is the same for every closed line, since no current escapes the annulus. But (59) implies that

$$|\mathbf{J}_\perp| \frac{\Delta V}{|\nabla V|} = \frac{c}{B} \Delta P$$

where ΔP is the pressure drop across the annulus. So we have

$$I(v) = c \Delta P \oint \frac{ds}{B} = c \Delta P I_0. \quad (78)$$

Since the pressure difference, ΔP , is a flux label the proof is complete.

The conclusion—that Hamada coordinates always exist in scalar pressure equilibria—is comforting, but unfortunately it begs a serious question: the singularity of the vacuum limit. Suppose, as in stellarator geometry, that the flux surfaces are constructed from external currents exclusively. Then I_0 need not be the same on each closed line; indeed, typical vacuum fields in existing devices *display* variation of I_0 on rational surfaces. When plasma is then introduced, it can satisfy (59) only if plasma currents are sufficiently strong to modify the field geometry and adjust I_0 on each rational surface. As Grad (Grad, 1967) has emphasized, this scenario is problematic in general; it becomes especially implausible at low plasma pressure. The issue remains an object of research.

3.7 Ampère's Law

Averaged Closure Relations

As will be emphasized in Chapter 6, a prominent general goal of theoretical plasma physics is to construct a closed set of equations for the evolution

of the electromagnetic field. This is accomplished by combining Maxwell's equations with additional information ("constitutive relations") specifying the current and charge densities in terms of the fields.

The equilibrium setting provides a helpful introduction to the question of closure. For example, (76) can be viewed as a constitutive relation, specifying (part of) the plasma current density independently of Maxwell's equations. We note that its combination with (2.54)—an approximate Maxwell equation—leads to further specification of the current, as in (75). A more powerful combination involves Ampère's law, (2.56), to which we next turn our attention.

The steady-state relation

$$\frac{4\pi}{c} \mathbf{J} = \nabla \times \mathbf{B}$$

has, in Hamada coordinates, the components [recall (2.33)]

$$\frac{4\pi}{c} J^v = \frac{\partial B_\zeta}{\partial \theta} - \frac{\partial B_\theta}{\partial \zeta}, \quad (79)$$

$$\frac{4\pi}{c} J^\theta = \frac{\partial B_v}{\partial \zeta} - \frac{\partial B_\zeta}{\partial v}, \quad (80)$$

$$\frac{4\pi}{c} J^\zeta = \frac{\partial B_\theta}{\partial v} - \frac{\partial B_v}{\partial \theta}. \quad (81)$$

Consider first (79). The left-hand side has been shown to vanish; for the right-hand side, we use (71) and (72) to find, after some manipulation,

$$\chi' \left(\frac{\partial}{\partial \theta} + q \frac{\partial}{\partial \zeta} \right) (B J_{||}) = \left(J^\theta \frac{\partial}{\partial \theta} + J^\zeta \frac{\partial}{\partial \zeta} \right) B^2$$

or

$$\mathbf{B} \cdot \nabla (B J_{||}) = (\mathbf{J} \cdot \nabla) B^2. \quad (82)$$

Since its right-hand side measures the variation of B on a flux surface, this relation can be viewed as an alternative description of return current.

We consider the other components of Ampère's law only in averaged form. Recalling (44), we introduce the abbreviated notation

$$\overline{A} = \langle A \rangle = (2\pi)^{-2} \oint d\theta d\zeta A, \quad (83)$$

and find

$$\frac{4\pi}{c} J^\theta = -\overline{B}'_\zeta, \quad \frac{4\pi}{c} J^\zeta = \overline{B}'_\theta, \quad (84)$$

since the current components are flux labels, equal to their averages. We substitute these forms into the averages of (71) and (72) to obtain the

differential equations

$$\bar{B}'_\zeta + \frac{4\pi P'}{\langle B^2 \rangle} \bar{B}_\zeta = -\frac{4\pi \chi'}{c \langle B^2 \rangle} \langle B J_{\parallel} \rangle ,$$

$$\bar{B}'_\theta + \frac{4\pi P'}{\langle B^2 \rangle} \bar{B}_\theta = \frac{4\pi q \chi'}{c \langle B^2 \rangle} \langle B J_{\parallel} \rangle , \quad (85)$$

for the covariant field components. Of course the solutions depend upon the average parallel current appearing on the right-hand side. Determining $\langle B J_{\parallel} \rangle$ is an objective of transport theory, discussed in Chapter 8.

Observe that

$$\bar{B}_\theta + q \bar{B}_\zeta = \left\langle B_\theta + \frac{B^\zeta}{B^\theta} B_\zeta \right\rangle = \left\langle \frac{B^2}{B^\theta} \right\rangle = \frac{1}{\chi'} \langle B^2 \rangle .$$

Hence the relations (85) combine to give

$$\bar{B}'_\theta + q \bar{B}'_\zeta = -\frac{4\pi P'}{\chi'} \quad (86)$$

a compact expression of force balance. Since the right-hand side of (86) is positive for normal pressure gradients, the field components B_θ and B_ζ can be said to contribute to force balance in so far as they increase with minor radius—the usual sense of diamagnetism. In experimental devices, B_θ indeed contributes in this sense (i.e., $J^\zeta > 0$; recall that \bar{B}_θ vanishes on the magnetic axis). However B'_ζ can have either sign. When it is positive the plasma is said to be diamagnetic with respect to the toroidal field; otherwise one speaks of a paramagnetic plasma. The direction of the poloidal current indicates which case pertains.

Poloidal Beta

The poloidal beta, β_P , measures the plasma pressure in terms of the poloidal magnetic field (recall the discussion in Chapter 1); one definition is

$$\beta_P = \frac{8\pi \langle P \rangle}{B_P^2(\alpha)} , \quad (87)$$

where α is the plasma radius and the brackets indicate an average over the plasma volume. In §3.12 we shall show that, in large aspect ratio axisymmetric geometry, the sign of the poloidal current is proportional to $\beta_P - 1$. Here we note that a similar conclusion will pertain in general, because of (85).

The point is that (85) can also be expressed as

$$B^\theta \bar{B}'_\theta + B^\zeta \bar{B}'_\zeta = -4\pi P'$$

since $B^\theta = \chi'$. It is clear that the left-hand side here roughly measures the radial derivative of $(\frac{1}{2})(\langle B_P^2 \rangle + \langle B_T^2 \rangle)$; that is

$$(B_P^2 + B_T^2)' \approx -8\pi P'$$

as in cylindrical geometry. Since $B_P(0) = 0 = P(\mathbf{a})$ we can integrate to obtain $B_P^2(\mathbf{a}) + B_T^2(\mathbf{a}) - B_T^2(0) \approx 8\pi P$ or, after dividing by $B_P^2(\mathbf{a})$,

$$\beta_P \approx 1 + \frac{B_T^2(\mathbf{a}) - B_T^2(0)}{B_P^2(\mathbf{a})}. \quad (88)$$

The point of (88) is that the diamagnetic effect on B_T is measured by $\beta_P - 1$. If β_P is less than unity, then the toroidal field profile is typically paramagnetic. For the same reason $\beta_P - 1$ prescribes the sense of the poloidal plasma current.

Typical experimental devices have poloidal betas not far from unity, with $B_P \ll B_T$. Equation (88) then implies that B_T varies little over the radius of the discharge. Note that devices with $B_P \ll B_T$ are inherently inefficient: the relatively large toroidal field component contributes only marginally to balancing the pressure gradient. “Current-free” stellarators and reversed-field pinch devices are example of confinement concepts in which this disadvantage is ameliorated.

Magnetic Curvature

By the curvature of an arbitrary vector field $\mathbf{A}(\mathbf{x})$, we mean a vector, pointing towards the local center of curvature, whose magnitude is the inverse radius of curvature. It is easy to see that the curvature vector is given by the change in the unit vector along a field line, $\mathbf{a} \cdot \nabla \mathbf{a}$, where $\mathbf{a} \equiv \mathbf{A}/A$.

The curvature of the magnetic field is denoted by

$$\kappa \equiv \mathbf{b} \cdot \nabla \mathbf{b}.$$

We shall find that considerations of magnetic curvature enter virtually every aspect of magnetic confinement physics. Here we point out the relation between curvature and plasma current.

Any unit vector satisfies $\mathbf{b} \cdot \nabla \mathbf{b} = -\mathbf{b} \times \nabla \times \mathbf{b}$; therefore

$$\begin{aligned} \kappa &= -\mathbf{b} \times \nabla \times \mathbf{b} = -\mathbf{b} \times \left[\frac{1}{B} \nabla \times \mathbf{B} - \mathbf{B} \times \nabla \left(\frac{1}{B} \right) \right] \\ &= \frac{4\pi}{c} \frac{\mathbf{J} \times \mathbf{B}}{B^2} + \frac{\nabla_\perp B}{B} \end{aligned} \quad (89)$$

where the notation follows (62). Note that κ is always orthogonal to \mathbf{b} :

$$\mathbf{b} \cdot \kappa = 0.$$

For scalar-pressure equilibrium we have, from (59),

$$B^2 \kappa = 4\pi \nabla P + B \nabla_{\perp} B,$$

or, since $\mathbf{b} \cdot \nabla P = 0$,

$$\kappa = \frac{1}{2} B^2 \nabla_{\perp} (8\pi P + B^2). \quad (90)$$

Here we see, incidentally, that the plasma and magnetic pressures ($B^2/8\pi$) must balance in a straight ($\kappa = 0$) system.

An obvious consequence of (89) or (90) is that κ is mainly determined by ∇B in a low-beta system:

$$\kappa \approx \frac{\nabla_{\perp} B}{B}, \quad \text{for } \beta \ll 1. \quad (91)$$

This low beta approximation is commonly used.

In the stability literature, κ is usually considered in terms of its “normal” and “geodesic” components. The *normal curvature*, κ_n , is simply the covariant radial component:

$$\kappa_n \equiv \kappa_r,$$

while the *geodesic curvature*, κ_g , is the covariant ζ -component:

$$\kappa_g \equiv \kappa_{\zeta}.$$

Thus we have

$$\kappa = \kappa_n \nabla r + \kappa_g (\nabla \zeta - q \nabla \theta). \quad (92)$$

3.8 Tensor Pressure Equilibrium*

CGL Pressure Tensor

Simple considerations of magnetized particle motion, two versions of which will be presented in Chapters 4 and 6, lead to the following form for the pressure tensor of a magnetized plasma:

$$\mathbf{P} = \mathbf{P}_{\text{CGL}} \equiv \mathbf{b}\mathbf{b}P_{\parallel} + (\mathbf{I} - \mathbf{b}\mathbf{b})P_{\perp} \quad (93)$$

where P_{\parallel} and P_{\perp} are the parallel and perpendicular pressures. The subscript stands for Chew, Goldberger and Lowe, who emphasized the importance of this tensor for magnetized plasma dynamics (Chew, Goldberger, et al., 1956). It is clear that P_{\perp} represents the thermal energy associated with gyration, while P_{\parallel} measures the thermal motion along the magnetic

field. The difference between the parallel and perpendicular pressures is the **pressure anisotropy**, for which we use the abbreviation

$$P_\Delta \simeq P_{\parallel} - P_{\perp}.$$

Thus we can write

$$\mathbf{P}_{\text{CGL}} = \mathbf{I}P_{\perp} + \mathbf{b}\mathbf{b}P_\Delta. \quad (94)$$

The scalar pressure case is described simply by $P_\Delta = 0$.

It is clear that particle collisions, in equilibrating parallel and perpendicular energies, will reduce P_Δ , and therefore that a collision-dominated plasma is described accurately by scalar pressure. It does not follow, however, that a confined plasma is necessarily anisotropic at low collisionality: even in the nearly collisionless limit, particle confinement times are much longer than the relevant collision times, allowing anisotropy to relax. We will find in Chapter 5 that, for a *sufficiently isolated* plasma, P_Δ is proportional to the parameter

$$\delta \sim (\text{ion gyroradius})/(\text{plasma scale-size})$$

(the same parameter used in the guiding-center expansion in §2.4). Thus P_Δ is no larger than other effects omitted from (59), and its inclusion in (60) is not generally consistent. That is, (59) provides a consistent lowest-order description of plasma equilibrium, even at low collisionality. Anisotropy is consistently included in higher δ -order, where it can have important consequences.

Equilibrium anisotropy is nonetheless worth considering, because not all confined plasmas are sufficiently isolated for P_Δ to equilibrate. The conventional example is mirror confinement: because of end losses, particle lifetimes in mirror systems are not always much longer than a collision time. Even in toroidal systems, certain auxiliary heating methods may drive significant P_Δ , although little anisotropy is predicted or observed in present machines.

Plasma Current

We briefly consider the anisotropic equilibrium current (Spies and Nelson, 1974). From (94) we compute

$$\nabla \cdot \mathbf{P} = \nabla P_{\perp} + \mathbf{b} [\nabla_{\parallel} P_\Delta + P_\Delta \nabla \cdot \mathbf{b}] + P_\Delta \boldsymbol{\kappa},$$

where $\nabla_{\parallel} \equiv \mathbf{b} \cdot \nabla$. Simple manipulation, using the identity

$$\nabla \cdot \mathbf{b} = -\frac{\nabla_{\parallel} B}{B},$$

then gives

$$\nabla \cdot \mathbf{P} = \nabla P_{\perp} + \mathbf{B} \nabla_{\parallel} \left(\frac{P_{\Delta}}{B} \right) + P_{\Delta} \kappa . \quad (95)$$

Upon substituting this form into (60), we also use (89) for κ ; the result is

$$\nabla P_{\perp} + \mathbf{B} \nabla_{\parallel} \left(\frac{P_{\Delta}}{B} \right) + \frac{P_{\Delta}}{B} \nabla_{\perp} B = \frac{\sigma}{c} \mathbf{J} \times \mathbf{B} , \quad (96)$$

where

$$\sigma \equiv 1 - 4\pi \frac{P_{\Delta}}{B^2} = 1 + 4\pi \frac{(P_{\perp} - P_{\parallel})}{B^2} . \quad (97)$$

Alternatively observe that

$$\frac{B^2}{4\pi} \nabla_{\perp} \sigma = -B \nabla_{\perp} \left(\frac{P_{\Delta}}{B} \right) + \frac{P_{\Delta}}{B} \nabla_{\perp} B ,$$

and therefore

$$\frac{1}{c} \mathbf{K} \times \mathbf{B} = \nabla P_{\parallel} - \frac{P_{\Delta}}{B} \nabla B , \quad (98)$$

where

$$\mathbf{K} \equiv \frac{c}{4\pi} \nabla \times (\sigma \mathbf{B}) , \quad (99)$$

is sometimes called the "Northrop-Whiteman current (Northrop and Whiteman, 1964)."

The parallel component of (98), $\nabla_{\parallel} P_{\perp} + B \nabla_{\parallel} (P_{\Delta}/B) = 0$ or

$$\nabla_{\parallel} P_{\perp} - \frac{P_{\Delta}}{B} \nabla_{\parallel} B = 0 \quad (100)$$

can be solved for either pressure if the other is known. It reveals a key feature of anisotropic equilibria: P_{\parallel} cannot be a flux label unless B is a flux label. Indeed, kinetic arguments suggest dependence on both r and the field magnitude, $P(r, B)$, for both pressures. This form is frequently assumed, although it is compelling only in special circumstances.

In addition to lacking simple isobars, (98) has the annoying feature of permitting radial current: there is no analogue of (64) in the anisotropic case. We have

$$\mathbf{J}_{\perp} = \frac{c}{\sigma B} \left[\mathbf{b} \times \nabla P_{\perp} + \frac{P_{\Delta}}{B} \mathbf{b} \times \nabla_{\perp} B \right] ,$$

with radial component

$$\mathbf{J} \cdot \nabla r = \frac{c}{\sigma B} (\nabla r \times \mathbf{b}) \cdot \left[\nabla_{\perp} P_{\perp} + \frac{P_{\Delta}}{B} \nabla_{\perp} B \right] .$$

The fact that this must satisfy the ambipolarity condition $(\mathbf{J} \cdot \nabla r) = 0$ is now a nontrivial constraint. (Equilibrium anisotropy is not problematic, at least conceptually, in mirror geometry, where flux surfaces and radial ambipolarity play little role.)

Total Stress Tensor

The force balance equation is sometimes written in terms of the total stress tensor, including plasma stress as well as the Maxwell terms. This quantity is given by

$$T_{\alpha\beta} \equiv (\delta_{\alpha\beta} - b_\alpha b_\beta) T_\perp + b_\alpha b_\beta T_\parallel$$

with

$$T_\perp = P_\perp + \frac{B^2}{8\pi}, \quad T_\parallel = P_\parallel - \frac{B^2}{8\pi}.$$

Thus the relation

$$\nabla \cdot \mathbf{T} = 0 \tag{101}$$

can be seen to reproduce to (60). The fact that magnetic energy adds to P_\perp reflects transverse magnetic pressure; that it subtracts from P_\parallel reflects magnetic field-line tension.

Part 3: Axisymmetric Systems

3.9 Magnetic Field

Two coordinate systems are commonly used in axisymmetric geometry. Symmetry coordinates, discussed in §3.4, are flux coordinates specialized to provide partial orthogonality, as in (51). The other useful set, Shafrazenov coordinates, specifically pertain to large aspect ratio geometry; they are not flux coordinates. We discuss Shafrazenov coordinates in §3.12; otherwise, symmetry coordinates are used exclusively below, suppressing the zero subscript as usual.

A key property of symmetry coordinates was anticipated in §3.4: the covariant component B_ζ is a flux label, as in (55). This is a consequence of the radial component of Ampère's law,

$$\frac{4\pi}{e} J^r = \frac{1}{\sqrt{g}} \left(\frac{\partial B_\zeta}{\partial \theta} - \frac{\partial B_\theta}{\partial \zeta} \right). \tag{102}$$

Since force balance requires $J^r = 0$ and axisymmetry requires $\partial B_\theta / \partial \zeta = 0$, we have $\partial B_\zeta / \partial \theta = 0$ and $B_\zeta \equiv I$ depends only on \mathbf{r} . As a result we can write

$$\mathbf{B} = I(r) \nabla \zeta + \nabla \zeta \times \nabla \chi. \tag{103}$$

This mixed representation of \mathbf{B} (covariant for B_T , contravariant for B_P) is often more convenient than the general (contravariant) flux representation

of (14). It shows in particular that the toroidal field $B_T = I|\nabla\zeta| = I/R$ varies on flux surfaces only through the variation of the major radius. The corresponding poloidal component has magnitude $B_P = |\nabla\chi|/R = \chi'|\nabla r|/R$. In many axisymmetric devices the poloidal field is relatively small, so that

$$B(r, \theta) \simeq \frac{I(r)}{R}. \quad (104)$$

3.10 Plasma Current

Grad-Shafranov Equation

We use (103) to analyze the other components of Ampère's law. From the vector identity $\nabla\xi \cdot \nabla \times \mathbf{A} = \nabla \cdot (\mathbf{A} \times \nabla\xi)$, for any ξ , we find

$$\nabla\xi \cdot \nabla \times \mathbf{B}_P = \nabla \cdot [(\nabla\xi \times \nabla\chi) \times \nabla\xi] = \nabla \cdot [\nabla\chi(\nabla\xi \cdot \nabla\xi) - \nabla\xi(\nabla\chi \cdot \nabla\xi)]. \quad (105)$$

Then the choice $\xi = \theta$ yields

$$\nabla\theta \cdot \nabla \times \mathbf{B}_P = -\nabla\xi \cdot \nabla(\nabla\chi \cdot \nabla\theta) = 0$$

by axisymmetry (note also that the symmetry angle $\zeta = -\varphi$ satisfies $\nabla \cdot \nabla\zeta = 0$). Hence the poloidal current comes exclusively from \mathbf{B}_T :

$$\frac{4\pi}{c} J^\theta = \nabla\theta \cdot \nabla \times [I(r)\nabla\zeta] = -I'(r)\nabla\theta \cdot \nabla\zeta \times \nabla r.$$

That is

$$J^\theta = -\frac{c}{4\pi} \frac{I'}{\sqrt{g}} = -\frac{c}{4\pi} \frac{II'}{q'\chi'R^2}. \quad (106)$$

For the toroidal current we choose $\xi = \zeta$ in (105) to find

$$J^\zeta = \frac{c}{4\pi} \nabla \cdot [\nabla\chi(\nabla\xi \cdot \nabla\xi)] = \frac{c}{4\pi} \nabla \cdot (R^{-2}\nabla\chi), \quad (107)$$

in view of the orthogonality expressed by (51). It is not surprising that the spatial structure of the poloidal flux is determined by the toroidal current; but note that the simple form of (107) depends upon axisymmetry.

Next consider the force balance relation, (59). Since $B^r = 0 = J^r$, only the radial component is interesting:

$$\sqrt{g} B^\theta (q J^\theta - J^\zeta) = c P'. \quad (108)$$

After substitution from (106) and (107) we find

$$R^2 \nabla \cdot (R^{-2} \nabla\chi) \chi' = -II' - 4\pi R^2 P'$$

or

$$R^2 \nabla \cdot (R^{-2} \nabla \chi) = -I \frac{dI}{d\chi} - 4\pi R^2 \frac{dP}{d\chi}. \quad (109)$$

This important result is called the Grad-Shafranov equation (Batemann, 1980). The operator on the left-hand side is often abbreviated by

$$\Delta^* \equiv R^2 \nabla \cdot (R^{-2} \nabla). \quad (110)$$

The Grad-Shafranov equation is a second order, elliptic partial differential equation for the function $\chi(\mathbf{x})$. Together with appropriate boundary data, it determines the flux surface configuration in an axisymmetric system. Of course the right hand side must be presumed known: the pressure and toroidal field profiles are to be found from other physical considerations. Notice that the profiles must be specified as functions of χ , the quantity whose spatial dependence is to be determined—a mathematical peculiarity that decisively affects the schemes used to solve (108). We obtain an explicit, approximate solution in §3.12.

The axisymmetric version of (109) is more complicated, and less important. The point is that plasma currents have relatively little influence on most axisymmetric field geometries. In distinction, axisymmetric devices depend heavily on plasma currents, which provide in particular most of the poloidal field. Thus tokamak experimental programs devote considerable attention to solving the Grad-Shafranov equation.

Return Current

The axisymmetric identity,

$$\sqrt{g} \nabla \mathbf{r} \times \nabla \theta = \frac{\sqrt{g} I}{q \chi'} \nabla \zeta = R^2 \nabla \zeta, \quad (111)$$

allows

$$\mathbf{J} = \sqrt{g} (J^\theta \nabla \zeta \times \nabla \mathbf{r} + J^\zeta \nabla \mathbf{r} \times \nabla \theta)$$

to be expressed as

$$\mathbf{J} = \sqrt{g} J^\theta \nabla \zeta \times \nabla \mathbf{r} + J^\zeta R^2 \nabla \zeta,$$

analogous to (103). Since $\nabla \zeta \times \nabla \mathbf{r} = \mathbf{B}_P/\chi' = (\mathbf{B} - I \nabla \zeta)/\chi'$ we can write

$$\mathbf{J} = \sqrt{g} J^\theta \frac{\mathbf{B}}{\chi'} + R^2 \nabla \zeta \left[J^\zeta - \frac{\sqrt{g} I}{R^2 \chi'} J^\theta \right]$$

$$= \sqrt{g} J^\theta \frac{\mathbf{B}}{\chi'} + R^2 \nabla \zeta (J^\zeta - q J^\theta),$$

where (111) was used again. Here the first and second terms can be simplified using (106) and (108) respectively, with the result

$$\mathbf{J} = -\frac{c}{4\pi} \frac{dI}{d\chi} \mathbf{B} - c R^2 \nabla \zeta \frac{dP}{d\chi}, \quad (112)$$

conveniently summarizing the form of the current density in any axisymmetric system.

Two consequences are that

$$J^\zeta = -\frac{c}{4\pi R^2} I \frac{dI}{dX} - c \frac{dP}{dX}, \quad (113)$$

as in (109), and that

$$J_{||} = -\frac{c}{4\pi} B \frac{dI}{dX} - c \frac{I}{B} \frac{dP}{dX}. \quad (114)$$

Equation (114) is evidently the axisymmetric version of (71). Presuming as usual that B varies on flux surfaces, we see that its two terms have distinctive θ -dependence and cannot cancel: toroidicity requires a parallel current. Thus we observe again the return current, originating in force balance and quasineutrality, discussed in §3.6.

Diamagnetism

In §3.7 we noted that poloidal currents do not always contribute to confinement: the force $\mathbf{J}_P \times \mathbf{B}_T$ can add to the pressure gradient, rather than opposing it. Poloidal current contributes to confinement only in the “toroidally diamagnetic” case, with $J_P \propto I'(r) > 0$, which is not always achieved in tokamak experiments. We also noted that, because of the relatively large toroidal field, confinement efficiency would improve if this diamagnetic poloidal current were increased.

In the extreme case, J_T is locally negligible and confinement is provided by J_P alone. Equation (113) then implies

$$\frac{d}{dX} I^2 = -8\pi R^2 \frac{d}{dX} P. \quad (115)$$

Significantly, this annihilation of the toroidal current is most easily satisfied on the inside—smaller R —region of the torus. That is, strong toroidal diamagnetism pushes the toroidal current outwards in major radius.

More important is the observation that any further increase in dI/dX implies a local reversal of J_T . One can imagine containing oppositely directed toroidal currents, with restoring forces supplied by external conductors. However, since such a configuration is unlikely to be stable, (115) effectively limits the rate of variation of the toroidal field. The constraint can be expressed roughly as

$$\left| \frac{d \log I^2}{dr} \right| \leq \left| \frac{d \beta_T}{dr} \right|, \quad (116)$$

where [compare (87)]

$$\beta_T = \frac{8\pi P}{B_T^2}$$

is the toroidal beta. Equation (116) particularly restricts tokamaks, in which β_T is quite small (no more than a few percent). In this case the function $I(r)$ is nearly constant, so that toroidal field variation comes primarily from the $1/R$ factor:

$$B_T \approx \text{const}/R \quad (\text{in tokamak geometry}). \quad (117)$$

It should be mentioned that (117) can be contravened: for example omnigenous geometries, in which the field magnitude is flux label, can be constructed.

Magnetic Curvature

In §3.7 we noted the pervasive importance of magnetic curvature, $\kappa = \mathbf{b} \cdot \nabla \mathbf{b}$, and derived the identity (89)

$$\kappa = \frac{\nabla_{\perp} B}{B} + \frac{4\pi}{c} \frac{\mathbf{J} \times \mathbf{B}}{B^2}. \quad (118)$$

Here we obtain explicit expressions for the covariant components of (118) in the axisymmetric case.

Consider first the radial component. Simple manipulation gives

$$\kappa_r = \frac{\partial}{\partial r} \log B - \chi' \frac{4\pi}{cB^2} (J^{\zeta} - qJ^{\theta})$$

Thus (106) and (107) imply

$$\kappa_r = \frac{\partial}{\partial r} \log B - \frac{\chi'}{B^2} \left[\nabla \cdot (R^{-2} \nabla \chi) + \frac{qI'}{\sqrt{g}} \right].$$

Since $q\chi'/\sqrt{g} = B^{\zeta} = B_{\zeta}/R^2$, the last term here involves

$$B^{\zeta} B'_{\zeta} = \frac{1}{2} \frac{\partial B_T^2}{\partial r} + B_T^2 \frac{\partial}{\partial r} \log R.$$

Then, since

$$\frac{\partial}{\partial r} \log B = \frac{1}{2B^2} \frac{\partial}{\partial r} (B_P^2 + B_T^2),$$

the terms involving radial derivatives of B_T cancel, leaving

$$\kappa_r = \frac{1}{2B^2} \frac{\partial B_P^2}{\partial r} - \frac{B_T^2}{B^2} \frac{\partial}{\partial r} \log R - \frac{\chi'}{B^2} \nabla \cdot (R^{-2} \nabla \chi).$$

Next observe that, since $B_P = |\nabla\chi/R|$,

$$\begin{aligned}\frac{\partial B_P^2}{\partial r} &\approx -2B_p^2 \frac{\partial}{\partial r} \log R + R^{-2} \frac{\partial}{\partial r} |\nabla\chi|^2 \\ &= -2B_p^2 \frac{\partial}{\partial r} \log R + 2R^{-2} \nabla\chi \cdot \nabla\chi'\end{aligned}$$

so we have

$$\kappa_r = -\frac{\partial}{\partial r} \log R + \frac{1}{(BR)^2} \nabla\chi \cdot \nabla\chi' - \frac{\chi'}{B^2} \nabla \cdot (R^{-2} \nabla\chi) .$$

But

$$\frac{1}{(BR)^2} \nabla\chi \cdot \nabla\chi' \sim \frac{\chi'}{B^2} \nabla \cdot (R^{-2} \nabla\chi) = -\frac{\chi'}{B^2} \nabla \cdot (R^{-2} \nabla r) ,$$

whence, finally,

$$\kappa_r = -\frac{\partial}{\partial r} \log R - \left(\frac{B_p}{B}\right)^2 R^2 \nabla \cdot (R^{-2} \nabla r) . \quad (119)$$

Here the first term is evidently the curvature of a purely toroidal line ($q = \infty$), with radius of curvature R . The second term accounts for the helical twist of \mathbf{B} on the flux surface; its corresponding radius appears in the cylindrical limit, where $R \approx \text{const}$ and $R^2 \nabla \cdot (R^{-2} \nabla r) \approx \nabla \cdot (\mathbf{r}/r) = 1/r$. Thus, for large aspect ratio surfaces with circular cross section,

$$\kappa_r \approx -\frac{\partial}{\partial r} \log R - \left(\frac{B_p}{B}\right)^2 \frac{1}{r} . \quad (120)$$

The remaining two components of $\boldsymbol{\kappa}$ are much simpler. We assume $J^r = B^r = 0$, so that the first term in (118) has only a radial component. Then, from

$$\nabla_{\perp} B = \nabla B - \mathbf{b} \nabla_{\parallel} B ,$$

we easily find

$$\kappa_{\theta} = (1 - b_{\theta} b^{\theta}) \frac{\partial}{\partial \theta} \log B = \left(\frac{B_T}{B}\right)^2 \frac{\partial}{\partial \theta} \log B , \quad (121)$$

while the identity $\mathbf{b} \cdot \boldsymbol{\kappa} = 0$ implies

$$\kappa_{\zeta} = -\frac{\kappa_{\theta}}{q} . \quad (122)$$

The results (119) and (121) are exact and quite general, pertaining for scalar or tensor pressure, so long as the radial current vanishes.

3.11 Equilibrium Electric Field

Faraday's Law

Equation (112), for the current density in an axisymmetric system, is fully general and frequently useful, as we shall see. However it obscures what is, in many axisymmetric devices, the most important source of plasma current: an externally induced electric field. Thus the Ohmic tokamak, in particular, obtains its poloidal magnetic field, as well as its thermal energy, from externally driven toroidal currents—that is, from a toroidal electric field E_T . This E_T -driven current, often called the Ohmic current, is contained in the first term of (112); the gradient dI/dr will be seen, in §8.4, to involve a certain average of the driving electric field.

From Faraday's law [(2.46) expressed in terms of the scalar potential Φ and vector potential \mathbf{A}],

$$\mathbf{E} = -\nabla\Phi - \frac{1}{c} \frac{\partial \mathbf{A}}{\partial t}, \quad (123)$$

it is clear that axisymmetry forces any toroidal field to be electromagnetic:

$$E_\zeta = -\frac{1}{c} \frac{\partial A_\zeta}{\partial t}.$$

Thus the gauge freedom implicit in

$$\mathbf{B} = \nabla \times \mathbf{A}$$

is restricted by the requirement that $A_\zeta \neq 0$. In particular, the contravariant component,

$$B^\theta = -\frac{1}{\sqrt{g}} \frac{\partial A_\zeta}{\partial r},$$

is consistent with the flux-representation formula, (22), only if $A_\zeta + \chi$ is a spatial constant. It is customary to choose the constant to vanish, and thus to write

$$A_\zeta = -\chi(r, t). \quad (124)$$

The fact that A_ζ must be a flux label at each time could have been anticipated from $B^r \propto \partial A_\zeta / \partial \theta$.

Thus the toroidal component of Faraday's law is simply

$$E_\zeta = \frac{1}{c} \frac{\partial \chi}{\partial t}. \quad (125)$$

Alternatively one can rewrite (124) and (125) in terms of vector rather than covariant components:

$$A_T = -\frac{\chi}{R}, \quad E_T = \frac{1}{Rc} \frac{\partial \chi}{\partial t}. \quad (126)$$

The critical role of E_T in maintaining equilibrium justifies treating it as an equilibrium field, despite the time derivative appearing in (125). However, it should be pointed out that the rate of change entering (125) is quite slow—no faster than other processes, such as radial diffusion, which our equilibrium considerations otherwise omit. Thus a thorough treatment of the role of E_T must be deferred to Chapter 8, where the slow diffusion time scale is studied. Here we consider the incorporation of E_T into the equilibrium field description.

Flux Surface Motion

Equation (126) shows that the poloidal flux in an axisymmetric system with toroidal electric field must vary in time. The poloidal magnetic field can remain constant, as we shall see, but the flux surface on which χ has a particular value will move. The velocity of this surface, \mathbf{V}_f , is a quantity of some interest; it is defined by

$$\frac{\partial \chi}{\partial t} + \mathbf{V}_f \cdot \nabla \chi = 0. \quad (127)$$

Thus an observer moving at \mathbf{V}_f would find $\chi = \text{constant}$. If E_T is positive each constant- χ surface moves toward the magnetic axis. Only the radial component of \mathbf{V}_f is meaningful.

The most striking property of (127) is that, at least in the tokamak case, it predicts rapid motion. Recalling $|\nabla \chi| = RB_p |\nabla r| \cong RB_P$, we see from (126) that

$$|V_f| \cong c \frac{E_T}{B_P}. \quad (128)$$

This speed exceeds the $\mathbf{E} \times \mathbf{B}$ drift associated with E_T whenever, as in the tokamak case, B_P is relatively small. In fact (128) predicts that a typical flux surface will traverse a sizable fraction of the plasma radius during a confinement time.

Equation (127) allows the surfaces not only to move, but also to change shape in time. It is not hard to see that shape change, which requires the increment of \mathbf{B} to depart from its original surface, is proportional to $\nabla \chi \cdot \partial \mathbf{B} / \partial t$. Since $\mathbf{B} \cdot \nabla \chi$ vanishes identically at all times, we have

$$\nabla \chi \cdot \frac{\partial \mathbf{B}}{\partial t} = -\mathbf{B} \cdot \nabla \left(\frac{\partial \chi}{\partial t} \right) = -c \mathbf{B} \cdot \nabla E_\zeta \quad (129)$$

from (128). We conclude that if $E_\zeta = RE_T$ is a flux label, then the surfaces of constant χ expand or contract without change in shape. Indeed, the “constant shape assumption,”

$$E_\zeta(\mathbf{x}) = E_\zeta(r)$$

is commonly used in studies of tokamak evolution.

Notice here that the toroidal flux, Ψ_T , does not change at the same rate as χ . While at any time the set of flux surfaces is simultaneously labelled by Ψ_T or χ , the values of the fluxes on a chosen surface evolve independently. Indeed, because Ψ_T is primarily controlled by external field coils, it is nearly constant over the duration of a typical tokamak discharge. The conventional tokamak case, in which $B \cdot \nabla \zeta$ is a temporal constant and E_ζ is a flux label, is characterized by the following useful identity:

$$E_\zeta(r) = \frac{\langle E_{\parallel} B \rangle}{I(R^{-2})}. \quad (130)$$

The point is that $\nabla \zeta \cdot \nabla \times \mathbf{E} = 0$ implies $\mathbf{E} = -\nabla \Phi + E_\zeta \nabla \zeta$; (130) then quickly follows from (129).

Because of its approximate time-independence, Ψ_T is sometimes used as a basis for the radial variable, defining

$$\Psi_T = \pi B_{T0} \frac{r^2}{2}, \quad (131)$$

where B_{T0} is some constant, representative value of the toroidal field.

Finally we verify that variation of χ does not require variation of the poloidal magnetic field. The point is that we could have

$$\chi(r, t) = \chi_1(r) + \chi_2(t), \quad (132)$$

where each function on the right-hand side depends strictly on a single variable. It is clear that χ_1 alone determines \mathbf{B}_P , which is therefore constant in time; E_T on the other hand is determined exclusively by χ_2 . Equation (132), the general requirement for a static poloidal magnetic field, roughly describes the equilibrium electromagnetic field in most tokamak experiments. Of course the static \mathbf{B}_P is a special case of a constant-shape field.

3.12 Large Aspect Ratio Approximation

Shafranov Geometry

A common axisymmetric toroidal geometry, typical of tokamaks as well as some pinch devices, has circular boundary in the poloidal plane. Then the outermost flux surface, effectively determined by interaction with the boundary, can be presumed nearly circular (that is, circular in poloidal cross section). In general, the interplay of plasma forces and toroidal curvature will distort interior surfaces away from circularity. It was first noted by Shafranov that, for the special case of small plasma pressure and large aspect ratio, the inner flux surfaces will remain approximately circular (Shafranov, 1966).

Shafranov geometry refers to an approximate toroidal equilibrium—a large aspect-ratio, small beta, solution to the Grad-Shafranov equation—characterized by nested flux surfaces with circular cross sections. It is not a cylindrical equilibrium; toroidal curvature is manifested in a relative shift of the centers of the circles corresponding to different surfaces. The geometry is depicted in Figure 5.

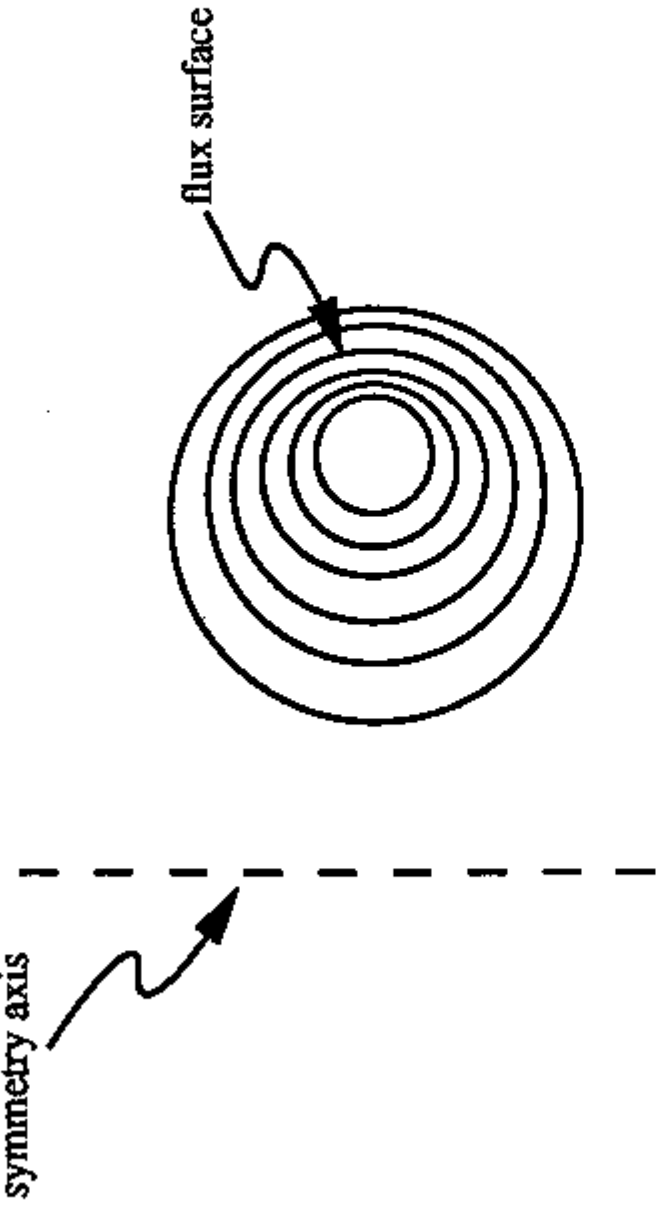


Figure 5. Displaced circular flux surfaces of Shafranov geometry.

The origin of the Shafranov shift is easily understood. First, a pressurized torus will always tend to expand in major radius, simply because more surface area is available on its outer (larger R) side. The force associated with this tendency, familiar to anyone who has inflated an unconfined inner tube, has been called the “tire tube force” (Freidberg, 1987). Expansion in R is also driven by hoop forces associated with toroidal plasma current; clearly the hoop force will dominate at low beta.

Shafranov Coordinates

Shafranov coordinates (r_S, θ_S, ζ_S) are defined, in terms of the usual cylindrical coordinates (R, φ, Z) , by

$$\begin{aligned} R &= R_c(r_S) + r_S \cos \theta_S , \\ \varphi &= -\zeta_S , \\ Z &= r_S \sin \theta_S . \end{aligned} \quad (133)$$

Here the function $R_c(r)$ remains to be determined; it evidently locates the center of that circular coordinate surface whose minor radius is r . It follows

in particular that

$$R_e(0) = R_0 \quad (134)$$

is the major radius of the magnetic axis, and that

$$R'_e(r_S) \equiv \frac{dR_e}{dr_S} < 0$$

for the physical case of an outwardly shifted magnetic axis. The displacement of the magnetic axis is measured by $R_0 - R_e(r_s)$.

We connect these coordinates to toroidal equilibrium theory by the following statement: If the aspect ratio is sufficiently large,

$$\epsilon \equiv \frac{a}{R_0} \ll 1, \quad (135)$$

and the plasma pressure sufficiently small,

$$\beta_P = \mathcal{O}(1), \quad (136)$$

then the Grad-Shafranov equation has a solution χ of the form

$$\chi(\mathbf{x}) = \chi(r_S) + \mathcal{O}(\epsilon^2). \quad (137)$$

with relatively small shift:

$$R'_e(r_S) = \mathcal{O}(\epsilon). \quad (138)$$

In other words, for suitably chosen $R_e(r_S)$, r_S is an approximate flux label, and therefore a suitable radial coordinate.

Two comments are in order:

(i) The shifted-circle equilibrium of (137) is not very accurate. Experimental aspect ratios are not very large; only the first order terms in ϵ are balanced; and it is known that noncircularity (ellipticity) appears promptly in second order. On the other hand the simplicity of the Shafranov solution has an obvious appeal, especially in pedagogical contexts.

(ii) Even through first order, where r_S is a flux label, Shafranov coordinates are not flux coordinates. We shall see that the angular choice given in (137) does not yield straight field lines in the appropriate sense. On the other hand a flux-coordinate version is easily constructed.

Note that the validity and importance of Shafranov geometry is unaffected by any weaknesses of the coordinates: the outward shift is real, however one wishes to describe it. Indeed measurements of the shift are regularly used as an experimental diagnostic. A salient virtue of the coordinates is that they allow straightforward calculation of the shift.

Before showing that shifted circles do indeed approximately satisfy the Grad-Shafranov equation, we examine some features of the corresponding magnetic field. From here on the S -subscripts are suppressed.

We use (103) to express the field components in Shafranov coordinates, consistently neglecting terms of order ϵ^2 . For the toroidal field, $B_T = I/R$, we quickly find

$$B_T(r, \theta) = B_{T0}(r) \left[1 - \frac{r}{R_0} \cos \theta \right], \quad (139)$$

where $B_{T0}(r) = I/R_0$. For the poloidal field, $B_P = \chi' \nabla \zeta \times \nabla r$, we notice from (132) that

$$\nabla r = (1 + R'_t \cos \theta)^{-1} (\sin \theta \nabla Z + \cos \theta \nabla R), \quad (140)$$

where ∇Z and ∇R are cylindrical unit vectors. Thus, again neglecting $\mathcal{O}(\epsilon^2)$, we have

$$B_P = B_{P0}(r) \left[1 + \frac{r}{R_0} \Lambda \cos \theta \right] \quad (141)$$

where $B_{P0}(r) = \chi'/R_0$ and the shift enters through

$$\Lambda \equiv - \left(1 + \frac{R_e R'_e}{r} \right). \quad (142)$$

Equation (138) implies that both terms in Λ are comparable: $\Lambda = \mathcal{O}(1)$. The Shafranov Jacobian is given by

$$\sqrt{g_s} = r R (1 + R_e \cos \theta) = r R_e \left[1 - \frac{r}{R_0} \Lambda \cos \theta \right]. \quad (143)$$

Therefore, using (36), the flux surface average can be expressed as

$$\langle A \rangle = \oint \frac{d\theta}{2\pi} \left[1 - \frac{r}{R_0} \Lambda \cos \theta \right] A. \quad (144)$$

We compute the safety factor in Shafranov geometry from the definition, (6), using (5) for Ψ_T . The latter gives

$$\frac{d\Psi_T}{dr} = \oint d\theta \sqrt{g_s} \frac{I}{R} = 2\pi \frac{r I}{R_0} + \mathcal{O}(\epsilon^2) = 2\pi r B_{T0} + \mathcal{O}(\epsilon^2) \quad (145)$$

Since $d\Psi_P/dr = 2\pi \chi' = 2\pi B_{P0} R_0$ we have

$$q = \frac{r B_{T0}}{R B_{P0}}. \quad (146)$$

This simple form is formally identical with the “cylindrical q ,” referred to in Chapter I and denoted by q_c . The point is that first order corrections from toroidicity vanish in the θ -average of (145). Although the r in (146) is distinct from the cylindrical radius, because the surfaces are not concentric, we shall refer to (146) as the cylindrical q .

It is noteworthy that q does not measure the local field line pitch,

$$\frac{\mathbf{B} \cdot \nabla \zeta}{\mathbf{B} \cdot \nabla \theta} = q \left[1 - \frac{r}{R_e} (2 + \Lambda) \cos \theta \right]$$

which varies on flux surfaces. Thus, as we have remarked, Shafranov coordinates are not flux coordinates.

Experimental devices are nearly always described in terms of the toroidal current,

$$I_T = \int r dr d\theta J_T$$

and the toroidal field. For circular cross-section one quickly finds $B_P = 2I_T/a c$ from Ampère's law, and therefore $q(a) = (c/2)a^2 B_{T0}/I_T R_0$. Since I_T is conventionally measured in Ampère's, rather than statampères, the practical formula is

$$q(a) = 5a^2 \frac{B_T}{RI_A} \quad (147)$$

where I_A is the toroidal current measured in Amperes (other quantities are measured in cgs units as usual). Elongated machines have noncircular cross section with "horizontal" radius (i.e., radius in the toroidal plane) a and vertical radius $\kappa_e a$, where $\kappa_e > 1$ is the *elongation parameter*. It is not hard to generalize (147) to obtain

$$q(a) = 5\kappa_e a^2 \frac{B_T}{RI_A}, \quad (148)$$

allowing for elongation.

Finally we turn our attention to the Grad-Shafranov equation, seeking a shifted-circle equilibrium as described by (135)–(138). By expanding the equation as a power series in ϵ , we find that the zeroth and first order terms can indeed balance, provided the functions $B_{P0}(\mathbf{r})$, $B_{T0}(\mathbf{r})$ and $R_c(r)$ are appropriately chosen. In higher order, force balance requires noncircularity of the surfaces, as we have remarked.

The differential operator in the Grad-Shafranov equation is expressed in Shafranov coordinates using

$$\nabla \cdot (R^{-2} \nabla \chi) = \frac{1}{\sqrt{g_s}} \left(\frac{\partial}{\partial r} \sqrt{g_s} R^{-2} \chi' \nabla_r \cdot \nabla_r + \frac{\partial}{\partial \theta} \sqrt{g_s} R^{-2} \chi' \nabla_\theta \cdot \nabla_\theta \right).$$

The ϵ -expansion of (109) is straightforward if somewhat tedious. In lowest (ϵ^0) order one finds

$$\frac{1}{r} \frac{d}{dr} r \chi = -I \frac{dI}{dX} - 4\pi R_0^2 \frac{dp}{dX},$$

or, after manipulation,

$$\frac{d}{dr} [r^2 (B_{P0}^2 + B_{T0}^2)] = 2r B_{T0}^2 - 8\pi r^2 \frac{dP}{dr}. \quad (149)$$

The first-order terms, all of which are proportional to $\cos \theta$, give

$$\left(1 - \frac{R_c}{r} R'_c\right) \frac{d}{dr} \left(\frac{r}{R_c} \chi' \right) - \frac{R_c}{r} \frac{d}{dr} \left[\frac{r}{R_c} \left(\frac{r}{R_c} + R'_c \chi' \right) \right] + \frac{R'_c}{r} \chi' = -8\pi r R_c \frac{dP}{d\chi}$$

which simplifies to

$$\frac{d}{dr} [(1 + \Lambda)r^2 B_{P0}^2] = r B_{P0}^2 - 8\pi r^2 \frac{dP}{dr}. \quad (150)$$

Equations (149) and (150) are the two dominant Fourier components of the Grad-Shafranov equation. (The fact that no unbalanced Fourier components, such as $\sin \theta$ terms, occur, is of course essential to the validity the shifted-circle equilibrium.) Thus, like the exact version of (109), they are to be solved for $\chi(\mathbf{x})$, given the pressure and toroidal field profiles. The only departure from (109) is the way in which $\chi(\mathbf{x})$ enters. In Shafranov geometry, the poloidal flux is parameterized through two one-dimensional functions, $B_{P0}(r)$ and $\Lambda(r)$; the first prescribes the value of χ on its contours, while the second determines the contour configuration.

For unspecified pressure and toroidal field profiles, the solutions to (149) and (150) can be expressed in terms of an average over the volume bounded by a flux surface. In the absence of angle-dependence, as in the present case, this average reduces to a simple radial average, given by

$$\langle f \rangle_v \equiv \frac{2}{r^2} \int_0^r dr' r' f(r'). \quad (151)$$

Thus (149) integrates to yield

$$B_{P0}^2(r) + B_{T0}^2(r) = \langle B_{T0}^2 \rangle_v(r) - 8\pi [P(r) - \langle P \rangle_v(r)].$$

In this regard, it is convenient to define the plasma poloidal beta as

$$\beta_P(r) \equiv 8\pi \frac{\langle P \rangle_v(r)}{B_{P0}^2(r)}. \quad (152)$$

This definition differs slightly from that used in a previous, more qualitative discussion; recall (86) *et seq.* We have

$$\beta_P(r) = 1 + \frac{B_{T0}^2(r) - \langle B_{T0}^2 \rangle_v(r)}{B_{P0}^2(r)} + 8\pi P(r),$$

or, if the pressure vanishes on the flux surface labelled by $r = a$,

$$\beta_P(a) = 1 + \frac{B_{T0}^2(a) - \langle B_{T0}^2 \rangle_v(a)}{B_{P0}^2(r)}, \quad (153)$$

as in (87). We have already pointed out the relation between toroidal diamagnetism and the sign of $\beta_P - 1$; (153) makes this relation explicit in the large aspect ratio case.

Turning to (150) we similarly integrate to obtain

$$(1 + \Lambda) B_{P0}^2(r) = \frac{1}{2} \langle B_{P0}^2 \rangle_v(r) + 8\pi \{ \langle P \rangle_v - P(r) \}, \quad (154)$$

and an additional integration provides the expression

$$\left[\frac{R_c(r)}{R_0} \right]^2 = 1 - \left(\frac{r}{R_0} \right)^2 \left\{ \frac{1}{2} \left\langle \frac{\langle B_{P0}^2 \rangle_v}{B_{P0}^2} \right\rangle_v + 8\pi \left\langle \frac{\langle P \rangle_v - P}{B_{P0}^2} \right\rangle_v \right\}. \quad (155)$$

Here the term involving $\langle B_{P0}^2 \rangle_v$ reflects the hoop force, while the pressure terms (tire-tube force) give $\mathcal{O}(\beta_P)$ corrections. Note that this result is consistent with the ordering ansatz of (138) only if

$$\beta_P = \mathcal{O}(1)$$

in the ϵ -ordering. Since (146) implies $B_P/B_T = \mathcal{O}(\epsilon)$ for $q \sim 1$, we see that

$$\beta_T = \mathcal{O}(\epsilon^2) \quad (156)$$

for consistency of a shifted-circle equilibrium. The ordering (156) is sometimes said to refer to a “low-beta” tokamak. However the results pertain to any axisymmetric device with large aspect ratio and moderate poloidal beta.

The term “Shafranov shift” is often used to denote the displacement of the outermost flux surface, $R_c(a)$, from the geometric center of the circular vacuum chamber, $R_c(b)$:

$$\Delta_s \equiv R_c(a) - R_c(b); \quad (157)$$

this quantity is positive for the outward shift. Note we specifically assume here the existence of a vacuum “envelope” as discussed in §3.5. In view of (142),

$$\Delta_s = \int_a^b dr \frac{r}{R_c} (1 + \Lambda) \quad (158)$$

where the integrand is provided by (154). Before substitution we express (154) in more convenient form. First note that for $r > a$, the pressure vanishes and (152) allows us to write

$$1 + \Lambda = \frac{1}{2} \frac{\langle B_{P0}^2 \rangle_v(r)}{B_{P0}^2(r)} + \beta_P(r), \quad \text{for } a < r < b. \quad (159)$$

Second, observe that $\langle B_{P0}^2 \rangle_v(r) = 8U(r)/r^2$ is proportional to the poloidal magnetic field energy per unit length,

$$U(r) = 2\pi \int_0^r dr' r \frac{B_{P0}^2(r')}{8\pi};$$

while B_{P0}^2 measures the square of the driving toroidal current, I_T : $B_{P0}(r) = 2I_T(r)/cr$. It follows that the ratio $\langle B_{P0}^2 \rangle_v(r)/B_{P0}^2(r)$ measures the poloidal self-inductance per unit length of the plasma. Denoting this “internal inductance” by $l_i = 2c^2U/I_T^2$, we can express (159) as

$$1 + \Lambda(r) = \frac{1}{2} l_i(r) + \beta_P(r).$$

But in the vacuum envelope, $B_{P0}(r) \propto 1/r$, whence

$$\beta_P(r) = \beta_P(a), \quad l_i(r) = l_i(a) + 2 \ln\left(\frac{r}{a}\right), \quad \text{for } a < r < b,$$

and we have, finally,

$$1 + \Lambda(r) = \frac{1}{2} l_i(a) + \beta_P(a) + \ln\left(\frac{r}{a}\right), \quad \text{for } a < r < b. \quad (160)$$

The integral in (158) is now easy and yields

$$\Delta_s = \frac{b^2}{2R_0} \left\{ \left(1 - \frac{a^2}{b^2}\right) \left[\frac{l_i(a)}{2} + \beta_P(a) - \frac{1}{2} \right] + \ln\left(\frac{b}{a}\right) \right\}. \quad (161)$$

Here a and b , as the limiter and wall radii respectively, can be presumed known, while the internal inductance is measurable whenever the poloidal field profile can be determined. Then (161) provides a diagnostic for the plasma pressure.

Since an excessive shift will inefficiently lose plasma to the limiter scrape-off, it is customary in tokamak devices to control the shift with an externally provided, vertical magnetic field, B_v . The interaction of toroidal plasma current with B_v pushes the plasma inwards in major radius so that (161) becomes

$$\Delta_s = \frac{b^2}{2R_0} \left\{ \left(1 - \frac{a^2}{b^2}\right) \left[\frac{l_i(a)}{2} + \beta_P(a) - \frac{1}{2} \right] + \ln\left(\frac{b}{a}\right) \right\} - \frac{B_v}{B_{P0}(b)}.$$

A device with perfectly conducting walls would manufacture any needed vertical field from image currents. With conventional conductors, however, image currents typically decay within experimental times, making vertical field coils necessary. Note that the vertical field is simply a homogeneous solution to the Grad-Shafranov equation; the poloidal flux, χ , includes that of B_v . It is omitted from (160) and (161) only because of symmetries assumed in computing l_i .

3.13 Summary

A magnetic surface, or flux surface, is a smooth surface whose normal is everywhere orthogonal to the magnetic field. Thus the field lines lie

everywhere in the surface; the generic flux surface is densely covered by a single line. When the confining field never vanishes and never intersects a material wall, each flux surface must be a topological torus. Magnetic confinement is based on nested toroidal flux surfaces.

Perfect flux surfaces, corresponding to integrable magnetic fields, are an idealization. But they appear to provide a sensible approximation to physical confining fields, at least for sufficiently quiescent plasmas.

General toroidal coordinates, (r, θ, ζ) , are defined such that the radial variable, r , is constant on flux surfaces, while θ and ζ provide respectively poloidal and toroidal angle variables for the surface. Any quantity that is constant on flux surfaces, and therefore depends on position through r alone, is called a flux label.

The poloidal and toroidal magnetic fluxes Ψ_P and Ψ_T provide a general definition of rotational transform, $\iota \equiv 2\pi d\Psi_P/d\Psi_T$, which can be seen to measure the average helical pitch of a field line on the surface. An equivalent measure of field-line pitch is the safety factor, $q = 2\pi/\iota$, or $q = d\Psi_T/d\Psi_P$. Significantly, q is a flux label.

On surfaces with rational values of q , field lines are closed, and many lines are needed to cover the surface. Low-order rational magnetic surfaces have distinctive stability properties. An irrational surface is densely covered by a single line. In the presence of magnetic shear, $dq/dr \neq 0$, it is obvious that rational surfaces are exceptional.

For any set of toroidal coordinates the magnetic field can be expressed as

$$\mathbf{B} = \nabla F \times \nabla(a\theta - \zeta) + \nabla F \times \nabla G_0$$

where a and F are arbitrary flux labels and G_0 is an arbitrary function periodic in both angles. Flux coordinates are coordinates chosen to eliminate the G_0 term; with this choice, it can be shown that

$$\mathbf{B} = \nabla \chi \times \nabla(q\theta - \zeta) = \frac{1}{2\pi} (\nabla \zeta \times \nabla \Psi_P + \nabla \Psi_T \times \nabla \theta).$$

Here either form is called the flux representation of \mathbf{B} . The primary advantage of flux coordinates is that the local field-line pitch, $d\theta/d\zeta = \mathbf{B} \cdot \nabla \theta / \mathbf{B} \cdot \nabla \zeta$, becomes a flux label, equal to the global pitch. That is, $\mathbf{B} \cdot \nabla \theta / \mathbf{B} \cdot \nabla \zeta = 1/q(r)$.

Flute perturbations are constant along the magnetic field and are therefore flux labels on any irrational surface: $\mathbf{B} \cdot \nabla h = 0$. On a rational surface, a flute perturbation can depend upon the field line label, $q\theta - \zeta$, as well as r , while maintaining physical periodicity. The Fourier coefficients H_{mn} of such a perturbation satisfy $(m - nq)H_{mn}(r) = 0$. These components nicely decouple only when flux coordinates are used.

A magnetic differential equation has the form

$$\mathbf{B} \cdot \nabla f = S(\mathbf{x}),$$

where S is a prescribed source and f is to be determined. In a sheared magnetic field, the form of the source is crucially restricted; solutions can be found only if the Fourier coefficient $(S/B^\theta)_{mn} = 0$ on any rational surface where $q = m/n$.

The flux surface average of any quantity q is a volume average, over the infinitesimal shell enclosed by two neighboring flux surfaces. A radially local, normalized annihilator of the magnetic operator, the flux surface average satisfies the useful identity,

$$\langle \nabla \cdot \mathbf{A} \rangle = \frac{d}{dV} \langle \mathbf{A} \cdot \nabla V \rangle .$$

It follows that $\langle \nabla r \cdot \nabla \times \mathbf{A} \rangle = 0$, for any vector \mathbf{A} , and most importantly,

$$\langle \mathbf{B} \cdot \nabla f \rangle = 0 ,$$

for any function f .

Several sets of coordinate systems are useful in describing plasma behavior in toroidal magnetic fields. The most generally important coordinate sets are two special cases of flux coordinates: Hamada coordinates, (r_H, θ_H, ζ_H) , in which the angle variables are chosen to make the Jacobian a constant; and symmetry coordinates, (r_0, θ_0, ζ_0) , which are partially orthogonal in the sense that $\nabla \zeta_0 \cdot \nabla r_0 = 0 = \nabla \zeta_0 \cdot \nabla \theta_0$.

It can be shown that symmetry coordinates exist in axisymmetric geometry, where ζ is ignorable. Hamada coordinates can be constructed for any toroidal geometry for which the specific volume of a flux tube, $I_0 \equiv \oint ds/B$, is a flux label.

In scalar pressure equilibrium the magnetic flux surfaces become surfaces of constant pressure, or isobars. The diamagnetic current lies on the isobars, so that the total current density has no component normal to the surface: $J^r = 0$.

Effective energy confinement demands close control of plasma interaction with boundary walls. Wall contact is usually minimized by providing a low pressure envelope between the plasma and the vacuum chamber.

While the ambipolarity condition, $\langle J^r \rangle = 0$, is automatically satisfied in scalar pressure equilibrium, the (electromagnetic) quasineutrality condition,

$$\mathbf{B} \cdot \nabla \left(\frac{J_{\parallel}}{B} \right) = -\nabla \cdot \mathbf{J}_{\perp} ,$$

is usually satisfied only in the presence of return currents, parallel to \mathbf{B} . In Hamada coordinates, one finds that the quasineutrality equation, viewed as a magnetic differential equation, is soluble whenever Hamada coordinates exist.

The flux line specific volume, $I_0 \equiv \oint ds/B$, is easily shown to be a flux label in any scalar-pressure equilibrium. Thus Hamada coordinates exist. However, this result is singular in the vacuum limit, since I_0 varies

on (rational) surfaces for typical vacuum fields. Such fields are presumably subject to topology change when plasma is introduced.

The surface-averaged, covariant field components satisfy

$$\overline{B}'_\theta + q \overline{B}'_\zeta = -\frac{4\pi P'}{\chi'}$$

where the two terms on the left-hand side reflect toroidal and poloidal plasma currents respectively. The poloidal field is virtually always diamagnetic, $\overline{B}'_\theta > 0$; but the toroidal field is often paramagnetic.

The field curvature, $\kappa \equiv \mathbf{b} \cdot \nabla \mathbf{b}$, is given in general by

$$\kappa = \frac{4\pi}{\chi'} \frac{\mathbf{J} \times \mathbf{B}}{B^2} + \frac{\nabla_{\perp} B}{B}$$

and, for scalar pressure equilibrium, by

$$\kappa = \frac{1}{2B^2} \nabla_{\perp} (8\pi P + B^2).$$

The most important generalization of scalar pressure, at least with regard to equilibrium physics, is the CGL pressure tensor,

$$\mathbf{P} = \mathbf{I} P_{\perp} + \mathbf{b} \mathbf{b} P_{\Delta}$$

where $P_{\Delta} = P_{\parallel} - P_{\perp}$ measures the pressure anisotropy. Anisotropic force balance shows that neither pressure component is a flux label, unless the anisotropy vanishes. Furthermore J' does not generally vanish in the anisotropic case; indeed, even ambipolarity becomes nontrivial. The total stress tensor, including plasma pressure as well as electromagnetic stress, has the same form.

Most large confinement devices are designed to be axisymmetric. Axisymmetry simplifies various design and construction issues; it guarantees equilibrium flux-surface integrity; and it yields, typically, smaller radial transport rates. Of course it also provides relatively simple and explicit theoretical analysis.

The magnetic field in an axisymmetric toroidal system is conveniently expressed as

$$\mathbf{B} = I(r) \nabla \zeta + \nabla \zeta \times \nabla \chi,$$

where I is a flux label measuring the toroidal field, ζ is the symmetry angle and χ is the poloidal flux. The configuration of flux surfaces is described by the function $\chi(\mathbf{x})$. From Ampère's law and scalar-pressure force balance one obtains the Grad-Shafranov equation,

$$R^2 \nabla \cdot (R^{-2} \nabla \chi) = -I \frac{dI}{d\chi} - 4\pi R^2 \frac{dP}{d\chi},$$

which determines $\chi(\mathbf{x})$ for given pressure and toroidal field profiles.

The left-hand side of the Grad-Shafranov equation measures the toroidal current density: $J^\zeta = (c/4\pi)\nabla \cdot (R^{-2}\nabla \chi)$. A useful expression for the entire plasma current is given by

$$\mathbf{J} = -\frac{c}{4\pi} \frac{dI}{d\chi} \mathbf{B} - cR^2 \nabla \zeta \frac{dP}{d\chi},$$

showing that the pressure gradient drives a parallel current—the return current required by quasineutrality. Externally driven currents are implicitly included in the $dI/d\chi$ term.

The toroidal field in low beta axisymmetric systems is not always diamagnetic, in the sense of decreasing outwards from the magnetic axis. In a common case, $\beta_T \ll \beta_P \sim 1$ and confinement depends upon the poloidal field alone. In the diamagnetic case, the maximal logarithmic gradient of $I(r)$ is measured by β_T .

The field curvature in an axisymmetric system is $\kappa = \kappa_n \nabla r + \kappa_g (\nabla \zeta - q \nabla \theta)$ where

$$\kappa_n = \frac{\partial}{\partial r} \log R - \left(\frac{B_P}{B} \right)^2 R^2 \nabla \cdot (R^{-2} \nabla \mathbf{r})$$

is the normal (covariant radial) component and

$$\kappa_g = -\frac{1}{q} \left(\frac{B_T}{B} \right)^2 \frac{\partial}{\partial \theta} \log B,$$

is the geodesic (covariant toroidal) component.

The poloidal flux, χ , can be identified with the (covariant) toroidal component of the vector potential, $A_\zeta = -\chi(r, t)$. It follows that an electromagnetically induced, toroidal electric field, $E_\zeta = c^{-1} \partial \chi / \partial t$, causes poloidal flux surfaces to move radially. If $E_\zeta = E_T/R$ is a flux label, then flux surface motion occurs without change in shape—an important simplification that it often presumed to hold. The toroidal flux surfaces typically move more slowly, and the field components \mathbf{B}_P and \mathbf{B}_T need not vary in time at all.

Hoop forces and plasma pressure push the magnetic surfaces in a toroidal system outwards in major radius, compressing flux surfaces in the large- R region of the torus. In large aspect ratio geometry, the outward shift can be displayed analytically, through asymptotic solution to the Grad-Shafranov equation. The simplest case, with circular cross section and $\beta_P < 1$, is conveniently described by Shafranov coordinates, (r_S, θ_S, ζ_S) , where

$$R = R_c(r_S) + r_S \cos \theta_S, \quad \varphi = -\zeta_S, \quad Z = r_S \sin \theta_S.$$

The radial variation of $R_c(r_S)$, giving the major radius of the surface with minor radius r_S , manifests the outward shift.

By solving the Grad-Shafranov equation in zeroth order in inverse aspect ratio one finds that

$$\beta_P(a) = 1 + \frac{B_{T0}^2(a) - \langle B_{T0}^2 \rangle_v(a)}{B_{P0}^2(r)},$$

where the S -subscript is suppressed, and the angular brackets indicate a volume (radial) average. Thus the relation between toroidal diamagnetism and $\beta_P - 1$ is displayed. In first ε -order one finds that the nonconcentricity of the circular surfaces is described by

$$-\frac{R_c}{r} R'_c(r) = \frac{1}{2} \frac{\langle B_{P0}^2 \rangle_v(r)}{B_{P0}^2(r)} + 8\pi \frac{(P)_v(r) - P(r)}{B_{P0}^2(r)},$$

where self-consistency requires $\beta_P \approx 1$.

Further Reading on Confined Plasma Equilibrium:

- Bateman, 1980
- Freidberg, 1987
- Grad, 1967
- Kruskal and Kulsrud, 1958
- Newcomb, 1959
- Shafranov, 1966
- Taylor, 1974

Exercises

1. Show that the radial distance between two neighboring flux surfaces is given by $d\tau \equiv dF/|\nabla F|$, where F is any flux label. Then show that the flux surface average can be expressed as

$$\langle A \rangle = \int dS \frac{A}{|\nabla V|},$$

where dS is the area element on a magnetic surface.

2. Compute the flux surface average of $\nabla \chi \cdot \nabla \theta \times \nabla \zeta$.
3. For what value of the constant C does the differential equation

$$\frac{df}{d\theta} = \sin^2 \theta - C$$

have periodic solutions?

4. Show that Hamada coordinates exist, irrespective of force balance, in an axisymmetric system. Hint: use symmetry coordinates to evaluate the integral in (46).

5. Show explicitly that (52) follows from (51).
 6. The “standard tokamak”—a fictitious but conveniently representative device—has the following parameters:

toroidal field (B_T)	50 kG
major radius (R_0)	300 cm
minor radius (a)	80 cm
safety factor (q)	$q \approx 1$ (on axis) $q \approx 3$ (at edge)
central density (n)	10^{14} cm^{-3}
central temperature ($T_i = T_e = T$)	10 kev

Estimate (one significant figure) the following quantities in the standard tokamak:

- (a) toroidal plasma current;
 - (b) diamagnetic current density;
 - (c) return current density.
7. Estimate β and β_P in the standard tokamak.
 8. Estimate the thermal (plasma) energy in the standard tokamak, in Joules. Assume the volume-averaged density and temperature are about half their central values. Compare your result to the thermal energy in a cup of coffee and to the electrical energy in a 60 Amp-hr automobile battery.
 9. Show, using (63) and Ampere's law, that \mathbf{J}_\perp has the correct direction to be called a “diamagnetic” current.
 10. Virial theorem. Use the identity
- $$\partial(x_\beta A_{\alpha\beta})/\partial x_\alpha = A_{\alpha\alpha} + x_\beta \partial A_{\alpha\beta}/\partial x_\alpha ,$$
- for any tensor with Cartesian components $A_{\alpha\beta}$, to deduce the integral relation
- $$\int_V d^3x T_{\alpha\alpha} = \int_S d^2x n_\alpha T_{\alpha\beta} x_\beta$$
- where \mathbf{T} is the total stress tensor of §3.8 and V is an arbitrary volume with boundary S . Use this result to conclude that confined plasma equilibrium requires external conductors. See (Shafranov, 1966).
11. Large aspect-ratio flux coordinates. Find approximate symmetry coordinates, the special choice of flux coordinates discussed in §3.4, for the shifted-circle geometry considered in §3.12, as follows. Distinguishing the flux and Shafranov coordinates with “ f ” and “ S ” subscripts respectively, show that through $O(\epsilon)$ we must have
- $$r_f = r_S , \quad \theta_f = \theta_S + \epsilon P(\theta_S) , \quad \zeta_f = \zeta_S ,$$

- Then find the periodic function P by imposing (56), dropping $\mathcal{O}(\varepsilon^2)$.
12. Use (78) to show that an axisymmetric system without poloidal field cannot satisfy force balance. It follows that any system lacking poloidal magnetic field must be asymmetric; such devices are called bumpy tori.
 13. **Elliptic geometry.** In the simplest example of noncircular tokamak geometry, the magnetic surfaces are elliptical in poloidal cross-section (Harris, 1974). [Note that conventional Shafranov geometry becomes slightly elliptical when $\mathcal{O}(\varepsilon^2)$ -terms are included.] For large aspect-ratio and moderate beta, the corresponding equilibrium is similar to that of Shafranov, the flux-surfaces being approximately described by shifted ellipses.

Examine shifted-ellipse case, in a manner parallel to §3.12, as follows:

- (i) Choose coordinates (r_e, θ_e, ζ_e) such that [in the notation of (133)]

$$R = R_e(r_e) + r_e \cos \theta_e , \quad \varphi = -\zeta_e , \quad Z = \kappa r_e \sin \theta_e .$$

Here the elongation parameter κ is a number of order unity.

- (ii) After assuming the the poloidal flux depends mainly on r_e , as in (137), express the Grad-Shafranov equation in terms of (r_e, θ_e, ζ_e) . Neglect $\mathcal{O}(\varepsilon^2)$ terms as usual.
- (iii) Decompose this result into $\cos(m\theta)$ -components, with $m = 0, 1, 2$, and 3. Your $m = 2$ component should have the form

$$(\kappa^2 - 1) \left[\frac{1}{2} (r_e \chi')' - \chi' \right] = 0 ,$$

requiring, for $\kappa \neq 1$,

$$\chi \propto r_e^2 .$$

This fixed radial form for the poloidal flux is the salient characteristic of the large aspect-ratio, shifted-ellipse geometry.

Chapter 4

Kinetic Description of a Magnetized Plasma

4.1 General Kinetic Equation

Electrodynamical Closure

Any physical theory must provide a *closed*, predictive system, from which all unknown quantities can in principle be determined. The key closure issue in plasma physics concerns Maxwell's equations, which become a closed system for the electrodynamic field only when the sources—the electric current and charge densities—are appropriately specified. Usually Maxwellian closure is provided by *constitutive relations*. These specify the sources in terms of the fields,

$$\rho_c = \hat{\rho}_c[\mathbf{E}, \mathbf{B}; \mathbf{x}, t], \quad (1)$$

where ρ_c is the charge density, \mathbf{J} is the current density and the right-hand sides represent operators on the fields. The operators may be nonlinear and nonlocal, and, as indicated, they may explicitly depend on (\mathbf{x}, t) . Evidently a salient objective of plasma physics is to determine constitutive relations.

In a formal sense, kinetic theory meets this objective directly: it provides, for each particle species in the plasma, a *distribution function* $f_s(\mathbf{x}, \mathbf{v}, t)$, such that $f_s(\mathbf{x}, \mathbf{v}, t)d\mathbf{x}d\mathbf{v}$ is the number of species- s particles near point \mathbf{x} , having velocity \mathbf{v} , at time t . Then we have

$$\begin{aligned} \rho_c(\mathbf{x}, t) &= \sum_s e_s \int d^3 v f_s(\mathbf{x}, \mathbf{v}, t), \\ \mathbf{J}(\mathbf{x}, t) &= \sum_s e_s \int d^3 v \mathbf{v} f_s(\mathbf{x}, \mathbf{v}, t), \end{aligned} \quad (2)$$

where e_s is the charge of species s . Thus it suffices to determine each f_s , as a function or functional of the fields, \mathbf{E} and \mathbf{B} .

The *kinetic equation* for each distribution specifies its evolution in terms of given fields,

$$\mathcal{K}(\mathbf{E}, \mathbf{B}; \mathbf{x}, \mathbf{v}, t) \cdot f = 0 , \quad (3)$$

thus allowing closure in principle. In (3) \mathcal{K} represents an operator (generally an integro-differential operator) on f , whose form will be considered presently; species subscripts are suppressed.

Because its solution evidently closes Maxwell's equations, (3) is an obvious central focus of theoretical plasma physics. Yet a closure strategy based exclusively on (3) is rarely effective, for two complementary reasons. First, kinetic theory, set in the six dimensions of phase space, is difficult: analytic solutions to (3) are rare and numerical ones expensive. Second, attacking the closure problem through (3) is inefficient. For closure requires only the two lowest *moments* of f : its zeroth moment, the density,

$$n \equiv \int d^3 v f ,$$

and its first moment, the flow velocity,

$$n\mathbf{V} \equiv \int d^3 v f \mathbf{v} .$$

Of course the solution to (3) contains enormously more information. In other words, the distribution function itself does not matter: closure of Maxwell's equations involves only an equivalence class of distributions, whose members, however various, have the same density and flow.

Practical closure strategies avoid confronting the full kinetic equation any more than is necessary. Usually one attempts to express the two necessary moments in terms of other, more accessible quantities. In the end (3) must be consulted, but only in approximate form. That is, one finds a way to compute the charge and current densities to sufficient accuracy from rather crude, but relatively tractable, kinetic theory.

In Chapter 6 we show explicitly how moments of (3) can be manipulated to reduce the burden on kinetic theory. Our main objective here is to derive useful approximations to the kinetic equation. We take advantage in particular of a small parameter that always pertains to a magnetized plasma: the gyroradius. However, it is helpful to begin by considering the exact version of the operator \mathcal{K} .

Microscopic Kinetic Equation

Suppose for simplicity that atomic and nuclear reactions are absent, so that the particles of each plasma species are conserved. Then each distribution function must be constant along particle trajectories:

$$\frac{\partial f}{\partial t} + \mathbf{v} \cdot \nabla f + \mathbf{a} \cdot \frac{\partial f}{\partial \mathbf{v}} = 0 , \quad (4)$$

where \mathbf{a} , the acceleration, is given by the Lorentz force (2.45):

$$\mathbf{a}(\mathbf{x}, \mathbf{v}, t) = \frac{d\mathbf{v}}{dt} = \frac{e}{m} \left[\mathbf{E}(\mathbf{x}, t) + \frac{1}{c} \mathbf{v} \times \mathbf{B}(\mathbf{x}, t) \right]. \quad (5)$$

Here e and m are the particle charge and mass; the species label is suppressed.

The form of (4) presumes that f is expressed in terms of the Cartesian phase-space variables; however, the generalization to arbitrary coordinates is straightforward. Observe that the left hand side of (4) measures the change of f along a particle trajectory:

$$f[\mathbf{x}(t), \mathbf{v}(t), t] - f[\mathbf{x}(t - \Delta t), \mathbf{v}(t - \Delta t), t - \Delta t].$$

This (scalar) difference is modified in an obvious way when the trajectories are expressed in terms of non-Cartesian coordinates, $z^i, i = 1, \dots, 6$: $f[z_i(t), t] - f[z_i(t - \Delta t), t - \Delta t]$. Thus we obtain the kinetic equation

$$\frac{\partial f}{\partial t} + \frac{dz^i}{dt} \frac{\partial f}{\partial z^i} = 0,$$

where a sum over the repeated index is implied. The z^i can be any smooth functions of \mathbf{x} and \mathbf{v} , so long as the transformation $(\mathbf{x}, \mathbf{v}) \rightarrow (z^1, \dots, z^6)$ is nonsingular.

Of course the forces in (4) include not only externally imposed forces, but also the full electromagnetic interactions of all the particles in the system. Thus the function $\mathbf{a}(\mathbf{x}, \mathbf{v}, t)$, depending upon the positions and velocities of all the particles, is not only pathologically jagged (varying on all spatial and temporal scales down to the classical limit) but also essentially indeterminate. We refer to such forces, and to the corresponding distribution f , as microscopic. The useful force and distribution are averaged quantities:

$$\bar{f} \equiv \langle f \rangle_{\text{ensemble}}, \quad \bar{\mathbf{a}} \equiv \langle \mathbf{a} \rangle_{\text{ensemble}}.$$

These are smooth functions, expressing the pertinent physics of an ensemble of macroscopically equivalent plasmas.
Unfortunately the evolution of \bar{f} is not simply determined by $\bar{\mathbf{a}}$. An ensemble average of the kinetic equation

$$\frac{\partial \bar{f}}{\partial t} + \mathbf{v} \cdot \nabla \bar{f} + \left\langle \mathbf{a} \cdot \frac{\partial f}{\partial \mathbf{v}} \right\rangle = 0$$

shows that \bar{f} would decouple from the fluctuation $(\mathbf{a} - \bar{\mathbf{a}})$ only if \mathbf{a} and f were statistically independent—i.e., only in the absence of interactions. In the interacting case $\left\langle \mathbf{a} \cdot \frac{\partial f}{\partial \mathbf{v}} \right\rangle \neq \bar{\mathbf{a}} \cdot \frac{\partial f}{\partial \mathbf{v}}$ and an equation of the form of (4) no longer pertains.

A statistical accounting of the interactions, or particle *collisions*, is the primary task of classical kinetic theory. It provides an approximate, closed, *kinetic equation* for the mean distribution \bar{f} . All kinetic equations have the form

$$\frac{\partial f}{\partial t} + \mathbf{v} \cdot \nabla f + \mathbf{a} \cdot \frac{\partial f}{\partial \mathbf{v}} = C(f), \quad (6)$$

where the overbars are suppressed, and where C denotes the so-called collision operator, accounting for the residual effects of particle correlations. There is no exact version of the collision operator, but only a sequence of more accurate (and less tractable) forms. Fortunately the most useful versions—always closely related to the well-known Fokker-Planck operator—lead to roughly similar predictions.

Equation (6) is traditionally named according to which version of the collision operator it contains. Thus one has, for example, the “Boltzmann equation,” or, in the case we will focus on presently, the “Fokker-Planck equation.” For the present, however, it is convenient to leave C unspecified, supposing only that it represents collisional effects accurately. We can then assume that (6), or its more general version,

$$\frac{\partial f}{\partial t} + \frac{d\mathbf{z}^i}{dt} \frac{\partial f}{\partial \mathbf{z}^i} = C, \quad (7)$$

includes the physics on all scales of practical interest. Hereafter we shall refer to (7) as the “exact” or “general” kinetic equation.

Small Gyroradius Ordering

By a *magnetized plasma* we mean, roughly, one much larger than the gyroradii of its constituent charged particles. Thus if L is the scale length characterizing the plasma, and ρ a thermal gyroradius, then the plasma is magnetized if the parameter

$$\delta \equiv \frac{\rho}{L} \quad (8)$$

is much less than one [recall (2.61)].

Unfortunately the simple statement

$$\delta \ll 1 \quad (9)$$

leaves open several detailed ordering issues of importance. Equation (6) provides a convenient context for studying such details; for this reason, and to prepare for later derivation of approximate forms of (6), we next consider each of its terms.

Of course the largest term in (6) is that corresponding to Larmor gyration:

$$\frac{e}{mc} \mathbf{v} \times \mathbf{B} \cdot \frac{\partial f}{\partial \mathbf{v}} \sim \Omega f,$$

where Ω is the gyrosfrequency, (2.55):

$$\Omega_s \equiv \frac{e_s B}{m_s c} \quad (10)$$

for plasma species s . We use Ω , together with the thermal speed, (2.55),

$$v_{ts} \equiv \left(\frac{2T_s}{m_s} \right)^{1/2}, \quad (11)$$

to explicitly define the thermal gyroradius

$$\rho_s \equiv \frac{v_{ts}}{\Omega_s}. \quad (12)$$

We assume that all species temperatures are comparable; then the gyroradii of all ion species may be presumed comparable, while the electron gyroradius is smaller according to

$$\rho_e \sim \left(\frac{m_e}{m_i} \right)^{1/2} \rho_i. \quad (13)$$

Evidently the same distinction pertains to the parameter δ ; we will call a plasma magnetized only if its ions are magnetized,

$$\delta_i \sim \left(\frac{m_i}{m_e} \right)^{1/2} \delta_e \ll 1.$$

Sometimes, especially in the experimental literature, a plasma is called magnetized only if its collision frequency ν , where

$$Cf \sim \nu f,$$

is small compared to Ω . Without adopting this usage, we nonetheless assume

$$\frac{\nu}{\Omega} \sim \delta, \quad (14)$$

a condition that almost always pertains in practice.

Note that in (14) and below the symbol “~” is used in the asymptotic sense. Thus (14) is synonymous with $\nu/\Omega = \mathcal{O}(\delta)$ and allows as a special case $\nu/\Omega \ll \delta$.

The partial time derivative in (6) will be assumed small in the sense

$$\frac{\partial f}{\partial t} \sim \delta \Omega f. \quad (15)$$

This conservative ordering does not apply to certain auxiliary heating schemes, in which external radiation is tuned to resonate with gyration, but otherwise describes plasma motions of interest. The stronger version

$$\frac{\partial f}{\partial t} \sim \delta^3 \Omega f, \quad (16)$$

is called the *transport ordering* and will be seen to describe a quiescent plasma, evolving according to collisional dissipation alone.

The convective term, $\mathbf{v} \cdot \nabla f$, is more complicated, since plasma motions can involve disparate lengths. We must distinguish between a slow scale length, denoted by L , and a fast scale length, denoted by λ . Thus L might measure a toroidal minor radius, or density gradient scale-length, while λ could refer to the wave length of a linear disturbance, or the thickness of some boundary layer. We will assume that confined plasma equilibrium varies exclusively on the slow scale, L ; any fast variation will be associated with small, but not necessarily linear, departures from equilibrium. (Note that not all perturbations vary rapidly; many important disturbances have scale-lengths indistinguishable from those of the equilibrium.) Scale separation affects the present ordering arguments only if the fast scale is comparable to the Larmor radius,

$$\lambda \sim \rho , \quad (17)$$

as can occur in the ion case [it rarely describes electron dynamics: recall (13)]. Thus we decompose the distribution into terms varying slowly (f_{slow}) and rapidly (f_{fast}):

$$f = f_{\text{slow}} + \Delta f_{\text{fast}} . \quad (18)$$

Here we have introduced a parameter Δ , measuring the amplitude of the rapidly varying perturbation. Note that we must have $\Delta \ll 1$: the plasma is just as effectively demagnetized by $\Delta \sim 1$ as by $\delta \sim 1$.

It is convenient to express $\mathbf{v} \cdot \nabla f$ in terms of the *transit frequency*,

$$\omega_t \equiv \frac{v_t}{L} . \quad (19)$$

Then (18) yields

$$\mathbf{v} \cdot \nabla f \sim \omega_t f_{\text{slow}} + \Delta \Omega f_{\text{fast}} . \quad (20)$$

Notice that

$$\frac{\omega_t}{\Omega} = \delta ,$$

so the two terms in (20) are of order δ and Δ .

Acceleration due to \mathbf{E} is usefully decomposed into components parallel and perpendicular to \mathbf{B} :

$$\mathbf{E} = \mathbf{b} E_{\parallel} + \mathbf{E}_{\perp} \equiv \mathbf{E}_{\parallel} + \mathbf{E}_{\perp} .$$

The contribution from E_{\parallel} is described by

$$\frac{e}{m} \mathbf{E}_{\parallel} \cdot \frac{\partial f}{\partial \mathbf{v}} \sim \frac{e}{m} \frac{E_{\parallel}}{v_t} f \equiv \nu_E f . \quad (21)$$

The natural ordering

$$\frac{\nu_E}{\Omega} \sim \delta \quad (22)$$

is not only in accord with experiment, but mandatory, if we wish to treat situations near equilibrium. The point is that only two terms in (6) affect acceleration in the direction of the magnetic field: the collisional term, and the ν_E -term. We have treated the former as $\mathcal{O}(\delta)$; if the latter is larger, $\nu_E/\Omega \sim 1$, then the lowest order parallel dynamics consists of free acceleration along \mathbf{B} . Such unbalanced acceleration (charged-particle “runaway”) is inconsistent with any approach to equilibrium.

The perpendicular components,

$$\mathbf{E}_\perp \equiv \mathbf{E} - \mathbf{E}_\parallel \quad (23)$$

are expressed in terms of the $\mathbf{E} \times \mathbf{B}$ drift,

$$\mathbf{V}_E \equiv c \frac{\mathbf{E} \times \mathbf{B}}{B^2},$$

yielding the estimate $(e/m)\mathbf{E}_\perp \cdot \partial f / \partial \mathbf{v} = (V_E/v_t)\Omega f$. There are two cases of interest: the *drift ordering*,

$$\frac{V_E}{v_t} \sim \delta, \quad (24)$$

and the *MHD ordering*,

$$\frac{V_E}{v_t} \sim 1. \quad (25)$$

Clearly the two assumptions, (24) and (25), lead to quite different pictures of plasma evolution. In the MHD-ordered case, electric drifts, with their associated nonlinear inertial terms (such as centrifugal force), dominate the dynamics; in the drift ordering, the electric drift enters only in concert with other slow motions, such as the curvature or gradient- B drifts. While the most violent perturbations may be described by (25), the more prevalent ones, at least in modern confinement devices, are consistent with (24). Indeed, the replacement of (25) by (24) as the more realistic ordering is one indicator of progress in plasma confinement: even tokamak disruptions are not fast enough for the MHD ordering.

One consequence of the drift ordering is to forbid rapid time variation of the magnetic field. For, if \mathbf{A} is the vector potential,

$$\mathbf{B} = \nabla \times \mathbf{A}, \quad (26)$$

then \mathbf{B} and \mathbf{A} clearly vary on the same time scale. Since \mathbf{A} contributes to \mathbf{V}_E through $(\partial \mathbf{A} / \partial t) \times \mathbf{B}$, the drift ordering requires $(\partial \mathbf{A} / \partial t) \times \mathbf{B} / B^2 \sim \delta v_t$, or, in view of (26),

$$\frac{1}{B} \frac{\partial B}{\partial t} \sim \delta \omega_t = \delta^2 \Omega. \quad (27)$$

It follows in particular that the drift ordering is electrodynamically consistent with the transport ordering of (16).

A simpler characterization of both electric field terms is possible in the electrostatic (or predominantly electrostatic) case. Thus, if \mathbf{E} is estimated by $-\nabla\Phi$, then

$$\frac{e}{m} \mathbf{E} \cdot \frac{\partial f}{\partial \mathbf{v}} \sim \frac{e\Phi}{T} \left(\omega_t + \frac{\Delta v_t}{\lambda} \right) f, \quad (28)$$

where we allow for both spatial scales, as in (20), and normalize the potential by the thermal energy, T . In view of (17) we have

$$\frac{e}{m} \mathbf{E} \cdot \frac{\partial f}{\partial \mathbf{v}} \sim \frac{e\Phi}{T} \Omega (\delta + \Delta) f.$$

Here the first term reproduces (24) while the second, proportional to Δ , allows for rapid variation of Φ .

Let us summarize our results. For a magnetized plasma, the various operators in the exact kinetic equation, (6), are ordered as follows:

$$\begin{aligned} & \frac{e}{mc} \mathbf{v} \times \mathbf{B} \cdot \frac{\partial}{\partial \mathbf{v}} \sim \Omega ; \\ & \frac{\partial}{\partial t} \sim \delta\Omega, C \sim \nu \sim \delta\Omega ; \\ & \mathbf{v} \cdot \nabla \sim \omega_t + \frac{\Delta v_t}{\lambda} \sim (\delta + \Delta)\Omega ; \\ & \frac{e}{m} E_{\parallel} \cdot \frac{\partial}{\partial \mathbf{v}} \sim \delta\Omega, \frac{e}{m} E_{\perp} \cdot \frac{\partial}{\partial \mathbf{v}} \sim \frac{V_E}{v_t} \Omega . \end{aligned} \quad (29)$$

There are three cases in which the kinetic equation can be approximately solved. The simplest has neither fast variation nor rapid $\mathbf{E} \times \mathbf{B}$ motion,

$$\Delta = 0, \frac{V_E}{v_t} \sim \delta. \quad (30)$$

In this drift-ordered case, all terms in the kinetic equation are of order δ compared to gyration. The corresponding approximation to (6) is called the *drift-kinetic* equation; it is derived in the following subsection. The drift-ordering has especially wide application; it describes confined plasma equilibrium, as well as transport processes and a wide variety of plasma instabilities.

The MHD-ordered case assumes slow variation, but permits $\mathbf{E} \times \mathbf{B}$ motion rapid enough to compete with gyration:

$$\Delta = 0, \frac{V_E}{v_t} \sim 1. \quad (31)$$

(If the E were both large and electrostatic, it would have to vary on the fast scale, so strictly speaking we must rule out large electrostatic fields.) The corresponding kinetic theory is rather complicated in general (Rosenbluth

and Rostoker, 1958), but relatively simple in the linear limit, essentially because the MHD particle velocity is simply

$$\mathbf{v} \cong \mathbf{V}_E + \mathbf{b} v_{\parallel} .$$

The MHD-ordered *fluid* theory—called simply MHD—is of special importance and usefulness; it is studied in Chapter 7.

Finally, the gyro-ordered case forbids large V_E while allowing sharp variation of all perturbations. As we have remarked, it is rarely applicable to electron kinetic theory: few disturbances of interest vary on the scale of ρ_e . While the small parameter Δ is usually treated as independent of δ , there are mild advantages in assuming

$$\Delta \sim \delta , \quad \frac{V_E}{v_t} \sim \delta . \quad (32)$$

The approximate kinetic equation derived from (6) and (32) is the *gyrokinetic equation*. It is used to study those plasma instabilities whose wavelengths are comparable to ρ . We derive the gyrokinetic equation in §4.3.

4.2 Drift-kinetic Equation

Distribution of Guiding Centers

A kinetic equation describing magnetized plasma motions is much simpler than (6) because it suppresses details of the short scale-length of gyration: it is averaged over the gyro-scale. When the orbit of a gyrating particle is averaged in this way, what survives is a drifting magnetic dipole—the guiding center studied in Chapter 2. The distribution of guiding centers will be denoted by \bar{f} , where the overbar refers to the gyrophase average.

We recall from Chapter 2 that the guiding-center drift is dominated by simple streaming along \mathbf{B} ,

$$\mathbf{v}_{gc} = \mathbf{b} v_{\parallel} + \mathcal{O}(\delta) ; \quad (33)$$

its higher order version, $\mathbf{v}_{gc} = \mathbf{b} v_{\parallel} + \mathbf{v}_D + \mathcal{O}(\delta^2)$, is given by (2.87):

$$\mathbf{v}_D = \mathbf{V}_E + \frac{1}{\Omega} \mathbf{b} \times \left(\frac{\mu}{m} \nabla B + v_{\parallel}^2 \boldsymbol{\kappa} + v_{\parallel} \frac{\partial}{\partial t} \mathbf{b} \right) \quad (34)$$

The magnetic (dipole) moment of a guiding center is $\boldsymbol{\mu} = -\mathbf{b}\mu$, where [recall (2.88)]

$$\mu = \frac{mv_{\perp}^2}{2B} .$$

In view of (2.89) we may assume

$$\frac{d\mu}{dt} = \mathcal{O}(\delta). \quad (35)$$

Because of (35), gyration becomes an “internal” process, analogous to electron spin. It is coupled to external degrees of freedom by means of the mirror force of (2.86),

$$\mathbf{F}_m = -\nabla(\mu B). \quad (36)$$

The corresponding potential energy, μB , adds to the electrostatic energy $e\Phi$ to produce the total guiding-center energy,

$$U = \frac{mv_{||}^2}{2} + e\Phi + \mu B, \quad (37)$$

since, as in (33), $mv_{||}^2/2$ is the (lowest order) guiding-center kinetic energy. This quantity evolves according to

$$\frac{dU}{dt} = e \frac{d\Phi}{dt} + \mu \frac{dB}{dt} + \mathbf{v}_{gc} \cdot (e\mathbf{E} + \mathbf{F}_m), \quad (38)$$

assuming that the change in kinetic energy is given by the usual product of force and velocity; here the derivatives are taken along the guiding-center trajectory, $d/dt = \partial/\partial t + \mathbf{v}_{gc} \cdot \nabla$. In view of (35) and Faraday’s law, (2.46),

$$\mathbf{E} = -\nabla\Phi - \frac{1}{c} \frac{\partial \mathbf{A}}{\partial t}, \quad (39)$$

where \mathbf{A} is the vector potential, the guiding-center change of energy is

$$\frac{dU}{dt} = e \frac{\partial\Phi}{\partial t} + \mu \frac{\partial B}{\partial t} - \frac{e}{c} \mathbf{v}_{gc} \cdot \frac{\partial \mathbf{A}}{\partial t}. \quad (40)$$

Note that (40) is equivalent to $dU/dt = \partial U/\partial t$, reflecting the Hamiltonian character of guiding-center motion; recall §2.4.

Each guiding center can be specified by its position, its magnetic moment and its energy: (\mathbf{x}, μ, U) . Only two velocity variables are needed because the gyration angle has been averaged away. Hence, as in (7), the distribution of guiding centers evolves according to

$$\frac{\partial \bar{f}}{\partial t} + \mathbf{v}_{gc} \cdot \nabla \bar{f} + \frac{dU}{dt} \frac{\partial \bar{f}}{\partial U} + \frac{d\mu}{dt} \frac{\partial \bar{f}}{\partial \mu} = C. \quad (41)$$

The only unknown coefficient in (41) is $d\mu/dt$; as noted in (35), this quantity can be comparable to the other coefficients, because the μ of (35) is only a lowest order approximation to the magnetic moment. However, in the drift-kinetic context, it is almost always neglected, for two reasons.

First, detailed calculation shows that the estimate of (35) can be refined to give

$$\frac{d\mu}{dt} = \mathcal{O}(\beta\delta) \quad (42)$$

where $\beta = 8\pi p/B^2$ is small in most cases. Second, for the most important applications, the lowest order distribution is isotropic in velocity space, depending only on position and energy. Then the derivative $\partial\bar{f}/\partial\mu$ becomes first order and we have

$$\frac{d\mu}{dt} \frac{\partial\bar{f}}{\partial\mu} = \mathcal{O}(\delta^2\beta) . \quad (43)$$

This quantity is negligible compared to the other terms in (41).

The drift-kinetic equation therefore has the approximate form

$$\frac{\partial\bar{f}}{\partial t} + (\mathbf{v}_\parallel + \mathbf{v}_D) \cdot \nabla \bar{f} + \left[e \frac{\partial\Phi}{\partial t} + \mu \frac{\partial B}{\partial t} - \frac{e}{c} \mathbf{v}_\parallel \cdot \frac{\partial \mathbf{A}}{\partial t} \right] \frac{\partial\bar{f}}{\partial U} = C . \quad (44)$$

Here we have recalled (40) and omitted terms of order δ^3 or $\delta^2\beta$.

Perturbation Theory

Next we embark on a more formal derivation of the drift-kinetic equation. Our purpose is to verify such statements as (38) and (42), and also to obtain certain intermediate results that turn out to be widely useful. In particular we derive an expression for the gyrophase-dependent part of the distribution,

$$\tilde{f} = f - \bar{f} , \quad (45)$$

that has several applications.

We represent the velocity as

$$\mathbf{v} = \mathbf{u} + \mathbf{s} , \quad (46)$$

where

$$\mathbf{u} \equiv \mathbf{b}v_\parallel = \mathbf{b}\mathbf{u}_\parallel , \quad (47)$$

$$\mathbf{s} \equiv \mathbf{v}_\perp = s(\mathbf{e}_2 \cos \gamma - \mathbf{e}_3 \sin \gamma) = s\hat{\mathbf{s}} .$$

The gyrophase angle, γ , is defined as in §2.4, and following (2.58) the unit vectors $(\mathbf{b}, \mathbf{e}_2, \mathbf{e}_3)$ are orthogonal and right-handed. We also abbreviate the vector gyroradius as

$$\rho = \frac{\mathbf{b} \times \mathbf{s}}{\Omega} = \rho(\mathbf{e}_2 \sin \gamma + \mathbf{e}_3 \cos \gamma) = \rho\hat{\rho} . \quad (48)$$

It can be seen (Fig. 2.3) that ρ indeed follows the particle in its gyromotion. The Lorentz equation of motion, (2.45), is then expressed as

$$\frac{d}{dt}(\mathbf{u} + \mathbf{s}) = \frac{e}{m} \mathbf{E} - \Omega s \hat{\rho} . \quad (49)$$

Here and below the notation d/dt is reserved for the time derivative following the exact (not guiding-center) orbit.

Multiplication of (49) by \mathbf{s} , \mathbf{v} , and $\hat{\rho}$ yields, respectively,

$$\frac{d\mu}{dt} = -\frac{\mu}{B} \frac{dB}{dt} - \frac{mu}{B} \mathbf{s} \cdot \frac{d\mathbf{b}}{dt} + \frac{e}{B} \mathbf{s} \cdot \mathbf{E} \quad (50)$$

$$\frac{dU}{dt} = e \frac{\partial \Phi}{\partial t} - \frac{\mathbf{v}}{c} \cdot \frac{\partial \mathbf{A}}{\partial t} \quad (51)$$

and

$$\frac{d\gamma}{dt} = \Omega + \mathbf{e}_3 \cdot \frac{d\mathbf{e}_2}{dt} - \frac{u}{s} \hat{\rho} \cdot \frac{d\mathbf{b}}{dt} - \frac{e}{ms} \hat{\rho} \cdot \mathbf{E}. \quad (52)$$

Equations (50) and (51) follow quickly from (49), but the derivation of (52), whose right-hand side begins with the “gyro-term,” Ω , is somewhat more complicated. First note that $\hat{\rho} \cdot d\mathbf{u}/dt = u \hat{\rho} \cdot d\mathbf{b}/dt$ and

$$\hat{\rho} \cdot \frac{d\mathbf{s}}{dt} = s \hat{\rho} \cdot \frac{d}{dt} (\mathbf{e}_2 \cos \gamma - \mathbf{e}_3 \sin \gamma).$$

Then, since $\mathbf{e}_3 \cdot d\mathbf{e}_2/dt = -\mathbf{e}_2 \cdot d\mathbf{e}_3/dt$, $\mathbf{e}_2 \cdot d\mathbf{e}_2/dt = 0$, and so on, we find

$$\hat{\rho} \cdot \frac{d\mathbf{s}}{dt} = -s \frac{d\gamma}{dt} + s \mathbf{e}_3 \cdot \frac{d\mathbf{e}_2}{dt}$$

and the result, (52), follows.

At this point we explicitly adopt the drift-kinetic orderings of (29) and (30). These imply that all terms on the right-hand sides of (50)–(52), with the obvious exception of the gyro-term in (52), are $\mathcal{O}(\delta)$:

$$\frac{1}{\Omega} \frac{d\mu}{dt} = \mathcal{O}(\delta), \quad \frac{1}{\Omega} \frac{dU}{dt} = \mathcal{O}(\delta)$$

and

$$\frac{1}{\Omega} \frac{d\gamma}{dt} = 1 + \mathcal{O}(\delta).$$

Hence the kinetic equation (7) can be expressed as

$$\frac{\partial \tilde{f}}{\partial \gamma} = -\frac{(\mathcal{L} - C)}{\Omega} f \quad (53)$$

where the operator

$$\mathcal{L} = \mathbf{v} \cdot \nabla + \frac{d\mu}{dt} \frac{\partial}{\partial \mu} + \frac{dU}{dt} \frac{\partial}{\partial U} + \left(\frac{d\gamma}{dt} - \Omega \right) \frac{\partial}{\partial \gamma}$$

contains only slow coefficients:

$$\mathcal{L} \sim C \sim \delta\Omega . \quad (54)$$

Note that this ordering of the operators is meaningful only if f varies on scales longer than the gyroradius. That is, if we allowed $\nabla f \sim f/\rho$, then $\mathcal{L}f \sim \mathbf{v} \cdot \nabla f \sim \Omega f$, and all terms in (53) would be formally comparable. Similarly the μ and U variation of f must be moderate: $\mu \partial f / \partial \mu \sim U \partial f / \partial U \sim 1$.

Equation (53) is an exact transcription of (7); so far, we have only transformed the coordinates. The drift-kinetic equation is obtained from (53) by averaging over the gyrophase, taking into account the γ -dependence of both f and the coefficients. The gyrophase average is explicitly defined by (2.66):

$$\overline{A} = \langle A \rangle \equiv \oint \frac{d\gamma}{2\pi} A(\mathbf{x}, U, \mu, \gamma) \quad (55)$$

the integral being performed at fixed \mathbf{x} , U and μ as indicated. We also at this point specifically identify the distribution of guiding centers with the gyrophase-averaged distribution, $\langle f \rangle = \tilde{f}$.

Two conclusions can be drawn from (53). First, the gyrophase-dependent distribution, $\tilde{f} = f - \bar{f}$ must be relatively small. Indeed, since only f enters the left-hand side, it is clear that

$$\tilde{f} \sim \delta\bar{f} . \quad (56)$$

The second conclusion from (53) is the solvability condition,

$$((\mathcal{L} - C)f) = 0 , \quad (57)$$

which follows from the periodicity of f with respect to γ . Equation (57) is an abstract form of the drift-kinetic equation; its relation to (44) is considered presently.

The lowest order form of (57) has some interest. If we use (56) to neglect \tilde{f} , then we find

$$\langle (\mathcal{L} - C)\tilde{f} \rangle = \overline{\mathcal{L}}\tilde{f} - \overline{C}\tilde{f} = 0 . \quad (58)$$

From (50)–(52) we find

$$\left\langle \frac{d\mu}{dt} \right\rangle = -\frac{\mu}{B} \frac{\partial B}{\partial t}$$

$$\left\langle \frac{dU}{dt} \right\rangle = e \left(\frac{\partial \Phi}{\partial t} - \frac{\mathbf{u}}{c} \cdot \frac{\partial \mathbf{A}}{\partial t} \right)$$

whence

$$\overline{\mathcal{L}} = \frac{\partial}{\partial t} + \mathbf{u} \cdot \nabla - \frac{\mu}{B} \frac{\partial B}{\partial t} \frac{\partial}{\partial \mu} + e \left(\frac{\partial \Phi}{\partial t} - \frac{\mathbf{u}}{c} \cdot \frac{\partial \mathbf{A}}{\partial t} \right) \frac{\partial}{\partial U} . \quad (59)$$

Although the drift kinetic equation given by (58) and (59) is easily interpreted, it is too crude for most applications. In particular, it misses the guiding-center drift \mathbf{v}_D of (34). To capture such first order effects, we need to include \tilde{f} .

Gyrophase Dependence

We next approximately solve (53) for \tilde{f} as function of \tilde{f} . Our procedure is recursive, rather than perturbative; that is, we derive a single equation, including the effects of various δ -orders, rather than a sequence of equations for the various contributions (f_0, f_1, \dots) to f . The result is not markedly more accurate than that of conventional perturbation theory, but it is substantially more convenient.

In a perturbative theory, one would use (56) to replace f by \bar{f} on the right-hand side of (53):

$$\Omega \frac{\partial \tilde{f}}{\partial \gamma} = -(\mathcal{L} - C)\bar{f}.$$

However, this equation has as its solvability condition (58), which we have found to be insufficiently accurate. To obtain a more accurate equation, terms of the second order would have to be considered (similarly to the analysis in §2.4). The recursive theory proceeds from the equivalent, exact relation

$$\Omega \frac{\partial \tilde{f}}{\partial \gamma} = -(\mathcal{L} - C)f + \langle (\mathcal{L} - C)f \rangle,$$

Now approximating f by \bar{f} yields

$$\Omega \frac{\partial \tilde{f}}{\partial \gamma} = -(\mathcal{L} - C)\bar{f} + \langle (\mathcal{L} - C)\bar{f} \rangle \quad (60)$$

a differential equation whose solvability is guaranteed for any \tilde{f} . Equation (60) constitutes a first recursion in the solution of (53); fortunately no additional recursions are necessary.

While we have yet to discuss, or even specify, a collision operator C , we anticipate the fact that the difference $C\bar{f} - \bar{C}\bar{f}$ on the right-hand side of (60) is safely neglected here. [For a like-species, Fokker-Planck operator it can be shown that the collisional terms precisely cancel.] The remaining terms in (60) come from

$$\tilde{\mathcal{L}} = \mathcal{L} - \bar{\mathcal{L}}$$

which is given implicitly by (50)–(51) and (59); note that the γ -derivative terms in \mathcal{L} are irrelevant.

The indefinite γ -integral for \tilde{f} is accomplished using the identities

$$\hat{s} = \frac{\partial \hat{\rho}}{\partial \gamma}, \quad \frac{\partial \hat{s}}{\partial \gamma} = -\hat{\rho} \quad (61)$$

and

$$\begin{aligned} \int d\gamma \hat{s}\hat{s} &= \frac{1}{2} [\hat{\rho}\hat{s} + \gamma(\mathbf{I} - \mathbf{b}\mathbf{b})] , \\ \int d\gamma \hat{\rho}\hat{\rho} &= \frac{1}{2} [\hat{\rho}\hat{s} + \gamma(\mathbf{I} - \mathbf{b}\mathbf{b})] , \end{aligned} \quad (62)$$

where

$$\mathbf{I} = \mathbf{b}\mathbf{b} + \hat{\rho}\hat{\rho} + \hat{s}\hat{s}$$

is a unit dyadic. We have discarded integration constants, which are finally fixed by the requirement $\langle \tilde{f} \rangle = 0$. With these remarks, (60) is straightforwardly integrated; one finds that

$$\tilde{f} = \rho \cdot \mathbf{h} + g \quad (63)$$

where

$$\mathbf{h} = -\nabla \bar{f} - \frac{e}{c} \left[\mathbf{b} \times \mathbf{v}_D \frac{\partial \bar{f}}{\partial \mu} - \frac{\partial \mathbf{A}}{\partial t} \frac{\partial \bar{f}}{\partial U} \right], \quad (64)$$

$$g = \frac{u\mu}{\Omega} \frac{\partial \bar{f}}{\partial \mu} \left(\hat{\rho}\hat{s} : \nabla \mathbf{b} - \frac{1}{2} \mathbf{b} \cdot \nabla \times \mathbf{b} \right), \quad (65)$$

and \mathbf{v}_D is given by (34).

The simplest version of these results is apparent directly from (53), and instructive. If we neglect time variation of the fields and assume a nearly isotropic \bar{f} , so that $\partial \bar{f} / \partial \mu$ is small, then we have simply

$$\Omega \frac{\partial \tilde{f}}{\partial \gamma} \cong -\mathbf{s} \cdot \nabla \bar{f}, \quad (66)$$

and (61) yields

$$\tilde{f} \cong -\rho \cdot \nabla \bar{f}, \quad (66)$$

as in the first term of (64). We will find that the result (66) has special importance; for example, all the classical perpendicular transport coefficients are easily derived from this expression. Hence we briefly digress to comment upon its interpretation.

It has been noted that (54) makes sense only if f is presumed to vary slowly. In the presence of rapid gyration, the distribution avoids fast variation by depending upon only constants of motion, or near constants of motion, such as U and μ . In this sense the position of the guiding center is

also \mathbf{a} near invariant, because it changes at the rate $\omega_i = \delta\Omega$ rather than Ω . Denoting the guiding-center position by

$$\mathbf{X} = \mathbf{x} - \boldsymbol{\rho}, \quad (67)$$

we expect any slowly varying f to depend on gyrophase, at fixed \mathbf{x} , only through \mathbf{X} :

$$f(\mathbf{x}, U, \mu, \gamma) = F(\mathbf{X}, U, \mu),$$

for some distribution of guiding centers, F . Since F is presumed to vary slowly on the gyroradius scale, it is appropriate to expand

$$F(\mathbf{x} - \boldsymbol{\rho}, U, \mu) = F(\mathbf{x}, U, \mu) - \boldsymbol{\rho} \cdot \nabla F,$$

and thus to conclude, from (66), that $F = \bar{f}$.

In other words (66) reflects the simple fact that \bar{f} is an approximate distribution of guiding centers, as we assumed in (44).

Gyrophase Average

Upon substituting the expression of (63)–(65) into (57),

$$\langle \mathcal{L}(\bar{f} + \tilde{f}) \rangle = C\bar{f},$$

we obtain a drift kinetic equation that differs from (44) only in details. However, the evaluation of the gyrophase average is complicated enough to deserve some comment. The most awkward term is $\langle \mathcal{L}(\boldsymbol{\rho} \cdot \mathbf{h}) \rangle$, where \mathbf{h} is given by (64). (Indeed, the term $\langle \mathcal{L}g \rangle$ can be seen to vanish.) It is most conveniently evaluated using the identity

$$\langle \mathcal{L}G \rangle = \left\langle \frac{dG}{dt} \right\rangle,$$

for any G , where the time derivative is performed along the orbit, using (50)–(52). Thus

$$\langle \mathcal{L}(\boldsymbol{\rho} \cdot \mathbf{h}) \rangle = \left\langle \boldsymbol{\rho} \cdot \frac{d\mathbf{h}}{dt} \right\rangle + \left\langle \frac{d\boldsymbol{\rho}}{dt} \right\rangle \cdot \mathbf{h}$$

since \mathbf{h} is independent of gyrophase. For the second term we start with

$$\left\langle \frac{d\boldsymbol{\rho}}{dt} \right\rangle = \left\langle \frac{1}{\Omega} \right\rangle \left\langle \frac{d\mathbf{b}}{dt} \times \mathbf{s} \right\rangle + \frac{1}{\Omega} \mathbf{b} \times \left\langle \frac{ds}{dt} \right\rangle + \mathbf{b} \times \left\langle s \frac{d}{dt} \frac{1}{\Omega} \right\rangle.$$

The first term here

$$\left\langle \frac{1}{\Omega} \frac{d\mathbf{b}}{dt} \times \mathbf{s} \right\rangle = \left\langle \frac{1}{\Omega} \left(\frac{\partial \mathbf{b}}{\partial t} + \mathbf{v} \cdot \nabla \mathbf{b} \right) \times \mathbf{s} \right\rangle = \left\langle \frac{1}{\Omega} (\mathbf{s} \cdot \nabla \mathbf{b}) \times \mathbf{s} \right\rangle$$

$$= -\frac{\mu B}{\Omega} \mathbf{b}(\mathbf{b} \cdot \nabla \times \mathbf{b})$$

corresponds to a guiding-center drift

$$\mathbf{u}_D \equiv \frac{s^2}{2\Omega} \mathbf{b}(\mathbf{b} \cdot \nabla \times \mathbf{b})$$

parallel to \mathbf{b} . The remaining terms are computed from (49), which implies

$$\frac{d\mathbf{s}}{dt} = \frac{e}{m} \mathbf{E} - \Omega s \hat{\rho} - \frac{du}{dt}.$$

We thus find that

$$\left\langle \frac{d\rho}{dt} \right\rangle = -\mathbf{v}_D - \mathbf{u}_D.$$

We still need to compute

$$\left\langle \rho \cdot \frac{d\mathbf{h}}{dt} \right\rangle = \langle \rho s \rangle : \nabla \mathbf{h} + \left\langle \rho \frac{d\mu}{dt} \right\rangle \cdot \frac{\partial \mathbf{h}}{\partial \mu} + \left\langle \rho \frac{dU}{dt} \right\rangle \cdot \frac{\partial \mathbf{h}}{\partial U}.$$

It is not hard to show that

$$\left\langle \rho \frac{d\mu}{dt} \right\rangle = -\mu \mathbf{v}_D, \quad \left\langle \rho \frac{dU}{dt} \right\rangle = -\mu \mathbf{b} \times \frac{\partial \mathbf{A}}{\partial t}$$

and that, for any vector \mathbf{V} ,

$$\langle \hat{\rho} \mathbf{s} \rangle : \nabla \mathbf{V} = \frac{1}{2} \mathbf{b} \cdot \nabla \times \mathbf{V}.$$

Hence

$$\left\langle \rho \cdot \frac{d\mathbf{h}}{dt} \right\rangle = \frac{1}{2} \mathbf{b} \cdot \nabla \times \mathbf{h} - \mu \mathbf{v}_D \cdot \frac{\partial \mathbf{h}}{\partial \mu} - \mu \mathbf{b} \times \frac{\partial \mathbf{A}}{\partial t} \cdot \frac{\partial \mathbf{h}}{\partial U}.$$

After substituting from (64) and combining terms we obtain the drift kinetic equation

$$\begin{aligned} \frac{\partial \bar{f}}{\partial t} + (\mathbf{v}_{||} + \mathbf{v}_D + \mathbf{u}_D) \cdot \nabla \bar{f} + \left. \frac{d\mu}{dt} \right|_{g_c} \frac{\partial \bar{f}}{\partial \mu} \\ + \left[e \frac{\partial \Phi}{\partial t} + \mu \frac{\partial B}{\partial t} - \frac{e}{c} (\mathbf{v}_{||} + \mathbf{v}_D + \mathbf{u}_D) \cdot \frac{\partial \mathbf{A}}{\partial t} \right] \frac{\partial \bar{f}}{\partial U} = C. \end{aligned} \quad (68)$$

with

$$\left. \frac{d\mu}{dt} \right|_{g_c} = -\frac{u}{\Omega} \nabla \cdot \left(\mathbf{b} \times \frac{\partial \mathbf{b}}{\partial t} \right) - \frac{1}{B} (\mathbf{b} \cdot \nabla \times \mathbf{b}) \mathbf{b} \cdot \frac{\partial \mathbf{A}}{\partial t}$$

$$+ \frac{uB}{\Omega} \mathbf{b} \cdot \nabla \left(\frac{u \mathbf{b} \cdot \nabla \times \mathbf{b}}{B} \right). \quad (69)$$

It is clear that (68) includes several terms missing from the earlier version, (44). Specifically:

- (i) higher order corrections to the velocity appear, multiplying $\partial \mathbf{A} / \partial t$ in the coefficient of $\partial \bar{f} / \partial \mu$;
- (ii) the change in the lowest order magnetic moment, in (69), brings in $\partial \bar{f} / \partial \mu$;
- (iii) the parallel drift \mathbf{u}_D has been introduced.

Although of some academic interest, these refinements are rarely important; (44) is a sufficiently accurate drift kinetic equation for virtually all applications.

The most interesting corrections, occurring in both $d\mu/dt$ and \mathbf{u}_D , are proportional to

$$\mathbf{b} \cdot \nabla \times \mathbf{b} = \frac{1}{B} \mathbf{b} \cdot \nabla \times \mathbf{B} = \frac{4\pi}{cB} J_{||}, \quad (70)$$

the parallel current. It can be shown that these terms are related to higher-order corrections to the magnetic moment. The equilibrium estimate

$$J_{||} \sim J_{\perp} \sim \frac{cP}{LB} \quad (71)$$

shows that

$$\frac{v_t}{\Omega} \mathbf{b} \cdot \nabla \times \mathbf{b} \sim \beta \delta,$$

as anticipated in (42).

It should be pointed out that in many devices, including tokamaks, plasma current flows predominantly along the field, $J_{||} \gg J_{\perp}$. Then the first estimate in (71) is contradicted and (42) may become marginal. Still, the terms of (68) that large- $J_{||}$ might require seem unlikely to have dramatic effects. In particular, we are aware of no *applications* of the parallel drift in the literature, despite numerous derivations and discussions of \mathbf{u}_D .

An alternative version of the drift-kinetic equation is often convenient; it uses, instead of the total energy U , the kinetic energy

$$w \equiv U - e\Phi = \frac{mv^2}{2}.$$

Since

$$\left. \frac{\partial}{\partial t} \right|_U = \left. \frac{\partial}{\partial t} \right|_w + e \left. \frac{\partial \Phi}{\partial t} \right. \frac{\partial}{\partial w}$$

we find that (44) becomes

$$\frac{\partial \bar{f}}{\partial t} + (\mathbf{v}_{||} + \mathbf{v}_D) \cdot \nabla \bar{f} + \left[\mu \frac{\partial B}{\partial t} + e(\mathbf{v}_{||} + \mathbf{v}_D) \cdot \mathbf{E} \right] \frac{\partial \bar{f}}{\partial w} = C. \quad (72)$$

4.3 Gyrokinetic Equation*

Scale Length Ordering

The gyrokinetic equation is a gyrophase-averaged kinetic equation that allows for sharp spatial variation of field perturbations, as in (20). It is applied to the study of plasma instabilities, some of which indeed have wavelengths comparable to ρ . We have already pointed out that unless the sharply varying perturbations are small, no simplified kinetic description is pertinent: the plasma is unmagnetized. For this reason the gyrokinetic equation is usually studied in its linear approximation.

We distinguish unperturbed and perturbed quantities by means of subscripts, writing

$$Y = Y_0 + Y_1$$

where Y represents an arbitrary field or distribution function, and

$$\frac{Y_1}{Y_0} \sim \Delta \ll 1. \quad (73)$$

Here the parameter Δ measures the perturbation, as in §4.1. For simplicity, we suppress the 0-subscript in the case of the unit vector, $\mathbf{b} \equiv \mathbf{B}_0/B_0$, and the gyrofrequency, $\Omega \equiv eB_0/mc$. The quantity Y_0 , strictly distinguished by its relatively slow spatial variation, is traditionally identified with the “equilibrium” value of Y . Specifically it is assumed that

$$\frac{\partial Y_0}{\partial t} = 0. \quad (74)$$

Of course equilibrium fields are not strictly constant; in the context of transport theory, based on the drift-kinetic equation, their variation is treated carefully. But gyrokinetic theory concerns instability, not transport, and interesting instabilities can be presumed to evolve rapidly compared to transport.

The basic gyrokinetic ordering allows field perturbations to vary sharply, while the variation of unperturbed quantities is slow (*magnetized*):

$$\nabla Y_1 \sim \frac{Y_1}{\rho}, \quad \nabla Y_0 \sim \frac{Y_0}{L},$$

with $\rho/L = \delta \ll 1$. A refinement of this ordering, in which the parallel and perpendicular scale lengths are distinguished, is most commonly used. Thus we write

$$\nabla_{\parallel} Y_1 = \frac{Y_1}{L_{\parallel}}, \quad \nabla_{\perp} Y_1 = \frac{Y_1}{L_{\perp}}$$

and assume, refining (17), that

$$L \sim L_{\parallel} \gg L_{\perp} \sim \rho. \quad (75)$$

In other words, only the perpendicular scale length is allowed to be short. The justification for (75) is simply that, for reasons discussed in Chapter 7, the perturbations most likely to effect confinement are nearly constant in the direction of the confining field.

Guiding Center Coordinates

A relatively transparent derivation of the gyrokinetic equation uses the phase-space coordinates (\mathbf{X}, μ, U) , where \mathbf{X} is the position of the guiding center, defined by equation (67), $\mu \equiv mv_1^2/2B_0$, and $U \equiv mv^2/2 + e\Phi$. Note that U involves the full electrostatic potential,

$$\Phi = \Phi_0 + \Phi_1 ,$$

while μ is defined in terms of the unperturbed magnetic field. The parallel and perpendicular components of \mathbf{v} are defined as in (46), $\mathbf{v} = \mathbf{b}u + \mathbf{s}$, in terms of the unperturbed magnetic field. The gyrophase angle is defined as usual by (47).

Aside from the variable change $\mathbf{x} \rightarrow \mathbf{X}$, the derivation of the gyrokinetic equation proceeds in close analogy to that of the drift-kinetic equation. There are however two complications. First, the use of \mathbf{X} makes extension of the gyrokinetic theory to higher order in δ awkward. The problem is that averaging at fixed \mathbf{X} is straightforward only if, in particular, the gyroradius ρ is known in terms of \mathbf{X} . It is clear from the definition [recall (48)],

$$\mathbf{X}(\mathbf{x}, \mathbf{v}) \equiv \mathbf{x} - \boldsymbol{\rho} = \mathbf{x} - \frac{1}{\Omega(\mathbf{X})} \mathbf{b} \times \mathbf{s} , \quad (76)$$

that the \mathbf{X} -dependence of $\boldsymbol{\rho}$ must be determined iteratively. Thus, in lowest order,

$$\boldsymbol{\rho}(\mathbf{X}, \mathbf{v}) = \frac{1}{\Omega(\mathbf{X})} \mathbf{b}(\mathbf{X}) \times \mathbf{s} , \quad (77)$$

the result we will use. In next δ -order, however, we must include the correction from

$$\boldsymbol{\rho}(\mathbf{x}, \mathbf{v}) = \boldsymbol{\rho}(\mathbf{X} + \boldsymbol{\rho}, \mathbf{v});$$

$$\boldsymbol{\rho}(\mathbf{X}, \mathbf{v}) = \frac{1}{\Omega(\mathbf{X})} \mathbf{b}(\mathbf{X}) \times \mathbf{s} + \boldsymbol{\rho}(\mathbf{X}, \mathbf{v}) \cdot \nabla \boldsymbol{\rho}(\mathbf{X}, \mathbf{v}) + \dots$$

This nuisance complicates the higher order theory, and explains why some gyrokinetic derivations avoid the guiding-center variable altogether.

The second complication resides in the equation itself. Independently of how it is derived, the gyrokinetic equation is an integro-differential, rather than simply differential, relation. Indeed, if some field varies significantly over the distance ρ , then its gyroaverage at fixed \mathbf{X} cannot be a local function of position. This *awkwardness* is conventionally treated by assuming

an eikonal form for the rapid spatial dependence, as we consider presently. Even with the eikonal ansatz, however, the fully explicit form of the gyrokinetic equation is not simple: it incorporates essentially nonlocal physics.

Equations of Motion

We calculate the rates of change of the gyrokinetic variables, beginning with

$$\frac{d\mu}{dt} = \frac{d\mu}{dt}\Big|_{\mathbf{v}} + \frac{\partial\mu}{\partial\mathbf{v}} \cdot \frac{d\mathbf{v}}{dt}. \quad (78)$$

The first term is computed from

$$\mu = \frac{m}{2B_0}[v^2 - (\mathbf{b} \cdot \mathbf{v})^2],$$

with the result

$$\frac{d\mu}{dt}\Big|_{\mathbf{v}} = -\frac{\mu}{B_0}\mathbf{v} \cdot \nabla B_0 - \frac{mu}{B_0}\mathbf{s} \cdot (\mathbf{v} \cdot \nabla)\mathbf{b}.$$

Here we have recalled (74). Notice also that, since we are presently seeking exact formulae, the coordinate change, $\mathbf{x} \rightarrow \mathbf{X}$, is postponed. The second term in (78) is found from

$$\frac{\partial\mu}{\partial\mathbf{v}} = \frac{ms}{B_0}$$

and the Lorentz law, (5), which can be expressed as

$$\frac{d\mathbf{v}}{dt} = \frac{e}{m}\mathbf{E} - \Omega s \hat{\rho} + \frac{e}{mc}\mathbf{v} \times \mathbf{B}_1.$$

Here of course $\mathbf{E} = \mathbf{E}_0 + \mathbf{E}_1$. Thus we have

$$\frac{d\mu}{dt} = \dot{\mu}_0 + \dot{\mu}_1,$$

where

$$\dot{\mu}_0 = -\frac{\mu}{B_0}\mathbf{v} \cdot \nabla B_0 - \frac{mu}{B_0}\mathbf{s} \cdot (\mathbf{v} \cdot \nabla)\mathbf{b} + \frac{e}{B_0}\mathbf{s} \cdot \mathbf{E}_0, \quad (79)$$

$$\dot{\mu}_1 = \frac{e}{B_0}[\mathbf{s} \cdot \mathbf{E}_1 - \frac{us}{c}\hat{\rho} \cdot \mathbf{B}_1]. \quad (80)$$

The quantity $d\gamma/dt$ is computed similarly from

$$\frac{d\gamma}{dt} = \frac{d\gamma}{dt}\Big|_{\mathbf{v}} + \frac{\partial\gamma}{\partial\mathbf{v}} \cdot \frac{d\mathbf{v}}{dt},$$

with $\partial\gamma/\partial\mathbf{v} = -\hat{\rho}/s$ and

$$\frac{d\gamma}{dt}\Big|_{\mathbf{v}} = \mathbf{e}_1 \cdot (\mathbf{v} \cdot \nabla) \mathbf{e}_2 + \frac{u}{s} \hat{\rho} \cdot (\mathbf{v} \cdot \nabla) \mathbf{b}.$$

One finds

$$\frac{d\gamma}{dt} = \omega_0 + \omega_1,$$

with

$$\omega_0 \equiv \Omega + \mathbf{e}_3 \cdot (\mathbf{v} \cdot \nabla) \mathbf{e}_2 + \frac{u}{s} \hat{\rho} \cdot (\mathbf{v} \cdot \nabla) \mathbf{b} - \frac{e}{ms} \hat{\rho} \cdot \mathbf{E}_0,$$

and

$$\omega_1 = -\frac{e}{ms} \hat{\rho} \cdot \mathbf{E}_1 + \Omega \left(\mathbf{b} - \frac{\mathbf{u}}{s} \hat{\mathbf{s}} \right) \cdot \mathbf{B}_1. \quad (81)$$

It is easy to compute

$$\frac{dU}{dt} = e \left[\frac{\partial \Phi_1}{\partial t} - \frac{\mathbf{v}}{c} \cdot \frac{\partial \mathbf{A}_1}{\partial t} \right], \quad (82)$$

where \mathbf{A}_1 is the perturbed vector potential; recall (51). It is consistent to treat the two terms on the right hand side of (82) as comparable:

$$\frac{1}{c} \mathbf{v} \cdot \mathbf{A}_1 \sim \Phi_1. \quad (83)$$

Finally we need

$$\frac{d\mathbf{X}}{dt} = \mathbf{v} \cdot \nabla \mathbf{X} + \frac{d\mathbf{v}}{dt} \cdot \frac{\partial \mathbf{X}}{\partial \mathbf{v}}.$$

In Cartesian-component form,

$$\frac{dX_\alpha}{dt} = v_\beta \frac{\partial X_\alpha}{\partial x_\beta} + \frac{dv_\beta}{dt} \frac{\partial X_\alpha}{\partial v_\beta}.$$

From (76) we find

$$\frac{\partial X_\alpha}{\partial v_\beta} = -\frac{1}{\Omega} \epsilon_{\alpha\beta\gamma} b_\gamma$$

where $\epsilon_{\alpha\beta\gamma}$ is the unit antisymmetrical tensor, and

$$\frac{\partial X_\alpha}{\partial x_\beta} = \delta_{\alpha\beta} + \frac{1}{\Omega^2} \epsilon_{\alpha\kappa\lambda} v_\kappa \left(\Omega \frac{\partial b_\lambda}{\partial x_\alpha} - b_\lambda \frac{\partial \Omega}{\partial x_\alpha} \right)$$

There follows, respectively,

$$\mathbf{v} \cdot \nabla \mathbf{X} = \mathbf{v} + \frac{1}{\Omega} \left[\mathbf{v} \times (\mathbf{v} \cdot \nabla) \mathbf{b} - \frac{1}{B} \mathbf{v} \times \mathbf{b} (\mathbf{v} \cdot \nabla) \mathbf{B} \right]$$

and

$$\frac{d\mathbf{v}}{dt} \cdot \frac{\partial \mathbf{X}}{\partial \mathbf{v}} = \mathbf{v}_E - \mathbf{s} - \frac{1}{B} \mathbf{b} \times (\mathbf{v} \times \mathbf{B}_1)$$

where, as usual,

$$\mathbf{v}_E = \frac{\mathbf{c}\mathbf{E} \times \mathbf{b}}{B_0} = \mathbf{v}_{E0} + \mathbf{v}_{E1}.$$

Finally, then

$$\frac{d\mathbf{X}}{dt} = \mathbf{V}_0 + \mathbf{V}_1,$$

with

$$\mathbf{V}_0 \equiv \mathbf{u} + \mathbf{v}_{E0} + \mathbf{v} \times (\mathbf{v} \cdot \nabla) \left(\frac{\mathbf{b}}{\Omega} \right) + \rho \frac{(\mathbf{v} \cdot \nabla) B_0}{B_0}, \quad (84)$$

$$\mathbf{V}_1 \equiv \mathbf{v}_{E1} - \mathbf{v} \frac{\mathbf{b} \cdot \mathbf{B}_1}{B_0} + \mathbf{B}_1 \frac{\mathbf{u}}{B_0}. \quad (85)$$

Gyrophase Average

We can express the exact kinetic equation, (7), as

$$\frac{\partial f}{\partial t} + \frac{d\mathbf{X}}{dt} \cdot \frac{\partial f}{\partial \mathbf{X}} + \frac{d\mu}{dt} \frac{\partial f}{\partial \mu} + \frac{dU}{dt} \frac{\partial f}{\partial U} + \frac{d\gamma}{dt} \frac{\partial f}{\partial \gamma} \approx 0, \quad (86)$$

where the coefficients are given by (79)–(85). The collision operator has been omitted for simplicity; in fact gyrokinetic applications rarely attempt detailed or rigorous treatment of collisional effects. It is convenient to note here the following orderings, implicit in (79)–(85):

$$\begin{aligned} V_0 &\sim v_t + \mathcal{O}(\delta v_t), \quad V_1 \sim \Delta v_t; \\ \dot{\mu}_0 &\sim \omega_t \mu, \quad \dot{\mu}_1 \sim \Delta \Omega \mu; \\ \frac{dU}{dt} &\sim \Delta \omega_t U; \\ \omega_0 &= \Omega + \mathcal{O}(\omega_t), \quad \omega_1 \sim \Delta \Omega. \end{aligned} \quad (87)$$

The argument from (86) is closely analogous to that based on (53), with technical differences arising from the appearance two small parameters, δ and Δ , in (86). (Here, for clarity, we treat δ and Δ as independent parameters.) The orderings (87) show that $\Omega \partial f / \partial \gamma = \mathcal{O}(\delta \Omega) + \mathcal{O}(\Delta \Omega)$, so the distribution is as usual nearly independent of gyrophase: we write, in the notation of the previous section,

$$f = \bar{f} + \tilde{f}, \quad \tilde{f} = \mathcal{O}(\delta) + \mathcal{O}(\Delta). \quad (88)$$

In lowest order, \tilde{f} is neglected and the gyrokinetic equation is obtained from the simple average

$$\frac{\partial \bar{f}}{\partial t} + (\mathbf{V}_0 + \mathbf{V}_1) \cdot \frac{\partial \bar{f}}{\partial \mathbf{X}} + \left\langle \frac{d\mu}{dt} \right\rangle \frac{\partial \bar{f}}{\partial \mu} + \left\langle \frac{dU}{dt} \right\rangle \frac{\partial \bar{f}}{\partial U} = 0. \quad (89)$$

Equation (89) is a sufficiently accurate gyrokinetic equation for most applications of interest. Notice that \bar{f} involves only the slow spatial variation; it is independent of γ at fixed \mathbf{X} . The gyrokinetic equation is constructed to describe this slow response, in the presence of sharply varying electromagnetic fields.

Unlike the drift-kinetic case, gyrokinetic theory does not ordinarily need the function \bar{f} . Indeed, f is needed only in the exceptional case when μ -dependence of the lowest order, unperturbed distribution occurs—i.e., when f_0 is anisotropic. We consider the anisotropic case presently.

Our present task is to evaluate the gyrophase averages of (80), (82), (84), and (85). We consider first (84), for the unperturbed guiding-center velocity. It can be averaged without regard to the distinction between \mathbf{x} and \mathbf{X} ; equilibrium quantities vary slowly, and second order (in δ) corrections are not of interest. Hence we perform the average as in the drift-kinetic case, with the result

$$\langle \mathbf{V}_0 \rangle = \mathbf{u} + \mathbf{v}_{D0}, \quad (90)$$

where

$$\mathbf{v}_{D0} = \mathbf{v}_{E0} + \frac{1}{\Omega} \mathbf{b} \times (\mu \nabla B_0 + \mathbf{u}^2 \boldsymbol{\kappa}).$$

This drift differs from that of (34) only because it neglects $\partial B_0 / \partial t$ terms, as in (74). For the perturbed velocity, one straightforwardly finds

$$\langle \mathbf{V}_1 \rangle = \frac{c}{B_0} \langle \mathbf{E}_1 \rangle \times \mathbf{b} + \frac{\mathbf{u}}{B_0} \langle \mathbf{B}_{1\perp} \rangle - \frac{1}{B_0} \langle B_{1\parallel} \mathbf{s} \rangle \quad (91)$$

where the \perp and \parallel subscripts are defined with respect to \mathbf{b} . The electromagnetic fields must remain inside the averages because of their variation on the short spatial scale.

Very similar analysis shows that

$$\left\langle \frac{d\mu}{dt} \right\rangle = \langle \dot{\mu}_1 \rangle = \frac{e}{m B_0} s \left[\langle \hat{\mathbf{s}} \cdot \mathbf{E}_1 \rangle - \frac{\mathbf{u}}{c} \langle \hat{\rho} \cdot \mathbf{B}_1 \rangle \right]. \quad (92)$$

Here the approximate adiabatic invariance of μ has obviated an unperturbed contribution. To see explicitly the cancellation of the unperturbed terms, we use the identity

$$\langle \hat{\mathbf{s}} \hat{\mathbf{s}} \rangle = \frac{1}{2} (\mathbf{I} - \mathbf{b}\mathbf{b}),$$

where \mathbf{I} is the unit dyadic. It follows that

$$\langle \hat{\mathbf{s}} \hat{\mathbf{s}} \rangle : \nabla \mathbf{b} = \frac{1}{2} \nabla \cdot \mathbf{b} = -\frac{1}{2} \frac{\nabla B_0}{B_0},$$

and therefore that

$$\left\langle -\frac{\mu}{B_0} \mathbf{v} \cdot \nabla B_0 - \frac{\mathbf{u} \cdot \mathbf{s}}{B_0} \mathbf{s} \cdot (\mathbf{v} \cdot \nabla) \mathbf{b} \right\rangle = 0.$$

Finally we have, from (82),

$$\left\langle \frac{dU}{dt} \right\rangle = e \left[\left\langle \frac{\partial \Phi_1}{\partial t} \right\rangle - \frac{1}{c} \left\langle \mathbf{v} \cdot \frac{\partial \mathbf{A}_1}{\partial t} \right\rangle \right]. \quad (93)$$

The energy change also vanishes in the unperturbed case.

We next substitute (90)–(93) into (89), linearize, and suppress overbars for convenience. The result is

$$\frac{\partial f_1}{\partial t} + \langle \mathbf{V}_0 \rangle \cdot \frac{\partial f_1}{\partial \mathbf{X}} = - \langle \mathbf{V}_1 \rangle \cdot \frac{\partial f_0}{\partial \mathbf{X}} - \left\langle \frac{dU}{dt} \right\rangle \frac{\partial f_0}{\partial U}. \quad (94)$$

Two aspects of (94) require comment. First, our use of the total energy as a coordinate makes part of the linearization implicit; that is

$$f(U) = f_0(U_0 + U_1) + f_1(U_0) + \mathcal{O}(\Delta^2) = f_0(U_0) + \frac{\partial f_0}{\partial U} U_1 + f_1(U_0) + \mathcal{O}(\Delta^2).$$

In other words the full first order response is not f_1 but

$$f_1 \rightarrow f_1(U_0) + e\Phi_1 \frac{\partial f_0}{\partial U}. \quad (95)$$

The second comment concerns the gyrophase averages, which are evidently more complicated objects than in the drift-kinetic case. Consider, for example,

$$\langle \mathbf{E}_1 \rangle \equiv \oint \frac{d\gamma}{2\pi} \mathbf{E}_1(\mathbf{X} + \boldsymbol{\rho}) \quad (96)$$

The integral is to be performed at fixed \mathbf{X} , with $\boldsymbol{\rho} = (s/\Omega)(\mathbf{e}_3 \cos \gamma + \mathbf{e}_2 \sin \gamma)$. Such an average cannot in general be expressed in closed form; as we have remarked, gyrokinetic theory inherently involves integral operators.

A local version of the gyrokinetic equation is obtained through the “eikonal approximation.” This common simplification assumes that the rapid variation of each perturbed field can be expressed as

$$Y_1(\mathbf{x}) = Y_A^*(\mathbf{X}) e^{i\mathbf{k}_\perp \cdot \mathbf{x}} \quad (97)$$

where the amplitude \mathbf{Y}_A^* , as well as the perpendicular wave number \mathbf{k}_\perp , vary slowly. Equation (91) is often written in terms of a conventional eikonal, $\mathbf{k}_\perp \cdot \mathbf{x} \rightarrow S(\mathbf{x})$, but the departures of S from a strictly linear function do not enter gyrokinetic analyses.

Thus we have

$$\langle Y_1 \rangle(\mathbf{x}) = Y_A \left\langle e^{i\mathbf{k}_\perp \cdot \boldsymbol{\rho}} \right\rangle,$$

where the modified amplitude $Y_A \equiv \exp(i\mathbf{k}_\perp \cdot \mathbf{X}) Y_A^*$ is also slowly varying. From the identity

$$J_n(z) \equiv \oint \frac{d\gamma}{2\pi} e^{-iz\cos \gamma} e^{iz \sin \gamma}$$

where J_n is the Bessel function, we find that

$$\langle e^{i\mathbf{k}_\perp \cdot \boldsymbol{\rho}} \rangle = J_0(k_\perp \rho) \quad (98)$$

allowing $\langle Y_1 \rangle$ to be expressed in closed form. Similarly one finds

$$\langle \hat{s} e^{i\mathbf{k}_\perp \cdot \boldsymbol{\rho}} \rangle = i J_1(k_\perp \rho) \frac{\mathbf{k}_\perp \times \mathbf{b}}{k_\perp} \quad (99)$$

and

$$\langle \hat{\rho} e^{i\mathbf{k}_\perp \cdot \boldsymbol{\rho}} \rangle = i J_1(k_\perp \rho) \frac{\mathbf{k}_\perp}{k_\perp}. \quad (100)$$

Substitution of these expressions into (87) and (91)–(93) yields a useful version of the “eikonalized” gyrokinetic equation. However, a more common form—one that is simpler but less generally accurate—may be obtained as follows. Starting with the perturbed Lorentz force,

$$\mathbf{F}_1 \equiv \mathbf{E}_1 + \frac{1}{c} \mathbf{u} \times \mathbf{B}_1,$$

one notes that

$$\langle \mathbf{V}_1 \rangle = \frac{c}{B_0} \langle \mathbf{F}_1 \rangle \times \mathbf{b} - \frac{1}{B_0} \langle B_{1\parallel} \mathbf{s} \rangle. \quad (101)$$

We next use the scalar and vector potentials,

$$\mathbf{E}_1 = -\nabla \Phi_1 - \frac{1}{c} \frac{\partial \mathbf{A}_1}{\partial t}, \quad \mathbf{B}_1 = \nabla \times \mathbf{A}_1, \quad (102)$$

to write

$$\mathbf{F}_1 = -\nabla \Phi_1 - \frac{1}{c} \frac{\partial \mathbf{A}_1}{\partial t} + \frac{u}{c} \mathbf{b} \times \nabla \times \mathbf{A}_1,$$

where a familiar vector identity yields

$$\mathbf{b} \times \nabla \times \mathbf{A}_1 = \nabla A_{1\parallel} - \nabla_\parallel \mathbf{A}_1 - \mathbf{A}_1 \times \nabla \times \mathbf{b} - (\mathbf{A}_1 \cdot \nabla) \mathbf{b}. \quad (103)$$

At this point we approximate by neglecting the last two terms in (103). These terms involve only derivatives of the equilibrium field, while the terms we retain,

$$\mathbf{b} \times \nabla \times \mathbf{A}_1 \cong \nabla A_{1\parallel} - \nabla_\parallel \mathbf{A}_1 \quad (104)$$

involve the shorter scale length of the perturbed field. The weakness of this approximation is that the parallel gradient of a perturbed field is not presumed large; recall (75). Thus (104) is strictly justified only by a subsidiary ordering that distinguishes between L and L_\parallel . We are content to point out that the omitted terms do not dramatically change the predictions of the equation.

With (104) we have

$$\mathbf{F}_1 = -\nabla \Phi_1 - \frac{u}{c} \nabla A_{1\parallel} - \frac{1}{c} \left(\frac{\partial}{\partial t} + \mathbf{u} \cdot \nabla \right) \mathbf{A}_1 \quad (105)$$

or, in the eikonal approximation,

$$\mathbf{F}_1 = -i\mathbf{k}_\perp \left(\Phi_1 - \frac{\mathbf{u}}{c} A_{1\parallel} \right) - \frac{1}{c} \left(\frac{\partial}{\partial t} + \mathbf{u} \nabla_\parallel \right) \mathbf{A}_1 - \mathbf{b} \left(\nabla_\parallel \Phi_1 - \frac{\mathbf{u}}{c} \nabla_\parallel A_{1\parallel} \right).$$

Here only the first term, involving \mathbf{k}_\perp , is important. The last term, parallel to \mathbf{b} , cannot contribute to (95); the second term, proportional \mathbf{A}_1 , is smaller than the first by δ , since $\partial/\partial t \sim \mathbf{u} \cdot \nabla \sim \omega_t \sim \delta k_\perp \mathbf{u}$. (We note that this smaller term does enter the anisotropic case, discussed below.) Hence, after performing the gyroaverages and using (93) we find that (95) becomes

$$\langle \mathbf{V}_1 \rangle = i \frac{c}{B_0} J_0(k_\perp \rho) \left(\Phi_A - \frac{\mathbf{u}}{c} A_{\parallel A} \right) \mathbf{k}_\perp \times \mathbf{b} - i \frac{s}{B_0} J_1(k_\perp \rho) B_{\parallel A} \frac{\mathbf{k}_\perp \times \mathbf{b}}{k_\perp}. \quad (106)$$

Similar manipulation yields

$$\left\langle \frac{dU}{dt} \right\rangle = -i\omega e \left[J_0(k_\perp \rho) \left(\Phi_A - \frac{\mathbf{u}}{c} A_{\parallel A} \right) + J_1(k_\perp \rho) \frac{s}{ck_\perp} B_{\parallel A} \right]. \quad (107)$$

Here we expressed the time derivative in terms of a wave frequency,

$$\frac{\partial Y_1}{\partial t} \rightarrow -i\omega Y_1,$$

for convenience. We substitute (101) and (102) into (94) to obtain the gyrokinetic equation

$$\begin{aligned} \frac{\partial \bar{f}_1}{\partial t} + \mathbf{V}_0 \cdot \frac{\partial \bar{f}_1}{\partial \mathbf{X}} + C \bar{f}_1 &= i\omega e \left[J_0(k_\perp \rho) \left(\Phi_A - \frac{\mathbf{u}}{c} A_{\parallel A} \right) + \frac{s}{ck_\perp} J_1(k_\perp \rho) B_{\parallel A} \right] \\ &\quad \cdot \left[\frac{\partial f_0}{\partial U} + \frac{c}{eB_0} \mathbf{k} \times \mathbf{b} \cdot \nabla f_0 \right], \end{aligned} \quad (108)$$

where \mathbf{V}_0 is given by (84) and collisions have been (conventionally and sensibly, if not rigorously) taken into account by the insertion of a linearized collision operator, C , on the left-hand side. Equation (108) is the most commonly used version of the gyrokinetic equation. The absence of an eikonal factor, $\exp(-i\mathbf{k}_\perp \cdot \rho)$, in (108) reflects the fact, noted with regard to (94), that $f_1 \equiv \bar{f}_1$ contains only slow spatial variation.

Anisotropic Case

In Chapter 8 we will discuss the unperturbed distribution function, f_0 , in some detail. Here we anticipate the general conclusion that f_0 usually displays some anisotropy: it depends upon the direction of \mathbf{v} and therefore upon μ . One source of such dependence is already visible in (66). However,

unless anisotropy is driven externally, as in certain heating and current drive schemes, it occurs only in first δ -order:

$$\frac{\partial f_0}{\partial \mu} = \mathcal{O}(\delta) .$$

In that case (108) remains a consistent lowest order description, omitting only $\mathcal{O}(\delta\Delta)$ corrections to the source terms on the right-hand side (including numerous corrections of this order that are unrelated to anisotropy).

What is relevant, therefore, is the possibility of *zeroth-order* anisotropy of the unperturbed distribution. The point is that if $\mu \frac{\partial f_0}{\partial \mu} \sim U \frac{\partial f_0}{\partial U} \sim f_0$, then (89) contains terms of order $\Delta\Omega$, and our neglect of $\tilde{f} = \mathcal{O}(\Delta)$, while strictly consistent, omits a significant part of the linear perturbation. It turns out that the form of (108) is unaffected by these corrections; the only difference is that the linear perturbation f_1 must include two additional terms, as in (95).

Assuming then that $\frac{\partial f_0}{\partial \mu} = \mathcal{O}(1)$, we find that $\mathcal{O}(\Delta\Omega)$ -terms occur on the right-hand side of (94):

$$-\dot{\mu}_1 \frac{\partial f_0}{\partial \mu} = \mathcal{O}(\Delta\Omega) ,$$

where $\dot{\mu}_1$ is given by (80). In the approximation of (104) we have

$$\dot{\mu}_1 = \frac{e}{B_0} \mathbf{s} \cdot \mathbf{F}_1 , \quad (109)$$

where \mathbf{F}_1 is given by (105); in lowest order,

$$\dot{\mu}_1 = -\frac{e}{B_0} \mathbf{s} \cdot \left(\nabla \Phi - \frac{\mathbf{u}}{c} \nabla A_{\parallel} \right) .$$

These terms could be eliminated by appropriate change of variables, but it is simpler to integrate them directly. Thus making the usual decomposition in (86), $f = \tilde{f} + f$, we find the lowest order relation

$$\frac{\partial \tilde{f}}{\partial \gamma} = -\dot{\mu}_1 \frac{\partial f_0}{\partial \mu} = \frac{e}{B_0} \mathbf{s} \cdot \left(\nabla \Phi - \frac{\mathbf{u}}{c} \nabla A_{\parallel} \right) \frac{\partial f_0}{\partial \mu} .$$

Here gyrophase dependence occurs both in \mathbf{s} and in the fields, which are evaluated at $\mathbf{x} = \mathbf{X} + \rho(\gamma)$. We note, however, that (61) implies

$$\frac{\partial}{\partial \gamma} Y(\mathbf{X} + \rho) = \mathbf{s} \cdot \nabla Y \quad (110)$$

so integration is trivial:

$$\tilde{f} = \frac{e}{B_0} \left[\Phi - (\Phi) - \frac{\mathbf{u}}{c} (A_{\parallel} - \langle A_{\parallel} \rangle) \right] \frac{\partial f_0}{\partial \mu} .$$

where the integration constant has been chosen to make $\langle \tilde{f} \rangle = 0$. In the eikonal approximation, with $\tilde{f} = \exp(i\mathbf{k}_\perp \cdot \rho) \tilde{f}_A$ as usual, we have

$$\tilde{f}_A = \frac{e}{B_0} \left[\Phi_A - \frac{u}{c} A_{\parallel A} \right] \left[1 - e^{-i\mathbf{k}_\perp \cdot \rho} J_0(k_\perp \rho) \right] \frac{\partial f_0}{\partial \mu}. \quad (111)$$

This function is to be added to the gyrophase averaged \bar{f}_1 .

A similar correction term, proportional to $\partial f_0 / \partial \mu$, enters the expression for \bar{f} . Its origin is the term $\langle \dot{\mu}_1 \rangle \partial \bar{f} / \partial \mu$ in (89); however, it stems from the second, higher order term in (105). Thus we use (109),

$$\langle \dot{\mu}_1 \rangle = \frac{e}{B_0} \langle \mathbf{s} \cdot \mathbf{F}_1 \rangle,$$

and observe from (110) that $-\langle \mathbf{s} [\nabla \Phi - (u/c) \nabla A_{\parallel}] \rangle = 0$. Hence the only term to survive the average is

$$\langle \dot{\mu}_1 \rangle = -\frac{e}{cB_0} \left\langle \mathbf{s} \cdot \left(\frac{\partial}{\partial t} + \mathbf{u} \cdot \nabla \right) \mathbf{A}_1 \right\rangle.$$

In the eikonal approximation,

$$\begin{aligned} \langle \dot{\mu}_1 \rangle &= -i \frac{e}{cB_0} J_1(k_\perp \rho) s \mathbf{k}_\perp \times \mathbf{b} \cdot \left(\frac{\partial}{\partial t} + \mathbf{u} \cdot \nabla \right) \frac{\mathbf{A}_{1A}}{k_\perp}, \\ &= \frac{e}{cB_0} J_1(k_\perp \rho) s \left(\frac{\partial}{\partial t} + \mathbf{u} \cdot \nabla \right) \frac{B_{\parallel A}}{k_\perp}, \end{aligned}$$

where the second form results from rearranging the triple product $\mathbf{k}_\perp \times \mathbf{b} \cdot \mathbf{A}_1 = -\mathbf{b} \cdot \mathbf{k}_\perp \times \mathbf{A}_1$.

Hence anisotropy yields an additional source term, to be appended to the right-hand side of (108):

$$-\frac{e}{cB_0} J_1(k_\perp \rho) s \left(\frac{\partial}{\partial t} + \mathbf{u} \cdot \nabla \right) \frac{B_{\parallel A}}{k_\perp} \frac{\partial f_0}{\partial \mu}. \quad (112)$$

This term can be taken into account, at least approximately, as follows. Since terms of order $\delta \Delta$ are omitted, we are allowed the replacement

$$\left(\frac{\partial}{\partial t} + \mathbf{u} \cdot \nabla \right) B_{\parallel A} \rightarrow \left(\frac{\partial}{\partial t} + \mathbf{v}_0 \cdot \nabla \right) B_{\parallel A}.$$

We similarly ignore the collisional contribution, to identify the operator appearing in (112) with that on the left hand side of (108). It is then clear that (112) has the simple effect of adding to \bar{f}_1 a term proportional to $B_{\parallel A} / k_\perp \partial f_0 / \partial \mu$. That is,

$$\bar{f}_1 \rightarrow \bar{f}_1 - \frac{e}{cB_0} J_1(k_\perp \rho) s \frac{B_{\parallel A}}{k_\perp} \frac{\partial f_0}{\partial \mu}.$$

We can summarize these results as follows. When the unperturbed distribution is **isotropic** in lowest order, the linear perturbation of the distribution is simply given by (95) together with the solution to (108). More generally the perturbed distribution is given by

$$\begin{aligned} f_1 &= \bar{f}_1 + e\Phi_A e^{ik_{\perp}} \mathbf{k}_{\perp} \cdot \boldsymbol{\rho} \frac{\partial f_0}{\partial U} + \frac{e}{B_0} \left(\Phi_A - \frac{u}{c} A_{\parallel A} \right) \left[e^{ik_{\perp}} \cdot \boldsymbol{\rho} - J_0(k_{\perp} \rho) \right] \frac{\partial f_0}{\partial \mu} \\ &\quad - \frac{e}{cB_0} \frac{B_{1\parallel A}}{k_{\perp}} s J_1(k_{\perp} \rho) \frac{\partial f_0}{\partial \mu}, \end{aligned} \quad (113)$$

where \bar{f}_1 denotes the solution to (108).

Relatively general versions of the gyrokinetic equation, avoiding the eikonal approximation, are given by (89) and its linearized version, (94). Of course these forms are also more compact. It should be said, however, that applications of gyrokinetic theory, compelled by the need for explicitness and localization, invariably use the eikonal form.

4.4 Guiding-center Phase Space

Trapping

A dominant term in both the drift-kinetic and gyro-kinetic equations, the parallel streaming term $u \nabla_{\parallel} f$, is more complicated than may be apparent. The point is that, unlike v_x , say, in the ordinary convective term $\mathbf{v} \cdot \partial f / \partial \mathbf{x}$, the parallel velocity u is not a phase-space coordinate. Instead the coordinates are (μ, U) and position, \mathbf{x} , in terms of which

$$u(\mu, U, \mathbf{x}) = \pm \left\{ \frac{2}{m} [U - \mu B(\mathbf{x}) - e\Phi(\mathbf{x})] \right\}^{1/2}, \quad (114)$$

in view of (37). In other words, the symbol u abbreviates a rather complicated function of the magnetic and electrostatic field configurations; in particular, the function has a square-root singularity with ambiguous sign. Most of the difficulty in solving guiding-center kinetic equations results from this complication, the main features of which we consider here.

To begin we point out that (114) strictly pertains only in the drift-kinetic case. In gyrokinetic theory, one would append a zero subscript to Φ , and evaluate both fields at the guiding center position, \mathbf{X} , rather than \mathbf{x} . Fortunately neither change affects the present discussion; we keep to the drift-kinetic case for concreteness.

The physics underlying (114) is the modulation in speed experienced by the guiding center as it streams through regions of varying field and potential magnitude. Most importantly, (114) describes particle trapping—the

fact that guiding centers with sufficiently large magnetic moments are reflected by field gradients and prevented from penetrating regions of stronger field. Of course this circumstance is the root of magnetic mirror confinement; calling the reflected particles “trapped” reflects primarily mirror physics traditions. Particles with smaller magnetic moments, able to traverse the strong field regions, are called untrapped, “circulating,” or (in the language we will most often use) “passing.”

Here a very elementary point seems worth mentioning. When trapping is first uncovered from the point of view of equations like (114), it may seem to have some supra-mechanical origin: particles stop and turn around for no reason other than to preserve the reality of the streaming speed. Of course the bounce occurs as an ordinary, Newtonian response to electro-magnetic force—the mirror force of (36), acting on any magnetic dipole in a nonuniform external field, together with ordinary electrostatic fields. The parallel components of these forces are explicit in (2.87).

In the classic magnetic mirror field the passing particles are promptly lost through the mirrors at each end of the machine; only trapped particles are confined. In toroidal geometry, where both types of particles are confined, the trapped and passing orbits still differ qualitatively: only the passing particles are able to follow field lines over the full range of poloidal or toroidal angle.

We assume that the functions $\Phi(x)$ and $B(x)$ are sufficiently well-behaved that the equation $u = 0$ prescribes a smooth surface in coordinate space, for each (μ, U) . We call this surface the *bounce surface* and denote it by S_b :

$$S_b(\mu, U) \equiv \{\mathbf{x}_b | U - \mu B(\mathbf{x}_b) - e\Phi(\mathbf{x}_b) = 0\} . \quad (115)$$

The points \mathbf{x}_b of S_b are similarly called *bounce points*. The trapped orbits, or trapped particles, are simply those possessing bounce points. It is evident that no particle can penetrate its bounce surface.

In mirror geometry, for example, the bounce surfaces are caps at each end of the machine. In tokamaks, the bounce surfaces are approximately vertical cylinders whose axes coincide with the toroidal symmetry axis; recall that the tokamak B depends mainly on major radius, as in (3.104).

It should be kept in mind that only in the collisionless case are μ and U fixed: physical trajectories will preserve these invariants only in so far as the collision frequency is smaller than the transit frequency. On the other hand we shall find that the structure imposed on phase space by trapping is generally relevant.

In mirror devices, a steep electrostatic potential trough at each end (end “sheath”) helps to trap and confine electrons; then trapping results from both magnetic and electrostatic fields. In toroidal geometry, on the other hand, trapping is almost purely magnetic. To understand why, we recall that guiding-center motion is predominantly along the confining field, as in (33). Furthermore, rapid electron streaming along field lines short-

circuits potential variation in the parallel direction, so that

$$\nabla_{\parallel} \left(\frac{e\Phi}{T} \right) = \mathcal{O}(\delta). \quad (116)$$

We can conclude that

$$\mathbf{v}_{gc} \cdot \nabla \Phi = \mathcal{O}(\delta). \quad (117)$$

An explicit demonstration of (116) is provided in §5.3.

Thus the electrostatic term in (114) has little effect on orbits. Indeed, over the course of any chosen orbit, the kinetic energy

$$w = U - e\Phi \quad (118)$$

is an approximate invariant. We have already noted, in (72), the simple form of the kinetic equation when w is used. It turns out that w is a more convenient energy variable than U in most toroidal confinement contexts; in fact the simplest analysis of trapping uses as coordinates neither U nor μ , but w and the ratio μ/w . We next consider some properties of these new variables.

Pitch-angle Variable

The pitch-angle variable is denoted by λ and defined by

$$\lambda \equiv \frac{\mu}{w}. \quad (119)$$

Whenever electrostatic trapping can be neglected, as in (117), λ is manifestly a lowest-order invariant, whose use does not change the form of the drift-kinetic equation. [Modifications to the gyrokinetic equation, coming from $\partial/\partial\mu = (1/w)\partial/\partial\lambda$ are trivial.] Its name reflects the fact that

$$\lambda B = \frac{v_1^2}{v^2} = \sin^2 \Theta \quad (120)$$

is the squared sine of the angle, Θ , between \mathbf{B} and \mathbf{v} —the angle that prescribes the pitch of a particle's helical Larmor orbit. An advantage of λ is the simple form it gives to (114):

$$w(\lambda, w, \mathbf{x}) = \pm \left(\frac{2w}{m} \right)^{1/2} [1 - \lambda B(\mathbf{x})]^{1/2}. \quad (121)$$

There is an additional advantage, that will play a role in Chapter 5: the set (λ, w, γ) , unlike (μ, U, γ) , provides orthogonal coordinates in velocity space.

The bounce surface now consists of points $\mathbf{x}_b(\lambda)$ such that

$$B(\mathbf{x}_b) = \frac{1}{\lambda}. \quad (122)$$

Clearly any orbit with $1/\lambda$ greater than the maximum of B has no bounce surface; thus the passing region of velocity space is characterized by $0 < \lambda < 1/B_M$, where B_M is the maximum of B on a flux surface. It is convenient to denote the upper limit of the passing region by λ_c , the critical λ for trapping:

$$\lambda_c \equiv \frac{1}{B_M}. \quad (123)$$

On the other hand, the full domain of $\lambda, 0 < \lambda < 1/B(\mathbf{x})$, is a function of position: only particles with sufficiently small pitch angle can reach a given point \mathbf{x} . We are thus led to the following decomposition of velocity space:

$$0 < \lambda < \lambda_c : \quad \text{passing region} ; \quad (124)$$

$$\lambda_c < \lambda < 1/B(\mathbf{x}) : \quad \text{trapped region}.$$

A typical configuration is sketched in Figure 1. The surface $\lambda = \lambda_c$, separating classes of orbits with differing topology, is called the separatrix in velocity space. We shall see presently that it is similar to the separatrix occurring in the phase space of a simple pendulum.

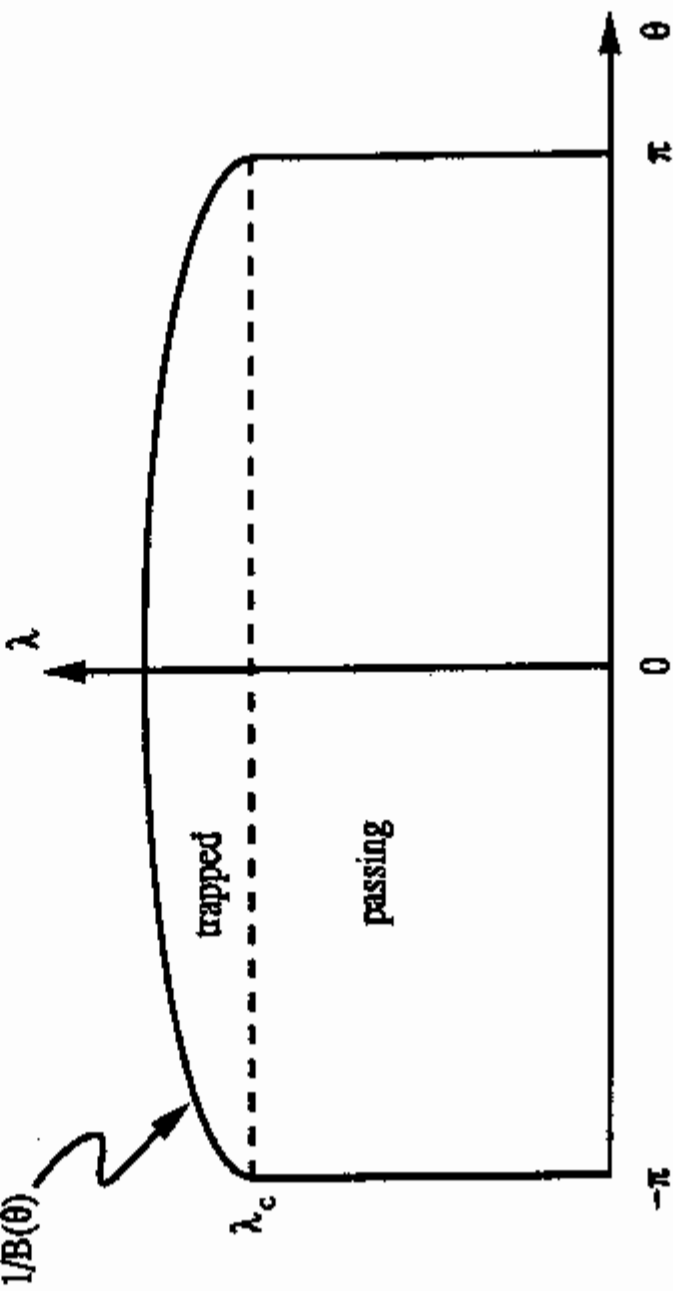


Figure 1. Phase domains in the (λ, θ) -plane.

Discrete Variable and Bounce Condition

To specify a point in guiding-center phase space, the variables λ, w and \mathbf{x} are not sufficient. Because of the square root occurring in (114), the sign

of the parallel velocity is also required. We denote the sign by

$$\sigma = \frac{u}{|u|} = \pm 1. \quad (125)$$

The variable σ enters analysis of guiding-center kinetic equations in surprisingly critical ways. The basic point is that σ is a dynamical invariant only for passing particles—only if $\lambda < \lambda_c$.

The distribution f is properly expressed as

$$f(\mathbf{x}, \mathbf{v}) \rightarrow f(\mathbf{x}, \lambda, w, \sigma) = f_\sigma(\mathbf{x}, \lambda, w), \quad (126)$$

where on the right we introduce the convention of indicating σ -dependence by a subscript. Now observe that σ is not defined on the bounce surface, where a trapped guiding-center reverses; to insure that the distribution has a definite value on S_b we must require

$$f_+(\mathbf{x}_b, \lambda, w) = f_-(\mathbf{x}_b, \lambda, w) \quad (127)$$

at each bounce point $\mathbf{x}_b(\lambda)$. Equation (29) is called the *bounce condition*; it provides critical boundary data for the distribution in all kinetic studies of trapping.

The importance of the bounce condition is especially clear in toroidal geometry. Consider for simplicity the axisymmetric case, in which the variation of B along any orbit depends only on $\cos \theta$. We choose the domain of θ to be $\{-\pi, \pi\}$, with $\theta = 0$ at the toroidal midplane on the outside (larger R) of the toroidal surface. Since $B(\theta) = B(-\theta)$, the bounce points, or *bounce angles*, $\theta_b(\lambda)$, occur in pairs:

$$B(\pm \theta_b) = \frac{1}{\lambda}. \quad (128)$$

The distribution of passing particles, which traverse an entire magnetic surface, is constrained by periodicity in the usual way:

$$f_\sigma(\theta = \pi, \lambda, w) = f_\sigma(\theta = -\pi, \lambda, w), \quad \text{for } \lambda < \lambda_c. \quad (129)$$

But since trapped particles are confined to the region $|\theta| < \theta_b < \pi$, (129) is meaningless for $\lambda > \lambda_c$: there is no periodicity condition in the *trapped region of phase space*. The missing constraint is of course provided by the bounce condition, which now takes the simplified form,

$$f_+(\theta = \pm \theta_b, \lambda, w) = f_-(\theta = \pm \theta_b, \lambda, w), \quad \text{for } \lambda > \lambda_c. \quad (130)$$

Orbital Average*

We seek here an operator that plays a role in phase space analogous to that played by the flux-surface average in coordinate space. We recall that

$\langle A \rangle_s$, the flux-surface average of $A(\mathbf{x})$, annihilates the differential operator $\mathbf{B} \cdot \nabla A = B \nabla_{\parallel} A$. The orbital average, denoted by $\langle F \rangle_o$, annihilates the corresponding operator $u \nabla_{\parallel} F$, where $F(\mathbf{x}, \mathbf{v})$ is some phase-space function—usually a distribution function. (Strictly speaking, F can be any function whose velocity moments are physically well-behaved functions of position.)

It is clear from the argument of Chapter 3 [cf. (3.40)] that $\langle \cdot \rangle_o$ must differ from the flux-surface average by a factor of B/u (aside from normalization); the point is that the orbital average is a time average, and $dt = (B/u)(ds/B)$. Indeed for passing particles we have, with the normalization to insure $\langle 1 \rangle_o = 1$,

$$\langle F \rangle_o = \frac{\left\langle \frac{FB}{u} \right\rangle_s}{\left\langle \frac{B}{u} \right\rangle_s} \quad (\text{passing region}). \quad (131)$$

In the trapped region of phase space, however, this definition must be modified. First of all, the integral in (131) does not exist in the trapped region, where u cannot be defined over the entire flux surface. This difficulty is easily remedied; we merely set the integration limits in (3.36) at the bounce surface, instead of $-\pi$ and π . We denote by $\langle A \rangle_b$ the flux-surface average with this appropriately restricted integration domain; $\langle A \rangle_b$ is a surface-average over the accessible part of the flux surface.

Unfortunately the operation $\langle FB/u \rangle_b / \langle B/u \rangle_b$, although meaningful, does not generally annihilate $\nabla_{\parallel} F$ in the trapped region. The problem is that F need not be periodic in the trapped region: its moments will be periodic and well-behaved provided only that F satisfies the bounce condition, (130). Again, the remedy is straightforward. Noticing that

$$\sum_{\sigma} \sigma f_o(r, \theta = \pm\theta_b, \lambda, w) = \sum_{\sigma} \frac{u}{|u|} f_o(r, \theta = \pm\theta_b, \lambda, w) = 0$$

for any f satisfying the bounce condition, we infer the normalized annihilator

$$\langle F \rangle_o \equiv \frac{1}{2} \sum_{\sigma} \frac{\left\langle \frac{FB}{|u|} \right\rangle_b}{\left\langle \frac{B}{|u|} \right\rangle_b} \quad (\text{trapped region}). \quad (132)$$

Note that $\langle F \rangle_o$ is necessarily independent of σ in the trapped region—as expected, since the orbits of trapped particles have no preferred direction.

The reader can verify that (131) and (132) indeed insure that

$$\langle \sigma | u | \nabla_{\parallel} f \rangle_o = 0 \quad (133)$$

for any function $f = f_o(\mathbf{x}, \lambda, w)$ that satisfies the bounce condition.

An explicit expression for the orbital average is easily written down in the axisymmetric case. We use (3.57) to find

$$\begin{aligned} \langle F \rangle_o &= \frac{\int_{-\pi}^{\pi} \frac{B}{u} R^2 F d\theta}{\int_{-\pi}^{\pi} \frac{B}{u} R^2 d\theta}, \quad \text{for } \lambda < \lambda_c, \\ \langle F \rangle_o &= \frac{\frac{1}{2} \sum_{\sigma} \int_{-\theta_b}^{\theta_b} \frac{B}{|u|} R^2 F d\theta}{\int_{-\theta_b}^{\theta_b} \frac{B}{|u|} R^2 d\theta}, \quad \text{for } \lambda > \lambda_c. \end{aligned} \quad (134)$$

An alternative version is derived from (3.37); for $\lambda < \lambda_c$ we have

$$\left\langle \frac{F B}{u} \right\rangle_o = \oint d\theta \frac{F B}{u \mathbf{B} \cdot \nabla \theta} \quad (135)$$

Noting that $u \mathbf{B} \cdot \nabla \theta / B = u^\theta$, the contravariant θ -component of the parallel velocity, we can write

$$\frac{\left\langle \frac{F B}{u} \right\rangle_o}{\left\langle \frac{B}{u} \right\rangle_o} = \frac{\oint d\theta}{\oint d\theta} \frac{\frac{d\theta}{u^\theta}}{\frac{1}{u^\theta}} \quad \text{for } \lambda < \lambda_c.$$

The denominator in this expression is the *transit time* required for a passing particle to encircle the minor axis; it is denoted by

$$\tau_t \equiv \oint \frac{d\theta}{|u^\theta|}. \quad (136)$$

The corresponding time for the trapped region is the *bounce time*, the poloidal period of a trapped particle orbit:

$$\tau_b \equiv \int_{-\theta_b}^{\theta_b} \frac{d\theta}{|u^\theta|}. \quad (137)$$

Thus the orbital average is expressed as

$$\begin{aligned} \langle F \rangle_o &= \frac{1}{\tau_t} \int_{-\pi}^{\pi} \frac{F d\theta}{|u^\theta|}, \quad \text{for } \lambda < \lambda_c, \\ \langle F \rangle_o &= \frac{1}{2\tau_b} \int_{-\theta_b}^{\theta_b} \frac{F d\theta}{|u^\theta|}, \quad \text{for } \lambda > \lambda_c. \end{aligned} \quad (138)$$

It should be clear that the definitions that

$$\lim_{\lambda \rightarrow \lambda_c} \theta_b(\lambda) = \pi \quad (139)$$

and therefore that

$$\lim_{\lambda \rightarrow \lambda_c} \tau_b = \lim_{\lambda \rightarrow \lambda_c} \tau_i. \quad (140)$$

Actually (140) has questionable meaning since, as we shall see, neither side of the equation is finite. The singularity in the orbital time on the separatrix is considered in more detail below.

Banana Orbits*

In axisymmetric geometry it is appropriate to view particle orbits in poloidal cross-section: one projects the three-dimensional orbit onto a surface of fixed toroidal angle. (In Chapter 3 we used such a surface, denoted by S_T , to study field line trajectories.) Then the orbits of passing particles appear as simple closed curves surrounding the magnetic axis, which appears as a point; the curves do not quite coincide with flux surfaces because of first-order drift motion across the magnetic field. Trapped orbits have a more interesting appearance: they reverse at $\theta = \pm\theta_b$, avoiding the inner region of the torus, while traversing the region $\{-\theta_b < \theta < \theta_b\}$ twice in each period. In combination with radial drifts, this bounce motion produces orbits whose poloidal cross-sections have a crescent shape, as shown in Figure 2. They are traditionally called *banana orbits*.

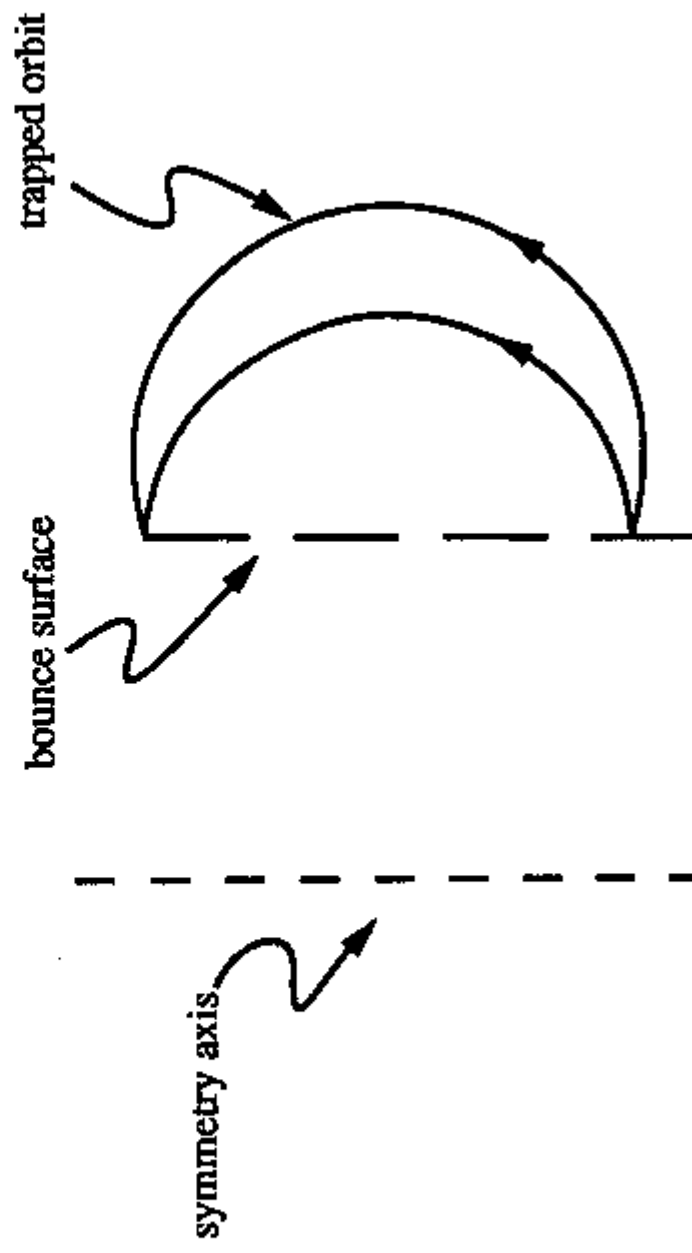


Figure 2. Poloidal cross section of trapped guiding-center orbit.

It is sometimes convenient to distinguish not just two, but three categories of guiding-center orbits. Thus we consider the deeply trapped parti-

cles, with nearly maximal pitch-angle variables:

$$\lambda \approx \lambda_m = \max_{\theta} \frac{1}{B} \quad (\text{deeply trapped}) ; \quad (141)$$

the *far-untrapped* particles, with λ well below λ_c ; and the *boundary layer* particles, close to the separatrix:

$$\lambda \approx \lambda_c \quad (\text{boundary layer}) . \quad (142)$$

The boundary layer, whose width in λ depends upon collisional effects not considered here, includes both trapped and passing particles. Particles in the layer play a special role in various transport and instability contexts, essentially because they are exceptionally slow.

A helpful model for the various regions of guiding-center phase space is provided by the nonlinear pendulum. The pendulum angle with respect to its stable equilibrium position can be identified directly with poloidal angle θ , and the different phase-space regions for nonlinear pendulum dynamics correspond closely to those of toroidally confined guiding-centers. Full rotation of the pendulum about its axis, $\Delta\theta > 2\pi$, corresponds to the motion of passing particles. Small deflections of the pendulum, leading to weak oscillation with $\Delta\theta \ll 1$, correspond to deeply trapped particles. The boundary layer is a thin region enclosing the pendulum separatrix, corresponding to swings that bring the pendulum tip just barely to (or barely beyond) the vertical position at $\theta = \pi$.

What should be noticed is that, while the pendulum always moves slowly near its turning points $\pm\theta_b$, its motion is exceptionally slow when $|\theta_b|$ is close to π , essentially because the vertical position provides an (unstable) equilibrium. Exactly on the separatrix, the period of the pendulum becomes logarithmically infinite.

It is therefore not surprising that the bounce-time—and therefore, in view of (140), the transit time—is singular on the separatrix:

$$\tau_b \rightarrow \infty , \text{ for } \lambda \rightarrow \lambda_c . \quad (143)$$

Indeed, for realistic geometries, τ_b has the same logarithmic singularity as the pendulum period. What is physically significant is not the singularity but rather the very slow motion of boundary layer particles as they approach $\theta = \pi$. Such particles, like the pendulum near its unstable equilibrium point, are sensitive to small perturbations. In particular, they can easily be tipped across the separatrix—not only because of their proximity to the separatrix, but also because of their slowness. Thus processes ordinarily considered feeble—with growth or accumulation times long compared to a typical bounce time—can be virulent on the scale of a boundary-layer bounce time.

Velocity Integration

At any point \mathbf{x} we can choose Cartesian velocity coordinates with z -axis, say, along the magnetic field (i.e., such that $u = v_z$). Then, from the velocity gradients,

$$\frac{\partial \mu}{\partial \mathbf{v}} = \frac{m v_{\perp}}{B}, \quad \frac{\partial U}{\partial \mathbf{v}} = m \mathbf{v}, \quad \text{and} \quad \frac{\partial \gamma}{\partial \mathbf{v}} = \frac{\mathbf{b} \times \mathbf{v}}{v_{\perp}^2}$$

it is easy to compute the Jacobian determinant $\partial(\mu, U, \gamma)/\partial(v_x, v_y, v_z) = m^2 u/B$ and infer

$$d^3 v = \frac{B}{m^2 |u|} d\mu dU d\gamma = \frac{w B}{m^2 |u|} d\lambda dw d\gamma.$$

To integrate over the full range of \mathbf{v} we must take into account the two branches of $u = \sigma|u|$; thus we have

$$\int d^3 v = \sum_{\sigma} \int \frac{w B}{m^2 |u|} d\lambda dw d\gamma. \quad (144)$$

For the guiding-center case there is no γ -dependence, so

$$\int d^3 v = \frac{2\pi B}{m^2} \sum_{\sigma} \int_0^{1/B} d\lambda \int_0^{\infty} dw \frac{w}{|u|}. \quad (145)$$

Note the spatial dependence of the integration limit, $1/B$. Similarly

$$\int d^3 v = \frac{B}{m^2} \sum_{\sigma} \oint d\gamma \int_{e\Phi}^{\infty} dU \int_0^{U-e\Phi/B} d\mu \frac{1}{|u|}. \quad (146)$$

Often one is interested in the flux-surface average of a velocity integral, $\langle \int d^3 v F(\mathbf{x}, \mathbf{v}) \rangle_s$; such integrals must be evaluated with care when guiding-center variables are used. We suppose that F is a distribution function multiplied by some smooth function of \mathbf{v} ; in particular, F must satisfy the bounce condition. From (145),

$$\left\langle \int d^3 v F \right\rangle_s = \frac{2\pi}{m^2} \sum_{\sigma} \int_0^{\infty} dw w \left\langle \int_0^{\lambda_c} d\lambda \frac{B}{|u|} F + \int_{\lambda_c}^{1/B} d\lambda \frac{B}{|u|} F \right\rangle_s.$$

A key point is that the flux-surface average can be brought inside the λ -integral trivially only for $\lambda < \lambda_c$. In the trapped region, we must first rearrange the limits of the λ - and (implicit) θ -integrals, not only because $1/B$ depends on θ , but also because of the restricted θ -domain for $\lambda > \lambda_c$. Thus, if the θ -integration is performed first, it is taken between bounce points, so that

$$\langle \dots \rangle_s \rightarrow \langle \dots \rangle_b$$

and then the λ -integral extends up to λ_m [recall (141)]. That is, as can be seen from Fig. 1,

$$\left\langle \int_{\lambda_e}^{1/B} d\lambda \frac{B}{|u|} F \right\rangle_s = \int_{\lambda_e}^{\lambda_m} d\lambda \left\langle \frac{B}{|u|} F \right\rangle_b \quad (147)$$

We compare this result to (131) and (132) to conclude, after simple manipulation, that

$$\left\langle \int d^3v F \right\rangle_s = \frac{2\pi}{m^2} \sum_\sigma \int_0^\infty dw w \int_0^{\lambda_m} d\lambda \left\langle \frac{B}{|u|} \right\rangle_b \langle F \rangle_\sigma. \quad (148)$$

In other words the flux-surface average of a moment of the distribution is a simple integral of its orbital average—essentially because the weight function B/u occurs in each.

4.5 Application: Flow of a Magnetized Plasma

Magnetization current

The decomposition of f into its gyro-averaged and gyrophase-dependent parts, as in (45), leads naturally to a decomposition of the plasma current:

$$\mathbf{J} = \mathbf{J}_{gc} + \mathbf{J}_m. \quad (149)$$

Here \mathbf{J}_{gc} is the current of guiding centers, while \mathbf{J}_m , the magnetization current, is given by

$$\mathbf{J}_m = c \nabla \times \mathcal{M}, \quad (150)$$

where \mathcal{M} is the plasma magnetization. The physical picture underlying (149) is quite simple: each guiding center represents a gyrating particle, carrying a magnetic moment $\boldsymbol{\mu} = -b\boldsymbol{\mu}$. Nonuniformity in the spatial distribution of magnetic moments yields a magnetization current, which must be added to the current resulting from motion of the guiding center. The fact that current results from the curl of \mathcal{M} is well-known from elementary magnetostatics; an especially helpful discussion is due to Spitzer (Spitzer, 1962).

The decomposition (149) is conveniently made for each plasma species. Recalling that $\mathbf{J} = \sum_s e n_s \mathbf{V}_s$, with

$$n_s \mathbf{V}_s \equiv \int d^3v f_s \mathbf{v}, \quad (151)$$

we write

$$n_s \mathbf{V}_s = n_s \mathbf{V}_{ges} + c \nabla \times \mathbf{M}_s. \quad (152)$$

Evidently

$$\begin{aligned}\mathbf{J}_{gc} &= \sum_s e_s n_s \mathbf{V}_{ges}, \\ \mathcal{M} &= \sum_s e_s \mathbf{M}_s.\end{aligned}\tag{153}$$

Our goal in this section is to explicitly evaluate (151), using the result (63) of drift-kinetic theory. We will find that the plasma velocity is indeed given by the sum of the mean flow of guiding centers,

$$n\mathbf{V}_{gc} \equiv \int d^3v \bar{f} (\mathbf{u} + \mathbf{v}_D + \mathbf{u}_D),\tag{154}$$

plus the curl of the plasma magnetization,

$$e\mathbf{M} \equiv \int d^3v \bar{f} \mu.\tag{155}$$

(Species subscripts are suppressed.) In (154), \mathbf{v}_D and \mathbf{u}_D are the perpendicular and parallel drifts of (68); the right-hand side of (155) is the obvious (single-species) magnetic moment per unit volume. In other words, (152) is satisfied with very natural definitions of its two terms.

Notice that $n\mathbf{V}$ has the same divergence as $n\mathbf{V}_{gc}$; hence, with regard to particle conservation, the two flows are equivalent. More generally, however, the distinction between guiding-center motion and plasma motion is crucial. It explains, for example, the diamagnetic current of (3.63): no guiding center executes a ∇P -drift! Thus (152), which we will call the “magnetization law,” has pervasive importance.

Surprisingly the magnetization law is not always appreciated. One can find in the literature confusions between \mathbf{V}_{gc} and \mathbf{V} , as well as misunderstandings concerning \mathcal{M} . For this reason, in preparation for the discussion of Chapter 6, and because the proof nicely explicates issues introduced in previous sections, we next verify (152) in detail.

Drift Velocity

To begin we consider the guiding-center velocity

$$\mathbf{v}_{gc} \equiv \mathbf{u} + \mathbf{v}_D + \mathbf{u}_D.\tag{156}$$

We derive expressions for \mathbf{v}_{gc} that simplify the proof of (152), and are also useful in other contexts. For simplicity we restrict attention to the time-independent case, thus expressing the perpendicular drift of (34) as

$$\mathbf{v}_D = \frac{1}{\Omega} \mathbf{b} \times \left[\left(u^2 + \frac{\mu B}{m} \right) \frac{\nabla B}{B} + \frac{e}{m} \nabla \Phi \right] + \frac{u^2}{\Omega} \frac{(\nabla \times \mathbf{B})_\perp}{B}.\tag{157}$$

Here (3.89) was used to write the magnetic curvature as

$$\kappa = \frac{\nabla_{\perp} B}{B} - \frac{\mathbf{b} \times (\nabla \times \mathbf{B})}{B}.$$

The point of (157) is that its last term, proportional to the perpendicular current density and therefore to ∇P , is relatively small in a low-beta plasma. The other terms together comprise the “low-beta drift,” which we will denote by \mathbf{v}_d , thus expressing (157) as

$$\mathbf{v}_D = \mathbf{v}_d + \frac{u^2}{\Omega}(\nabla \times \mathbf{B})_{\perp}. \quad (158)$$

Notice that in a scalar-pressure equilibrium, where $J^r = 0$, the second term has no radial component. Hence the radial equilibrium drift is given by \mathbf{v}_d , for any plasma beta:

$$v_D^r = v_d^r. \quad (159)$$

At this point we specifically adopt U and μ as our velocity coordinates. Then (114) is pertinent,

$$\nabla u = -\frac{1}{um}(\mu \nabla B + e \nabla \Phi),$$

and the low-beta drift can be expressed as

$$\mathbf{v}_d = -u\mathbf{b} \times \nabla \left(\frac{u}{\Omega} \right). \quad (160)$$

Since

$$\frac{u}{B} \nabla \times \left(\frac{\mathbf{B}u}{\Omega} \right) = \frac{u^2}{\Omega B} \nabla \times \mathbf{B} + \mathbf{v}_d,$$

and

$$\mathbf{u}_D = \frac{\mu}{m\Omega}(\nabla \times \mathbf{B})_{||}, \quad (161)$$

the full guiding-center velocity is

$$\mathbf{v}_{gc} = \frac{u}{B} \left[\mathbf{B} + \nabla \times \left(\frac{\mathbf{B}u}{\Omega} \right) \right] - \frac{1}{\Omega} \left(u^2 - \frac{\mu B}{m} \right) \frac{(\nabla \times \mathbf{B})_{||}}{B}. \quad (162)$$

Velocity Moment

We next evaluate (151):

$$n\mathbf{V} = \int d^3v (\mathbf{u} + \mathbf{s})(\bar{f} + \tilde{f}) = n\mathbf{V}_{||} + n\mathbf{V}_{\perp}, \quad (163)$$

where

$$n\mathbf{V}_{||} \equiv \int d^3v \mathbf{u}\bar{f}, \quad n\mathbf{V}_{\perp} \equiv \int d^3v \mathbf{s}\tilde{f}. \quad (164)$$

Of course the averaged distribution is not known, so the parallel flow cannot be made more explicit. Our objective is to express the perpendicular flow,

$$n\mathbf{V}_\perp \equiv \int d^3v s(\mathbf{e}_2 \cos \gamma - \mathbf{e}_3 \sin \gamma) \tilde{f} \quad (165)$$

in terms of \tilde{f} ; the result will verify (152).

Notice that the right hand side of (152) is computed from \tilde{f} exclusively, while (165) involves only \tilde{f} . The point is that, as is clear from (63), \tilde{f} is a functional of \tilde{f} , so that moments of the two distributions are not independent. A more interesting observation is that one can compute various perpendicular flows—such as the energy or momentum flow (perpendicular stress)—from \tilde{f} , provided that magnetization effects are taken into account. We will return to this comment in Chapter 6.

From (65) we observe that g , having only $\cos^2 \gamma$ and $\sin^2 \gamma$ components, cannot contribute to (165). With this remark and (64) we see that the steady-state perpendicular flow is

$$n\mathbf{V}_\perp = \mathbf{F}_1 + \mathbf{F}_2 , \quad (166)$$

$$\begin{aligned} \mathbf{F}_1 &= - \int d^3v s \rho \cdot \nabla \tilde{f} , \\ \mathbf{F}_2 &= - \int d^3v s \frac{e}{c} \left[\rho \cdot \mathbf{b} \times \mathbf{v}_D \frac{\partial \tilde{f}}{\partial \mu} \right] . \end{aligned}$$

The identity

$$\oint \frac{d\gamma}{2\pi} \hat{\rho} \cdot \mathbf{A} = \frac{1}{2} \mathbf{b} \times \mathbf{A}$$

implies

$$\mathbf{F}_1 = \frac{1}{2\Omega} \mathbf{b} \times \int d^3v s^2 \nabla \tilde{f} ,$$

$$\begin{aligned} \mathbf{F}_2 &= \frac{m}{2B} \mathbf{b} \times \int d^3v s^2 (\mathbf{b} \times \mathbf{v}_D) \frac{\partial \tilde{f}}{\partial \mu} , \\ &= - \int d^3v \mu \mathbf{v}_D \frac{\partial \tilde{f}}{\partial \mu} . \end{aligned}$$

We next evaluate \mathbf{F}_2 by partial integration. Noticing, from (146), that $d^3v u$ is independent of μ (a fact we use repeatedly below), and temporarily disregarding the surface term at $\mu = (U - e\Phi)/B$, we find

$$\mathbf{F}_2 = \int d^3v |u| \tilde{f} \frac{\partial}{\partial \mu} \left(\frac{\mu}{|u|} \mathbf{v}_D \right)$$

At this point we recall (158) to distinguish two contributions to \mathbf{F}_2 . From \mathbf{v}_d we obtain the term

$$\int d^3v |u| \tilde{f} \frac{\partial}{\partial \mu} \left(\frac{\mu}{|u|} \mathbf{v}_d \right) = \int d^3v \tilde{f} \mathbf{v}_d + \int d^3v |u| \tilde{f} \frac{\partial}{\partial \mu} \left[-\mathbf{b} \times \nabla \left(\frac{|u|}{\Omega} \right) \right] ,$$

or, since $\partial|u|/\partial\mu = -B/(m|u|)$,

$$\int d^3v |u| \bar{f} \frac{\partial}{\partial\mu} \left(\frac{\mu}{|u|} \mathbf{v}_d \right) = n \mathbf{V}_d + \frac{c}{e} \int d^3v |u| \mu \bar{f} \mathbf{b} \times \nabla \left(\frac{1}{|u|} \right), \quad (167)$$

where

$$n \mathbf{V}_d \equiv \int d^3v \bar{f} \mathbf{v}_d. \quad (168)$$

The other contribution to \mathbf{F}_2 comes from

$$-(\nabla \times \mathbf{B})_\perp \int d^3v \mu \frac{u^2}{B\Omega} \frac{\partial \bar{f}}{\partial\mu} = \frac{(\nabla \times \mathbf{B})_\perp}{\Omega} \int d^3v \bar{f} \frac{|u|}{B} \frac{\partial}{\partial\mu} \left(\frac{|u|}{u} \right). \quad (169)$$

There is no boundary contribution, since $|u|\mu$ vanishes at $\mu = (U - e\Phi)/B$. After performing the derivative we have

$$\begin{aligned} -(\nabla \times \mathbf{B})_\perp \int d^3v \mu \frac{u^2}{B\Omega} \frac{\partial \bar{f}}{\partial\mu} &= \frac{(\nabla \times \mathbf{B})_\perp}{\Omega} \int d^3v \frac{\bar{f}}{B} \left(u^2 - \frac{\mu}{m} B \right) \\ &= \frac{(\nabla \times \mathbf{B})_\perp}{m\Omega B} (P_{\parallel} - P_{\perp}). \end{aligned} \quad (170)$$

Here the parallel and perpendicular pressures, introduced in (3.98), are given in terms of \bar{f} by

$$\begin{aligned} P_{\parallel} &= \int d^3v \bar{f} m u^2, \\ P_{\perp} &= \int d^3v \bar{f} \mu B. \end{aligned} \quad (171)$$

Now \mathbf{F}_2 is given by the sum of the right-hand sides of (167) and (170). Before summarizing this result we note that the second term of (167) helpfully combines with \mathbf{F}_1 :

$$\begin{aligned} \frac{1}{2\Omega} \mathbf{b} \times \int d^3v s^2 \nabla \bar{f} + \frac{c}{e} \int d^3v |u| \mu \bar{f} \mathbf{b} \times \nabla \left(\frac{1}{|u|} \right) \\ = \int d^3v |u| \frac{\mu B}{m\Omega} \mathbf{b} \times \nabla \left(\frac{\bar{f}}{|u|} \right) = \nabla \times \mathbf{B} \int d^3v \frac{\mu}{m\Omega} \bar{f} - \nabla \times \int d^3v \frac{\mu \mathbf{B}}{m\Omega} \bar{f} \\ = \nabla \times \mathbf{B} \frac{P_{\perp}}{m\Omega B} - \nabla \times \left(\mathbf{B} \frac{P_{\perp}}{m\Omega B} \right). \end{aligned} \quad (172)$$

Hence we have

$$\begin{aligned} n \mathbf{V}_{\perp} &= \mathbf{F}_1 + \mathbf{F}_2 = n \mathbf{V}_d + \nabla \times \mathbf{B} \cdot \frac{P_{\perp}}{m\Omega B} - \nabla \times \left(\mathbf{B} \frac{P_{\perp}}{m\Omega B} \right) \\ &\quad + (\nabla \times \mathbf{B})_{\perp} \frac{P_{\parallel} - P_{\perp}}{m\Omega B}. \end{aligned} \quad (173)$$

Now we gather the pieces. From (158) and (171) we have

$$n\mathbf{V}_D = n\mathbf{V}_d + (\nabla \times \mathbf{B})_{\perp} \frac{P_{\parallel}}{m\Omega B}$$

and from (161),

$$n\mathbf{U}_D \equiv \int d^3v \tilde{f} u_D = (\nabla \times \mathbf{B})_{\parallel} \frac{P_{\perp}}{m\Omega B}.$$

Therefore (173) is

$$n\mathbf{V}_{\perp} = n\mathbf{V}_D + n\mathbf{U}_D - \nabla \times \left(\mathbf{B} \frac{P_{\perp}}{m\Omega B} \right)$$

whence

$$n\mathbf{V} = n\mathbf{V}_{\parallel} + n\mathbf{V}_D + n\mathbf{U}_D - \frac{c}{e} \nabla \times \left(\mathbf{b} \frac{P_{\perp}}{B} \right) \quad (174)$$

in agreement with (152), provided that we choose

$$\mathbf{M} = -\mathbf{b} \frac{P_{\perp}}{eB} \quad (175)$$

as in (155) (recall that $\boldsymbol{\mu} = -\mathbf{b}\boldsymbol{\mu}$).

This demonstration is incomplete for three reasons. First, we have omitted the partial time derivative terms, including the electromagnetic contribution to \mathbf{v}_E and the $\partial \mathbf{A}/\partial t$ term in \tilde{f} . The straightforward demonstration that (152) remains valid when these terms are included is left to the reader. Second, bringing the gradient operator outside the integral, in deriving (172), is cavalier. It is not sufficient to observe that $\nabla[d^3v(|u|/B)] = 0$: spatial dependence also occurs in the integration limits. Thus we have, for any function F ,

$$\begin{aligned} \nabla \int d^3v \frac{|u|}{B} F(\mu, U, \mathbf{x}) &= \int d^3v \frac{|u|}{B} \nabla F \\ &\quad + \nabla \left(\frac{U - e\Phi}{B} \right) 2\pi B \sum_{\sigma} \int dU F \left(\frac{U - e\Phi}{B}, U, \mathbf{x} \right). \end{aligned} \quad (176)$$

(There is no similar contribution from the U -integration limit, $e\Phi/m$, because at this limit the domain of μ vanishes.) The case of (172) is slightly more complicated because it corresponds to $F = (\mu B/m\Omega)(\tilde{f}/|u|)$, which is singular at $\mu = \mu_M \equiv (U - e\Phi)/B$. We fix this by temporarily modifying the integration limit: $\mu_M \rightarrow \mu_M - \Delta$, eventually letting $\Delta \rightarrow 0$. Thus the omitted term is

$$\begin{aligned} -2\pi B \sum_{\sigma} \int dU \mathbf{b} \times \nabla \mu_M \frac{\mu_M B}{m\Omega} \frac{\tilde{f}}{|u|} \Big|_{\mu_M - \Delta} . \end{aligned} \quad (177)$$

The third reason that (174) is incomplete is our neglect in \mathbf{F}_2 of the surface term, at $\mu = \mu_M$, from the partial integration leading to (167). The missing term is also singular, since $\nabla u \propto 1/u$, so we again replace μ_M by $\mu_M - \Delta$ to write it as

$$\begin{aligned} 2\pi B \sum_{\sigma} \int dU \bar{f}_{\mu} \mathbf{b} \times \nabla \left(\frac{|u|}{\Omega} \right) & \\ = 2\pi B \sum_{\sigma} \int dU \frac{\bar{f}_{\mu}}{\Omega} \mathbf{b} \times \nabla(|u|) & \Bigg|_{\mu_M - \Delta} . \end{aligned} \quad (178)$$

The sum of the two omitted terms, (176) and (177), is

$$2\pi B \sum_{\sigma} \int dU \left[\frac{\bar{f}_{\mu}}{|u|\Omega} \mathbf{b} \times \left(u \nabla u - \frac{B}{m} \nabla \mu_M \right) \right] \Bigg|_{\mu_M - \Delta} = 0 . \quad (179)$$

The point here is that the quantity in square brackets is proportional to Δ , while $|u| \Big|_{\mu_M - \Delta} \propto \Delta^{1/2}$. Hence the end-point singularity is only apparent, and our proof of the magnetization law is complete.

Maxwellian Case

The Maxwellian distribution function is defined by

$$f_M(\mathbf{x}, \mathbf{v}) = \frac{1}{(\sqrt{\pi} v_t)^3} n e^{-v^2/v_t^2} , \quad (180)$$

where n is the density and the thermal speed v_t is defined by (11),

$$v_t = \left(\frac{2T}{m} \right)^{1/2} .$$

Note that spatial dependence at fixed energy U enters not only through $n(\mathbf{x})$ and $T(\mathbf{x})$ but also through the potential, $\Phi(\mathbf{x})$. Thus when the guiding-center variables $(\mathbf{x}, \mu, U, \gamma)$ are used, we write

$$f_M(\mathbf{x}, \mathbf{v}) = \frac{1}{(\sqrt{\pi} v_t)^3} n \exp \left[\frac{-(U - e\Phi)}{T} \right] , \quad (181)$$

in order to compute

$$\nabla f_M = f_M \left[\nabla \ln n + \frac{e \nabla \Phi}{T} + \left(\frac{U - e\Phi}{T} - \frac{3}{2} \right) \nabla \ln T \right] . \quad (182)$$

In Chapter 5 we show that equilibrium in closed confinement systems is characterized by

$$\bar{f} = f_M + \mathcal{O}(\delta), \quad \tilde{f} = -\rho \cdot \nabla f_M + \mathcal{O}(\delta^2) \quad (183)$$

so it is natural to evaluate the plasma flow when \bar{f} is Maxwellian. We denote this lowest order flow by

$$n\mathbf{V}_{\perp 1} = - \int d^3v s\rho \cdot \nabla f_M = \frac{1}{2\Omega} \mathbf{b} \times \int d^3v s^2 \nabla f_M,$$

since it is evidently first order in δ . Here we have recalled (166) *et seq.*, noting that $\partial f_M / \partial \mu = 0$. According to (182),

$$n\mathbf{V}_\perp = \frac{1}{2\Omega} \mathbf{b} \times \int d^3v s^2 f_M \left[\nabla \ln n + \frac{e\nabla\Phi}{T} + \left(\frac{U - e\Phi}{T} - \frac{3}{2} \right) \nabla \ln T \right].$$

Integrals of the sort occurring here are common enough to deserve comment. Convenient integration variables are $\xi = u/v$ and $\eta = v/v_t$, in terms of which

$$s^2 = v_t^2(1 - \xi^2)\eta^2, \quad \frac{U - e\Phi}{T} - \frac{3}{2} = \eta^2 - 3/2$$

and

$$\int d^3v f_M = \frac{2}{\sqrt{\pi}} n \int_{-1}^1 d\xi \int_0^\infty d\eta \eta^2 e^{-\eta^2}; \quad (184)$$

both the ξ and η integrals are usually elementary. In the present case we find

$$n\mathbf{V}_{\perp 1} = \frac{p}{m\Omega} \mathbf{b} \times \left(\nabla \ln p + \frac{e\nabla\Phi}{T} \right), \quad (185)$$

where $p = nT$ is the (single species) pressure. This combination of diamagnetic drift and electrostatic $\mathbf{E} \times \mathbf{B}$ drift is of course familiar. (Table 4.1 summarizes the various velocity-space coordinates used in this book.)

Similar calculations provide the mean drift of guiding centers,

$$n(\mathbf{V}_{d1} + \mathbf{U}_{d1}) = \frac{p}{m\Omega} \left(2\mathbf{b} \times \nabla \ln B + \frac{e\nabla\Phi}{T} \right) + \nabla \times \mathbf{B} \frac{p}{m\Omega B}, \quad (186)$$

and the lowest order magnetization,

$$\mathbf{M}_1 = -\mathbf{b} \frac{p}{eB}. \quad (187)$$

Since

$$c\nabla \times \mathbf{M}_1 = -\frac{p}{m\Omega B} \nabla \times \mathbf{B} + \frac{1}{m\Omega} \mathbf{b} \times \nabla p - 2 \frac{p}{m\Omega} \mathbf{B} \times \nabla \ln B, \quad (188)$$

these results are consistent with magnetization law. We see that the magnetization flow converts the ∇B -drift of guiding centers into a ∇p -drift of its plasma species.

Name	Definition	Comment
energy	$U = \frac{1}{2}mv^2 + e\Phi$	
magnetic moment	$\mu = \frac{mv_\perp^2}{2B}$	
gyrophase angle	$\gamma = \tan^{-1} \left(\frac{-v_{\perp 3}}{v_{\perp 2}} \right)$	See (2.57)
kinetic energy	$w = \frac{mv^2}{2} = U - e\Phi$	
pitch-angle variable	$\lambda = \frac{\mu}{w} [= \frac{1}{B} \sin^2 \Theta]$ $\xi = \frac{u}{v} [= \cos \Theta]$	Θ , the pitch angle, is not used as a coordinate $u \equiv v_{\parallel} \equiv \mathbf{b} \cdot \mathbf{v}$
ξ		

Table 1. Velocity coordinates

4.6 Summary

Closure of Maxwell's equations depends on only the two lowest moments of the distribution function, $f_s(\mathbf{x}, \mathbf{v}, t)$, for each plasma species s ; in this sense the kinetic theory that determines f provides more information than is needed. Yet kinetic analysis is rarely avoidable. All rigorous closure schemes involve, at least implicitly, solution of some kinetic equation.

The general kinetic equation prescribes the evolution of the one-particle distribution function for each plasma species, for given electric and magnetic fields. It accounts for microscopic, interaction-scale fluctuations statistically, by means of a collision operator. While the collision operator is necessarily approximate, we consider the general kinetic equation to be exact as long as it applies to all length scales larger than the interaction scale.

The electrodynamics of a magnetized plasma can be closed by means of approximate kinetic equations, set in the contracted phase space of guiding-center motion. Guiding-center kinetic theory is pertinent when the gyroradius is small,

$$\frac{\rho}{L} = \delta \ll 1,$$

and the gyrofrequency is large,

$$\frac{\omega}{\Omega} = \mathcal{O}(\delta).$$

Here L denotes a typical scale length and ω a typical frequency for macroscopic variation.

Examination of each term in the general kinetic equation reveals three varieties of guiding-center kinetic theory. The *drift-kinetic* equation pertains when all macroscopic quantities vary on the scale L , and when the plasma flow is small, $V \sim \delta v_t$. It applies to plasma equilibrium, to transport and to many forms of plasma instability. The *gyrokinetic* equation addresses instability specifically. It distinguishes between unperturbed or “equilibrium” quantities, which vary slowly ($\nabla \sim 1/L$) and perturbed quantities—associated with a wave or instability—that are allowed to change over the width of a gyroradius ($\nabla \sim 1/\rho$). It therefore involves two small parameters: the measure of the field perturbation, Δ , as well as the gyroradius parameter δ . The *MHD-ordered* kinetic equation allows for rapid $\mathbf{E} \times \mathbf{B}$ drifts, $v_E \sim v_t$, as can characterize violent instability.

All guiding-center kinetic equations are obtained from gyrophase averages of the general kinetic equation. In the drift kinetic case, the average is performed at fixed magnetic moment μ , energy U and spatial coordinate \mathbf{x} ; the gyrophase-dependent part of the distribution is included as a small but crucial correction. On the other hand, the gyrokinetic average is performed at fixed μ , U and guiding-center position, $\mathbf{X} = \mathbf{x} - \boldsymbol{\rho}$. Since field quantities are allowed to vary over the distance ρ , the result is nonlocal: its coefficients involve spatial averages of the electromagnetic field. An eikonal *ansatz* is commonly employed to make the nonlocal aspects more tractable. Solution to guiding-center kinetic equations invariably hinges on a single technical feature: the square-root form of the parallel velocity function $u(\mu, U, \mathbf{x})$. The most important physical manifestation of this function is the trapping of charged particles in regions of relatively weak magnetic field. But its importance extends beyond trapping effects, essentially because (unless the collisionality parameter ν/ω_i is very large) the operator $u \nabla_{\parallel}$ dominates the kinetic equation. Thus the discrete variable, $\sigma = u/|u|$, assumes a surprisingly central role, along with such useful devices as the bounce condition and the orbital average.

The form of the magnetized-plasma distribution function provides a crucial relation between guiding-center motion and plasma flow: the “magnetization law.” The point is that each guiding center bears a magnetic moment; the distribution of such moments gives the plasma a magnetization whose curl contributes to flow in a familiar yet very important way. The natural definition shows the magnetization to be proportional to the perpendicular plasma pressure.

Further Reading on Kinetic Equations:

- Hastie, Taylor, et al., 1967
- Rutherford and Freiman, 1968
- Hazeltine, 1973
- Antonsen and Lane, 1980

Catto, Tang, et al., 1981
Littlejohn, 1983

Exercises

- Let N be the number of particles inside some fixed volume V . Suppose that the distribution function f vanishes on the boundary of V . Use (4.4) to prove that in this case N must be a constant: $dN/dt = 0$.
- Express the general kinetic equation in terms of cylindrical coordinates (r, θ, z) , using the velocity variables $(v^r = dr/dt, v^\theta = r d\theta/dt, v^z = dz/dt)$.
- A disruption in the Standard Tokamak¹ is observed to carry plasma over an appreciable fraction of the minor radius in a time Δt . How small must Δt be in order for the disruption to be described by the MHD ordering?
- Verify the identities in (62).
- Criticize the ordering given by (71), by using Ampère's law to estimate J_\parallel in terms of B_P . Thus show that $J_\parallel/J_\perp \sim B/B_P$.
- The derivation of the drift kinetic equation implicitly assumes $\partial f/\partial\mu \leq f/\mu$. Identify the step in which this assumption enters. At low collision frequency, boundary layers in velocity space can occur, giving the distribution relatively steep dependence on μ : $\partial f/\partial\mu \sim f/\Delta\mu \gg f/\mu$. Use the steady-state version of (69) to derive an expression for the smallest $\Delta\mu$ that is consistent with drift-kinetic theory.
- Explicitly demonstrate the annihilation property of the orbital average, (133), in the axisymmetric case.
- Verify the velocity-space Jacobian of (144). Then, using the Maxwellian distribution of (181), explicitly perform each integral in (146) to verify that
$$\int d^3v f_M = n .$$
- Using the estimate $\nabla B/B \sim 1/R$, compute the order of magnitude of the drift velocity in the Standard Tokamak,¹ in centimeters per second. Similarly discuss the relative size of the two terms in (158), for poloidal

¹Recall problem 5 of chapter 3.

drift motion in the Standard Tokamak.

10. Often the last term in (162), involving $(\nabla \times \mathbf{B})_{||}$, is omitted. Show that in that case one may write

$$\mathbf{v}_{gc} = \frac{\mathbf{u}}{B} \nabla \times \mathbf{A}^*, \quad \mathbf{A}^* = \mathbf{A} + \mathbf{B} \frac{\mathbf{u}}{\Omega}.$$

Show that $A_\zeta^* = R^2 \nabla \zeta \cdot \mathbf{A}^*$ is conserved by guiding-center motion in an axisymmetric system.

11. Prove that

$$\oint \frac{d\gamma}{2\pi} \hat{s} \hat{\rho} \cdot \mathbf{A} = -\frac{1}{2} \mathbf{b} \times \mathbf{A}$$

for any vector \mathbf{A} .

12. Consider a large aspect-ratio tokamak in which $B \simeq B_0(1 - r \cos \theta / R_0)$. Suppose that some (fictitious) instability has removed all the trapped ions, so that the ion distribution is approximated by

$$f = \begin{cases} f_M, & \lambda < \lambda_c \\ 0, & \lambda > \lambda_c. \end{cases}$$

Compute the ion density, n_i , and stress anisotropy $P_{i\parallel} - P_{i\perp}$, in this case.

13. Carefully perform each integral to verify (184) and (185).

14. Explain in a few sentences the origin of the minus sign in the magnetization, (187).

15. **FLR profile broadening.** In a magnetized plasma, no fluid variable can vary on a scale narrower than the gyroradius. To show this explicitly, consider the ion guiding-center distribution given by

$$\bar{f}(\mathbf{x}, \mathbf{v}) = f_M \frac{n_{gc}(\mathbf{X})}{n_M},$$

where f_M is a Maxwellian with constant density n_M and $n_{gc}(\mathbf{X})$ gives the spatial distribution of ion guiding centers. Assume slab geometry, with uniform magnetic field in the z -direction and spatial variation only in the x -direction.

- (a) Show that the ion density at some point \mathbf{x} is generally given by

$$n(x) = \frac{1}{\sqrt{\pi}} \int ds e^{-s^2} n_{gc}(x + s\rho), \quad \rho = \frac{v_t}{\Omega}.$$

(b) Show that a region of flat profile ($d^2 n / dx^2 = 0$) is unaffected by FLR. Thus it is profile-curvature that is broadened, not profile slope.

(c) Evaluate $n(x)$ explicitly and exactly in the following two cases:

$$(i) \quad n_{gc}(x) = \sqrt{\pi} \rho \delta(x) ;$$

$$(ii) \quad n_{gc}(x) = n_M e^{-x^2/a^2} .$$

Chapter 5

Coulomb Collisions

5.1 General Collision Operator

Physical Constraints

We noted in Chapter 4 that the evolution of the macroscopic distribution depends in part upon particle interactions that are effectively random. The collision operator provides a statistical account of such interactions; we survey its key properties here. To begin we consider requirements that any physical collision operator, whatever the basic scattering process, is expected to satisfy.

1. *Bilinearity.* Any collisional process should be dominated by binary scattering events, tertiary and higher order collisions being relatively rare. When several particle species are present, a binary collision operator can be expressed in the form

$$C_s = \sum_{s'} C_{ss'}(f_s, f_{s'}) , \quad (1)$$

where $C_{ss'}$ describes the effects on species s , the “scattered” species, of collisions with particles of species s' , the “background” species. Of course f_s and $f_{s'}$ are the distribution functions for the scattered and background species respectively.

Bilinearity, the statement that the operators $C_{ss'}(f_s, f_{s'})$ are linear in each argument, is a natural consequence of the binary collision assumption. Note that bilinearity makes the like-species term in (1), $C_{ss}(f_s, f_s)$, a quadratic function of its argument.

In general there is no simple relation between $C_{ss'}$ and $C_{s's}$. The two objects appear in different kinetic equations—only $C_{ss'}$ enters the kinetic equation for f_s , and, when the masses of the two species are disparate, have quite different forms.

2. *Classical dissipation.* The collision operator must cause entropy to

increase. Specifically, it should satisfy an *H*-theorem of the form

$$\frac{d}{dt} \left|_c S \geq 0; \quad \frac{d}{dt} \left|_c S = 0 \Leftrightarrow C_{ss'} = 0, \right. \right. \quad (2)$$

where S measures the plasma entropy and $d/dt|_c$ denotes the collisional rate of entropy production, excluding local changes due to entropy flow. A related, very reasonable, expectation is that $C_{ss'}$ will precisely vanish only in classical thermodynamic equilibrium, when both distributions are Maxwellian at the same temperature:

$$C_{ss'} = 0 \Leftrightarrow f_s = f_{sM}, \quad f_{s'} = f_{s'M}, \quad \text{and} \quad T_s = T_{s'}, \quad (3)$$

where f_M is the Maxwellian distribution given by (4.180).

3. *Galilean invariance.* Collisional processes should not change if a common, uniform velocity \mathbf{V} is imparted to both species:

$$C_{ss'}(f_s(\mathbf{v} - \mathbf{V}), f_{s'}(\mathbf{v} - \mathbf{V})) = C_{ss'}(f_s(\mathbf{v}), f_{s'}(\mathbf{v})). \quad (4)$$

4. *Spatial symmetry.* The collision operator $C_{ss'}$ should have translational symmetry, in the sense of depending on position only through f_s and $f_{s'}$. It should also reflect the rotational symmetry of the underlying collisional process. For example, an isotropic operator describes a collision process that is equally effective in all directions.

Rotational symmetry is problematic in the Coulomb case. The point is that the effective Coulomb interaction extends over a distance of λ_D , the Debye length. When λ_D is shorter than a thermal gyroradius ρ , then colliding orbits are unaffected by the magnetic field and collisions are isotropic. In the opposite limit, however, orbits are dominated by gyromotion, the scattering dynamics are sensitive to the direction of \mathbf{B} , and the corresponding operator is anisotropic: it has cylindrical, rather than spherical, symmetry.

Because the anisotropic operator is extremely complicated, almost all applications of the Coulomb operator use its isotropic form—as we shall in this book. But it must be acknowledged that in high-temperature experiments the (electron) Debye length is comparable to, or even slightly smaller than, the electron gyroradius. (The regime $\rho_e \sim \lambda_{D_e}$ is easily consistent with $\nu_e \ll \Omega_e$, and therefore can occur in a fully magnetized plasma.) Only collisions between ions are genuinely isotropic in such cases.

Fortunately the few existing calculations using the anisotropic electron operator have not revealed dramatic departures from predictions of the simpler, isotropic form. Indeed, typical corrections are proportional to $\log(\rho_e/\lambda_{D_e})$, which is close to unity.¹

5. *Local mechanical conservation.* The collision operator should conserve particles, momentum and energy at each spatial point.

¹ See, for example (Ware, 1989).

Of course fusion reactions, the objects of plasma confinement, do not conserve particles or kinetic energy. Similarly, various wave-particle effects can convert particle momentum, for example, into electromagnetic form; even if electromagnetic momentum is reabsorbed elsewhere in the plasma, it is no longer conserved locally. However, regardless of the importance of such processes, they need not be treated as *collisional* processes: by convention they are excluded from the operator C . Indeed, excluding non-locally conserving mechanisms from C has several advantages, helping in particular to distinguish what is meant by a collisional event.

Explicit forms for the conservation laws will be considered presently.

Linearized Operator

We will find in §5.3 that, under quite general conditions, confined plasmas are described by nearly Maxwellian distributions. It therefore makes sense to study the action of the collision operator on a distribution of the form

$$f_s = f_{sM} + f_{s'1} .$$

Here f_M is given by (4.180), while the correction, f_1 , is measured by a small parameter ε : $f_1/f_M = \mathcal{O}(\varepsilon)$. Bilinearity of the collision operator implies that (without approximation)

$$\begin{aligned} C_{ss'}(f_s, f_{s'}) &= C_{ss'}(f_{sM}, f_{s'M}) + C_{ss'}(f_{sM}, f_{s'1}) \\ &\quad + C_{ss'}(f_{s'1}, f_{s'M}) + C_{ss'}(f_{s'1}, f_{s'1}) . \end{aligned} \quad (5)$$

The first term vanishes when $T_s = T_{s'}$, as in (3); because temperature equilibration between electrons and ions is very slow, however, this term cannot be discarded in general. The two terms linear in f_1 constitute the linearized operator, which is denoted by

$$C_{ss'1}(f_1) \equiv C_{ss'}(f_{sM}, f_{s'1}) + C_{ss'}(f_{s'1}, f_{s'M}) . \quad (6)$$

Then we have

$$C_{ss'}(f_s, f_{s'}) = C_{ss'}(f_{sM}, f_{s'M}) + C_{ss'1}(f_1) + \mathcal{O}(\varepsilon^2) . \quad (7)$$

In the like-species case, $C_{ss'1}$ is a linear operator on $f_{s'1}$; for unlike species collisions, both perturbed distributions are clearly involved. Thus, in (6) and (7), the notation “ f_1 ” refers to both species—an abbreviated notation that we use generally. It is important to note, however, that f_s and $f_{s'}$ appear in quite different roles. Since $C_{ss'}$ appears in the kinetic equation for species s , only its action on $f_{s'1}$ affects the nature of the linear operator in that equation. The contribution to $C_{ss'}$ from $f_{s'1}$ enters as an inhomogeneous term, providing collisional coupling to the kinetic equation for species s' .

Perturbed Maxwellians

Galilean invariance, (4), implies that

$$C_{ss'} [f_{sM}(\mathbf{v} - \mathbf{V}), f_{s'M}(\mathbf{v} - \mathbf{V})] = C_{ss'} [f_{sM}(\mathbf{v}), f_{s'M}(\mathbf{v})], \quad (8)$$

where $f_M(\mathbf{v} - \mathbf{V})$ is a displaced or moving Maxwellian, given by

$$f_M(\mathbf{v} - \mathbf{V}) = \frac{1}{\pi^{3/2} v_t^3} n \exp \left[-\frac{(\mathbf{v} - \mathbf{V}) \cdot (\mathbf{v} - \mathbf{V})}{v_t^2} \right];$$

here \mathbf{V} , which may depend upon position, is the common flow velocity of the two species. One is usually interested in subsonic flow, in the sense that,

$$\frac{V}{v_t} = \mathcal{O}(\epsilon).$$

Then we can expand

$$f_M(\mathbf{v} - \mathbf{V}) = f_M(\mathbf{v}) + f_{d1}(\mathbf{v}) + f_{d2}(\mathbf{v}) + \mathcal{O}(\epsilon^3). \quad (9)$$

using the convenient notations,

$$f_{d1}(\mathbf{v}) \equiv 2 \frac{\mathbf{V} \cdot \mathbf{v}}{v_t^2} f_M, \quad (10)$$

$$f_{d2}(\mathbf{v}) \equiv \frac{1}{2} \left[\left(\frac{\mathbf{v} \cdot \mathbf{V}}{v_t^2} \right)^2 - \left(\frac{V}{v_t} \right)^2 \right] f_M, \quad (11)$$

for the first and second order perturbations of a displaced Maxwellian. Perturbations proportional to f_M , like the f_d , are often written in normalized form:

$$\hat{f} \equiv \frac{f}{f_M}. \quad (12)$$

Thus the normalized first-order displacement is

$$\hat{f}_{d1} = 2 \frac{\mathbf{V} \cdot \mathbf{v}}{v_t^2}. \quad (13)$$

We next substitute (9) into (8) and expand the left-hand side as in (5). It is clear that the first, Maxwellian, term coincides with the right-hand side of (7) and cancels, leaving

$$C_{ss'1}(f_{d1}) + C_{ss'1}(f_{d2}) + C_{ss'}(f_{s,d1}, f_{s',d1}) + C_{ss'}(f_{s',d1}, f_{s,d1}) = \mathcal{O}(\epsilon^3).$$

Since this result must hold for any value of ϵ , we can consider separately terms of each ϵ -order and conclude that

$$C_{ss'1}(f_{d1}) = 0; \quad (14)$$

$$C_{ss'1}(f_{d2}) + C_{ss'}(f_{sd1}, f_{s'd1}) + C_{ss'}(f_{s'd1}, f_{sd1}) = 0. \quad (15)$$

Equation (14) requires the linearized operator to vanish when acting on any distribution whose normalized form is linear in \mathbf{v} . This result has wide importance; it depends only on bilinearity and Galilean invariance, without regard to the specific scattering mechanism. The second and third terms in (15), nonlinear in f_1 , occur in some transport studies; the point of (15) is to allow the replacement of a nonlinear operator by a linear one.

To generalize (14), we can include perturbations in the density and temperature of the Maxwellian, in addition to the velocity displacement \mathbf{V} :

$$n = n_0 + n_1, \quad T = T_0 + T_1.$$

Restricting attention to the first order terms, we expand

$$f_M = f_{M0}(1 + \hat{f}_{M1}),$$

where \hat{f}_{M1} , the perturbed Maxwellian, is given by

$$\hat{f}_{M1} = \hat{f}_{d1} + n_1 \frac{d}{dn} \ln f_M + \frac{d}{dT} \ln f_M.$$

Since

$$\frac{d}{dn} \ln f_M = \frac{1}{n}, \quad \frac{d}{dT} \ln f_M = \frac{1}{T} \left(\frac{v^2}{v_T^2} - \frac{3}{2} \right), \quad (16)$$

we obtain

$$\hat{f}_{M1} = \hat{f}_{d1} + \frac{n_1}{n_0} + \left(\frac{v^2}{v_T^2} - \frac{3}{2} \right) \frac{T_1}{T_0}. \quad (17)$$

Now we can infer from (3) that

$$C_{ss'1}(\hat{f}_{M1}) = 0, \quad (18)$$

by essentially the same argument we used to derive (14). Here only the T_1 -term provides new information: we see that C_1 vanishes on any normalized perturbation that depends on velocity only through the factor $(v^2/v_T^2 - 3/2)$.

Of course (15) can be similarly generalized. Thus we find that the second-order correction f_{M2} must satisfy

$$C_{ss'1}(f_{M2}) = -C_{ss'}(f_{s'M1}, f_{s'M1}) - C_{ss'}(f_{s'M1}, f_{s'M1}). \quad (19)$$

Like (14) and (15), (18) and (19) can be viewed as constraints on the form of the collision operator.

Collisional Conservation Laws

The local conservation laws discussed previously are expressed in terms of moments of the collision operator. For example, the conservation of particles is expressed as

$$\int d^3v C_{ss'} = 0, \quad (20)$$

in terms of the “zeroth moment” of $C_{ss'}$. The first (vector) moment of C ,

$$\mathbf{F}_{ss'} \equiv \int d^3v m_s \mathbf{v} C_{ss'}, \quad (21)$$

specifies the rate at which the momentum of species s is changed by collisions with species s' . We will refer to \mathbf{F} as the collisional *friction force* (“friction force density” would be more precise). In a plasma with several ion species, the total friction force exerted on species s is

$$\mathbf{F}_s = \sum_{s'} \mathbf{F}_{ss'},$$

Collisional momentum conservation is expressed by

$$\mathbf{F}_{ss'} + \mathbf{F}_{s's} = 0. \quad (22)$$

This conservation law is *detailed*: momentum is separately preserved in each collision between pairs of particles. Of course (22) requires $\mathbf{F}_{ss} = 0$. The non-detailed version,

$$\sum_s \mathbf{F}_s = 0, \quad (23)$$

is sometimes more directly useful.

The second moment of $C_{ss'}$ measures the rate at which species s gains kinetic energy through collisions with species s' :

$$W_{ss'}^L \equiv \int d^3v \frac{1}{2} m_s v^2 C_{ss'}, \quad (24)$$

This quantity is sometimes called the (collisional) energy exchange. Detailed conservation of energy is expressed as

$$W_{ss'}^L + W_{s's}^L = 0. \quad (25)$$

The “ L ” superscript in (24) and (25) reminds us that $\frac{1}{2} m v^2$ is the kinetic energy measured in the lab frame. It is often convenient to measure energy exchange in terms of the relative velocity, $\mathbf{v} - \mathbf{V}_s$, where \mathbf{V}_s is the mean velocity of species s , defined by (4.151). In this frame the energy exchange is

$$W_{ss'} \equiv \int d^3v \frac{1}{2} m_2 (\mathbf{v} - \mathbf{V}_s)^2 C_{ss'}, \quad (26)$$

In view of (20) and (21) we have

$$W_{ss'} = W_{ss'}^L - \mathbf{V}_s \cdot \mathbf{F}_{ss'}. \quad (27)$$

Hence the energy conservation law (25) becomes

$$W_{ss'} + W_{s's} + (\mathbf{V}_s - \mathbf{V}_{s'}) \cdot \mathbf{F}_{ss'} = 0. \quad (28)$$

Here (22) was used to eliminate $\mathbf{F}_{s,s'}$. The non-detailed form is

$$\sum_s (W_s + \mathbf{V}_s \cdot \mathbf{F}_s) = 0, \quad (29)$$

where

$$W_s \equiv \sum_{s'} W_{ss'}. \quad (30)$$

We next consider the explicit form of $C_{ss'}$ for Coulomb collisions.

5.2 Coulomb Operator

Fokker-Planck Scattering

The Coulomb collision operator can be characterized as a *Fokker-Planck* operator, with rotational and Galilean symmetry; indeed, this description effectively determines the form of the operator. We therefore review some general properties of Fokker-Planck operators.

The essential feature of a Fokker-Planck operator—distinguishing it from, for example, the Boltzmann collision integral—is that it represents the effects of soft collisions: each scattering event makes only a small change in particle velocity. In the Coulomb case the dominant importance of soft collisions follows from the long-range nature of the Coulomb interaction.

Since the orbits of particles subject to Fokker-Planck scattering are smooth, without sudden changes in direction, the *collision time* associated with Fokker-Planck scattering is not the interval between individual binary events. Instead it measures the accumulated time required for many such events to produce an effective large-angle scattering. For this reason the Fokker-Planck collision time, denoted by τ , is sometimes defined as the “90° scattering time.” For example, in the Coulomb case, the time between individual interactions is roughly the plasma period, ω_p^{-1} , an extremely short interval compared to the Coulomb collision time. (In typical confinement experiments, $\omega_p^{-1} \sim 10^{12}$ sec, while the Coulomb collision time is close to 10^{-4} sec.)

The general form of a Fokker-Planck operator is

$$C_{ss'} = \frac{\partial}{\partial \mathbf{v}} \cdot \left[\mathbf{D}(f_{s'}) \cdot \frac{\partial f_s}{\partial \mathbf{v}} + \mathbf{d}_c(f_{s'}) f_s \right] \quad (31)$$

where \mathbf{D} is a velocity-space diffusion tensor, while the vector \mathbf{d}_c , sometimes called “dynamical friction,” represents collisional drag. It is through the Fokker-Planck combination of drag and diffusion that entropy increases, providing the relaxation described by (3). Note that the divergence form of (31) insures particle conservation.

Both \mathbf{D} and \mathbf{d}_c depend on moments of the background species, $f_{s'}$. On the other hand, the collision operator acts on the scattered species, f_s , differentially. It follows that, while $C_{ss'}$ is an integro-differential operator, $C_{s's'}$ is a strictly differential operator—a circumstance that simplifies the treatment of collisional effects.

Equation (31) implies that the collision time can be estimated as

$$\tau \sim \frac{v_{ts}^2}{D}, \quad (32)$$

where v_{ts} is as usual the thermal speed of species s .

Landau Operator

An especially compact form of the Coulomb collision operator is due to Landau:

$$C_{ss'} = \frac{\gamma_{ss'}}{2} \frac{\partial}{\partial \mathbf{v}} \cdot \int d^3 v' \mathbf{U} \cdot \left[\frac{f'_{s'}}{m_s} \frac{\partial f_s}{\partial \mathbf{v}} - \frac{f_s}{m_s} \frac{\partial f'_{s'}}{\partial \mathbf{v}'} \right]. \quad (33)$$

Here, following the convention of Boltzmann, the primes denote evaluation at \mathbf{v}' :

$$f' \equiv f(\mathbf{v}'). \quad (34)$$

The tensor \mathbf{U} has components

$$U_{\alpha\beta} = \frac{1}{u^3} (u^2 \delta_{\alpha\beta} - u_\alpha u_\beta), \quad (35)$$

where we use the traditional notation,

$$\mathbf{u} = \mathbf{v} - \mathbf{v}'. \quad (36)$$

Although elsewhere we use \mathbf{u} to denote the parallel velocity, confusion is unlikely. It is worth noting that the form of \mathbf{U} is primarily fixed by symmetry: Galilean invariance allows it to depend upon \mathbf{v} and \mathbf{v}' only through \mathbf{u} , while rotational symmetry imposes the form

$$U_{\alpha\beta} = S(u)(u^2 \delta_{\alpha\beta} - \alpha u_\alpha u_\beta)$$

where S is some scalar function and α is constant. The choice $\alpha = 1$ enforces (3), through the identity

$$\mathbf{u} \cdot \mathbf{U} = \mathbf{U} \cdot \mathbf{u} = 0, \quad (37)$$

while the $S = u^{-3}$ dependence, which is Coulomb-specific, reflects familiar properties of the Rutherford cross-section.

Similarly specific to Coulomb scattering is the coefficient $\gamma_{ss'}$, given by

$$\gamma_{ss'} \equiv \frac{4\pi e_s^2 e_{s'}^2}{m_s} \ln \Lambda, \quad (38)$$

where $\ln \Lambda$ is the "Coulomb logarithm."

$$\Lambda = 12\pi n \lambda_D^3.$$

The logarithmic factor reflects Debye shielding, which limits the range of the Coulomb interaction at the Debye length. Unfortunately, quantum effects confound this simple prescription: at thermonuclear temperatures the plasma parameter Λ in (38) must be replaced by a more complicated function, such that (Braginskii, 1965)

$$\ln \Lambda = \begin{cases} 23.4 - 1.15 \ln n + 3.45 \ln T_e, & \text{for } T_e < 50 \text{eV}, \\ 25.3 - 1.15 \ln n + 2.3 \ln T_e, & \text{for } T_e > 50 \text{eV}, \end{cases}$$

where T_e is measured in electron Volts and n is measured in cm^{-3} . Nonetheless, for confinement applications the final result is simple: the $\ln \Lambda$ factor rarely differs from the value

$$\ln \Lambda \approx 17, \quad (39)$$

by any significant amount.

By comparing (31) and (33) we see that the diffusion tensor is

$$\mathbf{D} = \frac{\gamma_{ss'}}{2m_s} \int d^3 v \mathbf{U} f_{s'} . \quad (40)$$

Since $U \sim 1/u$, (41) yields the estimate $D \sim n_{s'} \gamma_{ss'} / (m_s v_{t>})$ where $v_{t>}$ is the larger of the two thermal speeds, v_{ts} or $v_{ts'}$. Hence (32) implies

$$\tau_{ss'} \sim \frac{m_s v_{t>} v_{ts}^2}{n_{s'} \gamma_{ss'}} . \quad (41)$$

The form of the *linearized* Landau operator is easily derived from the definition, (6). We write $f_s = f_{sM}(1 + \hat{f}_s)$ and find, after simple manipulation,

$$C_{ss'1} = \frac{\gamma_{ss'}}{2} \frac{\partial}{\partial \mathbf{v}} \cdot \int d^3 v' f_{sM} f'_{s'm} \mathbf{U} \cdot \left[\frac{1}{m_s} \frac{\partial \hat{f}_s}{\partial \mathbf{v}} - \frac{1}{m_{s'}} \frac{\partial \hat{f}'_{s'}}{\partial \mathbf{v}'} \right. \\ \left. - \frac{m_s}{T_s} \left(1 - \frac{T_s}{T_{s'}} \right) (\hat{f}_s + \hat{f}'_{s'}) \mathbf{v} \right]. \quad (42)$$

RMJ Operator

One can use the identities

$$U_{\alpha\beta} = \frac{\partial^2 u}{\partial u_\alpha \partial u_\beta} = \frac{\partial}{\partial u_\alpha} \left(\frac{u_\beta}{u} \right) \quad (43)$$

$$\frac{\partial}{\partial u_\beta} U_{\alpha\beta} = -2 \frac{u_\alpha}{u^3} = 2 \frac{\partial}{\partial u_\alpha} \left(\frac{1}{u} \right) \quad (43)$$

and

$$\frac{\partial^2}{\partial u_\alpha \partial u_\beta} U_{\alpha\beta} = -8\pi\delta(\mathbf{u}) \quad (44)$$

to deduce numerous other forms for the Coulomb collision operator. An especially useful form, making (31) explicit, is due to Rosenbluth, MacDonald and Judd (RMJ) (Rosenbluth, MacDonald, et al., 1957).

We introduce the functions

$$G_s(\mathbf{v}) = \int d^3 v' f_{s'} u \quad (45)$$

and

$$H_s(\mathbf{v}) = \int d^3 v' f_{s'} \frac{1}{u}. \quad (46)$$

It is then easily seen, from (43) and (44), that the Landau operator can be expressed as

$$C_{ss'} = \frac{\gamma_{ss'}}{2} \left\{ \frac{1}{m_s} \frac{\partial^2}{\partial v_\alpha \partial v_\beta} \left(f_s \frac{\partial^2 G_{s'}}{\partial v_\alpha \partial v_\beta} \right) \right. \\ \left. - 2 \left(\frac{1}{m_s} + \frac{1}{m_{s'}} \right) \frac{\partial}{\partial v_\alpha} \left(f_s \frac{\partial H_{s'}}{\partial v_\alpha} \right) \right\}. \quad (47)$$

The functions G and H conveniently express the contribution of the background distribution $f_{s'}$ to the diffusion and drag terms in (31). They are called "Rosenbluth potentials" because of the identities

$$\nabla_v^2 G_s \equiv \frac{\partial^2 G_b}{\partial v_\alpha \partial v_\alpha} = 2H_s, \quad (48)$$

$$\nabla_v^2 H_s = -4\pi f_s. \quad (48)$$

Here again (43) and (44) were used. Thus, in particular, H resembles an electrostatic field, with charge density f_s , in velocity space. (Strictly speaking RMJ define the potentials in terms of species sums of G_s and $H_{s'}$.)

The Maxwellian case,

$$G_{sM} \equiv G_s(f_M), \quad H_{sM} \equiv H_s(f_M)$$

has special importance. By expanding u and $1/u$ in spherical harmonics, as in conventional potential theory, and noting that only the first, isotropic term survives the integral, one finds that

$$\begin{aligned} G_{sM} &= \frac{n_s v_{ts}}{2\eta} [\eta \operatorname{erf}'(\eta) + (1 + 2\eta^2) \operatorname{erf}(\eta)] \\ H_{sM} &\approx \frac{n_s}{v_{ts}\eta} \operatorname{erf}(\eta). \end{aligned} \quad (49)$$

Here η is the normalized speed,

$$\eta \equiv \frac{v}{v_{ts}}, \quad (50)$$

erf is the error function and $\operatorname{erf}'(\eta) = (2/\sqrt{\pi}) \exp(-\eta^2)$ is its derivative. With (49) it is easy to find the form of $C_{ss'}$ when both species are Maxwellian:

$$\begin{aligned} C_{ss'}(f_{sM}, f_{s'M}) &= -2 \frac{\gamma_{ss'} n_{s'}}{m_{s'} v_{ts'} v_{ts}^2} \left(1 - \frac{T_{s'}}{T_s} \right) f_{sM} \\ &\times \left[\frac{\operatorname{erf}(\eta)}{\eta} - \left(1 + \frac{m_{s'} T_s}{m_s T_{s'}} \right) \operatorname{erf}'(\eta) \right]. \end{aligned} \quad (51)$$

This object indeed vanishes in the equal temperature case.

As an application of (51) we compute the energy exchange $W_{ss'}^L$ of (24):

$$\begin{aligned} W_{ss'}^L &= -8\pi \frac{\gamma_{ss'} n_{s'}}{m_{s'} v_{ts'}} \frac{v_{ts}}{(T_s - T_{s'})} \int d\eta \eta^4 \left[\frac{\operatorname{erf}(\eta)}{\eta} - \left(1 + \frac{m_{s'} T_s}{m_s T_{s'}} \right) \operatorname{erf}'(\eta) \right] \\ &= -\frac{4}{\sqrt{\pi}} \frac{\gamma_{ss'} n_s n_{s'} (T_s - T_{s'})}{m_{s'} (v_{ts}^2 + v_{ts'}^2)^{3/2}}. \end{aligned} \quad (52)$$

This result is evidently valid for arbitrary mass ratio.

Small Mass-ratio Approximations

In a pure plasma the only unlike-species collision operators are $C_{e\epsilon}$ and C_{ie} . Both can be expressed quite simply if we neglect terms of order $(v_{ti}/v_{te})^{1/2} \sim (m_e/m_i)^{1/2}$. Here we obtain the simplified forms, following the review by Braginskii (Braginskii, 1965).

The derivation presumes that thermal speeds for both species can be defined, and that $T_i \sim T_e$; indeed, we routinely estimate

$$v^n f_s \sim v_t^n f_s. \quad (53)$$

This does not require f , to be strictly Maxwellian, but it rules out certain exotic distributions. For example, our results become questionable if either species has a significant suprathermal population, such as a fast beam.

Consider first the approximation to C_{ei} , describing the scattering of electrons by much more massive ions. Energy change in such collisions—as in the bouncing of a tennis ball off a brick wall—is extremely inefficient. It follows that the species energy exchange W_{ei} is very small; but more importantly it follows that energy *scattering*—alteration of the energy dependence of f_e —is small. In lowest order, the operator describes scattering in angle only, as if the ions were fixed scatterers. A gas with fixed, isotropic scattering sites, called a *Lorentz gas*, has been studied in the context of neutral gas diffusion; it is found to be described by the operator

$$C_{LG}(f) \equiv \nu v_t^3 \frac{\partial}{\partial v_\alpha} V_{\alpha\beta} \frac{\partial f}{\partial v_\alpha}, \quad (54)$$

where ν is an energy-dependent collision frequency and the tensor $V_{\alpha\beta}$ is given by $U_{\alpha\beta}$, evaluated at $\mathbf{v}' = 0$:

$$V_{\alpha\beta} = \frac{1}{v^3} (v^2 \delta_{\alpha\beta} - v_\alpha v_\beta). \quad (55)$$

The form of (55) forbids energy scattering. The point is that the energy derivative, $\partial f / \partial w$, would enter (54) with a factor of $\partial w / \partial v_\alpha = m v_\alpha$; since (37) implies $v_\alpha V_{\alpha\beta} = 0$, energy-derivative terms cannot occur.

In the guiding-center case, the operator C_{LG} describes diffusion in pitch-angle alone. Pitch-angle diffusion is generally important, in that terms similar to (54) occur in any Fokker-Planck operator, for arbitrary mass ratio. Indeed, such terms often dominate other collisional effects, so that (54), the Lorentz gas or *pitch-angle scattering* operator, has frequent application. To demonstrate the relation between C_{ei} and C_{LG} , we identify the leading order terms, with respect to v_{ti}/v_{te} , in (33). The second term, with its explicit $(1/m_i)$ -factor, is evidently negligible; careful expansion of $U_{\alpha\beta}$ shows that, through first order in v_{ti}/v_{te} , the remaining term becomes

$$\int d^3 v' f'_i U_{\alpha\beta} \cong n_i U_{\alpha\beta} (\mathbf{v} - \mathbf{V}_i). \quad (56)$$

Here \mathbf{V}_i is defined by (4.151), and the notation $U_{\alpha\beta}(\mathbf{v} - \mathbf{V}_i)$ simply indicates the replacement

$$\mathbf{u} = \mathbf{v} - \mathbf{v}' \rightarrow \mathbf{v} - \mathbf{V}_i$$

in (35). Keeping in mind that only first order terms are retained, we can write

$$C_{ei} = \frac{n_i \gamma_{ei}}{2m_e} \frac{\partial}{\partial v_\alpha} U_{\alpha\beta} (\mathbf{v} - \mathbf{V}_i) \frac{\partial f_e}{\partial v_\beta}. \quad (57)$$

Equation (57) obviously has the form of (54), with corrections due to ion flow: it is a *Lorentz-gas operator* in the ion rest frame.

Because of its Lorentz gas character, (57) cannot describe collisional energy exchange. That process, like energy scattering, is of higher order in the mass ratio:

$$W_{ei}^L = \mathcal{O}\left(\frac{m_e}{m_i}\right). \quad (58)$$

Fortunately we have already determined the dominant terms in the energy exchange: while (52) neglects non-Maxwellian parts of the distributions, it is exact with regard to the mass ratio, and sufficiently accurate for most applications.

We next consider, using (6), the linearized version of (57). We begin by expanding

$$U_{\alpha\beta}(\mathbf{v} - \mathbf{V}_i) \equiv V_{\alpha\beta} + \frac{1}{v^3} (v_\alpha V_{i\beta} + v_\beta V_{i\alpha} + \delta_{\alpha\beta} \mathbf{v} \cdot \mathbf{V}_i) - 3 \frac{v_\alpha v_\beta}{v^5} \mathbf{v} \cdot \mathbf{V}_i,$$

where $V_{\alpha\beta}$ is defined by (55). From the identities

$$\frac{\partial f_e}{\partial v_\beta} = f_{eM} \left\{ \frac{\partial \hat{f}_e}{\partial v_\beta} - 2 \frac{v_\beta}{v_{te}^2} (1 + \hat{f}_e) \right\} \quad (59)$$

and

$$\frac{\partial}{\partial v_\alpha} \left[\frac{V_\alpha}{v} + \frac{v_\alpha \mathbf{v} \cdot \mathbf{V}}{v^3} \right] = 0,$$

we find

$$C_{ei1} = \frac{n_i \gamma_{ei}}{2m_e} f_{eM} \frac{\partial}{\partial v_\alpha} \left[V_{\alpha\beta} \frac{\partial \hat{f}_e}{\partial v_\alpha} - 4 \frac{V_{i\alpha}}{v_{te}^2 v} \right]. \quad (60)$$

The following consistency check is instructive. Suppose the collisional process is viewed from a reference frame moving with the ions. Then the linearized operator must have the form

$$C_{ei1} = \frac{n_i \gamma_{ei}}{2m_e} f_{eM} \frac{\partial}{\partial v_\alpha} \left[V_{\alpha\beta} \frac{\partial \hat{f}'_e}{\partial v_\alpha} \right], \quad (61)$$

where \hat{f}'_e is the electron perturbation seen in the moving frame. Recalling (13) we see that

$$\hat{f}'_e = \hat{f}_e - 2 \frac{\mathbf{v} \cdot \mathbf{V}_i}{v_{te}^2}.$$

Substitution of this form into (61) indeed reproduces (60), explicitly confirming the Galilean invariance of the operator.

As an application of (60), we compute the friction force of (21). Consider first the general form, for arbitrary mass ratio. From the Landau operator one finds

$$\mathbf{F}_{ii'} = -\gamma_{ii'} \left(1 + \frac{m_*}{m_{i'}} \right) \int d^3 v d^3 v' f_i f_{i'} \frac{\mathbf{u}}{v^3},$$

or

$$\mathbf{F}_{ss'} = -\gamma_{ss'} \left(1 + \frac{m_s}{m_{s'}} \right) \int d^3 v H_{s'} \frac{\partial f_s}{\partial \mathbf{v}}, \quad (62)$$

since $\int d^3 v' f'_s \mathbf{u}/\mathbf{u}^3 = -\partial H_{s'}/\partial \mathbf{v}$. While (62) is sometimes useful, (60) is most directly applicable to our present task: a small mass-ratio approximation to F_{ei} . After partial integration we have

$$F_{eiy} = -\frac{1}{2} \gamma_{ei} n_i \int d^3 v \left[V_{\alpha\beta} \frac{\partial \hat{f}_e}{\partial v_\alpha} - 4 \frac{V_{i\beta}}{v_{te}^2} \right] \frac{\partial}{\partial v_\beta} v_\gamma f_{eM}$$

where

$$\frac{\partial}{\partial v_\beta} v_\gamma f_{eM} = f_{eM} \left[\delta_{\beta\gamma} - 2 \frac{v_\beta v_\gamma}{v_{te}^2} \right].$$

It is not hard to show that

$$\int d^3 v f_{eM} \frac{1}{v} f_{eM} \left[\delta_{\beta\gamma} - 2 \frac{v_\beta v_\gamma}{v_{te}^2} \right] = \frac{2}{3} \sqrt{\pi} \frac{n_e}{v_{te}} \delta_{\beta\gamma};$$

therefore

$$F_{eiy} = -\frac{1}{2} \gamma_{ei} n_i \int d^3 v f_{eM} V_{\alpha\gamma} \frac{\partial \hat{f}_e}{\partial v_\alpha} + \frac{m_e n_e}{\tau_{ei}} V_{i\gamma}. \quad (63)$$

Here the electron-ion momentum exchange time,

$$\tau_{ei} \equiv \frac{3\sqrt{\pi} m_e v_{te}^3}{4 n_i \gamma_{ei}}, \quad (64)$$

has been introduced; note its consistency with the estimate (41). In the first term of (63), we integrate by parts, recall $v_\alpha V_{\alpha\gamma} = 0$, and use (43) to conclude

$$\mathbf{F}_{ei} = -\gamma_{ei} n_i \int d^3 v f_e \frac{\mathbf{v}}{v^3} + \frac{m_e n_e}{\tau_{ei}} \mathbf{V}_i. \quad (65)$$

We use this form in Chapter 6.

Next we consider the small mass-ratio approximation to C_{ie} . The derivation is based on (47); we assume nearly Maxwellian f_e , and neglect the correction term f_{e1} except where it appears with $1/m_e$, as in the last term of the integrand. Thus, in particular, G_e is computed from the electron Maxwellian, as given by (49), and we find, to lowest order in $v/v_{te} \sim v_{ti}/v_{te}$,

$$\frac{\partial^2}{\partial v_\alpha \partial v_\beta} G_{eM} \cong \frac{4}{3\sqrt{\pi}} \frac{n_e}{v_{te}} \delta_{\alpha\beta}.$$

Similarly

$$\frac{\partial H_{eM}}{\partial v_\beta} \cong -\frac{4}{3\sqrt{\pi}} \frac{n_e}{v_{te}} v_\beta,$$

so we only need to compute

$$\frac{\partial H_{e\beta}}{\partial v_\beta} \cong \int d^3v f_e \frac{v_\beta}{v^3}.$$

Here (63) provides

$$\frac{\partial H_{e1}}{\partial v_\beta} \cong -\frac{F_{ei\beta}}{\gamma_{ei} n_i} + \frac{m_e n_e}{\gamma_{ei} n_i \tau_{ei}} V_{i\beta}.$$

We substitute these results into (47) and find, after some manipulation,

$$C_{ie} = \frac{1}{m_i n_i} \mathbf{F}_{ei} \cdot \frac{\partial f_i}{\partial \mathbf{v}} + \frac{m_e}{m_i} \frac{n_e}{n_i \tau_{ei}} \frac{\partial}{\partial \mathbf{v}} \cdot \left[(\mathbf{v} - \mathbf{V}_i) f_i + \frac{T_e}{m_i} \frac{\partial f_i}{\partial \mathbf{v}} \right]. \quad (66)$$

This form is apparently due to Braginskii; its first term, reflecting friction with the electrons, is usually dominant and easily interpreted. Thus the main collisional effect of electrons on ions is to provide, in the ion equation of motion, an effective electric field,

$$\mathbf{E} \rightarrow \mathbf{E}_{\text{eff}} \equiv \mathbf{E} - \frac{\mathbf{F}_{ei}}{e_i n_i}. \quad (67)$$

The remaining terms in (66) describe, together, velocity diffusion as well as energy exchange; indeed, straightforward calculation from (24),

$$W_{ie}^L = \int d^3v \frac{1}{2} m_i v^2 C_{ie},$$

yields

$$W_{ie}^L = 3 \frac{m_e n_e}{m_i \tau_{ei}} (T_e - T_i), \quad (68)$$

in agreement with the small mass-ratio limit of (52).

Collision Times

A basic estimate of "detailed" scattering rates is provided by (41):

$$\tau_{ss'} \sim \frac{m_s^2 v_{t>} v_{ts}^2}{n_s' e_s^2 e_s'^2 \ln \Lambda}. \quad (69)$$

Since we rule out extreme temperature ratios, $v_{t>}$ becomes v_{te} whenever electrons are involved. In view of (1), the total scattering rate for species s is given by

$$\nu_s = \frac{1}{\tau_s} \sim \sum_{s'} \frac{1}{\tau_{s'}}. \quad (70)$$

These formulae provide useful estimates and scalings for various collisional processes.

We begin with the observation that (69) implies

$$\tau \sim T^{3/2}. \quad (71)$$

Since the transit frequency ω_t [recall (4.19)] is proportional to $T^{1/2}$, we see that the “collisionality parameter,” $\nu/\omega_{t,i}$, decreases rapidly with increasing temperature:

$$\nu/\omega_{t,i} \sim T^{-2}; \quad (72)$$

it is safely presumed small for electrons and hydrogen ions under thermonuclear conditions. The temperature regime in which $\nu/\omega_{t,i} \ll 1$ is often called the “collisionless” regime—despite the fact that collisions continue to play a role even as $\nu/\omega_{t,i} \rightarrow 0$. The opposite case is described as “collision-dominated.” Note that here and below we ignore the weak parametric dependence of the Coulomb logarithm; recall (39).

Turning to the mass and charge dependence of (69), we first point out the strong variation with atomic number Z :

$$\tau_{ii} \propto Z_i^{-4} m_i^{1/2}. \quad (73)$$

Here the first factor, although mildly counteracted by the second, usually ensures that impurity ions with moderate or large Z will be collision-dominated, even when hydrogen ions at the same temperature are collisionless.

The effect of electron scattering on any ion species is quite weak:

$$\frac{\tau_{ie}}{\tau_{ii}} \sim \frac{Z^2 n_i}{n_e} \frac{v_{te}}{v_{ti}}. \quad (74)$$

This ratio is large enough, even for $Z = 1$, to justify omitting C_{ie} entirely in many cases. Electrons, on the other hand, are sensitive to ion impact, as can be seen from (69). For $Z = 1$ we have

$$\tau_{ee} \sim \tau_{et}. \quad (75)$$

For larger ionic charge, (69) shows that the electron collision frequency is dominated by ion scattering:

$$C_e = C_{ei} + \mathcal{O}\left(\frac{1}{Z_{\text{eff}}}\right), \quad (76)$$

where

$$Z_{\text{eff}} \equiv \frac{1}{n_e} \sum_i Z_i^2 n_i, \quad (77)$$

is called the “effective Z ” of the plasma. Notice that quasineutrality implies

$$Z_{\text{eff}} = \frac{\sum_i Z_i^2 n_i}{\sum_i Z_i n_i},$$

so that Z_{eff} indeed scales like Z , rather than Z^2 .

The estimate (76) suggests a convenient, explicit measure of the electron collision frequency. Starting with (64), we replace $n_i e_i^2 = n_i Z_i^2 e^2$ by $n_e Z_{\text{eff}} e^2$ to obtain

$$\tau_e = \frac{3}{16\sqrt{\pi}} \frac{m_e^2 v_{te}^3}{e^4 \ln \Lambda Z_{\text{eff}} n_e}. \quad (78)$$

This definition, apparently introduced by Braginskii, has become a widely recognized standard. Similarly standard is the ion collision time,

$$\tau_i = \frac{3\sqrt{2}}{16\sqrt{\pi}} \frac{m_i^2 v_{ti}^3}{(Ze)^4 \ln \Lambda n_i}, \quad (79)$$

which pertains to ion-ion scattering, as (74) shows to be appropriate; note the factor of $\sqrt{2}$ in the coefficient.

For comparable ion and electron temperatures,

$$\frac{\tau_i}{\tau_e} \sim \left(\frac{m_i}{m_e} \right)^{1/2}; \quad (80)$$

electron collisions are more frequent. Note, however, that (80) also describes the corresponding ratio of transit times. Hence electrons and ions at similar temperatures will have the same collisionality parameter ν/ω_t .

Pitch-angle Variables*

Such expressions as (33) and (47) are valid only if the velocity components v_α are defined in a Cartesian coordinate system. Unfortunately in most applications it is convenient to use curvilinear velocity coordinates, such as the pitch-angle variables of §4.4. Therefore our expression for the collision operator must be generalized.

It is not hard to express the Coulomb operator in invariant form, valid for any coordinate choice. We use the tensor notation discussed in Chapter 2; covariant derivatives with respect to velocity are indicated with commas: $F_{,\alpha} \equiv \partial F / \partial v^\alpha$ [recall (2.27)]. Thus (47) generalizes to

$$C_{\alpha\alpha'} = \frac{\gamma_{\alpha\alpha'}}{2m_s} \left\{ [f_s g^{\alpha\kappa} g^{\beta\lambda} G_{\beta',\kappa,\lambda}]_{,\alpha,\beta} - 2 \left(1 + \frac{m_s}{m_{s'}} \right) f_s g^{\alpha\kappa} H_{s',\kappa} \right\}_{,\alpha} \quad (81)$$

where $g^{\alpha\beta}$ is the (contravariant) metric tensor for whatever velocity coordinates are used.

We restrict attention to pitch-angle variables, (λ, w, γ) . From §4.4 we have

$$\mathbf{v} = \mathbf{b}\sigma \left[2 \frac{w}{m} (1 - \lambda B) \right]^{1/2} + \left(2\lambda B \frac{w}{m} \right)^{1/2} (\mathbf{e}_2 \cos \gamma - \mathbf{e}_3 \sin \gamma) . \quad (82)$$

Hence

$$d\mathbf{v} \cdot d\mathbf{v} = g_{11}(d\lambda)^2 + g_{22}(dw)^2 + g_{33}(d\gamma)^2 ,$$

with

$$g_{11} = \frac{wB}{2m\lambda(1 - \lambda B)}, \quad g_{22} = \frac{1}{2mw}, \quad g_{33} = \frac{2w\lambda B}{m} . \quad (83)$$

Since pitch-angle variables are orthogonal, no off-diagonal coefficients occur. This advantage is not shared by, for example, the variables (μ, U, γ) . Because of orthogonality the contravariant components $g^{\alpha\beta}$ are simple inverses of their covariant counterparts:

$$g^{11} = \frac{2m\lambda(1 - \lambda B)}{wB}, \quad g^{22} = 2mw, \quad g^{33} = \frac{m}{2w\lambda B} . \quad (84)$$

From (83) or (84) we obtain the Jacobian $g^{1/2} = Bw/(m|u|)$, as noted in (4.144) (we have returned to denoting the parallel velocity by u).

Equation (81) involves tensors of the form

$$S_{,\alpha,\beta} = \frac{\partial^2 S}{\partial \xi^\alpha \partial \xi^\beta} - \Gamma_{\alpha\beta}^\kappa \frac{\partial S}{\partial \xi^\kappa} \quad (85)$$

where (ξ^1, ξ^2, ξ^3) represent the velocity coordinates (λ, w, γ) ; hence the Christoffel symbol must be evaluated. Straightforward calculation, using (2.31) yields

$$\Gamma_{11}^1 = \frac{2\lambda B - 1}{2\lambda(1 - \lambda B)}, \quad \Gamma_{12}^1 = \frac{1}{2w}, \quad \Gamma_{33}^1 = -2\lambda(1 - \lambda B);$$

$$\Gamma_{11}^2 = -\frac{wB}{2\lambda(1 - \lambda B)}, \quad \Gamma_{22}^2 = -\frac{1}{2w}, \quad \Gamma_{33}^2 = -2w\lambda B;$$

$$\Gamma_{13}^3 = \frac{1}{2\lambda}, \quad \Gamma_{23}^3 = \frac{1}{2w} . \quad (86)$$

All other components vanish. Equations (85) and (86) are generally applicable; for the particular calculation of

$$\begin{aligned} \nabla_v^2 S &= \frac{2m\sqrt{1 - \lambda B}}{wB} \frac{\partial}{\partial \lambda} \lambda \sqrt{1 - \lambda B} \frac{\partial S}{\partial \lambda} \\ &\quad + \frac{2m}{\sqrt{w}} \frac{\partial}{\partial w} w^{3/2} \frac{\partial S}{\partial w} + \frac{m}{2w\lambda B} \frac{\partial^2 S}{\partial \gamma^2} \end{aligned} \quad (87)$$

we can more simply use (2.26) and (2.32). Note that the first, pitch-angle scattering term can also be expressed as

$$\nabla_v^2 S|_{\text{pitch-angle}} = \left(\frac{m}{w}\right)^2 \frac{u}{B} \frac{\partial}{\partial \lambda} \lambda u \frac{\partial S}{\partial \lambda} \quad (88)$$

in view of (4.121).

Finally we substitute (84)-(86) into (81) to express the collision operator in (λ, w, γ) -coordinates. Because of orthogonality, the result has fewer terms than might be expected. Nonetheless, we present only the linearized version. We also neglect γ -derivatives, since in guiding-center kinetic theory (drift- or gyro-kinetic) the distribution is independent of gyrophase. For like-particle collisions we find, suppressing the species subscript,

$$\begin{aligned} C_1 &= \gamma f_M \left\{ 4\pi \frac{f_M \hat{f}}{m} + \frac{\Phi}{wB} (1 - \lambda B)^{1/2} \frac{\partial}{\partial \lambda} \left[\lambda (1 - \lambda B)^{1/2} \frac{\partial \hat{f}}{\partial \lambda} \right] \right. \\ &\quad \left. + \frac{n m v_t}{2\eta} \left(\text{erf} - \eta \text{erf}' \right) \frac{\partial^2 \hat{f}}{\partial w^2} + \frac{1}{T} (2\eta \text{erf} - \text{erf}) \frac{\partial \hat{f}}{\partial w} \right) \\ &\quad - \frac{m}{T} H_1 + m \frac{\eta^4}{2} \left[\frac{\partial^2 G_1}{\partial w^2} + \frac{1}{2w} \frac{\partial G_1}{\partial w} \right] \} \end{aligned} \quad (89)$$

where $\eta = (2w/T)^{1/2}$ as in (50), the error functions are evaluated at η ,

$$\Phi \equiv \frac{n}{2v_t} \frac{1}{\eta^3} [\eta \text{erf}'(\eta) + (2\eta^2 - 1)\text{erf}(\eta)], \quad (90)$$

and the 1-subscripts indicate linearized contributions:

$$G_1 \equiv G - G_M, \quad H_1 \equiv H - H_M. \quad (91)$$

With regard to the unlike-species collision operators, we consider only the small mass-ratio approximations. For C_{ei1} , we have (60); note that any ion flow \mathbf{V}_i from \hat{f}_i must be parallel to the magnetic field, since $\mathbf{v} \cdot \mathbf{V}_i$ would otherwise depend on γ . Thus we find

$$C_{ei1} = \frac{3\pi^{1/2}}{4\tau_e} \left(\frac{T_e}{w}\right)^{3/2} f_{eM} \frac{u}{Bw} \left[\frac{\partial}{\partial \lambda} \lambda u \frac{\partial \hat{f}}{\partial \lambda} + \frac{w}{T_e} BV_{||i} \right]. \quad (92)$$

Here we have recalled (78) to make the replacement

$$\gamma_{ei} = \frac{3\pi^{1/2}}{4} \frac{m_e v_{te}^3}{n_i \tau_e},$$

thus allowing for electron collisions with multiple ion species.

It is clear from (88) that the derivative term in (92) represents diffusion in pitch angle. That C_{ee} involves only pitch-angle diffusion is a result of the large mass-ratio that we anticipated in the derivation of (60). Energy scattering of the electrons enters in higher $(m_e/m_i)^{1/2}$ -order and, more importantly, through C_{ee} ; notice the third term of (89). It follows in particular that energy scattering of electrons is a relatively weak effect for large Z_{eff} [recall (76)].

It is also clear from (89) and (92) that like- and unlike-species scattering yield pitch-angle diffusion operators of the same form—a form that is essentially set by rotational symmetry, as in (88).

5.3 Application: The Equilibrium Distribution

Entropy Source

We have required the collision operator to be dissipative in the sense of satisfying an H -theorem. Here we verify that the Coulomb operator has this property, using the Landau form of (33).

It may be recalled that Boltzmann's H-theorem describes the rate of entropy production. The entropy (entropy density) for species s is defined as

$$S_s(\mathbf{x}, t) = - \int d^3v f_s \ln f_s . \quad (93)$$

Hence the rate of change of entropy is

$$\frac{\partial S_s}{\partial t} = - \int d^3v \frac{\partial f_s}{\partial t} (1 + \ln f_s) . \quad (94)$$

This local change reflects entropy flow as well as entropy production; to include only the latter, we simply replace the time derivative in the integrand by the collision operator:

$$\frac{\partial f_s}{\partial t} \rightarrow C_s .$$

Then the first term in (94) vanishes by particle conservation. The surviving term, giving the entropy source, or entropy production rate, for species s will be denoted by

$$\Theta_s \equiv - \int d^3v \ln f_s C_s . \quad (95)$$

Similarly the total entropy source is denoted by

$$\Theta = - \sum_s \int d^3v \ln f_s C_s . \quad (96)$$

At this point we specialize to the explicit operator (33). After substitution into (96) we have

$$\begin{aligned}\Theta = -\frac{1}{2} \sum_{s,s'} m_s \gamma_{ss'} & \int d^3 v d^3 v' \ln f_s \frac{1}{m_s} \\ & \cdot \frac{\partial}{\partial v_\alpha} \left\{ U_{\alpha\beta} \left[\frac{1}{m_s} f'_{s'} \frac{\partial f_s}{\partial v_\beta} - \frac{1}{m_{s'}} f_{s'} \frac{\partial f'_{s'}}{\partial v'_\beta} \right] \right\}.\end{aligned}$$

Partial integration and some rearrangement gives

$$\begin{aligned}\Theta = \frac{1}{2} \sum_{s,s'} m_s \gamma_{ss'} & \int d^3 v d^3 v' f_s f'_{s'} \frac{1}{m_s} \ln f_s \frac{\partial}{\partial v_\alpha} \\ & \cdot U_{\alpha\beta} \left[\frac{1}{m_s} \frac{\partial \ln f_s}{\partial v_\beta} - \frac{1}{m_{s'}} \frac{\partial \ln f'_{s'}}{\partial v'_\beta} \right].\end{aligned}\quad (97)$$

The remaining argument is familiar from classical Boltzmann kinetic theory: we simultaneously interchange

$$s \leftrightarrow s', \quad \mathbf{v} \leftrightarrow \mathbf{v}',$$

noticing that the first factor in (97), $m_s \gamma_{ss'}$, is symmetric under this transformation [recall (38)], while the last factor, in square brackets, is antisymmetric. Hence, after combining (97) with its interchanged version, we have

$$\Theta = \frac{1}{4} \sum_{s,s'} m_s \gamma_{ss'} \int d^3 v d^3 v' f_s f'_{s'} A_\alpha U_{\alpha\beta} A_\beta, \quad (98)$$

where we abbreviate

$$A_\alpha \equiv \frac{1}{m_s} \frac{\partial \ln f_s}{\partial v_\alpha} - \frac{1}{m_{s'}} \frac{\partial \ln f'_{s'}}{\partial v'_\alpha}.$$

Finally we observe that, for an arbitrary vector \mathbf{a} ,

$$\mathbf{a}_\alpha U_{\alpha\beta} \mathbf{a}_\beta = \mathbf{u}^3 [(a\mathbf{u})^2 - (\mathbf{a} \cdot \mathbf{u})^2] \geq 0. \quad (99)$$

Hence (98) implies

$$\Theta \geq 0, \quad (100)$$

for any distributions f_s and $f'_{s'}$.

Equation (100), ensuring positive entropy production, verifies the first part of the H -theorem. To show that relaxation always produces Maxwellian distributions we note from (99) that $A_\alpha U_{\alpha\beta} A_\beta$ can vanish only if $A_\alpha = Ku_\alpha$, for some constant K . In this case we must have

$$\frac{\partial \ln f_s}{\partial v_\alpha} = Km_s v_\alpha, \quad (101)$$

so that each f_s is indeed Maxwellian. Since C_s then vanishes, we have verified (2): if Θ vanishes, then C_s must vanish. Finally, since $K = 1/T$ cannot depend on species, we see that collisional equilibrium must have equal species temperatures, as in (3).

That the collision operator, and therefore the entropy source, vanishes for the case of equal-temperature Maxwellian distributions is quickly apparent from (33). It is also transparent physically: Maxwellian distributions cannot be further randomized. What is less obvious is that *no other* distribution yields $\Theta = 0$: collisions cannot balance an entropy increase in one part of velocity space with a corresponding decrease elsewhere. Whenever the entropy production vanishes, (101) tell us that collisions have fully and finally randomized the distribution functions.

Lowest Order Maxwellians

Classical thermodynamic equilibrium refers to a stationary state whose temperature is uniform and whose density variation is determined by the (chemical) potential. From the point of view of the kinetic equation (4.6) this equilibrium corresponds to the trivial solution

$$\begin{aligned} C(f, f) = 0 &= \mathbf{v} \cdot \nabla f - \frac{e\nabla\Phi}{m} \cdot \frac{\partial f}{\partial \mathbf{v}} \\ \Rightarrow f &= f_M, \quad \nabla T = 0, \quad \nabla \left[n \exp \frac{e\Phi}{T} \right] = 0. \end{aligned} \quad (102)$$

We will use the term *Maxwell-Boltzmann distribution* to identify the density variation prescribed by (102). In Chapter 1 we emphasized that the state of a confined plasma is far from thermodynamic equilibrium. Here we note, from (102), that the thermodynamic equilibrium state is not confined, or even affected, by magnetic fields (a consequence of Van Leeuwen's theorem²). The confined state, on the other hand, is strongly affected by B , has typically strong temperature gradients and, being quasineutral, cannot display Maxwell-Boltzmann density variation for both signs of charge. Indeed, all the hardware of confinement is designed precisely to impede plasma relaxation to the state described by (102).

Yet we will find that (102), in an approximate and one-dimensional sense, does pertain to a confined plasma. To lowest order in δ , the distribution function of a confined plasma is Maxwellian; and, also to lowest order, the *parallel* gradients of its temperature and density are constrained much as in (101). The reason for this agreement is simply that the fastest processes occurring in an ensemble of guiding-centers—parallel streaming and collisions—are the very processes least affected by the magnetic field.

² An instructive discussion is provided by Peierls, *Surprises in Theoretical Physics*, Princeton University Press, Princeton, 1979, §4.4.

To make these statements more precise we recall the drift kinetic equation, (4.44):

$$\frac{\partial \bar{f}}{\partial t} + (\mathbf{u} + \mathbf{v}_D) \cdot \nabla \bar{f} + \left[e \frac{\partial \Phi}{\partial t} + \mu \frac{\partial B}{\partial t} - \frac{e}{c} \mathbf{v}_{\parallel} \cdot \frac{\partial \mathbf{A}}{\partial t} \right] \frac{\partial \bar{f}}{\partial U} = C. \quad (103)$$

This equation is attacked by expanding the distribution \bar{f} in powers of δ ,

$$\bar{f} = f_0 + f_1 + \dots, \quad f_n = \mathcal{O}(\delta^n), \quad (104)$$

and attempting an order-by-order solution. Here we are content with the lowest order function, f_0 . Since $v_D = \mathcal{O}(\delta)$, the only zeroth order terms in the drift-kinetic operator are those describing parallel streaming and collisions, so f_0 must satisfy

$$u \nabla_{\parallel} f_{s0} = C_s(f_0, f_0). \quad (105)$$

We next show that the only solution to this equation is that in which both sides vanish; that is, (105) requires

$$f_{s0} = f_{sM}, \quad \nabla_{\parallel} f_{sM} = 0. \quad (106)$$

It is clear that relaxation to the Maxwellian occurs during a collision time, τ , while relaxation of parallel gradients occurs over a transit time ω_t^{-1} . Note that the relative magnitudes of these times—whose ratio gives the collisionality parameter ν/ω_t —has not been specified. Relaxation is predicted for all collisionality regimes, so long as the gyroradius is small. It should also be noted that (106) provides the basic justification for most of the developments of Chapter 3.

The proof of (106) is straightforward and similar to the neutral gas case. We multiply both sides of (105) by $\ln f_{s0}$, integrate over velocity, sum over species, and perform a flux surface average. In view of (95) the right-hand side becomes $\langle \Theta \rangle$, while the left-hand side is

$$\sum_s \left\langle \int d^3 v \frac{u}{B} \mathbf{B} \cdot \nabla f_s \right\rangle = \left\langle \mathbf{B} \cdot \nabla \sum_s \int d^3 v \frac{u}{B} f_s \right\rangle = 0. \quad (107)$$

Here we have recalled (4.144) and (3.41). Then (105) implies $\langle \Theta \rangle = 0$, or, since Θ is never negative, $\Theta = 0$. Hence the f_s must be Maxwellian, as in (106).

Notice that this argument depends on the H-theorem, as in (2) and (3), but not on any details of the collision operator. More importantly, it depends upon the existence of an annihilator for the the operator $\mathbf{B} \cdot \nabla$, as in (107). This is a physical requirement: in mirror geometry, where end losses forbid such an annihilator, the proof fails—and indeed, experimental mirror-machine distributions can be strongly non-Maxwellian. But in

Chapter 3 we showed that such an annihilator, the flux-surface average, can be constructed in any toroidal geometry in which flux surfaces can be identified.

Experimental observations in closed confinement devices confirm the Maxwellian nature of f_0 . However it is often observed that temperature equilibration between ions and electrons fails. This is easily understood: as noted in (58), energy exchange is inefficient for disparate masses. The temperature difference $T_e - T_i$ (all ion species are typically close in temperature) can be taken into account, using the small mass-ratio m_e/m_i . However, in this Chapter we simplify the discussion by assuming all species temperatures are equal.

Recalling (4.181),

$$f_M(\mathbf{x}, \mathbf{v}) = \frac{1}{\pi^{3/2} v_t^3} n \exp \left[-\frac{U - e\Phi}{T} \right] \quad (108)$$

we infer from (107) [*cf.* (4.182)] that

$$\nabla_{\parallel} \ln n_s + \nabla_{\parallel} \frac{e_s \Phi}{T_s} + \left[\frac{U - e_s \Phi}{T_s} - \frac{3}{2} \right] \nabla_{\parallel} \ln T_s = \mathcal{O}(\delta), \quad (109)$$

for each plasma species s . The error term on the right-hand side of (109) is indicated for two reasons. First, as noted in the discussion leading to (4.95), the variable U must enter the perturbation expansion, because of its Φ -dependence. Thus the parallel gradient in (106) is strictly performed at constant $U_0 = (1/2)m\mathbf{v}^2 + e\Phi_0$, rather than at constant U , and only f_0 should appear in (109). The right-hand side of (109) accounts for this distinction. Secondly, the $\mathcal{O}(\delta)$ terms account for any differences between the density and temperature of the Maxwellian and those of the full distribution function: $n \equiv \int d^3v f_M$ may differ from $\int d^3v f_M$, for example. Since (109) must hold for all U we have

$$\nabla_{\parallel} T_s = \mathcal{O}(\delta), \quad (110)$$

and

$$\nabla_{\parallel} \left[n_s \exp \left(\frac{e_s \Phi}{T_s} \right) \right] = \mathcal{O}(\delta), \quad (111)$$

as in (102). It follows that we can write $n_s = N_s \exp(-e_s \Phi/T_s)$, with $\nabla_{\parallel} N_s = \mathcal{O}(\delta)$, and thus express the quasineutrality condition as

$$\sum_s e_s N_s \exp \left(-\frac{e_s \Phi}{T_s} \right) = \mathcal{O}(\delta).$$

Therefore

$$\nabla_{\parallel} \left\{ \sum_s e_s N_s \exp \left(-\frac{e_s \Phi}{T_s} \right) \right\} = \left\{ \sum_s \frac{e_s^2 N_s}{T_s} \exp \left(-\frac{e_s \Phi}{T_s} \right) \right\} \nabla_{\parallel} \Phi = \mathcal{O}(\delta).$$

Here the coefficient of $\nabla_{\parallel}\Phi$,

$$\sum_s \frac{e_s^2 N_s}{T_s} \exp\left(-\frac{e_s \Phi}{T_s}\right) \geq 0$$

is positive definite. Hence we may conclude

$$\nabla_{\parallel}\Phi = \mathcal{O}(\delta). \quad (112)$$

This important result was anticipated in (4.116).

Because no choice of flow velocity \mathbf{V} can make $\nabla_{\parallel}(\mathbf{u} \cdot \mathbf{V})$ vanish uniformly in velocity space, we see that (106) forces f_0 to be Maxwellian in the lab frame, without zeroth-order flow:

$$\frac{V}{v_t} = \mathcal{O}(\delta). \quad (113)$$

Unfortunately this result stems from the drift ordering, (4.24), and is not a general consequence of collisional relaxation. The point is that rapid flows require large electric fields, not treated by the drift-kinetic equation (103). In the case of rapid flow, $V/v_t = O(1)$, the magnetic moment coordinate μ must be defined in the moving frame, and the corresponding kinetic equation is more complicated. Rapidly flowing equilibria are briefly considered in Chapter 8.

Since our proof of the H-theorem assumes well-behaved flux surfaces, it is appropriate to express results like (106) in terms of flux coordinates. Thus we infer from (106) that the lowest-order distribution satisfies

$$f_0(\mathbf{x}, \mathbf{v}) = f_M(r, U_0), \quad (114)$$

and that the electrostatic potential is approximately a flux function,

$$\Phi(\mathbf{x}) = \Phi_0(r) + \mathcal{O}(\delta). \quad (115)$$

Quadratic Entropy Production

We have found that in a closed confinement system each distribution has the form

$$f = f_M(1 + \hat{f}), \quad \hat{f} = \mathcal{O}(\delta). \quad (116)$$

Therefore the entropy production rate can be expressed in terms of \hat{f} , by inserting (116) into (96). The leading term, proportional to $C(f_M, f_M)$, obviously vanishes. Furthermore first order terms cannot contribute, because collisional particle and energy conservation imply that

$$\sum_s \int d^3 v \ln f_{s,M} C_{s,1} = 0.$$

Thus the leading term in Q is quadratic:

$$\Theta = \Theta_2 + \mathcal{O}(\delta^3), \quad (117)$$

$$\Theta_2 \equiv - \sum_s \int d^3v \hat{f}_s C_{1s}(\hat{f}).$$

By measuring the entropy produced by \hat{f} , Θ_2 describes the relaxation of any perturbed state to thermodynamic equilibrium. It is thus the central object of linear transport theory.

A natural extension is the bilinear form

$$\Theta_2[f, g] = - \sum_{ss'} \int d^3v \hat{f}_s C_{1ss'}(\hat{g}), \quad (118)$$

where \hat{f} and \hat{g} are two arbitrary distribution-function perturbations. From (42) we find, after partial integration,

$$\Theta_2[f, g] = \sum_{ss'} \int d^3v \int d^3v' f_{sM} f_{s'M} \frac{m_s \gamma_{ss'}}{2} \cdot \frac{1}{m_s} \frac{\partial \hat{f}_s}{\partial v_\alpha} U_{\alpha\beta} \left[\frac{1}{m_s} \frac{\partial \hat{g}_s}{\partial v_\beta} - \frac{1}{m_{s'}} \frac{\partial \hat{g}'_{s'}}{\partial v'_\beta} \right].$$

This expression can be symmetrized in precisely the same manner as (97), with the result

$$\Theta_2[f, g] = \sum_s \int d^3v \int d^3v' f_{sM} f_{s'M} \frac{m_s \gamma_{ss'}}{2} \cdot \left[\frac{1}{m_s} \frac{\partial \hat{f}_s}{\partial v_\alpha} - \frac{1}{m_{s'}} \frac{\partial \hat{f}'_{s'}}{\partial v'_\alpha} \right] U_{\alpha\beta} \left[\frac{1}{m_s} \frac{\partial \hat{g}_s}{\partial v_\beta} - \frac{1}{m_{s'}} \frac{\partial \hat{g}'_{s'}}{\partial v'_\beta} \right]. \quad (119)$$

The symmetry

$$\Theta_2[f, g] = \Theta_2[g, f], \quad (120)$$

manifest in (119), plays a crucial role in transport theory. As will be shown in Chapter 8, it enforces *Onsager symmetry* on the transport coefficients, and furthermore permits a variational treatment of the kinetic equation.

Equation (119) also shows that

$$\Theta_2[f, f] \geq 0 \quad (121)$$

and that it vanishes only for Maxwellian perturbations, as defined by (17):

$$\Theta_2[f, f] = 0 \Leftrightarrow \hat{f} = \hat{f}_{M1}. \quad (122)$$

These conclusions are direct corollaries of the general results (100) and (101).

First Order Perturbation

Consider first the linearized kinetic equation,

$$u \nabla_{\parallel} h = C_1(h) \quad (123)$$

where C_1 is the linearized operator of (6). Its solution is denoted by h to emphasize the homogeneous nature of (123). We can apply to (123) the same procedure used for its nonlinear version, (105), and come to an analogous conclusion: after multiplying both sides by $\hat{h} \equiv h/f_M$, integrating over velocity and performing a flux surface average, we find that $(\Theta_2) = 0 \Rightarrow \Theta_2 = 0$. Hence, by (122), the unique solution to (123) is

$$\hat{h} = \hat{f}_{M1}, \quad \nabla_{\parallel} \hat{f}_{M1} = 0, \quad (124)$$

where \hat{f}_{M1} is given by (17). This conclusion, like (121) and (122), also follows directly from the general H -theorem; cf. (105) and (106). Since it is clear from (124) that we can replace f_0 by $f_0 + h$ without physical change, a correction of this form can always be neglected.

We consider next the first order terms in the ion version of (103), without electron scattering [recall (74)]. We confine our attention to the equilibrium state, using the transport ordering of (4.16) to neglect time derivatives. Thus we have

$$u \nabla_{\parallel} f_1 - C_1(f_1) = -\mathbf{v}_D \cdot \nabla f_0. \quad (125)$$

It is convenient to introduce the distribution function $k(\mathbf{x}, \mathbf{v})$, defined as the collisionless solution to (125):

$$u \nabla_{\parallel} k = -\mathbf{v}_D \cdot \nabla f_0, \quad (126)$$

with $k(u=0)=0$. The solvability condition for (126) is obtained using the orbital average of (4.131) and (4.132). Since the average annihilates the left-hand side of (126) we must have $(\mathbf{v}_D \cdot \nabla f_0)_o = 0$, or, in view of (114),

$$(\mathbf{v}_D \cdot \nabla X)_o = 0. \quad (127)$$

The physical requirement expressed by (127) is that the orbit remains bound, on the average, to a single flux surface. It is clearly necessary for the confinement of collisionless orbits, although easily verified only in the axisymmetric case. We presume (127) holds and assume k to be a known function. Then, writing

$$f_1 = k + g, \quad (128)$$

we have to solve

$$u \nabla_{\parallel} g - C_1(g) = C_1(k) \quad (129)$$

for the function g . Notice that (124) allows us to disregard solutions to the homogeneous version of (129).

The result given by (128) and (129) is used in Chapter 6 to provide insight into plasma flow; it also provides the basis for collisionless (“banana” regime) kinetic theory, as shown in Chapter 8. On the other hand, these equations do not supply any simple formula for g : the mathematical problem posed by (129) involves the phase-space issues discussed in §4.4, the complexity of C_1 and the general awkwardness of toroidal magnetic field curvature. It has been solved only approximately, and only in limiting cases.

For axisymmetric systems, there is one easily accessible consequence of (129). We first recall (4.159) to write

$$\mathbf{v}_D \cdot \nabla \chi = -u\mathbf{b} \times \nabla \left(\frac{u}{\Omega} \right) \cdot \nabla \chi \quad (130)$$

for any confinement geometry. Next, specializing to axisymmetry, we let $G(r, \theta)$ be an arbitrary function and consider the quantity

$$\mathbf{B} \times \nabla G \cdot \nabla \chi = \frac{\partial G}{\partial \theta} I \nabla \zeta \times \nabla \theta \cdot \nabla \chi = -IB^\theta \frac{\partial G}{\partial \theta} .$$

Thus we have the useful identity

$$\mathbf{B} \times \nabla G \cdot \nabla \chi = -I\mathbf{B} \cdot \nabla G \quad (131)$$

for any function G in an axisymmetric system. For the radial drift, the identity implies

$$\mathbf{v}_D \cdot \nabla \chi = Iu\nabla_{||} \left(\frac{u}{\Omega} \right) . \quad (132)$$

This expression manifestly satisfies (127) and yields, for (126),

$$u\nabla_{||} k = -Iu\nabla_{||} \left(\frac{u}{\Omega} \right) \frac{df_M}{d\chi} ,$$

whence

$$k = -\frac{Iu}{\Omega} \frac{df_M}{d\chi} . \quad (133)$$

What is most interesting about the distribution k is that it is almost a displaced Maxwellian. Indeed, since (16) provides

$$\frac{df_M}{d\chi} = f_M \left[\frac{d \ln n}{d\chi} + \frac{e}{T} \frac{d\Phi}{d\chi} + \left(\frac{v^2}{v_t^2} - \frac{3}{2} \right) \frac{d \ln T}{d\chi} \right] , \quad (134)$$

we see, recalling the discussion following (15), that the right-hand side of (129) is proportional to the radial (ion) temperature gradient: $C_1(k) \propto dT/d\chi$. (We needn’t require both species to have the same velocity displacement, since electron scattering is neglected.) Thus, by linearity and (124),

$$g \propto \frac{dT}{d\chi} . \quad (135)$$

In §8.6 we infer from (135) that the poloidal plasma flow in an axisymmetric system is proportional to $dT_i/d\chi$. An equally striking conclusion is evident here: if the temperature gradient is locally negligible in any region of an axisymmetric system, then $g = 0$ and the first order distribution is simply

$$f = -\frac{Iu}{\Omega} \frac{df_M}{d\chi}, \quad (136)$$

independently of the collisionality regime, or even of the nature of the collision process. All that is required is that the collision mechanism satisfy the general requirements listed at the beginning of §5.1. It should be noted that the gyrophase-dependent correction term, $-\rho \cdot \nabla f_M$, represents a similarly simple velocity shift in the isothermal case.

Thus, in axisymmetric systems, equilibrium kinetic theory is non-trivial only because of the temperature gradient. Temperature variation [as well as temperature perturbation: recall (17)], on the other hand, can distort the distribution in a complicated way, depending not only on energy, as in (134), but more importantly on pitch-angle: the general solution to (129), for example, is an elaborate function of both w and λ .

5.4 Summary

A physically reasonable collision operator, reflecting the dominant influence of binary interactions, should be bilinear in the distribution functions of the colliding species. The operator should satisfy an H-theorem, forcing relaxation to a Maxwellian distribution. It should have spatial symmetries appropriate to the underlying process, as well as Galilean invariance. Finally a local collision operator is expected to conserve particles, momentum and energy at each spatial point.

The Coulomb collision operator, $C(f, f)$, satisfies these constraints, with spherical symmetry. It is in addition a Fokker-Planck operator, in the sense of representing cumulative effects of many, very weak, scattering events. This Fokker-Planck character, together with the symmetry and conservation laws, essentially determines the form of the operator.

Of the numerous equivalent versions of the Coulomb operator, those due to Landau and to RMJ are especially useful. The latter provides a simple formula for the collisional energy exchange between two species, as well as small-mass-ratio approximations for scattering between electrons and ions.

Electrons scatter off ions almost as they would off fixed obstacles; since electron energy is nearly conserved in such encounters, the operator C_{ei} describes primarily diffusion in angle. The effect on ions of electron scattering, on the other hand, is dominated by simple friction, without diffusion—as expected for ion motion through the hail of electrons.

Ion and electron collision rates are in proportion to the respective thermal speeds, so that the collisionality ratio, ν/ω_t , is typically the same for both species. The electron collision time for an impure plasma depends prominently on an effective average, Z_{eff} , of the ion atomic number. All the linearized operators are easily expressed in terms of the velocity coordinates λ and w .

Applications of the Coulomb operator often involve the entropy production rate, Θ —the quantity whose increase is guaranteed by the H-theorem. The non-negative character of Θ is exploited, in the δ -ordered drift-kinetic equation, to determine the equilibrium state. It is found that in any confinement system possessing flux surfaces, the lowest-order equilibrium distribution is a Maxwellian, constant along the confining field. While relaxation to this state involves both the collision and transit times, it occurs in any collisionality regime. A consequence is that each species' density obeys a Maxwell-Boltzmann spatial distribution along \mathbf{B} ; quasineutrality then requires the parallel variation of the electrostatic potential to be small.

When the entropy production rate is expanded about the equilibrium state, its leading term is Θ_2 , a quadratic form in the non-Maxwellian correction. This quantity provides a bilinear form whose symmetry guarantees Onsager symmetry of plasma transport coefficients and permits a variational solution of the drift-kinetic equation.

Examination of the first-order drift-kinetic equation shows the general form of its solution. In the special case of an isothermal, axisymmetric plasma, one can write down the exact solution for any collisionality: in the absence of temperature gradients, the kinetic theory of tokamak equilibrium would be easy.

Further Reading on Collision Operators:

- Rosenbluth, MacDonald, and Judd, 1957
- Braginskii, 1965
- Fried, 1966
- Ichimaru, 1973
- Hinton, 1983

Exercises

1. Verify (52) for the energy exchange rate in the Maxwellian case.
2. Starting with (33), show explicitly that the like-particle collision operator conserves momentum: $\int d^3v \, m_s \mathbf{v} C_{ss'} \equiv 0$.

3. Relate the diffusion tensor \mathbf{D} of (40) to derivatives of the Rosenbluth potential. Then use (49) to compute \mathbf{D} explicitly for the case of a Maxwellian distribution.

4. The *Krook collision operator* is a model linearized operator defined by

$$C_K(f_1) \equiv -\nu \left[f_1 - \frac{n_1}{n_M} f_M \right]$$

where ν is a constant representing the collision frequency and $n_1 \equiv \int d^3v f_1$. Discuss this operator in terms of the general physical constraints imposed in §5.1. Specify in particular which conservation laws C_K obeys.

5. Suppose that the electron distribution is a displaced Maxwellian, moving at the ion velocity \mathbf{V}_i . By evaluating the integral in (65), show that in this case the friction force \mathbf{F}_{ei} vanishes exactly, as it should.
6. Collisionality. A precise measure of the collisionality parameter ν/ω_i is given by the ratio of times τ_e/τ_i , where τ_e is the Coulomb collision time, given for ions and electrons by (78) and (79), and τ_i is the transit time defined by (4.136).
- (a) How does this ratio scale with species mass? with temperature?
- (b) Consider the Standard Tokamak³ with $Z_{\text{eff}} = 1$. At what temperatures are the ion and electron collisionalities approximately unity?
7. Charge exchange. An important atomic interaction occurring near the plasma boundary is charge exchange: a neutral H-atom from the wall delivers its electron to an ion from the plasma interior. If the ion distribution is denoted by f_i and the neutral distribution by f_n , then the charge-exchange operator is represented approximately by

$$X(f_i, f_n) = \int d^3v' \sigma_x |\mathbf{v} - \mathbf{v}'| [f_i(\mathbf{v}) f_n(\mathbf{v}') - f_n(\mathbf{v}) f_i(\mathbf{v}')],$$

where σ_x is the charge exchange cross-section. The operator appears in the ion kinetic equation alongside the Coulomb collision operator, $C(f_i)$. The product $\sigma_x |\mathbf{v} - \mathbf{v}'|$ is a weak function of velocity, often taken to be constant.

- (a) It is physically obvious that charge exchange conserves both ions and neutrals. Verify that the operator X has this conservation property, analogous to (20).

³Recall problem 5 of chapter 3

- (b) The charge-exchange mean-free path, λ_x , is defined as the average distance travelled by a neutral between charge exchange events. Assuming that both distributions are roughly Maxwellian, with comparable temperatures, estimate λ_x in terms of σ_x and the ion density.
- (c) When λ_s is sufficiently short, the lowest order neutral distribution satisfies $X(f_i, f_n) \approx 0$. An obvious solution is $f_n = N(\mathbf{x})f_i$, where N is an arbitrary function of position. Modify the H-theorem argument of (98) to show that $f_n = N(\mathbf{x})f_i$ is the **only** solution.
8. **Slowing down.** Alpha particles, the ash of fusion reactions, are born in a $D-T$ plasma at 3.5 Mev. Sufficiently well-confined alphas ultimately equilibrate to the ion temperature T_i , but one expects a “slowing-down” tail of hot alphas, with distribution $f_{\alpha h}$ and thermal speed v_h . The slowing-down distribution is determined primarily by energy scattering with Maxwellian scatterers.

- (a) Assuming the $f_{\alpha h}$ depends only on kinetic energy w , show that the relevant collision operator is

$$C_{\text{slow}} = \sum_s C(f_{\alpha h}, f_s M)$$

$$= \sum_s \left(\frac{\gamma_{\alpha s} n_s v_{st}^3}{2v} \frac{\partial}{\partial w} \right) \left\{ \phi \left(\frac{v}{v_{st}} \right) \left[\frac{\partial f_{\alpha h}}{\partial w} + \frac{m_\alpha}{T_s} f_{\alpha h} \right] \right\}$$

where

$$\phi(x) = \text{erf}(x) - x \text{erf}'(x).$$

- (b) Under typical conditions ($T_i \approx T_e \cong 10$ keV) $v_{ti} \ll v_h \ll v_{te}$. Show that in this case the slowing-down operator is approximated by

$$C_{\text{slow}} \approx \frac{1}{\tau_s} \frac{m_i}{m_\alpha} \left(\frac{v_e}{v} \right)^3 w \frac{\partial}{\partial w} \left[\phi_s(v) \left(f + \frac{T}{m_\alpha} \frac{\partial f_{\alpha h}}{\partial w} \right) \right] \quad (137)$$

where the slowing-down time is $\tau_s \equiv (m_i n_i / m_e n_e) \tau_e$, the critical speed satisfies $v_e^3 \equiv (3\pi^{1/2}/4)(m_e/m_i)v_{te}^3$ and $\phi_s(v) \equiv (2m_\alpha/m_i)[(n_i/n_e) + (v/v_e)^3]$.

9. The slowing down distribution $f_{\alpha h}$ is determined by the obvious balance

$$C_{\text{slow}}(f_{\alpha h}) = S_\alpha \delta(w - w_0)$$

where S_α measures the fusion source and w_0 is the birth energy, 3.5 meV. Using the results of Problem 8, and neglecting contributions of order

$\exp(-v_h^2/v_{ti}^2)$, show that

$$f_{ah} = \frac{s}{\phi_s}, \quad \text{for } w < w_0,$$

$$f_{ah} = \frac{s}{\phi_s} \exp \left[\frac{m_\alpha}{T} (w - w_0) \right], \quad \text{for } w > w_0,$$

where $s \equiv (m_\alpha/m_i)(\tau_s/2\pi v_c^3)S_\alpha$.

10. Equation (136) for the perturbed guiding-center distribution in the isothermal case, can be compared to (4.66), for the perturbation in \tilde{f} . The comparison is made in terms of a toroidally confined plasma with thermal speed v_t , gradient scale-length L , poloidal magnetic field B_P and toroidal field B_T .

- (a) Compare the sizes of the two perturbations in a typical tokamak and in a reversed-field pinch.
- (b) While (4.66) is generally valid, (136) requires constant temperature. What is the origin of this difference?
- (c) Discuss the physical analogy between the two distributions, using (4.33).

11. In a general axisymmetric system, we expect the *collisionless* distribution to have the form

$$f(\mathbf{x}, \mathbf{v}) = F(p_\zeta, \mu, U)$$

where p_ζ is the (covariant) angular momentum, $p_\zeta = mv_\zeta + (e/c)A_\zeta$, and the function F is unspecified. After recalling (3.124), use an appropriate gyroradius expansion to relate F to perturbation given by (128) and (133). Thus (128) is derived from angular momentum conservation.

Chapter 6

Fluid Description of Magnetized Plasma

6.1 Moments of Distribution Function

General Moments

In a fluid description of plasma motion, the distribution function $f(\mathbf{x}, \mathbf{v}, t)$ is represented by some small set of its velocity moments, the so-called fluid variables. The essential advantage of fluid theory is the lower dimensionality of coordinate space, compared to phase space. Just as importantly, the concreteness of fluid variables—they are, after all, the quantities most commonly measured in experiments—permits relatively straightforward physical argument.

The most pertinent moments are obtained from the first four powers of the velocity. We have already used the density of species s ,

$$n_s \equiv \int d^3 v f_s, \quad (1)$$

and the flow velocity, \mathbf{V}_s ,

$$\mathbf{n}_s \mathbf{V}_s \equiv \int d^3 v f_s \mathbf{v}. \quad (2)$$

Here, using the conventions of Braginskii (Braginskii, 1965) we introduce the energy flux,

$$\mathbf{Q}_s \equiv \int d^3 v f_s \frac{1}{2} m_s v^2 \mathbf{v}; \quad (3)$$

the heat flux,

$$\mathbf{q}_s \equiv \int d^3 v f_s \frac{1}{2} m_s |\mathbf{v} - \mathbf{V}_s|^2 (\mathbf{v} - \mathbf{V}_s); \quad (4)$$

the stress tensor (momentum flux),

$$\mathbf{P}_s \equiv \int d^3 v f_s m_s \mathbf{v} \mathbf{v}; \quad (5)$$

the pressure tensor,

$$\mathbf{P}_s \equiv \int d^3 v f_s m_s (\mathbf{v} - \mathbf{V}_s) (\mathbf{v} - \mathbf{V}_s); \quad (6)$$

and the energy-weighted stress,

$$\mathbf{R}_s \equiv \int d^3 v f_s \frac{1}{2} m_s v^2 \mathbf{v} \mathbf{v}. \quad (7)$$

The trace of the pressure tensor measures the scalar pressure,

$$p_s \equiv \frac{1}{3} Tr(\mathbf{P}_s) = \frac{1}{3} \int d^3 v f_s m_s (\mathbf{v} - \mathbf{V}_s) \cdot (\mathbf{v} - \mathbf{V}_s), \quad (8)$$

and the temperature ("kinetic" temperature) of species s is defined by

$$T_s \equiv \frac{p_s}{n_s}. \quad (9)$$

The relation between \mathbf{Q} and \mathbf{q} , or between \mathbf{P} and \mathbf{p} , should be clear: the former (capitalized) quantity is measured in the "lab" frame, while the latter (lower-case) quantity is measured in the rest-frame of the species under consideration. The language—"energy" vs. "heat," or "stress" vs. "pressure"—is conventional, if not especially helpful. It is easily shown that

$$\mathbf{P}_s = \mathbf{p}_s + m_s n_s \mathbf{V}_s \mathbf{V}_s \quad (10)$$

and that

$$\mathbf{Q}_s = \mathbf{q}_s + \mathbf{V}_s \cdot \mathbf{p}_s + \frac{3}{2} p_s \mathbf{V}_s + \frac{1}{2} m_s n_s V_s^2 \mathbf{V}_s. \quad (11)$$

The advective inertial term, distinguishing \mathbf{P} from \mathbf{p} in (10), is comparable to p whenever the velocity \mathbf{V} approaches the thermal or the sound speed. We will see, for example, that the inertial term plays a key role in MHD-ordered fluid theory; it also enters the understanding of certain externally driven tokamak equilibria. However, the drift ordering has $V = \mathcal{O}(\delta v_t)$, so that the inertial terms in (10) are relatively small:

$$\mathbf{P} = \mathbf{p} + \mathcal{O}(\delta^2); \quad (12)$$

recall (5.113).

Moments of Guiding-Center Distribution

The distribution functions for each species in a magnetized plasma are approximated by the gyro-averaged, guiding-center distribution, as in (4.56). It is therefore appropriate to consider the form of various moments when \tilde{f} is omitted.

The density is obviously indifferent to \tilde{f} , while the velocity depends straightforwardly on both \tilde{f} and \bar{f} , as noted in (4.164); similar comments pertain to the heat and energy flows. The stress tensor is more interesting: if \tilde{f} is omitted from (5), \mathbf{P} becomes diagonal in the $(\mathbf{b}, \mathbf{e}_2, \mathbf{e}_3)$ system.

Consider

$$\mathbf{P}[\bar{f}] = \int d^3v \bar{f} m(\mathbf{u} + \mathbf{s})(\mathbf{u} + \mathbf{s}) .$$

It is clear that the integral over gyrophase will annihilate terms with one power of \mathbf{s} , along with off-diagonal terms involving products of \mathbf{e}_2 with \mathbf{e}_3 . In the surviving terms we can average the γ -dependence to obtain

$$\mathbf{P}[\bar{f}] = \int d^3v \bar{f} m[\mathbf{b}\mathbf{b}u^2 + \frac{1}{2}(\mathbf{e}_2\mathbf{e}_2 + \mathbf{e}_3\mathbf{e}_3)s^2]$$

or

$$\mathbf{P}[\bar{f}] = \mathbf{b}\mathbf{b}P_{\parallel} + (\mathbf{I} - \mathbf{b}\mathbf{b})P_{\perp} \quad (13)$$

where \mathbf{I} is the unit dyadic and we recall

$$\begin{aligned} P_{\parallel} &= \int d^3v \bar{f} mu^2, \\ P_{\perp} &= \int d^3v \bar{f} \mu B . \end{aligned} \quad (14)$$

as in (4.171).

Equation (13) has precisely the CGL form of (3.93):

$$\mathbf{P}[\bar{f}] = \mathbf{P}_{\text{CGL}} . \quad (15)$$

Thus the simplest conclusion of drift-kinetic theory—the statement that \tilde{f} is small when δ is small—implies that the stress in a magnetized plasma is approximated by the CGL stress:

$$\mathbf{P} = \mathbf{P}_{\text{CGL}}[1 + \mathcal{O}(\delta)] . \quad (16)$$

This argument is essentially that used in the original CGL work. In §6.3 we will find that (16) can also be derived from purely fluid considerations.

Equations (4.56) and (16) apply to any magnetized plasma; in the special case of a **confined plasma**, stronger conclusions pertain. Indeed, we have shown that the lowest order distributions in a slowly evolving, toroidally confined plasma must be **Maxwellian** [recall (5.106)]. It follows

that $P_{||} - P_{\perp} = \mathcal{O}(\delta)$: the lowest order stress and pressure of a confined plasma are isotropic. More explicitly we have

$$\mathbf{P} = \mathbf{I}p + [\mathbf{P}_{\text{CGL}} - \mathbf{I}p]_1 + [mn\mathbf{V}\mathbf{V} + \Pi]_2 . \quad (17)$$

Here Π represents any non-diagonal terms in \mathbf{P} , other than the explicitly given inertial term. We will study Π presently; it is sometimes called the “viscosity tensor,” although it need not have the form of an ordinary fluid viscosity. The main point of (17) is that the first bracketed term is $\mathcal{O}(\delta)$, and the second $\mathcal{O}(\delta^2)$.

In the same approximation (11) becomes

$$\mathbf{Q} = \mathbf{q} + \frac{5}{2} p\mathbf{V} + \mathcal{O}(\delta^2) , \quad (18)$$

a formula familiar from thermodynamics. The $(5/2)$ -factor includes the two ways a moving fluid transports energy: simple advection of the energy density $\frac{3}{2} p$, as well as mechanical work.

Similar comments pertain to the tensor \mathbf{R} , which has the lowest-order form

$$\mathbf{R}[\bar{f}] = \mathbf{b}\mathbf{b}R_{||} + (\mathbf{I} - \mathbf{b}\mathbf{b})R_{\perp} + \mathcal{O}(\delta) , \quad (19)$$

for any magnetized plasma, but which becomes

$$\mathbf{R}[f_M] = \mathbf{I}R + \mathcal{O}(\delta) \quad (20)$$

in the toroidal confinement case. Here R is given by

$$R = \frac{2}{3} \int d^3v f_{sM} \frac{1}{2} m v^4 = \frac{5}{2} \frac{p}{m} T . \quad (21)$$

6.2 Moments of Kinetic Equation

Conservation Laws

Here we consider velocity moments of the general kinetic equation, (4.6). Note that these relations, obtained by multiplying (4.6) by appropriate powers of \mathbf{v} and integrating, are exact. In particular they do not depend upon detailed or Coulomb-specific properties of the collision operator.

There are four moments of elementary interest: two *even* moment equations, describing the evolution of density,

$$\frac{\partial n}{\partial t} + \nabla \cdot (n\mathbf{V}) = 0 , \quad (22)$$

and pressure,

$$\frac{3}{2} \frac{\partial}{\partial t} \left[p + \frac{1}{2} mnV^2 \right] + \nabla \cdot \mathbf{Q} = W + \mathbf{V} \cdot (\mathbf{F} + e\mathbf{E}) ; \quad (23)$$

and two odd moment equations, describing the momentum,

$$\frac{\partial}{\partial t} mn\mathbf{V} + \nabla \cdot \mathbf{P} - en \left(\mathbf{E} + \frac{1}{c} \mathbf{V} \times \mathbf{B} \right) = \mathbf{F}, \quad (24)$$

and the energy flux,

$$\frac{\partial \mathbf{Q}}{\partial t} + \nabla \cdot \mathbf{R} - \frac{3}{2} \frac{e}{m} p \mathbf{E} - \frac{1}{2} en V^2 \mathbf{E} - \frac{e}{m} \mathbf{E} \cdot \mathbf{P} - \frac{e}{mc} \mathbf{Q} \times \mathbf{B} = \mathbf{G}. \quad (25)$$

Three moments of the collision operator, W , \mathbf{F} and \mathbf{G} , occur in (22)-(25). Thus (23) and (24) involve the energy exchange,

$$W = \int d^3v \frac{1}{2} m(\mathbf{v} - \mathbf{V})^2 C,$$

and friction force,

$$\mathbf{F} = \int d^3v m \mathbf{v} C,$$

introduced in §5.1, while (25) involves

$$\mathbf{G} \equiv \int d^3v \frac{1}{2} m v^2 \mathbf{v} C, \quad (26)$$

an energy-weighted friction, with no established name.

An alternative version of (24) is expressed in terms of the pressure tensor rather than the stress tensor. We use (10) and (22) to find that

$$mn \left(\frac{\partial \mathbf{V}}{\partial t} + \mathbf{V} \cdot \nabla \mathbf{V} \right) + \nabla \cdot \mathbf{P} - en \left(\mathbf{E} + \frac{1}{c} \mathbf{V} \times \mathbf{B} \right) = \mathbf{F}. \quad (27)$$

We assume that the reader is familiar with the derivation of (22)-(25). Their physical interpretation depends upon a single fact: if k is some fluid density whose flux is \mathbf{K} , then $S_k \equiv \partial k / \partial t + \nabla \cdot \mathbf{K}$ gives the rate at which k is created or externally introduced. S_k measures, in other words, the “nonconservation” of k . For example, (23) states that fluid energy $(3/2)[p + (1/2)mnV^2]$, whose flux is \mathbf{Q} , is not conserved because of collisional exchange, $W + \mathbf{F} \cdot \mathbf{V}$, and because of electromagnetic work, $en\mathbf{E} \cdot \mathbf{V}$.

The even moment equations (22) and (23) are more specifically contracted even moments: we have multiplied by v^2 rather than $\mathbf{v} \cdot \mathbf{v}$. An uncontracted equation for the evolution of \mathbf{P} is of some interest, as we shall find in §6.3. But the contracted even moment equations have special importance: by describing the decay or sustenance of plasma density and energy, they directly address the key confinement issues. Thus, if one had a predictive understanding of each flux and source term in the (22) and (23) all confinement questions would be answered.

Significantly, the form of (22) and (23) is independent of magnetic field; the even moments would look precisely the same if describing a neutral gas. This fact, an easy consequence of (4.6), displays the singular mechanism of magnetic confinement: the reduction of particle and energy *fluxes* by magnetic fields. It also shows that any fluid discussion of magnetization must emphasize the odd moments.

General Moment Equation

Before considering the odd moment equations in more detail, it is instructive to study the general moment of the kinetic equation. The N th moment of the distribution function is denoted by

$$M_{\alpha\beta\dots\tau}^{(N)} \equiv \int d^3v f v_\alpha v_\beta \dots v_\tau |_N \quad (28)$$

where the notation $|_N$ indicates that N factors of \mathbf{v} occur. (We insist here upon Cartesian velocity coordinates, and do not distinguish between upper and lower indices.) Thus, for example

$$M^{(0)} = n, \quad M_\alpha^{(1)} = n V_\alpha, \quad M_{\alpha\beta}^{(2)} = \frac{1}{m} P_{\alpha\beta},$$

and so on. $M^{(N)}$ is a tensor whose rank is at most N ; the rank is less than N in the case of contraction, such as the energy flux of (3):

$$Q_\alpha = \frac{1}{2} m M_{\alpha\beta\beta}^{(3)}.$$

Whenever the rank is not essential to the argument, we will suppress indices, writing

$$M_{\alpha\beta\dots\tau}^{(N)} \rightarrow M^{(N)}$$

for simplicity. We also adopt the convention

$$M^{(K)} = 0, \quad \text{for } K < 0.$$

The N th moment of the kinetic equation contains two terms involving more than the definition (28). First, we need the N th moment of the collision operator, denoted by

$$C_{\alpha\beta\dots\tau}^{(N)} \equiv \int d^3v C v_\alpha v_\beta \dots v_\tau |_N = [\delta_{\alpha\kappa} M_{\beta\dots\tau}^{(N-1)}]_\alpha \quad (29)$$

Second, we need to evaluate, by partial integration of the acceleration term,

$$\int d^3v f \frac{\partial}{\partial v_\kappa} v_\alpha v_\beta \dots v_\tau |_N = [\delta_{\alpha\kappa} M_{\beta\dots\tau}^{(N-1)}]_\alpha. \quad (30)$$

Here the double brackets denote the symmetrized tensor—a sum over permutations of the index α , using all subscripts of M :

$$\left[\delta_{\alpha\kappa} M_{\beta\gamma\dots\sigma\tau}^{(N-1)} \right]_{\alpha} \equiv \delta_{\alpha\kappa} M_{\beta\gamma\dots\sigma\tau}^{(N-1)} + \delta_{\beta\kappa} M_{\alpha\gamma\dots\sigma\tau}^{(N-1)} + \dots + \delta_{\tau\kappa} M_{\beta\gamma\dots\sigma\alpha}^{(N-1)}. \quad (31)$$

For the case $N = 2$, the operation $[M^{(2)}]$ simply adds to $M^{(2)}$ its transpose.

Next we express the exact kinetic equation as

$$\frac{\partial f}{\partial t} + v_{\mu} \frac{\partial f}{\partial x_{\mu}} + \frac{e}{m} E_{\mu} \frac{\partial f}{\partial v_{\mu}} + \Omega \epsilon_{\mu\kappa\lambda} v_{\kappa} b_{\lambda} \frac{\partial f}{\partial v_{\mu}} = C.$$

After multiplying by N factors of \mathbf{v} , we use (27), (29) and (30) to derive an equation for the evolution of the N th moment:

$$\begin{aligned} \frac{\partial}{\partial t} M_{\beta\gamma\dots\sigma}^{(N)} &+ \frac{\partial}{\partial x^{\alpha}} M_{\alpha\beta\dots\sigma}^{(N+1)} - \frac{e}{m} \left[E_{\beta} M_{\gamma\dots\sigma}^{(N-1)} \right]_{\beta} \\ &- \Omega b_{\lambda} \left[\epsilon_{\beta\kappa\lambda} M_{\kappa\gamma\dots\sigma}^{(N)} \right]_{\beta} = C_{\beta\gamma\dots\sigma}^{(N)}, \end{aligned} \quad (32)$$

or, in an abbreviated but transparent notation,

$$\frac{\partial \mathbf{M}^{(N)}}{\partial t} + \nabla \cdot \mathbf{M}^{(N+1)} - \frac{e}{m} \left[\mathbf{E} \mathbf{M}^{(N-1)} \right] + \Omega \left[\mathbf{b} \times \mathbf{M}^{(N)} \right] = \mathbf{C}^{(N)}. \quad (33)$$

The infinite set of equations (33), for all $N > 0$, contains precisely the same information as the original kinetic equation. However, as the reader may recall, certain physical effects—the most famous being Landau damping—are not contained in any finite subset. By suitable choice of N , and appropriate tensor contraction, we can reproduce from (33) each of the moment equations (22)–(25). [Equations (22) and (23) are independent of \mathbf{B} because total contraction annihilates the term involving Ω .]

Most importantly, (33) highlights the key property of exact moment equations: they couple each moment to its hierarchical neighbors, ruling out any rigorous, finite closure. We next consider the fluid closure problem in more detail; we will find in §6.3 that (33) provides the key to a partial, yet extremely useful, closure scheme.

Fluid Closure

The evolution of each exact fluid moment depends on the next higher moment. This discouraging observation, a fundamental obstacle in determining the evolution of any fluid, has engendered essentially three strategies:

1. *Kinetic theory*: one abandons fluid theory and returns to (4,6).

2. *Truncation*: one neglects, at some level, the next higher moment.
3. *Asymptotic closure*: one identifies a small parameter ϵ and solves the kinetic equation perturbatively, obtaining a distribution that is rigorously accurate to some order in ϵ ; then, crucially, one derives a fluid description of *higher order accuracy* by using that distribution to evaluate certain moments.

The first approach deals with a single scalar relation, the kinetic equation, requiring nothing more complicated than boundary and initial conditions to determine its unique solution. Furthermore, as we observed in Chapter 4, solution of the kinetic equation directly provides the constitutive relations needed to close Maxwell's equations.

The advantages of the kinetic approach, especially using the drift-kinetic or gyrokinetic approximation, are obvious. Kinetic analysis forms the basis for much important plasma confinement physics. It is even, in a sense, inescapable: every fluid theory is based, at least implicitly, on kinetic information. But kinetic plasma physics has the disadvantages mentioned in Chapter 4: it is technically difficult, being set in six-dimensional (or five-dimensional) phase space; and it is inefficient, since Maxwellian closure depends, not on the details of the distribution, but only on its two lowest moments. More generally one suspects that a simplified description, however approximate or non-rigorous, provides the quickest route to physical insight.

The second approach, truncation, can be crude, as in numerous calculations that assume any moment without a name (i.e., $N > 2$) is negligible, or careful and elegant, as in thirteen-moment theory (Herdan and Lilley, 1960). Truncation is evidently exact at zero temperature, when the plasma is described by n and \mathbf{V} alone (beam model).

At finite temperature, truncation involves uncontrolled approximation and lacks clear-cut limits of validity. It is nonetheless extremely useful. We will find in §6.4 that various versions of MHD are best viewed as truncation theories; yet few branches of plasma physics have provided as much physical understanding as MHD. We will consider examples of this procedure presently.

The third approach, asymptotic closure, is rigorous, in the sense of perturbation theory. It rests on a judicious combination of the kinetic equation and its moments. The model for asymptotic closure is Chapman-Enskog theory of neutral gas transport. In that case the small parameter is the ratio of mean free path λ to scale length L ; the fluid equations appear as solvability conditions for the perturbative kinetic theory. The application of this procedure to plasma fluid equations has been implemented by Chapman and Cowling, by Spitzer, and by Braginskii. In particular, Braginskii (Braginskii, 1965) provides a closed set of fluid equations for magnetized plasma evolution, the "Braginskii equations," that have frequent and effective application.

Unfortunately the mean free path is usually not small in magnetic confinement contexts. In the next section we explore, *inter alia*, the possibility of basing an asymptotic closure scheme on the parameter $\delta = \rho/L$.

6.3 Small Gyroradius Ordering

Perpendicular Velocity

Equation (24) provides a useful expression for the perpendicular plasma flow. Taking the cross product with \mathbf{b} we find that

$$n\mathbf{V}_\perp = \frac{1}{m\Omega} \mathbf{b} \times \left[\frac{\partial}{\partial t} m n \mathbf{V} + \nabla \cdot \mathbf{P} - e n \mathbf{E} - \mathbf{F} \right]. \quad (34)$$

The customary inference from (34) is that \mathbf{V}_\perp is given, in some approximation, by the sum of the $\mathbf{E} \times \mathbf{B}$ and diamagnetic drifts:

$$n\mathbf{V}_\perp \cong n\mathbf{V}_E + \frac{1}{m\Omega} \mathbf{b} \times \nabla p \quad (35)$$

with, as usual,

$$\mathbf{V}_E = c\mathbf{E} \times \mathbf{B}/B^2. \quad (36)$$

Despite its familiarity, this argument raises a number of questions. First, (34) is at best a differential equation for \mathbf{V} ; how was its solution reduced to algebra? Second, how do we justify neglecting the friction force and stress anisotropy? After all, (34) only restates (24), a relation whose “unclosed” aspect we have emphasized. Finally, in what sense is (35) better than (34)? It is clearly less accurate; have we made progress?

Such questions have intelligible answers only in the context of small gyroradius theory—only when the plasma is magnetized. Thus, recalling the discussion of Chapter 4, we assume

$$\delta \ll 1,$$

and then recognize the key feature of (34): the $1/\Omega$ -factor outside the square brackets. This plays the role of δ , since $\delta \equiv (1/\Omega)(v_t/L)$, giving (34) the form

$$n\mathbf{V}_\perp = \delta[\dots]. \quad (37)$$

It follows that, in order to compute \mathbf{V}_\perp to order δ^n , one needs to evaluate quantities inside the brackets only to order δ^{n-1} . For this reason alone, (34) does more than relate one unknown moment to other unknown moments. When δ is small, it provides a genuine advance.

Suppose for example one wants to compute, in a confined plasma, the first-order perpendicular flow. Then the bracketed terms in (34) are needed

only in the zero-gyroradius limit. We adopt the drift ordering of (4.15) and (4.24) to see that the acceleration term has no $\delta = 0$ contribution; similarly, in view of (4.14), there is no zeroth-order friction force. Since the zeroth-order stress tensor is provided by (17), we obtain a more detailed form of (35):

$$n\mathbf{V}_\perp = n\mathbf{V}_{\perp 1} + \mathcal{O}(\delta^2),$$

with

$$n\mathbf{V}_{\perp 1} \equiv \frac{1}{m\Omega}\mathbf{b} \times (\nabla p + en\nabla\Phi). \quad (38)$$

Here we have recalled that the \mathbf{E} is primarily electrostatic in the drift ordering:

$$\mathbf{E} = -\nabla\Phi[1 + \mathcal{O}(\delta)]. \quad (39)$$

This systematic derivation of (38) shows the conditions for its validity, provides estimates of its error, and allows higher order corrections to be calculated as needed. In these respects, the derivation could form part of an asymptotic closure scheme, as discussed in the previous section; we will consider this possibility presently.

The key feature of the derivation is that it produces first-order information about plasma flow, using only zeroth-order information about the distribution function. Thus it makes efficient use of kinetic theory. In contrast, the analysis of Chapter 4, while leading to the same result [recall (4.185)], required the first-order distribution function and much more elaborate analysis.

The general lesson is that appropriate manipulation of moment equations can significantly reduce the burden on kinetic theory. When attacking some new issue of confined plasma behavior, it is prudent to study moment equations first.

It is easy to generalize (38). The case of MHD-ordered flow is considered in §6.4; the higher-order corrections, in the drift-ordered case, are studied in §6.5. Here we relax the toroidal confinement assumption, treating an arbitrary magnetized plasma. Then the distribution function need not be Maxwellian; the only pertinent kinetic information is (4.56): $f = \bar{f} + \mathcal{O}(\delta)$.

It is clear that in this case the stress tensor has CGL form, and that the acceleration term continues to make no first order contribution (since $\partial/\partial t \sim V/v_t \sim \delta$). Some comment is appropriate, however, concerning the friction force. From the definition, (5.21), and the rotational symmetry of C , we see that

$$\mathbf{F}_\perp[\bar{f}] = \int d^3v m s C(\bar{f}) = 0;$$

the lowest order friction is parallel to the confining field. More specifically,

$$\mathbf{F}_\parallel \sim \nu nm v_t, \quad F_1 \sim \delta v nm v_t \quad (\text{general case}) \quad (40)$$

F_\parallel can be large enough to affect the first order flow, but it has the wrong direction: $(1/\Omega)\mathbf{b} \times \mathbf{F} = \mathcal{O}(\delta^2)$.

Although incidental to present purposes it is convenient to contrast (40) with the friction-ordering pertinent to a confined plasma. When $\bar{f} = f_M + \mathcal{O}(\delta)$, the lowest order contribution to F_{\parallel} vanishes by virtue of (5.3). Then we have

$$F_{\parallel} \sim F_{\perp} \sim \delta n m v_t \quad (\text{Maxwellian case}) . \quad (41)$$

Since $\nu/\Omega \sim \delta$, the friction makes a second-order contribution to \mathbf{V}_{\perp} . Of course similar comments pertain to the moment \mathbf{G} .

Returning to the general case we have found

$$n\mathbf{V}_{\perp} = n\mathbf{V}_E + \frac{1}{m\Omega} \mathbf{b} \times \nabla \cdot \mathbf{P}_{CGL} + \mathcal{O}(\delta^2) ,$$

or, from (3.95),

$$n\mathbf{V}_{\perp} = n\mathbf{V}_E + \frac{1}{m\Omega} \mathbf{b} \times [\nabla P_{\perp} + (P_{\parallel} - P_{\perp})\boldsymbol{\kappa}] + \mathcal{O}(\delta^2) . \quad (42)$$

A final comment on plasma flow is pertinent, however obvious: our manipulation of (24) has provided a useful recipe for the perpendicular flow, but no help at all concerning \mathbf{V}_{\parallel} . The flow is given (in the confined plasma case) by

$$n\mathbf{V} = n\mathbf{V}_{\parallel} + n\mathbf{V}_{\perp 1} + \mathcal{O}(\delta^2) , \quad (43)$$

where the first term is unspecified. Indeed, as the general solution to the homogeneous equation

$$\mathbf{b} \times n\mathbf{V} = 0 , \quad (44)$$

\mathbf{V}_{\parallel} is a sort of “manipulation constant,” analogous to the integration constant that appears when a differential equation is solved. We find next that when (34) is generalized to treat higher-order moments, there appears for each N an unknown tensor corresponding to $\mathbf{V}_{\parallel N}$.

General Perpendicular Flow

Here we apply the procedure leading to (43) to the general moment equation, (33). For clarity it is helpful first to express (33) in dimensionless form. Hence we introduce the dimensionless N th moment,

$$M^{(N)} \equiv \frac{M^{(N)}}{v_t^n}$$

and collision operator,

$$C^{(N)} \equiv \frac{C^{(N)}}{\nu v_t^n} .$$

We similarly normalize the coordinates (\mathbf{x}, t) :

$$\mathbf{x}' \equiv \mathbf{x}/L, \quad t' \equiv \omega t ,$$

in terms of a representative scale-length L and frequency ω . After substituting these definitions into (33), we divide each term by W and then suppress the primes. The result is

$$\frac{\omega}{\Omega} \frac{\partial \mathbf{M}^{(N)}}{\partial t} + \frac{\rho}{L} \nabla \cdot \mathbf{M}^{(N+1)} - \left[\frac{cE}{Bv_t} \mathbf{M}^{(N-1)} \right] + [\mathbf{b} \times \mathbf{M}^{(N)}] = \frac{\nu}{\Omega} \mathbf{C}^{(N)}. \quad (45)$$

Here it is instructive to review the discussion in §4.3, which treats each term of (45) in its original, kinetic context. We recall: that the plasma is considered magnetized when $\delta = \rho/L$ is small compared to unity; that, in the most important cases, the ratios ω/Ω and ν/Ω are no larger than δ ; that the remaining coefficient, cE/Bv_t , is also small in the drift ordering, but comparable to unity in the MHD ordering; and finally that the gyrokinetic case, in which M includes a rapidly varying perturbation, can be considered magnetized only if the perturbation is small.

But (45) also shows us something new: that the “upward” coupling of $\mathbf{M}^{(N)}$ to $\mathbf{M}^{(N+1)}$ is $\mathcal{O}(\delta)$. This observation suggests an iterative closure scheme that we consider next. For simplicity, our discussion assumes the drift-ordering, with $cE/Bv_t \sim \delta$, and no rapid variation.

We rearrange (45),

$$\begin{aligned} [\mathbf{b} \times \mathbf{M}^{(N)}] &= -\delta \left\{ \frac{\omega}{\delta\Omega} \frac{\partial \mathbf{M}^{(N)}}{\partial t} + \nabla \cdot \mathbf{M}^{(N+1)} \right. \\ &\quad \left. - \left[\frac{cE}{\delta Bv_t} \mathbf{M}^{(N-1)} \right] - \frac{\nu}{\delta\Omega} \mathbf{C}^{(N)} \right\}, \end{aligned} \quad (46)$$

giving it the form of (37); note that all the coefficients inside the curly brackets, $(\omega/\delta\Omega)$, $(cE/\delta Bv_t)$ and $(\nu/\delta\Omega)$, are at most of order unity. Thus $[\mathbf{b} \times \mathbf{M}^{(N)}]$ is computed to any order from lower-order knowledge of the moments on the right-hand side. If the collisional term $\mathbf{C}^{(N)}$ is temporarily disregarded, iteration would seem to provide any moment, to any desired degree of accuracy, from only the lowest order distribution function, f_0 !

Unfortunately this recipe does not magically eliminate the need for kinetic theory: even in the absence of collisions, there is no free closure. The difficulty concerns what we have called “manipulation constants,” the solutions $\mathbf{H}^{(N)}$ to the equation

$$[\mathbf{b} \times \mathbf{H}^{(N)}] = 0. \quad (47)$$

Because (47), like (44), has non-trivial solutions, we see that knowing $[\mathbf{b} \times \mathbf{M}^{(N)}]$ is distinctly different from knowing $\mathbf{M}^{(N)}$. The issue is acute because the $\mathbf{H}^{(N)}$ can in general be larger than other terms in $\mathbf{M}^{(N)}$. Indeed, (46) implies

$$\mathbf{M}^{(N)} = \mathbf{H}^{(N)} + \mathcal{O}(\delta). \quad (48)$$

That is, since the driving term on the right-hand side of (46) is $\mathcal{O}(\delta)$, the homogeneous solution can dominate.

It is not hard to appreciate the nature of the $\mathbf{H}^{(N)}$. We have noted that $\mathbf{H}^{(1)} = \mathbf{b}V_{\parallel}$. For $N = 2$ we have

$$[\mathbf{b} \times \mathbf{H}^{(2)}] = b_\lambda [\epsilon_{\alpha\kappa\lambda} H_{\kappa\sigma}^{(2)} + \epsilon_{\sigma\kappa\lambda} H_{\kappa\sigma}^{(2)}] = 0.$$

We choose the (locally Cartesian) coordinate basis $(\mathbf{b}, \mathbf{e}_2, \mathbf{e}_3)$ to find $b_\lambda = \delta_{\lambda 1}$ and therefore $\epsilon_{\alpha\kappa 1} H_{\kappa\sigma}^{(2)} + \epsilon_{\sigma\kappa 1} H_{\kappa\sigma}^{(2)} = 0$, which implies

$$H_{12}^{(2)} = H_{13}^{(2)} = H_{23}^{(2)} = 0,$$

and

$$H_{22}^{(2)} = H_{33}^{(2)}.$$

In other words,

$$\mathbf{H}^{(2)} = \mathbf{P}_{\text{CGL}}. \quad (49)$$

Thus (48) and (49) constitute a fluid demonstration of the CGL result, (16), obtained previously from kinetic theory.

It is not hard to see that any $\mathbf{H}^{(N)}$ of rank two (i.e., with two uncontracted indices) will have the CGL form, just as any $\mathbf{H}^{(N)}$ of rank one must be a vector oriented along \mathbf{B} . The general rule is that the $\mathbf{H}^{(N)}$ are moments of \bar{f} alone. Thus, in particular, they can be computed using only guiding-center kinetic theory.

The other set of moments that are not determined by the iteration scheme are the collisional moments $\mathbf{C}^{(N)}$. These quantities describe collisional dissipation. As key elements in plasma transport theory, they are studied in Chapter 8; but one elementary comment is appropriate here.

The $\mathbf{C}^{(N)}$ are computed from their definition, (29); the components that enter (46) involve \bar{f} , for which we can use (4.63). Significantly, (4.63) gives an expression for \bar{f} that is independent of the collision frequency, simply because it is not accurate enough to include the collisional contribution. Indeed, the calculation of \bar{f} through $\mathcal{O}(\nu/\Omega)$ is a formidable undertaking, evidently involving inversion of the collision operator. We see that (46) short-circuits that calculation: it provides the effect of collisions on any moment, through first order in ν , without needing the collisional contribution to f . Thus (46) offers enormous savings in the analysis of dissipation.

In the absence of dissipation, (46) has equally helpful application. First, it provides accurate formulae for most of the components of $\mathbf{M}^{(N)}$, and for the form of the tensor $\mathbf{H}^{(N)}$. In some cases this information is all that is needed. More generally, (46) allows us to compute fluid moments without knowledge of the gyrophase variation of f . It may be recalled, from §4.7, that direct calculation of the perpendicular velocity ($N = 1$) requires both \bar{f} and \tilde{f} . For larger N , the \tilde{f} -dependent magnetization terms appearing in (4.162) have much more complicated counterparts. Equation (46) allows us

to ignore such complications—just as (43) provides the perpendicular flow without mention of magnetization.

Thus (46) plays a role complementary to that of guiding center kinetic theory. The closure of magnetized fluid equations, based on small δ , depends on both kinetic and fluid results.

Magnetization Flows

In applying (46) to the calculation of specific moments, it is convenient to restore dimensional variables. Thus we write

$$[\mathbf{b} \times M^{(N)}] = -\frac{1}{\Omega} \left\{ \frac{\partial \mathbf{M}^{(N)}}{\partial t} + \nabla \cdot \mathbf{M}^{(N+1)} - \left[\frac{e\mathbf{E}}{m} M^{(N-1)} \right] - C^{(N)} \right\},$$

or, more explicitly,

$$\begin{aligned} b_\lambda [\varepsilon_{\beta\kappa\lambda} M_{\kappa\gamma\dots\sigma}^{(N)}]_\beta &= \frac{1}{\Omega} \left\{ \frac{\partial}{\partial t} M_{\beta\gamma\dots\sigma}^{(N)} \right. \\ &\quad \left. + \frac{\partial}{\partial x^\alpha} M_{\alpha\beta\dots\sigma}^{(N+1)} - \frac{e}{m} [E_\beta M_{\gamma\dots\sigma}^{(N-1)}]_\beta - C_{\beta\gamma\dots\sigma}^{(N)} \right\}, \end{aligned} \quad (50)$$

and consider two applications.

First we choose $N = 3$ and contract to obtain the energy flux of (3):

$$M_{\beta\gamma\gamma}^{(3)} = \frac{2}{m} Q_\beta.$$

Since

$$[E_\alpha M_{\gamma\sigma}^{(2)}]_\alpha = E_\alpha M_{\gamma\sigma}^{(2)} + E_\gamma M_{\sigma\alpha}^{(2)} + E_\sigma M_{\alpha\gamma}^{(2)},$$

becomes, after contraction,

$$\frac{1}{m} [E_\alpha P_{\gamma\gamma} + 2E_\gamma P_{\alpha\gamma}] = \frac{1}{m} [\mathbf{E} Tr(\mathbf{P}) + 2\mathbf{E} \cdot \mathbf{P}]_\alpha,$$

and since, according to (7),

$$M_{\alpha\beta\gamma\gamma}^{(4)} = \frac{2}{m} R_{\alpha\beta},$$

we have

$$\mathbf{b} \times \mathbf{Q} = -\frac{1}{\Omega} \left\{ \frac{\partial \mathbf{Q}}{\partial t} + \nabla \cdot \mathbf{R} - \frac{e}{2m} [\mathbf{E} Tr(\mathbf{P}) + 2\mathbf{E} \cdot \mathbf{P}] - Tr(\mathbf{C}^{(3)}) \right\}.$$

Finally, since $H_{\beta\gamma\gamma}^{(3)} = (2/m)b_\gamma Q_\parallel$,

$$\mathbf{Q} = \mathbf{b} Q_\parallel + \frac{\mathbf{b}}{\Omega} \times \left\{ \frac{\partial \mathbf{Q}}{\partial t} + \nabla \cdot \mathbf{R} - \frac{e}{2m} [\mathbf{E} Tr(\mathbf{P}) + 2\mathbf{E} \cdot \mathbf{P}] - Tr(\mathbf{C}^{(3)}) \right\}. \quad (51)$$

In Chapter 8 we use (51) to study collisional energy transport, which is contained in the term $C^{(3)}$. Here we are content with more elementary observations.

In the confined plasma case, (17) and (21) pertain and (51) becomes

$$\mathbf{Q}_\perp = \frac{5}{2} \frac{\mathbf{b}}{\Omega} \times \left[\nabla \frac{pT}{m} - \frac{e}{m} \mathbf{E}p \right] + \mathcal{O}(\delta^2),$$

$$= \frac{5}{2} \frac{p}{m\Omega} \mathbf{b} \times \nabla T + \frac{5}{2} T \left[n\mathbf{V}_E + \frac{1}{m\Omega} \mathbf{b} \times \nabla p \right] + \mathcal{O}(\delta^2) \quad (52)$$

After recalling (18) and (38) we see that

$$\mathbf{q}_\perp = \mathbf{q}_{11} + \mathcal{O}(\delta^2)$$

with

$$\mathbf{q}_{11} \equiv \frac{5}{2} \frac{p}{m\Omega} \mathbf{b} \times \nabla T. \quad (53)$$

This heat flow is obviously analogous to the first-order particle flow of (38). Like the latter, it reflects variation of the density and energy of magnetic moments, as discussed in §4.7. We refer to both $n\mathbf{V}_\perp$ and \mathbf{q}_{11} as *magnetization flows*, since both stem from plasma magnetization.

The magnetization flows are studied in Chapter 8, but it is appropriate to mention some elementary consequences of (38) and (53) here. The key fact is that magnetization flows are transverse to the gradients that drive them. More specifically, they are flows *within* a flux surface, rather than across surfaces:

$$\mathbf{q}_{11} \cdot \nabla \chi = 0 = \mathbf{V}_1 \cdot \nabla \chi. \quad (54)$$

Thus, at least in the drift ordering, particle and energy do not penetrate flux surfaces in first order. Equation (54) is in this sense the fluid expression of how confinement works.

The magnetization flows follow helical streamlines, normal to both $\nabla \chi$ and \mathbf{B}_\parallel , winding around the flux surfaces. The flows are not necessarily solenoidal, and generally require *return flows*, along the magnetic field, to avoid local accumulations; recall the return current discussed in §3.9. Thus equilibrium flux surfaces support rather complicated motions of particles and heat, parallel and transverse to the magnetic field, even when the plasma is entirely quiescent. The root of this elaborate flow pattern is Larmor gyration.

It should be pointed out that the pressure, temperature and electrostatic potential appearing in (38) and (53) should strictly have “0” subscripts. Allowing for first order perturbations p_1 , T_1 , and Φ_1 , that need not be flux functions, we see that *second-order* magnetization flow across flux surfaces is possible; for example,

$$\mathbf{q}_{12} = \frac{5}{2} \frac{p}{m\Omega} \mathbf{b} \times \nabla T_1 + \dots, \quad (55)$$

will in general have a radial component. In Chapter 8 we will find that second-order magnetization flows indeed contribute to plasma loss; however, they provide the dominant loss mechanism only in collisional regimes. The ellipsis in (55) emphasizes that there are in general other, larger contributions to q_{12} .

We conclude this discussion by emphasizing again the scant contribution of kinetic theory to results like (38) and (53). By taking advantage of small- δ , we needed only the very simplest result from Chapter 4: that each distribution is Maxwellian in lowest order.

Stress Tensor*

Our next application of (46) or (50) concerns the stress tensor. Setting $N = 2$ we have

$$\mathbf{b} \times \mathbf{P} + (\mathbf{b} \times \mathbf{P})^t = -\frac{1}{\Omega} \left\{ \frac{\partial \mathbf{P}}{\partial t} + m \nabla \cdot \mathbf{M}^{(3)} - en(\mathbf{E} \mathbf{V} + \mathbf{V} \mathbf{E}) - m \mathbf{C}^{(2)} \right\}. \quad (56)$$

Here the t -superscript indicates the matrix transpose. It is convenient to represent the right-hand side by the tensor

$$\mathbf{S} \equiv \frac{\partial \mathbf{P}}{\partial t} + m \nabla \cdot \mathbf{M}^{(3)} - en(\mathbf{E} \mathbf{V} + \mathbf{V} \mathbf{E}) - m \mathbf{C}^{(2)}, \quad (57)$$

so that (56) is simply

$$\mathbf{b} \times \mathbf{P} + (\mathbf{b} \times \mathbf{P})^t = -\frac{1}{\Omega} \mathbf{S}. \quad (58)$$

After recalling (17) we see that (58) determines the viscosity tensor, Π , and that it is $\mathcal{O}(\delta^2)$. Furthermore, because of the $1/\Omega$ -factor in (58), we can compute the viscosity tensor from the lowest order $\mathbf{S} = \mathcal{O}(\delta)$. Three other facts deserve attention.

1. \mathbf{S} is symmetric:

$$S_{\alpha\beta} = S_{\beta\alpha}, \quad (59)$$

a circumstance that simplifies the calculation of Π .

2. \mathbf{S} has no parallel component, in the sense that

$$\mathbf{b} \cdot \mathbf{S} \cdot \mathbf{b} = 0, \quad (60)$$

as the left-hand side of (58) clearly requires. Equation (60) yields a “parallel energy” conservation law—an exact evolution equation for P_{\parallel} —that has some interest but is rarely used.

3. \mathbf{S} has no trace:

$$S_{\alpha\alpha} = 0. \quad (61)$$

This fact, a consequence of (58) and the symmetry of \mathbf{P} , reproduces the energy conservation law (23).

We now turn to the solution of (58) for Π . The algebraic operator that inverts the left-hand side of (58) is slightly more complicated than the $N = 1$ version. The reader can verify that (58) is solved by

$$\mathbf{P} = \mathbf{P}^0 + \mathbf{H}^{(2)},$$

where $\mathbf{H}^{(2)}$ is any tensor having CGL form and

$$\mathbf{P}^0 \equiv \frac{1}{4\Omega} [\mathbf{b} \times \mathbf{S} + 3\mathbf{b}\mathbf{b} \times (\mathbf{b} \cdot \mathbf{S})],$$

In component form,

$$P_{\alpha\beta}^0 = \frac{1}{4\Omega} \{ \epsilon_{\beta\kappa\lambda} b_\kappa (S_{\alpha\lambda} + 3b_\alpha b_\gamma S_{\lambda\gamma}) + \epsilon_{\alpha\kappa\lambda} b_\kappa (S_{\beta\lambda} + 3b_\beta b_\gamma S_{\lambda\gamma}) \}. \quad (62)$$

Equation (62) simplifies in the usual coordinate system with axes $(\mathbf{b}, \mathbf{e}_2, \mathbf{e}_3)$. Then $b_\lambda = \delta_{1\lambda}$ and we find

$$P_{11}^0 = 0,$$

$$P_{12}^0 = -\frac{1}{\Omega} S_{13}, P_{13}^0 = -\frac{1}{\Omega} S_{12},$$

$$P_{23}^0 = \frac{1}{4\Omega} (S_{22} - S_{33}),$$

$$P_{22}^0 = -P_{33}^0 = -\frac{1}{2\Omega} S_{23}. \quad (63)$$

We used

$$S_{11} = 0 = S_{22} + S_{33}, \quad (64)$$

which follow from (60) and (61), to simplify some terms in (63). The remaining components of \mathbf{P}^0 are determined by symmetry.

We next interpret the various terms in $P_{\alpha\beta}^0$, choosing $\alpha = 2 = \beta$ for concreteness. From (62) and (57),

$$P_{22}^0 = -\frac{1}{2\Omega} \left\{ \frac{\partial P_{23}}{\partial t} + m \nabla \cdot \mathbf{M}_{23}^{(3)} - 2en(E_2 V_3 + E_3 V_2) - mC_{23}^{(2)} \right\}. \quad (65)$$

The last term on the right-hand side yields classical collisional viscosity, denoted by

$$\Pi_{c22} = \frac{m}{2\Omega} C_{23}^{(2)}. \quad (66)$$

In the confined plasma case, where the distribution has the form [recall (4.183)],

$$f = f_M + \bar{f}_1 - \rho \cdot \nabla f_M + \mathcal{O}(\delta^2) \quad (67)$$

it can be seen that $C^{(2)} = \mathcal{O}(\delta^2)$ and therefore

$$\Pi_\epsilon = \mathcal{O}(\delta^3). \quad (68)$$

The point is that the rotational symmetry of the collision operator implies

$$\int d^3v v_2 v_3 C(\bar{f}_1 - \rho \cdot \nabla f_M) = 0,$$

because the integrand has no γ -average. The integral

$$\int d^3v (v_2 v_2 - v_3 v_4) C(\bar{f}_1 - \rho \cdot \nabla f_M) = 0,$$

vanishes for the same reason, while ξ -asymmetry implies

$$\int d^3v v_1 v_2 C(\bar{f}_1 - \rho \cdot \nabla f_M) = 0 = \int d^3v v_1 v_4 C(\bar{f}_1 - \rho \cdot \nabla f_M).$$

The classical collisional viscosity tensor has second-order components only in the rapidly rotating case, as noted in Chapter 8.

The time-derivative term in (65) is similarly small in transport contexts; recall (4.16). With regard to instability theory, however, it is not always negligible and gives P_0 a frequency dependence akin to that of “AC” resistivity.

The remaining terms,

$$P_{g22} \equiv -\frac{m}{2\Omega} \left\{ \nabla M_{23}^{(3)} - 2\frac{e}{m} n(E_2 V_3 + E_3 V_2) \right\} \quad (69)$$

are primarily associated with *gyroviscosity*, or *magnetoviscosity*, to which we next turn our attention.

Gyroviscosity*

The gyroviscous tensor \mathbf{P}_g is analogous to the magnetization flows of (38) and (53); it represents a nondissipative transport of momentum, due to spatial variation of the density and energy of magnetic moments.

To calculate \mathbf{P}_g , we begin with

$$\mathbf{M}_{23}^{(3)} = \int d^3v f v v_2 v_3.$$

From (67) it can be seen that there is no contribution from \bar{f} :

$$\mathbf{M}_{23}^{(3)} = \int d^3v (-\rho \cdot \nabla f_M) v v_2 v_3.$$

Then straightforward calculation gives

$$\mathbf{M}_{23}^{(3)} = \frac{pT}{m^2\Omega} \left(\nabla \ln p + \nabla \ln T + \frac{e}{T} \nabla \Phi \right) \cdot (\mathbf{e}_2 \mathbf{e}_2 - \mathbf{e}_3 \mathbf{e}_3).$$

After recalling (38) and (53), we find after some manipulation that

$$\mathbf{M}_{23}^{(3)} = \frac{p}{m} \left[\mathbf{e}_2 \left(V_3 + \frac{2}{5} q_3 \right) + \mathbf{e}_3 \left(V_2 + \frac{2}{5} q_2 \right) \right].$$

Here only the coordinate subscripts on \mathbf{V}_{11} and \mathbf{q}_{11} are indicated. In computing the divergence of \mathbf{M} we omit contributions from magnetic field curvature, taking the unit vectors to be constant for simplicity. Then, using (39), we find

$$\begin{aligned} P_{g22} &\equiv -\frac{p}{2\Omega} (\mathbf{e}_2 \cdot \nabla V_3 + \mathbf{e}_3 \cdot \nabla V_2) \\ &\quad - \frac{1}{5\Omega} (\mathbf{e}_2 \cdot \nabla q_3 + \mathbf{e}_3 \cdot \nabla q_2) + mn \left(V_2^2 - \frac{1}{2} V^2 \right). \end{aligned}$$

A very similar argument provides P_{g33} and P_{g23} ; one finds that each component includes the term $-mnV^2/2$, which can therefore be absorbed into $\mathbf{H}^{(2)}$. We also recall (17) to subtract the advective inertial term and write

$$\Pi_g \equiv \mathbf{P}_g - mn\mathbf{V}\mathbf{V} + \frac{1}{2} mnV^2 \mathbf{I}.$$

We refer to Π_g as the gyroviscosity tensor; it has nonvanishing components

$$\begin{aligned} \Pi_{g22} &= -\Pi_{g33} = -\frac{p}{2\Omega} (\mathbf{e}_2 \cdot \nabla V_3 + \mathbf{e}_3 \cdot \nabla V_2) - \frac{1}{5\Omega} (\mathbf{e}_2 \cdot \nabla q_3 + \mathbf{e}_3 \cdot \nabla q_2), \\ \Pi_{g23} &= \Pi_{g32} = -\frac{p}{2\Omega} (\mathbf{e}_2 \cdot \nabla V_2 - \mathbf{e}_3 \cdot \nabla V_3) - \frac{1}{5\Omega} (\mathbf{e}_2 \cdot \nabla q_2 + \mathbf{e}_3 \cdot \nabla q_3). \end{aligned} \tag{70}$$

The components $\Pi_{g1\alpha} = \Pi_{g\alpha 1} (\alpha \neq 1)$, sometimes considered part of Π_g , are not specified here because they depend upon \bar{f}_1 . The point is that while (67) provides a general expression for f , the form of \bar{f}_1 depends upon solution of the guiding center kinetic equation; a general, closed form expression is not available. We will use a conventional *ansatz* to compute $\Pi_{g1\alpha}$ in §6.5.

The magnetic curvature terms, implicit in (69) but omitted in (70), are not hard to compute. Regardless of whether they are classified as “gyroviscous,” they are part of the second order stress and sometimes important. More generally we note that calculations of fluid moments based on slab geometry ($\mathbf{b}=\text{constant}$) can be applied to toroidal confinement problems only with care. On the other hand (69) pertains in any geometry.

Plasma Current

The perpendicular plasma current,

$$\mathbf{J}_\perp = \sum_s e_s n_s \mathbf{V}_{\perp,s}, \quad (71)$$

is computed from (34). Noting that $e_s/m_s \Omega_s = c/B$ is independent of species, recalling collisional momentum conservation, (5.25), and assuming quasineutrality,

$$\sum_s e_s n_s = 0, \quad (72)$$

we find the exact relation

$$\mathbf{J}_\perp = \frac{c}{B} \mathbf{b} \times \left[\frac{\partial}{\partial t} \rho_m \mathbf{v}_m + \nabla \cdot \mathbf{P}_t \right], \quad (73)$$

where

$$\rho_m \mathbf{v}_m \equiv \sum_s m_s n_s \mathbf{V}_s, \quad (74)$$

$$\rho_m \equiv \sum_s m_s n_s, \quad (74)$$

specifies the flow of the plasma center of mass and of course

$$\mathbf{P}_t \equiv \sum_s \mathbf{P}_s, \quad (75)$$

is the total plasma stress tensor.

Equation (73) can be compared to the corresponding kinetic formula, (4.2). The advantage of the fluid closure, in requiring less information about the distribution function, has already been emphasized. Yet we should stress that (73) does not specify the current parallel to \mathbf{B} . To find J_{\parallel} one needs f , the product of guiding-center kinetic theory.

Because of its role in electrodynamical closure, (73) is central to a variety of confinement issues. The steady-state version of (73) is at the heart of confined equilibrium theory, as is clear from Chapter 3. It is indispensable to the understanding of fluid stability, as shown in Chapter 7, and provides key information concerning certain transport issues, as shown in Chapter 8. Finally an approximate version of (73) will be seen, in the following section, to be part of the framework of MHD.

6.4 MHD Closure

MHD Flow

MHD is a model for magnetized plasma dynamics that is based on a single idea: the allowance for large perpendicular electric fields. Specifically, one allows \mathbf{E}_\perp to be so large that the $\mathbf{E} \times \mathbf{B}$ drift escapes the δ -ordering of (37); we have instead $V_E \sim v_t$ and

$$\mathbf{V}_\perp = \mathbf{V}_E + \mathcal{O}(\delta). \quad (76)$$

In this regard the reader may wish to review the discussion of the MHD and drift orderings in §4.1.

It is not hard to understand why this one term in \mathbf{V}_\perp is given special treatment. Magnetized plasmas have been observed—in early pinch experiments, for example—to move across the confining field at nearly thermal speeds,

$$V_\perp \sim v_t. \quad (77)$$

The point is that it is difficult to identify any other term in (34) that could effect such fast motion. Consider for example the contribution to \mathbf{V}_\perp from the divergence of the stress tensor:

$$V_\perp \sim \frac{1}{m\Omega} \mathbf{b} \times \nabla \cdot \mathbf{P} \sim \frac{nv_t^2}{m\Omega L} \sim v_t \frac{\rho}{L}.$$

This contribution cannot obey (77) in a magnetized plasma.

The $\mathbf{E} \times \mathbf{B}$ drift, on the other hand, can consistently yield rapid flow. Recall that

$$\mathbf{V}_E = \frac{c}{B} \mathbf{b} \times \left(\nabla \Phi + \frac{1}{c} \frac{\partial \mathbf{A}}{\partial t} \right). \quad (78)$$

In a strongly excited, nonlinear regime, the natural temporal ordering is

$$\left| \frac{\partial \mathbf{A}}{\partial t} \right| \sim \left(\frac{v_t}{L} \right) A.$$

where $L \gg \rho$ is as usual the scale length for fluid variation. Furthermore, since we expect $A \sim LB$,

$$\left| \frac{\partial \mathbf{A}}{\partial t} \right| \sim v_t B \quad (79)$$

and (77) follows. Indeed (79) can be used, instead of (77), as the essential assumption of MHD.

Note, on the other hand, that obtaining fast motion from the electrostatic term in (78) is problematic: the natural measure of potential change is $\Delta\Phi \sim T/e$, whence

$$\frac{c}{B} \nabla \Phi \sim \frac{cT}{eBL} \sim \frac{\rho}{L} u_t. \quad (80)$$

In other words, an MHD-ordered $\mathbf{E} \times \mathbf{B}$ drift can be electrostatic only if Φ varies on the scale of the gyroradius. Since plasma fluid variables can be expected to share the scale length of Φ , such variation is prohibited in a magnetized plasma.

Of course the MHD model, especially in its linearized form, is often used to describe mild perturbations, with $\partial A / \partial t \ll v, B$. Furthermore, one frequently considers “marginal stability” problems, with $\partial \mathbf{A} / \partial t \approx 0$. Although (77) is not obeyed in these cases, there is no inconsistency. The point is that in using MHD one is investigating the possibility of fast, violent motion. As part of such an investigation it may be useful, as a mathematical artifice, to examine limiting (very weak or very slow) regimes.

MHD theory is relatively simple because, after focussing on the case of rapid flow, it next omits all $O(\delta)$ corrections. The MHD velocity is therefore given by

$$\mathbf{V} = \mathbf{b} V_{\parallel} + \mathbf{V}_E . \quad (81)$$

where the parallel flow is at this point unspecified. Equation (81) is the fundamental assumption of MHD. Alternatively, we write

$$\mathbf{E} + \frac{1}{c} \mathbf{V} \times \mathbf{B} = 0 , \quad (82)$$

thus ensuring both (81) and

$$E_{\parallel} = 0 . \quad (83)$$

This is consistent with the neglect of δ -corrections, since, as noted in (2.61) or (4.22), E_{\parallel} must be of order δ .

We shall refer to (82) as the MHD “Ohm’s law.” This language is conventional; indeed, (82) is sometimes considered to be the “ideal” (that is, dissipationless) limit of the relation

$$\mathbf{E} + \frac{1}{c} \mathbf{V} \times \mathbf{B} = \eta \mathbf{J} . \quad (84)$$

It is true, as we shall see presently, that plasma current can be linearly related to a (sufficiently weak) electric field, although the actual relation is more complicated than (84). But it should be said that an Ohmic interpretation of (82) misses the point. The MHD Ohm’s law does not primarily reflect any balance between collision friction and electric acceleration. Rather, as we have emphasized, it is a simple consequence of (34) in the case of large perpendicular electric fields.

The coupling of plasma motion and field evolution implied by (82) has a peculiar consequence, demonstrated in introductory plasma physics treatments. Equation (82) says that the magnetic field lines can be imagined as moving with the plasma fluid, at the velocity \mathbf{V}_E (motion of field lines along \mathbf{B} is not physically meaningful). In MHD the field lines are locked to the fluid; one speaks of *frozen flux*. Thus even this preliminary investigation of rapid flow yields an interesting fact: **Can a magnetized plasma**

move, perpendicular to \mathbf{B} , at speeds comparable to its thermal speed? Yes, but only by dragging the field lines along with it. This crucial constraint is discussed more thoroughly in §7.6.

Of course the frozen flux constraint is broken by the resistive Ohm's law, (84). Indeed the resistive term, invoking magnetic field diffusion, crucially changes the relation between plasma motion and field evolution. We return to this matter presently.

MHD Truncation

Equation (82) is the point of MHD, but unfortunately it does not by itself provide a closed set of dynamical equations. One can obtain closure by combining (82) with an approximate guiding center kinetic equation, as discussed in Chapter 4. This asymptotic closure scheme (Rosenbluth and Rostoker, 1958), called "kinetic MHD," is rigorous but rather complicated, and especially unwieldy in nonlinear regimes. Much more commonly MHD is pursued using a simple fluid truncation that we consider here. It is summarized by the ansatz, for each plasma species,

$$f = f_M(\mathbf{v} - \mathbf{V}) + \mathcal{O}(\delta). \quad (85)$$

Here \mathbf{V} is given by (81), with the assumption that \mathbf{V}_{\parallel} , and therefore \mathbf{V} , is the same for each species. The correction term in (85) is necessary to allow for, *inter alia*, plasma current. Fortunately we need not compute it; the necessary information about \mathbf{J} is effectively provided by (73).

Equation (85) implies that the pressure tensor is isotropic,

$$\sum_s \mathbf{P}_s = \mathbf{I}P + \mathcal{O}(\delta) \quad (86)$$

and that the heat flux is negligible:

$$\sum_s \mathbf{q}_s = \mathcal{O}(\delta). \quad (87)$$

Recalling (10) and (11) and ignoring $\mathcal{O}(\delta)$, we see that

$$\sum_s \mathbf{P}_s = \mathbf{I}P + \rho_m \mathbf{V}\mathbf{V}, \quad (88)$$

$$\sum_s \mathbf{Q}_s = \frac{5}{2} \mathbf{p}\mathbf{V} + \frac{1}{2} \rho_m V^2 \mathbf{V}, \quad (89)$$

where ρ_m is defined by (74). These facts are sufficient to provide a closed system. Note that (86) and (88) introduce the convenient abbreviation, $P \equiv p_{\parallel}$.

It is possible to identify parameter regimes in which (85) appears as a lowest order result, rather than an *ansatz*. But such regimes are narrow, and not usually relevant to confinement experiments. The point is that large collision frequency is needed to justify the Maxwellian property; yet the collision-dominated theory, represented for example by the Braginskii equations, is not only invalid in most confinement contexts, it is also much more complicated than MHD. In the more realistic regime of long mean-free-path, kinetic MHD is applicable—and rigorously asymptotic in the sense of §6.2. Unfortunately it yields a distribution that is invariably non-Maxwellian.

Thus the truncation *ansatz* should not be considered rigorous. Nonetheless it appears to be physically relevant: the simplest MHD equations are often in good qualitative accord with experiment. Indeed, in most cases their predictions are not drastically unlike the rigorous results of kinetic MHD. The point is that stress anisotropy—the main phenomenon precluded by (85)—need not be crucial, even when it is large. As we emphasized in Chapter 3, only the first two moments of the distribution are needed to advance the electromagnetic field, and these moments need not be sharply affected by kinetic complications. A more explicit statement is discussed in Chapter 7: one finds, with regard to electromagnetic stability, that kinetic MHD introduces stabilizing terms that matter only in rather special circumstances.

In other words the important assumption of MHD is not (85), but rather the basic electric field ordering, (79). Thus (79) is a strong assumption, which restricts the MHD domain to the most violent fluid motions. Indeed, as was noted in Chapter 4, (79) is contradicted by most of the disturbances observed in present experiments; recall the discussion following (4.25).

Experimental observations suggest in particular that the diamagnetic flow is typically comparable to the $\mathbf{E} \times \mathbf{B}$ drift, making the two terms in (35) comparable. In other words, as we remarked in Chapter 4, contemporary experiments are best described by the drift-ordering of (4.24). Drift-ordered analogs to MHD—purely fluid theories that include the diamagnetic flow and related $\mathcal{O}(\delta)$ terms—are considered in §6.5.

To avoid confusion, one additional remark concerning (35) is appropriate. In fact MHD only partially neglects the diamagnetic drift. While diamagnetism is omitted from (76), its effect on the current is retained in (the MHD version of) (73): $\mathbf{J}_\perp = (c/B)\mathbf{b} \times \nabla P$. There is no inconsistency here. As noted in Chapter 2 the factor of electric charge in (71) is equivalent to $1/\delta$; hence, being multiplied by a large factor, \mathbf{J}_\perp depends upon the correction term in (85). This correction term contains the diamagnetic drift, the Maxwellian term in (85) providing no net current. However, in a manner that should by now seem familiar, we can avoid computing the correction by appropriate use of moment equations—in this case, by use of (73).

Closed System

The MHD equations are derived from species sums of (22)–(24), combined with (88) and (89). We begin with the equation of motion in the form of (27). Because of collisional momentum conservation and quasineutrality, its species sum simplifies to

$$\rho_m \left(\frac{\partial \mathbf{V}}{\partial t} + \mathbf{V} \cdot \nabla \mathbf{V} \right) + \nabla \mathbf{P}_t = \frac{1}{c} \mathbf{J} \times \mathbf{B}, \quad (90)$$

where \mathbf{P}_t is the total pressure tensor and the m-subscript on \mathbf{V} is suppressed. This relation is exact. In the MHD case we use (86),

$$\nabla \cdot \mathbf{P} = \nabla P \quad (91)$$

to conclude that

$$\rho_m \frac{d\mathbf{V}}{dt} + \nabla P = \frac{1}{c} \mathbf{J} \times \mathbf{B}. \quad (92)$$

Here d/dt is the advective derivative,

$$\frac{d}{dt} = \frac{\partial}{\partial t} + \mathbf{V} \cdot \nabla. \quad (93)$$

Next consider the species sum of the energy conservation laws, (23). Collisional energy conservation, (5.29), implies the exact relation

$$\frac{\partial}{\partial t} \left(\frac{3}{2} P + \frac{1}{2} \sum_s m_s n_s V_s^2 \right) + \nabla \cdot \mathbf{Q} = \mathbf{J} \cdot \mathbf{E}. \quad (94)$$

Because of (89) (and because the MHD flow is species-independent) the MHD version is

$$\frac{\partial}{\partial t} \left(\frac{3}{2} P + \frac{1}{2} \rho_m V^2 \right) + \frac{5}{2} \nabla \cdot (P\mathbf{V}) + \frac{1}{2} \nabla \cdot (\rho_m V^2 \mathbf{V}) = \mathbf{J} \cdot \mathbf{E}. \quad (95)$$

Cancellations occurring in (95) are important enough for detailed attention. We first combine (22) and (92) to find that

$$\frac{\partial}{\partial t} \left(\frac{1}{2} \rho_m V^2 \right) + \nabla \cdot \left(\frac{1}{2} \rho_m V^2 \mathbf{V} \right) + \mathbf{V} \cdot \nabla P \simeq \frac{1}{c} \mathbf{V} \cdot \mathbf{J} \times \mathbf{B},$$

where, in view of (82),

$$\frac{1}{c} \mathbf{V} \cdot \mathbf{J} \times \mathbf{B} = \mathbf{J} \cdot \mathbf{E}. \quad (96)$$

Hence

$$\frac{\partial}{\partial t} \left(\frac{1}{2} \rho_m V^2 \right) + \nabla \cdot \left(\frac{1}{2} \rho_m V^2 \mathbf{V} \right) + \mathbf{V} \cdot \nabla P = \mathbf{J} \cdot \mathbf{E}. \quad (97)$$

We subtract this result from (95) to get $(\partial/\partial t)\frac{3}{2}P + \frac{5}{2}$
 $nab \cdot (PV) - \mathbf{V} \cdot \nabla P = 0$, or

$$\frac{dP}{dt} + \frac{5}{3}P\nabla \cdot \mathbf{V} = 0, \quad (98)$$

the MHD pressure-evolution law. Note that (98) corresponds to adiabatic evolution: it follows from (22) if one assumes the adiabatic equation of state, $P\rho_m^{-5/3} = \text{constant}$. Indeed, adiabaticity is enforced by our neglect of heat flow in (87).

In some MHD literature (98) is replaced by an unspecified equation of state, $f(P, \rho_m) \approx 0$, allowing, for example, for isothermal evolution. It is not clear how one avoids (87), since the Maxwellian distribution is crucial to MHD. On the other hand, the use of differing equations of state rarely matters in practice.

We finally summarize the closed dynamical system of ideal MHD. There are four equations for the plasma fluid: an Ohm's law, (82); an equation of motion, (90) a mass conservation law, (22); and the adiabatic law, (98). These are combined with Ampere's law and Faraday's law to provide fourteen equations for the fourteen field quantities in $\mathbf{V}, \mathbf{J}, \mathbf{B}, \mathbf{E}, P$ and ρ_m :

$$\nabla \times \mathbf{B} = \frac{4\pi}{c} \mathbf{J}, \quad (99)$$

$$\frac{\partial \mathbf{B}}{\partial t} + c\nabla \times \mathbf{E} = 0, \quad (100)$$

$$\frac{d\rho_m}{dt} + \rho_m \nabla \cdot \mathbf{V} = 0, \quad (101)$$

$$\frac{dP}{dt} + \frac{5}{3}P\nabla \cdot \mathbf{V} = 0, \quad (102)$$

$$\rho_m \frac{d\mathbf{V}}{dt} + \nabla P = \frac{1}{c} \mathbf{J} \times \mathbf{B} \quad (103)$$

$$\mathbf{E} + \frac{1}{c} \mathbf{V} \times \mathbf{B} = 0. \quad (104)$$

Note that the fields \mathbf{J} and \mathbf{E} are easily eliminated using (99) and (104) respectively. Some manipulation then provides a more succinct system, consisting of (101), (102), and the relations

$$\rho_m \frac{d\mathbf{V}}{dt} + \nabla \left(P + \frac{B^2}{8\pi} \right) = \frac{\mathbf{B} \cdot \nabla \mathbf{B}}{4\pi}, \quad (105)$$

$$\frac{d\mathbf{B}}{dt} - \mathbf{B} \cdot \nabla V + \mathbf{B} \nabla \cdot \mathbf{V} = 0. \quad (106)$$

These are eight equations for the eight variables in p , ρ_m , \mathbf{B} and \mathbf{V} .

It is known from classical fluid theory that dissipation, even when very weak, can have qualitatively dramatic effects. The simplest way to explore this possibility, within the MHD ordering, is to replace (104) by the resistive Ohm's law, (84). The resulting system,

$$\frac{d\rho_m}{dt} + \rho_m \nabla \cdot \mathbf{V} = 0 ,$$

$$\frac{dP}{dt} + \frac{5}{3} P \nabla \cdot \mathbf{V} = 0 ,$$

$$\rho_m \frac{d\mathbf{V}}{dt} + \nabla \left(P + \frac{B^2}{8\pi} \right) = \frac{\mathbf{B} \cdot \nabla \mathbf{B}}{4\pi}$$

$$\frac{d\mathbf{B}}{dt} - \mathbf{B} \cdot \nabla \mathbf{V} + \mathbf{B} \nabla \cdot \mathbf{V} = \frac{c^2 \eta}{4\pi} \nabla^2 \mathbf{B} , \quad (107)$$

is called *resistive MHD*. Note that (107) assumes, for simplicity, that the resistivity η is a spatial constant. This assumption can in fact be justified only when the electron temperature is constant.

We defer discussion of the application of ideal and resistive MHD to Chapter 7. However, some elementary remarks on the significance of resistivity in (107) are appropriate here. The right-hand side of (107) corresponds to resistive diffusion of the magnetic field. We can readily estimate the corresponding magnetic field penetration time,

$$\tau_B = \frac{4\pi L^2}{c^2 \eta} \quad (108)$$

for a length scale L . In parameter regimes of confinement significance, τ is larger, by orders of magnitude, than any relevant time scale, i.e.

$$\tau_B \omega \gg 1 \quad (109)$$

for typical frequencies. Hence magnetic fields do not readily penetrate thermonuclear plasma—a circumstance with potent experimental implications.

Equation (109) reinforces the ideal relation, (82), in most MHD contexts. But as we have remarked, resistivity has a special significance regarding magnetic field evolution: it breaks the MHD constraint of frozen flux, allowing field lines to move through the plasma. We shall see in Chapter 7 that qualitatively distinct and often dangerous types of instability are thereby permitted. The related mathematical observation is that the resistive term in (107) changes the order of the differential equation, thus acting as a singular perturbation, however small its coefficient.

6.5 Generalization of MHD

Drift Ordering

We have noted that the fundamental ordering of MHD, $V \sim v_t$, is consistent with small δ only in the presence of rapid temporal change: $\partial/\partial t \sim v_t/L$. We have also noted that the dynamical phenomena observed in modern confinement experiments—including “MHD” activity, sawtooth oscillations and even disruptions—are rarely as violent or rapid as these orderings allow. The drift ordering, given by

$$V \sim \delta v_t , \quad (110)$$

$$\frac{\partial}{\partial t} \sim \frac{\delta v_t}{L} , \quad (111)$$

is much more commonly applicable.

It is tempting to directly extrapolate the MHD description to such mild perturbations, without change in form. The extrapolation seems especially natural since all the terms in (101), (102), and (104) remain formally comparable within the drift-ordering. In (103), the acceleration term becomes relatively small—an unsurprising and physically plausible statement that the plasma fluid evolves through a sequence of near equilibria.

But our derivation of MHD shows that it cannot describe drift-ordered evolution. The most obvious problem lies in the Ohm’s law, (82), which assumes the $\mathbf{E} \times \mathbf{B}$ drift to dominate all other contributions to \mathbf{V}_\perp . It is not hard to see that the diamagnetic drift¹,

$$n\mathbf{V}_p \equiv \frac{1}{m\Omega} \mathbf{b} \times \nabla p \quad (112)$$

is comparable to V_E in the drift-ordered case:

$$\mathbf{V}_p \sim \frac{1}{L\Omega} \frac{T}{m} = \frac{\rho}{L} v_t = \delta v_t .$$

Rigorous fluid closure in the drift ordering has been accomplished only for short mean-free path. In more realistic regimes of low collision-frequency, general solutions to the appropriate (drift- or gyro) kinetic equation are not available, so that the kinetic equation must remain part of the closed system. Indeed, many long mean-free path analyses use kinetic theory exclusively. [This circumstance is unsurprising and similar to the MHD case: recall that the only rigorous version of MHD, kinetic MHD, also makes essential use of guiding-center kinetic theory. The *ansatz* (84) is not generally valid.]

¹ We identify the diamagnetic drift with a p -subscript because the symbols “ δ ” and “ D ” have been appropriated in Chapter 4 for guiding-center drift velocities.

Nonetheless, for simplicity a fluid model of drift-ordered motion is desirable. Such systems are often called *finite Larmor radius* (FLR) models. Since they include $\mathcal{O}(\delta)$ terms that MHD neglects, this terminology is appropriate, and will be used here. But it is subject to misinterpretation. FLR theory always concerns magnetized plasma, and it usually concerns plasmas that are magnetized in the strong sense: in the language of Chapter 4, an FLR plasma is not ordinarily a gyrokinetic plasma. The Larmor radius is treated as nonzero because of relatively slow *temporal* variation, as in (111), rather than because of rapid spatial variation. What is studied in FLR fluid theory is a small-gyroradius plasma evolving so slowly that MHD-negligible effects dominate.

No FLR fluid system has the broad acceptance or stature of MHD. Indeed, the literature contains a multitude of FLR models, few of which agree in detail, and none of which attempts full rigor or generality. We next consider two closed systems that represent FLR physics. The first is quite general, and based on a single *ansatz* closely analogous to (85). Unfortunately this *ansatz* leads to equations that are unwieldy for pedagogical application. The second system, called the drift model, has a much simpler form, provides easy access to FLR physics and is remarkably accurate. But the approximations involved in its derivation, however plausible, are not completely systematic.

FLR Closure

The conceptually simplest drift-ordered closure is based on an assumption analogous to (85) of MHD. We assume

$$f = f_M(\mathbf{v}) \left[1 + 2 \frac{V_{\parallel} v_{\parallel}}{v_t^2} \right] - \rho \cdot \nabla f_M + \mathcal{O}(\delta^2). \quad (113)$$

This expression can be compared to the rigorous equilibrium distribution, (67); it differs in taking the gyrophase-averaged distribution \bar{f}_1 to be to a displaced Maxwellian,

$$\bar{f}_1 = \frac{V_{\parallel} v_{\parallel}}{v_t^2} f_M,$$

as in (5.10). The displacement is presumed small,

$$V_{\parallel} = \mathcal{O}(\delta), \quad (114)$$

so that the lowest order distribution is a stationary Maxwellian, as in the equilibrium case.

With regard to its MHD counterpart, (85), (113) differs mainly by specifying the first-order terms. Of course such terms are needed, in view of (110), to describe plasma motion: FLR theory must attend to the minutia that MHD ignores. A less obvious difference, concealed by terse notation,

is that the parallel flow speeds in (113) need not be the same for all species. The point is that (114) by itself enforces moderate parallel current, so that $V_{\parallel e}$ and $V_{\parallel i}$ can appreciably differ.

It should be clear that, despite such differences, (113) is very much in the spirit of the MHD *ansatz*. Its choice of a displaced Maxwellian with minimal FLR correction affords the simplest and probably the most natural extension of MHD. On the other hand, as in the MHD case, the FLR *ansatz* is not a general consequence of kinetic theory. Indeed, we shall find that even the equilibrium distribution of a confined plasma is rather complicated; it allows, unlike (113), for both parallel heat flow and pressure anisotropy in first-order. Thus, in the language of §6.2, use of (113) corresponds to *truncation* rather than to any asymptotic closure scheme. Indeed, (113) may be viewed as a simplified version of the more elaborate thirteen moment approximation—perhaps the most systematic, if still nonrigorous, truncation procedure.

The truncated FLR system is constructed from the exact moment equations, (22)–(24). Thus we need the particle and energy flows, the stress tensor, and two moments of the collision operator. By taking moments of (113) we compute the particle and energy flows

$$\mathbf{V} = \mathbf{b} V_{\parallel} + \mathbf{V}_E + \mathbf{V}_p + \mathcal{O}(\delta^2), \quad (115)$$

$$\mathbf{Q} = \frac{5}{2} n T \mathbf{V} + \mathbf{q} + \mathcal{O}(\delta^2), \quad (116)$$

with [recall (53)]

$$\mathbf{q} = \frac{5}{2} \frac{p}{m \Omega} \mathbf{b} \times \nabla T + \mathcal{O}(\delta^2). \quad (117)$$

Furthermore the method of §6.3 provides the stress tensor

$$\mathbf{P} = \mathbf{I} p + m n \mathbf{V} \mathbf{V} + \Pi_g + \mathcal{O}(\delta^3), \quad (118)$$

where Π_g denotes the gyroviscosity tensor. A crucial observation is that, according to (110),

$$m n V V \sim \Pi_g. \quad (119)$$

Unlike the MHD case, in FLR theory it is inconsistent to retain advective inertia without also keeping gyroviscosity. While we continue to suppress species subscripts, it should be noted that gyroviscous stress is proportional to mass, like the left-hand side of (119). It follows that electron dynamics are usually traced by keeping only the first, scalar pressure term in (118):

$$\mathbf{P}_e \cong \mathbf{I} p_e. \quad (120)$$

With regard to gyroviscosity: in §6.3 we computed all components of Π_g , except those depending on f_1 ; now using (113) we straightforwardly find the two remaining components. Thus, after multiplying (113) by $\mathbf{v} \mathbf{v} \mathbf{v}$

and integrating to compute $M_{12}^{(3)}$ and $M_{13}^{(3)}$, we follow the derivation of (70) and find that

$$\begin{aligned}\Pi_{g12} &= -\frac{p}{\Omega} (\mathbf{e}_3 \cdot \nabla V_{\parallel} + \mathbf{b} \cdot \nabla V_3) - \frac{2}{5\Omega} \mathbf{b} \cdot \nabla q_3, \\ \Pi_{g13} &= \frac{p}{\Omega} (\mathbf{e}_2 \cdot \nabla V_{\parallel} + \mathbf{b} \cdot \nabla V_2) + \frac{2}{5\Omega} \mathbf{b} \cdot \nabla q_2.\end{aligned}\quad (121)$$

Equations (70) and (121) can be expressed more compactly as follows. The gyroviscosity tensor corresponding to the FLR *ansatz*, (113) has the form

$$\Pi_g = \Pi_{\perp} + \mathbf{b}\Pi_{\parallel} + \Pi_{\parallel}\mathbf{b}, \quad (122)$$

where Π_{\perp} is the tensor

$$\begin{aligned}\Pi_{\perp} &= \frac{p}{2\Omega} [(\mathbf{b} \times \nabla)\mathbf{V}_{\perp} + \nabla(\mathbf{b} \times \mathbf{V}_{\perp})] \\ &\quad + \frac{1}{5\Omega} [(\mathbf{b} \times \nabla)\mathbf{q}_{\perp} + \nabla(\mathbf{b} \times \mathbf{q}_{\perp})],\end{aligned}\quad (123)$$

and Π_{\parallel} is the vector

$$\Pi_{\parallel} = \frac{p}{\Omega} [\mathbf{b} \times \nabla V_{\parallel} + \mathbf{b} \cdot \nabla(\mathbf{b} \times \mathbf{V}_{\perp})] + \frac{1}{5\Omega} \mathbf{b} \cdot \nabla(\mathbf{b} \times \mathbf{q}_{\perp}). \quad (124)$$

These forms, like (121), assume that the magnetic field is uniform; in that case it can be seen that (123) is automatically symmetric: $\Pi_{\perp\alpha\beta} = \Pi_{\perp\beta\alpha}$. Generalization to allow for field curvature is straightforward upon using covariant differentiation. Thus, for example, the second term in (123) has components

$$[\nabla(\mathbf{b} \times \mathbf{V}_{\perp})]_{\alpha\beta} = (g^{1/2} \epsilon_{\alpha\kappa\lambda} b^{\kappa} V_{\perp}^{\lambda})_{,\beta}.$$

Furthermore since field variation breaks the indicial symmetry, each term in (123) must be symmetrized by averaging with its transpose.

Finally we consider the dissipative terms. Collisional viscosity is negligibly small in the drift ordering, as we have observed in (68), and the energy exchange term, W , is generally negligible because of the small mass ratio; recall (5.68). But the distribution *ansatz* (113) allows for appreciable collisional friction. In the two-species case of primary interest, $\mathbf{F}_{ei} = -\mathbf{F}_{ie}$ is easily computed by substituting the electron version of (113) into (5.65). The result is

$$\mathbf{F}_{ei} = -\frac{m_e n}{\tau_{ei}} [\mathbf{V}_e - \mathbf{V}_i - \frac{2}{5} p_e \mathbf{q}_{\perp e}],$$

where the collision time is defined by (5.64) and $\mathbf{q}_{\perp e}$ is the heat flux of (117):

$$\mathbf{q}_{\perp e} = -\frac{5}{2} \frac{cp}{eB} \mathbf{b} \times \nabla T_e. \quad (125)$$

Therefore the friction can be expressed as

$$\mathbf{F}_{ei} = \frac{m_e}{e\tau_{ei}} \left[\mathbf{J} - \frac{3}{2} \frac{cn}{B} \mathbf{b} \times \nabla T_e \right]. \quad (126)$$

The quantity $e = |e_e| > 0$ is the magnitude of the electronic charge (we adhere to this convention everywhere except in equations where an implicit species subscript is suppressed).

The expressions (115)–(126) can be combined with the exact moment equations (22)–(24) for each species, to provide a closed description of the plasma fluid. Notice that the drift ordering allows us to neglect $\mathcal{O}(\varepsilon^2)$ -terms in the even moments, (22) and (23), while neglecting only $\mathcal{O}(\varepsilon_3)$ in the equation of motion, (24). Hence (115)–(118) have precisely the desired accuracy. By combining this description with Maxwell's equations, we obtain an FLR analog to the MHD system, (101)–(104).

Unfortunately, as we have noted, this system of equations is very complicated. Much of the complication stems from magnetic field curvature; for example, the divergence of the heat flow of (117) has contributions, not only from ∇T and ∇p , but also from $\nabla \times \mathbf{b}$ and $\nabla \Omega$. Additional complications arise from dissipation, especially in the presence of temperature gradients, from unequal species temperatures, and from compressibility. The resulting accumulation of terms burdens the calculation of even elementary results, and is especially discouraging when rooted in such nonrigorous assumptions as (113).

Hence we turn our attention to a simplified FLR system.

Drift Model

We will refer to the model presented here, which is drawn from the work of (Roberts and Taylor, 1962) and (Rosenbluth and Simon, 1965), as the drift model. The drift model is advantageous mainly for reasons of economy: it probably contains more physics per term than other formulations. Indeed, while taking into account the main effects of diamagnetic drifts, slow evolution and gyroviscosity, it remains remarkably similar to MHD. It is especially accurate in the case of uniform magnetic field, incompressibility, and uniform temperature.² Yet the model includes at least the gross effects of both temperature variation and field curvature.

The drift model avoids trivial complications by specializing to the two-species case and assuming equal species temperatures:

$$T_i = T_e. \quad (127)$$

Then quasineutrality makes both pressures the same, $p_i = p_e$; we nonetheless retain subscripts for pedagogical reasons. We continue to denote the

² With regard to the relative simplicity of the isothermal case, the discussion at the end of §5.3 should be recalled.

total pressure by

$$P \equiv p_i + p_e . \quad (128)$$

We similarly denote the center-of-mass velocity by \mathbf{V} , freely neglecting $\mathcal{O}(m_e/m_i)$ -terms to write

$$\mathbf{V} \cong \mathbf{V}_i . \quad (129)$$

In order to distinguish the fluid velocity from that of MHD we introduce the notation

$$\mathbf{V}_{\text{MHD}} \equiv \mathbf{V} - \mathbf{V}_{pi} , \quad (130)$$

where \mathbf{V}_{pi} is given by (112):

$$\mathbf{V}_{pi} = \frac{c}{enB} \mathbf{b} \times \nabla p_i = \frac{1}{2\Omega_i m_i n} \mathbf{b} \times \nabla P . \quad (131)$$

Notice that (130) and (131) specify \mathbf{V}_{MHD} in terms of \mathbf{V} , \mathbf{B} , and P . Of course (115) implies

$$\mathbf{V}_{\text{MHD}} \cong \mathbf{V}_E + \mathbf{b} V_{\parallel} ; \quad (132)$$

but this result, like (115), is not exact. In general the variable \mathbf{V} is affected by acceleration terms and must be determined from solution of the drift model.

The notation of (130) is useful in part because two distinct advective derivatives enter FLR fluid theory: the ordinary advective derivative

$$\frac{d}{dt} \equiv \frac{\partial}{\partial t} + \mathbf{V} \cdot \nabla , \quad (133)$$

as well as the MHD version,

$$\frac{d}{dt}|_{\text{MHD}} \equiv \frac{\partial}{\partial t} + \mathbf{V}_{\text{MHD}} \cdot \nabla \equiv \frac{\partial}{\partial t} + (\mathbf{V} - \mathbf{V}_{pi}) \cdot \nabla . \quad (134)$$

With these definitions we can express the drift model as follows:

$$\frac{dn}{dt} + n \nabla \cdot \mathbf{V} = 0 , \quad (135)$$

$$\frac{d}{dt}|_{\text{MHD}} P + \frac{5}{3} P \nabla \cdot \mathbf{V}_{\text{MHD}} = 0 , \quad (136)$$

$$\mathbf{E} + \frac{1}{c} \mathbf{V} \times \mathbf{B} + \frac{1}{en} \left(\frac{1}{2} \nabla P - \frac{1}{c} \mathbf{J} \times \mathbf{B} \right) = \eta \left[\mathbf{J} - \frac{3}{4} \frac{en}{B} \mathbf{b} \times \nabla \frac{P}{n} \right] , \quad (137)$$

$$m_i n \left[\frac{d\mathbf{V}_E}{dt} + \frac{d}{dt}|_{\text{MHD}} (\mathbf{b} V_{\parallel}) \right] + \nabla P = \frac{1}{c} \mathbf{J} \times \mathbf{B} . \quad (138)$$

Note that the drift model uses the same variables, $n = \rho_m/m_i$, P , \mathbf{B} and \mathbf{V} , as the MHD set that it generalizes, (101)-(104). We next discuss this model and its justification. A generally pertinent remark is that (135)-(137) neglect $\mathcal{O}(\delta^2)$ terms, while (138) neglects only $\mathcal{O}(\delta^3)$.

Density and Pressure Evolution*

Equation (135) does not differ from its MHD counterpart, (101); since both equations are exact the agreement is hardly surprising. The pressure evolution law, (136), is also similar to the MHD version (102); they differ only in that \mathbf{V}_{MHD} is no longer the fluid velocity.

It is easy to see why \mathbf{V}_p does not effect the pressure evolution. After applying the drift ordering to the species sum of (23) we find

$$\frac{3}{2} \frac{\partial P}{\partial t} + \nabla \cdot (\mathbf{Q}_i + \mathbf{Q}_e) = \mathbf{V} \cdot \nabla P. \quad (139)$$

Here the drift-ordered version of (97) was used to eliminate $\mathbf{J} \cdot \mathbf{E}$. Now (116) and (117) imply

$$\mathbf{Q}_s = \frac{5}{2} p_s \left[\frac{c}{e_s B} \mathbf{b} \times \left(\frac{1}{n} \nabla p_s + \nabla T_s \right) + \mathbf{V}_E + \mathbf{b} V_{\parallel} \right] + \mathcal{O}(\delta^2). \quad (140)$$

Notice that, because of equal temperatures, the terms involving gradients are opposite for the two plasma species, so that

$$\mathbf{Q} \equiv \mathbf{Q}_i + \mathbf{Q}_e = \frac{5}{2} P (\mathbf{V}_E + \mathbf{b} V_{\parallel}) + \mathcal{O}(\delta^2) \cong \frac{5}{2} P \mathbf{V}_{\text{MHD}}. \quad (141)$$

Since it is obvious that

$$\mathbf{V} \cdot \nabla P = \mathbf{V}_{\text{MHD}} \cdot \nabla P, \quad (142)$$

the form of (136) follows easily.

Actually (141) involves a mild swindle, since the parallel velocities of the two species can differ in the drift ordering [recall the discussion following (114)]. We should more strictly write

$$\mathbf{Q} = \frac{5}{2} P \left[\mathbf{V}_{\text{MHD}} - \frac{1}{2} \mathbf{b} \frac{J_{\parallel}}{en} \right].$$

This correction is rarely important because $\nabla \cdot [\mathbf{b} J_{\parallel}/en]$ is usually small compared to $\nabla \cdot \mathbf{V}_E$; see for example (185) and (186), below.

Generalized Ohm's Law*

The Ohm's law of the drift model, (137), is based on the electron version of (24), the equation of motion. After exploiting the small electron mass to neglect both acceleration and nonscalar stresses, as in (120), we find that

$$\nabla p_s + en \left(\mathbf{E} + \frac{1}{c} \mathbf{V}_e \times \mathbf{B} \right) = \mathbf{F}_e. \quad (143)$$

Since

$$\mathbf{V}_e = \mathbf{V}_i - \frac{\mathbf{J}}{en} \cong \mathbf{V} - \frac{\mathbf{J}}{en}, \quad (144)$$

we can express (143) in terms of \mathbf{V} and \mathbf{J} :

$$\mathbf{E} + \frac{1}{c} \mathbf{V} \times \mathbf{B} = \frac{1}{en} (\mathbf{F}_e - \nabla p_e + \frac{1}{c} \mathbf{J} \times \mathbf{B}). \quad (145)$$

The last term in (145) is sometimes called the *Hall term*.

Next we use (126) to evaluate the friction force. The coefficient of \mathbf{J} in \mathbf{F}_e/en is the plasma resistivity, denoted by

$$\eta = \frac{m_e}{e^2 n \tau_{ei}} = \frac{1}{\sigma_\perp}. \quad (146)$$

Its inverse $\sigma_\perp \equiv e^2 n \tau_{ei}/m_e = \omega_p^2 \tau_{ei}/4\pi$ is the *perpendicular conductivity*. Using (126) we find that (145) can be expressed as

$$\mathbf{E} + \frac{1}{c} \mathbf{V} \times \mathbf{B} + \frac{1}{en} \left(\nabla p_e - \frac{1}{c} \mathbf{J} \times \mathbf{B} \right) = \eta \left[\mathbf{J} - \frac{3}{2} \frac{cn}{B} \mathbf{b} \times \nabla T_e \right], \quad (147)$$

in agreement with (137), since $p_e = p/2$.

By combining (147) with the equation of motion (138) we obtain an equivalent statement of the generalized Ohm's law,

$$\begin{aligned} \mathbf{E} + \frac{1}{c} \mathbf{V} \times \mathbf{B} - \frac{\nabla p_i}{en} - \frac{m_i}{e} \left[\frac{d\mathbf{V}_E}{dt} + \frac{d}{dt} |\mathbf{M}_{\text{HD}}(\mathbf{b} V_{||})| \right] \\ = \eta \left[\mathbf{J} - \frac{3}{2} \frac{cn}{B} \mathbf{b} \times \nabla T_e \right]. \end{aligned} \quad (148)$$

This is just the ion equation of motion in the drift model. It is less convenient in applications but displays the departure of \mathbf{V} from the lowest order form of (115). In particular, (148) shows that \mathbf{V}_\perp includes a contribution from $\mathbf{E} \times \mathbf{B}$ acceleration—the so-called *polarization drift*.

Equation (147) can be compared to the simplest Ohm's law, (84). Clearly the generalized Ohm's law contains much more physics; in fact it treats perpendicular electron dynamics accurately. However, since it is not a rigorous consequence of drift-ordered kinetic theory, (147) misses some effects of parallel electron dynamics, such as parallel temperature gradients and electron stress anisotropy, that can matter in some circumstances. Even the Ohmic term in (147) is not quite right: as shown in Chapter 8, the physical conductivity is anisotropic, with

$$\sigma_{||} \cong 2\sigma_\perp. \quad (149)$$

Finally, the electron-inertial terms that we have omitted are occasionally important, despite the small mass ratio.

On the other hand, the deficiencies of (147) are not always critical. Indeed, various effects contained in (147) are reproduced—at considerable effort—by more rigorous kinetic investigation, and some of them have striking effects on plasma stability. In this sense the generalized Ohm's law exemplifies what fluid models are supposed to provide: a short-cut to physical insight.

Equation of Motion*

The FLR equation of motion, (138), is surprisingly simple, involving only the advective derivative of \mathbf{V}_E rather than that of \mathbf{V} . Since gyroviscosity is involved, the absence of $d\mathbf{V}_p/dt$ terms is sometimes called the “gyroviscous cancellation.” It is not restricted to the drift model but is a general and crucial feature of FLR acceleration. Our main goal here is to examine its origin.

It is easy to write the general FLR version of (138). Starting from the species-summed acceleration law, (90), we use (118) and (120) for the ion and electron stress tensors respectively. In terms of the exact “gyroacceleration” vector,

$$\mathbf{f}_i \equiv m_i n \frac{d\mathbf{V}}{dt} + \nabla \cdot \boldsymbol{\Pi}_{gi}, \quad (150)$$

we obtain simply

$$\mathbf{f}_i - \frac{1}{c} \mathbf{J} \times \mathbf{B} + \nabla P = 0. \quad (151)$$

Especially after recalling (121)–(124), we see that \mathbf{f}_i conceals a considerable mess; unravelling it is the main burden of any FLR fluid derivation. What can be shown is that $\mathbf{f}_i = \mathbf{f}_{i\perp} + \mathbf{b} f_{i\parallel}$, where

$$\mathbf{f}_{i\perp} = m_i n \frac{d\mathbf{V}_E}{dt} - \nabla_\perp \left[\frac{p_i}{2\Omega_i} \mathbf{b} \cdot \nabla \times (\mathbf{V}_E + \mathbf{V}_{pi}) \right], \quad (152)$$

$$f_{i\parallel} = m_i n \frac{\partial V_\parallel}{\partial t} + \mathbf{V}_{MHD} \cdot \nabla V_\parallel - \nabla_\parallel \left[\frac{p_i}{\Omega_i} \mathbf{b} \cdot \nabla \times (\mathbf{V}_E + \mathbf{V}_{pi}) \right]. \quad (153)$$

Notice that the terms involving $\mathbf{b} \cdot \nabla \times (\mathbf{V}_E + \mathbf{V}_{pi})$, the parallel vorticity, are neglected in the drift model: they do not appear in (138), which uses instead

$$\mathbf{f}_i \cong m_i n \left[\frac{d\mathbf{V}_E}{dt} + \frac{d}{dt} |_{MHD} (\mathbf{b} \mathbf{V}_\parallel) \right]. \quad (154)$$

The reason is that vorticity enters (152) and (153), not only with a factor of $1/\Omega \propto \delta$, but inside a gradient operator. Thus the vorticity terms add to ∇p in (152), where, as small corrections to the pressure, they lack dramatic

consequences. (A concrete discussion of the importance of the vorticity-gradient terms may be found at the end of §6.6.) It is *not* argued that the vorticity is small; indeed, vorticity, as computed from the curl of (138), can play a key role in applications of the drift model.

Before considering the derivation of (152) and (153) we must comment on geometrical approximations that are invariably used. It is supposed that the magnetic field, if not precisely uniform, varies relatively slowly:

$$\nabla B = \epsilon B/L \ll B/L, \quad (155)$$

where ϵ is some geometric small parameter, here unspecified. It is further supposed that variation along the direction of \mathbf{B} , of any quantity F , is relatively weak:

$$\mathbf{b} \cdot \nabla F = \epsilon F/L. \quad (156)$$

It is then not hard to see, using also (111), that

$$\nabla \cdot \mathbf{V} \ll V/L, \quad (157)$$

i.e., that the plasma is approximately incompressible. Thus the drift model computes \mathbf{f}_i for an incompressible plasma, immersed in a uniform magnetic field, without variation in the direction of the field. However, since all terms in \mathbf{f}_i are of order δ^2 or smaller, the result is consistent with the inclusion of both field variation and compressibility elsewhere in the model. The formal statement is that one neglects $\mathcal{O}(\delta^2 \epsilon)$ but not $\mathcal{O}(\delta^2)$ or $\mathcal{O}(\epsilon)$.

Here we are content to outline the demonstration of (152); the detailed proof (Hazeltine and Meiss, 1985) is tedious and not enlightening. Since acceleration terms are $\mathcal{O}(\delta^2)$ in the drift model, we can study them in the approximation of (115). From this point of view the striking feature of (152) is the absence of $\min d\mathbf{V}_p/dt$ terms. Hence we consider

$$\begin{aligned} m_i n \frac{d\mathbf{V}_{pi}}{dt} &= \frac{n}{\Omega_i} \frac{d}{dt} \left(\frac{1}{n} \mathbf{b} \times \nabla p_i \right) \\ &= -m_i \mathbf{V}_{pi} \frac{dn}{dt} + \frac{1}{\Omega_i} \mathbf{b} \times \frac{d}{dt} \nabla p_i. \end{aligned}$$

Here, in view of (135), the first term is proportional to $\nabla \cdot \mathbf{V}$ and negligible. An identical comment would pertain to the second term, if $(d/dt) \nabla p_i$ were the same as $\nabla(d\mathbf{V}_p/dt)$; but in fact

$$m_i n \frac{d\mathbf{V}_{pi}}{dt} - \nabla \frac{dp_i}{dt} = \mathbf{V} \cdot \nabla(\nabla p_i) - \nabla(\mathbf{V} \cdot \nabla p_i)$$

does not vanish. Instead, the quantity

$$m_i n \frac{d\mathbf{V}_{pi}}{dt} \cong \frac{1}{\Omega_i} \mathbf{b} \times [\mathbf{V} \cdot \nabla(\nabla p_i) - \nabla(\mathbf{V} \cdot \nabla p_i)]$$

nearly cancels with $\nabla \cdot \Pi_{gi}$; a glance at (123) confirms that similar terms occur in both. What survives is simply the vorticity gradient terms of (152).

Similar comments pertain to the derivation of the parallel acceleration, (153); the mild anisotropy between \mathbf{f}_\perp and f_\parallel is a curiosity that causes little difficulty in applications.

In summary, the simple form of the FLR equation of motion depends upon a cancellation between the diamagnetic acceleration, $m_i n d\mathbf{V}_{pi}/dt$, and gyroviscosity. Effectively, gyroviscosity disposes of terms coming from the commutator

$$[(\mathbf{V} \cdot \nabla) \nabla - \nabla(\mathbf{V} \cdot \nabla)] p_i .$$

The derivation of the equation is relatively straightforward for an incompressible plasma, in a uniform magnetic field, without variation along \mathbf{B} . (Indeed, these are the assumptions of the original derivations.) But the result can be more generally applied, at least in the common case of mild field variation and small parallel gradients. This result is given quite accurately by (152) and (153). In the drift model the vorticity-gradient terms are neglected for simplicity rather than by any rigorous ordering argument.

6.6 Application of the Drift Model: Drift Waves

Drift Frequency

As noted in Chapter 1, confined plasmas are noisy. Even when macroscopically stable, they display a wide range of low level fluctuations, involving both plasma parameters and the electromagnetic field. A large component of the noise is electrostatic: fluctuations in the electrostatic potential, with $\langle e\Phi/T \rangle_{rms} \sim 5\%$ or more. These fluctuations buzz away without interrupting the discharge, but they are not harmless. By causing small scale, random advection, they diminish plasma confinement (see Chapter 9).

The spectrum of electrostatic fluctuations is broad, extending from near zero frequency to the 100 kiloHertz range and beyond. But it typically has a distinguishable peak near a range of frequencies associated with plasma fluid drifts. That is, if \mathbf{k} is a wave vector characterizing the fluctuations, then the observed central frequency is near the *drift frequency*, $\omega_* \equiv \mathbf{k} \cdot \mathbf{V}_p$, where \mathbf{V}_p is the diamagnetic drift of (112).

Since \mathbf{V}_{pi} and \mathbf{V}_{pe} differ (at least) in sign, we should distinguish the electron and ion drift frequencies. Convenient formal definitions are

$$\omega_{*e} \equiv -\frac{c}{neB} \mathbf{k} \cdot \mathbf{b} \times \nabla p_e , \quad (158)$$

$$\omega_{*i} \equiv -\frac{c}{neB} \mathbf{k} \cdot \mathbf{b} \times \nabla p_i . \quad (159)$$

The minus sign in (158) reflects the negative electronic charge. The special

case $T_i = T_e$ allows the simplified notation

$$\omega_* = \omega_{*e} = -\omega_{*i}. \quad (160)$$

Of course the pressures in (158) and (159) refer to the equilibrium state.

It is clear that $\omega_* \sim \delta v_t$. Indeed the drift frequency is the archetypal frequency of the drift ordering, explaining its name. The prevalence of perturbations with

$$\omega \sim \omega_*, \quad (161)$$

in both experiments and theoretical calculations, is a major reason for studying drift-ordered evolution.

Because of the multitude of instabilities satisfying (161)—one speaks for example of “drift-tearing instability,” “drift-Alfvén waves,” and “drift-balloonning modes”—it is useful to identify the *drift wave* with some specificity. We shall use the term *drift wave* to label a (primarily) electrostatic disturbance, whose frequency ω satisfies

$$k_{\parallel} v_{ti} \ll \omega_* \sim \omega \ll k_{\parallel} v_{te}. \quad (162)$$

Here $k_{\parallel} = \mathbf{b} \cdot \mathbf{k}$ is the parallel wave vector. Thus, in particular, drift waves cannot propagate unless the electrons are warm; on the other hand they easily propagate in the equal temperature case, because of the small mass ratio. The physical point of (162) is that wave evolution appears slow to electrons, which therefore respond “adiabatically,” remaining close to Maxwell-Boltzmann equilibrium:

$$n_e \exp\left(-\frac{e\Phi}{T_e}\right) \cong \text{constant}. \quad (163)$$

For ions on the other hand, wave motion is too fast for parallel equilibration; the ion response essentially reflects perpendicular advection:

$$\frac{dn_i}{dt} \cong 0. \quad (164)$$

Indeed the simplest derivation of the drift-wave dispersion relation consists of linearizing (163) and (164) and then using quasineutrality to equate the two densities. (A derivation from the drift model, also very simple, is given below.) The conventional language summarizes (163) and (164) by calling the electrons “adiabatic,” the ions “hydrodynamic.” While this language may be questionable, it is deeply embedded in the literature and shall be used in this book. In particular, by “electron adiabaticity” we mean the state described by (163).

Electrostatic Perturbations

The electrostatic limit is that in which magnetic perturbations are negligibly small, so that $\mathbf{E} \cong -\nabla\Phi$, and the parallel gradient can be taken

along the unperturbed field lines: $\nabla_{\parallel} \cong \mathbf{b}_0 \cdot \nabla$. Drift waves are a prominent prediction of the drift model, (135)–(138), in the electrostatic limit. We simplify the derivation by assuming very small resistivity, taking the magnetic field to be uniform, and keeping only $\mathcal{O}(\delta^2)$ terms in the equation of motion. This last simplification is equivalent to neglecting the polarization drift, so that \mathbf{V} is evaluated in the approximation of (115). It provides an algebraic dispersion relation that differs from more accurate results—differential equations—in the omission of $\rho^2 \nabla^2 \sim \delta^2$ terms.

With these approximations it is easy to verify that

$$\nabla \cdot \mathbf{V}_E = 0, \quad (165)$$

$$\nabla \cdot \mathbf{V}_p = -\mathbf{V}_p \cdot \nabla \ln n, \quad (166)$$

$$\nabla \cdot \mathbf{b} V_{\parallel} = \mathbf{b} \cdot \nabla V_{\parallel} \equiv \nabla_{\parallel} V_{\parallel}. \quad (167)$$

Hence, after recalling (130)–(134), we find that (135) and (136) become simply

$$\frac{d}{dt} \Big|_{\text{MHD}} n = -n \nabla_{\parallel} V_{\parallel}, \quad (168)$$

$$\frac{d}{dt} \Big|_{\text{MHD}} P = -\frac{5}{3} P \nabla_{\parallel} V_{\parallel}. \quad (169)$$

Notice that the right-hand side of (166), which is proportional to ∇T (since $\mathbf{V}_p \propto \mathbf{b} \times \nabla n$ when $\nabla T = 0$), cancels with the advective derivative in (135). Hence only *parallel compressibility*—the right-hand side of (167)—enters the present analysis. More generally, one has in addition perpendicular compressibility, arising from magnetic field curvature, as well as electromagnetic contributions to \mathbf{V}_E . In Chapter 7 we will find that some of these terms can affect plasma stability.

The absence of \mathbf{V}_p from (168) and (169) is important; it shows in particular that the occurrence of ω_{\star} terms in drift-wave theory is not a simple artifact of equilibrium diamagnetic rotation. Indeed, ω_{\star} will be seen to enter (169) through radial $\mathbf{E} \times \mathbf{B}$ motion.

It will also be seen that (168) is not needed to describe drift waves. What is needed, in addition to (169), are the parallel components of the equation of motion, (138),

$$m_i n \frac{d}{dt} \Big|_{\text{MHD}} V_{\parallel} + \nabla_{\parallel} P = 0, \quad (170)$$

and of the (electrostatic) Ohm's law,

$$\frac{1}{2en} \nabla_{\parallel} P - \nabla_{\parallel} \Phi = \eta J_{\parallel}. \quad (171)$$

That is, electrostatic evolution is described by the variables Φ , P , and V_{\parallel} .

Next we linearize the model equations, (169)–(171). Consistent with the uniform magnetic field we use cylindrical geometry, with cylindrical radius r . Our notation expresses each fluid variable F as $F = F_0 + F_1$, where the equilibrium value, F_0 , depends only on r ,

$$\nabla F_0 = \hat{\mathbf{r}} F'_0(r),$$

and where

$$\nabla F_1 = ikF_1, \quad \frac{\partial F_1}{\partial t} = -i\omega F_1. \quad (172)$$

Radial derivatives are denoted by primes; the exponential factor $\exp(-i\omega t + ik \cdot \mathbf{x})$ is left implicit. We also use the abbreviation:

$$k_\perp = \mathbf{b} \times \hat{\mathbf{r}} \cdot \mathbf{k}. \quad (173)$$

Finally, while allowing for an equilibrium electrostatic field, we assume that $V_{\parallel 0}$ vanishes in equilibrium: $V_{\parallel 0} = 0$, $\mathbf{V}_{E0} = \mathbf{b} \times \hat{\mathbf{r}} c\Phi'_0/B$. Of course there is a $\mathbf{V}_{p0} = \mathbf{b} \times \hat{\mathbf{r}} (cp'_0/2n_0eB)$, but it is not needed.

Then the MHD-advection derivative assumes the linear form

$$\frac{d}{dt}|_{\text{MHD}} F = -i(\omega - \omega_E)F_1 - ik_\perp \frac{c\Phi'_1}{B} F'_0, \quad (174)$$

where

$$\omega_E \equiv \frac{k_\perp c\Phi'_0}{B}. \quad (175)$$

Furthermore, since

$$\omega_* = -k_\perp \frac{cT}{eB} \frac{P'_0}{P_0}, \quad (176)$$

(169) becomes

$$-i(\omega - \omega_E) \frac{P_1}{P_0} + i\omega_* \frac{e\Phi_1}{T} = -i\frac{5}{3} k_\parallel V_{\parallel 1}. \quad (177)$$

Notice that the drift frequency enters (177), not through equilibrium diamagnetic rotation, but through perturbed radial motion in the equilibrium pressure gradient. For $V_{\parallel 1} \equiv V_{\parallel 1}$ we use (170) and (174):

$$-i(\omega - \omega_E)V_{\parallel 1} = -ik_\parallel \frac{P_1}{m_i n_0}. \quad (178)$$

Equation (178) describes parallel acceleration due to the pressure perturbation; aside from the ω_E term it corresponds to the description of sound propagation in a neutral gas. We substitute (178) into (177) to find

$$\frac{P_1}{P_0} = \frac{\omega_* - \omega_E}{\omega - \omega_E} \frac{e\Phi_1}{T} + \frac{5}{3} \frac{k_\parallel^2}{m_i n_0 (\omega - \omega_E)^2} P_1.$$

Note here that $P_0 = 2n_0T$ implies $P_1/(m;n_0) = (P_1/P_0)(2T/m) = v_{ti}^2(P_1/P_0)$, where v_{ti} is the ion thermal speed. Thus we have

$$\frac{P_1}{P_0} \left[1 - \frac{5}{3} \frac{k_{\parallel}^2 v_{ti}^2}{(\omega - \omega_E)^2} \right] = \frac{\omega_*}{\omega - \omega_E} \frac{e\Phi_1}{T}, \quad (179)$$

showing that the pressure perturbation is modified by parallel sound wave propagation. Finally we linearize the Ohm's law, (171), to find $ik_{\parallel} P_1/(2en_0) = ik_{\parallel} \Phi_1$ or

$$\frac{P_1}{P_0} = \frac{e\Phi_1}{T}. \quad (180)$$

This is of course the adiabatic response of (163).

The drift-wave dispersion relation is obtained from (179) and (180):

$$1 - \frac{5}{3} \frac{k_{\parallel}^2 v_{ti}^2}{(\omega - \omega_E)^2} = \frac{\omega_*}{\omega - \omega_E}. \quad (181)$$

Note that an equilibrium radial electric field simply Doppler-shifts the wave frequency. From (163) we see that the left-hand side of (181) is nearly unity in the drift wave regime; hence $\omega \cong \omega_E + \omega_*$, and (181) is well approximated by

$$\omega \cong \omega_E + \omega_* \left[1 + \frac{5}{3} \frac{k_{\parallel}^2 v_{ti}^2}{\omega_*^2} \right]. \quad (182)$$

The combination $\omega_E + \omega_*$ that appears in (182) is the standard combination of pressure and potential gradients, occurring in, for example, the electron version of (35):

$$\mathbf{k} \cdot (\mathbf{V}_{E0} + \mathbf{V}_{pe0}) = \omega_E + \omega_*.$$

Equation (182) is the statement that the hydrodynamic ion response of (179) can match the adiabatic electron response of (180) if and only if the (Doppler-shifted) frequency is close to the drift frequency. The adiabaticity condition,

$$\omega \ll k_{\parallel} v_{te}$$

enters implicitly, through the neglect of electron inertia in (137).

Drift-Wave Stability*

The drift wave of (181) is purely oscillatory. Instability can result from a small, nonadiabatic contribution to the electron density perturbation,

$$\frac{n_1}{n_0} \rightarrow (1 - i\Delta) \frac{e\Phi_1}{T} \quad (183)$$

provided it has the proper phase:

$$\Delta > 0 .$$

Unfortunately the drift model, while providing a physical and accurate calculation of the real dispersion relation, is not reliable concerning Δ . Expressions for Δ that apply to contemporary experiments depend on kinetic effects, such as Landau damping and particle trapping, not contained in (135)–(138). Indeed, determining the stability of drift waves in parameter regimes of fusion interest involves considerable mathematical intricacy.

Yet the drift model does predict drift wave instability, $\Im(\omega) > 0$, because of electron dissipation. This result, if primitive, has some features in common with more sophisticated conclusions. Furthermore its derivation, involving ion acceleration and \mathbf{V}_{p0} , introduces concepts of general interest. In fact it provides a brief introduction to some of the ideas explored at greater length in Chapter 7.

Hence we compute Δ from the drift model. The key step is to allow for a small perturbed current, consistently with the electrostatic approximation. Thus (180) is replaced by

$$\frac{P_1}{P_0} = \frac{e\Phi_1}{T} - i\eta \frac{eJ_{\parallel}}{k_{\parallel} T} . \quad (184)$$

We compute the parallel current from quasineutrality,

$$\nabla_{\parallel} J_{\parallel} = -\nabla_{\perp} \cdot \mathbf{J}_{\perp} \quad (185)$$

and the drift model equation of motion, (138):

$$\mathbf{J}_{\perp} = \frac{m_i c}{B^2} \mathbf{B} \times (n \frac{d\mathbf{V}_E}{dt} + \nabla P) . \quad (186)$$

Here the diamagnetic term makes no contribution to the divergence, because \mathbf{B} is uniform.

The combination of (185) and (186) gives a version of the *shear-Alfvén law*, which will be an object of central interest in Chapter 7. Regarding the acceleration term, we note that $\mathbf{B} \times \mathbf{V}_E = -c\nabla_{\perp}\Phi$ and for simplicity neglect the variation of n (which is replaced by n_0 in linear theory) to find

$$\mathbf{J}_{\perp} \cong -\mathbf{k}_{\perp} \frac{n_0 m_i c^2}{B^2} (\omega + \omega_* - \omega_E) \Phi . \quad (187)$$

Notice that ω_* appears here with a positive sign; it is in fact ω_{*i} [recall (160)], stemming from \mathbf{V}_{p0} , and has the sign appropriate to the ionic charge:

$$\omega + \omega_* - \omega_E = \omega - \omega_{*i} - \omega_E .$$

It is clear from (185) that the parallel current driven by (187) is a *return current*, in the sense of §3.3. The destabilizing role of return currents in

drift-wave theory pertains generally, even when more elaborate physical processes are included.

After substituting (187) into (184) and (185) we find that (183) is reproduced with

$$\Delta = 2\omega_* \frac{m_i c^2}{B^2 n_0 \eta} \left(\frac{k_\perp}{k_\parallel} \right)^2. \quad (188)$$

The resulting dispersion relation predicts

$$\omega \cong \omega_E + \omega_* (1 + i\Delta). \quad (189)$$

It is said to describe the collisional *drift instability*.

It is helpful to rewrite Δ , using (146), in terms of basic frequencies of interest; one finds that

$$\Delta = 2 \frac{m_e}{m_i} \frac{\omega_*}{\Omega_i^2 \tau_{ei}} \left(\frac{k_\perp}{k_\parallel} \right)^2. \quad (190)$$

Here the first two factors are very small, as assumed in (189). Note in particular that small Δ implies small J_\parallel , thus preserving the primarily electrostatic nature of the drift wave.

Equation (190) shows that drift waves are strongly stabilized by large k_\parallel —a property shared, as we shall see, with the vast majority of plasma instabilities. It follows that drift-wave stability is sensitive to magnetic shear, and that analysis based on a uniform magnetic field is oversimplified (Antonsen, 1978). When magnetic shear is included, so that k_\parallel becomes a function of radius, the eigenmode develops rather elaborate radial structure. In this case, while (182) remains qualitatively pertinent, stability is determined by the higher-order (polarization drift) terms that we have neglected.

Finally we note that the effects of toroidicity on particle orbits, even at very low collision frequency, can produce a destabilizing Δ -correction, as in (183); the so-called *trapped particle modes* and their relatives are in fact drift waves, destabilized by toroidal curvature, and surviving despite the stabilizing effects of magnetic shear (Mikhailovskii, 1974).

Vorticity Correction*

We conclude this section with an example of physics that the drift model misses. Recall that the vorticity terms in (152) and (153) have been neglected; to see their significance, we continue to assume cylindrical symmetry with uniform \mathbf{B} and then compute

$$\mathbf{b} \cdot \nabla \times (\mathbf{V}_E + \mathbf{V}_{pi}) = \frac{c}{B} \nabla^2 \Phi + \frac{c}{eBn} \left[\nabla^2 P - \frac{1}{n} (\nabla \mathbf{n} \cdot \nabla P - \nabla_\parallel \mathbf{n} \nabla_\parallel P) \right]. \quad (191)$$

The effect on the perpendicular equation of motion is accounted for by the replacement

$$P \rightarrow P_{\perp*} \equiv P - \frac{T}{4\Omega_i^2 m_i} \left[\nabla^2 P + en\nabla^2\Phi - \frac{1}{n} \nabla_{\perp} n \cdot \nabla P \right]. \quad (192)$$

The corresponding replacement in the parallel equation of motion is

$$P \rightarrow P_{\parallel*} \equiv P - \frac{T}{2\Omega_i^2 m_i} \left[\nabla^2 P + en\nabla^2\Phi - \frac{1}{n} \nabla_{\perp} n \cdot \nabla_{\perp} P \right]. \quad (193)$$

Since $T/(\Omega^2 m_i) = (1/2)\rho_i^2$, these results have the rough form,

$$P_* \cong (1 - \rho_i^2 \nabla^2)P, \quad (194)$$

which is characteristic of FLR corrections. It corresponds to the gyrophase average $P = \langle p_*(\mathbf{X} + \boldsymbol{\rho}) \rangle$, discussed in Chapter 4, and reflects the smeared pressure profile seen by a gyrating ion.

The replacement of P by P_* has negligible effect on the drift wave. Indeed, $P_{\perp*}$ does not enter the drift-wave dispersion relation, while $P_{\parallel*}$ only slightly modifies the acoustic term, $k_{\parallel}^2 v_{ti}^2$, which is already small by (162). This circumstance is typical: the vorticity pressure corrections in (152) and (153) rarely affect stability. But they are not always unimportant. In particular the vorticity corrections enter equilibrium force balance, as considered in Chapter 3. By smearing the pressure gradient in the force balance equation—whose differential order is thereby changed—they help to resolve singularities that might otherwise arise on rational flux surfaces. It should be recalled that the drift-wave dispersion relation (181), based on (115), is not a rigorous prediction of the drift model. Without deriving the rigorous version here, we note that it contains FLR corrections of the form $-\rho_i^2 \nabla^2\Phi$, which, unlike the vorticity gradient terms, do affect drift-wave stability. The main effect is to replace the algebraic dispersion relation by a differential equation in radius, as we have mentioned.

6.7 Summary

Velocity moments of the general kinetic equation, expressing macroscopic conservation laws, provide expeditious physical insight. In particular, the (contracted) even moments, describing the evolution of plasma density and pressure, directly address the key issues of confinement. On the other hand, since the even moments do not contain the magnetic field, magnetic effects on particle and energy flow must be understood in terms of odd moment equations.

The efficient use of kinetic theory lies at the heart of all plasma fluid systems. Because coordinate space has fewer dimensions than phase space,

the moment or fluid equations are usually easier to solve than kinetic equations. However, reliable application of fluid theory depends ultimately upon kinetic information, since it requires a convincing closure scheme.

The small gyroradius parameter provides asymptotically rigorous, if only partial, closure for the fluid description of a magnetized plasma. That is, the perpendicular components of the N^{th} moment can be expressed in terms of lower order moments, to any desired accuracy. Thus one determines, from relatively crude kinetic information, accurate expressions for such important fluid quantities as the perpendicular particle and energy flows, and the gyroviscosity tensor.

Unfortunately this method leaves parallel components—"manipulation constants"—undetermined in each order. It follows that rigorous closure schemes, such as kinetic MHD or Chapman-Enskog theory, resort to kinetic theory to analyze dynamics along \mathbf{B} .

Fluid truncation schemes abandon asymptotic rigor in favor of clarity and simplicity. The primary example of such truncation is ordinary MHD, a closed system with demonstrated experimental relevance. The fundamental assumption of MHD theory is simply an allowance for large electric fields: the statement that the $\mathbf{E} \times \mathbf{B}$ drift is comparable to the thermal speed, outweighing any other contribution to plasma motion. When pursued rigorously, this assumption leads to a combination of fluid and kinetic theory called kinetic MHD. When, on the other hand, it is combined with an oversimplified if plausible kinetic *ansatz*, it leads to the famous fluid equations that underlie most confined plasma stability investigations.

The main weakness of MHD pertains to realism, rather than rigor: modern confinement experiments rarely exhibit electric fields or fluid velocities as large as MHD presumes. The observed motions, including those associated with instability and even disruption, are relatively slow, with $\mathbf{E} \times \mathbf{B}$ drifts no larger than diamagnetic drifts. The *drift ordering* approximates the plasma flow by a combination of $\mathbf{E} \times \mathbf{B}$ and diamagnetic motion, assuming both to be smaller than the thermal speed by the small gyroradius parameter, δ . Because it relegates dynamics to $\mathcal{O}(\delta)$ terms, which therefore must be reckoned with care, the drift ordering is said to provide FLR (finite Larmor radius) equations of motion.

As in the MHD-ordered case, the rigorous FLR system has recourse to kinetic theory—the drift or gyrokinetic equations of Chapter 4. But also like the MHD case, plausible assumptions about the lowest order distribution function can provide closed, reasonably tractable fluid equations. What is distinctive about FLR theory is the absence of any widely accepted truncation hypothesis, akin to the MHD *ansatz*. No FLR system has the wide acceptance of MHD; FLR fluid equations constructed in different contexts rarely coincide in detail.

We have examined two fluid descriptions of FLR physics. The first, relatively general FLR model is based on an especially natural kinetic **assumption—a close analog of the MHD ansatz**. Unfortunately, this sim-

plest assumption does not yield simple results: the general FLR system is burdened by numerous terms of dubious practical importance. Hence we resort to a simpler version, called the *drift model*, that is very similar to systems prevalent in the confinement literature. It incorporates crucial FLR physics in a form hardly more complicated than MHD. The key to its simplicity is the absence of diamagnetic acceleration terms—an artifact of gyroviscosity that pertains to any FLR model.

Application of plasma fluid theory is a major subject of Chapters 7 and 8, since fluid equations provide the simplest access to both stability and transport. Here we have studied a single application, the fluid description of *drift waves*. Disturbances with frequencies near the drift frequency seem to play an important role in present confinement experiments. Their oscillation frequency is an elementary consequence of diamagnetism and $\mathbf{E} \times \mathbf{B}$ motion across a radial pressure gradient, well described by the drift model. Ion acceleration in the wave drives a perpendicular current whose divergence does not vanish; the corresponding return current destabilizes the wave.

Further Reading on

Fluid Equations:

Braginskii, 1965
Bernstein and Trehan, 1960

MHD:

Bateman, 1980
Freidberg, 1987

Drift Waves:

Krall, 1968
Mikhailovskii, 1974

Exercises

1. Verify (10), for the pressure tensor, and (11), for the heat flux.
2. Cold plasma. In some beam plasmas the flow velocity far exceeds the thermal velocity. The cold plasma model idealizes this situation by taking each species temperature to vanish; the distributions are delta functions centered at the species flow speed \mathbf{V}_s .

Derive an exact set of closed fluid equations for a cold plasma with a single ion species. Discuss the relation between energy conservation, (23), and momentum conservation, (24), in the cold plasma case.

3. Compute all contravariant components of the stress tensor \mathbf{P}_{CGL} with respect to flux coordinates (r, θ, ζ) , in terms of P_{\perp} , P_{\parallel} and components of \mathbf{B} .
4. Express (60) explicitly as a law for evolution of the parallel stress tensor. Assume for simplicity that the magnetic field is uniform.

5. When unlike-species collisions are omitted (a common approximation to ion kinetics), the first nonvanishing collisional moment is $C^{(2)}$. Show that

$$C_{\alpha\beta}^{(2)} = -\frac{m\gamma}{2} (K_{\alpha\beta} + K_{\beta\alpha}),$$

$$K_{\alpha\beta} = \int d^3v \int d^3v' f_M f'_M (v_{\alpha} - v'_{\alpha}) U_{\beta\lambda} \left(\frac{\partial \hat{f}}{\partial v_{\lambda}} - \frac{\partial \hat{f}'}{\partial v'_{\lambda}} \right).$$

Here the tensor $U_{\alpha\beta}$ is defined by (4.37).

6. **Collisional viscosity.** We have noted that collisional viscosity is relatively small. It is also surprisingly easy to calculate, at least whenever the gyroaveraged distribution can be approximated by a displaced Maxwellian,

$$\bar{f} = f_M \left(1 + 2 \frac{v_{\parallel} V_{\parallel}}{v_t^2} \right). \quad (*)$$

- (a) Use $(*)$ and the method of (62) *et seq.* to derive an expression for Π_e as a collisional moment of the distribution $-\frac{1}{n} \mathbf{b} \times \mathbf{v} \cdot \nabla [(2V_{\parallel} v_{\parallel}^2/v_t^2) f_M]$.
- (b) Use the Krook model collision operator to compute the collisional viscosity component Π_{e12} . Assume for simplicity that \mathbf{B} , \mathbf{n} and T are spatially constant, and that $\mathbf{b} \cdot \nabla V_{\parallel} = 0$.

For comparison, the exact result is $\Pi_{e12} = -(6/5)[p_i/(\Omega_i^2 r_i)]\mathbf{e}_2 \cdot \nabla V_{\parallel}$. Even this version is straightforward, if rather lengthy, to calculate; if you try it, begin with the formula given in Problem 5.

7. Suppose that a symmetric second rank tensor T satisfies

$$\mathbf{e} \cdot \mathbf{T} \cdot \mathbf{e} = 0 = Tr(\mathbf{T}), \\ \mathbf{e} \times \mathbf{T} + (\mathbf{e} \times \mathbf{T})^* = \mathbf{S},$$

where \mathbf{e} is a specified unit vector and \mathbf{S} a known tensor. Show that a particular solution for T is

$$\mathbf{T} = -\frac{1}{4}\{[\mathbf{e} \times \mathbf{S} + 3\mathbf{e} \times (\mathbf{e} \cdot \mathbf{S})\mathbf{e}] + [\mathbf{e} \times \mathbf{S} + 3\mathbf{e} \times (\mathbf{e} \cdot \mathbf{S})\mathbf{e}]^T\}.$$

- 8.** Show that ideal MHD requires the electric field in the plasma rest frame to vanish.
- 9.** In the Standard Tokamak³, what radial electric field, in Volts/cm, is necessary for the poloidal $\mathbf{E} \times \mathbf{B}$ drift to satisfy the MHD ordering?
- 10.** Derive from (106) the MHD law for evolution of the field magnitude B . Compare the result to the pressure law, (102).
- 11.** Show that drift-wave consistency requires the wave-vector \mathbf{k} to satisfy

$$\left(\frac{m_e}{m_i}\right)^{1/2} \frac{\rho_i}{L} \ll \frac{k_{\parallel}}{k_{\perp}} \ll \frac{\rho_i}{L}.$$

Thus drift waves propagate in a direction nearly, but not exactly, perpendicular to the magnetic field.

- 12.** Derive the drift-wave dispersion relation for the cold-ion case—that is, the $v_{ti} \rightarrow 0$ limit of (181)—by linearizing (163) and (164).

³Recall problem 5 of Chapter 3

Chapter 7

Stability of Confined Plasmas

7.1 General Stability Considerations

The formal definition of stability is quite natural; it is based on intuitive ideas. Consider for example a simple pendulum—a rod suspended at one end in a gravitational field. There are two equilibria: the rod can either hang vertically down or be balanced vertically above the support. Naturally only the first of these positions is stable: any small deviation from the low equilibrium point leads to small oscillations about the equilibrium. When there is dissipation, such as friction, the oscillations decay, and the asymptotic state of the pendulum is its stable equilibrium point. By contrast, the second equilibrium point is unstable: nearby trajectories deviate from equilibrium by a distance which grows exponentially with time.

A confined plasma differs from the pendulum not only in being more complicated, but also because it is a driven system, forced away from its natural (thermodynamic) equilibrium state. Partly for this reason, as we noted in Chapter 1, confined plasmas are rarely completely stable: observed equilibria display a variety of unstable excitations. Some, such as disruptions, can destroy the discharge; others, such as sawtooth oscillations, saturate at tolerable amplitudes, apparently affecting confinement only by enhancing diffusion rates. The attempt to understand, predict and control plasma instability has been a major goal of the fusion research program since its beginning.

The general problem of stability can be formally expressed in terms of an evolution equation

$$\frac{d}{dt} \chi = N(\chi). \quad (1)$$

This may represent a set of ordinary differential equations, as for the pendulum, partial differential equations, as for MHD, or even integro-differential equations, as in kinetic theory. Suppose that we have determined an equilibrium point χ_0 :

$$N(\chi_0) = 0. \quad (2)$$

How do we study the stability of χ_0 ? We begin by considering some of the ideas and terminology used to characterize stability.

The most fundamental definition of stability (one that could be termed “stability” without any modifier) is

Lyapunov stability: an equilibrium χ_0 is stable if, for any neighborhood U of χ_0 , all initial conditions in some smaller neighborhood V stay in U .

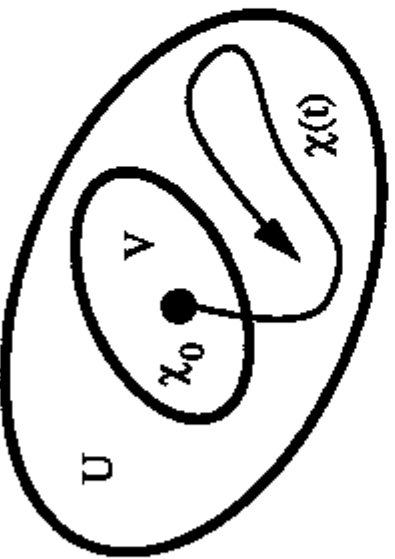


Figure 1. Lyapunov stability corresponds to the trajectory $\chi(t)$ remaining forever in U , if it started in V .

Thus a system is Lyapunov stable if the solution $\Delta\chi(t)$ of

$$\frac{d}{dt} \Delta\chi = N(\chi_0 + \Delta\chi) \quad (3)$$

stays bounded for all time. Unfortunately the Lyapunov criterion, while desirable, is usually too difficult to verify, since it seems to require the exact solution of the problem for $\Delta\chi$ for all time: note that (3) is in general nonlinear.

Acknowledging that a nonlinear system is usually intractable, and that we are interested mostly in showing that solutions starting “very” close to χ_0 stay close, we can study the linearization of (3). Expanding N about χ_0 gives

$$N(\chi_0 + \delta\chi) = N'(\chi_0)\delta\chi + \dots,$$

where $N'(\chi_0) = L$ is a linear operator, so the equation for $\delta\chi$ becomes

$$\frac{d}{dt} \delta\chi = L\delta\chi. \quad (4)$$

Study of the solutions to (4) yields the notion of

Linear stability: an equilibrium χ_0 is linearly stable if every solution to the linearized equation (4) is bounded as $t \rightarrow \infty$.

A slightly stronger notion of linear stability is:

Asymptotic linear stability: an equilibrium has asymptotic linear stability if every solution to (4) tends to zero as $t \rightarrow \infty$.

Note that a conservative system can never be asymptotically stable, since this would require contraction or dissipative behavior.

A common technique for studying linear stability is to compute the eigenvalues of the linear operator L . This leads to the notion of

Spectral stability: an equilibrium is spectrally stable if every eigenvalue of the linearized operator L has a nonpositive real part.

Unfortunately a system can be spectrally stable, but not linearly stable. The difference between the two notions is apparent even for a system of ordinary differential equations. Consider for example the 2×2 system,

$$\frac{d}{dt} \delta\chi = \begin{pmatrix} 0 & 1 \\ 0 & 0 \end{pmatrix} \delta\chi. \quad (5)$$

This system has a double eigenvalue at 0, and thus is spectrally stable; however there are solutions that blow up for large time, for example $\begin{pmatrix} t \\ 1 \end{pmatrix}$. Thus the system is not linearly stable. In general the notions of spectral and linear stability differ only when there are multiple eigenvalues on the imaginary axis.

Similarly a system can be linearly stable, and not Lyapunov stable.

Consider for example the differential equation

$$\frac{d}{dt} \chi = \begin{pmatrix} 0 & 1 \\ -1 & 0 \end{pmatrix} \chi + \begin{pmatrix} \chi_1(\chi_1^2 + \chi_2^2) \\ \chi_2(\chi_1^2 + \chi_2^2) \end{pmatrix}. \quad (6)$$

The equilibrium $\chi = 0$ is spectrally stable, since the eigenvalues are $\pm i$, and linearly stable, since all solutions of the linearized version are bounded. However, it is not Lyapunov stable, since by introducing $R = \chi_1^2 + \chi_2^2$, it can be seen that

$$\frac{d}{dt} R = 2R^2 \implies R(t) = \frac{R_0}{1 - 2R_0 t} \quad (7)$$

so that $R(t)$ approaches infinity in finite time for every initial condition, including those arbitrarily close to $R = 0$.

On the other hand, for ordinary differential equations, asymptotic linear stability does imply Lyapunov stability:

Poincaré-Lyapunov Theorem: If the linearization, (4), of a system of ordinary differential equations is asymptotically stable, and $N(\chi_0 + \Delta\chi) - L\Delta\chi \sim \mathcal{O}(\Delta\chi^2)$, then the equilibrium χ_0 is Lyapunov stable.

The situation is somewhat more complicated for partial differential equations: even if all the eigenvalues have negative real parts, they can still

accumulate on the imaginary axis, which can lead to instability of the nonlinear system. Furthermore a linear partial differential equation can have continuous components to its spectrum. In this case spectral stability does not imply linear stability, even if the eigenvalues are bounded away from the imaginary axis. Such problems are not merely academic; they arise in practice, as we will see.

There are two methods for showing that a partial differential equation is Lyapunov stable; unfortunately both are difficult to apply in practice. The first is somehow to find a *Lyapunov functional*. This is a functional $F[\chi]$ which has a minimum at the equilibrium point, $F[\chi_0] < F[\chi]$ for $\chi \neq \chi_0$, and which decreases with time: $dF/dt < 0$ for $\chi \neq \chi_0$. These conditions imply that the equilibrium is an attractor: all initial conditions eventually approach χ_0 .

The construction of such a functional is never easy, and clearly impossible for conservative systems. For conservative systems we can use a related idea: suppose that $F[\chi]$ is conserved by (1) and has a critical point at the equilibrium χ_0 . This happens, for example, when F is the Hamiltonian. The first variation of F , δF , then vanishes at χ_0 , and the second variation is the quadratic functional defined by

$$F[\chi + \xi] - F[\chi_0] \rightarrow \delta^2 F[\xi] \quad \text{as } \|\xi\| \rightarrow 0. \quad (8)$$

In this case we can use

Dirichlet's criterion (Energy Principle): If the second variation of F at χ_0 is uniformly positive definite:

$$\delta^2 F[\xi] \geq C \|\xi\|^2 \quad \text{for any } \xi \quad (9)$$

then χ_0 is Lyapunov stable.

The basic idea is that (9) implies that the surfaces of constant F must be ellipsoids near χ_0 ; since F is conserved the motion can never leave one of these ellipsoids. By assumption the first variation of F at the equilibrium is zero. Thus, by definition of the second variation,

$$F[\chi + \xi] = F[\chi_0] + \delta^2 F[\xi] + \varepsilon(\|\xi\|) \|\xi\|^2$$

and $\varepsilon \rightarrow 0$ as $\|\xi\|^2 \rightarrow 0$. In particular, by choosing $\|\xi\|$ so small that $|\varepsilon| < C/2$, we can conclude that

$$F[\chi + \xi] - F[\chi_0] > \frac{C}{2} \|\xi\|^2. \quad (10)$$

Now F is conserved, so the left-hand side of (10) is constant; therefore, $\|\xi\|^2$ is bounded for all time. Furthermore, by continuity, $F[\chi + \xi] \rightarrow F[\chi]$ as $\|\xi\|^2 \rightarrow 0$; therefore the size of the deviation also must vanish in this limit.

In general we think of $F[\chi]$ as the free energy of the system (Morrison and Kotschenreuther, 1990).

While the energy principle provides a sufficient condition, it is not necessary for stability: it is possible that χ_0 is stable even when the second variation is not positive definite. Showing stability in this case is an extremely delicate matter, however. The most sophisticated and elaborate results of the modern theory of dynamical systems (the Kolmogorov-Arnol'd-Moser Theorem, Arnol'd diffusion, Nekhoroshev's theorem, etc.) do not resolve the question. For more information on these matters consult (MacKay and Meiss, 1987).

Before applying these general stability considerations to plasma confinement we review the basic properties of electromagnetic perturbations in a plasma.

Part 1: Shear Alfvén Waves

7.2 Ideal MHD Waves

An infinite, homogeneous MHD plasma exhibits waves of three types: shear-Alfvén, compressional Alfvén and sound waves. These basic modes are still present in toroidal geometry, although they can be altered significantly. Here, for introductory purposes, we recall the dispersion relation for the homogeneous case.

We adopt the MHD model of §6.4, using the linearized equations to study spectral stability. Assume that the equilibrium consists of a stationary, homogeneous magnetized plasma, with $\mathbf{v} = 0$, $\rho_m = \rho_{m0}$, $P = P_0$, and that the magnetic field is constant, $\mathbf{B} = B_0 \hat{\mathbf{z}}$. Linearization of the MHD system (6.101), (6.105) and (6.106) about this state gives seven equations of motion for the perturbed fields, ρ_{m1} , \mathbf{v}_1 , and \mathbf{B}

$$\begin{aligned}\frac{\partial \rho_{m1}}{\partial t} &= -\rho_{m0}(\nabla \cdot \mathbf{v}_1), \\ \rho_{m0} \frac{\partial \mathbf{v}_1}{\partial t} &= -\nabla P_1 + \frac{1}{4\pi c} \mathbf{B}_0 \times (\nabla \times \mathbf{B}_1), \\ \frac{\partial \mathbf{B}_1}{\partial t} &= \nabla \times (\mathbf{v}_1 \times \mathbf{B}_0).\end{aligned}\quad (11)$$

The pressure is determined by the density through the equation of state $P = C\rho_m^{5/3}$, whence $P_1 = 5/3\rho_{m1}(P_0/\rho_{m0})$; thus there are seven unknown quantities in (11). Since the equilibrium quantities are constants, it is prof-

itable to Fourier transform the equations in both space and time:

$$\omega \rho_{m1} = \rho_{m0}(\mathbf{k} \cdot \mathbf{v}_1),$$

$$\omega \rho_{m0} \mathbf{v}_1 = \mathbf{k} P_1 + \frac{1}{4\pi c} \mathbf{B}_0 \times (\mathbf{k} \times \mathbf{B}_1), \quad (12)$$

$$\omega \mathbf{B}_1 = -\mathbf{k} \times (\mathbf{v}_1 \times \mathbf{B}_0).$$

Of course ω is the frequency and \mathbf{k} is the wave vector. The dispersion relation is obtained by demanding that the determinant of the matrix defined by (12) be zero. After some algebra we find

$$\omega \left(\omega^2 - k_{\parallel}^2 v_A^2 \right) [\omega^4 - \omega^2 k^2 (v_S^2 + v_A^2) + (k k_{\parallel} v_S v_A)^2] = 0. \quad (13)$$

Here v_A is the Alfvén speed, $k_{\parallel} \approx \mathbf{b} \cdot \mathbf{k}$, and $v_S = \sqrt{\frac{5}{3}(P_0/\rho_{m0})}$ is the sound speed. It is easy to see that the solutions of (13) for the eigenvalues ω are always real. Thus the homogeneous MHD system is spectrally stable. Each solution of (13) represents a mode of oscillation of the plasma. The seven modes are:

- 1) $\omega = 0$, $\mathbf{v}_1 = 0$, and $P_1 = \frac{1}{c} \mathbf{B}_0 \cdot \mathbf{B}_1$. This corresponds to a static displacement of the fluid to a neighboring equilibrium solution.
- 2) $\omega = \pm k_{\parallel} v_A$. This is the shear-Alfvén mode. It is incompressible, $\rho_1 \approx P_1 \approx 0$, and purely transverse: both \mathbf{v}_1 and \mathbf{B}_1 are perpendicular to \mathbf{B}_0 .

The quadratic equation for ω^2 given by the term in brackets in (13) yields two more distinct modes, the fast and slow magnetosonic waves, arising from the coupling between magnetic compression (Alfvénic) and fluid compression (sonic). These modes approximately decouple when the ratio $(v_S/v_A)^2 = \frac{5}{6}\beta$, which is typically the case. In this limit we obtain the solutions

- 3) $\omega = \pm k v_A$. This describes the compressional Alfvén mode. In this case the parallel velocity is $\mathcal{O}(\beta)$ compared to the perpendicular velocity, which must lie in the plane formed by \mathbf{B} and \mathbf{k} . The ratio $P_1/B_0 B_1 \sim \mathcal{O}(\beta)$, so most of the compressional energy is in the magnetic field.

- 4) $\omega = \pm k_{\parallel} v_S$. This describes the sound wave. In this case $\mathbf{k}_{\perp} \cdot \mathbf{v}_1 = 0$, so the compression is purely longitudinal. Since $\mathbf{B}_1 \cdot \mathbf{B}_0 = 0$, the compressional energy is primarily due to fluid motions.

A similar dispersion relation cannot be obtained in general for a toroidal system because the transformation of the differential equations (11) to an algebraic system (12), relied upon the homogeneity of the equilibrium. To proceed, we next develop simplified descriptions, which nonetheless exhibit the main features of the stability problem.

7.3 Shear-Alfvén Law

The salient issues for stability of toroidal equilibria can be understood in terms of a single equation, derived from the equation for conservation of momentum. We call this equation the *shear-Alfvén law*; it governs the low frequency dynamics of the plasma.¹ It displays, in model-independent form, the essential physics of stability and nonlinear evolution: rational surface singularities, interchange forces, current gradients, plasma vorticity, and magnetic nonlinearity. It also is helpful in motivating the essential spatial and temporal scales. We derive the shear-Alfvén law after characterizing the type of low-frequency perturbation that is most likely to be unstable in a toroidal system.

Flute Perturbations

Consider an arbitrary perturbation, $h(\mathbf{x}, t)$, of some variable describing a toroidally confined plasma. Use of flux coordinates, (r, θ, ζ) , permits the expansion of h in a Fourier representation (3.27). Such a decomposition is especially useful when the system has cylindrical symmetry and when the equations of motion are linear, for then each Fourier mode, $h_{mn}(r, t)$, evolves independently. However, in toroidal geometry the modes are coupled even in the linear limit. Nonlinearity also couples the modes, leading to such effects as energy cascades and chaos.

Despite the coupling, it is often convenient to identify perturbations by their dominant wave vector

$$\mathbf{k} = m \nabla \theta - n \nabla \zeta . \quad (14)$$

Here m , the poloidal mode number, and n , the toroidal mode number, are integers; the helicity of the harmonic is characterized by the ratio of the mode numbers, m/n . Recall that typical confined plasma equilibria are characterized by a magnetic field that also has a helicity, given by the safety factor q .

As we have seen for the homogeneous MHD system, there is a great difference between perturbations aligned with, and those perpendicular to, the magnetic field: these give rise to shear-Alfvén and compressional modes respectively. In the case of inhomogeneous plasmas, this difference is even more important. Modes that are predominantly aligned with the magnetic field tend to be the most dangerous perturbations; as in §3.3 we call such disturbances *flare-like modes*. The point is that modes with significant \mathbf{k}_{\parallel} must distort the magnetic field; as in the homogeneous MHD system, such distortion gives rise to a strong restoring force.

A perturbation is (nearly) aligned with the magnetic field when its

¹The shear-Alfvén law was also mentioned in (6.185) *et seq.*

parallel wavevector is zero (small). Using the definition of the safety factor (3.21), we find that the parallel wavevector

$$k_{\parallel} = \mathbf{k} \cdot \mathbf{b} = \mathbf{b} \cdot \nabla \theta(m - nq) = \frac{\chi'}{\sqrt{gB}} (m - nq) \quad (15)$$

depends on position through the contravariant component, b^{θ} , but most significantly through the factor $m - nq$. Since $q(r)$ depends on radius, the parallel wavevector can locally vanish. We will find that this leads to a singularity in the shear-Alfvén law, with profound physical consequences. Furthermore the parallel wavevector is globally small in systems with large aspect ratio. In fact, since $B_P \approx (r/R)B$, the ratio

$$\frac{k_{\parallel}}{k_{\perp}} \approx \frac{r}{Rq}, \quad (16)$$

is small even when there is no significant cancellation in $m - nq$.

There are two important consequences. The first is that the spatial scales for flute perturbations are larger than those for compressional modes. The second, which follows from the dispersion law (13), is that the time scale for flute modes is slow compared to compressional modes.

Scale separation is especially important in the plasma equation of motion. Beginning with the exact momentum law, (6.90), we express the total pressure tensor as $\mathbf{P}_t = \mathbf{I}P + \boldsymbol{\Pi}$ to write

$$\rho_m \frac{d\mathbf{V}}{dt} + \nabla \cdot \boldsymbol{\Pi} = -\nabla P + \frac{1}{c} \mathbf{J} \times \mathbf{B}. \quad (17)$$

Here we have arranged terms to emphasize the predominant balance between the pressure gradient and the $\mathbf{J} \times \mathbf{B}$ force—a balance that describes not only equilibrium, but also any evolution that is slower than a compressional Alfvén wave. In fact Amperé's law implies that $J_{\perp} \approx ck_{\perp}B$, so the bare $\mathbf{J} \times \mathbf{B}$ force has the magnitude

$$\frac{1}{c} \mathbf{J} \times \mathbf{B} \approx k_{\perp} \rho_m v_A^2. \quad (18)$$

This would imply $(d/dt)(v/v_A) \approx k_{\perp} v_A^2$, a time scale on the order of the compressional Alfvén mode. Evolution on slower time scales must evidently proceed through a sequence of near equilibrium states, in which the dominant part of the $\mathbf{J} \times \mathbf{B}$ force is shielded:

$$-\nabla P + \frac{1}{c} \mathbf{J} \times \mathbf{B} \sim \mathcal{O}\left(\frac{k_{\parallel}}{k_{\perp}}\right). \quad (19)$$

We will see that these slower, shielded motions are the most likely to be unstable.

Derivation of the Shear-Alfvén Law

A simple way to describe such slow evolution—which critically involves the error term in (19)—is obtained from manipulation of (17). As in neutral fluid dynamics we first eliminate the pressure gradient by taking the curl. It turns out that only one component of this curl is needed, the parallel component. The resulting equation will be called the shear-Alfvén law because it governs flute-like motions, similar to the Alfvén waves contained in (13). It should be emphasized that the shear-Alfvén law derived here is exact and fully general. It is in particular not tied to any fluid model, such as MHD.

The relevant electromagnetic forces are obtained from the term $\mathbf{B} \cdot \nabla \times (\mathbf{J} \times \mathbf{B})$, which can be expressed in terms of the curvature using (3.89). Denoting the left hand side of (17) by \mathbf{f} for convenience, we obtain the nonequilibrium generalization of (3.90),

$$\boldsymbol{\kappa} = \frac{4\pi}{B^2} (\nabla P + \mathbf{f}) + \frac{\nabla_{\perp} B}{B}. \quad (20)$$

Thus the electromagnetic term becomes

$$\begin{aligned} \mathbf{B} \cdot \nabla \times (\mathbf{J} \times \mathbf{B}) &= \nabla \cdot [(\mathbf{J} \times \mathbf{B}) \times \mathbf{B}] = -\nabla \cdot (B^2 \mathbf{J}_{\perp}) \\ &= B^2 \mathbf{B} \cdot \nabla \left(\frac{J_{\parallel}}{B} \right) - \frac{1}{B^2} \mathbf{B} \times (\mathbf{J} \times \mathbf{B}) \cdot \nabla_{\perp} B^2 \quad (21) \\ &= B^2 \mathbf{B} \cdot \nabla \left(\frac{J_{\parallel}}{B} \right) - \frac{c}{4\pi} \mathbf{B} \times \boldsymbol{\kappa} \cdot \nabla_{\perp} B^2. \end{aligned}$$

On the second line we have used the quasi-neutrality relation, $\nabla \cdot \mathbf{J} = 0$. Combining (21) with the left-hand side of (17) yields the exact shear-Alfvén law

$$c\mathbf{B} \cdot \nabla \times \mathbf{f} = B^2 \mathbf{B} \cdot \nabla \left(\frac{J_{\parallel}}{B} \right) - \frac{c}{4\pi} \mathbf{B} \times \boldsymbol{\kappa} \cdot \nabla B^2. \quad (22)$$

Alternatively we can use (20) to eliminate $\nabla_{\perp} B^2$ from (22) to give

$$c\mathbf{B} \cdot (\nabla \times \mathbf{f} - 2\boldsymbol{\kappa} \times \mathbf{f}) = B^2 \mathbf{B} \cdot \nabla \left(\frac{J_{\parallel}}{B} \right) + 2\mathbf{B} \times \boldsymbol{\kappa} \cdot \nabla P. \quad (23)$$

The left-hand side of (23) describes plasma inertia: the curl of the acceleration predominantly involves the fluid vorticity, $\nabla \times \mathbf{v}$. For this reason, (23) is sometimes called the vorticity equation. (Other contributions to the left-hand side involve details of the plasma response that are sensitive to collision frequency.) Roughly speaking (23) describes the plasma response to driving forces contained on its right-hand side, which we consider next.

Qualitative Features

The two terms on the right-hand side of the shear-Alfvén law (23) provide the driving forces (sources of free energy) for various plasma motions. The first term, involving the parallel current, gives rise to *current driven modes*. The second term, involving ∇P , gives rise to *pressure driven modes*. One could also refer to these, respectively, as “parallel current” and “perpendicular current” driven modes, since, as we see in (21), the two terms arise from the separation of the current into its perpendicular and parallel components. In general, a disturbance will be affected by both terms, although there are simple limits where one or the other can be neglected.

For a small departures from equilibrium, the parallel current term becomes

$$\mathbf{B} \cdot \nabla \left(\frac{J_{\parallel}}{B} \right) \approx \delta \mathbf{B} \cdot \nabla \left(\frac{J_{\parallel 0}}{B_0} \right) + \mathbf{B}_0 \cdot \nabla \left(\frac{\delta J_{\parallel}}{B_0} \right) \quad (24)$$

since, as shall be seen presently [*cf.* (37)], the perturbation in the magnitude of \mathbf{B} is relatively small. The first term in (24), called the *kink* term, is nonzero when there are gradients in the equilibrium parallel current. Typical current driven modes include the ideal kink and resistive tearing instabilities.

The second term in (24) is called the *line bending* term: it is loosely associated with bending of the magnetic field lines. The point is that δJ_{\parallel} is relatively small when $\delta \mathbf{B}$ and \mathbf{B} are parallel: it reflects perturbation in the *direction* of \mathbf{B} . The most important feature of the line-bending term is reflected in the singularity of the operator $\mathbf{B}_0 \cdot \nabla$ on mode rational surfaces, as discussed in §3.3. The line bending term tends to be stabilizing: energy that goes into bending the magnetic field is unavailable for fluid motions. The fact that the line bending term is small near mode rational surfaces, obviating its stabilizing effect, determines the character of most of the electromagnetic instabilities of toroidal plasmas.

The last term in (23) is called the *interchange* term because it is responsible for the Rayleigh-Taylor instability, an instability involving the exchange of fluid elements with different densities. The stability of an interchange mode depends upon the interaction of magnetic curvature with pressure gradients. In fact, as we will see, its stability depends upon the scalar $\kappa \cdot \nabla P$. Situations in which $\kappa \cdot \nabla P > 0$ tend to be unstable, so this type of curvature is referred to as “unfavorable.”

Together, the kink and interchange terms are called the *Newcomb* terms. The central fact of fluid stability theory is that instability usually results when either of the Newcomb terms dominates the line bending term. We will attempt to give some understanding of the resulting panoply of modes in the following sections.

Radial Boundary Layers

Certain features of confined plasma instabilities can be understood from a schematic expansion of the shear-Alfvén law. For any field quantity $h(\mathbf{x}, t)$, we let $h_0(\mathbf{x})$ represent its equilibrium value and $\delta h(\mathbf{x}, t)$ the perturbation:

$$h(\mathbf{x}, t) = h_0(\mathbf{x}) + \delta h(\mathbf{x}, t).$$

Then, neglecting second order terms, we may express the shear-Alfvén law in the form,

$$\mathbf{B}_0 \cdot \nabla \left(\frac{\delta J_{\parallel}}{B_0} \right) = \delta N + \delta^2 N + \mathbf{V} \cdot \delta \mathbf{f} + \delta \mathbf{V} \cdot \delta \mathbf{f}. \quad (25)$$

Here δN represents the linearized Newcomb terms, i.e. the interchange and kink terms; the operator \mathbf{V} represents that on the left-hand side of (23), related to the vorticity; and the two $\mathcal{O}(\delta^2)$ terms represent the nonlinear contributions. The main point of (25) is to isolate the operator $\mathbf{B}_0 \cdot \nabla \sim k_{\parallel}$, which is singular on rational surfaces.

Suppose first that the nonlinear contributions are neglected, and that V is relatively small. The resulting equation

$$\mathbf{B}_0 \cdot \nabla \left(\frac{\delta J_{\parallel}}{B_0} \right) = \delta N \quad (26)$$

is a linear description of neighboring equilibria. It is a magnetic differential equation for δJ_{\parallel} , and is well posed providing the right-hand side satisfies the appropriate Newcomb condition (3.33) on any rational surface in the plasma. Instabilities that satisfy this constraint include the ideal interchange and kink modes.

Typically these conditions are not satisfied. Then other terms in the shear-Alfvén law must be included, to avoid divergence of the (m, n) -Fourier coefficient of J_{\parallel} near the rational surface. In these cases, the additional terms can be relatively small, and serve only to resolve the singularity of (26) near rational surfaces; far from such surfaces (26) remains approximately valid.

Thus the shear-Alfvén law leads to a classic boundary layer problem: the exterior of the boundary layer (or “current layer”) is described by (26), while its interior description must include one or more of the additional terms from (25) to resolve the singularity. Solution of the boundary-layer problem follows, in general, the classical prescription: one solves the interior and exterior equations separately, allowing enough freedom in boundary values to asymptotically match the two solutions. Since there are several neglected terms in (26), there are several ways to resolve the singularity (including linear and nonlinear theory). Each results in a characteristic boundary layer structure, and boundary layer width. Examples are treated in §7.8 and §9.1.

First, however, we consider approximate versions of the shear-Alfvén law.

7.4 Flute Reduction

A formal flute reduction of the shear-Alfvén law can be accomplished by introducing a small parameter ϵ such that $k_{\parallel} \sim O(\epsilon k_{\perp})$. This can be exploited by separating spatial dependence into two parts, fast and slow, and expressing functions as

$$f(\mathbf{x}, t) = f(\mathbf{x}_f, \mathbf{x}_s, t),$$

where $\mathbf{x}_f = \mathbf{x}/\epsilon$, and $\mathbf{x}_s = \mathbf{x}$. Derivatives must now be taken with respect to both sets of variables

$$\nabla = \frac{1}{\epsilon} \nabla_f + \nabla_s, \quad (27)$$

where $\nabla_f = \partial/\partial\mathbf{x}_f$, etc. Although the space of independent variables has been enlarged in (27) (from four to seven dimensions), an expansion in the small parameter ϵ will actually yield equations that are much simplified. A perturbation expansion of this form is known as a “multiple scale” expansion.

Equilibrium quantities are assumed to depend only on the slow scale; perturbed quantities may depend on both \mathbf{x}_f , and \mathbf{x}_s . Formally, we have

$$\mathbf{B} = \mathbf{B}_0(\mathbf{x}_s) + \epsilon \mathbf{B}_1(\mathbf{x}_f, \mathbf{x}_s, t), \quad \mathbf{E} = \mathbf{E}_0(\mathbf{x}_s) + \epsilon \mathbf{E}_1(\mathbf{x}_f, \mathbf{x}_s, t), \quad (28)$$

$$P = P_0(\mathbf{x}_s) + \epsilon P_1(\mathbf{x}_f, \mathbf{x}_s, t), \quad (28)$$

$$\mathbf{V} = \epsilon \mathbf{V}_1(\mathbf{x}_f, \mathbf{x}_s, t), \quad \Pi = \epsilon \Pi_1(\mathbf{x}_f, \mathbf{x}_s, t),$$

and so forth. The fact that \mathbf{V} and Π are $O(\epsilon)$ reflects the assumption that the equilibrium is static and isotropic.

Since k_{\parallel} is assumed small, the choice of fast variables is constrained by the requirement that they be perpendicular to the equilibrium field

$$\mathbf{B}_0 \cdot \nabla_f = 0. \quad (29)$$

Equation (29) is a homogeneous magnetic differential equation; its solutions were discussed in §3.5 in terms of flux coordinates. If the fast dependence is limited to the flux coordinate, then the reduced equation applies to modes that vary rapidly near a particular rational surface. If an additional fast dependence on $\zeta - q\theta$ is allowed, then ballooning modes, §7.10, can be treated. Here we make no a priori choice of fast coordinates; the resulting reduced equations will be valid for either case.

Flute-reduced Shear-Alfvén Law

We next substitute the expansions (28) into the shear-Alfvén law. Because the strong forces have already been annihilated, it is necessary to keep only the lowest order terms. For clarity, we consider the effect of the ordering on each of the terms in (23) separately. A representation for the perturbed magnetic field may be obtained from $\nabla \cdot \mathbf{B} = 0$. According to (27) and (28),

$$0 = \nabla \cdot \mathbf{B}_0 + \nabla_f \cdot \mathbf{B}_1 + \epsilon \nabla_s \cdot \mathbf{B}_1 = \nabla_f \cdot \mathbf{B}_1 + \mathcal{O}(\epsilon),$$

which implies that \mathbf{B}_1 can be represented in terms of two scalar fields:

$$\mathbf{B}_1 = \nabla_f \psi \times \mathbf{B}_0 + B_{\parallel} \mathbf{b}_0. \quad (30)$$

Here $\psi(\mathbf{x}_f, \mathbf{x}_s, t)$ is the normalized parallel vector potential; it is defined to have the dimensions of length. The contribution of B_{\parallel} to $\nabla_f \cdot \mathbf{B}_1$ is zero by virtue of (29); note that B_{\parallel} is the linear correction to the field magnitude, B .

The exact parallel gradient operator is expressed as

$$\mathbf{B} \cdot \nabla = (\mathbf{B}_0 + \epsilon \mathbf{B}_1) \cdot \left(\frac{1}{\epsilon} \nabla_f + \nabla_s \right) = \mathbf{B}_0 \cdot \nabla_s + \mathbf{B}_1 \cdot \nabla_f + \mathcal{O}(\epsilon),$$

where (29) has been used to eliminate the $\mathcal{O}(\epsilon^{-1})$ term. A compact representation for this operator is obtained using (30)

$$\nabla_{\parallel} \equiv \frac{\mathbf{B} \cdot \nabla}{B_0} = \mathbf{b}_0 \cdot \nabla_s - [\psi,] + \mathcal{O}(\epsilon), \quad (31)$$

where the bracket represents the nonlinear terms, and is defined by

$$[\psi, \varphi] \equiv \mathbf{b}_0 \cdot \nabla_f \psi \times \nabla_f \varphi. \quad (32)$$

The current is obtained from Ampère's law, which is expanded as

$$\mathbf{J} = \mathbf{J}_0 + \frac{c}{4\pi} \nabla_f \times \mathbf{B}_1 + \mathcal{O}(\epsilon) = \mathbf{J}_0 - \frac{c}{4\pi} \left(\mathbf{B}_0 \nabla_f^2 \psi + \frac{1}{B_0} \mathbf{B}_0 \times \nabla_f B_{\parallel} \right) + \mathcal{O}(\epsilon). \quad (33)$$

Note that although the perturbing field is small, there is an $\mathcal{O}(1)$ correction to the equilibrium current. The parallel component of (33) is

$$\frac{J_{\parallel}}{B} = \frac{J_{\parallel 0}}{B} - \frac{c}{4\pi} \nabla_f^2 \psi + \mathcal{O}(\epsilon). \quad (34)$$

Thus, from (31) and (34), the first of the Newcomb terms in (23) is obtained in reduced form.

In general, the expansion of the interchange term of (23) yields three separate linear terms, as well as a host of nonlinear terms. The flute-like

ordering implies that only one of these terms is important. This significant reduction follows from expanding the curvature

$$\boldsymbol{\kappa} = \mathbf{b} \cdot \nabla \mathbf{b} = \mathbf{b}_0 \cdot \nabla_s \mathbf{b}_0 + \mathcal{O}(\epsilon) ,$$

showing that there is no $\mathcal{O}(1)$ correction to the equilibrium curvature. Alternatively the exact relation (20) implies that

$$\boldsymbol{\kappa} = \boldsymbol{\kappa}_0 + \frac{4\pi}{B_0^2} \nabla_f P_1 + \nabla_f \frac{B_{\parallel}}{B_0} + \mathcal{O}(\epsilon) . \quad (35)$$

Therefore the second term in (35) must vanish:

$$\frac{4\pi}{B_0^2} \nabla_f P_1 + \frac{\nabla_f B_{\parallel}}{B_0} = 0 . \quad (36)$$

This important relation is simply the expression of perturbed pressure balance; it also follows from the $\mathcal{O}(1)$ terms of the equation of motion (17) using the flute ordering. Equation (36) can be used to eliminate B_{\parallel} in favor of P_1 :

$$B_{\parallel} = -\frac{4\pi P_1}{B_0} . \quad (37)$$

Consider next the inertial terms in the shear-Alfvén law. The perturbed velocity has the general form

$$\mathbf{V}_1 = \mathbf{V}_{\perp} + V_{\parallel} \mathbf{b}_0 , \quad (38)$$

where $\mathbf{V}_{\perp} = \mathbf{b}_0 \times (\mathbf{V}_1 \times \mathbf{b}_0)$. Thus the advective derivative is

$$\frac{d}{dt} = \frac{\partial}{\partial t} + \mathbf{V}_{\perp} \cdot \nabla_f + \mathcal{O}(\epsilon) .$$

The angular acceleration is given by

$$\mathbf{B} \cdot \nabla \times \left(\rho_m \frac{d\mathbf{V}}{dt} \right) = \rho_m \mathbf{B}_0 \cdot \nabla_f \times \frac{d\mathbf{V}_1}{dt} + \mathcal{O}(\epsilon) .$$

After some manipulation, this term can be expressed in terms of the parallel vorticity, defined by

$$U = \mathbf{b}_0 \cdot \nabla_f \times \mathbf{V}_1 = \mathbf{b}_0 \cdot \nabla_f \times \mathbf{V}_{\perp} ,$$

and the divergence $\nabla_f \cdot \mathbf{V}_1 = \nabla_f \cdot \mathbf{V}_{\perp}$:

$$\mathbf{b} \cdot \nabla \times \left(\rho_m \frac{d\mathbf{V}}{dt} \right) = \rho_m \left(\frac{\partial}{\partial t} + \mathbf{V}_{\perp} \cdot \nabla_f \right) U + U \nabla_f \cdot \mathbf{V}_{\perp} + \mathcal{O}(\epsilon) . \quad (39)$$

Note that the parallel velocity explicitly cancelled from (39). The remaining term is the Coriolis-like expression

$$\mathbf{B} \cdot \boldsymbol{\kappa} \times \mathbf{f} = \mathbf{B}_0 \cdot \boldsymbol{\kappa}_0 \times (\nabla_f \cdot \boldsymbol{\Pi}_1) + \mathcal{O}(\epsilon) , \quad (40)$$

which depends solely on the anisotropic pressure.

Substitution of these results into (23) gives the reduced shear-Alfvén law

$$\rho_{m0} \left(\frac{d}{dt} U + U \nabla \cdot \mathbf{V}_\perp \right) = -\frac{B_0^2}{4\pi} \nabla_\parallel \nabla_\perp^2 \psi + 2\mathbf{b}_0 \times \boldsymbol{\kappa}_0 \cdot \nabla_\perp \cdot (P_1 \mathbf{I} + \boldsymbol{\Pi}_1) . \quad (41)$$

Here, since the only component of the slow dependence which enters is in the \mathbf{B}_0 direction, we have suppressed all the “g” and “f” subscripts; note that the fast gradient is equivalent to ∇_\perp . Furthermore we have used (31) for the parallel gradient.

Closure Relations: Resistive MHD

The reduced shear-Alfvén law depends on the five perturbed fields U , \mathbf{V}_\perp , ψ , $\boldsymbol{\Pi}_1$ and P_1 . Before applying it to stability analysis, we must find closure relations for these quantities. We consider first the relatively simple closure provided by resistive MHD, (6.107).

At this point it is convenient to introduce the scalar and vector potentials

$$\Phi = \epsilon^2 B_0 \varphi(\mathbf{x}_f, \mathbf{x}_s, t) \quad (42)$$

$$\mathbf{A} = \mathbf{A}_0(\mathbf{x}_s, t) + \epsilon^2 (\mathbf{B}_0 \psi + \mathcal{A}_\perp(\mathbf{x}_f, \mathbf{x}_s, t)) .$$

The potential φ has been defined with the dimensions of length, to be consistent with ψ . According to (30) $\nabla_f \times \mathcal{A}_\perp = B_\parallel \mathbf{b}_0$.

The first closure relation needed is Ohm’s law. In equilibrium, Ohm’s law expresses the balance between the inductive electric field, $-1/c \partial \mathbf{A}_0 / \partial t$ and the equilibrium resistive diffusion $\eta \mathbf{J}_0$. Of course this evolution is very slow, and consistently neglected in stability analysis. The parallel components of the perturbed Ohm’s law use the perturbed part of the parallel electric field

$$\mathbf{B} \cdot \mathbf{E} = -\mathbf{B} \cdot \nabla \Phi - \frac{1}{c} \frac{\partial}{\partial t} \mathbf{B} \cdot \mathbf{A} = -\epsilon^2 B_0^2 \left(\frac{1}{B_0} \nabla_\parallel B_0 \varphi + \frac{1}{c} \frac{\partial \psi}{\partial t} \right) ,$$

and the parallel current, (34). In order that the parallel electric field and ηJ_\parallel balance we must assume $\eta \sim \mathcal{O}(\epsilon^2)$. In this case the parallel component of Ohm’s law becomes

$$\frac{1}{c} \frac{\partial \psi}{\partial t} + \frac{1}{B_0} \nabla_\parallel B_0 \varphi = \frac{\eta c}{4\pi} \nabla_f^2 \psi . \quad (43)$$

The perpendicular component of Ohm’s law gives an expression for the perpendicular velocity, (38). To first order we obtain the electrostatic $\mathbf{E} \times \mathbf{B}$ drift:

$$\mathbf{V}_{1\perp} \equiv c \mathbf{B}_0 \times \nabla_f \varphi . \quad (44)$$

We will require the second order terms below; these can be written

$$\begin{aligned} \mathbf{V}_{2\perp} &= \frac{c}{B_0} \mathbf{b}_0 \times \left(\nabla_s (B_0 \varphi) + \frac{1}{c} \frac{\partial \mathcal{A}_\perp}{\partial t} \right) - \frac{\eta c^2}{B_0^2} (\nabla_s P_0 + \nabla_f P_1) \\ &\quad - \frac{c}{B_0} B_\parallel \mathbf{b}_0 \times \nabla_f \varphi - V_\parallel \mathbf{b}_0 \times \nabla_f \psi . \end{aligned} \quad (45)$$

The curl of (44) gives an expression for the parallel vorticity

$$U = c \nabla_f^2 \varphi , \quad (46)$$

and for the advective derivative

$$\frac{d}{dt} = \frac{\partial}{\partial t} + c[\varphi, \cdot] , \quad (47)$$

where the bracket is defined by (32).

The remaining unknown quantities in the shear-Alfvén law (40) are the perturbed scalar and tensor pressures. We recall from §6.4 that $\Pi = 0$ in MHD. To obtain a closure relation for the scalar pressure, we apply the flute ordering to the MHD energy equation (6.102). The result, through $\mathcal{O}(\epsilon)$, is

$$\frac{\partial}{\partial t} P_1 + c[\varphi, P_1] + c \mathbf{b}_0 \cdot \nabla_f \varphi \times \nabla_s P_0 = -\frac{5}{3} (P \nabla \cdot \mathbf{V})_\epsilon . \quad (48)$$

Here the subscript on the right-hand side, which measures plasma compressibility, indicates that it must be evaluated to $\mathcal{O}(\epsilon)$. Note that (38) and (29) imply that the fast divergence of \mathbf{V}_1 vanishes:

$$\nabla_f \cdot \mathbf{V}_1 \approx 0 .$$

The evaluation of the remaining terms in the divergence is a tedious process, resulting in

$$\begin{aligned} (\nabla \cdot \mathbf{V})_\epsilon &= \nabla_s \cdot \mathbf{V}_1 + \nabla_f \cdot \mathbf{V}_2 = 2c \mathbf{b}_0 \cdot \boldsymbol{\kappa}_0 \times \nabla_f \varphi + \frac{4\pi c}{B_0^2} \mathbf{b}_0 \cdot \nabla_f \varphi \times \nabla_s P_0 \\ &\quad - \frac{d}{dt} \frac{B_\parallel}{B_0} - \frac{\eta c^2}{B_0^2} \nabla_f^2 P_1 + \nabla_\parallel V_\parallel - \frac{V_\parallel}{B_0^2} \mathbf{B}_0 \cdot \nabla_s B_0 . \end{aligned}$$

Here the first four terms represent contributions from the perpendicular compressibility, and the last two from the parallel compressibility. Note that the perpendicular compressibility is absent in simplified geometries, such as that used for studying drift waves in §6.6.

Upon substituting this expression into (48), the second and third terms can be moved onto the left-hand side, using (37) to eliminate B_\parallel to give

$$\begin{aligned} \left(1 + \frac{5}{6} \frac{8\pi P_0}{B_0^2} \right) \left(\frac{\partial}{\partial t} P_1 + c[\varphi, P_1] + c \mathbf{b}_0 \cdot \nabla_f \varphi \times \nabla_s P_0 \right) \\ = \frac{5}{3} P_0 \left[2c \mathbf{b}_0 \cdot \nabla_f \varphi \times \boldsymbol{\kappa}_0 + \frac{\eta c^2}{B_0^2} \nabla_f^2 P_1 - \nabla_\parallel V_\parallel + \frac{V_\parallel}{B_0^2} \mathbf{B}_0 \cdot \nabla_s B_0 \right] . \end{aligned}$$

We simplify this result by introducing a constant measure of B_0 ,

$$\bar{B} \sim B_0, \quad \nabla \bar{B} = 0,$$

with the corresponding Alfvén speed,

$$v_A^2 \equiv \frac{\bar{B}^2}{B^2},$$

For example, \bar{B} might be B_0 evaluated on the magnetic axis. We also introduce the parameter

$$\hat{\beta} \equiv \frac{2v_S^2}{v_A^2 + \bar{B}^2 v_S^2 / B_0^2}. \quad (49)$$

Finally we normalize the equilibrium and perturbed pressures according to

$$\beta \equiv \frac{8\pi P_0}{\bar{B}^2}, \quad p = \frac{8\pi P_1}{\bar{B}^2}. \quad (50)$$

The pressure equation becomes

$$\begin{aligned} \frac{\partial}{\partial t} p + c[\varphi, p] + c\mathbf{b}_0 \cdot \nabla_f \varphi \times \nabla_s \beta \\ = \hat{\beta} \left(2c\mathbf{b}_0 \cdot \nabla_f \varphi \times \kappa_0 + \frac{\eta c^2}{8\pi} \nabla_f^2 p - \nabla_{||} V_{||} + V_{||} \mathbf{b}_0 \cdot \nabla_s B_0 \right). \end{aligned} \quad (51)$$

Here the left-hand side represents the advection of the pressure. The first term on the right-hand side is due to perpendicular compressibility, and the last two terms to parallel compressibility. The diffusive term on the right-hand side represents resistive diffusion.

Finally, since equation (51) has introduced the parallel velocity into the flute-reduced system, we must obtain an evolution equation for it. This is easily obtained from the parallel component of the equation of motion (6.103):

$$\rho_{m0} \left(\frac{\partial V_{||}}{\partial t} + c[\varphi, V_{||}] \right) = -\nabla_{||} P_1 + \mathbf{b}_0 \cdot \nabla_s \mathbf{P}_0 \times \nabla_f \psi. \quad (52)$$

Collecting (41), (43), (51), and (52) results in the system of four equations

comprising flute-reduced MHD

$$\frac{1}{v_A^2} \frac{d}{dt} U = -B_0^2 \bar{B}^2 \nabla_{\parallel} J + \mathbf{b}_0 \cdot \boldsymbol{\kappa}_0 \times \nabla_{\perp} p$$

$$\frac{1}{c} \frac{\partial \psi}{\partial t} + \frac{1}{B_0} \nabla_{\parallel} B_0 \varphi = \frac{\eta c}{4\pi} J$$

$$\frac{d}{dt} V_{\parallel} = -\frac{1}{2} v_A^2 (\nabla_{\parallel} p - \mathbf{b}_0 \cdot \nabla \beta \times \nabla \psi) \quad (53)$$

$$\frac{d}{dt} p + c \mathbf{b}_0 \cdot \nabla_{\perp} \varphi \times \nabla \beta$$

$$= \hat{\beta} \left(2c \mathbf{b}_0 \cdot \nabla_{\perp} \varphi \times \boldsymbol{\kappa}_0 + \frac{\eta c^2}{8\pi} \nabla_{\perp}^2 p - \nabla_{\parallel} V_{\parallel} + V_{\parallel} \mathbf{b}_0 \cdot \nabla B_0 \right).$$

Here we have used the abbreviations

$$\begin{aligned} U &= c \nabla_{\perp}^2 \varphi, & J &= \nabla_{\perp}^2 \psi \\ \nabla_{\parallel} &\equiv \mathbf{b}_0 \cdot \nabla - [\psi,] \quad (54) \\ \frac{d}{dt} &= \frac{\partial}{\partial t} + c[\varphi,]. \end{aligned}$$

An even simpler set of equations results from (53) if $\hat{\beta}$ is ordered with ϵ . In the above derivation, we made the nominal assumption $\hat{\beta} = O(1)$. It is often more realistic to take $\hat{\beta}$ smaller. Assuming $\hat{\beta} = O(\epsilon)$, we can omit all $\hat{\beta}$ terms in (53). In that case V_{\parallel} becomes uncoupled from the other perturbed fields, so its evolution can be ignored. The resulting system is known as *high-beta reduced MHD*

$$\begin{aligned} \frac{1}{v_A^2} \frac{d}{dt} U &= -\frac{B_0^2}{\bar{B}^2} \nabla_{\parallel} J + \mathbf{b}_0 \cdot \boldsymbol{\kappa}_0 \times \nabla_{\perp} p \\ \frac{1}{c} \frac{\partial \psi}{\partial t} + \frac{1}{B_0} \nabla_{\parallel} B_0 \varphi &= \frac{\eta c}{4\pi} J \quad (55) \\ \frac{d}{dt} p &= c \mathbf{b}_0 \cdot \nabla \beta \times \nabla_{\perp} \varphi. \end{aligned}$$

Note that the geometrical simplification used to derive reduced MHD has suppressed the compressional modes of oscillation. The point is that the ordering $k_{\parallel} < k_{\perp}$ makes the compressional Alfvén frequency much larger than the shear-Alfvén frequency. Hence, as shown by (37), reduced MHD presumes the compressional modes to have equilibrated.

Large Aspect Ratio Reduced MHD

For large aspect ratio, additional geometric simplification can be applied to the flute-reduced equations. Furthermore, according to (16), k_{\parallel} is in this case small over the entire plasma, so the flute-reduced equations are globally valid. The resulting model, known simply as “reduced MHD,” has attained prominence in the literature since its first derivation by H.R. Strauss (Strauss 1976). It can be used both for equilibrium and stability studies.

In this case the small parameter is taken explicitly to be the inverse aspect ratio

$$\varepsilon = \frac{a}{R_0} . \quad (56)$$

The vacuum magnetic field is $\mathbf{B}_0 = \hat{\zeta} I/R$ with $R = R_0 + r \cos \theta$. The separation into slow and fast coordinates can be seen in the gradient

$$R_0 \nabla = \frac{1}{\varepsilon} a \nabla_{\perp} + \left(1 + \frac{r}{R_0} \cos \theta \right)^{-1} \frac{\partial}{\partial \zeta} , \quad (57)$$

which is to be compared with (27). Thus the slow scale is measured by R_0 and the fast scale by a . The fast variables indeed satisfy (29).

The full magnetic field is, from (30),

$$\mathbf{B} = \overline{B} \hat{\zeta} + \varepsilon \left[\hat{\zeta} \left(B_{\parallel} - \overline{B} \frac{r}{a} \cos \theta \right) - \overline{B} \hat{\zeta} \times \nabla \psi \right] , \quad (58)$$

where $\overline{B} = I/R_0$, and we have kept the $\mathcal{O}(\varepsilon)$ terms from the variation of R . In view of (57) and (58) the parallel gradient becomes

$$R_0 \nabla_{\parallel} = \left(\frac{\partial}{\partial \zeta} - a[\psi, 1] \right) + \mathcal{O}(\varepsilon) . \quad (59)$$

The bracket is simply

$$[\varphi, \psi] = \hat{\zeta} \cdot \nabla \varphi \times \nabla \psi , \quad (60)$$

where again the gradients are “fast” gradients.

In lowest order the curvature is simply the toroidal curvature,

$$\kappa_0 = \mathbf{b}_0 \cdot \nabla \mathbf{b}_0 = \hat{\zeta} \cdot \nabla \hat{\zeta} = -\frac{1}{R_0} \hat{\mathbf{R}} + \mathcal{O}(\varepsilon) = -\frac{1}{R_0} \nabla x \quad (61)$$

where

$$x \equiv r \cos \theta .$$

Using (57)–(61) in (55) yields the model

$$\frac{1}{v_A^2} \frac{d}{dt} U = -\nabla_{||} J - \frac{1}{R_0} [x, p]$$

$$\frac{1}{c} \frac{\partial \psi}{\partial t} + \nabla_{||} \varphi = \frac{\eta c}{4\pi} J \quad (62)$$

$$\frac{d}{dt} p = c[\beta, \varphi].$$

Part 2: Ideal Stability

A complete treatment of plasma stability is difficult to present in a single chapter. Some of the complications are essential—for example the issues of rational surface singularities and magnetic curvature—while others arise from toroidal geometry and from the large number of equations of motion in any reasonable closure. In order to avoid obscuring the central issues in a geometric fog, we begin the discussion of ideal stability using a simplified system that displays the most important physical effects. We exhibit more of the geometric details in the last part of §7.6, with a discussion of the ideal MHD energy principle.

7.5 Cylindrical Reduced MHD

In this section we study reduced MHD stability in cylindrical geometry, without toroidal curvature. The cylindrical model is quite tractable, yet it still contains the shear-Alfvén mode and exhibits the rational surface singularity that dominates any study of toroidal stability. Indeed, the following treatment is similar to fully toroidal MHD studies in both its methods and its results.

For coordinates we use (r, θ, ζ) , where r is the cylindrical radius, θ is the azimuth, and ζ represents the cylindrical axis (ranging from 0 to 2π). By imposing periodic boundary conditions in ζ , we effect toroidal topology, while ignoring toroidal curvature.

At equilibrium we set $U = \varphi = 0$, $p = p_0(r)$, and $\psi = \psi_0(r)$. The latter gives an equilibrium poloidal field, and a safety factor, from (58), given by

$$\frac{1}{q} \equiv \frac{\mathbf{B} \cdot \nabla \theta}{\mathbf{B} \cdot \nabla \zeta} = -\frac{a}{r} \psi'_0. \quad (63)$$

Since the only coupling to the pressure in (55) occurs through the curvature, we must include curvature in some fashion. Instead of (61) we will use the

simple cylindrical expression

$$\kappa = \kappa_r(r)\tilde{f},$$

noting that κ_r depends only on the minor radius. Strict application of the ϵ -ordering makes this term is negligible compared to toroidal curvature, so its predictions have only limited application to the toroidal case. Nonetheless the model helpfully exhibits the significance of magnetic field curvature.

Our task is to determine the spectral stability of reduced MHD about this equilibrium. Thus we linearize the equations, using a Fourier expansion for all of the perturbed quantities in the angle variables. For example

$$\psi = \psi_0 + \sum_{m,n} \tilde{\psi}_{m,n}(r) e^{i(m\theta - n\zeta)}, \quad (64)$$

Because the equilibrium is independent of θ and ζ , the equations for the various components $\tilde{\psi}_{m,n}$ decouple. Thus we can consider each mode separately. Note, however, that this decoupling requires the curvature be independent of θ . In the actual reduced MHD model the θ dependence of κ couples the poloidal harmonics, complicating the analysis.

Linearized Reduced MHD

To linearize about the equilibrium, we must compute quantities such as $\nabla_{\parallel} f$, from (59). Using the expansion (64) for both f and ψ and suppressing the (m,n) subscripts yields

$$\begin{aligned} \nabla_{\parallel} f &= \left(\frac{1}{R_0} \frac{\partial}{\partial \zeta} - \epsilon[\psi_0,] \right) \tilde{f} e^{i(m\theta - n\zeta)} + \epsilon[f_0, \tilde{\psi}] e^{i(m\theta - n\zeta)} \\ &\approx \left[\frac{i}{R_0} \left(\frac{m}{q} - n \right) \tilde{f} + i\epsilon m \frac{f'_0}{r} \tilde{\psi} \right] e^{i(m\theta - n\zeta)}. \end{aligned}$$

Notation is simplified by introducing the parallel wavenumber (15), which, for the cylindrical case, becomes

$$k_{\parallel} \approx \frac{1}{R_0} \left(\frac{m}{q} - n \right), \quad (65)$$

since $X'/\sqrt{g} = B_0/R_0 q$. Evidently, k_{\parallel} is explicitly a function of r through $q(r)$. Similarly the perpendicular wavenumber is

$$k_{\perp} = \frac{m}{r}. \quad (66)$$

Of course the “true” k_{\perp} includes derivatives with respect to r , but radial derivatives cannot be included in the Fourier representation because the equilibrium is r dependent. Thus

$$\nabla_{\parallel} f \Rightarrow ik_{\parallel} \tilde{f} + i\epsilon k_{\perp} f'_0 \tilde{\psi}, \quad (67)$$

where the “ \Rightarrow ” entails discarding the exponential factor. Similarly the perpendicular gradient is

$$\nabla_{\perp} f \Rightarrow \left(\hat{r} \frac{\partial}{\partial r} + i\hat{\theta}k_{\perp} \right) \tilde{f},$$

and the perpendicular Laplacian has the form

$$\nabla_{\perp}^2 f \Rightarrow \frac{1}{r} \frac{\partial}{\partial r} (r\tilde{f}') - k_{\perp}^2 \tilde{f}.$$

Linearizing the remaining terms in (55), and suppressing the tildes, yields the model

$$\begin{aligned} v_A^{-2} \dot{J} &= -ik_{\parallel} J - iek_{\perp} J'_0 \psi + ik_{\perp} \kappa_r p \\ \dot{\psi} &= -ick_{\parallel} \varphi, \\ \dot{p} &= ick_{\perp} \beta' \varphi. \end{aligned} \quad (68)$$

where $\dot{f} = df/dt$.

To study spectral stability, we assume time dependence of the form $e^{-i\omega t}$. Then the three equations (68) can be combined into a single eigenvalue equation for φ . When $\omega \neq 0$ we find

$$\frac{\omega^2}{v_A^2} \nabla_{\perp}^2 \varphi = k_{\parallel} \nabla_{\perp}^2 k_{\parallel} \varphi + \epsilon k_{\parallel} k_{\perp} J'_0 \varphi + k_{\perp}^2 \kappa_r \beta' \varphi, \quad (69)$$

while the zero frequency case has $\varphi = 0$ and

$$k_{\parallel} \nabla_{\perp}^2 \psi = -\epsilon k_{\perp} J'_0 \psi + k_{\perp} \kappa_r p \quad (\omega = 0). \quad (70)$$

The left-hand side of (69) is the linear vorticity, representing inertia; its right hand side consists of the line bending, kink and interchange terms respectively. These equations represent the cylindrical version of (13). In fact if $J'_0 = p'_0 = 0$, and k_{\parallel} is a constant (no shear), then (69) reduces to $\omega^2 - (k_{\parallel} v_A)^2 = 0$, which is the shear-Alfvén dispersion law. On the other hand, (70) is the expression of neighboring equilibrium. Thus in going from (13) to (69) and (70) we have lost the compressional Alfvén and sound waves, but introduced the complications of an inhomogeneous equilibrium.

To proceed we express the equilibrium current in terms of the safety factor:

$$J'_0 = \frac{d}{dr} \nabla_{\perp}^2 \psi_0 = -\frac{d}{dr} \left[\frac{1}{r} \frac{d}{dr} \frac{r^2}{aq} \right] = -\frac{1}{me} \frac{d}{dr} \left[\frac{1}{r} (r^2 k_{\parallel})' \right].$$

As a consequence, the line bending and kink terms neatly combine to give²

$$k_{\parallel} \nabla_{\perp}^2 k_{\parallel} \varphi + \epsilon k_{\parallel} k_{\perp} k_{\perp} J'_0 \varphi = \frac{1}{r^2 \partial_r} \left[k_{\parallel}^2 r^3 \frac{\partial}{\partial r} \left(\frac{\varphi}{r} \right) \right] + \frac{k_{\parallel}^2}{r^2} (1 - m^2) \varphi. \quad (71)$$

²To verify (71) it is much easier to expand both sides of the equation, rather than deriving the right-hand side from the left.

The fact that the last term in (71) is proportional to $(1 - m^2)$ is significant: it shows that the $m = 1$ mode has behavior quite distinct from the $m \neq 1$ modes. Similarly the vorticity can be written as

$$U = \nabla_{\perp}^2 \varphi = \frac{1}{r^2} \frac{\partial}{\partial r} \left[r^3 \frac{\partial}{\partial r} \left(\frac{\varphi}{r} \right) \right] + \frac{1}{r^2} (1 - m^2) \varphi. \quad (72)$$

Substituting both (71) and (72) into (69) yields the eigenvalue equation

$$\begin{aligned} & \frac{1}{r^2} \frac{\partial}{\partial r} \left\{ [\omega^2 - (k_{\parallel} v_A)^2] r^3 \frac{\partial}{\partial r} \left(\frac{\varphi}{r} \right) \right\} \\ & + [\omega^2 - (k_{\parallel} v_A)^2] \frac{(1 - m^2)}{r^2} \varphi - (k_{\perp} v_A)^2 \beta' \kappa_r \varphi = 0. \end{aligned} \quad (73)$$

This equation is similar in many aspects to its fully toroidal version, even when unreduced MHD is used. The manipulations we have used to arrive at (73) also resemble those applied to more detailed models.

Properties of the Eigenvalue Equation

Equation (73) is an eigenvalue problem for $\varphi(r)$ with eigenvalue ω^2 ; to solve it requires specification of the boundary conditions. Note that the plasma velocity is

$$\mathbf{v} = \hat{\zeta} \times \nabla \varphi \Rightarrow \hat{\theta} \frac{\partial \tilde{\varphi}}{\partial r} - ik_{\perp} \tilde{\varphi} \hat{\mathbf{r}}. \quad (74)$$

In order that the velocity be finite at $r = 0$, we must insist that $k_{\perp} \varphi$ remain finite. Thus, by (66),

$$\varphi(0) = 0 \quad (75)$$

(when $m = 0$, this is not required, however; see below). The choice of the remaining boundary condition depends upon physical considerations. One idealized situation is that of a perfectly conducting wall at $r = a$. Then the radial velocity must be zero at the wall,

$$\varphi(a) = 0 \quad (\text{Conducting Wall}). \quad (76)$$

This also implies that the radial component of \mathbf{B} vanishes. The angular components are unrestricted because of the absence of viscosity or resistivity.

An alternative situation is that of a plasma vacuum interface at $r = r_v < a$. Here the velocity need not vanish; however, the solution to (73) must match with a solution to the equations in the vacuum region. We will not treat this case, restricting our attention to so-called *internal modes*, in which the plasma boundary is fixed. For a detailed discussion of the free boundary case in ideal MHD consult, for example, (Freidberg, 1987).

Equation (73), which we denote as $L_\omega \varphi = 0$, with the boundary conditions (75) and (76), is a self-adjoint equation for φ . In fact, assuming that φ and χ satisfy the boundary conditions but are otherwise arbitrary, we have

$$\langle \chi L_\omega \varphi \rangle \equiv \int_0^a r dr \chi L_\omega \varphi = \int_0^a r dr \varphi L_\omega \chi = \langle \varphi L_\omega \chi \rangle . \quad (77)$$

An immediate consequence of self-adjointness is that the eigenvalues ω^2 must be real. To see this let φ denote a square-integrable³ eigenfunction of L_ω , i.e. $L_\omega \varphi = 0$; then φ^* is the eigenfunction for ω^* : $L_{\omega^*} \varphi^* = 0$. Consider the relation

$$0 = \langle \varphi^* L_\omega \varphi \rangle - \langle \varphi L_{\omega^*} \varphi^* \rangle = \langle \varphi^* (L_\omega - L_{\omega^*}) \varphi \rangle .$$

The last inner product can be simplified, using (69):

$$0 = (\omega^2 - \omega^{*2}) \langle \varphi^* \nabla_\perp^2 \varphi \rangle = (\omega^2 - \omega^{*2}) \int_0^a r dr |\nabla_\perp \varphi|^2 , \quad (78)$$

which requires $\omega^2 = (\omega^2)^*$. Furthermore, if ω^2 is real, then L_ω is real, and we can assume that φ is also real.

Thus we see that spectral instability corresponds to the existence of an eigenmode with negative ω^2 (this is generally true in ideal MHD). Furthermore the boundary between stability and instability is always the point $\omega = 0$. This important fact simplifies the discussion of stability for ideal models considerably. When a mode becomes unstable—for example when some of the parameters of a system are changed—it must do so by passing through $\omega = 0$; this circumstance is known as *exchange of stability*.

The fact that the coefficient of the second derivative in (73) can vanish complicates its solution. Indeed the only generally important singular points (in the usual sense of singularities of an ordinary differential equation) occur when $\omega^2 = (k_{\parallel} v_A)^2$ and are intimately related to the shear-Alfvén modes. Typically at a singular point $r = r_s$, the shear will not vanish ($k'_{\parallel} \neq 0$). Thus the coefficient of the second derivative near the singular point,

$$r^2 [\omega^2 - (k_{\parallel} v_A)^2] \approx -2(r_s v_A)^2 k'_{\parallel} (r_s) k'_{\parallel}(r - r_s) , \quad (79)$$

vanishes as the first power of $r - r_s$. It follows that the singular point is regular, and can be treated by the power series (Fröbenius) method. However special consideration must be given to the fact that the eigenvalue enters into the definition of the singular point. As we will see below, this circumstance leads to the existence of a continuous spectrum.

³ There may also be eigenfunctions like the Alfvén continuum, which are not square-integrable.

Alfvén Modes

We begin by treating the case in which the plasma pressure is negligible ($\beta = 0$). Then (73) reduces to

$$\frac{\partial}{\partial r} \left\{ [\omega^2 - (k_{\parallel} v_A)^2] r^3 \frac{\partial}{\partial r} \left(\frac{\varphi}{r} \right) \right\} + [\omega^2 - (k_{\parallel} v_A)^2] (1 - m^2) \varphi = 0. \quad (80)$$

Suppose ω^2 is positive, and $\omega^2 = k_{\parallel}^2(r_0)$ for some point $r_0 < a$. In the neighborhood of r_0 (80) has the form

$$(x\varphi')' + x \frac{1 - m^2}{r_0^2} \varphi = 0 \quad (81)$$

where $x = r - r_0$; thus (80) has a regular singular point at r_0 (it happens to be a modified Bessel equation). When $m^2 \neq 1$, the solution of (81) is

$$\varphi = c_1 + c_2^{\pm} \ln|x| + O(x, x \ln x),$$

where c_1 and c_2^{\pm} are constants and we allow for different slopes, c_2^{\pm} , on either side of the singularity. Using this, a singular solution to (80) with the boundary conditions (75) and (76) can be constructed: the two boundary conditions give two relations for the three constants, leaving one arbitrary (the overall amplitude). Since this solution can be constructed for any r_0 , there is a solution for any ω^2 for which $\omega^2 = k_{\parallel}^2(r_0)$ for some $0 < r_0 < a$, a range of frequencies. This class of solutions is the *Alfvén continuum*.

When $m^2 = 1$ equation (80) can be integrated once to give

$$[\omega^2 - (k_{\parallel} v_A)^2] r^3 \frac{\partial}{\partial r} \left(\frac{\varphi}{r} \right) = A. \quad (82)$$

As $r \rightarrow 0$, (82) implies that $\varphi \sim A/r$; this can satisfy the boundary condition (75) only if $A = 0$. The next integration requires some care when $\omega^2 - (k_{\parallel} v_A)^2$ vanishes. In this case we have an equation of the form $(r - r_0)f(r) = 0$, whose most general solution is not $f(r) = 0$, but $f(r) = B\delta(r - r_0)$, where $\delta(x)$ is the Dirac delta function. Thus the general solution to (82) is

$$\left(\frac{\varphi}{r} \right)' = B\delta(r - r_0) \Rightarrow \frac{\varphi}{r} = B\Theta(r - r_0) + C, \quad (83)$$

where $\Theta(x)$ is the step function,

$$\Theta(x) = \begin{cases} 1, & x > 0 \\ 0, & x < 0 \end{cases}.$$

Applying the boundary condition (76) implies that $C = -B$, and therefore

$$\varphi(r) = rB\Theta(r_0 - r), \quad m^2 = 1. \quad (84)$$

Because φ/r is proportional to the radial velocity, this mode represents a rigid displacement of the plasma inside the singular surface r_0 .

The parallel wavenumber k_{\parallel} typically has a zero in the plasma: according to (65) this occurs at the rational surface

$$q(r_s) = m/n.$$

It follows that the Alfvén continuum extends to $\omega = 0$, as in Fig. 7.2. However when $\omega = 0$ (69) and (73) are not valid and we must use (70) instead; we defer the discussion of this case.

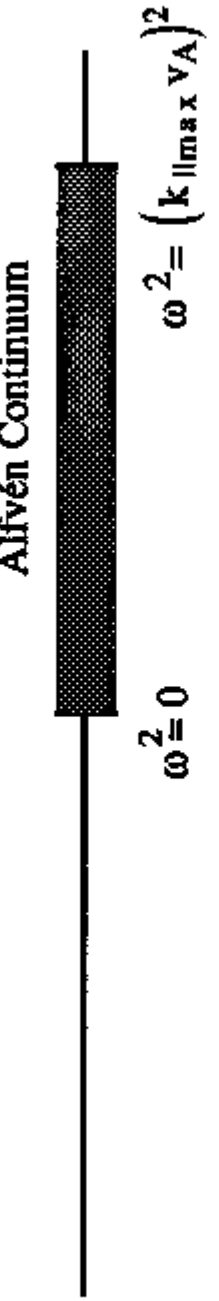


Figure 2. Continuous Spectrum for the Alfvén continuum.

The Alfvén modes have real frequency, but because the spectrum is continuous, stability is not determined by an eigenvalue analysis: a superposition of these modes could grow or decay algebraically with time. To determine which occurs it is necessary to solve the initial value problem represented by the time-domain version of (80). This approach, which is analogous to the treatment of Landau damping, shows that any smooth initial state in fact decays with time.

Alfvén modes are important in applications to plasma heating. Effects such as resistivity, and toroidal curvature can significantly modify these modes. The latter leads to gaps in the continuous spectrum, analogous to the band gaps in a solid state lattice.

Kink Modes

Non-singular solutions to (80) are known as *kink modes*. They represent helical deformations or kinking of the plasma column. Since we have neglected the interchange term, kink mode evolution is driven by the imbalance between the line bending term and the kink term.

For any such solution the inner product $\langle \varphi L_{\omega} \varphi \rangle$ must vanish. Thus

$$\begin{aligned} & - \int_0^a dr r^3 [\omega^2 - (k_{\parallel} v_A)^2] \left[\left(\frac{\varphi}{r} \right)' \right]^2 \\ &= \int_0^a dr r [\omega^2 - (k_{\parallel} v_A)^2] (m^2 - 1) \left(\frac{\varphi}{r} \right)^2. \end{aligned} \quad (85)$$

If an unstable solution exists, then $\omega^2 = -\gamma^2$ is negative, and the left-hand side of (85) must be positive. However, if $m^2 > 1$, then its right-hand side is

negative and the mode is stable. Thus the only possible unstable solutions to (85) have $m^2 = 0$ and 1.

When $m^2 = 1$, we have already solved (80), to obtain (82); however in this case $\omega^2 < 0$, so that there is no singular surface. Then B in (83) vanishes, and C must vanish as well, due to the boundary condition at the wall.

Finally when $m = 0$, $k_{\parallel} = -n$ is a constant, and (80) reduces to the simple equation

$$\frac{\partial}{\partial r} \left[r^3 \frac{\partial}{\partial r} \left(\frac{\varphi}{r} \right) \right] + \varphi = r \frac{\partial}{\partial r} \left[r \frac{\partial}{\partial r} \varphi \right] = 0$$

This has the solution $\varphi = A + B \ln(r)$; the only nonsingular solution has φ constant, which is physically indistinguishable from $\varphi = 0$.

We conclude that there are no unstable kink modes for the cylindrical model with a conducting wall (internal modes). The case of free boundary modes, where there is a vacuum region surrounding the plasma, is more complicated; it is usually investigated numerically.

Neighboring Equilibria

When $\omega = 0$, the equations (68) become singular. In fact, if we assume a time dependence of $e^{-i\omega t}$, the only information obtained is (70), which is under-specified since it involves two unknowns. As an alternative we assume that φ is time-independent, i.e. that the velocity is constant. Then (68) implies that

$$\psi = -ick_{\parallel}\varphi t$$

$$p = ick_{\perp}\beta'\varphi t .$$

Substitution into the shear-Alfvén law gives

$$0 = k_{\parallel} \nabla_{\perp}^2 k_{\parallel} \varphi + \epsilon k_{\parallel} k_{\perp} J'_0 \varphi + k_{\perp}^2 \beta' \kappa_r \varphi , \quad (86)$$

which coincides with (69) for $\omega = 0$. However, in this case the solution corresponds to a steady drift away from the equilibrium. Here the discussion of (5) should be recalled.

The usual manipulations convert (86) into (73) with $\omega = 0$. We have already solved this for the zero β case: equation (85) implies that there can be no solution if $m^2 \neq 1$, other than the Alfvén continuum mode.

When $m = 1$, there is a solution if there is a rational surface in the plasma—a surface r_s on which $k_{\parallel}(r_s) = 0$. In Z-pinch devices there may be many such surfaces, with $q = 1/n$; recall (65). However, in tokamaks, $q > 1/2$ and the $m = 1$ rational surface must have $q = 1$. The solution is again (84), with r_0 now interpreted as r_s , the radius of the $q = 1$ surface. Because it is neutrally stable, the stability of $m = 1$ kink modes in tokamaks

is determined by higher order effects, such as toroidicity or resistivity. It is not surprising that (84) plays a central role in the perturbative analysis of such corrections.

We next consider the effects of nonzero β .

Pressure Driven Modes

When the plasma pressure is not negligible, the inner product $\langle \varphi L_\omega \varphi \rangle$ is identical to (85) with the addition of the interchange term:

$$\begin{aligned} & - \int_0^a dr r^3 [\omega^2 - (k_{\parallel} v_A)^2] \left[\left(\frac{\varphi}{r} \right)' \right]^2 \\ & = \int_0^a dr r [\omega^2 - (k_{\parallel} v_A)^2] (m^2 - 1) \left(\frac{\varphi}{r} \right)^2 + m^2 \int_0^a dr r \beta' \kappa_r \left(\frac{\varphi}{r} \right)^2. \end{aligned} \quad (87)$$

When $\omega^2 < 0$, the left-hand side is again positive and the first term on the right hand side is nonpositive when $m^2 \neq 0$. An immediate consequence is that no solution exists if the interchange term is negative. Thus it is sufficient that

$$\beta' \kappa_r < 0 \quad (88)$$

everywhere for the system to be spectrally stable. The interpretation of this sufficient condition for stability is relatively simple. Physically we are trying to confine plasma pressure with magnetic pressure. Equation (88) implies that the regions of high pressure should be contained within convex fields, as in Fig. 7.3. This sign for the curvature is often referred to as "favorable." Various confinement devices with "cusped" or mirror magnetic fields have been designed specifically to provide favorable curvature. Note that for the cylinder $\kappa_r < 0$, which is in the unfavorable direction. We will see that the derivation of a similar criterion in the tokamak is subtle because the curvature depends on θ as well as r ; however the toroidal version of (88) differs mainly in that a flux-surface average of curvature appears.

The violation of (88) is therefore a necessary condition for instability, but it is not necessarily sufficient. Since β' is typically small, the stabilizing, line bending term [the first term on the right hand side of (87)] dominates whenever $m^2 \neq 1$. Modes that are unstable must minimize the effect of the line bending term, for example by forcing φ to be small except in regions where $k_{\parallel} \ll 1$. These modes are known as localized interchanges; we will study them presently.

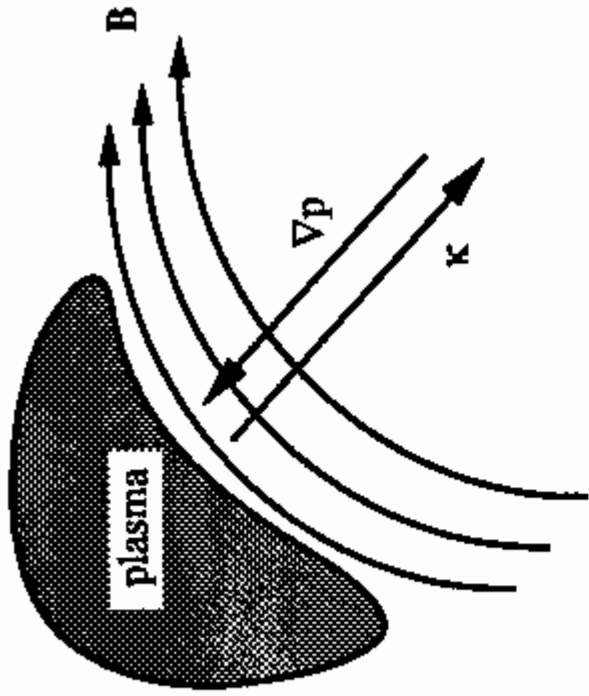


Figure 3. Favorable curvature corresponds to the plasma on the convex side of the field lines.

Sturmian Theory*

To treat (73) in more detail, we next introduce some basic results from the Sturmian theory of differential equations. The eigenvalue problem

$$\frac{\partial}{\partial x} \left(f(x, \lambda) \frac{\partial}{\partial x} \xi \right) - g(x, \lambda) \xi = 0, \quad (89)$$

with parameter λ , is known as a Sturmian system (Ince, 1956). We assume that f is positive and that both f and g are monotonically decreasing functions of λ . The first result deals with the solutions to the initial value problem:

Comparison theorem: Let $\xi(x, \lambda)$ be a solution to (89) obeying

$$\xi(a) = 0, \quad \xi'(a) = 1. \quad (90)$$

If $\lambda_1 < \lambda_2$, and $\xi(x, \lambda_1)$ has m zeros in the interval $a < x \leq b$, then $\xi(x, \lambda_2)$ has at least m zeros in that interval.

In fact, since $\xi(x, \lambda)$ is a continuous function of λ , then the zero crossings move monotonically towards $x = a$, as λ increases. Application of this fact to the boundary value problem gives the

Oscillation theorem: Suppose $\xi_n(x, \lambda_n)$ is a square-integrable solution of (89) obeying

$$\xi(a) = \xi(b) = 0, \quad (91)$$

and having n zeros in the interval $a < x < b$. Then there are n other eigenmodes $\xi_j(x, \lambda_j)$ for $0 \leq j < n$ which have j zeros in the interval and whose eigenvalues obey

$$\lambda_0 < \lambda_1 < \dots < \lambda_n .$$

Equation (73) can be put in the Sturmian form with $\xi = \varphi/r, \lambda = \omega^2$ and

$$\begin{aligned} f(r, \lambda) &= [(k_{\parallel} v_A)^2 - \lambda] r^3 \\ g(r, \lambda) &= [(k_{\parallel} v_A)^2 - \lambda] (m^2 - 1)r + 2m^2 r \beta' \kappa_r . \end{aligned} \quad (92)$$

In order to insure that $f > 0$, we must assume $\lambda < 0$. Thus the analysis applies to the unstable situation $\omega^2 = -\gamma^2$. However, $f(r)$ still vanishes at $r = 0$: (73) has a singular point at the origin. This implies that the boundary condition at $r = 0$ cannot be $\xi(0) = 0$. Rather, as we argued in (75),

$$r\xi(r) \rightarrow 0 \quad \text{as} \quad r \rightarrow 0 . \quad (93)$$

Near $r = 0$, (73) reduces to $\nabla_{\perp}^2 \varphi = 0$, so its behavior is $\varphi \sim Ar^m + Br^{-m}$. Thus, demanding that ξ be regular as $r \rightarrow 0$ selects one of the two solutions. Furthermore as we have seen above, the boundary condition (93) is one for which (89) is self-adjoint. This fact can be used to show that, with the modification (93), the Sturmian theorems apply to (73).

The function g is strictly decreasing when $m^2 > 1$. However, the theory extends to the case of nonincreasing $g, m^2 = 1$, provided there is no interval on which g is zero. Thus Sturmian theory is applicable except in peculiar cases, e.g. if $p_0(r)$ were flat over some interval.

The oscillation theorem then implies that if there exist unstable modes, then the most unstable eigenmode (smallest λ) has no zeros. Of course we can say nothing about the continuum case, $\lambda = \omega^2 > 0$, because then $f(x)$ is no longer positive.

Applying the comparison theorem to the $\omega^2 = 0$ equation yields a stability criterion. Suppose first that $k_{\parallel}(r)$ does not vanish, so that $f(r)$ is indeed positive for $r > 0$. We then find the solution that obeys the boundary condition (75) [but not necessarily (76)]. The comparison theorem implies that if this solution has a zero in the interval $0 < r < a$, then there is a solution that also satisfies the second boundary condition (76), with $\omega^2 < 0$. This would be an unstable mode. In other words, instability is predicted whenever the $\omega^2 = 0$ equation (satisfying the left-hand boundary condition) has a solution with a zero in the interval. This fact gives the zero-frequency equations special importance.

On the other hand, suppose there is a rational surface: $k_{\parallel}(r_s) = 0$. This surface is singular point for (73). As we will see in the next section, of the two solutions near the singular point, only one is regular. To apply the comparison theorem it is necessary to study the two regions, $0 < r < r_s$, and $r_s < r < a$ separately. In the first region, we find the solution that obeys the boundary condition (75). If this solution has a zero in the interval $(0, r_s)$, then there exists an unstable mode. The same argument applies to the solution which obeys the boundary condition (76) in the second region.

Thus the mode is unstable if it is unstable in either of the two intervals taken separately.

Thus the Sturmian theory has provided precise criteria for determining the existence of unstable modes. These criteria are often implemented numerically.

Localized Interchange modes

An analytical criterion for stability of pressure driven, cylindrical modes can be obtained from the comparison theorem by considering the neighborhood of the rational surface. We study (73) for $\omega^2 = 0$ to see if solutions are oscillatory in nature. In the neighborhood of a particular rational surface $k_{\parallel}^2(r_s) = 0$, the parallel wavenumber can be expanded as

$$k_{\parallel} \approx k'_{\parallel} x, \quad x = r - r_s, \quad (94)$$

Evaluating the remaining coefficients of (73) at r_s , yields the differential equation

$$\begin{aligned} \frac{\partial}{\partial x} \left(x^2 \frac{\partial}{\partial x} \varphi \right) + \left(\frac{x}{r_s} \right)^2 (1 - m^2) \varphi + D \varphi &= 0 \\ D &= \frac{m^2 \beta' \kappa_r}{(k'_{\parallel} r_s)^2}. \end{aligned} \quad (95)$$

This equation has a regular singular point at $x = 0$; thus we can expand the solution in the neighborhood of this singular point in a power series

$$\varphi = |x|^{\nu} \sum_{i=0}^{\infty} A_i x^i. \quad (96)$$

Substituting (96) into (95), and balancing like powers of x , yields equations for the coefficients A_j . The lowest order term is the indicial equation that determines ν :

$$\nu(\nu + 1) + D = 0 \Rightarrow \nu = \frac{-1 \pm \sqrt{1 - 4D}}{2}. \quad (97)$$

When $D < 1/4$, both exponents are real; the solutions do not oscillate and never vanish. The solution with $\nu > -1/2$ has finite energy, and is the proper one to choose for boundary conditions. However, when $D > 1/4$, both solutions oscillate, and do so infinitely often near $x = 0$. Thus, by the comparison theorem, there exist unstable eigenmodes in this case.

Stated conversely, $D < 1/4$ is necessary for the system to be stable. This stability criterion is known as the *Suydam criterion*. We can write it as

$$q^2 \beta' \left(\frac{Rq}{r_s} \right)^2 \kappa_r < \frac{q'^2}{4} \quad (\text{for stability}). \quad (98)$$

A comparison of (98) to (88) shows the stabilizing effects of shear. Thus positive $\beta' \kappa_r$ does not imply instability; there is a threshold based on the strength of the shear.

The toroidal version of the Suydam criterion, known as the Mercier criterion, will be derived in §7.11. It is remarkably similar; one merely replaces κ_r by an appropriate average.

We now turn our attention to analysis of the full (unreduced) MHD system.

7.6 Ideal MHD Stability*

Lagrangian for MHD

The energy principle for stability can be applied to MHD, yielding an extremely useful, necessary and sufficient, condition for stability. The traditional way to derive the energy principle is to manipulate the linearized equations of motion, putting them into the form of a second order differential equation for ζ , the Lagrangian displacement of the fluid. We proceed by a different route, using the Lagrangian for MHD. The primary advantage of our method is that it shows directly that the linearized equations are derived from an energy principle.

A Lagrangian description of fluid motion (not to be confused with the Lagrangian variational principle discussed in Chapter 2) is based on the positions of fluid elements as a function of time. Let $\mathbf{x}(\mathbf{r}, t)$, be the position of a fluid element as a function of initial position, \mathbf{r} , and time. Thus $\mathbf{x}(\mathbf{r}, 0) \equiv \mathbf{r}$. The fluid velocity at the point \mathbf{x} , which is the Eulerian quantity of interest, is then

$$\mathbf{v}(\mathbf{x}, t) = \dot{\mathbf{x}}(\mathbf{r}, t). \quad (99)$$

While this equation looks innocent, it is in fact highly nonlinear, since the Eulerian velocity is evaluated at the point $\mathbf{x}(\mathbf{r}, t)$. Thus the construction of the Lagrangian displacement from the Eulerian velocity is nontrivial. In general the time derivative of a function expressed in Lagrangian variables is related to the *advective derivative* of the function in Eulerian variables

$$\frac{d}{dt} f(\mathbf{r}, t) = \frac{d}{dt} f(\mathbf{x}(\mathbf{r}, t), t) = \left(\frac{\partial}{\partial t} + \mathbf{v} \cdot \nabla \right) f(\mathbf{x}, t). \quad (100)$$

Here, the notation is ambiguous, but the total time derivative on the left-hand side of (100) is taken at fixed \mathbf{r} , and the time derivative on the right-hand side is taken at fixed \mathbf{x} .

The equations for conservation of mass and flux become kinematic expressions in Lagrangian coordinates. Conservation of mass, (6.101) means

that the mass contained in the initial volume element $d^3\mathbf{r}$ is equal to the mass in the volume element $d^3\mathbf{x}$. Thus

$$\rho_m(\mathbf{r}, 0) d^3\mathbf{r} = \rho_m(\mathbf{x}, t) d^3\mathbf{x}. \quad (101)$$

Thus, if we let $\rho_m(\mathbf{r}, 0) = \rho_{m0}$, and recall that the transformation of volume elements is the Jacobian (2.1), then $\mathcal{J} = \det[\partial\mathbf{x}/\partial\mathbf{r}]$, and

$$\rho_m \mathcal{J} = \rho_{m0}. \quad (102)$$

A similar description holds for the magnetic field. The conservation of flux (6.106) can be rewritten as

$$\frac{d}{dt} \frac{\mathbf{B}}{\rho_m} = \left(\frac{\mathbf{B}_0}{\rho_{m0}} \cdot \nabla \right) \mathbf{v}. \quad (103)$$

This equation can be physically interpreted by noticing that it is the same equation as that for another Lagrangian quantity: the separation of two neighboring fluid elements. Let $\Delta\mathbf{x}(\mathbf{r}, t)$ be the infinitesimal distance between two fluid elements initially a distance $\Delta\mathbf{r}$ apart, thus

$$\Delta\mathbf{x} = \mathbf{x}(\mathbf{r} + \Delta\mathbf{r}, t) - \mathbf{x}(\mathbf{r}, t). \quad (104)$$

The rate of change of $\Delta\mathbf{x}$ is then

$$\frac{d}{dt} \Delta\mathbf{x} = \dot{\mathbf{x}}(\mathbf{r} + \Delta\mathbf{r}, t) - \dot{\mathbf{x}}(\mathbf{r}, t) = \mathbf{v}(\mathbf{x} + \Delta\mathbf{x}, t) - \mathbf{v}(\mathbf{x}, t) = (\Delta\mathbf{x} \cdot \nabla) \mathbf{v}(\mathbf{x}, t). \quad (105)$$

Equation (105) is identical to the linear differential equation (103), so if we choose $\Delta\mathbf{r} = \mathbf{B}_0/\rho_{m0}$ then $\Delta\mathbf{x} = \mathbf{B}/\rho_m$. Thus (105) implies that the flux, $\mathbf{B} \cdot d^2S = \rho_m \Delta\mathbf{x} \cdot d^2S = \rho_m d^3x$, is preserved along the flow, by virtue of (101). This is illustrated in Figure 7.4.

By virtue of the definition (104), the general solution to (105) is

$$\Delta\mathbf{x}(\mathbf{r}, t) = \Delta\mathbf{r} \cdot \nabla_{\mathbf{r}} \mathbf{x}(\mathbf{r}, t). \quad (106)$$

Here we use $\nabla_{\mathbf{r}}$ for the derivative with respect to \mathbf{r} . Note that $\Delta\mathbf{r} = \Delta\mathbf{x}(\mathbf{r}, 0)$ is simply the initial condition. Therefore the solution to (103) is similarly

$$\frac{\mathbf{B}}{\rho_m} = \left(\frac{\mathbf{B}_0}{\rho_{m0}} \cdot \nabla_{\mathbf{r}} \right) \mathbf{x}. \quad (107)$$

Equations (102) and (107) provide kinematic relations which determine the evolution of the density and magnetic field. The pressure is determined by the equation of state $P(\rho_m) = C\rho_m^{5/3}$. The only “equation of motion” which we need is the equation of conservation of momentum (6.105).

We next develop a variational principle for the equation of motion, starting with a physically transparent guess: the Lagrangian,

$$L[\mathbf{x}, \dot{\mathbf{x}}] = \int d^3x \left(\frac{\rho_m}{2} \dot{\mathbf{x}}^2 - \frac{3}{2} P(\rho_m) - \frac{1}{8\pi} B^2 \right). \quad (108)$$

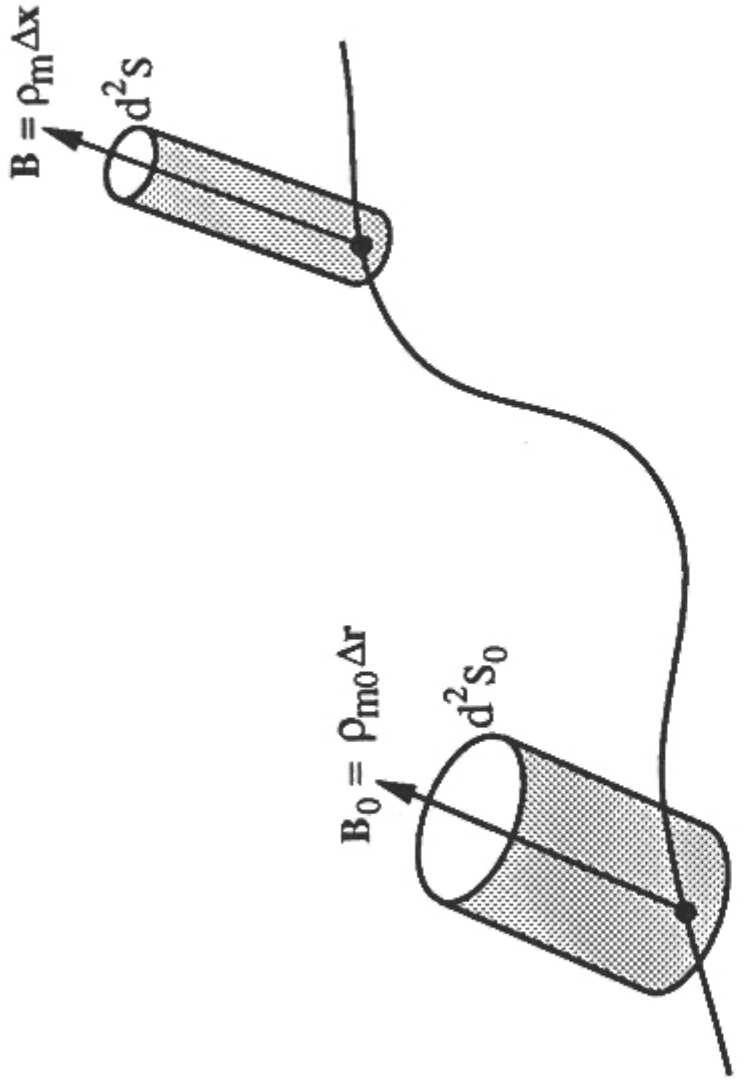


Figure 4. Conservation of magnetic flux according to (7.103).

This function is evidently the difference between the kinetic energy, $\frac{1}{2} \rho_m \dot{x}^2$, and the potential energy, which has contributions from the kinetic pressure and the magnetic pressure $\frac{1}{8\pi} B^2$. In order to show that this Lagrangian gives the correct equations of motion, as we do below, it is necessary to change the integration variable from \mathbf{x} to \mathbf{r} , using (102).

Alternatively the kinematic relations, (102) and (107) can be included in the Lagrangian using Lagrange multipliers

$$\begin{aligned} L[\mathbf{x}, \dot{\mathbf{x}}, \rho, \mathbf{B}, \Lambda, \Gamma] = & \int d^3 r \left[\frac{\rho_{m0}}{2} \dot{x}^2 - \frac{\rho_{m0}}{\rho_m} \left(\frac{3}{2} P(\rho_m) + \frac{B^2}{8\pi} \right) \right. \\ & \left. + \Lambda \left(\mathcal{J} - \frac{\rho_{m0}}{\rho_m} \right) + \Gamma \cdot \left(\frac{\mathbf{B}}{\rho_m} - \frac{\mathbf{B}_0}{\rho_{m0}} \cdot \nabla \mathbf{r} \mathbf{x} \right) \right], \end{aligned} \quad (109)$$

In this case $\rho(\mathbf{r}, t)$ and $\mathbf{B}(\mathbf{r}, t)$ can be treated as independent fields.

Variations with respect to Λ and Γ simply yield the kinematic constraints (102) and (107). Variation with respect to ρ_m and \mathbf{B} determines the values of the Lagrange multipliers

$$\begin{aligned} \Lambda &= P(\rho_m) + \frac{1}{8\pi} B^2 \\ \Gamma &= \frac{\rho_{m0}}{4\pi} \mathbf{B}. \end{aligned} \quad (110)$$

Thus Λ is the total pressure, in the sense of (3.101). Finally, the first vari-

ation with respect to \mathbf{x} gives

$$\int d^3r \left[\rho_{m0} \dot{\mathbf{x}} \cdot \delta \dot{\mathbf{x}} + \Lambda \delta \mathcal{J} - \Gamma \cdot \left(\frac{\mathbf{B}_0}{\rho_{m0}} \cdot \nabla \mathbf{r} \right) \delta \mathbf{x} \right] = 0. \quad (111)$$

To obtain the equation of motion we must compute the variation of \mathcal{J} with respect to \mathbf{x} . By definition (2.1) the Jacobian is

$$\varepsilon_{ijk} \mathcal{J} = \varepsilon_{lmn} \frac{\partial x^i}{\partial r^\ell} \frac{\partial x^j}{\partial r^m} \frac{\partial x^k}{\partial r^n}. \quad (112)$$

Thus letting $\mathbf{x} \rightarrow \mathbf{x} + \delta \mathbf{x}$ gives, to first order in $\delta \mathbf{x}$

$$\varepsilon_{ijk} \delta \mathcal{J} = \varepsilon_{lmn} \frac{\partial \delta x^i}{\partial r^\ell} \frac{\partial x^j}{\partial r^m} \frac{\partial x^k}{\partial r^n} + \text{cyclic}(i, j, k),$$

where the “cyclic” terms are the cyclic permutations in (i, j, k) . Inserting

$$\frac{\partial}{\partial r^\ell} \delta x^i = \frac{\partial x^\mu}{\partial r^\ell} \frac{\partial}{\partial x^\mu} \delta x^i$$

and using (112) gives

$$\delta \mathcal{J} = \mathcal{J} \frac{\partial}{\partial x^i} \delta x^i. \quad (113)$$

Substituting (113) into (111), and recalling that $\mathcal{J} d^3r = d^3x$, we can change integration variables, and then integrate the second term by parts.

In view of (106) the last term in (111) can be expressed as

$$\left(\frac{\mathbf{B}_0}{\rho_{m0}} \cdot \nabla \mathbf{r} \right) \delta \mathbf{x} = \left(\frac{\mathbf{B}_0}{\rho_{m0}} \cdot \nabla \mathbf{r} \right) (\mathbf{x} - \mathbf{r}) = \frac{\mathbf{B}}{\rho_m} - \frac{\mathbf{B}_0}{\rho_{m0}}, \quad (114)$$

where the second term arises because $\nabla \mathbf{r} \mathbf{r} = \mathbf{I}$. Furthermore the analysis leading to (106) also implies that $\delta \mathbf{r} = \delta \mathbf{x} \cdot \nabla \mathbf{r}$, whence $\frac{\mathbf{B}_0}{\rho_{m0}} = \left(\frac{\mathbf{B}}{\rho_m} \cdot \nabla \right) \mathbf{r}$ and we can rewrite (114) as

$$\left(\frac{\mathbf{B}_0}{\rho_{m0}} \cdot \nabla \mathbf{r} \right) \delta \mathbf{x} = \left(\frac{\mathbf{B}}{\rho_m} \cdot \nabla \right) \delta \mathbf{x}. \quad (115)$$

Inserting both (113) and (115) into (111) yields the equation of motion

$$\rho_m \ddot{\mathbf{x}} = -\nabla \Lambda - \frac{1}{4\pi} \mathbf{B} \cdot \nabla \mathbf{B}. \quad (116)$$

Note that the gradients here are taken with respect to \mathbf{x} , not \mathbf{r} , and that ρ_m , \mathbf{B} , and Λ are to be written as functions of \mathbf{x} and t .

MHD Energy Principle

To compute the second order terms in the energy, we expand the Lagrangian about a given solution $(\mathbf{x}, \rho, \mathbf{B})$, keeping terms up to second order. The first order terms vanish, because the expansion point is a solution of the MHD equations. Terms involving $(\delta\Lambda)^2$, $(\delta\Gamma)^2$, $\delta\mathbf{T} \cdot \delta\mathbf{B}$, $\delta\rho_m \delta\mathbf{B}$, etc. also cancel because of the equations of motion. The remaining second order terms simplify because of the relations (110) for Λ and Γ , and we find

$$\delta^2 L = \int d^3 r \left[\frac{\rho_{m0}}{2} (\delta\dot{x})^2 + \Lambda \delta^2 \mathcal{J} - \frac{1}{2} \rho_{m0} \frac{P'}{\rho_m^2} (\delta\rho_m)^2 - \frac{\rho_{m0}}{8\pi\rho_m} (\delta\mathbf{B})^2 \right]. \quad (117)$$

The second variation of the Jacobian can be computed using an analysis similar to (112)–(113) to yield

$$\delta^2 \mathcal{J} = \frac{\mathcal{J}}{2} (\nabla_i \delta x^i \nabla_j \delta x^j - \nabla_j \delta x^i \nabla_i \delta x^j) = \frac{\mathcal{J}}{2} [(\nabla \cdot \delta\mathbf{x})^2 - Tr(\nabla \delta\mathbf{x})^2]. \quad (118)$$

Using this and changing integration variables yields

$$\begin{aligned} \delta^2 L &= \frac{1}{2} \int d^3 x \left[\rho_m (\delta\dot{x})^2 - \Lambda [Tr(\nabla \delta\mathbf{x})^2 - (\nabla \cdot \delta\mathbf{x})^2] \right. \\ &\quad \left. - \frac{P'}{\rho_m} (\delta\rho_m)^2 - \frac{1}{4\pi} (\delta\mathbf{B})^2 \right]. \end{aligned} \quad (119)$$

The variations $\delta\rho_m$ and $\delta\mathbf{B}$ are constrained by the kinematic relations (112) and (107). Thus

$$\delta\rho_m = \rho_m (\nabla \cdot \delta\mathbf{x}), \quad \delta\mathbf{B} = (\mathbf{B} \cdot \nabla) \delta\mathbf{x} - \mathbf{B} (\nabla \cdot \delta\mathbf{x}). \quad (120)$$

It is not necessary to go beyond the first order terms in computing these variations, since they enter quadratically in (119). These variations are Lagrangian variations, carried out at fixed \mathbf{r} , rather than Eulerian variations, at fixed \mathbf{x} . In order to convert between the two, we could use the identity

$$\delta h|_{\mathbf{r}} = \delta h|_{\mathbf{x}} + (\delta\mathbf{x} \cdot \nabla) h. \quad (121)$$

which follows from (100).

Equation (119) has the form of kinetic energy minus potential energy. It can be transformed into a Hamiltonian using the usual relations (2.36). It is conventional to denote $\delta\mathbf{x}$ by $\boldsymbol{\xi}$ and the energy by $\delta^2 F$; the result is the second order term of the MHD energy:

$$\delta^2 F[\boldsymbol{\xi}] = \frac{1}{2} \int d^3 x \rho_m \dot{\boldsymbol{\xi}}^2 + \delta^2 W[\boldsymbol{\xi}], \quad (122)$$

where $\delta^2 W$ is the potential energy

$$\begin{aligned} \delta^2 W[\boldsymbol{\xi}] = & \frac{1}{2} \int d^3x \left\{ \left(P + \frac{B^2}{8\pi} \right) [Tr(\nabla \boldsymbol{\xi})^2 - (\nabla \cdot \boldsymbol{\xi})^2] \right. \\ & \left. + \frac{5}{3} P(\nabla \cdot \boldsymbol{\xi})^2 + \frac{1}{4\pi} [(\mathbf{B} \cdot \nabla) \boldsymbol{\xi} - \mathbf{B}(\nabla \cdot \boldsymbol{\xi})]^2 \right\}. \end{aligned} \quad (123)$$

Dirichlet's criterion (9) then states that a sufficient condition for the stability of the reference solution is that the energy be uniformly positive definite. Since the kinetic energy satisfies this criterion, it is only necessary to check the potential energy terms. Of these, the $(\delta\rho_m)^2$ and $|\delta\mathbf{B}|^2$ terms in $\delta^2 W$ are positive definite; the only indefinite term is the pressure term, resulting from $\delta^2 J$. This term is not displayed in an especially illuminating form in (123).

A more intuitive form for $\delta^2 W$, in which the terms in the shear-Alfvén law are made explicit, can be obtained by integrating some of the terms by parts, and carrying out extensive algebra. We begin by integrating the term $Tr(\nabla \boldsymbol{\xi})^2$ by parts, using $\nabla(P + B^2/8\pi) = \mathbf{B} \cdot \nabla \mathbf{B}$, and collecting the resulting terms involving the pressure. Some manipulation and partial integration on the remaining magnetic field terms then yields the form

$$\begin{aligned} \delta^2 W[\boldsymbol{\xi}] = & \frac{1}{2} \int d^3x \left[\frac{Q^2}{4\pi} - \frac{1}{c} \boldsymbol{\xi} \cdot \mathbf{J} \times \mathbf{Q} + \frac{5}{3} P(\nabla \cdot \boldsymbol{\xi})^2 \right. \\ & \left. + (\boldsymbol{\xi} \cdot \nabla P)(\nabla \cdot \boldsymbol{\xi}) \right] + \text{B.T.}, \end{aligned} \quad (124)$$

where $\mathbf{Q} = \nabla \times (\boldsymbol{\xi} \times \mathbf{B})$ is the Eulerian variation in \mathbf{B} [as opposed to the Lagrangian variation, (120)]. Here "B.T." stands for a boundary term, arising from the integration by parts, that must be considered when the plasma is surrounded by a vacuum region. We will not need the explicit form of B.T. here.

Some of the terms involving $\boldsymbol{\xi}_{\parallel}$ in (124) in can be shown to vanish:

$$\begin{aligned} & -\frac{1}{c} \boldsymbol{\xi}_{\parallel} \mathbf{b} \cdot \mathbf{J} \times \mathbf{Q} + (\boldsymbol{\xi} \cdot \nabla P)(\nabla \cdot \mathbf{b}\boldsymbol{\xi}_{\parallel}) \\ & = \frac{\boldsymbol{\xi}_{\parallel}}{B} \left[\frac{1}{c} \mathbf{J} \times \mathbf{B} \cdot \mathbf{Q} - \mathbf{B} \cdot \nabla(\boldsymbol{\xi} \cdot \nabla P) \right] \\ & = \frac{\boldsymbol{\xi}_{\parallel}}{B} \nabla \cdot [\nabla P \times (\boldsymbol{\xi} \times \mathbf{B}) - \mathbf{B}(\boldsymbol{\xi} \cdot \nabla P)] = 0. \end{aligned} \quad (125)$$

Furthermore, it is convenient to separate the parallel and perpendicular

components of \mathbf{Q} using

$$Q_{\parallel} = \mathbf{b} \cdot \nabla \times (\boldsymbol{\xi}_{\perp} \times \mathbf{B}) = -B(\nabla \cdot \boldsymbol{\xi}_{\perp} + 2\boldsymbol{\xi}_{\perp} \cdot \boldsymbol{\kappa}) + \frac{4\pi}{B} \boldsymbol{\xi}_{\perp} \cdot \nabla P,$$

Then we find, finally,

$$\begin{aligned} \delta^2 W[\boldsymbol{\xi}] &= \frac{1}{2} \int d^3x \left[\frac{Q_{\perp}^2}{4\pi} + \frac{B^2}{4\pi} |\nabla \cdot \boldsymbol{\xi}_{\perp} + 2\boldsymbol{\xi}_{\perp} \cdot \boldsymbol{\kappa}|^2 + \frac{5}{3} P(\nabla \cdot \boldsymbol{\xi})^2 \right. \\ &\quad \left. + (\boldsymbol{\xi}_{\perp} \cdot \nabla P)(\boldsymbol{\xi}_{\perp} \cdot \boldsymbol{\kappa}) - \frac{1}{c} J_{\parallel} \mathbf{b} \cdot (\mathbf{Q}_{\perp} \times \boldsymbol{\xi}_{\perp}) \right] + \text{B.T.} . \quad (126) \end{aligned}$$

Here the various terms from the shear-Alfvén law are explicitly displayed. The first term, $Q_{\perp}^2/4\pi$ is the line bending energy—it is the energy contained in the perpendicular field perturbation. The second and third terms are the magnetic and fluid compressional energies. These first three terms are positive and hence stabilizing. The last two terms involve pressure gradients and parallel currents; they are the interchange and kink energies, related to the analogous terms in the shear-Alfvén law (23). These can have either sign.

Our conclusion from (88) is confirmed: when $\nabla P \cdot \boldsymbol{\kappa} < 0$ the interchange energy is negative and destabilizing. Furthermore (126) makes explicit the fact that interchange instability requires both pressure gradients and curvature.

In (126), the parallel component of the displacement enters only in the fluid compressibility term, which is stabilizing. Minimization of this term occurs for a displacement satisfying $\nabla \cdot \tilde{\boldsymbol{\xi}} = 0$. Since (126) is always smaller for such displacements,

$$\delta^2 W[\tilde{\boldsymbol{\xi}}] \Big|_{\nabla \cdot \tilde{\boldsymbol{\xi}} = 0} \leq \delta^2 W[\boldsymbol{\xi}] , \quad (127)$$

it is clear that the most pessimistic stability criteria will be obtained for the incompressible limit.

A similar statement can be made for kinetic MHD, discussed in §6.4: it results in an energy principle that differs from (126) by the addition of positive terms (Kruskal and Oberman, 1958; Rosenbluth and Rostoker, 1959). Thus the most stringent ideal stability limits are obtained from incompressible MHD.

Part 3: Resistive Stability

In ideal models, the conservation of magnetic flux provides a strong constraint on plasma motions: it implies that the topology of field lines cannot change. In fact the Lagrangian interpretation of flux conservation, (103), implies that two fluid elements on the same field line at $t = 0$ remain on the same field line for all time: only when the ideal constraint is relaxed can the topology of field lines change. Thus it is clear that the kink and interchange stability results that we obtained in the ideal case are overly optimistic.

A change in topology of the magnetic field lines is known as *reconnection*. One envisions the field lines, which are toroidal helices, “breaking,” reconnecting, and creating new lines. Although the concept of a “field line” is not well defined when nonideal effects are included, it remains useful, since the slippage between fluid element trajectories and the magnetic field is typically slow. We defer the discussion of the new topologies created by reconnection to Chapter 9. Here we treat the linear effects arising from relaxing the ideal constraint.

Any study of ideal MHD stability involves geometrical complications because the modes extend over the entire plasma. In the shear-Alfvén law, the dominant balance between the line bending term and the kink and interchange is valid over most of the plasma. In fact, far from the rational surface singularity, the relatively small corrections to the ideal closure relations do not affect the evolution. Only when $k_{\parallel} \ll k_{\perp}$, i.e. only in the flute limit, do corrections to the ideal equations alter the dynamics in a significant way.

We will study two alternative scenarios for the flute behavior. In the first case the rational surface singularity is crucial; thus k_{\parallel} is inherently small in a boundary layer about the rational surface. Non-ideal terms then result in reconnection of the magnetic field, giving rise to “tearing instabilities” and magnetic islands. These form the subject of §7.7–7.9.

The second case has large k_{\perp} : the limit of large mode number. Then modes arise, driven mainly by the interchange term, that are localized to regions of unfavorable curvature. In toroidal geometry this implies a poloidal localization to the outside of the torus. We study these in §7.10–7.13.

7.7 Asymptotic Matching

Recall here the notation of (94): $\mathbf{x} = \mathbf{r} - \mathbf{r}_*$ denotes the radial variable in the neighborhood of a singular surface, \mathbf{r}_* . The boundary layer width will be denoted by w ; its value will be determined by which of the terms in the

shear-Alfvén law are used to resolve the singularity. Far from the singular layer, $|x| \gg w$, the inertial and resistive terms in the eigenmode equations become unimportant, but the geometrical complications of toroidal geometry are manifest. Thus the outer region equation is the neighboring equilibrium form of the shear-Alfvén law. We have already studied this for the cylindrical case, obtaining (86). This equation is to be solved in the outer region, with the appropriate boundary conditions (75) and (76). The solution will schematically look like Fig. 7.5.

Imagine integrating from $r = 0$, to obtain a solution for the region $r < r_s$, and from $r = a$ to obtain a solution for $r > r_s$. Near the rational surface both of these solutions will be singular in general; in fact the outer equation approaches (95) (the fully toroidal system is identical, except that D is replaced by the more complicated Mercier expression), and the solutions have the form

$$\varphi = \begin{cases} -A_L|x|^{\nu_-} + B_L|x|^{\nu_+}, & x < 0 \\ A_R|x|^{\nu_-} + B_R|x|^{\nu_+}, & x > 0 \end{cases} \quad (128)$$

where ν_{\pm} are the two roots (97). When $D > 1/4$ the system is ideally unstable, by the Suydam criterion, and there is no need to study boundary layer corrections. When $D < 1/4$, ν_{\pm} are real and $-1 \leq \nu_- \leq -1/2 \leq \nu_+ \leq 0$. If an ideal solution were to exist, then the energy of the mode must be finite; since the kinetic energy is proportional to φ^2 this implies that A_L and A_R would both have to vanish. While one of A_L and B_L (A_R and B_R) can be chosen arbitrarily, representing the overall amplitude of the solution, the ratios A_L/B_L and A_R/B_R are fixed by the boundary conditions at $r = 0$ and $r = a$ and do not typically vanish. It follows that there is no ideal solution in general. A separate, non-ideal treatment of the layer near r_s is called for.

Near the rational surface, $x \sim w \ll a$, effects such as resistivity and inertia become important and must be included to obtain "layer" equations. The solution of the layer equations is simplified by the boundary layer ordering. However, the layer system will be higher order: dissipative terms introduce additional derivatives, giving a fourth (or higher) order system.

In order to construct a complete solution to the problem, the layer solution must join smoothly to the outer solution in an intermediate region $w \ll x \ll a$. In order to match the outer solution, the inner solution must exhibit a power law with the same powers as (128). This requirement eliminates solutions of the inner equations that are exponentially growing or decaying. What remains are solutions involving two arbitrary constants

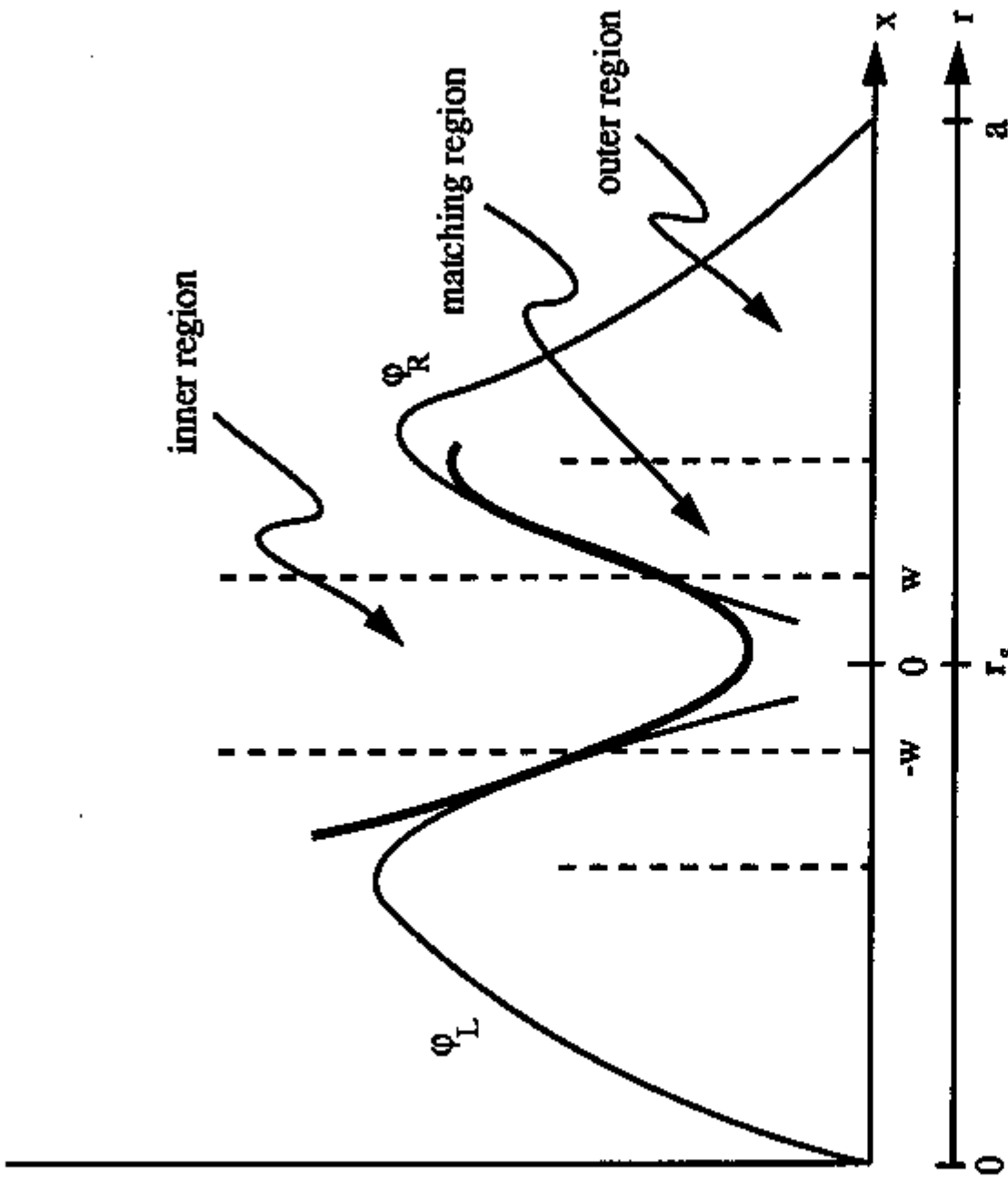


Figure 5. Sketch of an eigenfunction. The outer solutions φ_R and φ_L are labelled and the inner resistive solution is shown as the thicker line. They must smoothly match in a region $w \ll x \ll a$.

which, as we will see, have the form

$$\varphi = \begin{cases} -\varphi_0 |x|^{\nu_-} + \varphi_L |x|^{\nu_+}, & x < 0 \\ \varphi_0 |x|^{\nu_-} + \varphi_R |x|^{\nu_+} & x > 0 \end{cases} \quad (129)$$

in the matching region. Here φ_R can be expressed, by means of the layer equation, in terms of φ_0 and φ_L . There are thus two free parameters in the outer solutions, A_R and A_L , and two free parameters for the inner solution, φ_0 and φ_L . Matching is accomplished by choosing the amplitude of the left and right solutions to match the inner solution:

$$A_L = \varphi_0 = A_R.$$

Setting $\varphi_L = B_L$ then specifies the solution completely (up to an arbitrary amplitude). The remaining matching condition $\varphi_R = B_R$ provides

the dispersion relation; it specifies the frequency of the mode since the inner solution depends on the inertia, and hence on ω .

Alternatively, we can define

$$\Delta' \equiv \frac{B_L}{A_L} - \frac{B_R}{A_R}, \quad (130)$$

a quantity that is determined by the outer, ideal solution. Then the dispersion relation is determined by setting

$$\frac{\varphi_R - \varphi_L}{\varphi_0} = \Delta'. \quad (131)$$

For the zero β case the asymptotic form becomes $\varphi = \varphi_{L,R} + \varphi_0/x$, since $\nu_+ = 0$ and $\nu_- = -1$. In this case, as we will see, Δ' represents the total current in the boundary layer.

In the sheared slab geometry, $\mathbf{B} = \hat{\mathbf{z}} + \hat{\mathbf{y}}x/L_s$, and $\beta = \text{constant}$; Δ' can be computed analytically, with the result

$$\Delta' L_s = 2 \left(\frac{1}{k L_s} - k L_s \right),$$

where k is the wavenumber in the y direction (for the cylinder k is replaced by m/r). Verification of this form is left as an exercise. As we will see below the resistive stability criterion is $\Delta' < 0$ for the zero β case. Note that Δ' is negative when $k L_s > 1$. More generally, numerical computation is required to determine Δ' . For example, the cylindrical, zero β case was studied by Furth, Rutherford, and Selberg (1973). Here Δ' is found to be infinite for $m = 1$, because $D = 0$, $\nu_- = -1$ and $\nu_+ = 0$, and the analytic solution for φ (84), implies that $A_R = A_L = 0$ (of course Δ' is not infinite when $\beta' \neq 0$, but for $m = 1$ it is still large). Numerical computations show that Δ' is a decreasing function of m , analogous to the slab result. Like the slab version, it is positive only for low m : typically $m = 2$ and 3 for models in which the current profile is not too peaked.

7.8 Boundary Layer Theory

We next consider an axisymmetric equilibrium, using the flux coordinates (r, θ, ζ) , and the flux representation for \mathbf{B} (3.14). Equilibrium quantities may depend on r and θ . The flute-reduced equations are valid near a rational surface, $q(r_s) = m/n$, for modes of the proper helicity. We linearize in the usual way:

$$h(r, \theta, \zeta) \rightarrow h_0(r, \theta) + h_{mn}(r)e^{i(m\theta - n\zeta)}. \quad (132)$$

In the neighborhood of the rational surface, the geometry can be simplified by expanding all quantities for $x \sim w \ll a$. This ordering implies that the

“fast” coordinate is x , and the slow coordinates are (θ, ζ) . Thus the fast gradient is

$$\nabla_f = \nabla_\perp \rightarrow \nabla_r \frac{\partial}{\partial x}. \quad (133)$$

The linearized parallel gradient from (54) is

$$\nabla_{\parallel} = \mathbf{b}_0 \cdot \nabla = \frac{B^\theta}{B} \left(\frac{\partial}{\partial \theta} + q \frac{\partial}{\partial \zeta} \right) \Rightarrow ik_{\parallel} = i \frac{B^\theta}{B} (m - nq) \quad (134)$$

where the \Rightarrow indicates the action on the (m, n) Fourier component. Expanding in the neighborhood of r_s gives

$$k_{\parallel} \approx k'_{\parallel} x. \quad (135)$$

Here k'_{\parallel} is evaluated at r_s , but may depend on θ if the equilibrium is not circular.

Low-beta Tearing Modes

We first study the linear eigenmodes of flute-reduced MHD (53) in the low-beta limit. Thus the interchange term in (53) is neglected, and the shear-Alfvén law is decoupled from the pressure. Only two dynamical equations are required:

$$\begin{aligned} \frac{d}{dt} U &= -v_A^2 \nabla_{\parallel} \nabla_{\perp}^2 \psi \\ \frac{1}{c} \frac{\partial \psi}{\partial t} + \nabla_{\parallel} \varphi &= \frac{\eta c}{4\pi} \nabla_{\perp}^2 \psi \end{aligned} \quad (136)$$

where B_0 reduces to \bar{B} , which is constant in the boundary layer. In the low-beta limit, the equilibrium can be assumed to be circular. Thus both ∇r and k'_{\parallel} are constants on the rational surface. Substituting (128)-(135) into (136), and linearizing, yields

$$\omega \frac{\partial^2 \varphi}{\partial x^2} - \frac{v_A^2}{c} k'_{\parallel} x \frac{\partial^2 \psi}{\partial x^2} = 0 \quad (137)$$

$$\omega \psi - ck'_{\parallel} x \varphi = i \frac{\eta c^2}{4\pi} \frac{\partial^2 \psi}{\partial x^2}. \quad (138)$$

Here (137) is the linearized shear-Alfvén law; it balances plasma inertia against line bending, with no vestige of curvature. In fact the same equation could have been obtained in slab geometry. However, this equation does not correspond to a homogeneous medium because it contains the x dependence due to the variation of k_{\parallel} . In other words, what survives the reductions and

simplifications is toroidal topology (periodicity in θ and ζ) and magnetic shear.

Equations (137) and (138) can be easily combined to give a single fourth-order differential equation. Interestingly, however, two of the integrations can be carried out trivially. Upon defining

$$E \equiv \varphi',$$

which measures the radial electric field, we find that (137) becomes

$$E' = \frac{v_A^2}{c\omega} k'_\parallel x \psi'' \quad (139)$$

Noticing that

$$x\psi'' = (x\psi' - \psi)' = \left[x^2 \left(\frac{\psi}{x} \right)' \right]',$$

we can integrate (139) once to obtain

$$\omega E' - \frac{v_A^2}{c} k'_\parallel x^2 \left(\frac{\psi}{x} \right)' = C, \quad (140)$$

where C is an integration constant. Finally, dividing (138) by x , and differentiating using (140) gives

$$\left[1 - \left(\frac{v_A k'_\parallel x}{\omega} \right)^2 \right] E - i \frac{c^2}{4\pi} \frac{x^2}{\omega} \left(\frac{\eta E'}{x^2} \right)' = \frac{C}{\omega}. \quad (141)$$

Equation (141) for E is a second order differential equation. Its solution involves two arbitrary constants; solving for φ requires integrating once more. Thus there are four integration constants for the fourth order system. Equation (141) is valid only in the boundary layer, $x \sim w$. The boundary layer solution must smoothly connect to the ideal solution in the outer region. The outer solutions have the asymptotic form given by (128), which for zero β implies that $\varphi \sim B + A/x$ or $E \sim A/x^2$, for $|x| \ll a$.

The asymptotic form of the solutions to (141) is easily obtained. First consider the homogeneous equation. Assuming the eikonal form for $E \sim \exp[S(x)]$ implies $S'^2 = \alpha^2 x^2$, so $S = \pm \alpha x^2/2$, where α is positive if the growth rate $\gamma = -i\omega > 0$. Corrections to this form can be obtained by standard WKB techniques; however, we are only interested in the dominant behavior,

$$E \sim c_1 e^{\frac{\alpha}{2} x^2} + c_2 e^{-\frac{\alpha}{2} x^2} \quad |x| \gg w. \quad (142)$$

Matching is impossible unless c_1 vanishes. The c_2 term decays exponentially and gives a mode for which E (but not φ) is localized within the boundary layer. This corresponds to the large Δ' case, and is discussed below.

The inhomogeneous part of the solution to (141) is obtained by balancing the line bending term with the right-hand side, giving

$$E \rightarrow -\frac{C\omega}{(v_A k'_\parallel x)^2}, \quad |x| \gg w. \quad (143)$$

This connects onto the solution of the ideal equations. Since (143) is valid only far from the origin, we must allow for different integration constants, φ_R and φ_L , on either side:

$$\varphi \rightarrow \varphi_{R,L} + \frac{\varphi_0}{x}, \quad x \rightarrow \pm\infty \quad (144)$$

where $\varphi_0 = C\omega/(k'_\parallel v_A)^2$. Note that φ_R is determined by the choice of φ_L , since $\varphi_R = \varphi_L + \int E(y)dy$. Also, it follows from (138) that

$$\psi \rightarrow A_0 + A_{R,L}x, \quad x \rightarrow \pm\infty \quad (145)$$

where $A_0 = (ck'_\parallel/\omega)\varphi_0$.

The fourth order system is characterized by the integration constants, c_1 , c_2 , A_0 , and A_R . The constants A_R and A_L determine the total current in the layer:

$$\int_{-\infty}^{\infty} dx J = A_R - A_L. \quad (146)$$

As far as solutions of the boundary layer problem are concerned, Δ' is taken to be given by (130). Thus, (139) implies that

$$\int_{-\infty}^{\infty} dx J = A_0 \Delta'. \quad (147)$$

Combining (147) and (139) allows us to convert the differential equation (141), including the asymptotic limits (145), into an integro-differential equation⁴

$$\left[1 - \left(\frac{v_A k'_\parallel x}{\omega} \right)^2 \right] E - i \frac{c^2}{4\pi} \frac{x^2}{\omega} \left(\eta \frac{E'}{x^2} \right)' = \frac{1}{\Delta'} \int_{-\infty}^{\infty} dx \frac{E'}{x}, \quad (148)$$

which is to be solved with the simple boundary condition

$$E \rightarrow 0 \quad \text{as } |x| \rightarrow \infty. \quad (149)$$

A more transparent form of (148) involves two characteristic widths. First, the shear-Alfvén width, x_A , is the width at which the growth rate, $\gamma = -i\omega$, is locally equal to the shear-Alfvén frequency,

$$x_A = \frac{\gamma}{k'_\parallel v_A}. \quad (150)$$

⁴Equation (148) has been written in such a way as to be valid even when \tilde{v} depends on position, as it does for the current channel modes discussed later.

Second, the resistive skin depth, x_R , measures the size of the resistive term in (148):

$$x_R^2 = \frac{\eta c^2}{4\pi\gamma}. \quad (151)$$

Then (148) becomes

$$\left[1 + \left(\frac{x}{x_A} \right)^2 \right] E - (xx_R)^2 \left(\frac{E'}{x^2} \right)' = \frac{1}{\Delta'} \int_{-\infty}^{\infty} dx \frac{E'}{x}. \quad (152)$$

Notice that the highest derivative term in (152) is the resistive term. Thus resistivity, however small, is a singular perturbation, in that its inclusion changes the order of the system. On the other hand, resistivity resolves the ideal singularity at $x = 0$ exhibited by (143).

Eigenmode Classification

An important feature of (152) is the symmetry of its integro-differential operator under $x \rightarrow -x$. This implies that the eigenmode solutions can be chosen to have definite parity: $E = E_+(x)$ or $E_-(x)$ where

$$E_\sigma(x) = \sigma E_\sigma(-x), \quad \sigma = \pm 1.$$

We call these solutions even and odd, respectively. Notice that ψ and J must have the same parity as E , while φ has the opposite parity.

As we will see in Chapter 9, topology change is primarily associated with the even eigenmodes. We therefore call them *tearing modes*, following the terminology of Furth, Killeen and Rosenbluth (FKR) who first analyzed reconnection in the confined plasma context (Furth et al., 1963). The odd eigenmodes are called *twisting modes* (Strauss, 1979); they exemplify a class of instabilities that display boundary-layer behavior, but still satisfy the Newcomb condition (since $\psi(0)$ must vanish).

There is another criterion used to classify the eigenmodes: the size of Δ' . Noticing that Δ' has the units of inverse length, the case

$$\Delta'w \ll 1 \quad (153)$$

is called “small Δ' ”, while

$$\Delta'w \gtrsim 1 \quad (154)$$

is called “large Δ' .“ Since Δ' measures the slope of $\psi(x)$, we see that ψ is nearly constant (despite its large curvature, ψ'') when $\Delta'w$ is small. Thus when studying the small Δ' case, FKR simplified (138) by replacing ψ on the right-hand side by A_0 , a constant (the constant- ψ approximation). We will see that this is equivalent to the neglect of the inertial term in (152).

Large Δ' is associated either with steep slope or with negligibly small A_0 . In general one can treat this case by taking the limits

$$A_0 \rightarrow 0 \quad \text{or} \quad \Delta' \rightarrow \infty.$$

As we discussed above, Δ' is large in particular for $m = 1$; indeed, for the zero- β cylinder, $\Delta' \rightarrow \infty$ for $m = 1$.

Dispersion Relations: Estimates

The four terms in (152) can be identified as the inertia, line bending, resistive diffusion, and kink terms respectively. Simple estimates for the eigenvalues $\omega(k'_\parallel, \Delta', \eta)$ of (152) can be obtained by various balances among these terms. There are three relevant scale lengths: the radial width, w , of the radial electric field, the shear-Alfvén width, x_A , and the resistive width x_R . For example, using $E' \sim E/w$, we can estimate the resistive term in (152) as

$$(xx_R)^2 \left(\frac{E'}{x^2} \right)' \sim \left(\frac{x_R}{w} \right)^2 E.$$

Applying this argument to all four terms gives the relative orderings:

inertia	line bending	resistive diffusion	kink
1	$\left(\frac{w}{x_A} \right)^2$	$\left(\frac{x_R}{w} \right)^2$	$\frac{1}{\Delta' w}$

Since there are two unknown quantities, γ and w , determination of a dispersion relation requires two equations. These follow from a balance among any three of the four terms. Two of these balances lead to uninteresting behavior. First, neglecting the resistive term gives $x_A \sim w \sim 1/\Delta' \gg x_R$. This mode, which does not involve resistivity at all, is a singular Alfvén mode, considered in §7.5. Second, neglecting the line bending term implies that $x_R \sim w \sim 1/\Delta' \ll x_A$, which corresponds to slow resistive diffusion.

The case when the kink term is negligible corresponds to the large Δ' modes. The dispersion relation for this case results from the balance of inertia, line bending and resistive diffusion: $w \sim x_A \sim x_R \gg 1/\Delta'$. Using the definitions (150) and (151) gives

$$\gamma^3 \sim (k'_\parallel v_A)^2 \frac{\eta c^2}{4\pi}. \quad (155)$$

This is the dispersion relation for large Δ' modes.

Finally when the inertial term is negligible, the mode corresponds to a balance between line bending, resistive diffusion and kink terms, which gives

$$w \sim (x_A x_R)^{1/2} \quad (156)$$

and the dispersion relation

$$\Delta' \sim \left(\frac{x_A}{x_R^3} \right)^{1/2}. \quad (157)$$

Recalling the definitions of x_A and x_R yields the growth rate

$$\gamma \sim (\Delta')^{4/5} \left(\frac{\eta c^2}{4\pi} \right)^{3/5} (k'_\parallel v_A)^{2/5}. \quad (158)$$

This small- Δ' result corresponds to the tearing mode dispersion relation of FKR. Note that the sign of the kink term in (152) goes with that of $\Delta' E$. The sign of the resistive term on the left-hand should be that of γ_E for tearing parity, since $E'' \propto -E$ in this case. Thus we expect that the small Δ' modes will be unstable when

$$\Delta' > 0. \quad (159)$$

Dispersion Relation: Large Δ' *

An exact dispersion relation for (152) is simplest to obtain in the large Δ' case. By (154) the right-hand side of (152) can be neglected, yielding a second order differential equation. Using the substitution

$$E(x) = e^{-\frac{\alpha}{2}x^2} M(\alpha x^2),$$

with

$$\alpha = \frac{1}{x_R x_A} \quad (160)$$

and $z = \alpha x^2$, results in the differential equation

$$zM'' - \frac{2z+1}{2} M' - bM = 0$$

where $b = -\frac{1}{4}(1 - x_A^2 \alpha)$. This is a confluent hypergeometric equation;⁵ its two linearly independent solutions are denoted by

$$M(b, -\frac{1}{2}, \alpha x^2), \quad x^3 M\left(\frac{3}{2} + b, -\frac{5}{2}, \alpha x^2\right).$$

For large $|x|$ these solutions grow as $\exp(\alpha x^2)$, unless the first argument M is a negative integer, in which case M is a polynomial. Since exponential growth, as in (142), is ruled by the boundary condition (149), we obtain the two solutions

$$E_+^{(n)}(x) = e^{-\frac{\alpha}{2}x^2} M(-n, -\frac{1}{2}, \alpha x^2) \quad (161)$$

$$E_-^{(n)}(x) = e^{-\frac{\alpha}{2}x^2} x^3 M(-n, \frac{5}{2}, \alpha x^2)$$

*See Chapter 13 of (Abramowitz and I.A. Stegun, 1965).

where n is an integer and

$$x_A^2 \alpha = \begin{cases} 1 - 4n, & E_+ \\ -5 - 4n, & E_- \end{cases}. \quad (162)$$

These two solutions correspond to the exponentially decaying solution in (142). Combining (160) and (162) gives the dispersion relation.

In order that (161) decay as $|x| \rightarrow \infty$, we must demand that $\Re(\alpha) > 0$. Then (162) implies that $\Re(x_A^2) < 0$ except for $E_+^{(0)}$, when $\Re(x_A^2) > 0$. Since $x_A^2 \sim \gamma^2$, this provides restrictions on the phase of the growth rate as shown in Fig. 7.6. In fact there is only one unstable mode, $E_+^{(0)}$. This is

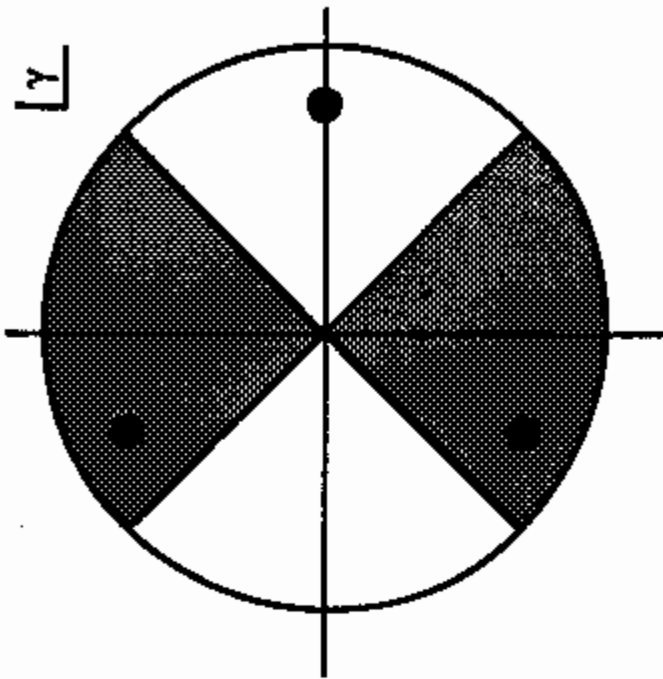


Figure 6. Complex γ Plane. Shaded regions are determined by $\Re(\gamma^2) < 0$. The dispersion relation has three solutions, given by the black points.

the large Δ' tearing mode. Using (160) and (162) we find its growth rate is exactly that given by the estimate (155). All other modes have growth rates with phases $\pm 2\pi/3$; thus all the remaining tearing and twisting modes are stable.

Dispersion Relation: Small Δ' *

To obtain a dispersion relation for the small Δ' modes, we neglect the inertial term in (152). Dividing the equation by x^2 , letting $E = \varphi'$, and integrating the equation once gives

$$\varphi'' - \left(\frac{x}{x_A x_R} \right)^2 \varphi = \frac{x}{\Delta' x_R^2} \int_{-\infty}^{\infty} \frac{\varphi''}{x} dx. \quad (163)$$

The homogeneous part of (163) is a parabolic cylinder equation.⁶ Using α as defined by (160), and letting $y^2 = \alpha x_r^2/2$, we obtain from (163),

$$\varphi_{yy} - 4y^2\varphi = \frac{y}{\Delta' x_r^2} \sqrt{\frac{2}{\alpha}} \int_{-\infty}^{\infty} \frac{\varphi_{yy}}{y} dy . \quad (164)$$

In order to solve (164), it is efficient to Fourier transform, letting $\varphi(y) = \int e^{iky} \varphi(k) dk$. Then $\partial/\partial y \rightarrow ik$, $y \rightarrow i\partial/\partial k$, and the right-hand side can be written in terms of the derivative of a Dirac delta function. Thus

$$\varphi_{kk} - \frac{1}{4}k^2\varphi = C\delta'(k) , \quad (165)$$

where

$$C = i \frac{1}{4\Delta' x_R^2} \sqrt{\frac{2}{\alpha}} \int_{-\infty}^{\infty} \frac{\varphi_{yy}}{y} dy . \quad (166)$$

Fourier transform converts large x behavior to small k behavior; thus the $k = 0$ singularity in (165) reflects the ideal singularity in the matching region. The two linearly independent solutions to the homogeneous part of (165) are the parabolic cylinder functions $U(0, k)$, and $V(0, k)$. The latter must be rejected because it grows exponentially for large k . The solution of the inhomogeneous equation is therefore

$$\varphi(k) = \begin{cases} A_+ U(0, k) & k > 0 \\ A_- U(0, k) & k < 0 . \end{cases} \quad (167)$$

The two coefficients A_+ and A_- can be obtained by integrating (165) across $k = 0$, to give

$$(A_+ - A_-)U(0, 0)\delta(k) = C\delta(k) . \quad (168)$$

Thus we can choose $A_+ = C/2U(0, 0)$, and $A_- = -C/2U(0, 0)$. To obtain the dispersion relation, we substitute (168) into (166) and find

$$\begin{aligned} 4\Delta' x_r^2 \sqrt{\frac{\alpha}{2}} C &= -i \int_{-\infty}^{\infty} \frac{\varphi_{yy}}{y} dy = -i \int_{-\infty}^{\infty} dk k^2 \varphi(k) \int_{-\infty}^{\infty} dy \frac{e^{iky}}{y} \\ &= \pi \int_{-\infty}^{\infty} dk k^2 \varphi(k) \\ &= \frac{4\pi C}{2U(0, 0)} \left[\int_0^{\infty} U_{kk}(0, k) dk - \int_{-\infty}^0 U_{kk}(0, k) dk \right] \\ &= -4\pi C \frac{U'(0, 0)}{U(0, 0)} . \end{aligned}$$

⁶ See Chapter 19 (Abramowitz and Stegun, 1965).

Evaluating the parabolic cylinder functions at zero gives⁷

$$\Delta' = \frac{2\pi}{\sqrt{\alpha}} \frac{x_R^2}{x} \frac{\Gamma(3/4)}{\Gamma(1/4)}. \quad (169)$$

Note that (169) differs from the estimate (157) only by a factor of 2.12.

The tearing mode is unstable when $\Delta' > 0$. As we discussed above, Δ' is commonly positive only for low- m modes. Corresponding disturbances are often seen in experiments. So called “micro-tearing” modes, for large m , may also be present, but are not accounted for by the simple models presented so far.

7.9 Kinetic Effects*

The MHD Ohm’s law is a vast oversimplification of the electron response. As we will see, the primary effect of a more careful treatment is to modify the conductivity for nonzero frequency and parallel wavenumber. In particular, the generalized conductivity $\sigma_*(\nu, \omega, k_{\parallel})$, reduces to the MHD conductivity at $\omega = k_{\parallel} = 0$, but can be significantly smaller at appreciable distances from the rational surface.

Electron Response

In this section we derive the electron response for the simplest kinetic model: the collisionless drift kinetic equation (4.72), in slab geometry, with $\nabla T = 0$. For the equilibrium we use the Maxwell-Boltzman distribution, (5.108) and (5.115), with $\mathbf{E}_0 = 0$. We assume large aspect ratio in order to neglect the ∇B and curvature drifts. Then, linearizing about the equilibrium with

$$\bar{f} = f_M + f_1, \quad (170)$$

gives

$$\mathcal{L}_0 f_1 = - \left(v_{\parallel} \mathbf{b}_1 + \frac{c}{B_0} \mathbf{b}_0 \times \nabla \Phi \right) \cdot \nabla f_M + e v_{\parallel} \mathbf{b}_0 \cdot \mathbf{E}_1 \frac{\partial f_M}{\partial w}, \quad (171)$$

where

$$\mathcal{L}_0 = \frac{\partial}{\partial t} + v_{\parallel} \mathbf{b}_0 \cdot \nabla - C_1 \quad (172)$$

is the lowest order drift kinetic operator. To solve (172), it is convenient to write

$$f_1 = -e \frac{\partial f_M}{\partial w} \Phi_1 + g_1 = f_M \frac{e\Phi}{T} + g_1. \quad (173)$$

⁷Equation (19.4.1) of (Abramowitz and Stegun, 1965).

Here the first term can be recognized as the linearization of the Maxwell-Boltzmann factor (5.102). In fact, if we were to neglect the electromagnetic terms in (171), and assume

$$\frac{\partial}{\partial t} \ll v_{\parallel} \mathbf{b} \cdot \nabla \quad (\text{adiabatic limit}), \quad (174)$$

then the second term of (173) would be small. Equation (174) implies that the electrons can sample the parallel structure of the perturbed potential before the latter changes appreciably. As in (6.162), when the first term of (173) dominates the second, the electron response is referred to as *adiabatic*. Note, however, that even in the electrostatic case (174) will break down in the vicinity of the rational surface.

Substituting (173) into (171) gives

$$\mathcal{L}_0 g_1 = Q \equiv -\frac{e}{T} f_M \frac{\partial}{\partial t} \left(\Phi_1 - \frac{v_{\parallel}}{c} A_{\parallel} \right) - \left(v_{\parallel} \mathbf{b}_0 + \frac{e}{m} \mathbf{b}_0 \times \nabla \Phi \right) \cdot \nabla f_M , \quad (175)$$

since $\mathbf{b}_0 \cdot \nabla f_M = 0$, and $C_1(\Phi_1, f_M) = 0$. To solve this equation we must invert the operator \mathcal{L}_0 . When collisions are important, inversion is difficult; however, in this section we neglect the effects of collisions, and inversion is relatively easy.

Since v_{\parallel} is approximately constant, we can use flux coordinates (r, θ, ζ) to write

$$g_1 = \tilde{g}(r, \mu, w) e^{i(\omega t + m\theta - n\zeta)} . \quad (176)$$

Such a representation would not be correct for trapped particles, where only a limited range of θ is accessible, but our large aspect ratio approximation neglects trapping. Now (172) gives

$$\mathcal{L}_0 g_1 \Rightarrow -i(\omega - k_{\parallel} v_{\parallel}) \tilde{g} , \quad (177)$$

where k_{\parallel} is given by (15). Thus inversion of \mathcal{L}_0 in this case involves nothing more than dividing by the factor $-i(\omega - k_{\parallel} v_{\parallel})$, displaying the familiar Landau resonance at $\omega = k_{\parallel} v_{\parallel}$. However, we will find that the most important aspect of \mathcal{L}_0^{-1} is usually not this resonance, but rather the radial variation of k_{\parallel} associated with magnetic shear.

Using the solution for g_1 from (175) and (176) gives

$$f_1 = f_M \frac{e\Phi}{T} + i \frac{Q}{\omega - k_{\parallel} v_{\parallel}} . \quad (178)$$

Integrating over v_{\parallel} to determine the density or current moments will yield expressions involving the *plasma dispersion function* $Z(z)$, which is defined by

$$Z(z) \equiv \frac{1}{\sqrt{\pi}} \int_{-\infty}^{\infty} dt \frac{e^{-t^2}}{t - z} , \quad \Im(z) > 0 \quad (179)$$

and by analytic continuation of the above integral for $\Im(z) < 0$. In this case the argument is given by

$$z = \frac{\omega}{|k_{\parallel}|v_{te}}, \quad (180)$$

where the absolute value allows (179) to be applied to unstable modes. Of particular interest is the velocity moment of (178)

$$nV_{\parallel e} = \int d^3v v_{\parallel} f_1 \approx \int d^3v v_{\parallel} g_1. \quad (181)$$

To compute $nV_{\parallel e}$, we first simplify (175). We use the representation (30) for \mathbf{B}_1 , noting that for the low-beta case, the B_{\parallel} term can be dropped, since it is proportional to the pressure perturbation, as in (37). Using the Fourier form (176) for Φ_1 and $A_{\parallel} = B_0 \psi$ we express Q as

$$Q \Rightarrow i \frac{e}{T} f_M (\omega - \omega_{*e}) \left(\tilde{\Phi} - \frac{v_{\parallel}}{c} \tilde{A}_{\parallel} \right), \quad (182)$$

where ω_{*} is the drift frequency

$$\omega_{*e} = -\frac{Tc}{e} \frac{1}{f_M} \frac{\partial f_M}{\partial r} \left(\frac{nB_{\theta} + mB_{\zeta}}{\sqrt{g} B^2} \right). \quad (183)$$

When $\nabla T = 0$, ω_{*} is the same as the diamagnetic rotation obtained in drift fluid model, since (6.112) implies that

$$\mathbf{V}_{pe} \cdot \nabla = \frac{1}{m\Omega_s} \mathbf{b} \times \nabla(n_s T_s) \cdot \nabla \Rightarrow i\omega_{*s}. \quad (184)$$

However, inclusion of ∇T invalidates this relation, even after a Maxwellian average; recall (4.185).

A simpler expression for ω_{*} holds at the rational surface. Since $B^2 = B^{\theta} B_{\theta} + B^{\zeta} B_{\zeta}$, (2.25) implies $B_{\theta} + q B_{\zeta} = \sqrt{g} B^2 / \chi'$. Hence we find

$$\omega_{*e}(r_s) = -n \frac{Tc}{e\chi'} \frac{1}{f_M} \frac{\partial f_M}{\partial r}. \quad (185)$$

A simple estimate is

$$\omega_{*e} \sim k_{\perp} \rho_e \frac{v_{te}}{a}.$$

Now we can integrate (181) straightforwardly and find

$$V_{\parallel e} = -i \frac{E_{\parallel}}{2T} \frac{\omega - \omega_{*e}}{k_{\parallel}^2} Z'(z). \quad (186)$$

It is noteworthy that the parallel flow depends on Φ and A_{\parallel} only through $E_{\parallel} = i(\omega A_{\parallel}/c - k_{\parallel}\Phi)$. This circumstance, which is unsurprising on physical grounds, survives both the inclusion of temperature gradients, and of collisions; however, it does depend on the neglect of the non-Maxwellian correction to f_M .

Current Channel Modes

The most important feature of (186) is its strong radial dependence. This is most straightforwardly expressed in terms of a new length

$$x_* = \left| \frac{\omega}{k'_\parallel v_{te}} \right|. \quad (187)$$

For $x \ll x_*$, $k'_\parallel v_t \ll \omega$, and thus $z \gg 1$. In this limit, $Z(z) \rightarrow 1/z$, so the parallel velocity becomes

$$V_{\parallel e} \rightarrow -\frac{i}{2} E_\parallel \frac{e}{m_e} \frac{\omega - \omega_{*e}}{\omega^2}, \quad x \ll x_*. \quad (188)$$

On the other hand, when k'_\parallel is large, $Z(z) \rightarrow -2z^2$, and

$$V_{\parallel e} \rightarrow i E_\parallel \frac{e}{T_e} \frac{\omega - \omega_{*e}}{k_\parallel^2}, \quad x \gg x_*. \quad (189)$$

which is relatively small. In fact, the estimate $\omega \sim \omega_*$ implies that (189) is $O(\delta^2)$ relative to (188). The region $|x| < x_*$, where the electron contribution to the parallel current is relatively large, is called the *current channel*.

The generalized Ohm's law is obtained from

$$J_\parallel = en(V_{\parallel i} - V_{\parallel e})$$

and therefore requires the ion, as well as the electron velocity. The ion response is more complicated than the electron response, since $O(\delta_i)$ terms are more important. However, in a kinetic treatment plasma dispersion functions still occur, with an argument involving $z_i = \omega/(k'_\parallel v_i) = (m_i/m_e)^{1/2} z_e$. Therefore $z_i \gg 1$ in the vicinity of the rational surface; unless the mode is so broad as to allow $k'_\parallel v_e \sim (m_i/m_e)^{1/2} \omega$, $V_{\parallel i}$ is given by the ion version of (188), and $V_{\parallel i} \ll V_{\parallel e}$. Thus, for reasonably localized perturbations, the generalized conductivity is approximated by⁸

$$\begin{aligned} J_\parallel &= \sigma_* E_\parallel \\ \sigma_* &= \frac{i}{4\pi} \omega_{pe}^2 \frac{\omega - \omega_{*e}}{k_\parallel^2 v_{te}^2} Z'(z). \end{aligned} \quad (190)$$

Near the rational surface, ω_* can be simplified using (185), and $k'_\parallel = k'_\parallel x$, so that $z = x_*/|x|$. Equation (190), with $\eta = 1/\sigma_*$, replaces (138). The analysis leading to (148) is unchanged, although it must be remembered that η is a strong function of x . Indeed, the rapid variation of σ_* implies

⁸ An elementary discussion of the case where $V_{\parallel i}$ cannot be neglected may be found in (Hazeltine and Meiss, 1985).

that our previous estimate for the resistive diffusion term, based on (151), must be reconsidered.

Near the rational surface, (190) becomes

$$\sigma_*(0) = \frac{i}{4\pi} \left(\frac{\omega_{pe}}{\omega} \right)^2 (\omega - \omega_*),$$

in view of (188). Correspondingly, the resistive length becomes

$$x_R^2 = \frac{\omega}{\omega - \omega_{*e}} \left(\frac{c}{\omega_{pe}^2} \right)^2. \quad (191)$$

Recalling that w represents the width of E while x_* represents the width of σ_* , we see that the resistive term in (148) is of order

$$-i \frac{c^2}{4\pi} \frac{x^3}{\omega} \left(\eta \frac{E'}{x^2} \right)' \sim i w^2 x_R^2 \left(\frac{E}{x_* w^3} \right) = i \frac{x_R^2}{x_* w} E. \quad (192)$$

As before, the large Δ' case is derived from a balance between inertia, line bending and resistive diffusion. Balancing the first two implies $w \sim x_A$, as for the resistive mode. The dispersion relation follows from the balance of (192) with inertia, implying

$$ix_R^2 \sim x_A x_*, \quad (193)$$

or, explicitly

$$\omega(\omega - \omega_{*e}) \sim -(k'_\parallel v_{te})^2 \left(\frac{c}{\omega_{pe}} \right)^2 \frac{v_A}{v_{te}} \quad (\text{large } \Delta'). \quad (194)$$

The actual dispersion relation differs from (194) by a factor of $\sqrt{\pi}/2$.

For the small Δ' case, inertia is negligible as before; balancing resistive diffusion and kink terms determines the dispersion relation

$$\Delta' \sim -i x_* / x_R^2,$$

and the remaining balance shows that

$$w^3 \sim x_A^2 / \Delta'. \quad (195)$$

This dispersion relation has the explicit form

$$\omega - \omega_{*e} \sim ik'_\parallel v_{te} \left(\frac{c}{\omega_{pe}} \right)^2 \Delta' \quad (\text{small } \Delta'), \quad (196)$$

showing that the mode has a real frequency ω_{*e} , and growth rate proportional to Δ' . Equation (196) is said to describe the “collisionless tearing mode.”

A more precise version of (196) can be obtained by returning to (137) and (138). Using the estimate $x\psi'' \sim \Delta'\psi$, and (195) for w , we find that (137) implies $(c/v_A)\varphi \sim \psi/w$. Thus the electrostatic term on the left-hand side of (138) is of order x/w relative to the electromagnetic term. Since the resistive term is only important within the current channel, $x < x_*$, we should compare x_* to w :

$$\frac{x_*}{w} \sim \frac{v_A}{v_{te}} (x_A \Delta')^{1/3}.$$

Now $v_A/v_{te} = (m_i/m_e \beta)^{1/2}$, which is typically $\mathcal{O}(1)$; however, small Δ' , (153), implies $\Delta' x_A \ll 1$. Thus the electrostatic term in (138) can be neglected, giving the simple differential equation

$$\frac{\partial^2 \psi}{\partial x^2} = -i \frac{4\pi\sigma_*\omega}{c^2} \psi = \frac{\omega(\omega - \omega_*)}{(k'_\parallel v_{te})^2} \left(\frac{\omega_{pe}}{c} \right)^2 \frac{1}{x^2} Z' \left(\frac{x_*}{|x|} \right) \psi. \quad (197)$$

The argument that $x_* \ll w$ also implies that the ψ appearing on the right-hand side of (197) is roughly a constant. We use this constant ψ approximation to integrate over the current channel and obtain

$$\Delta' = -2 \frac{(\omega - \omega_*)}{k'_\parallel v_{te}} \left(\frac{\omega_{pe}}{c} \right)^2 \int_0^\infty dx \frac{d}{dx} Z = -2i\sqrt{\pi} \frac{(\omega - \omega_*)}{k'_\parallel v_{te}} \left(\frac{\omega_{pe}}{c} \right)^2, \quad (198)$$

since $Z(x_*/x) \rightarrow i\sqrt{\pi}$ as $x \rightarrow \infty$. Equation (198) is a more exact version of (196).

Other Effects

The tearing mode frequency and growth rate are often small compared to the local collision frequency. A current channel may still form in this case, especially since the local mode frequency is often $\mathcal{O}(\omega_*)$. In this case collisional terms must be included when the operator \mathcal{L}_0 , (172), is inverted. The case $x_* \ll w$, but $\omega \ll \nu$ is known as the *semi-collisional* regime. The growth rate can be shown to be estimated by $\gamma_0(\nu/\omega_*)^{1/2}$ where γ_0 is the collisionless growth rate and ν a collision rate (Drake and Lee, 1977). The nomenclature refers to the fact that even though $\nu \gg \omega$, the existence of a current channel depends on long mean free path physics.

Temperature gradients can effect the growth rates of tearing modes in complicated ways, because of the energy-dependence of both ω_* and the Coulomb cross section. This topic is an area of current research.

A more detailed description of the ion response modifies the shear-Alfvén law through the inclusion of \mathbf{V}_{pi} in the equation of motion, (6.138). The result is to replace (136) by

$$\left(\frac{d}{dt} - i\omega_{pi} \right) U = -v_A^2 \nabla_\parallel \nabla_\perp^2 \psi,$$

where ω_{*i} is given by (184). The ultimate effect is to replace x_A^2 by

$$x_A^2 \Rightarrow -\frac{\omega(\omega - \omega_{*i})}{(k'_\parallel v_A)^2}, \quad (199)$$

since only the ω from the shear-Alfvén law is affected. This change is unimportant for the small Δ' mode, where inertia is neglected in any case; however, it does provide significant modifications to the large Δ' modes.

The inclusion of finite β and curvature terms changes the threshold for the tearing modes from $\Delta' > 0$ to $\Delta' > \Delta_{\text{crit}}$, where the threshold, Δ_{crit} can be large enough to be significantly stabilizing (Glasser et al., 1975). The point is that the average curvature in axisymmetric devices is typically favorable and therefore in competition with positive Δ' .⁹

Part 4: Poloidal Localization

In the following sections we consider perturbations driven primarily by the interaction of field curvature with pressure gradients, that is, by the interchange term in the shear-Alfvén law. As we have already seen in the cylindrical case, such modes can be destabilized if they are localized near a rational surface, and if the curvature and the pressure gradient point in the same direction. This simple picture must be modified in a torus, because the curvature, like most equilibrium quantities, depends on poloidal angle. It follows that a single helicity perturbation does not exist: various helicities are coupled by the poloidal variation of the equilibrium. Furthermore, since the toroidal curvature is unfavorable only on the outside of the torus, unstable interchange modes tend to be localized there.

Nevertheless, in order to minimize the line-bending restoring force, an interchange mode must have k'_\parallel small compared to k_\perp . For a single helicity this occurs naturally near the rational surface. However, it is harder to maintain with multiple helicities. The difficulty of resolving the conflict between small k'_\parallel and poloidal coupling implies that the interchange mode is more stable in toroidal geometry than in the cylindrical case.

A technique for reducing the dimensionality of a multiple-helicity system—essentially reducing partial differential equations to ordinary ones—was developed by several researchers, based on ideas of J.B. Taylor. It has become known as the *ballooning representation*. It applies most directly to the case where the modes are strongly localized poloidally, but not radially; indeed a “ballooning mode” can be thought of as a coupled set of modes with different helicities and nearly equal amplitudes. Each helicity is large near its corresponding rational surface; the mode itself, as a collection of various

⁹ Many of the effects mentioned here are discussed in more detail by (Crowley, Kulsrud, and Hahm, 1996).

helicities, varies slowly with radius. Poloidal localization is responsible for the term “ballooning”: these modes typically appear as aneurysms on the outer part of the torus.

Perturbations that balloon only weakly have a well defined helicity, and therefore tend to be localized in the neighborhood of a rational surface. The radially localized limit describes interchange modes; it was analyzed in the preceding section. Below we derive the Mercier criterion, which is the toroidal generalization of (98).

Perturbations that are somewhat less localized in radius are amenable to a multiple scale analysis, in which the parallel mode-width is assumed to exceed the scale of variation of κ . These modes can be unstable even when the Mercier criterion predicts stability.

In the strongly ballooning limit, modes are poloidally localized to the unfavorable curvature region, but have considerable radial extent. This case must be treated using the full apparatus of the ballooning representation. The analysis, a generalized WKB expansion, breaks up into two parts, local and global. The local theory consists of the solution of the ballooning equation, describing the structure of the mode on a given magnetic surface. A global eigenmode is constructed by combining local modes with the same eigenfrequency. This leads to a quantization condition for the frequencies. The details of the global treatment are beyond the scope of this book.

7.10 Ballooning Representation

WKB Theory

The analytical treatment of pressure-driven instabilities appears to be tractable only when the scale length of the perturbations is much smaller than that of the equilibrium. Since flute-like modes with $k_\perp a \gg 1$ are often the most unstable perturbations, this limit is also a fruitful one.

The natural technique for problems with disparate length scales is the eikonal or WKB analysis.¹⁰ Functions of interest are represented as

$$\Phi(\mathbf{x}) = \varphi(\mathbf{x}) \exp \left[\frac{i}{\varepsilon} S(\mathbf{x}) \right], \quad (200)$$

with $\nabla S(\mathbf{x}) \sim \nabla \varphi \sim \mathcal{O}(1)$. Here $S(\mathbf{x})$ is the eikonal, and $\varphi(\mathbf{x})$ is the envelope. By analogy with a Fourier expansion, the wavenumber is defined as $\mathbf{k}(\mathbf{x}) = \nabla S(\mathbf{x})$. In the standard WKB analysis, all the coordinates have both a fast an slow part, so \mathbf{k} is a vector of all the coordinates. We will see in the next section how this is modified for the case of flute instabilities.

The problem of interest is a linear differential equation for Φ , which

¹⁰See for example (Bender and Orzag, 1987), Chapter 10.

we can represent schematically as

$$L[\mathbf{x}, \nabla, \lambda]\Phi = 0;$$

here λ represents an eigenvalue. The ansatz (200) is substituted into this equation, giving

$$L \left[\mathbf{x}, \frac{i}{\epsilon} \mathbf{k}(\mathbf{x}) + \nabla, \lambda \right] \varphi = 0,$$

(this expression is schematic, in that the gradient operator may act on the \mathbf{x} dependence of both L and \mathbf{k}). Expansion in ϵ gives, to lowest order,

$$L_0[\mathbf{x}, i\mathbf{k}, \lambda] = 0, \quad (201)$$

which provides a dispersion relation for the modes, defining $\mathbf{k}(\mathbf{x}, \lambda)$. Thus, to lowest order, the differential equation is replaced by the algebraic equation (201). Typically (201) will have several branches; in the standard case when L is a second order operator, there are two. The various branches are labeled as $\mathbf{k}_j(\mathbf{x}, \lambda)$.

The shape of the envelope for each branch is obtained from the next order in the expansion, which is sometimes called the transport equation. Its form depends in detail on the operator L .

Ballooning Equation

In our case the eikonal, $S(\mathbf{x})$, represents the rapid perpendicular dependence, while the envelope, φ , determines the parallel structure. The separation into disparate scales, using the factor $1/\epsilon$, is completely analogous to the flute ordering of (27).

Since by assumption the eikonal represents only the perpendicular mode structure, we insist that

$$\mathbf{B} \cdot \nabla S(\mathbf{x}) = 0. \quad (202)$$

This leads to the natural definition of the perpendicular wavenumber

$$\mathbf{k}_\perp(\mathbf{x}) = \nabla S(\mathbf{x}). \quad (203)$$

Recalling (66), we see that $\mathbf{k}_\perp/\epsilon = m/r = nq/r$, so the limit $\epsilon \rightarrow 0$ corresponds to $n \rightarrow \infty$.

In this section it is convenient to use flux coordinates (q, θ, ζ) where the flux label is chosen to be the safety factor $q(v)$, and v is the Hamada coordinate, as in §3.6. A related coordinate system that will also be used is the field line system, (q, η, α) , with

$$\eta = \theta, \quad \alpha = \zeta - q(v)\theta. \quad (204)$$

In this coordinate system $\mathbf{B} \cdot \nabla$ becomes $\chi' \partial/\partial\eta$; thus η represents the parallel coordinate, while the coordinates (q, α) label a field line. When no confusion can arise, functions will be referred to in both coordinate systems by the same label: $f(q, \theta, \zeta) = f(q, \eta, \alpha)$.

As we have seen in §3.3, the general solution to the magnetic differential equation (202) is an arbitrary function $S(q, \alpha)$, (3.25). This function, however, cannot represent a physical perturbation: it does not satisfy the periodicity condition (3.26), except on rational surfaces, as in (3.31). The application of WKB theory to large- n toroidal eigenmodes therefore requires special consideration.

The ballooning representation is a modification of (200) that yields a periodic solution. The first step in its construction is counter-intuitive: we drop the poloidal periodicity requirement on the eikonal and envelope. Instead, we seek aperiodic solutions S and φ defined on the range $-\infty < \eta < \infty$, which is called the *covering space*. We continue to demand periodicity in ζ . As we have seen, a function $S(q, \alpha)$ that is toroidally periodic necessarily oscillates in θ with period $2\pi/q$. The envelope φ , on the other hand, will turn out to decay as $|\eta| \rightarrow \infty$, and usually be square integrable.

As in the general WKB analysis, the system of equations to be solved can be represented schematically as

$$L[\mathbf{x}, \nabla_{\perp}, \nabla_{\parallel}, \lambda]\Phi = 0 .$$

Here Φ may consist of several components, in which case L is a matrix operator. We will assume that each component of L is at most second order in ∇_{\perp} . After substitution from (200) the lowest order equation becomes

$$-\frac{1}{\varepsilon^2} L[\mathbf{x}, \mathbf{k}_{\perp}(\mathbf{x}), \nabla_{\parallel}, \lambda]\varphi = 0 , \quad (205)$$

for each branch of the solution. Notice that, unlike (201), (205) is an *ordinary* differential equation, determining the parallel structure of the envelope, φ . This equation is commonly referred to as the *ballooning equation*. It takes a more perspicuous form when written in field line coordinates:

$$\mathcal{L}\left[\eta, \frac{\partial}{\partial\eta}; q, \alpha, \mathbf{k}_{\perp}, \lambda\right]\varphi = 0 , \quad (206)$$

showing the explicit dependence on η , on the field line labels (q, α) , and on \mathbf{k}_{\perp} . Solutions of this equation on the covering space must fall to zero as $|\eta| \rightarrow \infty$; this requirement yields a well-defined eigenvalue problem for $\mathbf{k}_{\perp}(q, \alpha, \lambda)$.

Equation (206) is exactly what one would get naively, using the eikonal ansatz of (200). The additional insight is to allow solutions that are not poloidally periodic. Of course it is still necessary somehow to construct a physical (i.e. periodic) solution for Φ . This will be provided by a linear combination of the various branches of the solutions of (206).

For simplicity, we consider only the axisymmetric case. Then the equilibrium is ζ -independent, the operator L does not depend on α , and the dispersion relation is α -independent. After writing \mathbf{k}_\perp in terms of its covariant components in the field line coordinate system, we find

$$\mathbf{k}_\perp = k_\alpha \nabla \alpha + k_q \nabla q = k_\alpha (\nabla \alpha + \theta_k \nabla q) \quad (207)$$

where $\theta_k \equiv k_q/k_\alpha$ is fixed, by the dispersion relation, from the ballooning equation. Alternatively, in the Hamada coordinate system,

$$\mathbf{k}_\perp = k_\alpha [\nabla \zeta - q \nabla \eta + (\theta_k - \eta) \nabla q] . \quad (208)$$

The explicit η dependence of \mathbf{k}_\perp is a manifestation of the fact that S is not periodic, and therefore well defined only on the covering space. Indeed the equation (203) for S in terms of these components becomes

$$k_\alpha \theta_k = k_q \Rightarrow \theta_k \frac{\partial S}{\partial \alpha} = \frac{\partial S}{\partial q}$$

which, since θ_k is independent of α , has the explicit solution

$$S(q, \alpha) = S_0 \left(\alpha + \int dq \theta_k(q) \right) , \quad (209)$$

where S_0 is an integration constant (an additional integration constant corresponds to an irrelevant, constant shift in α). Although we have temporarily abandoned poloidal periodicity, (200) must be toroidally periodic, requiring $S_0 = -\varepsilon n$ for some integer n . Thus we have obtained the solution

$$\Phi(\mathbf{x}) = \varphi(\eta, q) \exp \left[-in \left(\alpha + \int dq \theta_k \right) \right] . \quad (210)$$

Finally we address the problem of constructing a periodic solution from (210). It is obtained by noting that (206) is really just one branch of the solution. Distinguishing the various branches with superscripts, we can express the general solution as

$$\Phi(\mathbf{x}) = \sum_j \alpha^j \varphi^j(\eta, q) \exp \left[-in \left(\alpha + \int dq \theta_k^j \right) \right] , \quad (211)$$

where the α^j are arbitrary coefficients. We next observe, crucially, that there must be an infinite set of related branches, as shown by the following simple argument. Since the equilibrium is periodic in $\theta = \eta$, the explicit η -dependence in the ballooning equation (206) is periodic as well. In fact the only aperiodic dependence arises from the explicit θ in \mathbf{k}_\perp , (208). Note that this dependence occurs in conjunction with θ_k . Therefore if one solution for θ_k^0 is known, then shifting η by $2\pi j$ yields another solution:

$$\theta_k^j(q) = \theta_k^0 - 2\pi j , \quad (212)$$

which has the envelope function $\varphi^j(\eta) = \varphi^0(\eta + 2\pi j)$. Thus (211) can be written

$$\Phi(q, \theta, n) = a(q) \sum_{j=-\infty}^{\infty} \varphi^0(\eta + 2\pi j, q) \exp \left[-in \left(\alpha - 2\pi qj + \int dq \theta_k^0 \right) \right]. \quad (213)$$

This final function is indeed periodic in θ , providing the sum converges. The representation (213) is known as the ballooning representation, and is often presented simply as an ansatz. Our presentation, which follows (Dewar and Glasser, 1983), permits a straightforward generalization to the nonaxisymmetric case, and a clear treatment of the global theory, which determines the radial envelope function $a(q)$.

Ballooning Transform*

The ballooning representation can also be viewed as a generalized transform analogous to the Fourier or Laplace transforms:

$$\Phi(q, \theta, \zeta) \rightarrow \varphi(\eta, q, n). \quad (214)$$

To accomplish this, first Fourier transform in ζ :

$$\Phi(q, \theta, \zeta) = \sum_{n=-\infty}^{\infty} \Phi(q, \theta, n) e^{-in\zeta}. \quad (215)$$

Then, using (213), we can express the ballooning transform as

$$\Phi(q, \theta, n) = \sum_{j=-\infty}^{\infty} \varphi(\theta + 2\pi j, q, n) e^{inq(\theta - \theta_0 + 2\pi j)}. \quad (216)$$

Here we have defined $q\theta_0 = \int \theta_k dq$. Now if φ is presumed to vary slowly in radius, it is possible to demonstrate that the inverse transform also exists (Hazeltine and Newcomb, 1990):

$$\varphi(\eta, q, n) = \int_{-\infty}^{\infty} ds \frac{\sin(\pi ns)}{\pi s} e^{-in(\eta - \theta_0)(q + s)} \Phi(q + s, \eta, n). \quad (217)$$

This can be most easily demonstrated by substituting (216) for Φ into (217) to obtain an identity. The integrand in (217) involves the filtering function $\sin(\pi ns)/\pi s$, which cuts off the rapid radial variation of Φ .

Although both Φ and its transform φ depend on q , it is appropriate to view q and η as conjugate variables, in a similar sense to the Fourier pair ζ and n . The transform relations imply that a function that is localized about some magnetic surface will fall off slowly in η . Conversely, one that is localized in η will be radially extended.

7.11 Ideal Stability

MHD Ballooning Equation

In this section we obtain the explicit ballooning equation, as well as approximations to the local dispersion relation, for pressure-driven modes in axisymmetric geometry. As we have seen in §7.4, the flute-like ordering $k_\perp \gg k_\parallel$ leads naturally to the flute-reduced equations (53). These equations are appropriate in the ballooning limit. To simplify the resulting dispersion relation, we specialize in this section to the ideal, incompressible limit, (55).

Because flute reduction eliminates the slow spatial scale, linearization of (55) leads directly to the set of equations corresponding to the operator L of (206). Linearization is accomplished simply by neglecting the bracket terms in (55):

$$\begin{aligned} \frac{1}{v_A^2} \frac{\partial}{\partial t} U &= -\frac{B_0^2}{B^2} \mathbf{b}_0 \cdot \nabla \nabla_\perp^2 \psi + \mathbf{b}_0 \cdot \boldsymbol{\kappa}_0 \times \nabla_\perp p \\ \frac{\partial \psi}{\partial t} &= -\frac{c}{B_0} \mathbf{b}_0 \cdot \nabla B_0 \varphi \\ \frac{\partial}{\partial t} p &= c \mathbf{b}_0 \cdot \nabla \beta \times \nabla_\perp \varphi. \end{aligned}$$

After differentiating the shear-Alfvén law with respect to time, these equations can be combined to yield a single equation for φ :

$$\begin{aligned} -\frac{\omega^2}{v_A^2} \nabla_\perp^2 \varphi &= -\frac{B_0^2}{B^2} \mathbf{b}_0 \cdot \nabla \left[\frac{\nabla_\perp^2}{B_0} (\mathbf{b}_0 \cdot \nabla) B_0 \varphi \right] \\ &\quad + \mathbf{b}_0 \cdot \boldsymbol{\kappa}_0 \times \nabla_\perp (\mathbf{b}_0 \cdot \nabla \beta \times \nabla_\perp \varphi), \end{aligned} \tag{218}$$

which is the toroidal version of (69). Since $B_0 \varphi = \Phi$ (by 42) appears in (218), it is more convenient to use Φ , the unnormalized electrostatic potential as the independent function, instead of φ .

In the ballooning representation each ∇_\perp in (218) is converted to $i\mathbf{k}_\perp$, leaving an ordinary differential equation in η . For the curvature, we use the covariant representation (3.91), to write

$$\boldsymbol{\kappa}_0 = \kappa_\nu \nabla v + \boldsymbol{\kappa}_g (\nabla \zeta - q \nabla \theta). \tag{219}$$

The first component of (219) is related to the normal curvature, κ_n , as $\kappa_n = \kappa_\nu dv/d\tau$. We refer to κ_ν as the normal curvature for simplicity. Using (219), (207), and the form (3.14) for \mathbf{B}_0 yields

$$\mathbf{b}_0 \cdot \boldsymbol{\kappa}_0 \times \nabla_\perp \rightarrow i\mathbf{b}_0 \cdot \boldsymbol{\kappa}_0 \times \mathbf{k}_\perp = -i \frac{B_0 k_\alpha}{\chi'} [\kappa_\nu + q'(\eta - \theta_k) \kappa_g],$$

where all derivatives are with respect to the flux label, v . Furthermore, noting that $\nabla \beta = \beta' \nabla v$, we obtain

$$\mathbf{b}_0 \cdot \nabla \beta \times \nabla_{\perp} \rightarrow i\beta' \frac{B_0 k_{\alpha}}{\chi'} .$$

Therefore, in the ballooning representation, (218) becomes the ballooning equation

$$-\tilde{\omega}^2 F^2 \Phi = \frac{\partial}{\partial \eta} F^2 \frac{\partial}{\partial \eta} \Phi + \tilde{\beta}' [\kappa_v + q'(\eta - \theta_k) \kappa_g] \Phi \quad (220)$$

where

$$\tilde{\beta}' = \beta' \frac{\overline{B}^2}{\chi'^2} , \quad \tilde{\omega} = \omega \frac{\overline{B}}{v_A \chi'} , \quad \Phi = B_0 \varphi . \quad (221)$$

Since $\chi' \sim B/qR$, the factor $\chi'/v_A B_0$ represents an Alfvén time and $\tilde{\omega}$ is a dimensionless frequency. Similarly $\tilde{\beta}'$ is a normalized (but not dimensionless) pressure gradient. The normalized perpendicular wavenumber is denoted by F :

$$F = \frac{k_{\perp} \chi'}{k_{\alpha} B_0} = \frac{\chi'}{B_0} |\nabla \zeta - q \nabla \theta + (\theta_k - \eta) \nabla q| \quad (222)$$

Notice that (220) is an ordinary differential equation, unlike the partial differential equation (218). The equilibrium explicitly enters (220) through F , β , κ_n , and κ_g , all of which depend only on the slow variables. These functions depend periodically on η .

Asymptotic Analysis: Mercier Criterion

The ballooning equation (220) is to be solved on the covering space, $-\infty < \eta < \infty$, for a square integrable function Φ . It has the form of a Sturmian eigenvalue problem (89), with eigenvalue $\lambda = \omega^2$. Thus the ballooning operator is self-adjoint, and its eigenvalues are real. Therefore, as is characteristic of MHD, modes are either stable or purely growing.

Recall that the Sturmian comparison and oscillation theorems, used in deriving the Suydam criterion (98), imply that if (220) has oscillatory solutions for $\omega^2 = 0$, then there are eigenvalues with $\omega^2 < 0$. Thus a stability criterion is obtained from the marginal equation.

The simplest criterion depends only on the asymptotic behavior of Φ for large $|\eta|$: if Φ oscillates in this limit then the system is certainly unstable. As $|\eta| \rightarrow \infty$ the perpendicular wavenumber becomes arbitrarily large; according to (208), $\mathbf{k}_{\perp} \rightarrow \eta k_{\alpha} \nabla q$. Using this limiting form in (222)

gives

$$F(\eta) \rightarrow \eta \frac{\chi'}{B_0} |\nabla q| \equiv \eta G(\eta). \quad (223)$$

Thus the marginal stability ballooning equation reduces to

$$\frac{\partial}{\partial \eta} G^2 \frac{\partial}{\partial \eta} \Phi = \mathcal{O}(\eta^{-1}); \quad (224)$$

the secular terms do not appear in leading order. Note that $G(\eta)$ is a periodic function of η , since it depends only on equilibrium quantities.

We can solve (220) in this limit by an asymptotic expansion of the form

$$\Phi(\eta) = \eta^\nu (\Phi_0 + \eta^{-1} \Phi_1 + \dots),$$

where the Φ_i are periodic functions of η . To order $\eta^{\nu+2}$, the equation reduces to (224), implying

$$\frac{\partial}{\partial \eta} \Phi_0 = \frac{A}{G^2}, \quad (225)$$

where A is an arbitrary constant. Let $\langle \rangle$ represent the η average over one period; in the field line coordinate system, this is just the flux surface average (3.44). Then (225) has the solvability condition

$$\left\langle \frac{A}{G^2} \right\rangle = 0, \quad (226)$$

which can be satisfied only if $A = 0$. Therefore Φ_0 is a constant, which can be equated to unity without loss of generality.

To the next order, $\eta^{\nu+1}$, we obtain from (220)

$$\frac{\partial}{\partial \eta} G^2 \left(\frac{\partial}{\partial \eta} \Phi_1 + \nu \right) + \tilde{\beta}' q' \kappa_g = 0. \quad (227)$$

This equation is solvable for a periodic Φ_1 if and only if the flux-surface average of κ_g is zero. To verify this, note that κ_g , as defined by (219), can be obtained from

$$\kappa_g = -\frac{\chi'}{B_0^2} \mathbf{B} \times \nabla v \cdot \boldsymbol{\kappa}. \quad (228)$$

Using the equilibrium condition (3.59), we can express (228) in terms of the perpendicular current, and using (3.89) and (3.82) gives

$$\kappa_g = -\frac{\chi'}{cP'} \mathbf{J}_\perp \cdot \boldsymbol{\kappa} = -\frac{\chi'}{cP'} \nabla \cdot \mathbf{J}_\perp = -\frac{\chi'}{2cP'} \mathbf{B}_0 \cdot \nabla \frac{J_\parallel}{B_0}.$$

It follows directly from the last relation that

$$\langle \kappa_g \rangle = 0, \quad (229)$$

since χ and P are flux functions.

Continuing with the solution of (227), we define the function h by

$$\kappa_g = \frac{\partial}{\partial \eta} h \quad (230)$$

The solution for Φ_1 is then

$$\frac{\partial \Phi_1}{\partial \eta} = -\nu - \frac{1}{G^2} (\tilde{\beta}' q' h - C). \quad (231)$$

The constant C is determined by the solvability condition for (231), which gives

$$\frac{\partial \Phi_1}{\partial \eta} = -\nu \left(1 - \frac{G^{-2}}{\langle G^{-2} \rangle} \right) - \frac{\tilde{\beta}' q'}{G^2} \left(h - \frac{\langle h G^{-2} \rangle}{\langle G^{-2} \rangle} \right). \quad (232)$$

Since we have shown that $\partial \Phi_0 / \partial \eta = 0$, it is the η -dependence of Φ_1 that represents the ballooning behavior. The two terms in (232) show that the flux surface dependence of the geodesic curvature, as well as the nonuniformity of the shear, drive ballooning in the present case.

The Mercier condition is finally obtained from the next order equation, which involves the line bending operator on Φ_2 . The solvability condition for this equation is

$$(\nu + 1) \left\langle G^2 \left(\frac{\partial \Phi_1}{\partial \eta} + \nu \right) \right\rangle + \tilde{\beta}' (\langle \kappa_v \rangle + q' (\kappa_g \Phi_1)) = 0. \quad (233)$$

Using (232) for Φ_1 in (233) yields

$$v(\nu + 1) + D_I = 0,$$

$$D_I = \tilde{\beta}' \left\langle \frac{1}{G^2} \right\rangle \left[\langle \kappa_v \rangle + \tilde{\beta}' q'^2 \left(\left\langle \frac{h^2}{G^2} \right\rangle - \frac{\langle h G^{-2} \rangle^2}{\langle G^{-2} \rangle} \right) - q' \left(\langle h \rangle - \frac{\langle h G^{-2} \rangle}{\langle G^{-2} \rangle} \right) \right], \quad (234)$$

which determines the exponent ν . The equation for ν is identical to (97), except that the D of (95) has been replaced by a more complicated expression.

When $D_I < 1/4$, $\Phi \sim \eta^\nu$ decays as $\eta \rightarrow \infty$. A square integrable asymptotic form is attained by choosing the smaller exponent, $\nu < -1/2$. However, when $D_I > 1/4$ the exponent is complex and Φ is oscillatory as $n \rightarrow \infty$. The Sturm comparison theorem then implies that there is an unstable eigenvalue with a square integrable Φ .

Thus the necessary condition for stability is $1/4 - D_I > 0$, the Mercier criterion. In view of (224), it can be rewritten as

$$\frac{q'^2}{4} - \tilde{\beta}' \left[\left\langle \frac{B^2}{|\nabla \chi|^2} \right\rangle (\kappa_v) + \left\langle \left(\tilde{\beta}' \frac{hB^2}{|\nabla \chi|^2} - q' \right) \left(h \left\langle \frac{B^2}{|\nabla \chi|^2} \right\rangle - \left\langle \frac{hB^2}{|\nabla \chi|^2} \right\rangle \right) \right\rangle \right] > 0 \quad (\text{stability}). \quad (235)$$

Here the first term can be interpreted as the stabilizing effect of shear; it reflects the fact that k_{\parallel} cannot be identically zero in a sheared field for a mode of finite extent. The second term, involving the normal curvature, shows the stabilizing effect of the average normal curvature. It corresponds to the curvature term in (95). The last terms in (235) represent the effects of geodesic curvature, which, although it has zero average, is important at large η due to shear. These terms can have either sign.

Recall from §7.10 that modes with large extent in η are narrow in q . Thus Mercier unstable modes are surface-localized, and can be recognized as interchange modes. Equation (232) implies that the ballooning effect (represented by Φ_1) is weak in the interchange limit. Thus it is not too surprising that the ballooning analysis gives a result similar to that obtained by more conventional interchange theory. It is remarkable, however, that the present result reproduces the Mercier criterion exactly. Furthermore, the ballooning analysis is considerably simpler than the conventional one, showing the power of the ballooning formalism.

Of course (235), which takes into account only the radially localized perturbations, is far from a sufficient stability criterion. We next consider a more general class of disturbance.

7.12 Model Equation*

Solution of the general ballooning equation is quite difficult analytically because of its awkward dependence on the explicit form of the equilibrium. The point is that no characterization of flux surfaces in terms of a parameter like Δ' is available. The only reasonable technique is to expand about a known, simple case, such as zero shear and β . This approach works well near the axis of a tokamak, for example, since the shear and β' are both zero there.

Here we introduce, without much justification, a model equation that has many of the features of the more rigorous expansions (except of course quantitative validity). The advantage is that analytical calculations are less burdensome, so that important ideas can be exposed without algebraic overload. The model is loosely based on Shafranov geometry; it is not rig-

orous because the expansions in the Shafranov case are based on $\beta \sim \epsilon^2$, while here we assume $\beta \sim \epsilon$.

To obtain the model, it is helpful to express the perpendicular wavenumber (208) as

$$k_\perp^2 = \frac{1}{|\nabla v|^2} \left[\left(\frac{B k_\alpha}{\chi'} \right)^2 + (k^v)^2 \right],$$

where k^v is the contravariant component of \mathbf{k}_\perp :

$$k^v = \mathbf{k}_\perp \cdot \nabla v \approx k_\alpha [q'(\theta_k - \eta) |\nabla v|^2 - q \nabla \theta \cdot \nabla v], \quad (236)$$

and we have used $B^2 = |\nabla \chi|^2 [q^2 |\nabla \theta|^2 + |\nabla \zeta|^2 - q^2 (\nabla v \cdot \nabla \theta)^2 / |\nabla v|^2]$. Thus (222) becomes

$$F^2 = \frac{1}{|\nabla v|^2} \left[1 + \left(\frac{\chi' k^v}{B k_\alpha} \right)^2 \right]. \quad (237)$$

Similarly the curvature can be rewritten using the contravariant component of the normal curvature:

$$\kappa^v = \kappa \cdot \nabla v = \kappa_v |\nabla v|^2 - \kappa_g q \nabla \eta \cdot \nabla v$$

from (219). Using (236) we find

$$\kappa_v + q'(\eta - \theta_k) \kappa_g = \frac{1}{|\nabla v|^2} \left(\kappa^v - \kappa_g \frac{k^v}{k_\alpha} \right). \quad (238)$$

The point here is that the secular dependence of both F^2 and the curvature comes from the same component k^v .

To obtain the model equation we use the shifted circle, Shafranov equilibrium. In this model $\nabla v \cdot \nabla \theta \propto -\sin \theta$, and the geodesic curvature can also be shown to be proportional to $-\sin \theta$. The normal curvature has a q -independent contribution, and the oscillatory component will be proportional to $\cos \theta$. Thus (220) becomes

$$-\omega^2 f^2 \varphi = \frac{\partial}{\partial \eta} f^2 \frac{\partial}{\partial \eta} \varphi + \rho \{ \bar{\kappa} + \cos \eta + [s(\eta - \theta_k) - \rho \sin \eta] \sin \eta \} \varphi \quad (239)$$

where $\rho, \bar{\kappa}$ and s are dimensionless measures of pressure gradient, average normal curvature, and shear respectively, and $f = |\nabla v| F$:

$$f^2 = 1 + [s(\eta - \theta_k) - \rho \sin \eta]^2.$$

The expressions for $\rho, \bar{\kappa}$ and s can be derived in terms of the Shafranov equilibrium explicitly,¹¹ but for our purposes it is more appropriate to

¹¹ See e.g. (Hazeltine and Meiss, 1985). The model ballooning equation also applies to a sharp boundary model (see Fredberg, 1987).

regard (239) as a model with only qualitative connection to a real system. Important effects neglected in this model include the higher harmonics in η , which can arise from noncircularity of the flux surfaces.

The Mercier criterion, (234), can be written using the model equation in the dimensionless form $\nu(\nu+1)s^2 + \rho\bar{\kappa} = 0$. Here the geodesic curvature terms cancel completely. This implies the instability criterion

$$\rho\bar{\kappa} > \frac{1}{4}s^2. \quad (240)$$

Weak Ballooning

When the mode extent is large in η compared to 2π , a multiple scale analysis can be applied to solve the ballooning equation. In this technique weak-ballooning effects are represented by slow modulation of the mode along the field line, and a first correction to the Mercier criterion is obtained. The most important result of this analysis is the discovery of a *second stability* region for large pressure gradients.

The primary analytical tool used is a subsidiary ordering on the length scale representing the shear. We assume

$$s \sim \delta^2,$$

where δ represents weak shear (and not the gyroradius ordering), as occurs, for example, near the axis where q has a minimum. The ballooning mode width is assumed to be $\mathcal{O}(1/s)$.

Due to the oscillatory curvature terms, the mode will have rapid oscillations on the scale $\eta \sim 2\pi$. In order that the modulation influence stability of the mode, the inertia term in (239) must be comparable to the slow-scale line bending term; this implies $\omega \sim \delta^2$. In order that pressure influence stability, we take $\rho \sim \delta$. Finally the Mercier criterion (240) must be near marginal, thus $\bar{\kappa} \sim \delta^3$.

To implement the ordering we allow variation in φ on two length scales, $\eta \sim 1$ and $\eta \sim 1/s$. The slow variable is naturally given by

$$z = s(\eta - \theta_k). \quad (241)$$

This is the scale which enters into the aperiodic terms in the ballooning equation. To allow a dependence on both z and η , the η derivatives are expanded as

$$\frac{\partial}{\partial\eta} \rightarrow \frac{\partial}{\partial\eta} + s\frac{\partial}{\partial z}, \quad (242)$$

showing that slow derivative enters at order δ^2 .

Expanding φ in powers of δ ,

$$\varphi(\eta) = \varphi_0(z, \eta) + \delta\varphi_1(z, \eta) + \dots,$$

and substituting into the model ballooning equation (239), yields equations determining the φ_i ; order by order. Integrating the $\mathcal{O}(\delta^0)$ equation once gives

$$\frac{\partial}{\partial \eta} \varphi_0 = \frac{A(z)}{1+z^2}. \quad (243)$$

We demand that there be no secular terms in η : all the slow-scale behavior is to be absorbed into the z -dependence. This yields the solvability condition

$$\left\langle \frac{A(z)}{1+z^2} \right\rangle = 0$$

where $\langle \dots \rangle$ denotes an average over η holding z fixed. Thus $A = 0$. Integrating (243) then gives $\varphi_0 = \varphi_0(z)$, an arbitrary function of z . This represents the envelope of the mode; its z -dependence will be fixed by a solvability condition at fourth order.

The $\mathcal{O}(\delta)$ equation is

$$\frac{\partial}{\partial \eta} (1+z^2) \frac{\partial}{\partial \eta} \varphi_1 + \rho(\cos \eta + z \sin \eta) \varphi_0 = 0.$$

The solvability condition for this equation is satisfied automatically since $\langle \sin \eta \rangle = \langle \cos \eta \rangle = 0$. Integrating twice gives

$$\varphi_1 = \rho \frac{(\cos \eta + z \sin \eta)}{1+z^2} \varphi_0 + C(z)$$

where $C(z)$ is another function undetermined at this order.

The second-order solvability condition is satisfied if the Mercier criterion is marginal to $\mathcal{O}(\delta^2)$, which is equivalent to $\bar{\kappa} \sim \delta^3$. The solution for φ_2 is

$$\varphi_2 = \frac{\rho^2}{4} \frac{(1-2z^2)\cos 2\eta + 3z \sin 2\eta}{(1+z^2)^2} + \rho \frac{\cos \eta + z \sin \eta}{1+z^2} C(z) + D(z)$$

where $D(z)$ is again undetermined; it represents the average part of φ_2 . The terms of interest here are those proportional to $e^{i2\eta}$. They will couple to $e^{i\eta}$ to give an average ballooning effect that determines the shape of the envelop φ_0 .

The third order solvability condition is trivially satisfied. At fourth order we obtain a nontrivial equation, the object of our analysis:

$$\begin{aligned} -\omega^2 (1+z^2) \varphi_0 &= 2\rho s \frac{\partial}{\partial z} (\cos \eta \varphi_1) + s^2 \frac{\partial}{\partial z} (1+z^2) \frac{\partial}{\partial z} \varphi_0 + \rho \bar{\kappa} \varphi_0 \\ &\quad - \rho^2 \langle \sin^2 \eta \varphi_2 \rangle + \rho \langle (\cos \eta + z \sin \eta) \varphi_3 \rangle. \end{aligned}$$

To obtain the equation for φ_0 , it is evidently necessary to solve only for the terms of φ_3 involving $\cos \eta$ and $\sin \eta$ (there are terms proportional to $e^{i3\eta}$

that do not affect the solvability condition). After considerable algebra we obtain

$$-\omega^2(1+z^2)\varphi_0 = s^2 \frac{\partial}{\partial z} (1+z^2) \frac{\partial}{\partial z} \varphi_0 + \left[\rho\bar{\kappa} + \frac{\rho^2(2s - \frac{3}{8}\rho^2)}{(1+z^2)^2} \right] \varphi_0 \quad (244)$$

which is the averaged or “distilled” ballooning equation for the envelope. Although the details of (244) depend on the specifics of the model, its qualitative behavior is similar to that obtained from more realistic equilibria.

The averaged curvature term $\rho\bar{\kappa}$ is the fourth-order term of the Mercier criterion and thus represents interchange effects. The last term in (244) describes the ballooning effects. The destabilizing term proportional to $s\rho^2$ arises from the interaction of the line bending with geodesic curvature. The stabilizing term results from the average of the rapid curvature oscillations. Note that as $z \rightarrow \infty$ the ballooning term vanishes and the Mercier analysis is recovered. Modes with structure at finite z are influenced by the ballooning term.

Equation (244) can be rewritten as a Schrödinger equation by letting

$$\varphi_0 = \frac{\phi(z)}{(1+z^2)^{1/2}},$$

whence

$$\begin{aligned} \omega^2\phi &= -s^2 \frac{\partial^2}{\partial z^2} \phi + V(z)\phi \\ V(z) &= \frac{1}{1+z^2} \left[-\rho\bar{\kappa} + \frac{s^2}{1+z^2} - \frac{\rho^2(2s - \frac{3}{8}\rho^2)}{(1+z^2)^2} \right]. \end{aligned} \quad (245)$$

It is clear that if $\rho\bar{\kappa} > 0$ then the potential in (245) is negative for sufficiently large z , which is the point of the Mercier criterion: this leads to instability. A simple sufficient condition for stability is $V(z) > 0$ for all z . This gives the criterion

$$\rho\bar{\kappa} < 0$$

$$s^2 + |\rho\bar{\kappa}| + \rho^2 \left(\frac{3}{8}\rho^2 - 2s \right) > 0. \quad (\text{stability}) \quad (246)$$

The first relation implies interchange stability, and the second ballooning stability. Equation (246) shows that ballooning modes are stable for sufficiently small pressure (ρ) and again at sufficiently large pressure. Rewriting (246) as

$$(s - \rho^2)^2 + |\rho\bar{\kappa}| - \frac{5}{8}\rho^4 > 0 \quad (\text{stability})$$

we obtain the two stability boundaries (see Figure 7.7)

$$s = \rho^2 \pm \left(\frac{5}{8}\rho^4 - |\rho\bar{\kappa}| \right)^{1/2}. \quad (247)$$

Instability occurs between these curves. There is a minimum ρ , $|8\bar{\kappa}/5|^{1/3}$, below which no instability occurs for any value of s . For larger pressures the two stability curves are approximately parabolas. The curves agree well with those obtained numerically for the model equation (239).

The fact that ballooning modes are stabilized at sufficiently large pressure gradients, confirmed by calculations using realistic equilibria, makes the operation of tokamaks theoretically feasible in an economically favorable regime of high β : the so-called "second stability" regime.

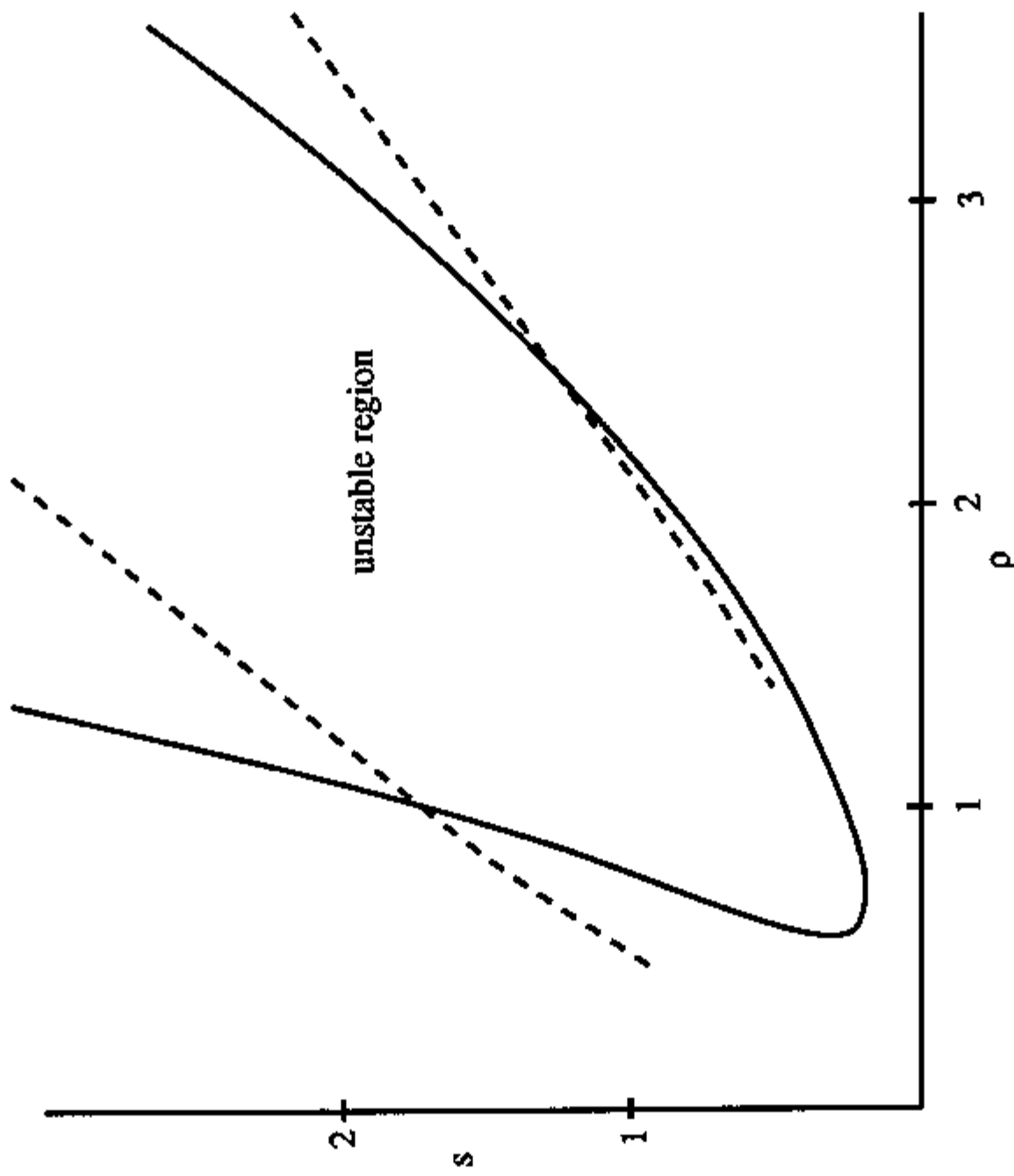


Figure 7. Ballooning stability boundaries from Eq. (247) and (249) for $\bar{\kappa} = 0.1$. The weak ballooning results, solid curve, are valid for small shear, and the strong ballooning results, dashed curves, are valid for strong shear.

Strong Ballooning

In the strong ballooning limit, the unstable mode is localized to a narrow range of η , typically near the outside of the torus, where the curvature is unfavorable. For this case the ballooning representation (211), shows that the mode is spread over a large range in radius, and hence contains many

helicities. To treat this case we expand the ballooning equation for small mode width. We will see that this approximation is valid in the regime $s \sim \rho \gg 1$.

The substitution

$$\varphi = \phi/f,$$

converts the model ballooning equation (239) into a Schrödinger equation

$$\omega^2 \phi = -\frac{\partial^2}{\partial \eta^2} \phi + V(\eta) \phi$$

$$V(\eta) = \frac{(s - \rho \cos \eta)^2}{f^4} - \rho \frac{\bar{\kappa} + \cos \eta}{f^2}. \quad (248)$$

Here we have set θ_k to zero for simplicity. The potential $V(\eta)$ oscillates on the scale $\eta \sim 1$, but for strong ballooning we are interested only in its behavior for $\eta \ll 1$. Expanding about $\eta = 0$ gives

$$V(\eta) = a + b^2 \eta^2 + \dots$$

$$a \approx -\rho(\bar{\kappa} + 1) + (s - \rho)^2$$

$$b^2 = \rho \left[s - \rho + \frac{1}{2} + (s - \rho)^2(\bar{\kappa} + 1) \right] - 2(s - \rho)^4.$$

Schrödinger's equation with this potential is Weber's equation (the harmonic oscillator), and the solutions are

$$\begin{aligned} \phi &= e^{-\frac{b}{2} \eta^2} H_j(\sqrt{b}\eta) & j = 0, 1, 2, \dots, \\ \omega^2 &= a + (2j + 1)b \end{aligned}$$

where H_j is the j th Hermite polynomial. Since b must be positive, it is clear that the lowest mode, $j = 0$, is the most unstable. Localization of the mode requires b to be large; when $s \sim \rho$ this in turn requires large ρ . The only consistent ordering is $s - \rho \sim \mathcal{O}(\rho^{1/2})$ which implies that the mode is always unstable:

$$\omega^2 = -c^2 + c(s - \rho) - (s - \rho)^2$$

$$c = [\rho(\bar{\kappa} + 1) - 2(s - \rho)^2]^{1/2}.$$

The localization approximation is certainly invalid if $b^2 < 0$; this determines two curves

$$s = \rho \pm \left[\frac{\rho}{2} (\bar{\kappa} + 1) \right]^{1/2} \quad (249)$$

outside of which the potential develops a local maximum at $\eta = 0$. The upper shear boundary, shown in Fig. 7.7, lies close “first stability” boundary

obtained by numerical solution of (239). Stability in this case is due to the positive shear-induced potential overwhelming the local well due to the curvature term. On the other hand the minus sign in (249) does not agree well with the “numerically determined ‘second stability’ boundary. This is due to quartic terms in V : the local maximum at $\eta = 0$ only causes a small dimple in the potential. Since the minimum of V now occurs for $\eta \neq 0$, the most unstable modes have $\theta_k \neq 0$. Keeping terms due to θ_k leads to an increase in the size of the unstable region over that predicted by (249). This effect could be analyzed by expanding V about its minimum.

In general, the instability we have found for $s \sim \rho$ is replaced by one that occurs when the local shear vanishes (Greene and Chance, 1981). Near such points the stabilizing effects of the line-bending term is minimized, and if the local curvature is unfavorable, instability results.

7.13 Non-Ideal Stability*

Unlike the equations for boundary layer analysis, the order of the ballooning equation does not increase when resistive terms are included. Resistivity causes the line-bending term of (220) to become

$$\frac{\partial}{\partial \eta} \frac{F^2}{1 + x_R^2 F^2} \frac{\partial}{\partial \eta} \phi. \quad (250)$$

The primary effect of this modification is a significant reduction of the stabilizing effect of the line-bending term for $\eta \sim s/x_R$. Thus the shear, which is important in the localization of the ideal mode, is defeated by the resistivity for large η . Resistivity permits the unstable modes to be extended in η by allowing the perturbed field lines to slip relative to the flow. A similar modification to the line bending occurs when FLR effects are added: the line bending term is reduced at large η . In addition the inertial term is modified by the change $\omega^2 \rightarrow \omega(\omega - \omega_{*i})$. The former has similar effects to resistivity, and the latter results in an increase in the pressure required for instability.

7.14 Summary

A plasma is regarded as stable if, beginning near an equilibrium state, it remains nearby for all time. It is usually impossible to prove that a toroidal equilibrium is stable in this sense. More modestly we can attempt to prove a system is linearly stable, or spectrally stable.

In a spectral analysis the linearized eigenmodes are studied. Low frequency modes in a confined plasma are typically flute-like in character: the

disturbances are predominantly aligned with the magnetic field. The fundamental equation governing flute evolution is the shear-Alfvén law (23); its terms define the issues relevant to plasma stability: rational surface singularity, interchange forces involving magnetic curvature and pressure, and line bending forces involving the parallel current. Ideal modes are termed shear-Alfvén, kink modes, or interchange modes depending upon the importance of the various terms in the shear-Alfvén law.

Fluid equations can be simplified using the assumption that disturbances are flute-like. The resulting models include flute-reduced MHD, (53) and large-aspect ratio reduced MHD.

For ideal MHD, the spectral stability problem reduces to an eigenvalue equation with eigenvalue ω^2 . It can be shown that ω^2 is real; thus the only possible spectral instabilities are purely growing. A simple necessary criterion for stability is the Suydam criterion (98), in the cylindrical case, and its generalization, the Mercier criterion (235), in the toroidal case. More generally the ideal MHD energy principle (126) is a quadratic form, which when positive definite guarantees that the system is linearly stable. When kink modes are stable, relaxation of the constraint imposed by the conservation of flux, (103), can lead to instability. Instabilities which rely upon reconnection of flux are called tearing modes. Near the rational surface, $|x| < w$, the equations for resistive modes are fourth order, (137) and (138), in the simplest case. Solution involves matching the layer solution with external, ideal solution. The character of the resulting eigenmodes depends on the matching parameter, Δ' , which is obtained from the ideal solutions far from the layer. Typically $\Delta'w \ll 1$ when $m \neq 1$, and the mode has growth rate (158). For $m = 1$, $\Delta'w > 1$, and the dispersion relation is (155).

Collisionless resolution of the rational surface singularity results in the formation of a current channel. The simplest current channel is formed by the large parallel conductivity of electrons near the rational surface. The resulting dispersion relations (194) and (196) have a real frequency given by the drift frequency.

Modes driven predominantly by the interaction of pressure gradients with magnetic curvature are most likely to be unstable when they are flute-like. The conflict between satisfying the condition $\mathbf{B} \cdot \nabla \approx 0$ in a sheared system, and poloidal periodicity, leads to the introduction of the ballooning representation. In this representation the linearized equations become ordinary differential equations along the field direction, e.g. (218). The parallel coordinate is taken to be infinite in extent, and the equations are to be solved for square integrable eigenfunctions.

The ballooning representation is particularly useful in the derivation of the Mercier criterion (235), for modes which are localized to a rational surface. It can also be used to derive more general stability conditions, such as (246) when the mode is extended. The latter criterion indicates the existence of two stability regions in the shear-pressure gradient plane.

The first stability region occurs for small pressure gradient and moderate shear; the second stability region occurs for large pressure gradient and small shear. The possible existence of a second stability region would be important in constructing and economical tokamak reactor.

Further Reading on

Ideal Stability:

Kruskal and Oberman, 1958
 Newcomb, 1960
 Greene and Johnson, 1962
 Jeffrey and Taniuti, 1966
 Bateman, 1980
 Freidberg, 1987

Resistive Stability:

Furth, 1985
 Kadomtsev, 1965
 White, 1986.

Ballooning Stability:

Connor, Hastie and Taylor, 1978
 Hazeltine and Meiss, 1985

Exercises

- Find conditions on $f(x)$ such that the first order differential equation $\dot{x} = f(x)$ has a fixed point at $x = 0$ and which has the property of: (a) spectral stability, (b) asymptotic linear stability, (c) Lyapunov stability, (d) global stability: all initial conditions approach $x = 0$ as $t \rightarrow \infty$.
- Lyapunov Stability.** Two dimensional, incompressible fluid motion is governed by the equation

$$\frac{\partial}{\partial t} U + [\varphi, U] = 0$$

where $[f, g] = \hat{z} \cdot \nabla f \times \nabla g$, and $U = \nabla^2 \varphi$ is the vorticity, and $\mathbf{V} = \hat{z} \times \nabla \varphi$ is the velocity. Consider a fluid in a bounded disk, with the condition $\varphi = \text{constant}$ on the boundary. (a) Show that $H = \frac{1}{2} \int d^2x |\nabla \varphi|^2$ and

$G = \int d^2x g(U)$ for any function $g(U)$ are conserved quantities. (b) Consider the functional $F[\varphi] = H + G$. Show that $\delta F = 0$ determines an equilibrium solution. (c) Show that $\delta^2 F$ is positive definite if $g'' > 0$, and therefore that the flow is (formally) Lyapunov stable when the velocity profile has no inflection points. Complete Lyapunov stability follows upon demonstrating (9), see (Arnol'd, 1965).

3. Derive (73) verifying (71) and (72).

4. Consider the equation

$$x^2\xi'' + 2x\xi' + (\omega^2x^2 - 2)\xi = 0$$

with the boundary conditions $\lim_{x \rightarrow 0} x\xi(x) = \xi(1) = 0$. (a) Show this is a Sturmian equation. (b) Obtain the variational principle and show that there are no solutions for $\omega^2 < 0$. (c) Convert the equation to the spherical Bessel equation and obtain the eigenvalues.

5. Show that the curvature of a helical field line in a cylindrical plasma, is $\kappa_r = -r/(Rq)^2$. Combining this with (98) gives a familiar form of the Suydam criterion.
6. Verify (124), keeping track of the partial integrations so as to obtain the boundary terms.
7. Derive the linearized energy, $\delta^2 W[\phi, \psi]$, for low-beta, large-aspect ratio reduced MHD, (62). Compare the result with (126).
8. θ -Pinch. Consider a cylindrical plasma, described by $\mathbf{B} = B(r)\hat{\mathbf{z}}$ and $P = P(r)$. Use the Fourier representation (64) for $\boldsymbol{\xi} = \xi_r \hat{\mathbf{r}} + \xi_\theta \nabla\theta + \xi_\zeta \nabla\zeta$ (note that the Fourier amplitudes are complex). The argument at the end of §7.6 implies that one can consider incompressible displacements $\boldsymbol{\xi}$. Use this to eliminate $\xi_{||} = \xi_\zeta$. (a) Show that (126) can be reduced to the form
- $$\delta^2 W = \frac{\pi}{2} R \int_0^a \frac{dr}{r} B^2 \left\{ \left| k\xi_\theta - \frac{im}{k} (r\xi_r)' \right|^2 + \left(\frac{n}{kR} \right)^2 \left[|(r\xi_r)'|^2 + k^2 r^2 |\xi_r|^2 \right] \right\}$$

where $k^2 = (m/r)^2 + (n/R)^2$. (b) Determine ξ_θ by minimizing $\delta^2 W$. (c) Substitute this into the above expression showing that $\delta^2 W$ is positive for $n \neq 0$. Thus the only possible unstable mode is that for $n = 0$, for which $\delta^2 W$ is zero.

- 9. Screw Pinch.** Consider the cylindrical field (62), with $P = P(r)$.

(a) Eliminate ξ_{\parallel} using the incompressibility constraint, and show that ξ_1 can be eliminated from $\delta^2 W$ algebraically, just as ξ_{θ} was in exercise (8). (b) The resulting expression is a quadratic form in ξ_r and ξ'_r . After judicious integration by parts to eliminate the $\xi_r \xi'_r$ terms, show that $\delta^2 W$ becomes

$$\begin{aligned} \delta^2 W = \frac{\pi}{2} R \int_0^a \frac{dr}{r} B^2 & \left\{ \left(\frac{rk_{\parallel}}{k} \right)^2 |\xi'_r|^2 \right. \\ & + \left[\left(\frac{n}{Rk} \right)^2 r \beta' + [(kr)^2 - 1] \left(\frac{k_{\parallel}}{k} \right)^2 - \frac{n^2}{(kR)^4} (n + mq) R k_{\parallel} \right] |\xi_r|^2 \left. \right\}. \end{aligned}$$

- (c) Taking the large aspect ratio limit, compare this result to the $\omega^2 = 0$ limit of (87), noting that $\varphi/r = \xi_r$.

- 10. Slab Model.** The sheared slab has the equilibrium field $\mathbf{B} = B_0 [\hat{\mathbf{z}} + \hat{\mathbf{y}} F(x/L_s)]$, where (x, y, z) are rectangular coordinates. Linearize ideal, zero-beta, reduced MHD (55) using the model $F = \tanh(x/L_s)$. Consider perturbations with $k_{\parallel}(x=0)=0$, and show that

$$\Delta' L_s = 2 \left(\frac{1}{kL_s} - kL_s \right)$$

- 11.** Use the approximate dispersion relation (158) to estimate the growth rate (γ), layer width (w), shear-Alfvén width (x_A) and resistive skin depth (x_R) of an $m \geq 2$ tearing mode in the Standard Tokamak (see Exercise 3.6). Use the estimates $\sigma_S \simeq 10^{18} \text{ sec}^{-1}$, $L_s \simeq qR$ and $\Delta' \simeq 1/a$. Discuss the physical significance of the ratio w/ρ_i .

- 12.** Consider a cylindrical system with uniform temperature and negligible magnetic curvature (but nonvanishing shear). Use the drift model of §6.5 to derive the linear electron response to $E_{\parallel i}$; compare your answer to the kinetic result, (190). See (Hazeltine and Meiss, 1985).

- 13.** Show that the electrostatic potential for the ideal $m = 1$ mode, at low beta, has the approximate form

$$\Phi = C/2 - (C/\pi) \tan^{-1}(x/x_A)$$

where C is a constant, $x = r - r_s$, and x_A is the shear-Alfvén width. See (Rosenbluth et al., 1973).

14. Show that the Mercier criterion (235) reduces to the Suydam criterion (98) in the appropriate limit. Note that q' means dq/dr in the former and dq/dv in the latter.

15. Show, starting with (3.120) or (3.121), that the flux surface average of the normal curvature, at low beta, is proportional to $q^2 - 1$. Thus the Mercier criterion reduces to

$$\frac{q'^2}{4} + \frac{\beta'}{r} q^2 (1 - q^2) > 0$$

showing that modes with $q > 1$ are stable. See (Ware and Haas, 1966).

16. Compute φ_3 and derived the averaged ballooning equation (244) for the envelope φ_0 .

17. Obtain the ballooning equation for resistive, flute-reduced MHD, deriving (250). Show that when $\eta \gg x_R^{-2}$ the line bending term is small, and in this limit the mode has the form $\Phi \sim e^{-(\eta/w)^2}$ and obtain the mode width, w .

Chapter 8

Collisional Transport

8.1 Introduction: Classical Perpendicular Transport

Minimal Dissipation

In the limit of vanishing gyroradius, charged particles simply stream along the magnetic field. Then lowest-order confinement is insured by the existence of closed, nested flux surfaces, as in a toroidal confinement system. At finite gyroradius, perpendicular guiding-center drifts allow particles to penetrate flux surfaces; in that case confinement requires the average radial excursion to vanish, as in (5.127). When such constraints are satisfied one has achieved equilibrium confinement,¹ and plasma loss can be blamed on the corruption of single-particle orbits by extraneous fields. Thus magnetic perturbations deform the lines of force, bringing them closer to a boundary or making them chaotic, while errant electric fields allow particles to move radially across \mathbf{B} .

It is helpful—albeit imprecise—to distinguish between two kinds of electromagnetic field perturbation. There are on the one hand coherent interactions, studied in Chapter 7, which can cause a bulk outward flow of plasma—as in MHD instability or tokamak disruption. On the other hand one has microscopic, effectively random excitations, possibly but not necessarily related to plasma instability. The corresponding escape of particle or energy is diffusive in nature, and presumed to stem from *fluctuations*, in the statistical mechanical sense. This second category of loss processes is the concern of plasma transport theory.

As we have noted, confined plasmas display a variety of fluctuations, including MHD activity, electrostatic noise, and so on. The rms fluctuation

¹Sometimes one hears of “single particle confinement” or “test particle confinement,” but these terms can be misleading. In a tokamak, for example, suitable flux surfaces and drift orbits depend upon equilibrium plasma currents; the vacuum-field trajectory of a single particle is not relevant. What is assumed to be confined is a test particle that responds to the macroscopic equilibrium fields—including fields that result collectively from other charged particles.

amplitude varies sharply in different experiments—in response, for example, to divertor operation, or external heating input—and the consequent change in transport rates is usually apparent. However, there is a minimum level of fluctuations that must be present, even in the most quiescent discharge. These are thermal fluctuations, resulting from particle discreteness; the corresponding minimal interactions are the Coulomb collisions studied in Chapter 5.

We shall use the term *collisional transport* to describe this irreducible minimum of dissipation, involving only Coulomb collisions. Although frequently outweighed in experiments by other transport mechanisms, collisional transport has special significance. It is always present, whatever additional dissipative processes may contribute. Being comparatively well understood, it provides a standard against which other transport mechanisms are usefully measured. It is especially useful pedagogically, because its consequences can be calculated with relative simplicity and rigor. Therefore we restrict attention in this chapter to collisional transport. Other varieties of dissipation are considered in Chapter 9.

Classical Diffusion

The simplest collisional transport process results from the interaction of Coulomb scattering with particle gyromotion. Called classical transport (Hinton, 1983), it is rarely a dominant loss mechanism, but it deserves attention because of its simplicity, and because it has many features in common with more virulent and complicated transport processes.

We recall that gyromotion, in the presence of gradients, drives a non-Maxwellian correction to the distribution,

$$\tilde{f} = -\rho \cdot \nabla f_M,$$

$$= -\frac{f_M}{\Omega} \mathbf{b} \times \mathbf{v}_\perp \cdot \left\{ \nabla \ln n + \frac{e \nabla \Phi}{T} + \left[\frac{U - e\Phi}{T} - \frac{3}{2} \right] \nabla \ln T \right\} \quad (1)$$

[see (4.66) and (4.182)]. While trying to relax this perturbation, Coulomb collisions engender a friction force,

$$\mathbf{F}_c \equiv \int d^3 v m v C (-\rho \cdot \nabla f_M), \quad (2)$$

whose effect on guiding centers is to induce a drift, analogous and additive to the $\mathbf{E} \times \mathbf{B}$ drift [see (5.67)]:

$$\mathbf{V}_E = -\frac{c}{B} \mathbf{b} \times \mathbf{E} \rightarrow -\frac{c}{B} \left[\mathbf{b} \times \left(\mathbf{E} + \frac{\mathbf{F}_c}{en} \right) \right]. \quad (3)$$

The corresponding perpendicular flow

$$n \mathbf{V}_c \equiv -\frac{c}{eB} \mathbf{b} \times \mathbf{F}_c, \quad (4)$$

is outward, and proportional to the driving gradients. This flow, which we shall find to have a diffusive character, is responsible for classical diffusion.

Consider for simplicity the case of a pure plasma, with a single ion species. The corresponding friction force was evaluated in §6.5; we recall (6.126) to write, for the force on electrons,

$$\mathbf{F}_e = \frac{n m_e}{T_{ei}} \left[\mathbf{V}_{\perp 1s} - \mathbf{V}_{\perp 1e} - \frac{3}{2} \frac{c}{eB} \mathbf{b} \times \nabla T_e \right]. \quad (5)$$

Here the $V_{\perp 1s}$ are the familiar first order flows, corresponding to (1), and given by

$$n \mathbf{V}_{\perp 1s} \equiv \frac{c}{e_s B} \mathbf{b} \times (\nabla p_s + e_s n \nabla \Phi) \quad (6)$$

as was found in §4.5 and §6.3. In combining (4)–(6), we note that the electric field terms cancel, and use the notation of §6.4,

$$P \equiv p_i + p_e.$$

Thus

$$n \mathbf{V}_e = -\frac{1}{(m_e \Omega_e^2 \tau_{ei})} \left[\nabla_{\perp} P - \frac{3}{2} n \nabla_{\perp} T_e \right]. \quad (7)$$

This result pertains in any equilibrium geometry, and for any regime of collisionality, as long as the plasma is magnetized. In particular we must require that $\nu \ll \Omega$; otherwise, the lowest order trajectory does not correspond to gyration and (1) is not applicable.

Several additional comments are in order:

1. The classical particle flow is *dissipative*. This is apparent from the first term of (7), showing that $n \mathbf{V}_e$ flows down the pressure gradient:

$$n \mathbf{V}_e \cdot \nabla P < 0. \quad (8)$$

It therefore degrades confinement, driving the system towards thermodynamic equilibrium, where $\nabla P = 0$. In other words, classical diffusion indeed tends to increase the entropy of the system. Note that the first-order flow of (6) is not dissipative in this sense.

The second term in (7), involving the temperature gradient, is not manifestly dissipative. However we will find, after computing the classical heat flow, \mathbf{q}_e , that entropy necessarily increases, even in the presence of temperature gradients, according to

$$n \mathbf{V}_e \cdot \nabla_{\perp} \ln P + \frac{\mathbf{q}_{ee}}{T_e} \cdot \nabla_{\perp} \ln T_e < 0. \quad (9)$$

2. Classical diffusion is independent of the electric field. We have already noted that the $\nabla \Phi$ terms of (6) cancel in (7). The fundamental reason is not hard to see: the electric field enters the perturbed distribution, (1), as a displacement of the Maxwellian, with velocity given by the same $\mathbf{E} \times \mathbf{B}$

drift for all plasma species. As long as the collision operator is Galilean invariant, in the sense of (5.4), any such common flow cannot affect the friction force.

3. Classical diffusion is proportional to the square of the gyroradius and thus $\mathcal{O}(\delta^2)$. This is clear from (7). If we define the classical diffusion coefficient D_c by

$$\mathbf{n} \mathbf{V}_c = -D_c \nabla n + \dots \quad (10)$$

(where the ellipsis refers to temperature gradient terms) then (7) implies $D_c = (m_e \Omega_e^2 \tau_{ei})^{-1} (T_i + T_e)$, or

$$D_c = \frac{1}{2} \nu_{ei} \rho_e^2 \left(1 + \frac{T_i}{T_e} \right), \quad (11)$$

where $\nu_{ei} \equiv 1/\tau_{ei}$. It follows that $V_c/v_t \sim \rho_e^2/(L \lambda_{\text{mfp}})$, where L is the density gradient scale-length and

$$\lambda_{\text{mfp}} \equiv \frac{v_t}{\nu} \quad (12)$$

is the collisional mean free path. In other words

$$\frac{V_c}{v_t} \sim \frac{L}{\lambda_{\text{mfp}}} \delta^2. \quad (13)$$

The second-order nature of V_c was noted in Chapter 6, and implicitly assumed in writing down, for example, (6). It deserves emphasis here because of its relation to the transport ordering,

$$\frac{\partial}{\partial t} \sim \delta^2 \omega_t \quad (14)$$

discussed in Chapter 4 [recall (4.16)]; here $\omega_t \equiv v_t/L$ is the transit frequency. It is clear (13) and (14) are together consistent with particle conservation.

4. Classical diffusion is intrinsically ambipolar,

$$\sum_s e_s n_s \mathbf{V}_{cs} = 0, \quad (15)$$

for any set of equilibrium gradients. This follows, for any number of ion species, from (4),

$$e_s n_s \mathbf{V}_{cs} \equiv -\frac{c}{B} \mathbf{b} \times \mathbf{F}_{cs} \quad (16)$$

and collisional momentum conservation, (5.23). Thus (11) for D_c applies to both species, despite the appearance of electron parameters only.

Note that ambipolarity, in the form of (3.66), characterizes any quasistatic system, whatever the transport mechanism. In general, however, ambipolarity is to be imposed as a constraint, providing additional information concerning equilibrium parameters. One speaks, for example, of the

“ambipolar field”—the electrostatic field required to eliminate equilibrium radial current. From this point of view, the significance of (15) is that classical ambipolarity obtains automatically, as an intrinsic property of the diffusion mechanism, without constraining the equilibrium state. (A more elaborate discussion of ambipolarity may be found in §9.5.).

A related observation is that classical diffusion is affected only by unlike species collisions. Indeed, the relevant distribution is determined by gyration, so that collisions enter only through the friction force, as in (2), and momentum conservation rules out any like-species contribution.

Random Walk Estimate

Before turning our attention to classical heat flow, we take note of a helpful interpretation of the diffusion formula, (11). The diffusion coefficient for a general random walk process is given by²

$$D_{\text{random walk}} = (\text{collision frequency}) \times (\text{step-size})^2 \quad (17)$$

where the step-size is the excursion between collisions. Evidently D_c describes a random walk of electrons, with step-size given by the gyroradius. Ions obey the same formula and, despite their much larger step size, have the same diffusion rate, because their wider orbits are only weakly perturbed by electron impact.

The process is sometimes pictured in terms of an electron gyrating about some field line, and then suffering a large-angle Coulomb collision. The resulting change in gyrophase causes the guiding center to jump to a neighboring field line, so that the electron executes a random walk, each step being measured by its gyroradius. The estimate $D_c \sim \nu_{ei} \rho_e^2$, in essentially exact agreement with (11), follows. This picture is faithful in that ν_{ei} is indeed the collision rate for large angle collisions, and also because the classical formula requires $\nu_{ei} \ll \Omega$. We recall from Chapter 5, however, that Coulomb collisions are individually very mild, the parameter ν_e corresponding to a large number of small-angle scattering events. Hence details of the picture should not be taken literally.

The sharp distinction between magnetized plasma transport and the diffusion process occurring in a neutral gas deserves emphasis. Neutral particles diffuse because of the random orientations of their collisionless trajectories; collisions act to *impede* the escape trajectory of a neutral, by imposing a finite mean free path, as in (12). Thus λ_{mfp} becomes the appropriate step-size, and the neutral random-walk diffusion coefficient is inversely proportional to ν :

$$D_n \sim \nu \lambda_{\text{mfp}}^2 \sim v_t^2 / \nu . \quad (18)$$

Magnetized particles, on the other hand, remain close to field lines and escape only because of collisions, with the result that D_c is proportional to

- v. Since the Coulomb collision frequency decreases with temperature [recall (5.71)], this fact is encouraging for magnetic confinement fusion.

Classical Heat Conductivity

By comparing the moment equations for plasma flow and plasma energy flow, (6.24) and (6.25), we see that there is an energy flow analogous to (4), with the friction force replaced by the energy weighted friction, \mathbf{G} . In terms of the heat flow \mathbf{q} [recall (6.18)] we have

$$\mathbf{q}_e = \frac{1}{\Omega} \mathbf{b} \times \mathbf{G}_e - \frac{5}{2} p \mathbf{V}_e ,$$

where \mathbf{G}_e is computed from (1):

$$\mathbf{G}_e \equiv \int d^3 v \frac{1}{2} m v^2 \mathbf{v} C(-\rho \cdot \nabla f_M) . \quad (19)$$

An important difference between \mathbf{q}_e and \mathbf{V}_e is apparent: in the absence of any dynamical conservation law for \mathbf{G} , \mathbf{q}_e is affected by like-species collisions. Indeed, for the case of ion heat flow, the integral in (19) is dominated by the like-species term, since $C_{ii} \gg C_{ie}$. This fact makes the calculation of \mathbf{G}_e somewhat more tedious than the friction case.

Equation (19) provides the estimates

$$G_{ci} \sim p v_{ti} \nu_{ii} (\rho_i / L)$$

and

$$G_{ce} \sim p v_{te} \nu_e (\rho_e / L) .$$

Since $\nu_e v_{te} \sim (m_i / m_e) \nu_i v_{ti}$ we see from (18) that

$$q_{ci} \sim \left(\frac{m_i}{m_e} \right)^{1/2} p V_e \sim \left(\frac{m_i}{m_e} \right)^{1/2} q_{ce} . \quad (20)$$

Thus the dominant classical transport process is ion heat conduction. We will see that this circumstance also describes more elaborate varieties of collisional transport. It is a consequence of the larger orbital excursion of ions in a magnetized plasma.

Detailed evaluation of the integral in (19) gives

$$\mathbf{q}_{ci} = -2(m_i \Omega_i^2 \tau_i)^{-1} p_i \nabla_\perp T_i , \quad (21)$$

$$\mathbf{q}_{ce} = -(m_e \Omega_e^2 \tau_{ei})^{-1} [4.66 p_e \nabla_\perp T_e - (3/2) T_e \nabla_\perp P] . \quad (22)$$

In (21), the ion collision time τ_i is that defined by (5.79); the numerical coefficient in (22) assumes unit ionic charge. It is clear that these heat flows are

dissipative; indeed, the thermodynamic inequality (9) is easily confirmed. We can read off from (21) and (22) the classical thermal conductivities,

$$\kappa_i = 2(m_i \Omega_i^2 \tau_i)^{-1} p_i, \quad (23)$$

$$\kappa_e = 4.66(m_e \Omega_e^2 \tau_{ei})^{-1} p_e. \quad (24)$$

Notice also that q_{ce} contains a pressure-gradient term, analogous to the $\nabla_\perp T_e$ term of (7). Both are “off-diagonal” terms, in the sense that particle flow is naturally driven by pressure gradients and heat flow by temperature gradients. The fact that both appear with the precisely the same coefficient is a manifestation of *Onsager symmetry*—a topic to which we return presently. Similar off-diagonal terms in q_{ci} would appear in higher $(m_e/m_i)^{1/2}$ -order.

Most of our previous comments concerning nV_c , such as electric field independence, also apply to q_c .

8.2 Fluid Evolution in a Torus

Transport Closure

Unfortunately the word “classical” has the same connotation regarding (11), (21) and (22) as it does in other domains of physics: observed transport rates are typically much faster. More surprisingly, even the theoretically predicted collisional transport rates exceed classical transport by an order of magnitude or more. (As we have noted, the observed transport is often larger still, reflecting noncollisional diffusion mechanisms.) Indeed, when toroidal transport is analyzed carefully, the classical terms appear as small corrections, often omitted.

We therefore begin a more systematic treatment of toroidally confined plasma transport. It is based on the transport ordering, (14), which is assumed to survive whatever transport enhancements may pertain. (Indeed any faster plasma decay would hardly be consistent with the notion of confinement.) We also use a now familiar assumption concerning plasma flow:

$$V \sim \delta v_t. \quad (25)$$

Thus the very rapid motions of MHD are ruled out.

These orderings, essentially defining what is meant by a quiescent, stable plasma, are applied first to the conservation laws for particles and energy, (6.22) and (6.23). In order to follow time evolution in the transport ordering, we retain $O(\delta^2)$ terms; all higher order terms are neglected. Because of (25), the energy law slightly simplifies and we have

$$\frac{\partial n}{\partial t} + \nabla \cdot (nV) = 0, \quad (26)$$

$$\frac{3}{2} \frac{\partial p}{\partial t} + \nabla \cdot \mathbf{Q} = \mathbf{W} + \mathbf{V} \cdot (\mathbf{F} + en\mathbf{E}) . \quad (27)$$

We found in Chapter 5 that, in the quasi-equilibrium described by the transport ordering, the density and pressure are nearly constant along \mathbf{B} . In this case $n \cong \langle n \rangle$, $p \cong \langle p \rangle$, where the brackets indicate flux-surface averages, and the main content of (26) and (27) should survive a flux-surface average. Indeed the form of the unaveraged equations is awkward, especially at low collisionality, where the macroscopic excursion of collisionless particles on the flux surface must be taken into account.

The flux surface average is performed using (3.40):

$$\langle \nabla \cdot \mathbf{A} \rangle = (d/dV) \langle \mathbf{A} \cdot \nabla V \rangle ,$$

where \mathbf{A} is any vector and $V(r)$ is the volume enclosed by the surface. Alternatively

$$\langle \nabla \cdot \mathbf{A} \rangle = \frac{1}{V} \frac{d}{dr} (V' \langle A^r \rangle) = \frac{1}{V'} (V' \langle A^r \rangle)' ,$$

where the primes denote radial derivatives and A^r is the contravariant radial component of \mathbf{A} . Hence (26) and (27) become

$$\left\langle \frac{\partial n}{\partial t} \right\rangle + \frac{1}{V'} (V' \Gamma)' = 0 , \quad (28)$$

$$\frac{3}{2} \left\langle \frac{\partial p}{\partial t} \right\rangle + \frac{1}{V'} (V' Q)' = \langle W \rangle + \langle \mathbf{V} \cdot (\mathbf{F} + en\mathbf{E}) \rangle \quad (29)$$

where the averaged radial *fluxes* of particle and energy are given respectively by

$$\Gamma \equiv \langle n V^r \rangle , \quad (30)$$

and

$$Q \equiv \langle Q^r \rangle . \quad (31)$$

Note that (6.54) insures that both Γ and Q are of order δ^2 , consistent with the transport ordering.

The objective of transport theory should be clear. We are to express the fluxes Γ and Q in terms of an appropriate set of thermodynamical forces, as in (7), (21) and (22), and to find similar expressions for the energy exchange terms on the right hand side of (29). Then (28) and (29), in combination with Maxwell's equations, yield a closed description of confined plasma evolution.

This closure scheme, called *transport closure*, can be compared to the MHD and FLR closures studied in Chapter 6. Transport closure is outstandingly simple and rigorous—an archetype of asymptotic closure methods. Its result is a set of differential equations in a single spatial variable and

time, for the density and temperature of each plasma species: a complete answer to central questions of confinement. Furthermore this prescription, although strongly dependent in detail on plasma parameters, can be calculated in any collisionality regime of interest.

Despite these impressive strengths, it should be said that transport closure in a torus is a peculiar theoretical object. It is especially important that the closed set has been averaged over a magnetic flux surface: there is no description of dynamics or variation within the surface, and the flux-label nature of equilibrium plasma parameters is essential to the system's completeness. In particular the closure scheme assumes that well behaved flux surfaces exist. Thus the peculiarities of transport closure sharply limit its application. It describes in principle the quasistatic evolution of a diffusing equilibrium, but it is too dependent on the transport ordering, and on the maintenance of various equilibrium symmetries, to describe much of anything else.

Before considering the radial fluxes in more detail we comment on the first terms of (28) and (29). We would like to write

$$\left\langle \frac{\partial n}{\partial t} \right\rangle = \frac{\partial}{\partial t} \langle n \rangle , \quad \left\langle \frac{\partial p}{\partial t} \right\rangle = \frac{\partial}{\partial t} \langle p \rangle \quad (32)$$

but (32) is not generally correct, because of motion or deformation of the flux surfaces in time. Recall that a magnetic surface with specified poloidal flux contracts significantly in a diffusion time, due to $E_T = (Rc)^{-1} \partial \chi / \partial t$. Furthermore the surfaces, whether defined by the poloidal or toroidal fluxes, may change shape on the same time scale. In using (32) we evidently assume, in the tokamak case, that the surfaces are defined in terms of the relatively invariant toroidal magnetic field, and that their shape is preserved during diffusive evolution. In other words we employ the constant shape assumption, as discussed in §3.11.

Radial Fluxes

We next derive helpful formulae for the radial fluxes, considering the particle flux of (30) first for convenience. Our discussion uses several results of Chapters 3–6, especially §5.3 and §6.3. We exploit small δ in precisely the usual fluid manner: the manipulation summarized by (6.46) is at the heart of transport closure. However, because the present analysis is specifically addressed to toroidal geometry, it differs in detail from that in Chapter 6. We first combine the tensor formula (2.24) with (3.22) to find that

$$(\mathbf{V} \times \mathbf{B})_\zeta = g^{1/2} \epsilon_{\zeta\alpha\beta} V^\alpha B^\beta = g^{1/2} V^r B^\theta = \chi' V^r ; \quad (33)$$

that is,

Note that (33) holds in an arbitrary toroidal system with flux coordinates (r, θ, ζ) ; there is no assumption of axisymmetry. The right-hand side is computed from the covariant ζ -component of the exact momentum conservation law, (6.24). After recalling (6.17),

$$\mathbf{P} = \mathbf{I}[p_0(\chi) + p_1(\chi, \theta, \zeta)] + \mathbf{P}_{\text{CGL}} + \mathcal{O}(\delta^2), \quad (34)$$

and neglecting third order terms we have

$$nV^r = \frac{c}{e\chi'} \left[\frac{\partial p_1}{\partial \zeta} + (\nabla \cdot \mathbf{P}_{\text{CGL}})_\zeta - enE_\zeta - F_\zeta \right] + \mathcal{O}(\delta^3). \quad (35)$$

This result may be compared with (6.42). It is not hard to see that the flux surface average of the first term must vanish,

$$\left\langle \frac{\partial p_1}{\partial \zeta} \right\rangle = \frac{\int d\theta d\zeta g^{1/2} \frac{\partial p_1}{\partial \zeta}}{\int d\theta d\zeta g^{1/2}} = 0,$$

in any system satisfying equilibrium force balance. For we have shown that Hamada coordinates exist in such a system, and since the Jacobian $g^{1/2}$ is constant in Hamada coordinates, the ζ -integral will annihilate $\partial p_1 / \partial \zeta$. The radial particle flux can therefore be expressed as

$$\Gamma = -\frac{c}{e\chi'} [\langle F_\zeta \rangle - ((\nabla \cdot \mathbf{P}_{\text{CGL}})_\zeta) + e \langle nE_\zeta \rangle], \quad (36)$$

showing its contributions from collisional friction, from anisotropy and from the electric field. This result pertains in any toroidal geometry, and is correct through second order in δ whenever the orderings (14) and (25) pertain. We also recall, from §6.3, that the second order flux is determined by (36) from *first order* expressions for \mathbf{F} and \mathbf{P}_{CGL} .

Equation (36) is attractively simple and even useful, but it misses a near cancellation of the terms on its right-hand side, due to parallel force balance. The point is that (6.24) implies

$$\nabla_{\parallel} p_1 = F_{\parallel} - (\nabla \cdot \mathbf{P}_{\text{CGL}})_{\parallel} + enE_{\parallel} + \mathcal{O}(\delta^3); \quad (37)$$

hence only the perpendicular components of \mathbf{F} , $\nabla \cdot \mathbf{P}$ and \mathbf{E} survive to affect Γ . Here it is helpful to introduce the “perpendicular- ζ ” component of a vector \mathbf{A} : the covariant ζ -component of \mathbf{A}_{\perp} , given by

$$A_{\perp\zeta} \equiv (\mathbf{A} - \mathbf{b} A_{\parallel})_\zeta = A_\zeta - b_\zeta A_{\parallel}. \quad (38)$$

Then (36) and (37) combine to yield the expression

$$\Gamma = -\frac{c}{e\chi'} [\langle F_{\perp\zeta} \rangle - ((\nabla \cdot \mathbf{P}_{\text{CGL}})_{\perp\zeta}) + \langle b_\zeta \nabla_{\parallel} p_1 \rangle + e \langle nE_{\perp\zeta} \rangle], \quad (39)$$

which, although more complicated than (36), is better suited for interpretation. The same result can be derived from (6.34) for $n\mathbf{V}_\perp$; in this regard the identity

$$A_{\perp\zeta} = \frac{\chi'}{B} \nabla r \times \mathbf{b} \cdot \mathbf{A}, \quad (40)$$

essentially a generalization of (5.131) to asymmetric geometry, is helpful.

It is clear that an expression similar to (39) can be written down for the energy flux, $Q \equiv (\mathbf{Q} \cdot \nabla r)$, using (6.25); essentially one replaces \mathbf{F} by \mathbf{G} and \mathbf{P} by \mathbf{R} . Thus, although we use (39) for concreteness, most of the following comments apply to both the particle and energy fluxes.

Neoclassical Transport

The first term on the right-hand side of (39) is evidently the classical radial particle flux:

$$\Gamma_c \equiv \langle n V_c^r \rangle = -\frac{c}{e\chi'} \langle F_{\perp\zeta} \rangle. \quad (41)$$

It seems to have a distinctive inevitability: gyration, in the presence of pressure or temperature variation, always produces collisional friction, so that Γ_c cannot vanish everywhere in a confined, magnetized plasma. The other contributions to Γ might be expected to decay, either from collisional randomization (removing stress anisotropy), sound wave propagation (relaxing the parallel pressure gradient), or plasma conductivity (dissipating the electric field). Indeed it is precisely this expectation that accounts for the word “classical”: the other terms in (39) were rarely considered in early investigations of plasma transport.

But the classical expectation is incorrect. In a true confinement system, the other terms in (39) are not only invariably present, but they dominate the total particle flux, exceeding the classical term by one or two orders of magnitude. Furthermore, the relative unimportance of Γ_c pertains even when—perhaps especially when—the underlying dissipative mechanism is ordinary Coulomb scattering.

This surprising circumstance follows from a single fact: physical confinement systems are necessarily toroidal. Because of the associated magnetic field curvature, plasma relaxation in a torus is very different from the cylindrical case. At low collisionality, toroidicity drives stress anisotropy, while at higher collisionality, it drives pressure variation along the magnetic field. Such nonclassical perturbations dramatically enhance the radial flux of plasma and plasma energy.

When transport rates are calculated from the Coulomb operator, but with detailed regard for curvature effects, the resulting coefficients are called **neoclassical**. [The vast literature on neoclassical theory has become fully international; however the basic ideas of the theory were first established by Soviet scientists, especially A.A. Galeev and R.Z. Sagdeev (Galeev

and Sagdeev, 1968).] Accordingly we express (39) as

$$\Gamma = \Gamma_c + \Gamma_{nc}, \quad (42)$$

where

$$\Gamma_{nc} = \frac{c}{e\chi'} \left(((\nabla \cdot \mathbf{P}_{CGL})_{\perp\zeta}) - \langle b_\zeta \nabla_{\parallel} p_1 \rangle - e \langle n E_{\perp\zeta} \rangle \right), \quad (43)$$

is the neoclassical particle flux. Of course a similar decomposition applies to the energy flux.

The first term in (43), reflecting stress anisotropy, contributes to Γ when the collision frequency is sufficiently small. It is variously called the “neoclassical,” “banana” or “banana-plateau” flux. We call it the *anisotropy flux*, using the notation

$$\Gamma_a \equiv \frac{c}{e\chi'} \langle (\nabla \cdot \mathbf{P}_{CGL})_{\perp\zeta} \rangle, \quad (44)$$

for simplicity. But Γ_a is in fact linked with banana orbits: when particle motion is sufficiently collisionless, $\nu \ll \omega_t$, the distributions of trapped and untrapped particles can significantly differ. The resulting anisotropy, in concert with collisions, yields a net averaged outward flux, Γ_a .

The parallel pressure-gradient term matters in the complementary regime, $\nu \ll \omega_t$. In this case anisotropy has been randomized by collisions, but the relatively short parallel mean-free path allows first-order pressure variation on the flux surface. Indeed, toroidal effects, essentially related to return flow, require such variation; see §8.6. The resulting flux is denoted by

$$\Gamma_p \equiv \frac{c}{e\chi'} \langle b_\zeta \nabla_{\parallel} p_1 \rangle \quad (45)$$

where the subscript follows the convention of (6.112). In the literature Γ_p is commonly called the “collisional” or “Pfirsch-Schlüter” flux.

Finally the electric field contributes to Γ_{nc} the term

$$\Gamma_E \equiv -\frac{c}{\chi'} \langle n E_{\perp\zeta} \rangle, \quad (46)$$

which is nothing more than $\mathbf{E} \times \mathbf{B}$ drift. It is worth mentioning, however, because of its role in turbulent transport. Thus if E and n are allowed to fluctuate in time, then a suitable temporal or ensemble average of (46) yields the major contribution to turbulent transport, at least in the electrostatic limit. We return to this matter in Chapter 9.

8.3 Axisymmetric Geometry

Surface Flows

At this point we concentrate on transport in axisymmetric systems, both for pedagogical reasons and because of the dominant experimental role of

axisymmetric devices. Our main focus is the radial particle and energy fluxes; but comment on the faster motion occurring on each flux surface is appropriate first.

We noted in §6.3 that the first-order flows of particles and heat, artifacts of plasma magnetization, lack radial components and do not contribute directly to transport. They are flows *on* the flux surface, rather than across it. We have also noted that toroidal curvature gives the magnetization flows a divergence, thereby requiring return flows along the magnetic field. Thus, for example,

$$n\mathbf{V}_1 = n\mathbf{V}_{\parallel 1} + n\mathbf{V}_{\perp 1},$$

where the second term is given by (6); the first term is considered here.

The key observation is that the transport ordering requires

$$\begin{aligned} \nabla \cdot (n\mathbf{V}_1) &= 0, \\ \nabla \cdot \mathbf{q}_1 &= 0. \end{aligned} \quad (47)$$

Otherwise, plasma or plasma energy would accumulate locally on flux surfaces, contradicting the presumed first-order equilibrium. To determine the form of these surface flows, which indirectly effect second-order evolution, we recall the discussion of return current in §3.10. Because diamagnetism drives a perpendicular current, $\mathbf{J}_\perp = cb \times \nabla P/B$, while quasineutrality requires $\nabla \cdot \mathbf{J} = 0$, we find that in symmetry coordinates \mathbf{J} must have the form given by (3.112),

$$\mathbf{J} = -\frac{c}{4\pi} \frac{dI}{d\chi} \mathbf{B} - cR^2 \nabla \zeta \frac{dP}{d\chi}. \quad (48)$$

Precisely the same argument can be applied to the magnetization flows, which are similarly divergence-free and have similarly specified perpendicular components [(6) and (6.53)].

Thus we find that

$$n\mathbf{V}_1 = -\frac{c}{e\chi'} (p' + en\Phi') R^2 \nabla \zeta + K(r)\mathbf{B}, \quad (49)$$

$$\mathbf{q}_1 = -\frac{5}{2} \frac{c}{e\chi'} pT' R^2 \nabla \zeta + L(r)\mathbf{B}. \quad (50)$$

The flux labels K and L , analogous to $dI/d\chi$ in (48), are essentially integration constants, to be determined from kinetic analysis. The parallel components of (49) and (50) provide the return flows

$$nV_{\parallel 1} = -\frac{cI}{eB\chi'} (p' + en\Phi') + K(r)B, \quad (51)$$

$$q_{\parallel 1} = -\frac{5}{2} \frac{cI}{eB\chi'} pT' + L(r)B. \quad (52)$$

As in the J_{\parallel} case, we see that each parallel flow has terms proportional to B and to $1/B$. As long as B is not a flux label, these terms have distinct θ -dependence, and the return flows cannot vanish.

Axisymmetric Fluxes

We now consider the second order radial fluxes in axisymmetric geometry, specializing the results of the previous section. The present discussion, like (49)–(52), uses symmetry coordinates (r, θ, ζ) implicitly. Such formulae as (43) simplify in the axisymmetric case because

$$\langle (\nabla \cdot \mathbf{T}_{\text{CGL}})_{\zeta} \rangle = 0 \quad (\text{axisymmetry}), \quad (53)$$

where \mathbf{T}_{CGL} is any tensor having CGL form. Equation (53) is a corollary of the more general result,

$$\langle (\nabla \cdot \mathbf{T})_{\zeta} \rangle = \frac{1}{V'} \langle \mathcal{V}' \langle T_{\zeta}^r \rangle' \rangle \quad (\text{symmetry coordinates}), \quad (54)$$

for any tensor \mathbf{T} having indicial symmetry: $T_{\alpha\beta} = T_{\beta\alpha}$. On the right-hand side we use conventional tensor notation with

$$T_{\zeta}^r = g_{\zeta\zeta} T^{\zeta r} \equiv R^2 \nabla \zeta \cdot \mathbf{T} \cdot \nabla \mathbf{r}. \quad (55)$$

Note that (55) vanishes for an axisymmetric CGL tensor; thus (53) follows from (54).

To verify (54), we begin with a simple property of symmetry coordinates:

$$\nabla(R^2 \nabla \zeta) = R(\nabla R \nabla \zeta - \nabla \zeta \nabla R), \quad (56)$$

where the second term reflects changes in the direction of $\nabla \zeta$. Now $(\nabla \cdot \mathbf{T})_{\zeta} = R^2 \nabla \zeta \cdot \nabla \cdot \mathbf{T}$, so (56) implies

$$\langle (\nabla \cdot \mathbf{T})_{\zeta} \rangle = \nabla \cdot (R^2 \nabla \zeta \cdot \mathbf{T}) - R \mathbf{T} \cdot (\nabla R \nabla \zeta - \nabla \zeta \nabla R). \quad (57)$$

Here the second term vanishes, because \mathbf{T} is a symmetric tensor. Hence we have

$$\langle (\nabla \cdot \mathbf{T})_{\zeta} \rangle = \langle \nabla \cdot (R^2 \nabla \zeta \cdot \mathbf{T}) \rangle. \quad (58)$$

The desired result, (54), follows immediately from (3.40).

As a point of minor interest, we note that our proof of (54) uses several properties of symmetry coordinates but only the *indicial symmetry* of \mathbf{T} , so it holds in general. However the corollary (53) does require axisymmetry: $\nabla \zeta \cdot \mathbf{T}_{\text{CGL}} \cdot \nabla \mathbf{r}$, where \mathbf{r} and ζ are symmetry coordinates, vanishes in general only when the stress is axisymmetric.

The axisymmetric version of (36) has become

$$\Gamma = -\frac{c}{e \chi'} [\langle F_{\zeta} \rangle + e \langle n E_{\zeta} \rangle], \quad (59)$$

with a simple interpretation: in the absence of collisions, plasma moves inwards at the rate

$$\Gamma(\nu = 0) = -\frac{c}{\chi'} \langle n E_\zeta \rangle = \langle n V_f \rangle , \quad (60)$$

where \mathbf{V}_f is the velocity of the poloidal flux surface, as in (3.127). For this reason the first, collisional term in (59) is sometimes called the *relative flux*—the plasma motion in the frame of the moving surface. Equivalently, note that when $E_{\parallel} = 0$ —and indeed E_{\parallel} should vanish in the collisionless case—(60) gives simply the $\mathbf{E} \times \mathbf{B}$ drift. Collisions decouple the plasma from the moving surface, as indicated by the first term in (59); they also allow a finite E_{\parallel} , making the response to E_ζ more complicated than any $\mathbf{E} \times \mathbf{B}$ drift.

The corresponding energy flux is

$$Q = -\frac{c}{e\chi'} \left[\langle m G_\zeta \rangle + \frac{5}{2} e \langle p E_\zeta \rangle \right] , \quad (61)$$

with a similar interpretation. A consequence of (61) is that Q_i is large,

$$Q_i \sim \left(\frac{m_i}{m_e} \right)^{1/2} Q_e \sim \left(\frac{m_i}{m_e} \right)^{1/2} T \Gamma , \quad (62)$$

just as in the classical case, (20). Note that Q , unlike Q_c , depends on more kinetic information than the \tilde{f} provided by (1), so verification of (62) awaits the kinetic treatment of §8.6 [see, for example, (188)]. But it is important enough to emphasize here: neoclassical theory predicts the dominant transport process to be ion thermal conduction. Unfortunately experimental tokamak plasmas do not respect (62): while experimental ion energy fluxes are often comparable to the neoclassical predictions, anomalous electron fluxes violate the mass-ratio ordering.

We have defined Γ in terms of the averaged, radial fluid velocity. However, since $\langle \nabla \times \mathbf{M} \cdot \nabla \mathbf{r} \rangle \equiv 0$, magnetization cannot contribute to Γ [recall (4.152)] and we could as well write it in terms of the guiding center velocity

$$\Gamma = \left\langle \int d^3 v \bar{f} v_D^r \right\rangle . \quad (63)$$

While this form lacks the explicit factor of δ represented by (c/e) in (59), it carries an implicit factor of δ , since $v_D^r = \mathcal{O}(\delta)$. Hence, as in other formulations, only the $\mathcal{O}(\delta)$ distribution is needed for second-order accuracy. The deficiency of (63) is its lack of an implicit collision-frequency factor, as is contained in the friction force of (59). The point is that to compute any flux proportional to ν , (41) would require finding the distribution through first order in n , a formidable task when ν/Ω_t is small. Hence (59), which like (4) requires the distribution only to the zeroth-order in ν , provides a major short-cut at low collisionality. Yet we will find that (63) has application in certain ranges of collisionality.

Comparison to Classical Flux

After decomposing the friction force into parallel and perpendicular components, we can use (41) and (42) to express (59) as

$$\Gamma_{nc} = -\frac{c}{e\chi'} [\langle F_{\parallel\zeta} \rangle + e \langle nE_\zeta \rangle] . \quad (64)$$

Thus neoclassical transport in an axisymmetric system results from toroidal electric fields and parallel friction. Similarly

$$q_{nc} = Q_{nc} - \frac{5}{2} p\Gamma = q_c - \frac{c}{e\chi'} \langle mG_{\parallel\zeta} \rangle , \quad (65)$$

We temporarily ignore E_ζ to note the suggestive relation

$$\Gamma_c \propto \langle F_{\perp\zeta} \rangle , \quad \Gamma_{nc} \propto \langle F_{\parallel\zeta} \rangle .$$

We have seen that F_\perp results from gyromotion; since $v_{gc} = v_\parallel + \mathcal{O}(\delta)$ it is clear that F_\parallel accordingly reflects guiding-center motion. The physical analogy is therefore

$$\Gamma_c \propto (\text{friction resulting from gyromotion}) ,$$

$$\Gamma_{nc} \propto (\text{friction resulting from guiding-center motion}) . \quad (66)$$

The corresponding kinetic-theoretical statement is

$$\Gamma_c \propto (\text{friction associated with } \tilde{f}) ,$$

$$\Gamma_{nc} \propto (\text{friction associated with } \bar{f}) . \quad (67)$$

Hence calculation of the neoclassical flux depends upon solution to the drift-kinetic equation. The crux of any such calculation is finding the guiding-center counterpart to (1).

The parallel between Γ_c and Γ_{nc} is accurate, even in asymmetric devices, and helpful in understanding neoclassical physics. However, (66) also reveals an important distinction between the two forms of transport. For, while the excursion of a Larmor orbit is necessarily small in a magnetized plasma, guiding-center orbits can traverse macroscopic regions of the plasma volume. As a result, local fluid variables are not generally adequate to describe a low-collisionality plasma.

On the other hand, transport closure is *radially* local. Because of the limited radial extent of guiding center motion, guaranteed by (5.127) and

$$\mathbf{v}_{gc} \cdot \nabla r = \mathcal{O}(\delta) ,$$

and because the basic fluid variables are flux labels in the quiescent state, the *flux-surface averaged* conservation laws provide a closed, local, fluid description.

The neoclassical particle flux resembles its classical counterpart in being intrinsically ambipolar,

$$\sum_s e_s \Gamma_{nec} = 0 , \quad (68)$$

and for the same reason: collisional momentum conservation (Rutherford, 1970). On the other hand the neoclassical flux, unlike Γ_e , is influenced by like-species collisions: while the friction force in (64) is necessarily that between unlike species, the guiding-center distribution function, rather more complicated than (1), is determined by both types of scattering.

A similar comment pertains to the dependence of Γ_{ne} on the electric field. In the classical case, \mathbf{E} entered only through the $\mathbf{E} \times \mathbf{B}$ drift, and Galilean invariance prohibited any effect on the flux. But the gyro-averaged distribution responds to $E_{||}$, and that response is not a simple Maxwellian displacement. Hence Γ_{ne} and Q_{ne} have terms proportional to (an appropriate average of) $E_{||}$.

Energy Exchange*

We consider next the energy exchange terms on the right-hand side of (27):

$$X_s \equiv W_s + \mathbf{V}_s \cdot (\mathbf{F}_s + e_s \mathbf{n}, \mathbf{E}) . \quad (69)$$

Here of course the terms involving W and \mathbf{F} measure collisional energy exchange between plasma species, while the term involving \mathbf{E} can be considered an exchange of energy between plasma and the electromagnetic field. For simplicity we restrict attention to the single ion-species case, assuming unit ionic charge. Our first observation is that W_s , defined by (5.26), is most easily computed for ions. The reason is that

$$W_i = W_{ie} \cong W_{ie}^L$$

is easily found from C_{ie} and the Maxwellian part of f_i ; recall (5.68). Omitting mass-ratio corrections we have

$$W_i = 3 \frac{m_e}{m_i} n \frac{T_i - T_e}{\tau_{ei}} . \quad (70)$$

In the case of W_{ei} , on the other hand, the friction correction of (5.27) is not negligible, because of the relatively large electron parallel flow associated with Ohmic heating. Hence W_{ei} is most easily computed from collisional energy conservation, (5.28): $W_{ei} = -W_i + (\mathbf{V}_i - \mathbf{V}_e) \cdot \mathbf{F}_e$. In other words we use

$$X_e = -X_i + \mathbf{J} \cdot \mathbf{E} . \quad (71)$$

Consider next

$$\langle \mathbf{V}_i \cdot (\mathbf{F}_i + en\mathbf{E}) \rangle = \langle \mathbf{V}_{i1} \cdot (\mathbf{F}_i + en\mathbf{E}) + \mathbf{V}_{i2} \cdot [-en\nabla\Phi(r)] \rangle$$

where the subscripts indicate the δ -ordering as usual. For the first order velocity we have (49), which yields

$$\langle \mathbf{V}_{i1} \cdot (\mathbf{F}_i + en\mathbf{E}) \rangle_1 = -\frac{c}{en\chi'}(p'_i + en\Phi') \langle F_{i\zeta} + enE_\zeta \rangle + K \langle \mathbf{B} \cdot (\mathbf{F}_i + en\mathbf{E}) \rangle ,$$

or, in view of (59),

$$\langle \mathbf{V}_{i1} \cdot (\mathbf{F}_i + en\mathbf{E}) \rangle_1 = (p'_i/n + e\Phi')\Gamma + K \langle \mathbf{B} \cdot (\mathbf{F}_i + en\mathbf{E}) \rangle .$$

Then, since $\langle \mathbf{V}_{i2} \cdot [-en\nabla\Phi(r)] \rangle = -e\Gamma\Phi'$, the radial potential-gradient terms precisely cancel:

$$\langle \mathbf{V}_i \cdot (\mathbf{F}_i + en\mathbf{E}) \rangle = \frac{p'_i\Gamma}{n} + K \langle B(F_{\parallel i} + enE_{\parallel i}) \rangle .$$

Similar manipulation, using (48) for \mathbf{J} , yields

$$\langle \mathbf{J} \cdot \mathbf{E} \rangle = -\frac{c}{4\pi\chi'} I' \langle E_{\parallel} B \rangle - \frac{c}{\chi'} p' \langle E_\zeta \rangle . \quad (72)$$

In summary we have found the energy exchange terms

$$\langle X_i \rangle = 3 \frac{m_e}{m_i} n \frac{T_i - T_e}{\tau_{ei}} + \frac{p'_i\Gamma}{n} + K \langle B(F_{\parallel i} + enE_{\parallel i}) \rangle , \quad (73)$$

$$\langle X_e \rangle = -\langle X_i \rangle - \langle \mathbf{J} \cdot \mathbf{E} \rangle . \quad (74)$$

The radial electric field is absent from these expressions because the energy loss associated with expansion through the potential, $-e\Gamma\Phi'$, is restored by $\mathbf{E} \times \mathbf{B}$ toroidal rotation through the force $\mathbf{F} + en\mathbf{E}$. This curious balance, peculiar to axisymmetric geometry, is significant. Together with the Galilean invariance, discussed in §8.1, it implies that Φ' appears nowhere in the averaged particle and energy conservation laws.

Observe that the exchange terms introduce an additional variable: the function $K(r)$. Hence K , along with the radial fluxes, must be computed from kinetic theory.

8.4 Entropy Production*

Fluid Entropy Source

In §5.3 we studied the rate of change of plasma (species-specific) entropy density

$$S = - \int d^3v f \ln f ,$$

using kinetic theory. Here we consider its fluid description. Our main purpose is to identify the thermodynamic forces and fluxes appropriate to confined plasma transport.

The lowest order entropy is computed from f_M ; one finds

$$S[f_M] \equiv S_0 = n \ln(T^{3/2}/n). \quad (75)$$

Here a term proportional to n , ill-defined without quantum mechanical considerations, has been ignored; it is ultimately irrelevant because of particle conservation. The rate of change

$$\frac{\partial S_0}{\partial t} = \frac{1}{T} \frac{3}{2} \frac{\partial p}{\partial t} - \frac{5}{2} \frac{\partial n}{\partial t} + S_0 \frac{\partial \ln n}{\partial t}$$

is computed from the even moment equations, (6.22) and (6.23). In the transport ordering it is consistent to neglect terms of higher than second order in δ ; thus we find

$$\frac{\partial S_0}{\partial t} + \nabla \cdot \left[\frac{1}{T} \mathbf{q} + S_0 \mathbf{V} \right] = \Theta, \quad (76)$$

where

$$\Theta_s = -\frac{1}{T_s} \mathbf{q}_s \cdot \nabla \ln T_s - n_s \mathbf{V}_s \cdot \nabla \ln p_s + \frac{1}{T_s} (W_s + \mathbf{V}_s \cdot \mathbf{F}_s) + \frac{e_s n_s}{T_s} \mathbf{V}_s \cdot \mathbf{E}. \quad (77)$$

The second law of thermodynamics makes it natural to interpret $(1/T)\mathbf{q} + S_0 \mathbf{V}$ as the entropy *flux*; hence, recalling the discussion of §6.2, we see that Θ measures the local rate at which entropy is created. In other words it is the entropy source, introduced in §5.3.

Equation (77) is easily interpreted. Entropy is created as heat flows down the temperature gradient, in the first term, and as particles flow down the pressure gradient, in the second. The third term, involving $W + \mathbf{V} \cdot \mathbf{E}$, reflects entropy increase due to heat exchange between species, while the last term measures the entropy produced when work is done by the electromagnetic field.

Transport Matrix

We next review, very briefly, some conventional transport formalism. A set of thermodynamic forces, \mathcal{A}_i , and fluxes, \mathcal{J}_i , are called “canonical” if they satisfy

$$\Theta = - \sum_{i=1}^N \mathcal{A}_i \cdot \mathcal{J}_i. \quad (78)$$

For example, for the classical electron entropy production of (9),

$$\Theta_e = -\mathbf{n} \mathbf{V} \cdot \nabla \ln p - \frac{\mathbf{q}}{T} \cdot \nabla \ln T,$$

one could choose

$$\mathcal{J}_1 = \mathbf{n}\mathbf{V}, \quad \mathcal{J}_2 = \mathbf{q}/T;$$

$$\mathcal{A}_1 = \nabla \ln p, \quad \mathcal{A}_2 = \nabla \ln T.$$

It is clear that the canonical property is preserved under various linear rearrangements, such as orthogonal transformations,

$$\mathbf{X}_i \rightarrow \mathbf{X}'_i = - \sum_{k=1}^N \mathbf{R}_{ik} \cdot \mathbf{X}_k, \quad (\mathbf{R}^{-1})_{ij} = \mathbf{R}_{ji} \quad (79)$$

as well as interchanges, $\mathcal{A}_i \leftrightarrow \mathcal{J}_i$. There are an infinity of canonical choices for the fluxes and forces.

The index labelling is physically motivated: one pairs each flux with its “canonically conjugate” force, chosen to make each term in (78) negative-definite in a dissipative system. For example, \mathcal{J}_1 is conjugate to \mathcal{A}_1 —particle flux is the natural response to a pressure gradient—in the sense of (8).

In linear transport theory each flux can be expressed as a linear combination of the forces:

$$\mathcal{J}_i = \sum_j L_{ij} \mathcal{A}_j. \quad (80)$$

The coefficients L_{ij} are the transport coefficients; one sometimes speaks of the *transport matrix*, with elements L_{ij} . Diagonal coefficients link each flux to its conjugate force, while off-diagonal coefficients allow for more subtle types of dissipation. Onsager showed that the off-diagonal coefficients are constrained by

$$L_{ij}(\mathbf{B}) = \pm L_{ji}(-\mathbf{B}) \quad (81)$$

whenever the underlying dissipative mechanism is symmetric under time reversal; the sign depends upon the symmetries of the corresponding force and flux with respect to reversal of \mathbf{v} . Notice that the *Onsager symmetry*, (81), is preserved by orthogonal transformations, (79); in fact it will be obeyed by any canonical choice of forces and fluxes. It is exemplified classically by (7) and (22): $L_{12} = L_{21} = 3n/(2m_e \Omega_e^2 \tau_{ei})$.

Onsager symmetry can be a useful calculational tool. However, any transport matrix computed from a collision operator that is self-adjoint, in the sense of (5.120), will automatically display Onsager symmetry (see Exercise 8.7). Hence (81), while useful as a check, plays no crucial role in the calculation of collisional transport coefficients.

Axisymmetric Forces

For present purposes we can consider a quantity somewhat simpler than Θ : the total heat production rate,

$$H \equiv \sum_s T_s \Theta_s . \quad (82)$$

Here the sum annihilates heat exchange between species, because of collisional energy conservation, (5.28). There remains

$$H = - \sum_s (\mathbf{q}_s \cdot \nabla \ln T_s + p_s \mathbf{V}_s \cdot \nabla \ln p_s) + \mathbf{J} \cdot \mathbf{E} . \quad (83)$$

Since transport closure involves only surface-averaged flows, the appropriate forces are obtained by averaging (83):

$$\langle H \rangle = - \sum_s T_s [q_s (\ln T_s)' + \Gamma_s (\ln p_s)'] + \langle \mathbf{J} \cdot \mathbf{E} \rangle , \quad (84)$$

where the last term is given by (72), and, as usual,

$$q_s = Q_s - \frac{5}{2} T_s \Gamma . \quad (85)$$

Notice that (72) includes a flux-surface motion term that precisely cancels the corresponding term in Γ , (59), leaving only the relative flux

$$\Gamma_{\text{rel}} \equiv - \frac{e}{e\chi'} \langle F_\zeta \rangle \quad (86)$$

in (84). We have then

$$\langle H \rangle = - \sum_s T_s \left\{ \frac{q_s}{T_s} (\ln T_s)' + \Gamma_{\text{rels}} (\ln p_s)' \right\} - \frac{c}{4\pi\chi'} I' \langle E_{\parallel} B \rangle . \quad (87)$$

This result holds for any number of ion species. It indicates that a suitable choice of thermodynamic forces is given by

$$\mathcal{A}_{1s} = (\ln p_s)', \quad \mathcal{A}_{2s} = (\ln T_s)', \quad \mathcal{A}_3 = \frac{c}{4\pi\chi'} I' \quad (88)$$

with corresponding fluxes

$$\mathcal{J}_{1s} = \Gamma_{\text{rels}}, \quad \mathcal{J}_{2s} = \frac{q_s}{T_s}, \quad \mathcal{J}_3 = \frac{\langle E_{\parallel} B \rangle}{T_s} . \quad (89)$$

Some of the neoclassical calculations in the literature have used differing sets of forces and fluxes, including noncanonical sets. (Indeed, beyond making Onsager symmetry manifest, canonical forces and fluxes have

no deep advantage.) While the various choices are essentially linear combinations of those in (88) and (89), two technical departures are worth mentioning.

The most important differences stem from the large mass ratio, which dictates separate consideration of Θ_i and Θ_e . Thus one usually studies (77) instead of (87); then K , describing first-order flow along \mathbf{B} , enters through (73) and (77), and the corresponding forces have a more complicated appearance. But they are linear combinations of the choices in (88) and (89). The point is that kinetic arguments, to be discussed presently, show that K can be expressed in terms of \mathcal{A}_2 and \mathcal{J}_3 :

$$K_s(r) = a_s \mathcal{A}_{2s} + b_s \mathcal{J}_3 . \quad (90)$$

Common choices of the electromagnetic terms, \mathcal{A}_3 and \mathcal{J}_3 , also depart from (88) and (89). For example, $\langle E_{\parallel} B \rangle$ is often interpreted as a force, rather than as a flux; the corresponding flux can be chosen to be the parallel current. In view of (48), such differences are merely formal: one can always eliminate I' in terms of J_{\parallel} , for example, using (3.114):

$$\langle J_{\parallel} B \rangle = -\mathcal{A}_3 \langle B^2 \rangle - \frac{cI}{\chi'} \sum_s p_s \mathcal{A}_{1s} . \quad (91)$$

What is more than formal—what is invariant under the various arrangements—is the particular average of E_{\parallel} that appears. Note that $\langle E_{\parallel} B \rangle$ does not correspond to an averaged $\mathbf{E} \times \mathbf{B}$ drift; indeed (38) and (46) show that the latter,

$$-\frac{c}{\chi'} \langle E_{\perp\zeta} \rangle = -\frac{c}{\chi'} \langle E_{\zeta} - b_{\zeta} E_{\parallel} \rangle = -\frac{c}{\chi'} \left\langle E_{\zeta} - I(r) \frac{E_{\parallel}}{B} \right\rangle ,$$

involves a quite different average of E_{\parallel} . Instead $\langle E_{\parallel} B \rangle$ measures the Poynting flux—the flux of electromagnetic energy—relative to the moving poloidal flux surface. This distinction is especially significant because parallel variation of the electrostatic field would contribute to $\langle E_{\perp\zeta} \rangle$ but never to $\langle E_{\parallel} B \rangle$: the definition of the average insures that $\langle \mathbf{B} \cdot \nabla \Phi \rangle = 0$. Hence \mathcal{J}_3 is exclusively electromagnetic.

8.5 Tokamak Transport: Basic Features

Random Walk Estimates

Radial transport in a torus exceeds that in an otherwise similar cylindrical system in so far as the poloidal magnetic field is relatively small:

$$\frac{B_P}{B_T} \ll 1 . \quad (92)$$

In typical confinement devices $B_P/B_T \cong r/(Rq)$ is close to 10^{-1} ; of course it is much smaller close to the magnetic axis. Indeed, the neoclassical enhancement factor at low collisionality—the most interesting and realistic case—is roughly $(B_T/B_P)^2$, corresponding to about two orders of magnitude in a typical tokamak.² On the other hand the complications of neoclassical transport hardly matter in a reversed-field pinch, where $B_P \gtrsim B_T$. Tokamak transport is neoclassically enhanced because the radial excursion of guiding centers, Δr , responds primarily to the poloidal field. We shall find that

$$\Delta r \sim \rho_P , \quad (93)$$

where $\rho_P \equiv (B/B_P)\rho$ is the *poloidal gyroradius*—the gyroradius a charged particle would have if it saw only the poloidal field. If collisions are so infrequent that the collisionless guiding-center orbits are actually traversed, that is, if

$$\nu \ll \omega_t , \quad (94)$$

then the random walk formula, (17), implies

$$D_{nc} \sim \nu \rho_P^2 , \quad (95)$$

in close analogy to the classical case, (11). Indeed, (11) and (95) neatly manifest the relation given in (66). Recall in particular that (11) requires, in parallel with (94), $\nu \ll \Omega$: that the *gyromotion* is collisionless.

The version of (95) usually given in the literature

$$D_{nc} \sim \left(\frac{r}{R}\right)^{1/2} \nu \rho_P^2 , \quad (96)$$

does not quantitatively differ, since the aspect ratio rarely exceeds 5. (The difference might seem important close to the magnetic axis, but we will find that neither formula applies at very small r .) However the distinction between (95) and (96) is qualitatively instructive, so we next derive the latter. Our argument makes frequent reference to the discussion in §4.4.

The radial excursion in a tokamak depends upon ρ_P rather than ρ because the time required to traverse a collisionless orbit is proportional to B/B_P , as shown by (4.136) and (4.137). To see this more simply, consider the canonical momentum conservation law,

$$\frac{dp_\zeta}{dt} = 0 \quad (97)$$

where

$$p_\zeta = mv_\zeta + \frac{e}{c} A_\zeta$$

² Strictly speaking, the smallness of B_P/B_T depends upon large aspect ratio, since $q \sim 1$. However B_P/B_T is a more reliable small parameter than r/R .

is the invariant angular momentum corresponding to axisymmetry. For guiding-center motion we have

$$v_\zeta \cong v_{\parallel\zeta} = \frac{I}{B} u$$

in the notation of Chapter 4. Furthermore, according to (3.124),

$$A_\zeta = -\chi .$$

Hence the guiding-center radial excursion, given by $\Delta p_\zeta = 0$, satisfies $mI\Delta(u/B) = (e/c)\chi'\Delta r$, or

$$\Delta r = \frac{mc}{e\chi'} I \Delta \left(\frac{u}{B} \right) \cong \frac{B_T}{\Omega_P} \Delta \left(\frac{u}{B} \right) , \quad (98)$$

where $\Omega_P \equiv eB_P/mc$ is the poloidal gyrofrequency. Here the quantity I is treated as constant because it is a flux label.

Equation (93) verifies the appearance of ρ_P in Δr , but to derive (96) a more explicit form is needed. For small r/R , Δu is estimated from (4.121):

$$|\Delta u| \cong \left| \frac{\partial u}{\partial B} \Delta B \right| \cong (2w)^{1/2} \frac{\lambda}{u} \Delta B \cong \frac{v}{u} \Delta B$$

while ΔB is found from (3.104):

$$\Delta B \cong \frac{r}{R} B . \quad (99)$$

The interesting feature is that, for large aspect ratio, the streaming speed is relatively small in the trapped region. That is, while

$$\left(\frac{u}{v} \right)_{\text{passing}} \sim 1 , \quad (100)$$

the trapped and nearly trapped particles have

$$\left(\frac{u}{v} \right)_{\text{trapped}} \sim \left(\frac{r}{R} \right)^{1/2} . \quad (101)$$

(The fact that u becomes very small for boundary-layer particles near their turning points is not relevant here.) Hence the largest excursion is that executed by trapped and nearly trapped particles; it is given by the *banana width* of a trapped particle,

$$\Delta r_b \sim \left(\frac{r}{R} \right)^{1/2} \rho_P . \quad (102)$$

The passing particle excursion is smaller by $(r/R)^{1/2}$.

For simplicity, the following qualitative arguments exploit this difference by neglecting the passing particle excursion altogether. Collisionless

Passing particle orbits are imagined to remain tied to a single flux surface, so that diffusion results from the random walk of trapped particles from one banana orbit to another. In this extreme limit of large aspect ratio—a hula-hoop tokamak—two additional aspect-ratio factors contribute to D_{nc} . Both are related to the phase-space volume of the trapped region. First, if only trapped particles contribute to neoclassical diffusion, the random walk formula must be multiplied by the fraction of such particles, \mathcal{F} , in the total population. Since the distribution is nearly Maxwellian, and since the width in $\xi = u/v$ of the trapped region is of order $(r/R)^{1/2}$,

$$\mathcal{F} \sim \left(\frac{r}{R}\right)^{1/2}. \quad (103)$$

The second factor is more interesting. Recall that in the classical case a large-angle scattering event is required to move a gyrating particle from one Larmor orbit to a new, uncorrelated gyration center. Thus the “effective” collision frequency—the frequency pertinent to (17)—for classical transport is the classical frequency, ν_c . In the neoclassical case the effective step is that from one banana to another; since the trapped region of phase space occupies only a narrow region of pitch angle,

$$\Delta\Theta \leq \left(\frac{r}{R}\right)^{1/2}$$

correspondingly weaker collisions become effective. [Here Θ is the pitch angle of (4.120), not to be confused with entropy production.] By considering the collisional random walk of a guiding center in pitch-angle space, we see that the effective collision frequency for scattering by $\Delta\Theta$ is

$$\nu_{\text{eff}} \sim \frac{\nu_c}{(\Delta\Theta)^2}, \quad (104)$$

since $\Delta\Theta$ is expected to grow with $t^{1/2}$. Hence

$$\nu_{\text{eff}} \sim \frac{R}{r} \nu_c.$$

These estimates combine to yield the banana diffusion estimate

$$D_b \sim \mathcal{F} \nu_{\text{eff}} (\Delta r_b)^2 \sim \left(\frac{r}{R}\right)^{1/2} \rho_P^2 \quad (105)$$

as in (96).

Notice that the collisionality condition, (94) is also modified at large aspect ratio: we must require that many banana orbits are executed between effective collisions. Since the trapped-particle bounce frequency $\omega_b = 1/n$ is of order $(r/R)^{1/2} \omega_t$, the requirement $\omega_b \gg \nu_{\text{eff}}$ becomes

$$\frac{\nu_c}{\omega_t} \ll \left(\frac{r}{R}\right)^{3/2} \quad (\text{banana regime}). \quad (106)$$

After noting that collision-dominated transport occurs only if

$$\nu_c \gg \omega_t \quad (\text{collision dominated regime}), \quad (107)$$

we see that at large aspect ratio there is an intermediate collision-frequency regime, where

$$1 \gg \frac{\nu_c}{\omega_t} \gg \left(\frac{r}{R}\right)^{3/2} \quad (\text{intermediate regime}) . \quad (108)$$

It is not hard to construct random walk estimates for diffusion in the collision-dominated and intermediate regimes. However, the existence and significance of the various regimes is best appreciated in the context of the drift-kinetic equation, to be considered presently. Here we are content with two remarks concerning the intermediate regime:

1. Diffusion in the intermediate regime turns out to be independent of ν . As a result, it is often called the *plateau regime*—language that we will use.

2. For realistic aspect ratios, the plateau regime is obviously narrow. Indeed it is clear that neither inequality in (108) can be satisfied very strongly, and that even a plasma whose thermal speed satisfies (108) will contain many particles whose speeds and collision frequencies contradict it. Indeed, plateau calculations that take into account correction terms or thermal broadening show that D is never really independent of ν .

Yet the plateau ordering is often pertinent, at least roughly. There is a parameter range in which the collisionality dependence of D becomes relatively weak, and even a banana-regime tokamak must include, close to its magnetic axis, a region in which (108) is satisfied. (Every fat tokamak contains a thin one!) For this reason, because qualitative features matter more than quantitative accuracy, and because the plateau analysis is outstandingly simple, we briefly consider plateau kinetic theory below. We conclude the present discussion by comparing the orbit description of transport to the fluid result, (59). Returning to angular momentum conservation, (97), we now take into account the time dependence of $A_\zeta = -X$. According to (3.125),

$$\frac{dA_\zeta}{dt} = -cE_\zeta - \chi' v^r ;$$

hence (97), with $\mathbf{v} \cong \mathbf{b}u$ as usual, implies

$$v^r = \frac{mc}{e\chi'} \mathbf{u} \cdot \nabla \frac{I\mathbf{u}}{B} - \frac{c}{\chi'} E_\zeta . \quad (109)$$

Here the first term may be recognized from (5.132): it is the familiar axisymmetric guiding center drift. The second term, measuring the velocity of a poloidal flux surface, is familiar from (3.128). Recall from Chapter 3 that the transport ordering makes flux surface motion a second order effect,

occurring on the same time scale as diffusion. Therefore, for consistency, we should include along with E_ζ the toroidal friction force, which contributes in the same order:

$$E_\zeta \rightarrow E_\zeta + \frac{F_\zeta}{en}, \quad (110)$$

as in (3). Of course this prescription, while plausible, is not rigorous: friction is not the only collisional process, and collisions are not the only second order process omitted from (109).

Nonetheless using (110), we obtain the radial drift

$$v^r = \frac{mc}{e\chi'} \mathbf{ub} \cdot \nabla \frac{Iu}{B} - \frac{c}{\chi'} E_\zeta - \frac{c}{en\chi'} F_\zeta. \quad (111)$$

At this point an orbital average, (4.138), annihilates the first term and provides an expression

$$\langle v^r \rangle_o = -\frac{c}{\chi'} \left\langle E_\zeta + \frac{F_\zeta}{en} \right\rangle_o, \quad (112)$$

obviously similar to (59). The annihilation of the first term under the orbital average, noted previously in (5.127), manifests equilibrium confinement: collisionless orbits do not escape the confinement region.

The orbital expression (112) cannot replace (59); aside from questions of rigor, one cannot compute fluxes without knowledge of the distribution functions. It is nonetheless instructive to view the electric and friction forces from the single-particle viewpoint. Note in particular that the frictional and electric terms in (112) must nearly balance, to avoid uncontrolled parallel acceleration of passing electrons to E_ζ is small. But the frictional balance is quite different for trapped particles: as their parallel motion is reversed, they experience the friction force in alternatively opposing directions, while subject to a relatively constant electromagnetic force. Thus the trapped particles respond primarily to the first term of (112), drifting inward at roughly the flux-surface velocity V_f [recall (3.128)]. This *trapped particle pinch effect* was discovered independently by Ware (Ware, 1970) and Galeev (Galeev, 1971); we denote it by Γ_{WG} .

In the banana regime, where our heuristic argument is most nearly valid, Γ_{WG} is estimated by nV_f times $(r/R)^{1/2}$, the fraction of trapped particles:

$$\Gamma_{WG} \sim \left(\frac{r}{R}\right)^{1/2} nc \frac{E_T}{B_P}. \quad (113)$$

(Of course the rigorous result involves E_T through the force $\langle E_{||} B \rangle$.) The trapped particle pinch is relatively weak in other collisionality regimes.

The transport process adjoint to Γ_{WG} , in the Onsager sense of (81), can be expressed as parallel plasma current driven by pressure gradients — the so-called *bootstrap current*. We survey the various neoclassical transport

processes in §8.6; a more detailed survey may be found in, for example, (Hinton and Hazeltine, 1976).

Drift Kinetic Theory at Large Aspect Ratio

In Chapter 5 we studied the first order ion drift-kinetic equation,

$$u \nabla_{\parallel} f_{i1} - C_{i1}(f_{i1}) = -\mathbf{v}_{iD} \cdot \nabla f_{iM}. \quad (114)$$

Here f_{i1} is the $\mathcal{O}(\delta)$ -correction to the ion Maxwellian $f_{i0} = f_{iM}$, C_{i1} is the linearized Coulomb collision operator, $u = v_{\parallel}$ and v_D is the first order drift velocity, whose radial component is given by the first term of (109):

$$v'_{iD} = \frac{I}{\chi'} u \nabla_{\parallel} \frac{u}{\Omega_i}. \quad (115)$$

The gradients are performed at fixed λ (pitch-angle variable) and U (energy). The present discussion, a continuation of the argument of §5.3, imposes the main ideas of neoclassical kinetic theory. Thus we outline the calculation of the guiding-center distribution f_1 , whose importance was emphasized in §8.3.

We first comment on a technical difference between (114) and the corresponding electron equation. Here it is convenient to use λ and $w = U - e\Phi$ as variables, so the basic drift-kinetic equation is (4.72); (115) remains valid because $\nabla_{\parallel}\Phi$ is higher order in δ . The point is that the source term on the right-hand side of (114) is proportional to ρ_i (*i.e.*, δ_i) and therefore large compared to the electric acceleration term:

$$\mathbf{v}_{iD} \cdot \nabla f_{iM} \gg \frac{e}{T_i} \mathbf{v}_{\parallel} \cdot \mathbf{E}_{f_{iM}}. \quad (116)$$

Because $\delta_e \ll \delta_i$ the corresponding inequality with electron parameters is not valid: electromagnetic acceleration competes with equilibrium drifts in fixing the first order electron response. In other words the electron counterpart to (114) is

$$u \nabla_{\parallel} f_{e1} - C_{e1}(f_{e1}) = -v_{eD} \cdot \nabla|_U f_{eM} - \frac{e}{T_e} u E_{\parallel} f_{eM}. \quad (117)$$

Though the last term in (117) does not introduce serious complication, we simplify the present discussion by focusing on the ion equation, (114).

In §5.3 we noted that (114) has a simple and exact solution whenever the temperature gradient vanishes. Unfortunately plasma temperatures must vary over the radius of any confinement system, so a deeper analysis is required. More unfortunately, such analysis is difficult. Equation (114) represents a competition between parallel streaming and Coulomb collisions with intricate consequences—especially in toroidal geometry, where

mirror forces make \mathbf{u} a function of position. Its solution is understood only for large aspect ratio, and only from separate calculations performed in the different collisionality regimes of (106)–(108). Our present purpose is to clarify the basic, physical point of such calculations, without exploring neoclassical theoretical technology in detail. Indeed, the argument summarized here is pertinent to a variety of kinetic issues involving non-uniform magnetic fields, including questions unrelated to neoclassical transport.

It is helpful to begin by changing velocity variables, from w and λ , to v and $\xi \equiv u/v$ (recall Table 4.1). We write

$$f_{11}(\mathbf{x}, \lambda, w) = F(\mathbf{x}, \xi, v)$$

and compute $\nabla f = \nabla|_{\xi, v} F + \frac{\partial F}{\partial \xi} \nabla|_{\lambda, w} \xi$, where

$$\nabla|_{\lambda, w} \xi = -\frac{1 - \xi^2}{\xi} \frac{\nabla B}{2B}.$$

The resulting first order equation is

$$\xi v \nabla_{\parallel} F - \frac{\nabla_{\parallel} B}{2B} v (1 - \xi^2) \frac{\partial F}{\partial \xi} - C_1(F) = Q, \quad (118)$$

where $Q = -\mathbf{v}_{iD} \cdot \nabla|_U f_{1M}$ represents the source. With its extra differential term acting on F , representing the mirror force, (118) appears to be a step backwards from (114)—as it is in some cases. Note however, that we have drastically simplified the coefficient of the streaming term:

$$\pm \left\{ \frac{2}{m} [w - \mu B(\mathbf{x})] \right\}^{1/2} \rightarrow \xi v. \quad (119)$$

If its first term were uniformly dominant, (118) would be an advance.

The three terms on the left-hand side of (118) are readily compared; they stand in the ratio $\omega_t : (r/R)\omega_t : \nu$. When collisions dominate, $\nu/\omega_t \gg 1$, (118) is amenable to a particularly straightforward analysis, valid for arbitrary toroidal geometry, that is studied in the following subsection. The interesting difficulties arise at low collisionality. Then (118) is analytically tractable only for large aspect ratio, making both the second and third terms on the left hand side relatively small. In that case we have, in lowest order,

$$\xi v \nabla_{\parallel} F \cong Q, \quad \text{for } \frac{\nu}{\omega_t} \ll 1, \quad \frac{r}{R} \ll 1,$$

with solution

$$F \cong F_* \equiv \frac{1}{\xi v} \int ds Q(s). \quad (120)$$

Here the integration variable s represents arc-length along \mathbf{B} .

Before criticizing (120) we point out that it indeed approximates the ion distribution function in a large aspect ratio tokamak: the distribution determined from more sophisticated analysis resembles F_* throughout most of phase space. The problem with F_* is its singularity at $\xi = 0^3$. The singularity is not integrable, and would imply an infinite radial flux:

$$\left\langle \int d^3v v_D^r F_* \right\rangle = \infty. \quad (121)$$

A finite value for the flux can be found only by resolving F in the singular region.

In other words, at small (r/R) and v/Ω_t , a *boundary layer* arises in the slowly-transiting, large pitch-angle region of velocity space. The collisionless distribution becomes so large for $\xi \cong 0$ that the structure of the layer—the manner in which the singularity is resolved—determines the nature of radial transport. This is the crux of neoclassical kinetic theory.

For the specific purpose of resolving a boundary layer in the variable ξ , one part of the collision operator clearly dominates: the pitch-angle scattering operator, describing diffusion in ξ . It is given by the first term in (5.87); after transforming variables $(\lambda, w) \rightarrow (\xi, v)$ we have

$$C_1 \cong C_{LG} \equiv \nu \frac{\partial}{\partial \xi} (1 - \xi^2) \frac{\partial}{\partial \xi}, \quad (122)$$

where $\nu = \gamma_{ii} \Phi_i(v)/(2v^2) \sim \nu_c$ is a measure of collision frequency whose v -dependence is not important here. In fact the present argument depends only on the small- ξ scaling,

$$C(F) \sim \frac{\nu F}{\xi^2}, \quad \xi \sim 0. \quad (123)$$

Similarly the mirror force term in (118),

$$M(F) \equiv \frac{\nabla_{||} B}{2B} v (1 - \xi^2) \frac{\partial F}{\partial \xi} \quad (124)$$

has the scaling

$$M(F) \sim \frac{r}{R} \omega_t \frac{F}{\xi}, \quad \xi \sim 0. \quad (125)$$

These estimates are to be compared with the streaming term of (118),

$$S(F) \equiv \xi v \nabla_{||} F \sim \omega_t \xi F. \quad (126)$$

Equations (123)–(126) show that two qualitatively different layer structures are possible. The layer associated with banana motion occurs when ξ

³When $\partial \Phi / \partial \theta = \mathcal{O}(\delta)$, as we have assumed, (5.157) shows that there is no singularity at $v = 0$.

becomes so small that the mirror force competes with streaming: $M \sim S$. We denote the corresponding value by ξ_b , whence $\omega_t \xi_b \sim (r/R)(\omega_t/\xi_b)$ or

$$M \sim S \Leftrightarrow \xi_b \sim \left(\frac{r}{R}\right)^{1/2}. \quad (127)$$

On the other hand, the collisional layer, where collisions are comparable to streaming, is bounded by the value ξ_c , where $\omega_t \xi_c \sim \nu/\xi_c^2$; that is,

$$C \sim S \Leftrightarrow \xi_c \sim \left(\frac{\nu}{\omega_t}\right)^{1/3}. \quad (128)$$

The important layer is that which is wider—the one first encountered as ξ decreases from $\xi \sim 1$. Thus the singularity is resolved primarily by bananas in the case $\xi_b > \xi_c$, or

$$\frac{\nu}{\omega_t} < \left(\frac{r}{R}\right)^{3/2}. \quad (129)$$

It is resolved by collisions, which randomize banana orbits, in the opposite case, $\xi_c > \xi_b$. It is clear from (106) and (108) that these two cases correspond respectively to the banana and plateau regimes. Now we have found that the lowest order kinetic equation is given in the two low-collisionality regimes by

$$\xi v \nabla_{\parallel} F - \left(\frac{\nabla_{\parallel} B}{2B}\right) v(1 - \xi^2) \frac{\partial F}{\partial \xi} \cong Q \text{ (banana regime)}; \quad (130)$$

$$\xi v \nabla_{\parallel} F - C_1(F) \cong Q \text{ (plateau regime)}. \quad (131)$$

When ξ_c is large banana motion is collisionally obliterated, but the opposite statement is not true: the banana layer always contains a collisional boundary layer inside it. The point is that even when (129) is strongly satisfied, some particles, near the trapped-passing separatrix, will move slowly enough to be Coulomb-deflected in one period. As the collisionality increases, this inner plateau layer grows, and fewer banana orbits remain intact. Such inner layer growth characterizes the banana-plateau transition region.

8.6 Tokamak Transport: Analysis and Results*

Collision-dominated Transport

Before discussing the solutions to (130) and (131), we briefly consider the simplest transport regime. When the collision frequency exceeds the transit frequency, so that

$$\Delta = \frac{\omega_t}{\nu} \ll 1$$

the largest term in (114) in the collision term. Then we have to solve, suppressing species subscripts,

$$C_1(f) = 0 . \quad (132)$$

Equations of the form of (132) were encountered in Chapter 5 [recall (5.123)], where we found the unique solution to be perturbed Maxwellian,

$$\hat{f}_{M1} = \frac{2V_{\parallel 1} u}{v_t^2} + \frac{p_1}{p_0} + \left(\frac{v^2}{v_t^2} - \frac{5}{2} \right) \frac{T_1}{T_0} \quad (133)$$

as in (5.18). Here the perturbations $V_{\parallel 1}$, p_1 and T_1 can depend on both r and poloidal angle θ , thus distinguishing \hat{f}_{M1} from the unperturbed Maxwellian. (Indeed, the perturbations can depend on toroidal angle as well: the present argument makes no essential use of axisymmetry.) An interesting feature is that T_1 , while first order in δ , can be of order Δ^{-1} . That is, if we indicate the ordering in Δ with a superscript,

$$\hat{f}_{M1}^{(-1)} = \left(\frac{v^2}{v_t^2} - \frac{5}{2} \right) \frac{T_1}{T_0} .$$

We will see that T_1 must be this large, while similarly large contributions to $V_{\parallel 1}$ and p_1 are ruled out by momentum conservation. Thus the $\mathcal{O}(\delta\Delta^0)$ version of (114) is

$$u \nabla_{\parallel} \hat{f}_{M1}^{(-1)} = C_1(f_1^{(0)}) \quad (134)$$

or

$$C_1(f) = f_M u \left(\frac{v^2}{v_t^2} - \frac{5}{2} \right) \nabla_{\parallel} \ln T , \quad (135)$$

when inessential labels are suppressed. By multiplying (134) by $m u$ and integrating over velocity, we can rule out a p_1 -term in $f^{(-1)}$, since $C_1 = C_{ii1}$ conserves momentum. Similarly, particle conservation of C_{ii} implies that $V_{1\parallel}^{(-1)}$ can be assumed to vanish.

It is a remarkable fact that the ion radial transport problem is readily solved once we extract certain *parallel* transport information from (135). None of the higher order terms in (114) need to be considered. Before explaining this simplification we comment on the intrinsic significance of (135).

The characteristic feature of (135) is that the unknown function appears only inside a linearized collision operator. Equations of this form were studied extensively by Lyman Spitzer in the early 1950s (Spitzer, 1962); they are called *Spitzer problems*, although their importance has engendered investigations by many scientists. The general Spitzer problem describes the collisional response to some gradient, or collection of gradients. It involves the magnetic field only obliquely, to set the direction of the parallel gradient. Noticing that small- Δ corresponds to short mean-free

path in the direction of \mathbf{B} , we are not surprised that the Spitzer problem closely resembles that of short mean-free path transport in a neutral gas.

After multiplying (135) by $\hat{f} = f_1/f_M$ and integrating to compute the entropy production [as in (5.117)], we find

$$\Theta_i = -\frac{q_{\parallel}}{T} \nabla_{\parallel} \ln T \quad (136)$$

the expected force-flux product; compare (77). Of course to compute

$$\frac{q_{\parallel}}{T} = \int d^3v f u \left(\frac{v^2}{v_t^2} - \frac{5}{2} \right)$$

we need to solve the Spitzer problem. While this task—accomplished either numerically, or variationally, using an extremal property of Θ —is too lengthy to be considered here, the form of the result is clear. Since the solution to (135) must be proportional to its right hand side and inversely proportional to ν , the heat flux will have the form

$$\frac{q_{\parallel}}{T_i} = -\kappa_{i\parallel} \nabla_{\parallel} \ln T_i, \quad (137)$$

with (“classical”) parallel heat conductivity

$$\kappa_{i\parallel} = \frac{p_i \tau_i}{m_i} \alpha. \quad (138)$$

Here $\tau_i \sim 1/\nu_{ii}$ is the ion collision time of (5.79) and α is a numerical coefficient; detailed analysis yields $\alpha \cong 3.9$. The $1/\nu$ -dependence of $\kappa_{i\parallel}$ betrays the unmagnetized character of parallel transport, as discussed in §8.1; recall (18).

Thus we have found that, in the collision-dominated regime, the ion drift-kinetic equation becomes, in lowest order, a Spitzer problem for ion parallel heat transport. Of course nearly the same statement describes the electron case, with modifications to account for the additional term on the right hand side of (117) and the need to retain ion scattering: $C_{ie} \sim C_{ee}$. The salient result of the electron analysis is a Spitzer problem with several driving terms, and finally a set of transport relations analogous to (137). The latter are given by

$$\frac{J_{\parallel}}{e} = L_{\parallel 11} A_{\parallel 1} + L_{\parallel 12} A_{\parallel 2}, \quad (139)$$

$$\frac{q_{e\parallel}}{T_e} = -L_{\parallel 12} A_{\parallel 1} - L_{\parallel 22} A_{\parallel 2}, \quad (140)$$

where the forces are

$$A_{\parallel 1} = \nabla_{\parallel} \ln p_e + \frac{e E_{\parallel}}{T_e}, \quad A_{\parallel 2} = \nabla_{\parallel} \ln T_e \quad (140)$$

and the electron parallel transport matrix is

$$L_{\parallel mn} = \frac{p_e \tau_e}{m_e} \alpha_{mn}, \quad (141)$$

with $\alpha_{11} \cong 1.98$, $\alpha_{12} \cong 1.38$ and $\alpha_{22} \cong 4.17$. Notice that the coefficient $L_{\parallel 11}$ corresponds to the parallel conductivity

$$\sigma_{\parallel} = 1.98 \frac{\tau_e e^2 n}{m_e}, \quad (142)$$

usually called *Spitzer conductivity*, whose magnitude was anticipated in (6.149).

The general significance of these formulae should be clear. When $v \gg \omega_r$, particles cannot freely stream along the magnetic field lines. They are so shaken by Coulomb interactions as to randomly wander back and forth along the field, slowly diffusing in order to dissipate (first δ -order) parallel pressure and temperature gradients. Only two questions remain to be answered: why should there be such gradients? And what has parallel relaxation to do with radial transport?

Considering first the source of parallel gradients, we recall that magnetization induces the perpendicular heat flow,

$$\mathbf{q}_{i\perp 1} = \frac{5}{2} \frac{p_i}{m_i \Omega_i} \mathbf{b} \times \nabla T_i,$$

whose divergence does not vanish. Therefore heat accumulates locally on each flux surface; the steady state is maintained by a return flow which, in the collisional regime, is diffusive and given by (137). We noted in §8.3 that this flow has the general form given by (52), which must therefore agree with (137). Thus we obtain the condition

$$-\kappa_{i\parallel} \nabla_{\parallel} T_i = -\frac{5}{2} \frac{cI}{eB\chi'} p_i T'_i + L_i(r)B.$$

Here the flux function L_i can be eliminated using the identity $\langle B \nabla_{\parallel} T \rangle = 0$, with the result

$$\kappa_{i\parallel} \nabla_{\parallel} T_i = \frac{5}{2} \frac{cI}{eB\chi'} p_i T'_i \left(1 - \frac{B^2}{\langle B^2 \rangle} \right). \quad (143)$$

At this point we see that the ordering $\nabla_{\parallel} T_i = \mathcal{O}(\delta \Delta^{-1})$, which implies $\kappa_{i\parallel} \nabla_{\parallel} T_i = \mathcal{O}(\delta)$, is indeed compulsory. In a collision-dominated plasma with nonuniform confining field, the radial temperature gradient induces a parallel temperature gradient of significant size.

Of course an analogous argument applies to the electron gradients. After comparing (139) to the electron version of (52) and the parallel com-

ponent of (48), we deduce the relations

$$L_{\parallel 11} A_{\parallel 1} + L_{\parallel 22} A_{\parallel 2} = -\frac{cI}{eBX'} P' \left(1 - \frac{B^2}{\langle B^2 \rangle} \right) + \frac{e}{T_e} L_{\parallel 11} \frac{B \langle E_{\parallel} B \rangle}{\langle B^2 \rangle},$$

$$L_{\parallel 12} A_{\parallel 1} + L_{\parallel 21} A_{\parallel 2} = -\frac{5}{2} \frac{cI}{eBX'} n T'_e \left(1 - \frac{B^2}{\langle B^2 \rangle} \right) + \frac{e}{T_e} L_{\parallel 12} \frac{B \langle E_{\parallel} B \rangle}{\langle B^2 \rangle}. \quad (144)$$

Again the parallel gradients are a collisional response to radial ones.

The second question, concerning radial transport, is already answered by (43): in the collision-dominated regime, when anisotropy is negligible, the radial particle flux Γ_p is determined by parallel gradients [that $\Gamma_a = \mathcal{O}(\omega_t/\nu)$ is easily verified from (133) and (134)]. After recalling (38) and (140) we can combine the fluxes Γ_p and Γ_E to find

$$\Gamma_{nc} = -\frac{c}{eX'} \left[p_e \left\langle \frac{IA_{\parallel 1}}{B} \right\rangle - e \langle n E_{\zeta} \rangle \right].$$

At this point we simplify by specializing to an axisymmetric system, and explicitly using the constant shape assumption. (The axisymmetric case involves more manipulation but gives a similar result.) Then $I \equiv B_{\zeta}$ and E_{ζ} become flux labels, with $E_{\zeta}(r) = \langle E_{\parallel} B \rangle / (I \langle R^{-2} \rangle)$, as noted in (3.130). Since n is an approximate flux label and $B_T = I/R$ we have

$$\Gamma_{nc} = -\frac{cI}{eX'} \left[p_e \left\langle \frac{A_{\parallel 1}}{B} \right\rangle - en \frac{\langle E_{\parallel} B \rangle}{\langle B_T^2 \rangle} \right]. \quad (145)$$

Analogous treatment provides the heat fluxes in terms of parallel gradients:

$$q_{enc} = \frac{5}{2} \frac{cI}{e} p_e T_e \left\langle \frac{A_{\parallel 2}}{B} \right\rangle, \quad (146)$$

$$q_{inc} = -\frac{5}{2} \frac{cI}{e} p_i \left\langle \frac{\nabla_{\parallel} T_i}{B} \right\rangle. \quad (147)$$

We emphasize that the fluxes on the left hand sides of (145)–(147) are radial, while the driving forces on the right are parallel to \mathbf{B} : these expressions are not manifestly dissipative. To obtain dissipative transport relations, we return to (143) and (144), which can be solved—the determinant of the L_{ij} being nonzero—for the parallel gradients in terms of the radial gradients and $\langle E_{\parallel} B \rangle$. Notice in particular that the right hand sides of (143) and (144) involve precisely the neoclassical fluxes and forces given by (88) and (89). Hence, after substitution, (145)–(147) acquire the standard form of (80), and the collision-dominated transport problem is solved.

Explicitly we find that (145)–(147) become

$$\begin{aligned}\Gamma_{ne} = & - \left(\frac{cI}{e\chi'} \right)^2 \frac{m_e}{\tau_e} \left(\langle B^{-2} \rangle - \langle B^2 \rangle^{-1} \right) (0.66P' - 0.55nT_e') \\ & + \frac{cI}{\chi'} n \langle E_{||} B \rangle \left(\langle B^2 \rangle^{-1} - \langle B_T^2 \rangle^{-1} \right),\end{aligned}\quad (148)$$

$$q_{enc} = -\frac{5}{2} \left(\frac{cI}{e\chi'} \right)^2 \frac{m_e T_e}{\tau_e} \left(\langle B^{-2} \rangle - \langle B^2 \rangle^{-1} \right) (1.95nT_e' - 0.55P'), \quad (149)$$

and

$$q_{inc} = -1.6 \left(\frac{cI}{e\chi'} \right)^2 \left(\frac{m_i T_i}{\tau_i} \right) \left(\langle B^{-2} \rangle - \langle B^2 \rangle^{-1} \right) nT_i'. \quad (150)$$

The third electron flux can taken to be the parallel current; it is evaluated by eliminating the $A_{||}$'s from (139), which becomes

$$J_{||} = \sigma_{||} \frac{B \langle E_{||} B \rangle}{\langle B^2 \rangle} - \frac{IcP'}{B} \left(1 - \frac{B^2}{\langle B^2 \rangle} \right). \quad (151)$$

Here the second term displays return current in fully explicit form; compare (3.114).

These results, like all neoclassical formulae, resemble their classical counterparts in most respects: for example, they are intrinsically ambipolar, independent of Φ' , and dominated by ion thermal conduction. In the present collision-dominated case the similarity even extends to magnitude. To compare (148) with classical diffusion, we isolate the coefficient of n' in (148) and recall $I/\chi' \cong B_T/B_P$ to write

$$\Gamma_{ne} = -D_{PS} n' + \dots$$

where D_{PS} , the Pfirsch-Schlüter diffusion coefficient, is given by

$$\begin{aligned}D_{PS} \cong & 0.66 \left(\frac{B_T}{B_P} \right)^2 \nu_e \rho_e^2 \left(\langle B^{-2} \rangle - \langle B^2 \rangle^{-1} \right) \cong 1.3 \left(\frac{B_T}{B_P} \right)^2 \nu_e \rho_e^2 \left(\frac{r}{R} \right)^2 \\ & \cong q^2 D_c.\end{aligned}\quad (152)$$

Thus Pfirsch-Schlüter diffusion is relatively innocuous—smaller than the estimate of (95)—because of the small factor $\langle B^{-2} \rangle - \langle B^2 \rangle^{-1} \cong 2(r/RB_0)^2$. On the other hand it is clear that, even in this case of collisionally impeded guiding-center motion, the transport coefficients depend upon the global structure of B on a flux surface.

Transport at Low Collisionality

Pfirsch-Schlüter diffusion involves global information because its derivation requires averaging parallel transport equations over flux surfaces. The analogous nonlocal aspect of banana diffusion arises from the need to average kinetic equations over the collisionless orbits. In both cases the objective is to eliminate parallel gradient terms, leaving a radial transport law of the appropriate form, as in (80). But the orbit-averaged kinetic equation is much harder to solve than (144).

Such complications are miraculously absent from plateau kinetic theory, which we therefore consider first. In the plateau regime we are to solve (131), keeping in mind that the small collisional term is included only to resolve the singularity at $\xi = 0$. For this reason details of the collision operator are irrelevant, and the simple model

$$C(F) = -\nu F \quad (153)$$

gives accurate results. The point is that, given any solution to (131), we are really interested only in the $\nu/\omega_t \rightarrow 0$ limit.

Now the first order differential equation

$$\xi v \nabla_{||} F + \nu F \cong \frac{\xi v}{qR} \frac{\partial F}{\partial \theta} + \nu F = Q \quad (154)$$

is elementary, especially since, at large aspect ratio,

$$Q \equiv -\mathbf{v}_{ID} \cdot \nabla|_U f_{iM} = Q_s \sin \theta . \quad (155)$$

After decomposing F into $\sin \theta$ and $\cos \theta$ components one finds

$$F_s = Q_s \frac{\nu \sin \theta - (\xi v/qR) \cos \theta}{(\xi v/qR)^2 + \nu^2} . \quad (156)$$

This form allows calculation of the fluxes from moments of v_D^r , as in (63):

$$\Gamma = \left\langle \int d^3 v v_D^r F \right\rangle . \quad (157)$$

Notice that only the $\sin \theta$ -component of F contributes. In the limit of interest this component is a delta function in ξ ,

$$\frac{\nu}{[(\xi v/qR)^2 + \nu^2]} \rightarrow \pi \delta \left(\frac{\xi v}{qR} \right) = \pi \frac{qR}{v} \delta(\xi) \quad (158)$$

so the integral is not hard to evaluate.

The form of (158) confirms the collision-frequency independence of plateau fluxes. Evidently plateau transport reflects an approximate resonance between slowly transiting particles and the stationary magnetic field

structure. We may also note that (156) corresponds to anisotropic pressure; as remarked in Chapter 6, equilibrium pressure anisotropy is commonly predicted in first δ -order, at low collisionality.

Of course (154) determines F only up to a constant of integration. The constant does not affect the radial fluxes, but it is needed to determine the quantity K discussed in Section 3. It is found from consideration of momentum conservation in higher ν/ω_t -order; we omit the details because an analogous and more interesting integration-constant issue arises in the banana regime, to which we now turn our attention.

The lowest order banana kinetic equation is (130). We remove the messy mirror-force term in this equation by reverting to the natural drift-kinetic variables λ and w . Then we have, for the ion distribution,

$$\mathbf{u} \nabla_{\parallel} f^{(0)} = -\mathbf{v}_D \cdot \nabla|_U f_M , \quad (159)$$

where the superscript denotes the ordering with respect to $\nu/\omega_t \ll 1$ and subscripts are omitted. Of course we could have obtained (159) directly from expansion of (114) in powers of ν/ω_t .

Equation (159) was studied in §5.3; its general, exact solution is

$$f^{(0)}(r, \theta, \lambda, w) = k(r, \theta, \lambda, w) + g(r, \lambda, w) , \quad (160)$$

where k is given by (5.133),

$$k = -\frac{Iu}{\Omega} \frac{df_M}{d\chi}|_U$$

$$= -\frac{Iu}{\Omega} f_M \left[\frac{d \ln n}{d\chi} + \frac{e}{T} \frac{d\Phi}{d\chi} + \left(\frac{v^2}{v_t^2} - \frac{3}{2} \right) \frac{d \ln T}{d\chi} \right] , \quad (161)$$

and g is an integration “constant,” satisfying $\nabla_{\parallel} g = 0$. Unlike the corresponding plateau contribution, g does contribute to the radial fluxes in the banana regime. In fact the most characteristic features of banana transport, including the special role of trapped particles, are manifested through g . The burden of banana kinetic theory is determine this function.

An equation for g is derived by considering the first order terms in (114): $\mathbf{u} \nabla_{\parallel} f^{(1)} - C_1(f^{(0)}) = 0$, or

$$\mathbf{u} \nabla_{\parallel} f^{(1)} - C_1(k + g) = 0 . \quad (162)$$

We eliminate $f^{(1)}$ from (162) by means of an orbital average; that is, we consider its solvability condition. This relation

$$\langle C_1(k + g) \rangle_o = 0 , \quad (163)$$

is called the *banana constraint*. As the basic kinetic equation for toroidal transport in the low-collisionality limit, the banana constraint evidently has the form of an orbitally averaged Spitzer problem for g :

$$\langle C_1(g) \rangle_o = \text{known function} . \quad (164)$$

We recall from §5.3 that the right hand side of (164), and therefore g , vanishes in the isothermal case. In general, however, (163) poses a formidable mathematical problem; it has been solved only approximately, to lowest order in $(r/R)^{1/2}$, by variational methods. Thus it can be shown that the functional $\langle \Theta_2(f, f) \rangle$ is extremal, in the sense that

$$\delta \langle \Theta_2(f, f) \rangle = 0 , \quad (165)$$

has (163) as its Euler equation (Rosenbluth et al., 1972). Indeed (165) is a special case of a more general variational principle that describes transport in a toroidal system for any collisionality (Hinton and Rosenbluth, 1973). The linearity of (163) implies that the extremal value of $\langle \Theta_2 \rangle$ must be a quadratic form in the forces:

$$\langle \Theta_2(f, f) \rangle = \sum_{i,j} L_{ij} A_i A_j ; \quad (166)$$

recall (78) and (80). Once this form is found—after using, for example, a trial function for g —the transport coefficients can be read off by inspection.

Rather than pursuing the variational treatment here, we infer directly from (163) the essential qualitative features of g . The first point to notice is that in the passing region, (163) is *almost* solved by the function

$$g = -k + \hat{f}_d f_M , \quad (167)$$

where

$$\hat{f}_d = \frac{2V_{i\parallel} u}{v_{ti}^2} \quad (168)$$

is a displacement in parallel velocity (only the parallel velocity can enter because the distributions have been averaged over gyrophase; pressure and temperature-perturbation terms are irrelevant, since they cannot depend on θ). This “almost” solution is ruled out only because g is a flux label, while k and \hat{f}_d , proportional to u , are not. But notice that in the far-untrapped region, u is nearly independent of θ . Hence (167) closely approximates the solution for $\lambda \ll \lambda_c$; moreover, for large aspect ratio the trapped region is small, so that small- λ result pertains over most of the λ -domain. In other words we have

$$g = -k + \hat{f}_d f_M + f_{loc} , \quad (169)$$

where the distribution f_{loc} is localized, in a sense to be described, to the region $\lambda \geq \lambda_c$.

An expression equivalent to (169) is

$$f = \hat{f}_d f_M + f_{loc} . \quad (170)$$

Thus, for large aspect ratio, the banana-regime distribution function differs from a displaced Maxwellian only by a function that is effectively localized

to the trapped and nearly trapped region. This result should be kept in mind whenever a quick sense of neoclassical prediction is desired. It explains in particular the proportionality of the radial fluxes to $(r/R)^{1/2}$, i.e., to the width of the trapped region, since it is obvious from (157) that a displaced Maxwellian cannot contribute to any radial flux. It also explains why neoclassical kinetic theory emphasizes the pitch-angle scattering part of the Coulomb collision operator. The point is that λ -scattering dominates other collisional processes when acting on f_{loc} ,

$$C_1(f_1) \cong C_{\text{LG}}(f_{\text{loc}}), \quad (171)$$

in the notation of (122).

The function g vanishes in the isothermal case because at constant temperature, k is itself a displaced Maxwellian. Thus we can choose, in (168),

$$V_{\parallel i} = -\frac{I}{\Omega_i \chi'} \frac{T_i}{m_i} \left[(\ln n)' + \frac{e}{T_i} \Phi' \right] \quad (\text{when } T_i' = 0), \quad (172)$$

and find that (169) is exact, with $f_{\text{loc}} = 0 = g$. For $T_i' \neq 0$, we infer the form of the displacement from linearity:

$$V_{\parallel i} = -\frac{I}{\Omega_i \chi'} \frac{T_i}{m_i} \left[(\ln n)' + \frac{e}{T_i} \Phi' + \alpha_i (\ln T_i)' \right], \quad (173)$$

where the coefficient α_i is determined from g and the localization requirement on f_{loc} . Thus only the temperature gradient term in (169) survives, and g has the form

$$g = -\frac{I}{\Omega_i \chi'} f_M' (\ln T)' u^*(\lambda). \quad (174)$$

Here the function u^* has the dimensions of u , but is independent of θ . For small λ it must be proportional to u , by (170), while for $\lambda \geq \lambda_c$, u^* (like u) becomes small: g is *localized to the passing region*. Equation (174) is the main result of our discussion. Together with (160), it provides the essential conclusion of neoclassical kinetic theory.

To see why u^* is small in the trapped region we recall the bounce condition, (4.130). This constraint forces g to be even in $\sigma = u/|u|$ in the trapped region, since it is independent of θ and even at the boundary. But the inhomogeneous term in (164) that drives g is proportional to k and odd; in fact, (4.134) shows that the orbital average annihilates the right hand side of (164) in the trapped region.

Another feature of (167)–(173) deserves mention. Observe that the radial electrostatic field enters the ion kinetic equation only through the Φ' term in (173)—that is, it enters only through a displacement of the Maxwellian in parallel velocity. We will find that the same statement pertains to electron kinetic theory. Hence the argument applied previously

to classical transport (§8.1) applies, and Galilean invariance rules out any contribution of Φ' to the neoclassical fluxes.

Finally we comment on the sense in which f_{loc} is localized. The rigorous version of (170) shows that the truly localized function is $\partial f_{loc}/\partial \lambda$, rather than f_{loc} itself. This is hardly surprising since, in view of (171), the lowest order banana constraint involves only $\partial f_{loc}/\partial \lambda$. The constant (independent of λ) part of f_{loc} is awkward to calculate but fortunately not needed: in lowest $(r/R)^{1/2}$ -order, the collisional momentum prescription (59) gives each flux in terms of λ -derivatives alone. As a result (170) reliably describes virtually all banana-regime transport issues.

The above argument pertains to ions; the electron version differs in two ways. First, the electron collision operator contains terms describing both like and unlike species collisions, since $C_{ei} \sim C_{ee}$. Recall that C_{ei} contains a term proportional to $V_{\parallel i}$; to simplify this awkward ion coupling we displace the electron distribution as described in §5.2:

$$f_{e1} = F_e + 2 \frac{u V_{\parallel i}}{v_{te}^2} f_{eM}; \quad (175)$$

recall (5.61). When acting on F_e , C_{ei} simply augments the pitch-angle scattering term in C_{ee} , as shown in (5.89) and (5.92), so that the collision operator is not significantly more complicated than C_{ii} . Of course the second term in (175) also enters the parallel streaming term, where it appears as an additional source; the function F_e is driven by

$$Q_e \rightarrow Q_e - \frac{2V_{\parallel i}}{v_{te}^2} f_{eM} u \nabla_{\parallel} u.$$

It follows, in view of (172), that the electron perturbation is driven by both electron and ion gradients.

The second distinctive feature of the electron equation is the E_{\parallel} term on its right hand side. This term is easily accommodated by introducing the electron Spitzer function f_S , defined to satisfy

$$C_{e1}(u E_{\parallel} f_S) = \frac{e}{T_e} u E_{\parallel} f_{eM}. \quad (176)$$

Equation (173) is a standard Spitzer problem—in fact it is the version of (135) first tackled by Spitzer and his collaborators; although not available in analytic form, f_S can be considered a known function. It allows us to express the electron version of (162) as

$$u \nabla_{\parallel} F_e - C_{e1}(F_e + u E_{\parallel} f_S) = Q_e \quad (177)$$

where

$$Q_e = -v_{eD} \frac{df_{eM}}{dr}|_U - \frac{2V_{\parallel i}}{v_{te}^2} f_{eM} u \nabla_{\parallel} u. \quad (178)$$

Starting from (177), the electron kinetic analysis is hardly different from the ion case treated previously. One finds that

$$F_e^{(0)} = k_e + g_e ,$$

where

$$k_e = f_{eM} \frac{I}{\chi' \Omega_e} \left(\frac{d}{dr} \ln f_{eM} \Big|_U - \frac{m_e}{T_e} V_{i\parallel} \right)$$

and the function g_e resembles the ion version, discussed above. In particular g_e satisfies the electron banana constraint,

$$\langle C_{e1}(k_e + g_e + uE_{\parallel}f_S) \rangle_o = 0 . \quad (179)$$

Here the fact that

$$\langle C_{e1}(uE_{\parallel}f_S) \rangle_o \equiv 0 , \quad \text{for } \lambda > \lambda_c , \quad (180)$$

which is clear from (4.136), diminishes the “Ohmic” response in the trapped region (Hinton and Oberman, 1969). The point is that since $\mathbf{v} \cdot \mathbf{E}_{\parallel}$ changes sign at each bounce, the parallel electric field does little work on trapped particles.

Only one other feature of the electron problem requires special comment. Suppose for simplicity that all gradients vanish. Then $V_{\parallel i} = 0$ and the parallel current is simply

$$J_{\parallel} = -e \int d^3 v u f_{e1} . \quad (181)$$

Here, unlike the case of the radial fluxes, the distribution appears without the collision operator. Hence knowledge of $\partial f / \partial \lambda$ is not sufficient to evaluate (181); it would appear that the small, nonlocalized piece of f_{e1} is needed. This ugly complication is avoided by means of the following artifice. One first uses (176) to write

$$J_{\parallel} = -\frac{T_e}{E_{\parallel}} \int d^3 v \frac{f_{e1}}{f_{eM}} C_{e1}(uE_{\parallel}f_S) ; \quad (182)$$

then self-adjointness of the collision operator, in the sense of (5.121), implies

$$J_{\parallel} = -\frac{T_e}{E_{\parallel}} \int d^3 v \frac{uE_{\parallel}f_S}{f_{eM}} C_{e1}(f_{e1}) . \quad (183)$$

Notice that (183) has the desired form, involving f_{e1} only inside C_{e1} ; thus the nonlocalized part of f_{e1} is eliminated.

Banana-regime Closure

As a concrete example of transport closure, we next consider the neoclassical fluxes in the banana regime—the final results of the kinetic analysis described above. For simplicity we treat the case of single ion species with ionic charge $Z = 1$. In this context one uses large aspect ratio approximations freely; aside from the explicit $(r/R)^{1/2}$ factors in the transport coefficients, the torus becomes essentially cylindrical. Note in particular that in this case, $g^{-1/2} \cong rR_0$, $E_\zeta \cong \mathcal{E}R_0$, $B^\theta = B_P/r$ and $\nabla r = \hat{r}$, the cylindrical unit vector.

The following transport relations are obtained by solving the ion and electron banana constraints, (163) and (179), and substituting the resulting distributions into the collisional moments (64), (65), and (183). The particle flux is given by

$$\Gamma = -D_b n \left[1.12 \left(1 + \frac{T_i}{T_e} \right) (\ln n)' + 0.43 (\ln T_e)' + 0.19 (\ln T_i)' \right] + 2.44 n \left(\frac{r}{R} \right)^{1/2} V_f^r , \quad (184)$$

where

$$D_b = \left(\frac{r}{R} \right)^{1/2} \frac{\rho_P^2}{\tau_e} \quad (185)$$

is the banana diffusion coefficient and V_f^r is the radial flux surface velocity of (3.127). In the constant shape case, (3.130) yields $V_f^r = -c \langle E_{\parallel} B \rangle / [I X' \langle R^{-2} \rangle]$, or, for large aspect ratio,

$$V_f^r = -c \frac{\mathcal{E}}{B_P} \quad (186)$$

where $\mathcal{E} = -c^{-1} \partial A_{\parallel} / \partial t$ is the electromagnetically induced parallel field. The heat fluxes are

$$q_e = -D_b p_e \left[-1.53 \left(1 + \frac{T_i}{T_e} \right) (\ln n)' + 1.81 (\ln T_e)' + 0.27 \frac{T_i}{T_e} (\ln T_i)' \right] + 1.75 p_e \left(\frac{r}{R} \right)^{1/2} V_f^r , \quad (187)$$

and

$$q_i = -0.48 D_b \left(\frac{m_i T_e}{m_e T_i} \right)^{1/2} n T_i' . \quad (188)$$

The parallel current density is

$$J_{\parallel} = \frac{p_e}{B_P} \left(\frac{r}{R} \right)^{1/2} \left[-2.44 \left(1 + \frac{T_i}{T_e} \right) (\ln n)' - 0.69 (\ln T_e)' + \frac{T_i}{T_e} (\ln T_i)' \right] + \left[1 - 1.95 \left(\frac{r}{R} \right)^{1/2} \right] \sigma_{\parallel} \mathcal{E} , \quad (189)$$

where σ_{\parallel} is the Spitzer conductivity of (142). In (189) we consider J_{\parallel} as a flux for convenience; however, as noted in Section 3, the parallel current can as well be considered as a force; recall (88). Indeed the large aspect-ratio version of Ampère's law, (3.107), suggests such an interpretation:

$$J_{\parallel} = \frac{c}{4\pi} \frac{1}{r} \frac{\partial}{\partial r} r B_P . \quad (190)$$

The corresponding flux is the Poynting flux of (89), here approximated by E ; thus (189) can be rearranged as

$$\begin{aligned} \mathcal{E} = - & \left[1 - 1.95 \left(\frac{r}{R} \right)^{1/2} \right]^{-1} \sigma_{\parallel}^{-1} \left\{ \frac{c}{4\pi} \frac{1}{r} \frac{\partial}{\partial r} (r B_P) - \frac{p_e}{B_P} \left(\frac{r}{R} \right)^{1/2} \right. \\ & \times \left. \left[-2.44 \left(1 + \frac{T_i}{T_e} \right) (\ln n)' - 0.69 (\ln T_e)' + \frac{T_i}{T_e} (\ln T_i)' \right] \right\} . \end{aligned} \quad (191)$$

Most of the terms in these equations have been discussed previously. Thus the last term in (184) displays the Ware-Galeev pinch effect, as estimated by (113). Equation (187) shows that a similar term occurs in the heat flux. In (188) we see again the dominance of ion thermal conduction, due to the large ion gyroradius, that also characterized classical and collision-dominated transport; cf. (20) and (150). The first term in (189) gives the bootstrap current, driven by ∇n , while the last term shows the reduction in conductivity due to magnetic trapping, as noted in (180).

We next display the conservation laws, (28) and (29) which, together with Ampère's law, provide the closed set of transport equations. Here the discussion of §8.3 should be recalled: the only nontrivial terms involve energy exchange, as given by (73) and (74) in terms of the flux label, K . It will be shown presently that K is simply the velocity moment of g , so it too is computed from the banana constraint—that is, from the explicit version of (174). We use this result, and the approximations

$$\langle B(F_{\parallel i} + e n E_{\parallel i}) \rangle \cong - \frac{e B_P B}{c} \Gamma , \quad (\mathbf{J} \cdot \mathbf{E}) \cong J_{\parallel} \mathcal{E} ,$$

to write the large aspect-ratio versions of (73) and (74) as

$$(X_i) = 3 \frac{m_e}{m_i} n \frac{T_i - T_e}{\tau_{ei}} + \Gamma [T_i (\ln n)' - 0.17 T_i'] ,$$

$$(X_e) = - \langle X_i \rangle - J_{\parallel} \mathcal{E} .$$

Then the conservation laws take the form

$$\frac{\partial n}{\partial t} + \frac{1}{r} (\mathbf{r}\Gamma)' = 0 , \quad (192)$$

$$\frac{3}{2} \frac{\partial p_e}{\partial t} + \frac{1}{r} \left[r \left(q_e + \frac{5}{2} T_e \Gamma \right) \right]' = -3 \frac{m_e}{m_i} n \frac{T_i - T_e}{T_{ei}} + J_{\parallel} \mathcal{E} - \Gamma [T_i (\ln n)' - 0.17 T_i'] , \quad (193)$$

$$\frac{3}{2} \frac{\partial p_i}{\partial t} + \frac{1}{r} (rq_i)' = 3 \frac{m_e}{m_i} n \frac{(T_i - T_e)}{T_{ei}} + \Gamma [T_i (\ln n)' - 0.17 T_i'] . \quad (194)$$

The final neoclassical equation is the poloidal component of Faraday's law,

$$\frac{\partial B^{\theta}}{\partial t} = c g^{-1/2} E'_{\zeta} .$$

It has the large aspect-ratio form

$$\frac{\partial B_P}{\partial t} = c \mathcal{E}' , \quad (195)$$

which is combined with (191) to track the evolution of the poloidal field. It is evident that (184)–(195) provide a closed set for the four variables n , $p_e = nT_e$, $p_i = nT_i$ and B_P .

Tokamak Plasma Rotation

Equilibrium rotation of a pure tokamak plasma is predicted to be rapid and primarily toroidal:

$$V_T \sim \frac{\rho_P}{r} v_{ti} \gg V_P \sim \frac{\rho}{r} v_{ti} , \quad (196)$$

where $V_{T(P)} \equiv \mathbf{B}_{T(P)} \cdot \mathbf{v}/B$. This is the essential prediction of equilibrium kinetic theory (Rosenbluth, Rutherford, et al., 1971; Hazeltine, 1974). We use the word "rapid" because, as indicated in (196), V_T exceeds simple magnetization flow $V_{\perp 1}$ (as well as V_P) by the neoclassical factor $B_T/B_P \sim 10$. It should be emphasized that (196) is independent of collisionality, and is instead a simple consequence of particle conservation, axisymmetry and the most elementary features of the collisional dissipation. Experimental disagreements with (196) can be attributed to the rotation damping effect of neutral impurities in the plasma.

We derive (196) using banana-regime kinetic theory for definiteness; it will be clear that a similar argument pertains in other collisionality regimes.

Indeed, most of the argument follows from the discussion in §5.3, which made no reference to the form or size of the collision operator. We first use (160) (derived in §5.3) to compute $V_{\parallel i} \cong V_{\parallel}$:

$$nV_{\parallel} = \int d^3v (k + g)u.$$

Only the ion flow is of interest here; we suppress the i -subscript from V . Since

$$\int d^3v f_M u^2 \left[(\ln p)' + \frac{e}{T} \Phi' + \left(\frac{v'^2}{v_t^2} - \frac{5}{2} \right) (\ln T)' \right] = \frac{p}{m} \left[(\ln p)' + \frac{e}{T} \Phi' \right]$$

we find

$$nV_{\parallel} = -\frac{cI_p}{eB\chi'} \left[(\ln p_i)' + \frac{e}{T_i} \Phi' \right] + \int d^3v gu. \quad (197)$$

We compare this result to (51) and conclude that

$$\int d^3v gu = K(r)B. \quad (198)$$

This relation between g and K , mentioned previously, is not surprising. Note that both functions appeared first as integration constants, and the flux-label nature of g can be seen, from (4.147), to imply that of K .

Yet (198) tells us something new: it shows that K must be proportional to the ion temperature gradient. Indeed, after substituting (174) into (198) we find

$$K = -\kappa \frac{I_c}{eB^2\chi'} nT'_i \quad (199)$$

where κ is a number whose value depends upon the details of u^* . It is clear from the derivation of (174) that $\kappa \sim 1$, and this information is sufficient to verify (196). In fact the value of κ is the only collisionality-dependent aspect of the present argument.

Finally, we substitute (199) into (49) to write the flow velocity in an axisymmetric system as

$$n\mathbf{V}_T = -\frac{c}{e\chi'} (p' + en\Phi') R^2 \nabla \zeta - \kappa \frac{I_c}{eB\chi'} nT'_i \mathbf{b}. \quad (200)$$

The toroidal and poloidal components of this flow,

$$\begin{aligned} nV_T &= -\frac{cR}{e\chi'} \left[p' + en\Phi' + \kappa \frac{B_T^2}{B^2} nT'_i \right] \\ &\cong -\frac{c}{eB_P} (p' + en\Phi' + \kappa nT'_i), \end{aligned} \quad (201)$$

$$nV_P = -\kappa \frac{I_c}{eB^2\chi'} nT'_i B_P \cong -\kappa \frac{c}{eB} nT'_i, \quad (202)$$

verify (196). That poloidal rotation is proportional to the temperature gradient is characteristic of axisymmetric confinement.

Notice that we have not determined V_T , because Φ' remains unknown. Indeed, (201) is sometimes used as a diagnostic for Φ' , when p' and V_T are experimentally known. As we have remarked, the radial electrostatic field appears nowhere in the closed set of transport equations, (184)–(195). Transport theory provides only an equation for the rate of change of V_T , considered in the following subsection.

Confined plasma velocities are sometimes estimated, or even calculated, as if $\mathbf{V} = \mathbf{v}_\perp$, apparently because the magnetization flow is more widely appreciated than the return flow incorporated into (200). It is therefore worth emphasizing that return flows are real, and just as inevitable as diamagnetism. In fact the largest contribution to \mathbf{V} , entering both terms in (200), is parallel to \mathbf{B} : whenever the poloidal field is relatively small,

$$V_\parallel \gg V_\perp . \quad (203)$$

Strongly driven plasmas, as in the case of unbalanced neutral-beam injection, are sometimes observed to rotate faster, at least marginally, than (196) suggests. Because the drift-kinetic equation presumes that any flow is at most first order in ρ_{Pi} , the results of Chapter 5 might seem suspect in the rapidly rotating case. However, allowing *ab initio* for much more rapid flow,

$$V \sim v_{ti} , \quad (204)$$

has surprisingly little effect on (196) (Hinton and Wong, 1985). Specifically, after the general kinetic equation is expressed in the moving plasma frame, a generalization of the H -theorem argument of §5.3 shows that only the toroidal velocity survives collisional relaxation. The equilibrium state has $\mathbf{V} = R\nabla\zeta V_T + \mathcal{O}(\delta)$, with

$$V_T = -\frac{cR}{\chi'}\Phi' \gg V_P = \mathcal{O}(\delta) , \quad (205)$$

very similar to (196). Indeed the fast equilibrium rotation speed is simply the large- Φ' limit of (201).

In other words, if external drives are allowed to “spin-up” a tokamak plasma to near sonic toroidal flow, the radial electrostatic field responds in accordance with (49)⁴. Equation (49) survives in large-velocity regimes because it reflects plasma magnetization and particle conservation; it is altered by external forces only in the extreme situation when such forces are strong enough to compete with the plasma pressure gradient.

Rapid poloidal rotation, damped by the poloidal variation of B , is harder to maintain. It is most likely to be found near the plasma edge, where sources of both particles and momentum can be virulent and very large radial electric fields are common.

⁴As we have remarked, the ordering $(eB/\chi')\Phi' \ll \text{str forces } \Phi \text{ to vary on the scale of the poloidal gyroradius}; (204) stretches the limits of drift-kinetic theory.$

Toroidal Acceleration

So far we have considered the particle fluxes only through second order in the gyroradius; the higher order terms are also of interest. We therefore return to the exact momentum conservation law, (6.24), restricting our attention for simplicity to the axisymmetric case⁵. Performing the same manipulation that led to (59), but now keeping all terms, we obtain

$$\Gamma_s = \frac{c}{e_s \chi'} \left(\left\langle \left\langle \frac{\partial}{\partial t} m_s n V_{s\zeta} \right\rangle \right\rangle + \frac{d}{dV} \langle P_{s\zeta}^V \rangle - e_s \langle n E_\zeta \rangle - \langle F_{s\zeta} \rangle \right). \quad (206)$$

Notice that the higher order terms are not intrinsically ambipolar; the radial current is

$$\langle J^r \rangle = \sum_s e_s \Gamma_s = \frac{c}{\chi'} \left(\left\langle \left\langle \frac{\partial}{\partial t} \rho_m V_{m\zeta} \right\rangle \right\rangle + \frac{d}{dV} \langle P_\zeta^V \rangle \right) \quad (207)$$

where $\rho_m \mathbf{V}_m$ is the center of mass flow and \mathbf{P} the total stress tensor, as in (6.90). Indeed, (55) is easily interpreted in terms of (6.90); after rearrangement we have

$$\left\langle \frac{\partial}{\partial t} \rho_m V_{m\zeta} \right\rangle = \frac{1}{c} \langle (\mathbf{J} \times \mathbf{B})_\zeta \rangle - \frac{d}{dV} \langle P_\zeta^V \rangle, \quad (208)$$

stating that the change of toroidal angular momentum on a flux surface is given by the electromagnetic torque on that surface, plus the net flow of angular momentum to neighboring surfaces.

The size of the viscous term in (208) is consistent with the transport ordering. Thus in §8.3 we showed that P_ζ^V must be $\mathcal{O}(\delta^2)$, but the flux-surface average is smaller:

$$\langle P_\zeta^V \rangle = \mathcal{O}(\delta^3). \quad (209)$$

We omit the detailed proof of (209), but it is not surprising if one begins with the guiding-center formula

$$\langle P_\zeta^V \rangle = \mathcal{V}' \left\langle \int d^3 v f \frac{I}{B} u v_B^r \right\rangle, \quad (210)$$

since $v_{ge\zeta} \cong b_\zeta u = (I/B)u$. Any second order contribution to $\langle P_\zeta^V \rangle$ must evidently come from f_1 ; but the appropriate drift-kinetic equation, (114), shows that f_1 has the wrong θ -dependence (and σ -dependence) to contribute to the flux-surface average in (210). Hence only f_2 contributes and (209) follows.

⁵Nearly the same formalism pertains in axisymmetric geometry, but the interpretation is no longer straightforward; recall the discussion following (8.58).

In §3.5 we noted that Ampère's law without the Maxwell term requires $\langle J^r \rangle$ to vanish. Here we restore the Maxwell term and use the identity $\langle \nabla \times \mathbf{B} \cdot \nabla r \rangle = 0$ to find

$$\langle J_r \rangle = -\frac{1}{4\pi} \left\langle \frac{\partial E^r}{\partial t} \right\rangle. \quad (211)$$

That is, *any averaged radial current must be balanced by an opposing displacement current*. It must be emphasized that this statement follows from the nature of flux surfaces, and not from ambipolarity; indeed, ambipolarity would require both sides of (211) to vanish.

In the case of slow evolution, described by the transport ordering, (207) and (211) yield an equation for the evolution of the radial electrostatic field, $\Phi(r)$. To derive this result, first note that the electron contributions to (207) are negligible, since $\rho_m \mathbf{V}_m \cong m_i n \mathbf{V}_i$ and $\delta_e \ll \delta_i$. For the same reason we can treat the density as constant: momentum and particle conservation enforce

$$\frac{\partial n'}{\partial t} = \mathcal{O}(\delta_e^2). \quad (212)$$

Second, recall that the radial electric field is dominated by $-\nabla \Phi$, so

$$E^r = -\Phi' |\nabla r|^2 = -\Phi' \left(\frac{RB_P}{\chi'} \right)^2. \quad (213)$$

Finally note that since each term in (207) is $\mathcal{O}(\delta^3)$, we can consistently use the first order expression, (200), for the toroidal velocity:

$$nV_\zeta = -\frac{cR^2}{e\chi'} \left[p' + en\Phi' + \kappa \frac{B_T^2}{B^2} nT'_i \right]. \quad (214)$$

Hence, after substituting (212)–(214) into (207) we have

$$\frac{\langle R^2 B_P^2 \kappa_P \rangle}{4\pi} \frac{\partial \Phi'}{\partial t} = -\frac{c^2 \langle R^2 \rangle m_i}{e} \left(\frac{\partial p'}{\partial t} + \kappa \left\langle \frac{B_T^2}{B^2} \right\rangle nT'_i \right) + c\chi' \frac{d}{d\gamma} \langle P_\zeta^V \rangle, \quad (215)$$

where κ_P is a “poloidal magnetic susceptibility” given by

$$\kappa_P = 1 + 4\pi m_i nc^2 \frac{\langle R^2 \rangle}{\langle R^2 B_P^2 \rangle}. \quad (216)$$

Equation (215) determines, in principle, the evolution of the electrostatic field in an intrinsically ambipolar system.

Note that the poloidal magnetic susceptibility is larger than the ordinary magnetic susceptibility because B_P^2 , rather than B^2 , occurs in the denominator. Usually the second term dominates,

$$\kappa_P \gg 1,$$
(217)

implying that the radial current could have been neglected. Indeed, (217) is the sole vestige of ambipolarity in the present context.

It is clear [from (194)–(196), for example] that conventional orderings would estimate the right-hand side of (215) as $\mathcal{O}(\delta_i^3)$, implying that $\Phi(r)$ evolves slowly. This circumstance, which is exacerbated by (217), means that neoclassical electrostatic relaxation is not predicted to occur during a collisional confinement time, and need not occur during the duration of the discharge.

In other words neoclassical relaxation of the radial electric field is rather feeble, and easily dominated by various noncollisional effects, such as turbulence or wall interactions. Indeed, experimental relaxation occurs more quickly: tokamak toroidal viscosity appears to be strongly anomalous. On the other hand, since neoclassical physics hardly entered the derivation of (215), a generalized description of toroidal acceleration will be very similar.

8.7 Summary

The minimum level of dissipation possible in a confined plasma is diffusion and heat conduction across \mathbf{B} due to Coulomb collisions. The simplest version of such dissipation is classical transport: a random walk of guiding centers, due to occasional ($\nu \ll \Omega$) large angle scatterings, from one field line to another. Since the corresponding step-size is the gyroradius, the classical diffusion coefficient is given by $D_c \sim \nu \rho^2$.

Classical transport is the only collisional transport process in an idealized cylindrical system. Real confinement systems are predicted to display additional losses, stemming ultimately from magnetic field curvature. Appearing in a fluid description as artifacts of stress anisotropy or parallel fluid gradients, the “neoclassical,” curvature-induced radial fluxes exceed classical transport whenever $B_T \gg B_P$. In other words, when end losses are avoided by bending the confinement cylinder into a torus, a price is paid in terms of enhanced radial loss. (Of course curvature takes a bigger toll in the context of plasma stability.)

At low collisionality, neoclassical diffusion has the same relation to guiding-center motion that classical diffusion has to gyromotion; the neoclassical process dominates because the radial excursion of a guiding center usually exceeds the gyroradius. In part because of the large poloidal and toroidal extent of guiding center orbits, neoclassical theory is not fully local: it describes evolution in terms of radius and time, using flux-surface averaged variables. In an axisymmetric system, the radial fluxes are advantageously expressed in terms of moments of the collisional operator; such expressions show, in particular, that axisymmetric particle transport is intrinsically ambipolar.

Transport in any system is conveniently summarized by its entropy

production rate, which has the canonical form of a sum of products of thermodynamic forces and fluxes. In the case of toroidal confinement, the canonical form is obtained after a flux-surface average. The averaged entropy production is used to identify a convenient set of forces and fluxes; one finds in particular that only the electromagnetically induced electric field enters. Off-diagonal elements of the corresponding transport matrix satisfy Onsager symmetry.

Equilibrium kinetic theory in a torus hinges upon the competition between guiding-center streaming along \mathbf{B} and Coulomb collisions. When guiding-center motion is dominated by collisions ($\nu > \omega_t$), streaming is sufficiently impeded to allow parallel gradients of pressure and temperature. Maintained by return flows, such gradients drive radial fluxes that exceed classical transport by roughly the square of the safety factor.

In the opposite case ($\nu < \omega_t$), the relatively strong transport enhancement results from a near singularity of the distribution function at small v_{\parallel} . The corresponding velocity-space boundary layer is resolved by either collisions or magnetic curvature, depending upon the collisionality and inverse aspect ratio. In either case, analytic solution of the drift-kinetic equation depends upon large aspect-ratio approximation.

Rotation of a pure axisymmetric toroidal plasma is dominated by flow along the magnetic field (return flow). The relatively fast toroidal motion is affected by the radial electrostatic field; since the closed set of transport equations does not involve Φ' , toroidal acceleration depends on third-order dissipation. Poloidal rotation is predicted to be relatively slow, for $B_T \gg B_P$, and proportional to the ion temperature gradient.

Further Reading on

Fundamentals and Classical Transport:

Robinson and Bernstein, 1962
Braginskii, 1965

Neoclassical Theory:

Bernstein, 1974
Galeev and Sagdeev, 1975
Hinton and Hazeltine, 1976
Fisch, 1987 (current drive)

Other Tokamak Transport Phenomena:

Hirshman and Sigmar, 1981 (impurity transport)
Kaye, 1985 (confinement scaling laws)
Fisch, 1987 (current drive)

Exercises

1. A direct calculation of classical transport would use the obvious formula

$$\mathbf{n}\mathbf{V} = \int d^3v \mathbf{v} f.$$

Describe how accurately the distribution f would be needed to compute $\mathbf{n}\mathbf{V}_c$ in this way; explain in a few sentences how this distribution would be computed. See (Rosenbluth and Kaufman, 1958).

2. Generalize (32), allowing for temporal change in the flux surface configuration. See (Hinton and Hazeltine, 1976).
3. Verify the identity (40) for arbitrary toroidal geometry.
4. Derive an equation, analogous to (39), for the radial heat flux, \mathbf{Q} .

5. Describe how the presence of an ion source would affect (49). Denoting the source by S [that is, $\partial n / \partial t + \nabla \cdot (\mathbf{n} \mathbf{V}) = S$], and assuming that S is constant in space and time, determine the modified form of (49).
6. Beginning with an exact moment equation, derive (61).

7. **Onsager symmetry.** Deduce the Onsager symmetry of classical transport coefficients from the self-adjointness property of the collision operator, (5.120), as follows.

- (a) Show from (1)–(4) that the classical particle flux can be expressed as

$$\mathbf{n}\mathbf{V}_c^r = \int d^3v \rho^r C \left\{ f_M \rho^r \left[A_1 + \left(\frac{v^2}{v_t^2} - \frac{5}{2} \right) A_2 \right] \right\}$$

where $A_1 \equiv d \ln p / dr + (e/T) d\Phi / dr$, $A_2 \equiv d \ln T / dr$. Deduce a corresponding expression for the heat flux q_c^r .

- (b) Conclude that the classical transport coefficient L_{12} is

$$L_{12} = \int d^3v \rho^r C \left[f_M \rho^r \left(\frac{v^2}{v_t^2} - \frac{5}{2} \right) \right].$$

- (c) Similarly compute L_{21} and show that (5.120) requires $L_{12} = L_{21}$. Of course a similar argument applies to other forms of collisional transport.

8. **Bananas.** Use the approximation $B(r, \theta) \cong B_0 [1 - (r/R) \cos \theta]$ to derive, from the invariance of p_ζ , μ and U , an explicit expression $r(\theta)$ for the banana orbit in a large aspect ratio tokamak. Sketch your result in

poloidal cross section (Hint: the two sides of the banana correspond to differing choices for the discrete variable σ .).

9. Calculate from (156) and (158) the lowest order stress anisotropy $P_{\parallel} - P_{\perp}$ in the plateau regime.
10. Use the random walk formula, (105) to derive an estimate for the particle diffusion coefficient in the plateau regime.

11. It was noted in Chapter 5 that when $Z \gg 1$, the electron collision operator is approximated by C_{ei} . Use (5.92), assuming $V_{\parallel i} = 0$ for simplicity, to solve the electron Spitzer problem (176) analytically for large Z . Thus obtain an explicit expression for f_S in the large Z case.

12. **Rotation direction.** It is conventional to assume that the poloidal and toroidal components of \mathbf{B} are positively oriented with respect to the coordinate axes: $\mathbf{B}_P \cdot \nabla \theta > 0$, $\mathbf{B}_T \cdot \nabla \zeta > 0$. However, confining fields in experimental tokamaks can have the opposite directions, depending upon the sense of the toroidal field coils and the driven toroidal current. In other words, the quantities $I = B_{\zeta}$ and $d\chi/dr$ can have either sign.

- (a) If r is a suitable radial coordinate and χ is the poloidal flux in the sense of (3.13), show that $d\chi/dr$ has the same sign as $\mathbf{J} \cdot \nabla \zeta$.
- (b) Assuming that the toroidal flow is given by (205), show that the product $V_T J_T$ has the same sign as the radial electric field $E_r = -d\Phi/dr$. Thus the toroidal flow and toroidal current are parallel or antiparallel, depending upon the direction of the radial electric field.

13. **Cylindrical confinement.** A straight cylindrical system, avoiding both neoclassical effects as well as the instabilities associated with toroidicity, might conceivably display only classical transport. If it were long enough, it would even satisfy the Lawson criterion. Investigate this confinement concept, as follows.

- (a) Show that the classical, perpendicular energy confinement time associated with a cylinder of radius a is estimated by

$$\tau_{\perp} \sim \left(\frac{a}{\rho}\right)^2 \tau_i$$

where ρ is the ion thermal gyroradius and τ_i the ion collision time of (5.79).

- (b) Show from (138) that the classical, axial energy confinement time

in a straight cylinder of length L is estimated by

$$\tau_{\parallel} \sim \left(\frac{L}{v_t} \right)^2 \frac{1}{\tau_i}$$

where v_t is the ion thermal speed and we have assumed $v_t \tau_i < L$.

- (c) Finally, suppose that mechanical constraints give the upper bounds $B \sim 100 \text{ kG}$, $n \sim 10^{14} \text{ cm}^{-3}$, and that $T \sim 10 \text{ keV}$ as usual. Compute the smallest possible length of the system.

Chapter 9

Nonlinear Processes

9.1 Magnetic Islands

As we noted in §7.3, the shear-Alfvén law implies that the nonideal corrections to MHD are most important near rational surfaces. The tearing instabilities studied in §7.7–8, growing near rational surfaces, led to helical magnetic perturbations that can change the surface structure. Here we consider the resulting formation of “magnetic islands.”

A change in topology of the magnetic field lines is known as *reconnection*: one envisions the field lines breaking and rejoining in a distinctive way, creating new lines. In the case of ideal evolution, such topology changes are forbidden. When the resistivity is small the slippage between fluid element trajectories and the magnetic field is typically slow, and the structure of the magnetic field still provides strong constraints on the motion.

In this section we will investigate the general properties of field lines in toroidal systems when their topology is allowed to change. In the next section we investigate the consequences of magnetic islands on tearing instabilities.

Field Line Hamiltonian

It is convenient here to represent a magnetic field in terms of its vector potential \mathbf{A} . In a general toroidal coordinate system (r, θ, ζ) , \mathbf{A} can be written

$$\mathbf{A} = A_r \nabla r + A_\theta \nabla \theta + A_\zeta \nabla \zeta \quad (1)$$

in terms of its covariant components. This form can be simplified by gauge transformation: first we define \bar{v} , Ψ and χ by

$$\bar{v} = \int^r dr' A_r(r', \theta, \zeta), \quad \Psi = A_\theta - \frac{\partial v}{\partial \theta}, \quad \chi = -A_\zeta + \frac{\partial v}{\partial \zeta},$$

so that \mathbf{A} becomes

$$\mathbf{A} = \Psi \nabla \theta - \chi \nabla \zeta + \nabla \bar{\psi}.$$

Since the last term does not affect \mathbf{B} , we can set

$$\mathbf{A} = \Psi \nabla \theta - \chi \nabla \zeta. \quad (2)$$

Consequently the magnetic field is expressed as

$$\mathbf{B} = \nabla \Psi \times \nabla \theta - \nabla \chi \times \nabla \zeta. \quad (3)$$

Equation (3) is a completely general representation for \mathbf{B} which, despite its superficial similarity to (3.15), does not mean that (χ, θ, ζ) are flux coordinates. In fact flux surfaces need not even exist. We will see below that (3) is a flux representation only when χ is a function solely of Ψ .¹

The forms (2) and (3) are especially convenient for studying magnetic field line trajectories. A field line is a path in space and so can be represented by functions $\mathbf{r}(\tau)$, $\theta(\tau)$ and $\zeta(\tau)$ where τ is any convenient parameter labelling points along the curve. Such a path $\mathbf{x}(\tau)$ is a field line if its tangent vector, $d\mathbf{x}/d\tau$, is everywhere parallel to \mathbf{B} :

$$\frac{d\mathbf{x}}{d\tau} \times \mathbf{B} = 0.$$

These equations for field lines can be obtained from a variational principle analogous to (2.40):

$$S = \int \mathbf{A} \cdot d\ell = \int \Psi d\theta - \chi d\zeta. \quad (4)$$

In other words, field lines are the paths that extremize S .

In some cases it is possible to choose one of the phase space coordinates as the parameter; for example, if $\tau = \zeta$, then $[\mathbf{r}(\zeta), \theta(\zeta), \zeta]$ describes a path; we will see that this works providing $B^\zeta \neq 0$. Then (4) can be rewritten as

$$S = \int \left(\Psi \frac{d\theta}{d\zeta} - \chi \right) d\zeta. \quad (5)$$

Equation (5) is formally identical to the phase-space action principle for a canonical Hamiltonian (2.38): one merely identifies time with ζ , the Hamiltonian with χ , and the canonical coordinates with (Ψ, θ) . The ability to use ζ as a time-like variable requires the coordinate transformation $(r, \theta, \zeta) \rightarrow (\Psi, \theta, \zeta)$ to be nonsingular, i.e. that the Jacobian $\nabla \Psi \cdot \nabla \theta \times \nabla \zeta = B^\zeta$ does not vanish. In this case χ can be considered a function of (Ψ, θ, ζ) , so the equations for a field line are Hamilton's equations for (5):

$$\frac{d}{d\zeta} \Psi = -\frac{\partial}{\partial \theta} \chi(\Psi, \theta, \zeta), \quad \frac{d}{d\zeta} \theta = \frac{\partial}{\partial \Psi} \chi(\Psi, \theta, \zeta). \quad (6)$$

¹ Even in this case, the symbol Ψ differs from the toroidal flux by a factor of 2π , which we ignore here for convenience.

These are nonlinear differential equations for $\Psi(\zeta)$ and $\theta(\zeta)$.

In the (Ψ, θ, ζ) coordinate system, (3) becomes

$$\mathbf{B} = \nabla\Psi \times \nabla\theta - \frac{\partial X}{\partial\theta} \nabla\theta \times \nabla\zeta + \frac{\partial X}{\partial\Psi} \nabla\zeta \times \nabla\Psi.$$

The contravariant components can be read off explicitly using (2.15). Thus the field line equations (6) are equivalently

$$\frac{d\Psi}{d\zeta} = \frac{B^\Psi}{B\zeta}, \quad \frac{d\theta}{d\zeta} = \frac{B^\theta}{B\zeta}, \quad (7)$$

as in (3.18). The system (Ψ, θ, ζ) is called a *canonical magnetic coordinate system*.

It is easy to see that an axisymmetric field yields an integrable Hamiltonian, that is, a set of equations of motion that can be solved to give non-chaotic field lines. Axisymmetry means that the fields are not ζ -dependent, so that X is a function of Ψ and θ only:

$$X = X(\Psi, \theta) \quad (\text{integrable}) . \quad (8)$$

The Hamiltonian is then independent of “time,” and thus a constant of the motion:

$$\frac{d}{d\zeta} X = \frac{\partial X}{\partial\Psi} \frac{d\Psi}{d\zeta} + \frac{\partial X}{\partial\theta} \frac{d\theta}{d\zeta} = 0.$$

Thus each field line lies on a flux surface $X = \text{constant}$. Because of the nature of the variables θ and ζ , these surfaces are tori; the trajectories lie on nested toroidal surfaces defined by various values of the energy X .

All axisymmetric systems are integrable. However, a typical, axisymmetric system is by no means integrable. In fact there is only one other known integrable case: that of helical symmetry. We will discuss in §9.3 the structure of magnetic field lines for the nonintegrable case. Here it is instructive to survey some principal ideas of §3.1 from a Hamiltonian perspective.

Flux coordinates, as defined by (3.12), are a special case of canonical coordinates: those for which X depends only on Ψ ,

$$X = X(\Psi) \quad (\text{flux coordinates}) . \quad (9)$$

This implies that the Hamiltonian, X , is in “action-angle” form: not only is X a constant of motion, but so is Ψ . Furthermore the equation for the poloidal angle reduces to

$$\frac{d\theta}{d\zeta} = \frac{\partial X}{\partial\Psi} = \frac{1}{q} \quad (10)$$

where $q = q(\Psi)$ is the safety factor. Thus the field lines wind around the tori with pitch $1/q$. In fact we can integrate (10) easily to obtain

$$\theta(\zeta) = \theta_0 + \zeta/q . \quad (11)$$

When $q = m/n$ is rational, (11) shows that θ returns to its initial value θ_0 (modulo 2π) after a finite number of toroidal circuits

$$\theta(2\pi m) = \theta_0 + 2\pi m/q = \theta_0 + 2\pi n. \quad (12)$$

Thus each field line is closed on the rational surface. When q is irrational, (12) shows that q never comes back to its initial value (modulo 2π). Thus the field lines on irrational surfaces never close; in fact they come arbitrarily close to any point on the surface.

In general $q(\Psi)$ varies from flux surface to flux surface: the field is sheared. In this case $q(\Psi)$ is almost always irrational. Thus most magnetic surfaces are densely covered by never-ending field lines.

Even when $X(\Psi, \theta)$ is not in action-angle form, the dynamics is easily described. A theorem of Poincaré implies that the field lines have, on the average, a pitch that is either rational or irrational; recall the argument in §3.3. The safety factor $q(\Psi)$ still exists, but it is not simply related to a derivative of X .

Reconnection

When the equilibrium magnetic field is integrable, any two fluid elements on an irrational magnetic surface are connected by a single field line. Under evolution governed by the ideal law (6.82), the fluid elements are still on a single field line at any later time. Fluid elements can never merge, by mass conservation; thus they remain on a topological torus, covered by a single field line. In the case of a system with shear, the same argument applies on every irrational surface, and since these are dense, every magnetic surface must remain toroidal.

Such *topology preserving* change in a magnetic field, enforced by ideal MHD, is atypical: a generic perturbation breaks the torus. This crucial circumstance is illustrated by the following simple example.

Suppose the unperturbed coordinates are flux coordinates, and that the perturbation is not large enough to violate $B\zeta \neq 0$. Then we can represent the full, perturbed field in the same coordinate system, except that the “Hamiltonian” will be modified

$$X \rightarrow X_0(\Psi) + \delta X(\Psi, \theta, \zeta).$$

Physical quantities must be periodic in θ and ζ , and since only derivatives of X enter \mathbf{B} , we can assume that X is periodic. Thus

$$X = X_0(\Psi) + \sum_{m,n} \delta X_{m,n}(\Psi) e^{i(m\theta - n\zeta)}, \quad (13)$$

yielding the equations of motion

$$\frac{d}{d\zeta} \Psi = -i \sum_{m,n} m \delta \chi_{m,n} e^{i(m\theta - n\zeta)} . \quad (14)$$

$$\frac{d}{d\zeta} \theta = \frac{1}{q} + \sum_{m,n} \delta \chi'_{m,n} e^{i(m\theta - n\zeta)} . \quad (14)$$

These equations are too difficult to solve analytically. In fact, as we will see in §9.3, they lead in general to magnetic chaos.

When $\delta\chi$ is small, the lowest order motion from (14) has $\Psi(\zeta) = \Psi_0 = \text{constant}$ and $\theta(\zeta)$ given by (11). To obtain the first correction, we use these lowest order results in the perturbation terms of (14). Then (14) can be integrated explicitly, giving, for example,

$$\Psi(\zeta) = \Psi_0 + \sum_{m,n} \frac{m q \delta \chi_{m,n}(\Psi_0)}{n q - m} e^{i[m\theta_0 - (n-m/q)\zeta]} . \quad (15)$$

This expression determines the radial motion of the field line to lowest order. However, it fails dramatically near rational surfaces: wherever $q(\Psi) \simeq m/n$ for some m and n , the denominator can become small enough to violate the assumption that the field line was only weakly perturbed. If $\delta \chi_{m,n}$ is nonzero for many (m, n) , as in the typically case, then (15) fails at almost all radii. (This issue is of course that addressed by the Newcomb condition in §3.3.)

One might think that with sufficiently clever manipulation, we could solve (14) in such a way that resonant denominators do not occur. In fact resonance is unavoidable; it signals the appearance of a new phenomena: the reconnection of field lines to form new topological structures. To illuminate the topology change, consider (14) near a particular rational surface with $q = q_s \equiv m_0/n_0$. Equation (15) suggests that the most important terms will be those having the helicity m_0/n_0 . After discarding all the other helicities in (13), we have

$$\chi \approx \chi_0 + \sum_{\mathbf{k}} \delta \chi_{km_0,kn_0} e^{i\mathbf{k}(m_0\theta - n_0\zeta)} ,$$

or, after reversing the Fourier transform,

$$\chi \approx \chi_0(\Psi) + \delta \chi \left(\Psi, \theta - \frac{\zeta}{q_s} \right) . \quad (16)$$

The Hamiltonian (16) is completely integrable: to integrate it, change coordinates from (Ψ, θ) to (Ψ, α) , where

$$\alpha = \theta - \frac{\zeta}{q_s} . \quad (17)$$

is a helical variable. The effective Hamiltonian in the new variables is obtained by applying the transformation (17) to (2):

$$\mathbf{A} = \Psi \nabla \alpha - \chi_h \nabla \zeta$$

where the helical flux is

$$\chi_h(\Psi, \alpha) = \chi(\Psi, \alpha) - \frac{1}{q_s} \Psi. \quad (18)$$

Since (18) is the Hamiltonian in the new coordinate system, and it is independent of ζ , the new field line equations are integrable.

Now (16) is valid only near Ψ_s , where $q(\Psi_s) = q_s$. Hence it is reasonable to set $\Psi = \Psi_s + x$, and expand, using $\chi'_0 = 1/q_s$ (the primes indicate derivatives with respect to Ψ),

$$\chi_h(x, \alpha) = -\frac{q'_s}{2q_s^2} x^2 + \delta \chi(\Psi_s, \alpha). \quad (19)$$

Here a constant term has been dropped since it does not affect the fields, and q'_s is the shear evaluated at the rational surface. The simplest case is that of the single harmonic $\delta \chi \propto \cos(m\alpha)$, when (19) becomes the pendulum Hamiltonian. In any case (19) has two topologically distinct types of orbits. When $\chi_h < \min(\delta \chi)$, the orbits are untrapped and able to tra-

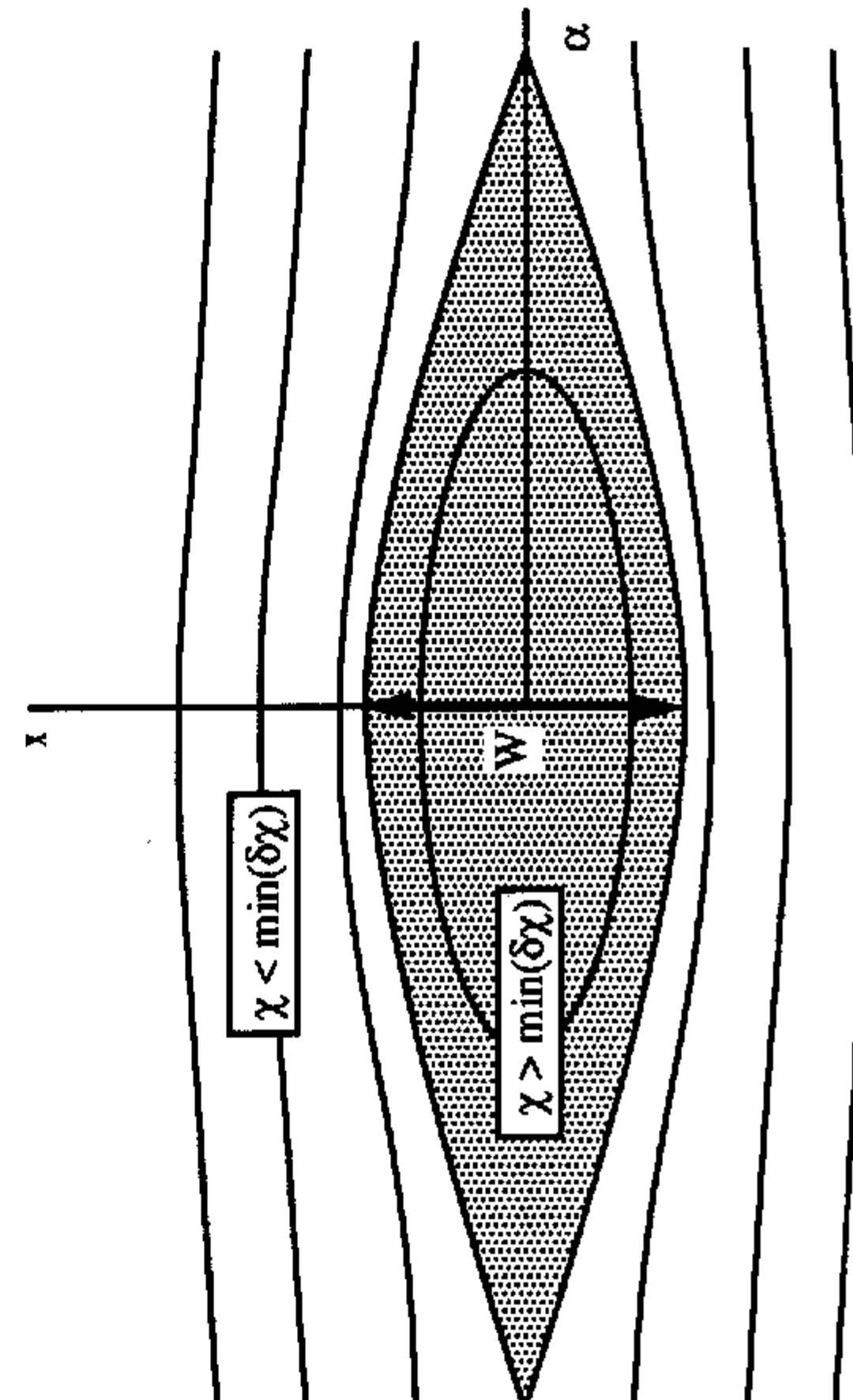


Figure 1. Contours of constant energy for the Hamiltonian (19). The shaded region is the magnetic island. It has width W given by (20). The boundary between trapped and untrapped field lines is the separatrix.

verse the entire range of α . The corresponding magnetic surfaces have the same topology as the original surfaces, being merely distorted. But when $\chi_h > \min(\delta\chi)$, the orbits are trapped: they oscillate over a limited range of α as ζ changes. The resulting magnetic surface consists of tubes that helically encircle the magnetic axis, appearing in cross section as islands. The field lines on the surfaces defined by $\chi_h = \min(\delta\chi)$ correspond to the separatrix of the island. See Fig. 9.2.

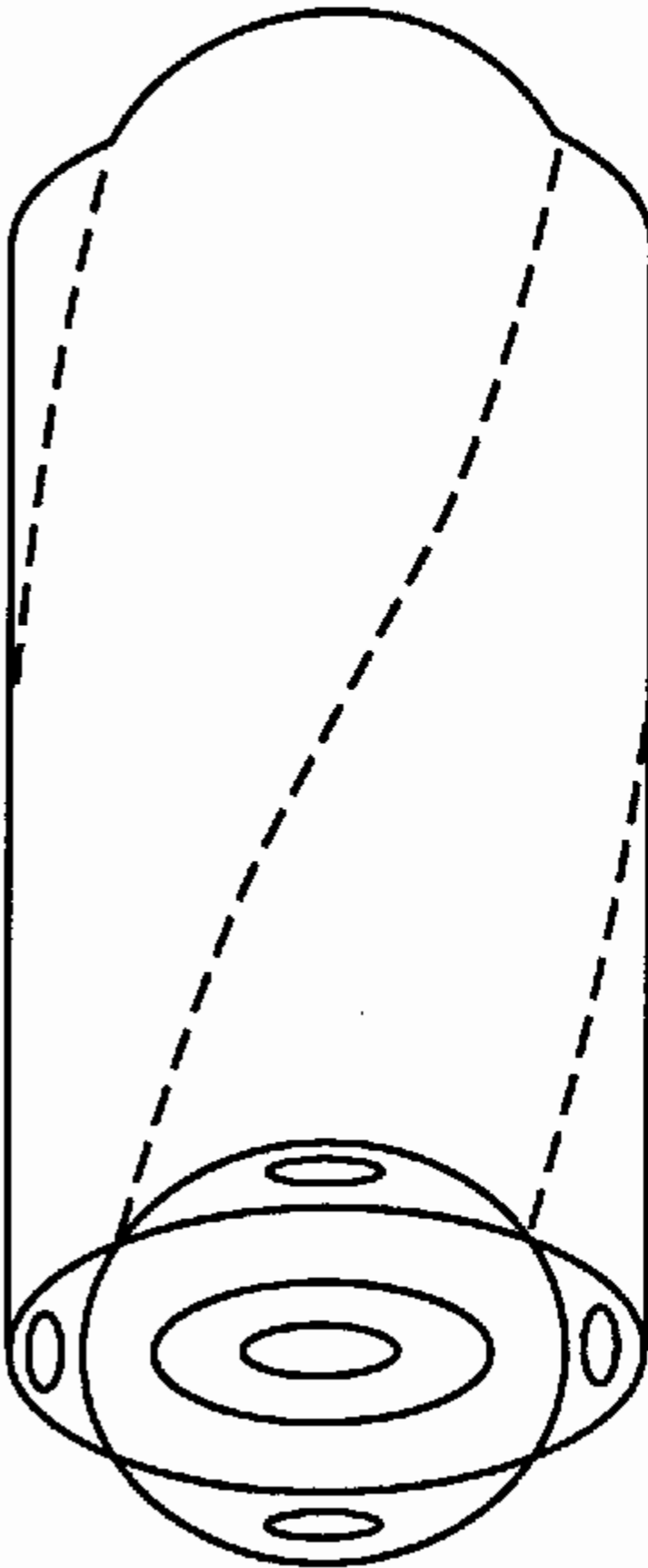


Figure 2. The $(m, n) = (4, 1)$ magnetic island configuration. Shown are the helical paths for the x -point field lines.

In the original (θ, ζ) coordinates there are m islands in any poloidal section, and n in any toroidal cross section. In such an island chain there are typically only two closed field lines with the original helicity of the rational surface: one, for $\chi_h = \max(\delta\chi)$, forms the center of the islands, corresponding to the “ o -point”. The other, for $\chi_h = \min(\delta\chi)$, forms the edge of the islands, or the “ x -point”. These field lines close after m toroidal and n poloidal circuits. The o -point field lines are at the center of the islands, which have a width

$$W = \sqrt{\frac{8q_s^2}{q'} \|\delta\chi\|} \quad (20)$$

measured in units of Ψ , where $\|\delta\chi\| = \max(\delta\chi) - \min(\delta\chi)$. Note that the width is proportional to the square root of the perturbation size. This is why the expansion leading to (15) failed.

When W is small, it is reasonable to expect the behavior of the full Hamiltonian (16) to be similar to that given by (19), when χ is close to the rational surface. Just how small α must be for (19) to apply is discussed in §9.3.

Islands and Linear Theory

Next we recall the discussion of magnetic perturbations in §7.3. The magnetic island structure that results from a generic field perturbation resolves the singularity of magnetic differential equation (7.26): adding the nonlinear Newcomb terms to (7.26) means that the operator $\mathbf{B}_0 \cdot \nabla$ is replaced by $\mathbf{B} \cdot \nabla$, the full magnetic field. This field no longer has a rational surface. The boundary layer width for the nonlinear system—the width over which the nonlinear terms are important—is the island width W . We will discuss the solution of the Newcomb equation for these fields in the next section.

An alternative way to resolve the singular layer is to add the linear vorticity terms to (7.26), as discussed in §7.8. If these terms dominate the nonlinear terms, then linear theory provides the appropriate resolution of the boundary layer. Unfortunately, since the nonlinear island width is proportional to $\sqrt{\delta\chi}$, and linear terms are proportional to $\delta\chi$ by definition, the former always appear to be more important than the latter for $\delta\chi \rightarrow 0$. To see that linear theory can nonetheless pertain, we must consider the boundary layer widths. The linear boundary layer width w depends on the frequency and collisionality regime of the instability. When

$$w \gg W \quad (21)$$

i.e., when the linear width exceeds the nonlinear width, then matching with the exterior region involves only linear theory. In the region $W \ll |x| \ll w$, one is well outside the separatrix, so the structure of the field lines is approximately given by linear theory, (15); that is, linear theory applies over most of the boundary layer. In the linear boundary layer the characteristic scale of the perturbation is governed by w , and the equations are not singular, so while there is indeed an island structure in the region $|x| < W$, it has negligible effect on the evolution of the instability.

It is only when the magnetic island becomes comparable to the linear boundary layer that the nonlinear terms begin to influence the matching problem. When $W \gg w$, then nonlinear theory governs the evolution.

9.2 Coherent Nonlinear Islands*

To treat the effects of nonlinearity on tearing mode evolution we return to the simplest of the fluid models: large aspect ratio, reduced MHD, as derived in §7.4. We study the nonlinear evolution of the simplest tearing mode: the resistive, small- Δ' mode, whose dispersion relation given by (7.157). The following analysis is due to Rutherford (Rutherford, 1973).

The equations of motion are given by (7.62), without the pressure

terms:

$$\begin{aligned} \frac{1}{v_A^2} \frac{d}{dt} U &= -\nabla_{\parallel} J \\ \frac{1}{c} \frac{\partial \psi}{\partial t} + \nabla_{\parallel} \varphi &= \frac{\eta c}{4\pi} J , \end{aligned} \quad (22)$$

where $\nabla_{\parallel} = \frac{1}{R_0} \frac{\partial}{\partial \zeta} - \epsilon[\psi,]$, and $J = \nabla_{\perp}^2 \psi$. Corresponding to the parallel gradient is the magnetic field $\mathbf{B}_0 = B_0(\hat{\zeta} + \epsilon \nabla \psi \times \hat{\zeta})$, obtained from the vector potential $\mathbf{A} = B_0(r^2/2\nabla\theta + a\psi \nabla\zeta)$. For comparison with the previous section we set $\chi = -B_0 a\psi$ and $\Psi = B_0 r^2/2$. Then (6) provides the equations for field line flow

$$\frac{r \frac{dr}{d\zeta}}{a} = \frac{\partial \psi}{\partial \theta}, \quad \frac{r \frac{d\theta}{d\zeta}}{a} = -\frac{\partial \psi}{\partial r}.$$

In the case of a tearing mode with helicity (m_0, n_0) , $\psi = \psi_0(r) + \delta\psi(\theta - \zeta/q_s)$, which is the same perturbation considered in (16). The helical Hamiltonian (18) becomes

$$\psi_h(r, \alpha) = \frac{r^2}{2aq_s} + \psi(r, \alpha)$$

Expanding in the neighborhood of $q(r_s) = q_s$, as in (19), gives

$$\psi_h(x, \alpha) \approx -\frac{r_s q'_s}{2a q_s^2} x^2 + \delta\psi(r_s, \alpha) . \quad (23)$$

For a linear tearing mode,

$$\delta\psi(r_s, \alpha) = \delta\psi(t) \cos(m_0 \alpha) \quad (24)$$

and (23) is equivalent to the pendulum Hamiltonian. Time enters the field lines equations only as a parameter.

We begin by considering the nonlinear shear-Alfvén law (22). We assume (and verify below) that the inertia term is negligible. Thus the island evolution is constrained by the relation

$$\nabla_{\parallel} J = 0 . \quad (25)$$

This of course is the nonlinear version of (7.26), the neighboring equilibrium equation. However (25) has an entirely different significance: rather than describing some “exterior” region, it is presumed to hold everywhere, including arbitrarily close to the equilibrium rational surface. It is not singular at the rational surface because it involves the nonlinear parallel gradient. Schematically

$$\nabla_{\parallel} J = \mathbf{b}_0 \cdot \nabla J + \mathbf{b}_1 \cdot \nabla J . \quad (26)$$

For a single helicity perturbation, the first term on the right-hand side of (26) vanishes at q_s . In linear theory this term alone acts on the perturbation, giving the linear singularity. Its nonlinear resolution results from the second term, which therefore plays a role similar to inertia in the linear case. The width W measures the region in which the second term, $\mathbf{b}_1 \cdot \nabla J \sim k_{\perp} \delta\psi J/W$, is comparable to the first, $\mathbf{b}_0 \cdot \nabla J \sim k'_{\parallel} W J$, consistent with $\delta\psi \sim W^2$ as usual.

Equation (25) implies that J is constant along the field lines. Therefore, since the field line flow is Hamiltonian, J is a function of the constants of motion of the flow (see also §3.5). In general there are two such constants, since there are two equations of motion; these can be taken to be the Hamiltonian defining the flux surface, and a field line label, representing the initial condition on the flux surfaces. However, as discussed in §3.3, any smooth function must be independent of field line label when there is shear. Thus we can express the solution of (25) as

$$J(r, \alpha) = J(\psi_h) \quad (27)$$

where $J(\psi_h)$ is an undetermined function.

To determine the evolution we use Ohm's law, (22). Notice that a flux surface average (with respect to the perturbed surfaces) will eliminate the electrostatic term,

$$\langle \nabla_{\parallel} \varphi \rangle = 0 .$$

However, since J is a flux function, the average leaves the right-hand side of Ohm's law unchanged. Hence we have

$$\left\langle \frac{\partial \psi}{\partial t} \right\rangle_{\psi_h} = \frac{\eta c^2}{4\pi} J . \quad (28)$$

This is effectively a diffusion equation for ψ ; however, it is highly nonlinear because of the flux surface average.

In fact, because electrostatic effects have been eliminated, (28) resembles the current channel equation (7.197), and it is amenable to a similar analysis. We integrate (28) over a radial width that much exceeds w and W , but within which the helical part of ψ , that is, the second term in (23), is nearly constant in radius; such a domain exists when

$$\Delta' W \ll 1 , \quad \Delta' w \ll 1 .$$

In this case (23) is valid over the layer: $\delta\psi$ can be considered constant in radius, while the axisymmetric part of ψ can be expanded about the rational surface. Further, to obtain the m th Fourier harmonic of (28), we multiply it by $\cos(m\alpha)$ and integrate over α . Recalling that Δ' is defined, by (7.147), to be the total helical current in the layer we see that

$$\int_{-\infty}^{\infty} dx \oint d\alpha \cos(m\alpha) \left\langle \frac{\partial \psi}{\partial t} \right\rangle_{\psi_h} = \frac{\eta c^2}{4} \int_{-\infty}^{\infty} dx J_m = \frac{\eta c^2}{4} \Delta' \delta\psi . \quad (29)$$

The flux surface average is given by (3.38). Converting to (x, α, ζ) coordinates, and noting that near the rational surface the Jacobian $\nabla x \cdot \nabla \alpha \times \nabla \zeta$ is constant we find

$$\langle A \rangle_{\psi_h} = \frac{\oint \frac{d\alpha}{|d\psi_h/dx|} A}{\oint \frac{d\alpha}{|d\psi_h/dx|}}. \quad (30)$$

The flux function is ψ_h given by (23).

Next we assume that the only disturbance with significant amplitude is a single tearing mode, with $\delta\psi$ having the form of (24). The validity of this assumption can be questioned on two grounds: there may be other harmonics present with the same helicity, and there may be different helicities present. Higher harmonics are not likely because Δ' is generally positive only for small values of m . Thus modes with high m are either linearly damped, or grow much more slowly, and will not reach the nonlinear regime as quickly. We will discuss the effect of multiple helicities presently. Substitution of (23) and (30) into (29) gives

$$2 \frac{\partial \delta\psi}{\partial t} \int_{-\infty}^{\delta\psi} d\psi_h \langle \cos(m\alpha) \rangle_{\psi_h}^2 \oint \frac{d\alpha}{|d\psi_h/dx|} = \frac{\eta c^2}{4} \Delta' \delta\psi \quad (31)$$

where we have changed integration variables from x to ψ_h . The crucial point of (31) is in the flux surface average $\langle \cos(m\alpha) \rangle^2$. When x exceeds the island width W , the flux surfaces of ψ_h nearly coincide with those of ψ , and are therefore α -independent. Hence the average of $\cos m\alpha$ nearly vanishes for $x \gg W$. For smaller x , that is, within or close to the island separatrix, averaging at fixed ψ_h involves a limited range of α , in which $\cos m\alpha$ is predominantly positive. Thus, because of (27), the m th Fourier component of J is localized to the island region.

Quantitatively we can see this localization by using (23) to obtain

$$\left| \frac{d\psi_h}{dx} \right| = \left| \frac{r_s q'_s}{aq_s^2} x \right| = \left[\frac{r_s q'_s}{aq_s^2} (\delta\psi \cos m\alpha - \psi_h) \right]^{1/2},$$

which implies that (31) can be written

$$\frac{\partial \delta\psi}{\partial t} = \frac{\eta c^2}{8C} \left(\frac{r_s q'_s}{aq_s^2} \right)^{1/2} \Delta' \sqrt{\delta\psi}. \quad (32)$$

Here C is a numerical coefficient, defined by

$$C = \int_{-1}^{\infty} dz \left(\int_0^{2\pi} d\theta \frac{\cos \theta}{\sqrt{z - \cos \theta}} \right)^2 \left(\int_0^{2\pi} d\theta \frac{1}{\sqrt{z - \cos \theta}} \right)^{-1}. \quad (33)$$

It is straightforward to express C in terms of elliptic functions, and show that $C \approx 0.7$.

Since the island width (in units of ψ) is $W = 4(\delta\psi a q_s / r_s q'_s)^{1/2}$, (32) can be simply expressed as

$$\frac{dW}{dt} = \frac{\eta c^2}{16C} \Delta'. \quad (34)$$

Thus, in the nonlinear regime, the island width grows linearly with time; this is the key conclusion of Rutherford's theory. The rate of growth of the tearing mode in this regime can be compared to the resistive diffusion time $\tau_R = 4\pi a^2/\eta c^2$, so that

$$\frac{1}{a} \frac{dW}{dt} \sim \frac{\Delta' a}{\tau_R}. \quad (35)$$

The growth is therefore much slower than during the (exponential) linear phase.

The Rutherford theory has been generalized to other collisionality regimes, and other $\delta\psi$ regimes. For the collisionless regime it is found that the island growth terminates at the current channel width x_* . More realistically however, the evolution becomes semi-collisional as the saturation is approached, and the ultimate behavior is similar to (34). In the large $\delta\psi$ case, the evolution continues to be exponential far into the nonlinear regime.

9.3 Multiple Helicity Fields: Island Overlap Criterion

When there are many helicities present, such as in (13), the single helicity approximation leading to the integrable Hamiltonian (18) may break down. To see when this occurs, consider first the effect of each helicity individually. Each helicity in (13) gives rise to an island with a width given by (20), $W_{m/n}$. For $|x| \gg W_{m/n}$ the perturbation due to the m/n island is small; indeed (15) implies that it falls off as the inverse of the distance from the surface. Thus when the two islands are separated by a distance much larger than the sum of their half widths, the single-helicity approximation should be reasonable for each rational surface independently. Otherwise, each island perturbs the surfaces of the other in a significant way, and the single helicity approximation is invalid.

Thus consider two islands, with widths W_1 and W_2 , and denote the distance between their rational surfaces by $\Delta\Psi_{12}$. Then the single helicity approximation breaks down when

$$\Delta\Psi_{12} \sim \frac{1}{2} (W_1 + W_2). \quad (36)$$

This is known as the *overlap criterion*, because in this case the separatrices of the islands appear to overlap (see Fig. 9.3). It was first formulated by Chirikov (Chirikov, 1979). Now the spectrum of perturbations does not

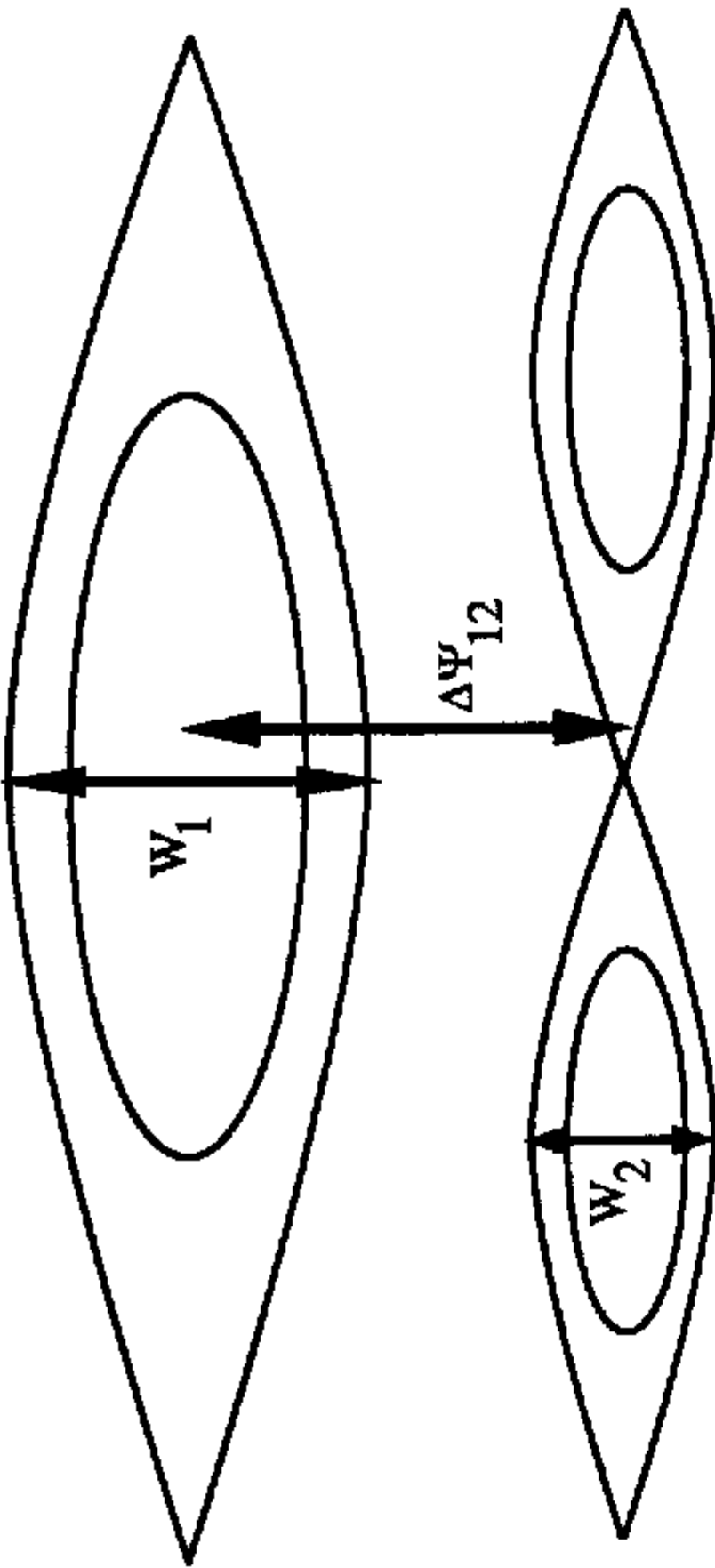


Figure 3. Magnetic islands and the overlap criterion.

simply consist of two islands, but one for each value of n ; thus the overlap criterion must be computed for each pair in turn. As $n \rightarrow \infty$ one might expect that all islands of any size overlap. However, this is not necessarily the case. Letting $q(\Psi_1) = m/n$ and $q(\Psi_2) = m'/n'$, and expanding for Ψ_2 close to Ψ_1 we see that

$$\Delta\Psi_{12} = \Psi_2 - \Psi_1 \approx \frac{1}{q'} \left(\frac{m'n - mn'}{nn'} \right). \quad (37)$$

The most stringent case occurs for the case of “neighboring” rationals, those for which

$$m'n - n'm = \pm 1$$

(for example 2/1 and 3/2 are neighbors in this sense). In this case $\Delta\chi$ decays for large n as $1/nm' \sim 1/n^2$. On the other hand, the island sizes are proportional to $\sqrt{\delta\chi_{m,n}}$, which typically decays more rapidly with n . In fact any smooth perturbation (one for which all derivatives exist) has a spectrum that decays at least exponentially in the mode numbers. Thus only small or moderate values of n are associated with island overlap.

Two neighboring islands, on nearby rational surfaces, which have similar amplitudes, overlap when the ratio

$$s = \frac{1}{2} \frac{W_1 + W_2}{\Delta\Psi_{12}} \approx nm\sqrt{8q' \parallel \delta\chi_{m,n} \parallel} \quad (38)$$

is larger than one. The parameter “ s ” is called the overlap parameter. [Numerical computations show that the magnetic surfaces between two islands are destroyed when $s \sim 1/2$ rather than $s \sim 1$. This is because of nonlinear effects that distort the island shapes, and give rise to islands with other helicities.]

A more formal statement is given by the KAM theorem (Arnol'd, 1978). Roughly speaking, this theorem states that if $\delta\chi$ is smooth enough and

small enough, then most of the original ($\delta\chi = 0$) magnetic surfaces survive the perturbation. These surfaces are those “far” from any of the rational surfaces. Being far from all rationals seems to be a rather stringent requirement since we have already seen that every rational magnetic surface is destroyed and replaced by an island. In the theorem, far from rationals is defined as

$$|nq - m| > C/n^\tau$$

for all (m, n) and some $\tau \geq 1$. It is a simple exercise to show that when $\tau > 1$ the set of such q 's is very large, provided that C is small; thus, as C approaches zero, almost all surfaces are far from rationals. In the KAM theorem the value chosen for C is linked to the size of the perturbation. The theorem ensures that for small amplitude perturbations, most magnetic surfaces are preserved, and the single helicity approximation gives a reasonable picture of their structure near rational surfaces.

When the island overlap criterion is satisfied, the field lines with helicities between those of the two overlapping islands are now caught by the islands. When a field line is trapped within one island, it has the helicity of that island; however, when the islands overlap, numerical solution of (13) shows that field lines move sometimes with one helicity and sometimes with the other. This transition from helicity to helicity occurs at intervals that depend sensitively on which field line is followed. Such “sensitive dependence on initial conditions” is called *chaos*.

An effective way to see the effect of overlapping islands is to view

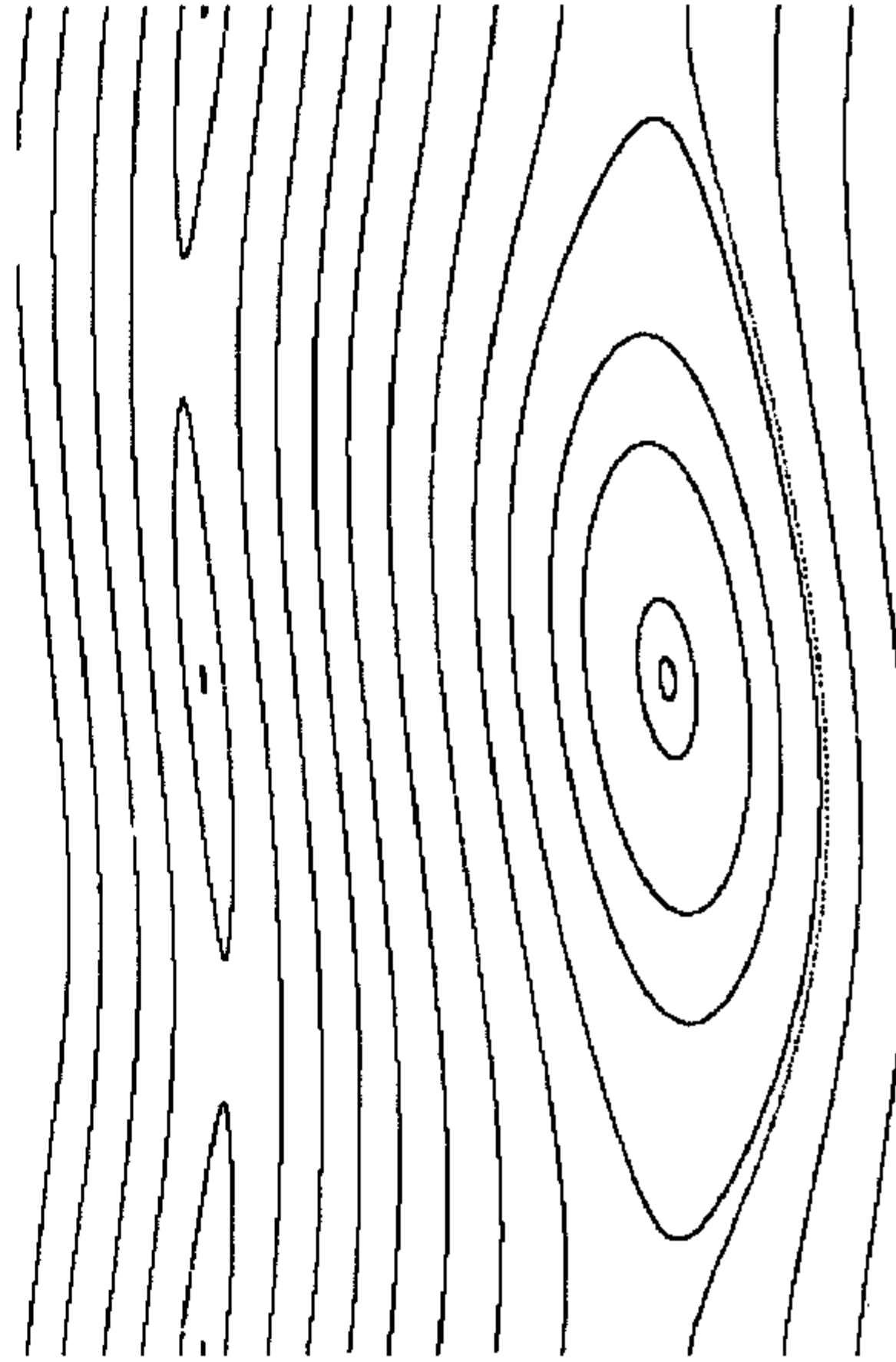


Figure 4. Cross section of magnetic field lines for nonoverlapping islands.

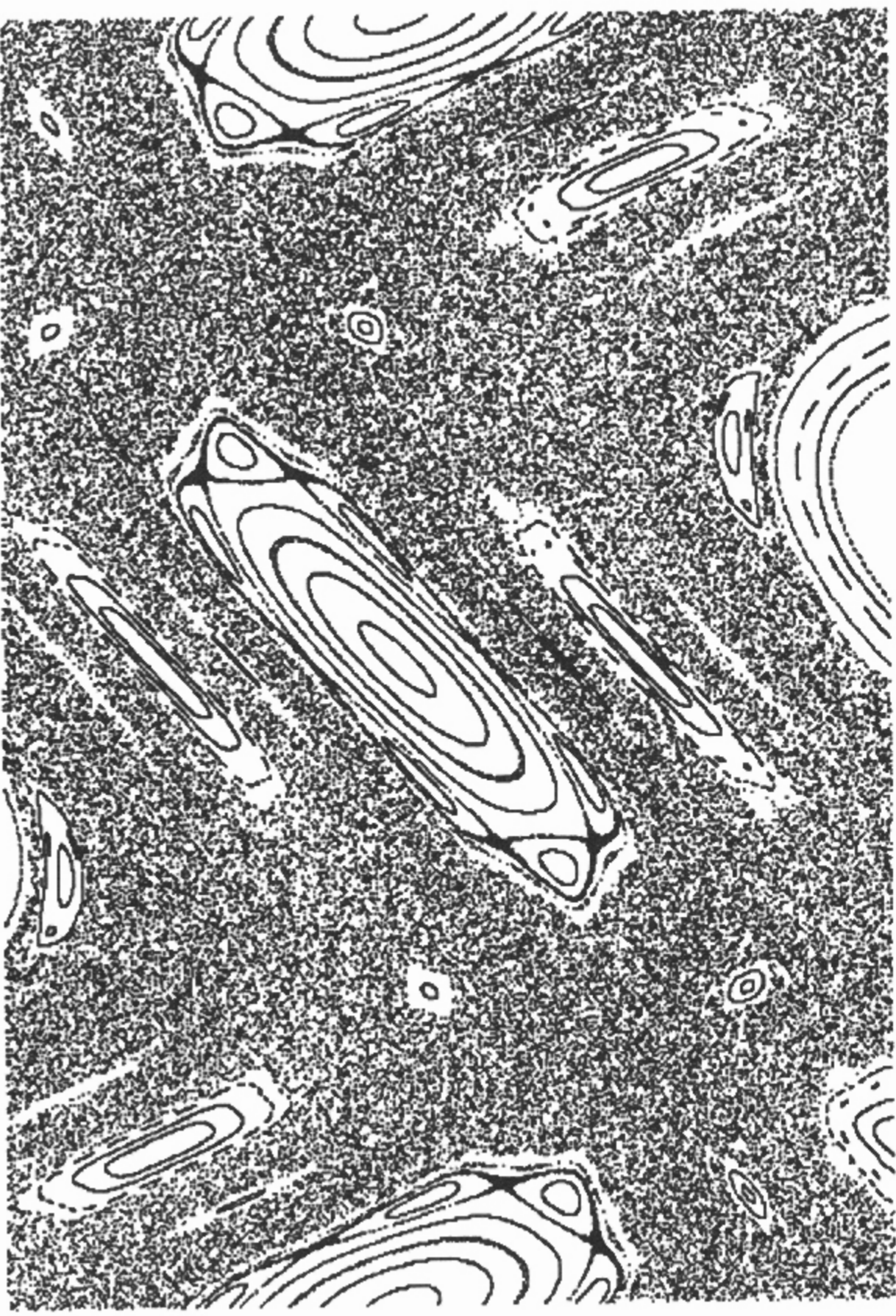


Figure 5. Magnetic field lines for overlapping islands, $s \sim 1$. The scattered points are on chaotic lines.

the field lines as they pierce a surface, such as the cap S_T discussed in §3.1. Upon each toroidal circuit, a field line pierces S_T , creating a dot. For irrational magnetic surfaces these dots eventually cover a curve on S_T . An example of such a plot is shown in Fig. 9.4 when $s < 1$. Here the horizontal coordinate is θ , and the vertical coordinate represents a small range in Ψ . Islands with two helicities are visible. As s increases the islands overlap. Then, while some lines are still trapped in islands, the field lines that are not near the o -points of the islands move chaotically across the islands. The resulting surface shows a random looking splatter of dots created by the chaotic lines. For $s \gg 1$, most field lines look chaotic, and the section consists of a nearly uniform splatter of dots.

When $s \gg 1$ the numerical analysis suggests that the field line motion resembles more a random process than a deterministic one. Numerically one observes that field lines beginning close together separate rapidly; in fact the separation is observed to grow exponentially with distance along the field:

$$d \sim e^{\lambda \zeta}$$

where λ is referred to as the Lyapunov exponent. This exponential divergence underlies the phrase “sensitive dependence on initial conditions;” any initial uncertainty in position grows exponentially with distance along the line.

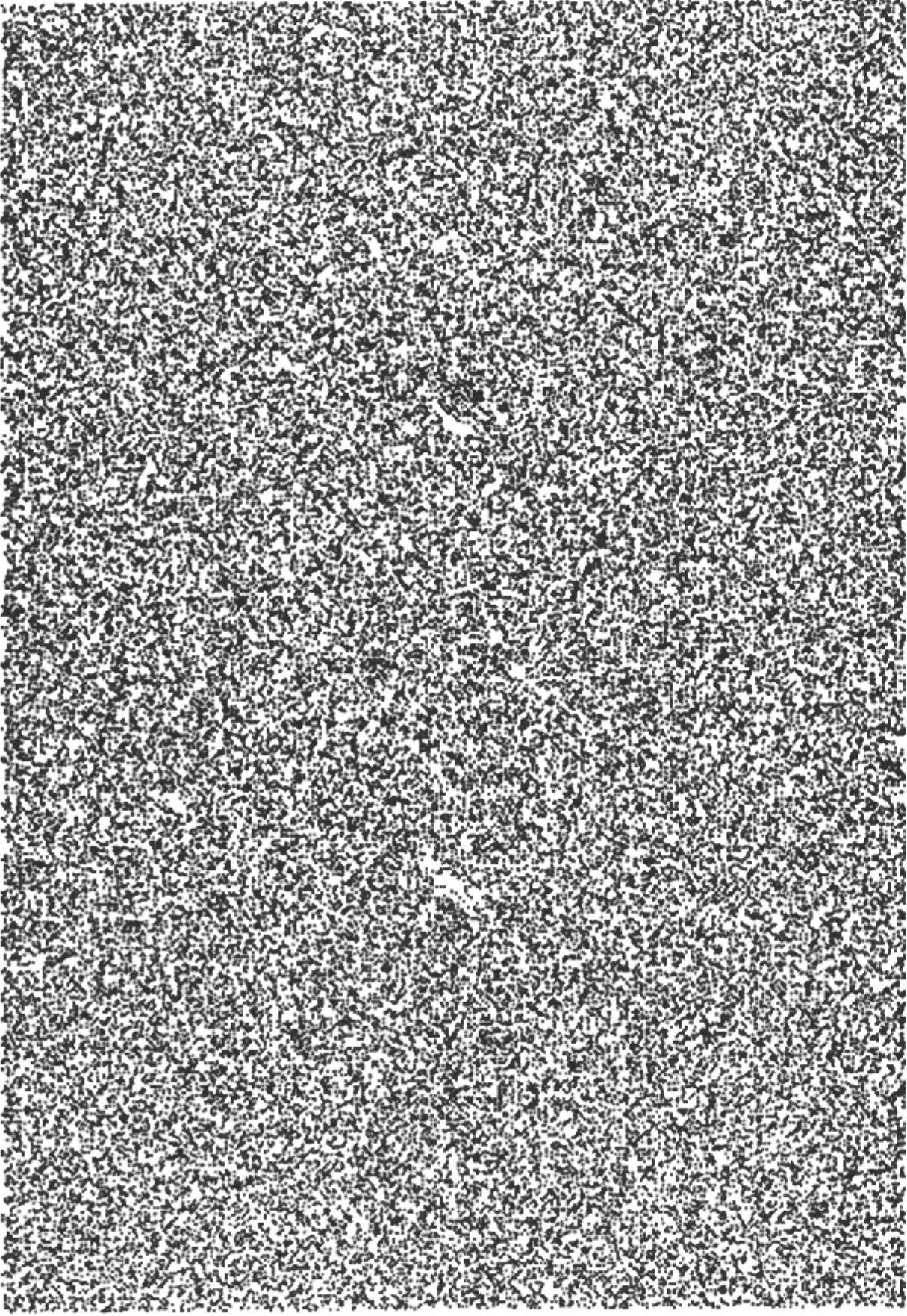


Figure 6. Magnetic field lines for $s \gg 1$, when most field lines appear chaotic.

Field Line Diffusion

When the magnetic islands are strongly overlapping, the angular position of the field line can be treated as a random variable. The basic idea is that small changes in radial position of a field line result in large changes in its poloidal position after a toroidal circuit; this is due to the shear.

To see this, consider again the equations of motion (14). Within an island width of the rational surface, the resonant terms in (14) are dominant. Using (11) to determine the θ evolution we find

$$\frac{d}{d\zeta} \Psi \approx -i \sum_{m,n} m \delta \chi_{m,n} e^{im\theta_0} \delta_{nq-m} . \quad (39)$$

Here the Kronecker δ represents a function which is nonzero over the width of the island. Thus after a toroidal circuit

$$\Delta \Psi \approx -2\pi i \sum_{m,n} m \delta \chi_{m,n} e^{im\theta_0} \delta_{nq-m} . \quad (39)$$

Next consider the evolution of poloidal angle, θ . The simple expression (11) is incorrect not only because of the neglect of the $\delta\chi$ terms in (14), but also because of the Ψ dependence of q : magnetic shear. To see the effect of shear, we note that the corresponding error in θ is

$$\Delta\theta \approx -\frac{q'}{q^2} \Delta\Psi .$$

Using the overlap parameter (38), this can be rewritten

$$m\Delta\theta \sim \frac{\pi s^2}{4m^2}. \quad (40)$$

Since $s > 1$ in the chaotic limit, the uncertainty in θ after a toroidal circuit can easily be $\mathcal{O}(1)$.

We conclude that on each circuit Ψ changes by an amount, (39), depending upon the initial angle θ_0 , while the angle is uncertain by $\mathcal{O}(1)$. Therefore, in repeated applications of (39), it is appropriate to treat θ_0 as a random variable. The radial motion thus resembles a random walk, with a step size $\Delta\Psi$ and time step $\Delta\zeta = 2\pi$. The corresponding diffusion coefficient is

$$D_M(q) \equiv \frac{\langle \Delta\Psi^2 \rangle_\epsilon}{2\Delta\zeta} = \pi \sum_{m,n} |m\delta\chi_{m,n}|^2 \delta_{nq-m}. \quad (41)$$

Here $\langle \dots \rangle_\epsilon$ represents an ensemble average over the variable θ_0 . Equation (41) is known as the *quasilinear* magnetic diffusion coefficient (Chirikov, 1979), because of the resemblance of its derivation to that of ordinary quasilinear theory. The diffusion coefficient changes with radius since the nonzero terms in the sum are the resonant ones.

To express (41) in more useful coordinates, note that a step $\Delta\Psi$ is equivalent to $\Psi_r \Delta r$, and that, according to (3), $B_T \sim \Psi_r/r$. Therefore

$$\Delta\Psi = rB_T\Delta r.$$

Furthermore (3) implies that the radial component of the perturbed field is

$$\delta B_{m,n} \approx \frac{m}{rR} \delta\chi_{m,n}.$$

Using these expressions in (41) gives

$$\frac{\Delta r^2}{2\Delta\zeta} = \pi R^2 \sum_{m,n} \left(\frac{\delta B_{m,n}}{B_T} \right)^2 \delta_{nq-m}. \quad (42)$$

Corrections to the quasilinear diffusion coefficient can be obtained by noting that the phase is not completely decorrelated after a single toroidal circuit. Keeping these correlations results in an asymptotic series for D in inverse powers of s ; the large s limit is (41) (Lichtenberg, 1982).

9.4 Anomalous Particle Transport

When the transport coefficients in experiments differ significantly from the neoclassical predictions, the transport is said to be “anomalous.” In fact it

is not uncommon for the diffusion coefficients inferred from tokamak experiments to exceed neoclassical predictions by two orders of magnitude or more, especially with regard to electron diffusion. The study of anomalous transport is a rapidly evolving field of current research. In this section we attempt only an introduction to the simplest anomalous diffusion laws.

Electromagnetic Transport

When the magnetic field lines are chaotic, the concept of particle confinement by toroidal surfaces is no longer valid, and it is reasonable to use the magnetic diffusion coefficient to obtain a test-particle diffusion coefficient. We concentrate on the electrons because of the experimental indications and because electron gyroradii are small enough to make the neglect of drift effects a reasonable first approximation (Rechester, 1978).

In a collisionless plasma, the electrons stream along the field lines with velocity v_{te} , and therefore make a toroidal circuit in time $\Delta t = 2\pi R/v_{te}$. Converting from the magnetic diffusion coefficient (42), which describes the radial diffusion per toroidal circuit, to a test particle diffusion coefficient, which describes the radial diffusion per unit time, gives

$$D_e = \frac{\Delta r^2}{2\Delta t} = \frac{\Delta\zeta}{\Delta t} \frac{\Delta r^2}{2\Delta\zeta} = \pi v_{te} R \sum_{m,n} \left(\frac{\delta B_{m,n}}{B_T} \right)^2 \delta_{nq-m}. \quad (43)$$

When there are collisions, some modification to (43) may be necessary. The primary effect is a reduction in particle diffusion because electrons no longer stream along the field lines. In fact, the streaming would be exactly cancelled if the electron makes a velocity reversing collision and travels along the same field line. However, as discussed in §8.1, the position of the guiding center jumps by $O(\rho_e)$ upon collision. Thus the electron moves to a new field line, which, because of field line chaos, rapidly diverges from the old line. The required condition for the validity of (43) is thus that the mean free path be longer than the Lyapunov length for the magnetic field. When the mean free path is short, diffusion due to magnetic chaos can be much more complicated (Krommes, 1984).

Electrostatic Transport

The dominant guiding center motion perpendicular to \mathbf{B} is the $\mathbf{E} \times \mathbf{B}$ drift. When the electrostatic field includes fluctuating components, $\mathbf{E} \times \mathbf{B}$ diffusion across flux surfaces can result. In the simplest model, we assume \mathbf{B} is constant. Then the perpendicular drift is strictly two-dimensional:

$$\frac{d\mathbf{x}}{dt} = \frac{e}{B} \mathbf{b} \times \nabla\Phi.$$

If we introduce the dimensionless time $\tau = \Omega t$, these equations can be expressed as

$$\frac{d\mathbf{X}}{d\tau} = \frac{\rho^2}{2} \mathbf{b} \times \nabla \left(\frac{e\Phi}{T} \right) . \quad (44)$$

where ρ is the thermal gyroradius as usual. The diffusion coefficient is defined in terms of the rate of growth of the mean square position, as

$$\mathbf{D} = \frac{\langle (\Delta \mathbf{X})^2 \rangle_\epsilon}{2\tau_0} = \frac{1}{2\tau_0} \int_0^{\tau_0} ds \int_{-\infty}^{\tau_0-s} d\tau \langle \dot{\mathbf{X}}(s) \dot{\mathbf{X}}(s+\tau) \rangle_\epsilon ,$$

where the average can be considered to be over initial conditions, or over an ensemble of Φ . We discuss the choice of the time τ_0 presently. When Φ is a stationary random process, or when Φ is time independent, the autocorrelation function in the integral is a function only of the time difference. Then the integral over s cancels the τ_0 in the denominator. Supposing that τ_0 is large compared to the autocorrelation time of the velocity, we find

$$D = \frac{1}{2} \int_0^\infty \langle \dot{\mathbf{X}}(0) \dot{\mathbf{X}}(\tau) \rangle_\epsilon d\tau , \quad (45)$$

which is a standard result. For $\mathbf{E} \times \mathbf{B}$ motion, we use (44) to obtain

$$\mathbf{D} = \frac{\rho^2 \Omega}{8} \int_0^\infty \left\langle \mathbf{b} \times \nabla \left(\frac{e\Phi(\mathbf{X}_0, 0)}{T} \right) \mathbf{b} \times \nabla \left(\frac{e\Phi(\mathbf{X}(\tau), \tau)}{T} \right) \right\rangle_\epsilon d\tau . \quad (46)$$

The inverse- B dependence of the coefficient, $\rho^2 \Omega \sim cT/eB$, is known as the Bohm scaling for diffusion.

Evaluation of the integral in (46) requires knowledge of the orbits, since Φ must be evaluated at $\mathbf{X}(\tau)$. In any case the integration can be estimated as a fluctuation strength times a dimensionless autocorrelation time, τ_{ac} , or $t_{ac} = \tau_{ac}/\Omega$. Thus we obtain

$$D \sim (\rho \Omega)^2 t_{ac} \left\langle \left(\frac{eE}{T} \right)^2 \right\rangle_\epsilon . \quad (47)$$

When the fields are sufficiently weak, the auto-correlation time can be computed from the frequency width of the field spectrum; more generally the autocorrelation time will depend on the particle orbits themselves, which are diffusing.

Present treatments of this fully nonlinear case are not fully satisfactory. They involve various assumptions about the statistics of the electric field—usually an assumption that \mathbf{E} is a stationary Gaussian random process, since it gives tractable integrals (Taylor and MacNamara, 1971). Unfortunately, one of the characteristics of a highly nonlinear system is that the Gaussian approximation often breaks down.

An alternative expression for D is obtained when the fluctuating fields are traced to some specific linear instability process, such as drift waves (Horton, 1984; Horton, 1989). In this case the particle flux can be treated as the average of $n\dot{\mathbf{X}}$. Using (44) for the velocity results in the vector flux [analogous to the radial flux (8.46)]

$$\mathbf{T} = n_0 \frac{cT}{eB} \mathbf{b} \times \left\langle \frac{n_1}{n_0} \nabla \frac{e\Phi}{T} \right\rangle_{\epsilon}. \quad (48)$$

Again the Bohm scaling appears explicitly. Evaluation of this flux requires knowledge of the correlation between density and potential fluctuations. In the case of linear modes, the result (6.183) implies that the flux is proportional to the phase shift Δ between n_1 and Φ . The phase shift is extremely sensitive to the instability mechanism, and does not apply to the fully nonlinear case where one would like to apply (48). In general (48) is most useful in experimental situations where the spectra of Φ and n can be simultaneously measured.

Diffusion coefficients such as (43) or (47) are not manifestly ambipolar: they seem to allow species of different charge to diffuse at different rates. Since ambipolarity has considerable importance, both intrinsically and as a diagnostic on transport anomaly, we next consider it in some generality.

9.5 Ambipolarity and Rotation*

In Chapter 8 we found that collisional diffusion in an axisymmetric system is intrinsically ambipolar, through second order in δ . Here we generalize that discussion, considering asymmetry, higher order terms in the particle flux and noncollisional transport mechanisms. The basic question being addressed is: to what extent and in what way does ambipolarity determine the electrostatic field?

Mobility

To begin we review an elementary transport process that relates a particle flux to the electric field: mobility. For simplicity suppose that the temperature gradient and toroidal electric field both vanish. Then one expects the radial particle fluxes to have the form

$$\Gamma_s = -D_s \left(n + \mu_s n \frac{e\Phi'}{T} \right) \quad (49)$$

in terms of the diffusion coefficients D_s , and mobility coefficients, or mobilities, μ_s . Mobility is crucial whenever the D_s are unequal. Since quasistatic

equilibrium (transport ordering) requires the total charge inside any flux surface to be very nearly constant, we can integrate (8.28) over the volume contained by an arbitrary surface and conclude that

$$\sum_s e_s \int \frac{dV}{V'} (V' \Gamma_s)' = \sum_s e_s \int dr (V' \Gamma_s)' = V' \sum_s e_s \Gamma_s = 0 . \quad (50)$$

Let us simplify as usual by considering the single ion species case: $\Gamma_e = \Gamma_i$. Then (49) and (50) determine the “ambipolar” potential,

$$\frac{e\Phi'}{T} = \frac{n'}{n} \frac{D_i - D_e}{\mu_e D_e - \mu_i D_i} . \quad (51)$$

We will use the word *forced ambipolarity* to describe this path to insuring constant plasma charge; it is the generic path, described in elementary plasma texts.

As noted in Chapter 8, very different considerations apply for axisymmetric collisional transport. First, axisymmetric systems (or, in the collision-dominated regime, all toroidal systems) are automatically ambipolar, satisfying (50) for any radial potential profile. Second, the mobilities in axisymmetric systems (or collision-dominated toroidal systems) vanish. Thus (51) becomes meaningless in the axisymmetric case: both its numerator and its denominator vanish. We use the term *intrinsic ambipolarity* to describe this situation.

Intrinsic ambipolarity in an axisymmetric systems results from collisional momentum conservation, as in (8.68). Notice that (8.68) applies to any dissipative process that conserves local momentum; it therefore constrains many noncollisional transport mechanisms. The lack of mobility should also be widely applicable; stemming from Galilean invariance of the collision operator, it pertains so long as Φ' enters the perturbed distributions only in the form of a displaced Maxwellian, as in (8.161). Hence intrinsic ambipolarity is a robust property of an axisymmetric system.

Quasilinear Theory

Consider the exact plasma acceleration law,

$$\frac{\partial(\rho_m \mathbf{V}_m)}{\partial t} + \nabla \cdot \mathbf{P} = \rho_c \mathbf{E} + \frac{1}{c} \mathbf{J} \times \mathbf{B} , \quad (52)$$

which differs from (6.73) only because the charge density, ρ_c , is included on the right hand side (the subscript on \mathbf{P}_t is suppressed). Here we allow for fluctuating fields, expressing each field variable in terms of its ensemble average and fluctuating contributions; for example

$$\Phi = \langle \Phi \rangle_\epsilon + \delta\Phi = \bar{\Phi} + \delta\Phi ,$$

where $\langle \delta\Phi \rangle_\epsilon \equiv 0$. Of course the field fluctuations will induce fluctuations in the plasma variables; for example

$$\mathbf{P} = \overline{\mathbf{P}} + \delta\mathbf{P}. \quad (53)$$

Here it should be noted that $\overline{\mathbf{P}}$, the nonfluctuating part of \mathbf{P} , is not the same as \mathbf{P} in the absence of fluctuations. However, we do not attempt to compute the rms field fluctuations contained in the averaged fluid variables, restricting our attention to the explicit contributions, from the right-hand side of (52). We also neglect the ensemble-averaged charge density. Thus the average of (52) is expressed as

$$\left\langle \frac{\partial(\rho_m \mathbf{V}_m)}{\partial t} \right\rangle_\epsilon + \nabla \cdot \overline{\mathbf{P}} - \frac{1}{c} \overline{\mathbf{J}} \times \overline{\mathbf{B}} = \langle \delta\rho_e \delta\mathbf{E} \rangle_\epsilon + \frac{1}{c} \langle \delta\mathbf{J} \times \delta\mathbf{B} \rangle_\epsilon.$$

Here the second term on the right-hand side is conveniently expressed in terms of the Maxwell stress tensor (recall §3.11),

$$\delta\mathbf{J} \times \delta\mathbf{B} = \frac{c}{4\pi} (\nabla \times \delta\mathbf{B}) \times \delta\mathbf{B} = \nabla \cdot \mathbf{T}_M, \quad (54)$$

and combined with the plasma stress, as in (3.101),

$$\mathbf{T} = \mathbf{P} + \mathbf{T}_M \quad (55)$$

to write

$$\left\langle \frac{\partial(\rho_m \mathbf{V}_m)}{\partial t} \right\rangle_\epsilon + \nabla \cdot \overline{\mathbf{T}} - \frac{1}{c} \overline{\mathbf{J}} \times \overline{\mathbf{B}} = \langle \delta\rho_e \delta\mathbf{E} \rangle_\epsilon. \quad (56)$$

Finally we assume that the ensemble-averaged magnetic field is axisymmetric, so that it has well-behaved, nested flux surfaces. In that case symmetry coordinates pertain, and the argument of §8.3 applies to (56). Performing the same manipulation that led to (8.59), we obtain, for the flux-surface average of the covariant ζ -component of (56),

$$\langle J^r \rangle_\epsilon = \frac{c}{\chi'} \left(\left\langle \frac{\partial}{\partial t} \rho_m V_{m\zeta} \right\rangle_\epsilon + \frac{d}{d\nu} \langle T_{\zeta}^y \rangle_\epsilon - \langle \delta\rho_e \delta E_\zeta \rangle_\epsilon \right). \quad (57)$$

Here the combined ensemble and flux-surface average is abbreviated by

$$\langle A \rangle_\epsilon \equiv \langle (A)_\epsilon \rangle_s. \quad (58)$$

Equation (57) closely resembles (8.207), and much of the discussion in §8.6 pertains. Notice that the last term in (57) is simply the species sum of the flux,

$$\Gamma_E = -\frac{c}{\chi'} \langle n E_\zeta \rangle, \quad (59)$$

discussed in (8.59); it corresponds of course to the diffusion process given by (48). The most interesting new features of (57) occur in the steady-state limit:

$$\langle J^r \rangle_\epsilon = \frac{c}{\chi'} \left(\frac{d}{d\nu} \langle T_{\zeta}^y \rangle_\epsilon - \langle \delta\rho_e \delta E_\zeta \rangle_\epsilon \right). \quad (60)$$

In so far as the right-hand side of (60) does not vanish, the system is not intrinsically ambipolar; then forced ambipolarity can be used to determine the electrostatic potential.

Our first observation is that most electrostatic perturbations are quasineutral,

$$\delta\rho_e \sim k^2 \lambda_D^2 e n_e \ll e n_e , \quad (61)$$

where k is typical wave number of the disturbance. In that case the last term in (60) is very small: quasineutrality implies intrinsic ambipolarity of the direct electrostatic flux.

A more interesting observation pertains to the first, "viscous" term on the right-hand side of (60). As pointed out by Waltz (Waltz, 1982), the derivative appearing in this term can significantly attenuate its contribution to the radial current. Attenuation occurs when the fluctuations contributing to T_ζ^V have a radial scale-size, δr , that is very small compared to the plasma radius. Then

$$\frac{d}{dV} \langle T_\zeta^V \rangle_\epsilon \sim \frac{\langle T_\zeta^V \rangle_\epsilon}{\delta V} \quad (62)$$

where $\delta V \cong 4\pi^2 R_0 r \delta r$ is the volume of an annulus of radial width Δr . In that case it is appropriate to average the corresponding flux—a third average!—over the annular volume corresponding to some intermediate radial scale, Δr , with

$$\delta r \ll \Delta r \ll a . \quad (63)$$

Explicitly, we obtain the macroscopically pertinent flux from the replacement

$$\frac{d}{dV} \langle T_\zeta^V \rangle_\epsilon \rightarrow \frac{1}{\Delta V} \int_{\Delta V} dV \frac{d}{dV} \langle T_\zeta^V \rangle_\epsilon , \quad (64)$$

where $\Delta V \cong 4\pi^2 R_0 r \Delta r$ is the volume of the annulus. Of course if $\langle T_\zeta^V \rangle$ varied slowly over ΔV , it would not be affected by the average. In the case of (63), however, the average sharply reduces the nonambipolar flux. The point is that since the values of $\langle T_\zeta^V \rangle_\epsilon$ at the integration end-points in (64) are uncorrelated, we can estimate

$$\frac{1}{\Delta V} \int_{\Delta V} dV \frac{d}{dV} \langle T_\zeta^V \rangle_\epsilon \sim \frac{\langle T_\zeta^V \rangle_\epsilon}{\Delta V} . \quad (65)$$

In view of (62), the effect is to reduce the contribution of $\langle T_\zeta^V \rangle_\epsilon$ by a factor of roughly $\delta r / \Delta r \ll 1$. Notice that this conclusion pertains to the direct electromagnetic flux, coming from $\langle T_{M\zeta}^V \rangle_\epsilon$, as well as any electrostatic or electromagnetic contributions to the mean plasma stress $\langle P_\zeta^V \rangle_\epsilon$.

Of course the fluctuations need not satisfy (63). Moreover, even when δr is small, a nonambipolar contribution of order $\delta r / \Delta r$ is not necessarily negligible. Yet it must be said that the electromagnetic contribution to

$\langle J^r \rangle_E$ is usually much smaller than might have been anticipated. In this sense, the intrinsic ambipolarity of an axisymmetric system survives, or nearly survives, the presence of fluctuating fields, and the determination of $\Phi(r)$ remains delicate.

9.6 Summary

Nonlinearity affects plasma evolution far from the equilibrium state. We have not attempted to give a full survey of its effects or even of the possible phenomena, which include nonlinear fluid motions, turbulence, wave-wave and wave-particle interactions, saturation and suppression of instabilities, and so on. Instead we have focused on a few topics whose experimental consequences are relatively well understood.

Magnetic field lines can be treated as a Hamiltonian system. When there are nested toroidal flux surfaces the field line trajectories are integrable, and the Hamiltonian corresponds to the toroidal flux. Only very special configurations are integrable, and most any perturbation of an integrable system will destroy integrability. The primary effect is the occurrence of magnetic islands at every rational surface. These islands can be treated independently if the distance between rational surfaces is large compared to the width of the islands. However, when the island sizes becomes comparable to their separation, the nonlinear interaction causes the field lines to become chaotic.

When a Hamiltonian system is far from the integrable limit, statistical approaches can be used to treat chaotic trajectories. The simplest approach is analogous to quasilinear theory, and leads to a diffusion coefficient depending only on the mean square level of the perturbing forces. For the case of magnetic field lines the implied radial diffusion implies a corresponding particle diffusion since the dominant particle motion is along the field. Similar analysis can be carried out for electrostatic fluctuations, which might arise, for example, from the drift wave instability.

The self-consistent treatment of the effects of nonlinearity was considered only for the case of a single magnetic island arising from the resistive tearing instability: the Rutherford problem. The effects of nonlinearity become important when the island size exceeds the linear resistive layer width; in the nonlinear stage the mode grows much more slowly than in the linear stage.

Anomalous diffusion, unlike collisional diffusion in an axisymmetric system, need not be intrinsically ambipolar, and therefore could determine an ambipolar electrostatic field. However, such circumstances as quasineutrality and short radial correlation lengths conspire to make intrinsic ambipolarity surprisingly robust.

Further Reading on

Hamiltonian Chaos:

Arnol'd, 1978
Lichtenberg and Lieberman, 1982
MacKay and Meiss, 1987

Coherent Nonlinear Evolution:

Rutherford, 1970
Rosenbluth, 1973

Anomalous Transport:

Horton, 1989
Krommes, 1984

Exercises

- 1. Two Wave Overlap.** A standard model Hamiltonian for calculations of island overlap is

$$H = \frac{1}{2} p^2 + A_1 \cos(k_1 x - \omega_1 t) + A_2 \cos(k_2 x - \omega_2 t).$$

- (a) Compute the overlap parameter s .
 - (b) Hamiltonian perturbation theory provides a method to compute higher order corrections to s . Assume that $A_2 \ll A_1$ and use a canonical transformation $F_2(P, x, t)$ to obtain a new set of coordinates, (P, X) , for which the coefficient of $\cos(k_2 X - \omega_2 t)$ is zero (Arnol'd, 1978; Goldstein, 1980).
 - (c) In the new coordinates the Hamiltonian will have additional harmonics, including one with phase $(k_1 + k_2) - (\omega_1 + \omega_2)t$. Use the amplitude of this resonance to compute a corrected value for s .
- 2.** It is sometimes argued that linear tearing-instability theory is rarely pertinent, because even the *equilibrium* confining field has islands, due to field errors, that violate (21). Examine this issue for the special case of the small- Δ' tearing mode, of §7.8. Let δX_e be the flux perturbation due to equilibrium field errors. Find the inequality, corresponding to (21), that δX_e must satisfy, in terms of plasma equilibrium parameters. Then, evaluating the parameters in the Standard Tokamak (recall

problem 3.6), with $L_s \sim R$, estimate how large a field error $|\delta B_e/B|$ is consistent with the linear theory of tearing modes.

3. Compare the diffusion coefficient (43) with neoclassical banana expression (8.96). Using parameters for the Standard Tokamak (recall problem 3.6) estimate the size of $\delta B/B$ in order that (43) dominate neoclassical transport.
4. Show that the contravariant radial component of (48) is consistent with (8.46).
5. Suppose that the electrostatic turbulence arises from a spectrum of linear drift waves, as discussed in §6.6.
 - (a) Evaluate the radial flux from (48) using the model (6.183) for the density.
 - (b) Experimental measurements of electrostatic turbulence typically yield $e\Phi/T \sim \rho_i/a$. Compute D for the Standard Tokamak (recall problem 3.6).
6. Generalize the argument of (62)–(65) by showing that the $\delta r/\Delta r$ reduction factor can apply to electric perturbations, $\delta \mathbf{E}$, as well as magnetic perturbations (without appeal to quasineutrality). Hint: eliminate ρ_c from (56) or (57).

Bibliography

- Adler, R., M. Bazin and M. Schiffer (1975), *Introduction to General Relativity* (McGraw-Hill, New York).
- Antonsen, T.M., Jr. (1978), "Stability of bound eigenmode solutions for the collisionless universal instability," *Phys. Rev. Lett.* **41**, 33-36.
- Antonsen, T.M., Jr. and B. Lane (1980), "Kinetic equations for low frequency instabilities in inhomogeneous plasmas," *Phys. Fluids* **23**, 1205-1214.
- Arnol'd, V.I. (1965), "Conditions for nonlinear stability of the stationary plane curvilinear flows of an ideal fluid," *Doklady Math. Nauk.* **162**, 773-777.
- Arnol'd, V.I. (1978), *Mathematical Methods of Classical Mechanics* (Springer, New York).
- Bateman, G. (1980), *MHD Instabilities* (The MIT Press, Cambridge).
- Bender, C.M. and S.A. Orszag (1987), *Advanced Mathematical Methods for Scientists and Engineers* (McGraw-Hill, New York).
- Berk, H.L. and A.A. Galeev (1967), "Velocity space instabilities in a toroidal geometry," *Phys. Fluids* **10**, 441-450.
- Bernstein, I.B. (1974), "Transport in axisymmetric systems," *Phys. Fluids* **17**, 547-558.
- Bernstein, I.B. and S.K. Trehan (1960), "Plasma oscillations (I)," *Nucl. Fusion* **1**, 3-41.
- Braginskii, S.I. (1965), "Transport processes in a plasma," in *Reviews of Plasma Physics*, M.A. Leontovich (ed.), (Consultants Bureau, New York).
- Catto, P.J., W.M. Tang and D.E. Baldwin (1981), "Generalized gyrokinetics," *Plasma Phys.* **23**, 639-650.
- Chen, F.F. (1974), *Introduction to Plasma Physics* (Plenum Press, New York).
- Chen, L. and A. Hasegawa (1974), "Plasma heating by spatial resonance of Alfvén waves," *Phys. Fluids* **17**, 1399-1403.
- Cheng, C.Z., L. Chen and M.S. Chance (1985), "High-n ideal and resistive shear Alfvén waves in tokamaks," *Ann. Phys.* **161**, 21-47.
- Chew, G.L., M.L. Goldberger and F.E. Low (1956), "The Boltzmann equation and the one-fluid hydromagnetic equations in the absence of par-

- ticle collisions," *Proc. R. Soc. Lond. A* **236**, 112-118.
- Chirikov, B.V. (1979), "A universal instability of many-dimensional oscillator systems," *Phys. Rep.* **52**, 265-379.
- Connor, J.W., R.J. Hastie and J.B. Taylor (1978), "Shear, periodicity, and plasma ballooning modes," *Phys. Rev. Lett.* **40**, 396-399.
- Cowley, S.C., R.M. Kulsrud and T.S. Hahm (1986), "Linear stability of tearing modes," *Phys. Fluids* **29**, 3230-3244.
- Dewar, R.L. and A.H. Glasser (1983), "Ballooning mode spectrum in general toroidal systems," *Phys. Fluids* **26**, 3038-3052.
- Drake, J.F. and Y.C. Lee (1977), "Kinetic theory of tearing instabilities," *Phys. Fluids* **20**, 1341-1353.
- Fisch, N.J. (1987), "Theory of current drive in plasmas," *Rev. Mod. Phys.* **59**, 175-234.
- Freidberg, J.P. (1987), *Ideal magnetohydrodynamics* (Plenum Press, New York).
- Fried, B.D. (1966), "Statistical mechanical foundations," in *Plasma Physics in Theory and Application*, W.B. Kunkel (ed.), (McGraw-Hill, New York).
- Furth, H.P. (1985), "Nonideal magnetohydrodynamic instabilities and toroidal magnetic confinement," *Phys. Fluids* **28**, 1595-1611.
- Furth, H.P., J. Killeen and M.N. Rosenbluth (1963), "Finite-resistivity instabilities of a sheet pinch," *Phys. Fluids* **6**, 459-484.
- Galeev, A.A. (1971), "Diffusion-electrical phenomena in a plasma confined in a tokamak machine," *Sov. Phys. JETP* **32**, 752.
- Galeev, A.A. and R.Z. Sagdeev (1968), "Transport phenomena in a collisionless plasma in a toroidal magnetic system," *Sov. Phys. JETP* **26**, 233-240.
- Galeev, A.A. and R.Z. Sagdeev (1975), "Neoclassical theory of diffusion," in *Advances in Plasma Physics*, **6**, A. Simon and W.B. Thompson (ed.), (John Wiley & Sons, New York).
- Glasser, A.H., J.M. Greene and J.L. Johnson (1975), "Resistive instabilities in general toroidal plasma configurations," *Phys. Fluids* **18**, 875-888.
- Goldstein, H. (1980), *Classical Mechanics* (Addison-Wesley, Reading, Mass.).
- Grad, H. (1967), "Toroidal containment of a plasma," *Phys. Fluids* **10**, 137-154.
- Greene, J.M. and M.S. Chance (1981), "The second region of stability against ballooning modes," *Nucl. Fusion* **21**, 453-464.
- Greene, J.M. and J.L. Johnson (1962), "Stability criterion for arbitrary hydromagnetic equilibrium," *Phys. Fluids* **5**, 510-517.
- Gross, R.A. (1984), *Fusion Energy* (John Wiley & Sons, New York).
- Hamada, S. (1962), "Hydromagnetic equilibria and their proper coordinates," *Nucl. Fusion* **2**, 23-37.
- Harris, E.G. (1974), "Equilibrium and stability of elliptical cross section tokamak," Oak Ridge National Laboratory Report #ORNL-TM-4666.

- Hastie, R.J., J.B. Taylor and F.A. Haas (1967), "Adiabatic invariants and the equilibrium of magnetically trapped particles," *Ann. Phys.* **41**, 302-338.
- Hazeltine, R.D. (1973), "Recursive derivation of drift-kinetic equation," *Plasma Phys.* **15**, 77-80.
- Hazeltine, R.D. (1974), "Rotation of a toroidally confined, collisional plasma," *Phys. Fluids* **17**, 961-968.
- Hazeltine, R.D., D. Dobrott and T. Wang (1975), "Kinetic theory of tearing instability," *Phys. Fluids* **18**, 1778-1786.
- Hazeltine, R.D. and J.D. Meiss (1985), "Shear-Alfvén dynamics of toroidally confined plasmas," *Phys. Rep.* **121**, 1-164.
- Hazeltine, R.D. and W.A. Newcomb (1990), "Inversion of the ballooning transformation," *Phys. Fluids B* **2**, 7-10.
- Herdan, R. and B.S. Liley (1960), "Dynamical equations and transport relationships for a thermal plasma," *Rev. Mod. Phys.* **32**, 731-741.
- Hinton, F.L. (1983), "Collisional transport in plasma," in *Basic Plasma Physics I*, A.A. Galeev and R.N. Sudan (ed.), (North Holland, New York).
- Hinton, F.L. and R.D. Hazeltine (1976), "Theory of plasma transport in toroidal confinement systems," *Rev. Mod. Phys.* **48**, 239-308.
- Hinton, F.L. and C.R. Oberman (1969), "Electrical conductivity of plasma in a spatially inhomogeneous magnetic field," *Nucl. Fusion* **9**, 319-327.
- Hinton, F.L. and M.N. Rosenbluth (1973), "Transport properties of a toroidal plasma at low-to-intermediate collision frequencies," *Phys. Fluids* **16**, 836-854.
- Hinton, F.L. and S.K. Wong (1985), "Neoclassical ion transport in rotating axisymmetric plasmas," *Phys. Fluids* **28**, 3082-3098.
- Hirshman, S.P. and D.J. Sigmar (1981), "Neoclassical transport of impurities in tokamak plasmas," *Nucl. Fusion* **21**, 1079-1201.
- Horton, W. (1984), "Drift wave turbulence and anomalous transport," in *Basic Plasma Physics II*, A.A. Galeev and R.N. Sudan (ed.), (North Holland, Amsterdam).
- Horton, W. (1989), "Nonlinear drift waves and transport in magnetized plasma," *Phys. Rep.* **192**, 1-177.
- Ichimaru, S. (1973), *Basic Principles of Plasma Physics* (W.A. Benjamin, Inc., Reading, Massachusetts).
- Jackson, J.D. (1975), *Classical Electrodynamics* (John Wiley & Sons, New York).
- Jeffrey, A. and T. Taniuti (ed.) (1966), *Magnetohydrodynamics, Stability, and Thermonuclear Containment* (Academic Press, New York).
- Kadomtsev, B.B. (1965), "Hydromagnetic stability of a plasma," in *Reviews of Plasma Physics*, M.A. Leontovich (ed.), (Consultants Bureau, New York).
- Kapitsa, P.L. (1979), "Plasma and the controlled thermonuclear reaction," *Rev. Mod. Phys.* **51**, 417-423.

- Kaye, S.M. (1985), "A review of energy confinement and local transport scaling results in neutral-beam-heated tokamaks," *Phys. Fluids* **28**, 2327-2343.
- Krall, N.A. (1968), "Drift waves," in *Advances in Plasma Physics*, A. Simon and W.B. Thompson (ed.), **1**, (Interscience, New York).
- Krall, N.A. and A.W. Trivelpiece (1973), *Principles of Plasma Physics* (McGraw-Hill, New York).
- Krommes, J.A. (1984), "Statistical descriptions and plasma physics," in *Basic Plasma Physics II*, A.A.S. Galeev R.N. (ed.), (North Holland, Amsterdam).
- Kruskal, M.D. and R.M. Kulsrud (1958), "Equilibrium of a magnetically confined plasma in a toroid," *Phys. Fluids* **1**, 265-274.
- Kruskal, M.D. and C.R. Oberman (1958), "On the stability of plasma in static equilibrium," *Phys. Fluids* **1**, 275-280.
- Lichtenberg, A.J. and M.A. Lieberman (1982), *Regular and Stochastic Motion* (Springer-Verlag, New York).
- Littlejohn, R.G. (1981), "Hamiltonian formulation of guiding center motion," *Phys. Fluids* **24**, 1730-1749.
- Littlejohn, R.G. (1983), "Variational principles of guiding center motion," *J. Plasma Physics* **29**, 111-125.
- MacKay, R.S. and J.D. Meiss (ed.) (1987), *Hamiltonian Dynamical Systems: a reprint selection* (Adam-Hilgar Press, London).
- Mikhailovskii, A.B. (1974), *Theory of Plasma Instabilities* (Consultants Bureau, New York).
- Morozov, A.I. and L.S. Solov'ev (1965), "The structure of magnetic fields," in *Reviews of Plasma Physics*, **2**, M.A. Leontovich (ed.), (Consultants Bureau, New York).
- Morozov, A.I. and L.S. Solov'ev (1966), "Motion of charged particles in electromagnetic fields," in *Reviews of Plasma Physics*, **2**, M.A. Leontovich (ed.), (Consultants Bureau, New York).
- Morrison, P.J. and M. Kotschenreuther (1990), "The free energy principle, negative energy modes, and stability," in *IV International Workshop on Nonlinear Processes in Physics, Nonlinear World*, **2**, V.G. Baryakhtar, et al. (eds.), (World Scientific, Singapore).
- Morse, P.M. and H. Feshbach (1953), *Methods of Theoretical Physics* (McGraw-Hill, New York).
- Newcomb, W.A. (1959), "Magnetic differential equations," *Phys. Fluids* **2**, 362-365.
- Newcomb, W.A. (1960), "Hydromagnetic Stability of a Diffuse Linear Pinch," *Ann. Phys.* **10**, 232.
- Northrop, T.G. (1963), *The Adiabatic Motion of Charged Particles* (Interscience-Wiley, New York).
- Northrop, T.G. and K.J. Whiteman (1964), "Minimum-B plasma equilibria with finite pressure," *Phys. Rev. Lett.* **12**, 639-640.
- Rechester, A.B. and M.N. Rosenbluth (1978), "Electron Heat Transport in

- a Tokamak with Destroyed Magnetic Surfaces," *Phys. Rev. Lett.* **40**, 38-41.
- Ribe, R.L. (1975), "Fusion reactor systems," *Rev. Mod. Phys.* **47**, 7-41.
- Roberts, K.V. and J.B. Taylor (1962), "Magnetohydrodynamic equations for finite Larmor radius," *Phys. Rev. Lett.* **8**, 197-198.
- Robinson, B.B. and I.B. Bernstein (1962), "A variational description of transport phenomena in a plasma," *Ann. Phys.* **18**, 110-169.
- Rose, D.J. and M. Clark Jr. (1961), *Plasma and Controlled Fusion* (The MIT Press, Cambridge, Massachusetts).
- Rosenbluth, M.N., R.Y. Dagazian and P.H. Rutherford (1973), "Nonlinear properties of the internal $m=1$ kink instability in the cylindrical tokamak," *Phys. Fluids* **16**, 1894-1902.
- Rosenbluth, M.N., R.D. Hazeltine and F.L. Hinton (1972), "Plasma transport in toroidal confinement systems," *Phys. Fluids* **15**, 116-140.
- Rosenbluth, M.N. and A.N. Kaufman (1958), "Plasma diffusion in a magnetic field," *Phys. Rev.* **109**, 1-5.
- Rosenbluth, M.N., W.M. MacDonald and D.L. Judd (1957), "Fokker-Planck equation for an inverse-square force," *Phys. Rev.* **107** 1-6.
- Rosenbluth, M.N. and N. Rostoker (1958), "Theoretical structure of plasma equations," *Phys. Fluids* **2**, 23-30.
- Rosenbluth, M.N., P.H. Rutherford, J.B. Taylor, E.A. Frieman and L.M. Kovrizhnikh (1971), "Neoclassical effects on plasma equilibria and rotation," *Plasma Physics and Controlled Nuclear Fusion Research* (IAEA, Vienna).
- Rosenbluth, M.N. and A. Simon (1965), "Finite Larmor radius equations with nonuniform electric fields and velocities," *Phys. Fluids* **8**, 1300-1325.
- Rutherford, P.H. (1970), "Collisional diffusion in an axisymmetric torus," *Phys. Fluids* **13**, 482-489.
- Rutherford, P.H. (1970), "Nonlinear growth of the tearing mode," *Phys. Fluids* **16**, 1903-1908.
- Rutherford, P.H. and E.A. Frieman (1968), "Drift instabilities in general magnetic field configurations," *Phys. Fluids* **11**, 569-585.
- Schmidt, G. (1979), *Physics of High Temperature Plasmas* (Academic Press, New York).
- Shafranov, V.D. (1966), "Plasma equilibrium in a magnetic field," in *Reviews of Plasma Physics*, **1**, M.A. Leontovich (ed.), (Consultants Bureau, New York).
- Shohet, J.L. (1971), *The Plasma State* (Academic Press, New York).
- Spies, G.O. and D.B. Nelson (1974), "Properties of magnetically confined plasma equilibria," *Phys. Fluids* **17**, 1879-1884.
- Spitzer, L., Jr. (1962), *Physics of Fully Ionized Gases* (John Wiley & Sons, New York).
- Stix, T.H. (1973), "Magnetic braiding in a toroidal plasma," *Phys. Rev. Lett.* **30**, 833-835.

- Strauss, H.R. (1976), "Dynamics of high β tokamaks," *Phys. Fluids* **20**, 1354-1360.
- Strauss, H.R., R.D. Hazeltine, S.M. Mahajan and D.W. Ross (1979), "Twisting modes," *Phys. Fluids* **22**, 889-895.
- Tataronis, J.A. (1975), "Energy absorption in the continuous spectrum of ideal MHD," *J. Plasma Phys.* **13**, 87-105.
- Taylor, J.B. (1974), "Bundle divertors and topology," Culham Laboratory Report #CLM-R 132.
- Taylor, J.B. (1976), "Does magnetic shear stabilize drift waves?" *Plasma Physics and Controlled Nuclear Fusion Research* (IAEA, Vienna).
- Taylor, J.B. (1986), "Relaxation and magnetic reconnection in plasmas," *Rev. Mod. Phys.* **58**, 741-763.
- Taylor, J.B. and B. McNamara (1971), "Plasma diffusion in two dimensions," *Phys. Fluids* **14**, 1492-1499.
- Teller, E. (1981), "Introduction," in *Fusion*, E. Teller (ed.), (Academic Press, London).
- Tendler, M. and D. Heifetz (1987), "Neutral particle kinetics in fusion devices," *Fusion Tech.* **11**, 289-310.
- Van Kampen, N.G. and B.U. Felderhof (1967), *Theoretical Methods in Plasma Physics* (North Holland, Amsterdam).
- Waltz, R.E. (1982), "Magnetic fluctuations, ambipolarity, charge filamentation, and plasma rotation in tokamaks," *Phys. Fluids* **25**, 1269-1278.
- Ware, A.A. (1970), "Pinch effect for trapped particles in a tokamak," *Phys. Rev. Lett.* **25**, 15-17.
- Ware, A.A. (1989), "Electron Fokker-Planck equation for collisions with ions in a magnetized plasma," *Phys. Rev. Lett.* **62**, 51-54.
- White, R.B. (1986), "Resistive reconnection," *Rev. Mod. Phys.* **58**, 183-207.
- White, R.B. (1989), *Theory of Tokamak Plasmas* (North Holland, Amsterdam).